Scientific Instruments

— and —

Phase Noise and Frequency Stability in Oscillators

Lectures for PhD Students and Young Scientists

Spring 2024

Updated March 22, 2024

Extended Version

Enrico Rubiola

CNRS FEMTO-ST Institute, Besancon, France

INRiM, Torino, Italy

Part 1: General

Part 2: Phase noise and oscillators

Part 3: The International System of Units SI

ORCID 0000-0002-5364-1835

home page http://rubiola.org

Copyright information

This document

- Is intended for classroom use
  - PhD students and guests attending the Enrico's lectures at the University of Bourgogne Franche Comté, France
- Has no lucrative purpose, even a donation is not possible.
  Teaching is already paid by my monthly salary
- Makes fair use of a very small amount of copyrighted material, intended to promote reading the original
  - Should you spot a problem, please email at enrico [at] rubiola [dot] org rather than making a fuss

Lecture 6

Scientific Instruments & Oscillators

Lectures for PhD Students and Young Scientists

Enrico Rubiola

CNRS FEMTO-ST Institute, Besancon, France

INRiM, Torino, Italy

Contents
- Phase Noise
- Allan variances

ORCID 0000-0002-5364-1835

home page http://rubiola.org

Learning material

E. Rubiola, F. Vernotte, The Companion of the Enrico's Chart for Phase Noise and Two-Sample Variances, IEEE Trans MTT, Early access, February 2023
https://ieeexplore.ieee.org/document/10050257

… and download the Enrico's Chart from
https://doi.org/10.5281/zenodo.4399218

Otherwise, both are on https://rubiola.org

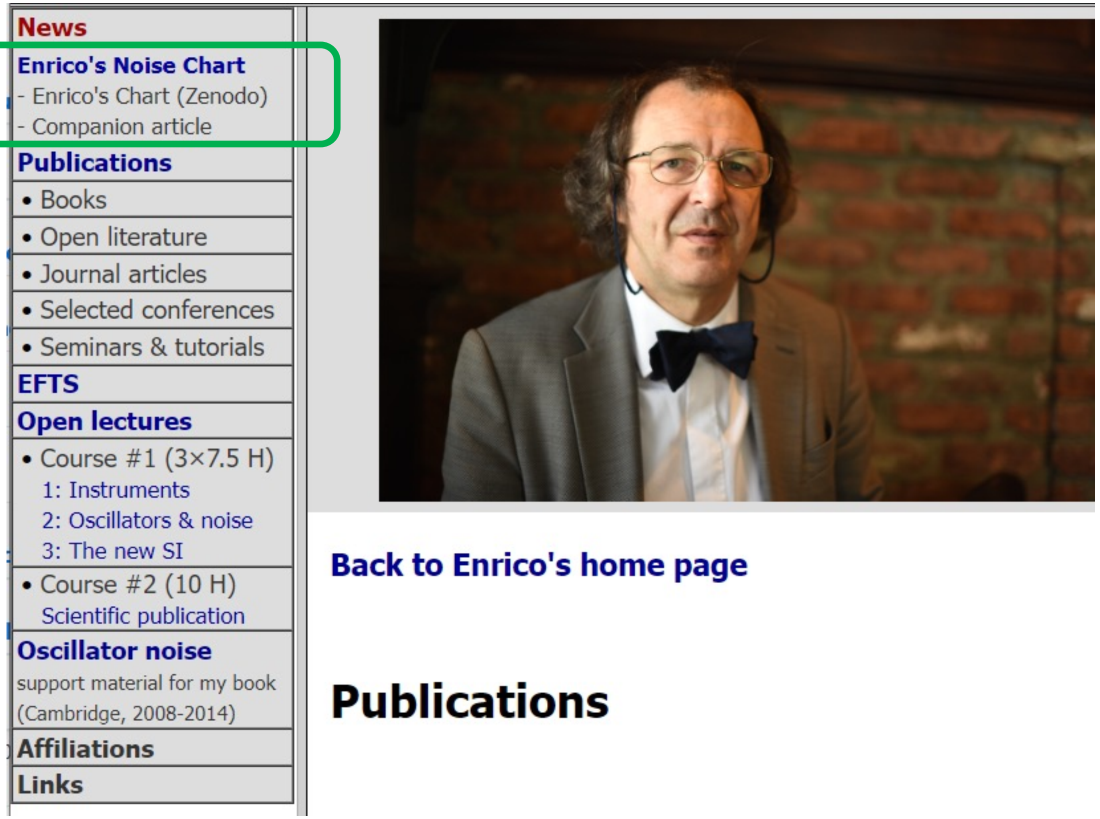

The Clock Signal

The clock signal

$$v(t) = V_0\,[1 + \alpha(t)]\cos\,[2\pi\nu_0 t + \varphi(t)]$$

- V_0: carrier amplitude
- $\alpha(t)$: fractional amplitude fluctuation
- ν_0: carrier frequency
- $\varphi(t)$: phase fluctuation

(regular) frequency	angular frequency	relation	context
ν	ω	$\nu = \omega/2\pi$	carrier
f	ω	$f = \omega/2\pi$	Fourier analysis, or modulation
ω is used as a shorthand for either $2\pi\nu$ or $2\pi f$			

The clock signal

Observed with an ideal oscilloscope

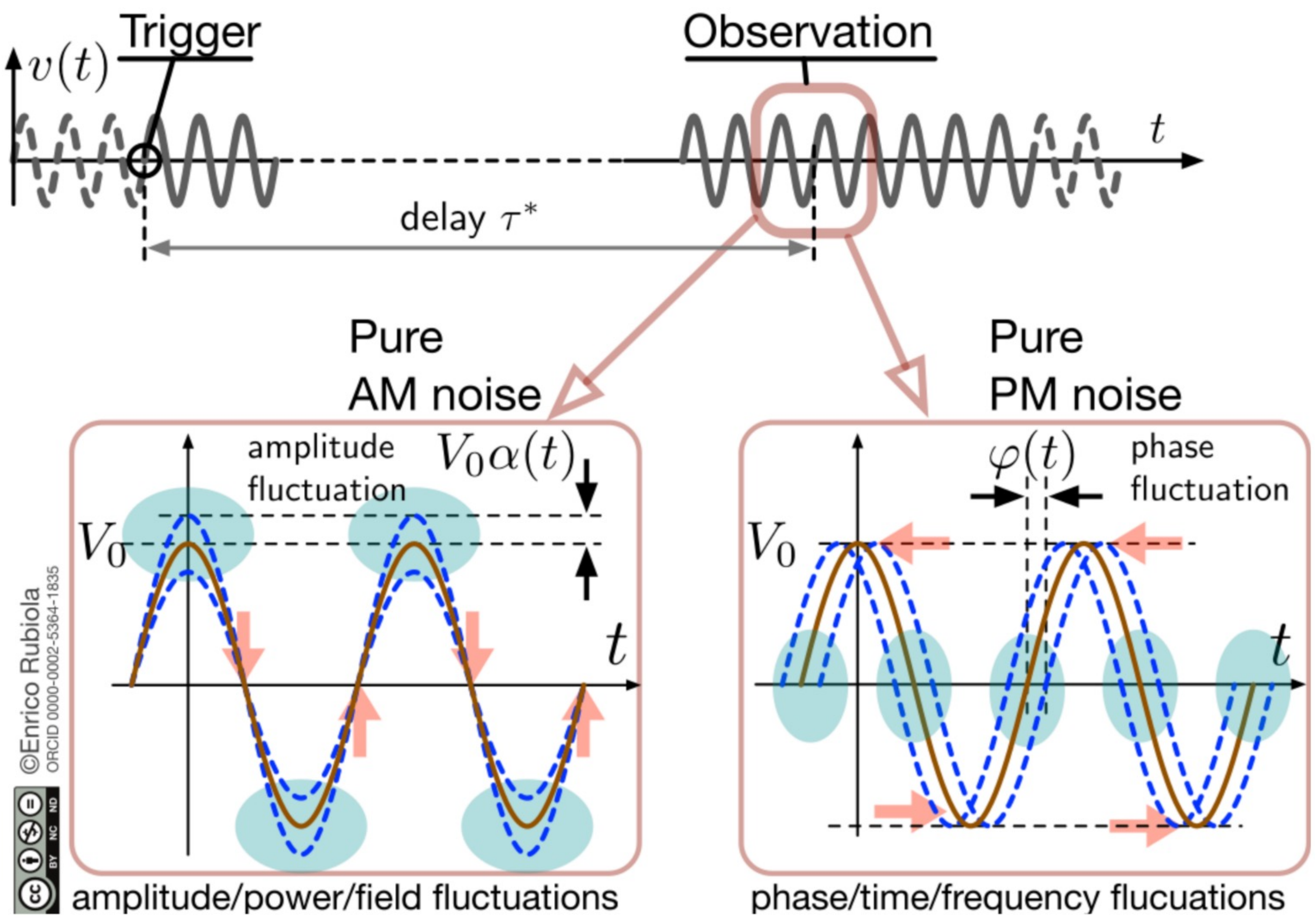

τ^* is not the same "τ" of the Allan variance

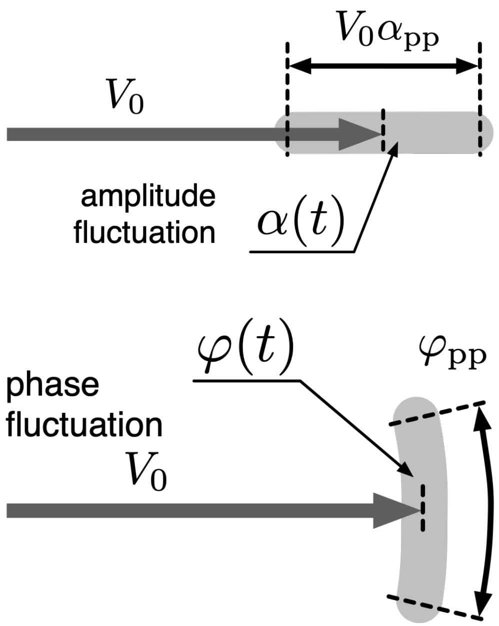

polar coordinates

$$v(t) = V_0\,[1+\alpha(t)]\cos[\omega_0 t + \varphi(t)]$$

Cartesian coordinates

$$v(t) = V_0 \cos\omega_0 t + n_c(t)\cos\omega_0 t - n_s(t)\sin\omega_0 t$$

Low noise approximation

$$\alpha(t) = \frac{n_c(t)}{V_0} \quad \text{and} \quad \varphi(t) = \frac{n_s(t)}{V_0}$$

A misleading representation

- The caption says instantaneous output voltage of an oscillator
- But the picture is a unrealistic representation of AM and PM noise
- The problem is that additive white noise is dominant
- Other, slower types of noise are our main concern

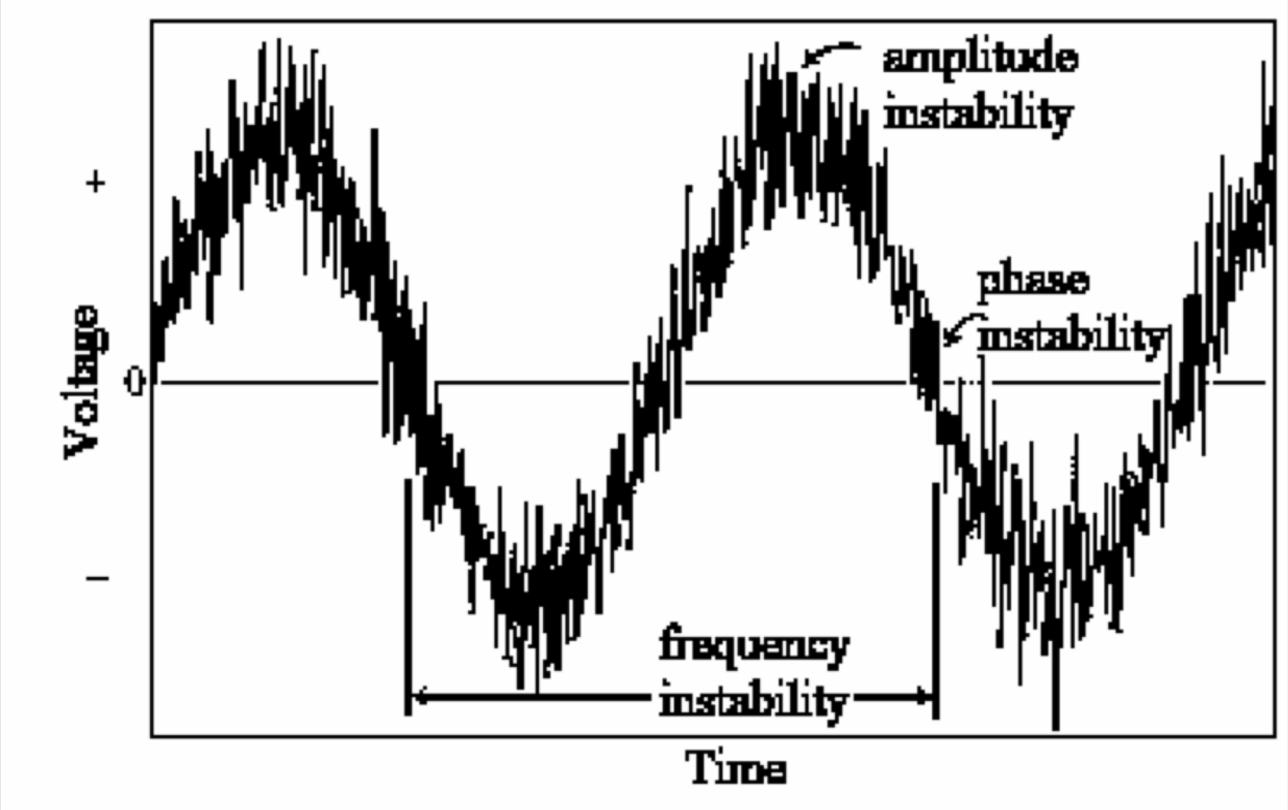

IEEE-1139-2009 - Ferre-Pikal E - IEEE Standard Definitions of Physical Quantities for Fundamental Frequency and Time Metrology, Random Instabilities - IEEE 2009, ISBN 978-0-7381-6855-5.pdf

Figure A.1—Instantaneous output voltage of an oscillator

Eye diagram

BPSK $v_{RF} = b_k \cos \omega t$, where $b_k = \pm 1$ is the k_{th} bit transmitted

Pure signal

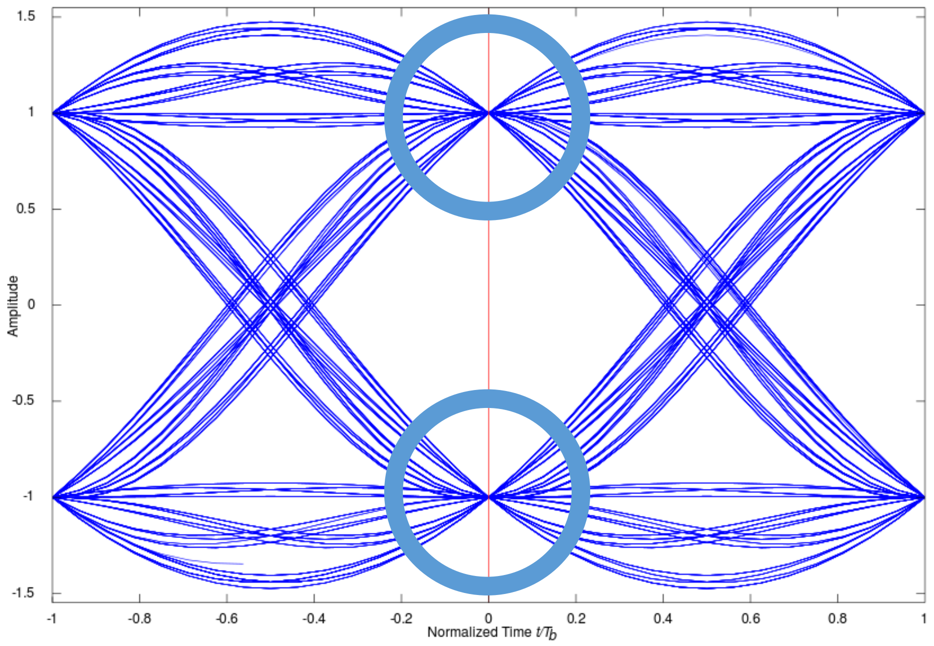

Signal corrupted by AM and PM noise

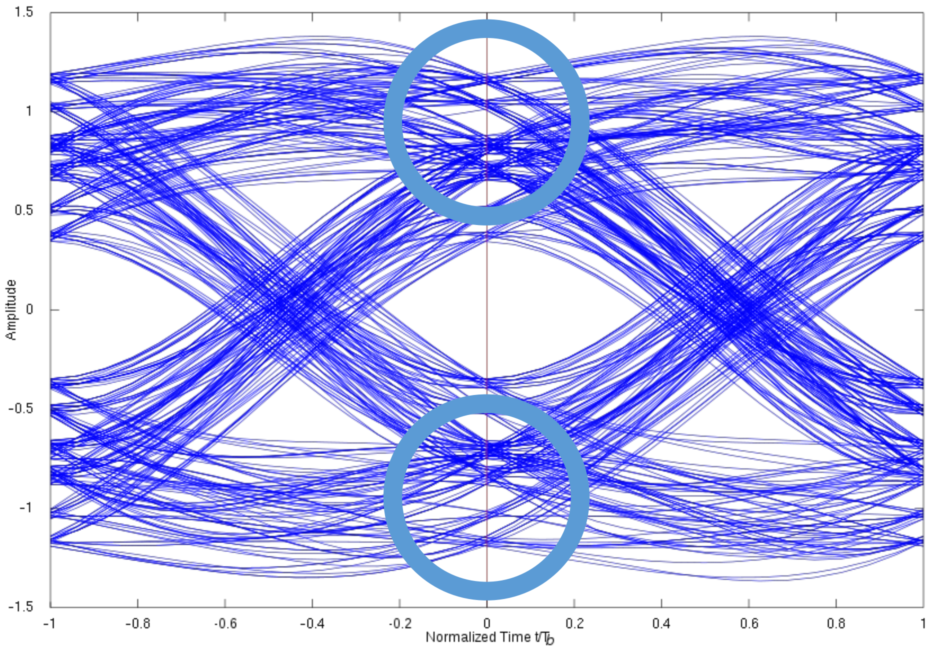

Timing impacts on the Bit Error Rate (BER)

The line width does not tell the true story

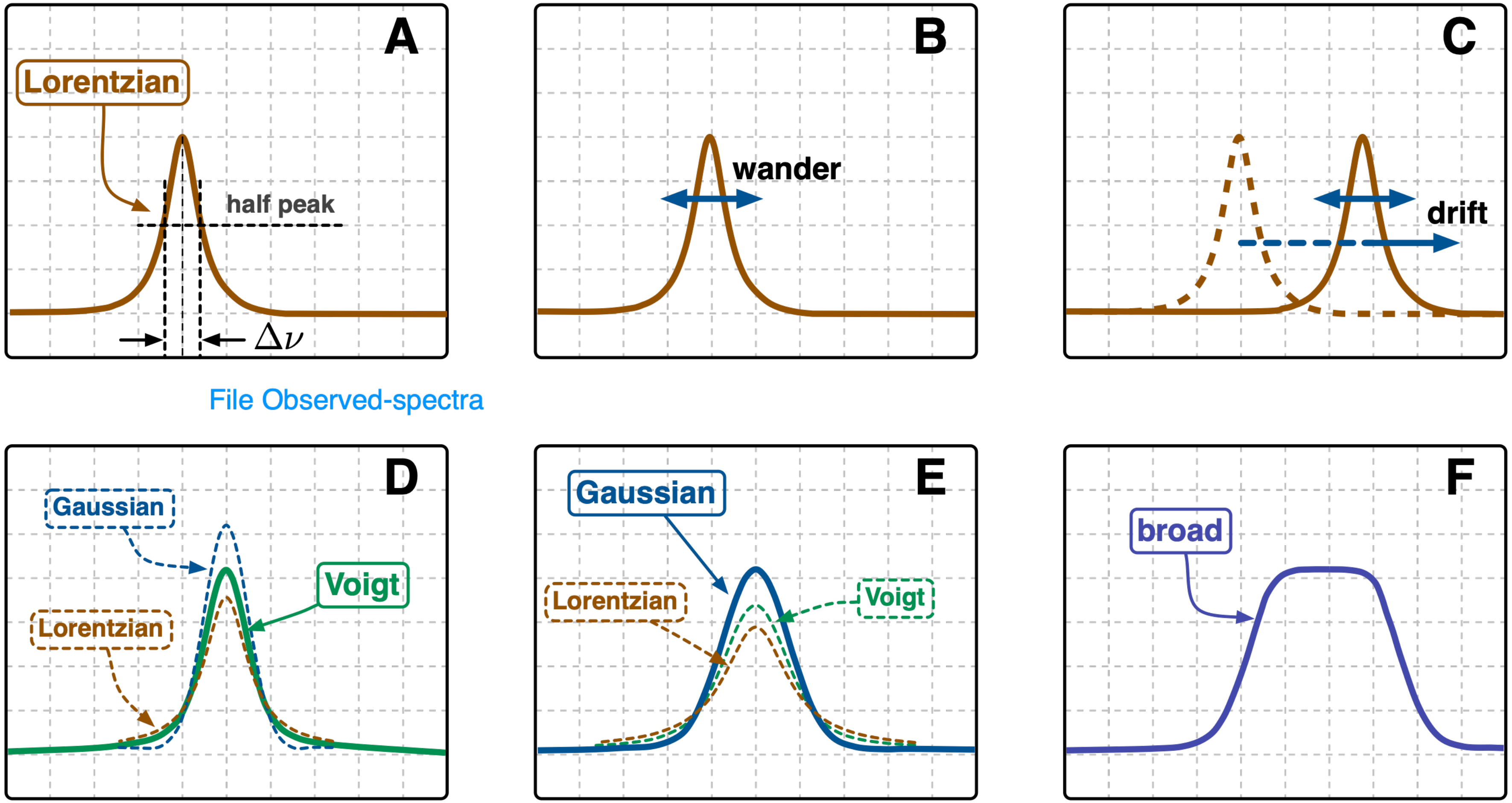

File Observed-spectra

- In the absence of noise, the clock signal is a Dirac δ(ν)
- Noise broadens the spectrum
- The difference between AM and PM noise is hidden here

The bath hub diagram

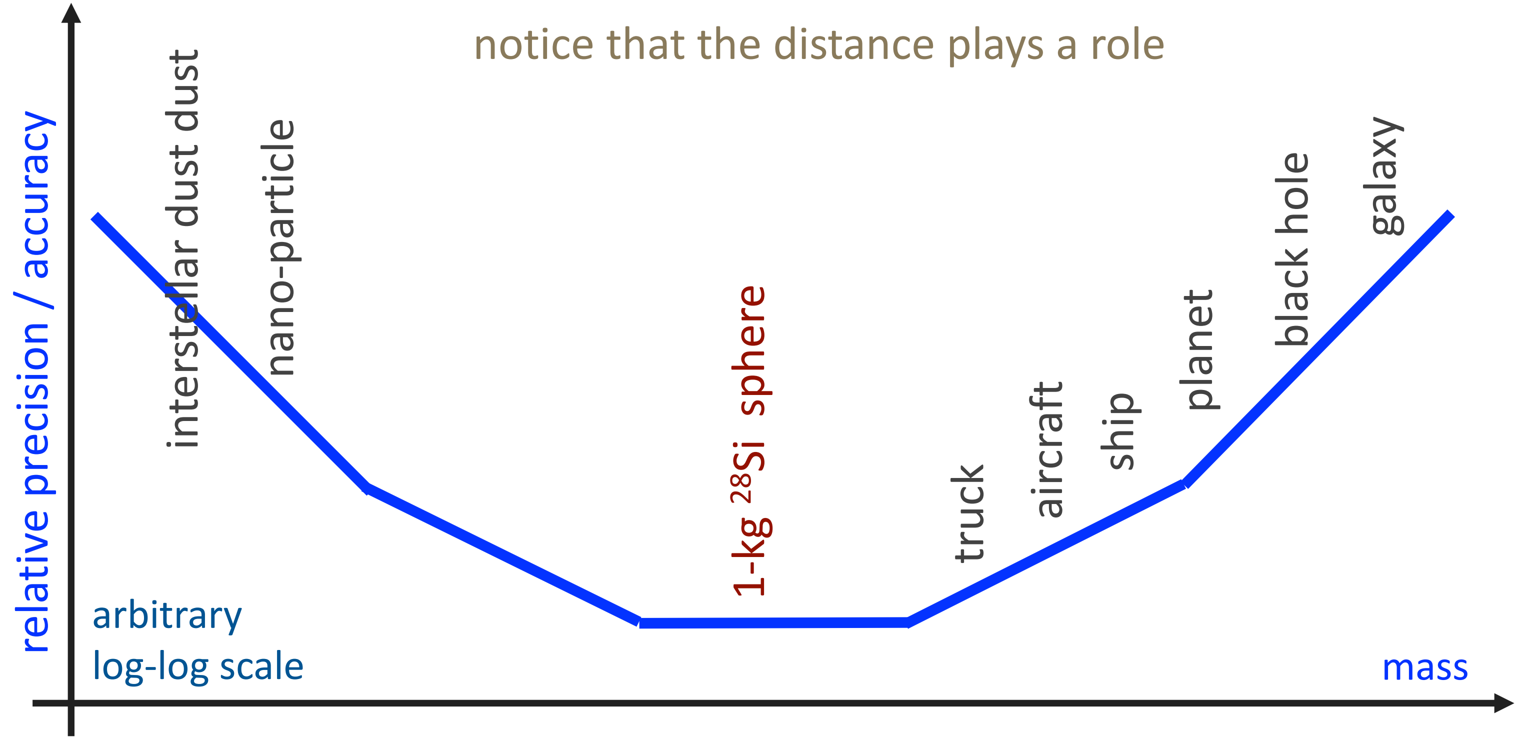

The same happens with *all physical quantities*, including time

notice that the *frequency* affects the resolution

The family of Allan variances

Precision is a function of the measurement time τ

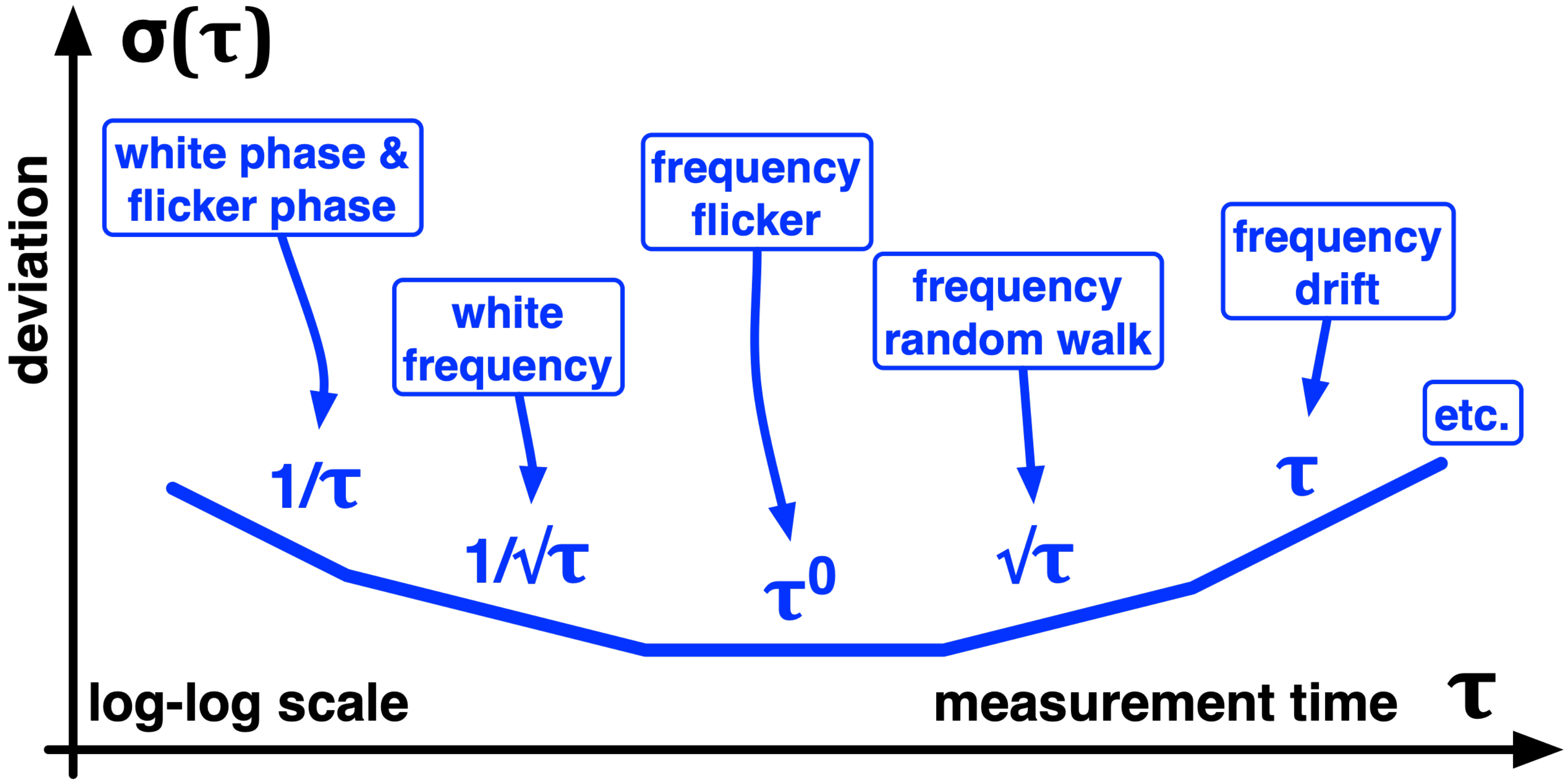

The noise types will be explained later

Representations of the Clock Signal

Analytic signal

Standard representation of signals in microwaves and optics

$$v(t) = V_0\,[1+\alpha(t)]\cos\left[\omega_0 t + \varphi(t)\right]$$

⇓

$$\mathring{v}(t) = V_0\,[1+\alpha(t)]\,e^{i\omega_0 t}e^{i\varphi(t)}$$

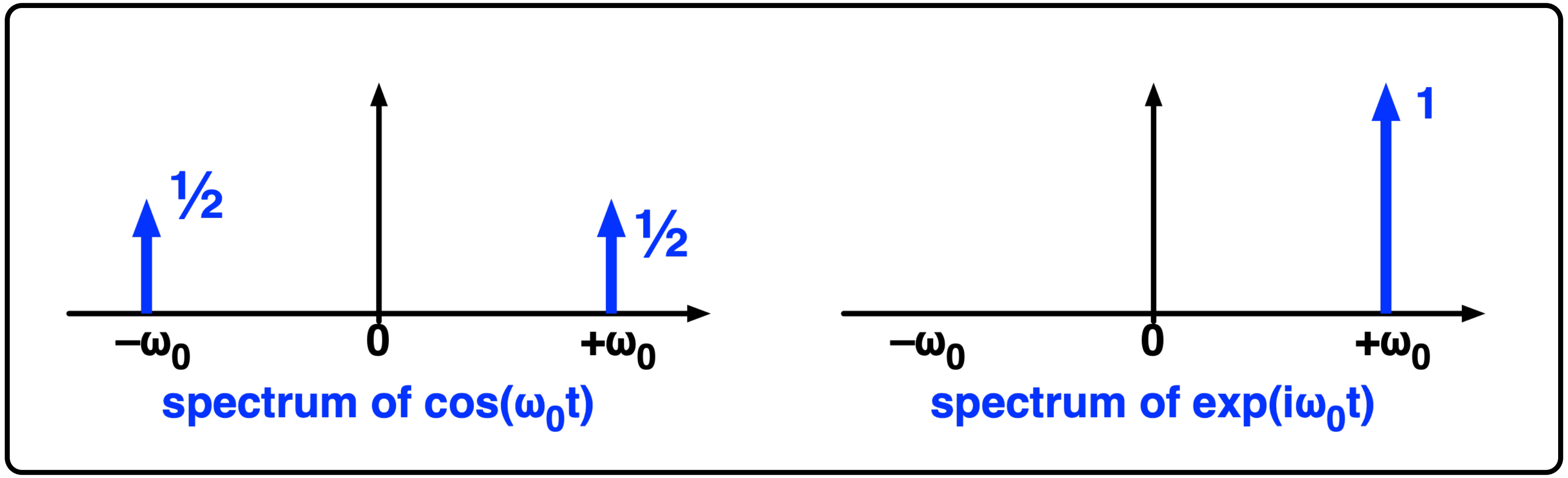

The analytic continuation

- Removes the negative frequencies
- Keeps the power

Low-pass process / pre-envelope

Often used in telecomm

Real signal $$v(t) = V_0\left[1+\alpha(t)\right]\cos\left[\omega_0 t + \varphi(t)\right]$$

Analytic signal $$\mathring{v}(t) = V_0\left[1+\alpha(t)\right]e^{i\omega_0 t}e^{i\varphi(t)}$$

freeze the $e^{i\omega t}$ oscillation

Low-pass process (pre-envelope) $$\tilde{v}(t) = V_0\left[1+\alpha(t)\right]e^{i\varphi(t)}$$

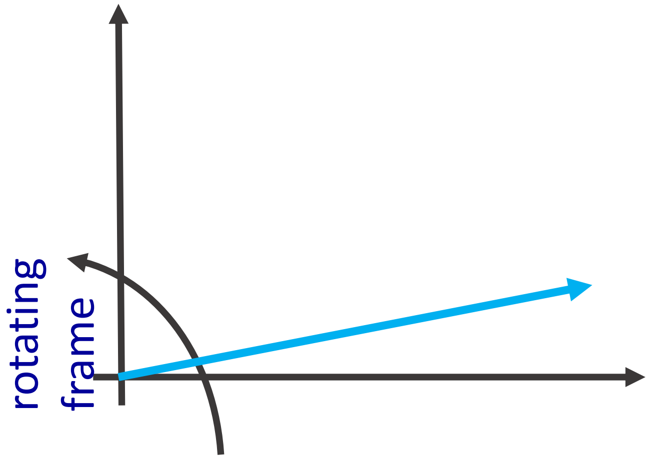

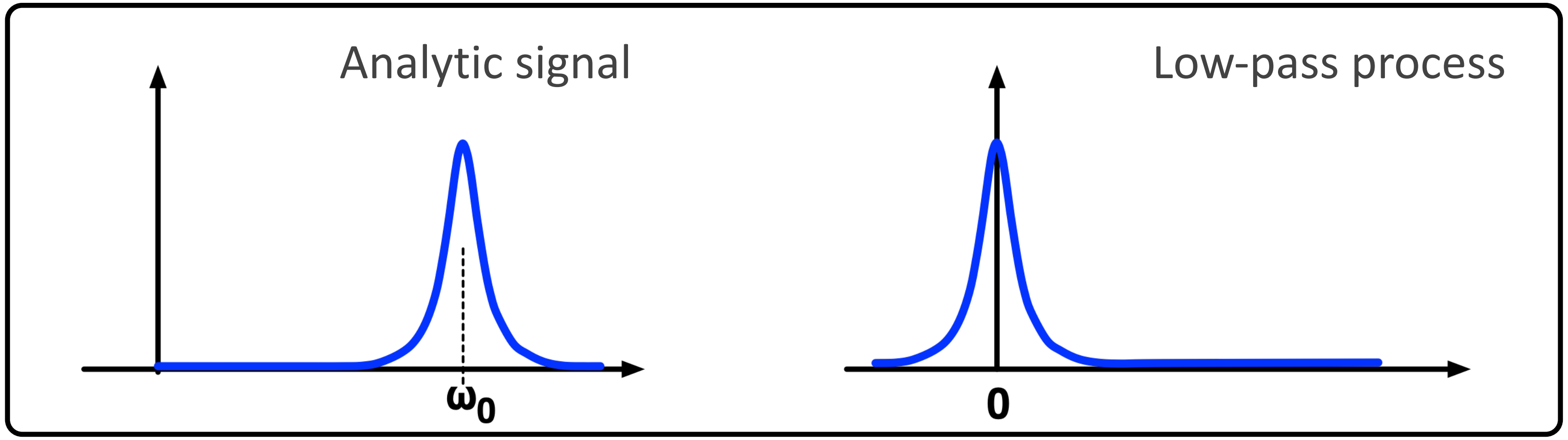

Phasor – Fresnel vector

amplitude fluctuation

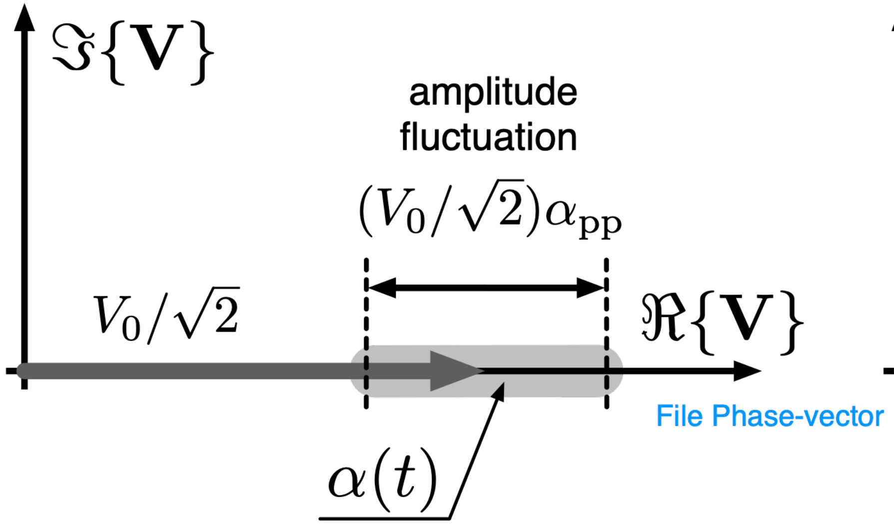

phase fluctuation

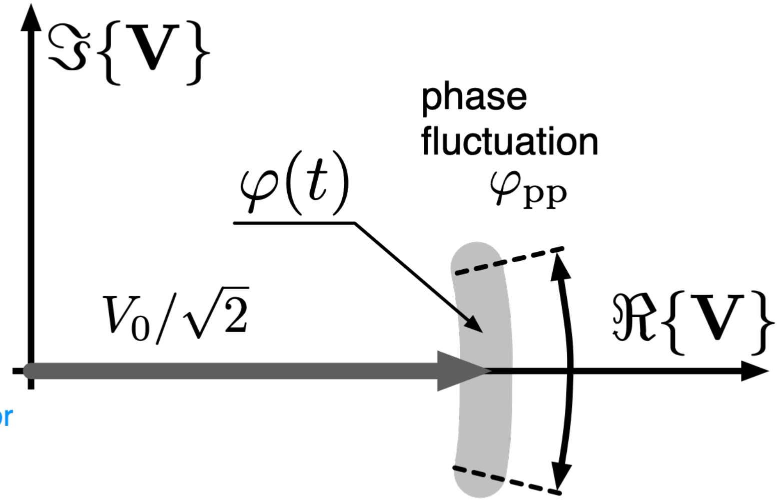

$$v(t) = V_0\left[1+\alpha(t)\right]\cos\left[\omega_0 t + \varphi(t)\right]$$

Freeze the $\omega_0 t$ oscillation, add an imaginary part

$$\mathbf{V} = \frac{V_0}{\sqrt{2}}\left[1+\alpha\right]\left[\cos\varphi + i\sin\varphi\right]$$

Strictly, the phase representation applies to static α and φ.
The extension to (slow) varying $\alpha(t)$ and $\varphi(t)$ is obvious

Notation

Power electronics

- RMS value
- $P = VI^*$

Microwaves

- Peak value

Modulation and sidebands

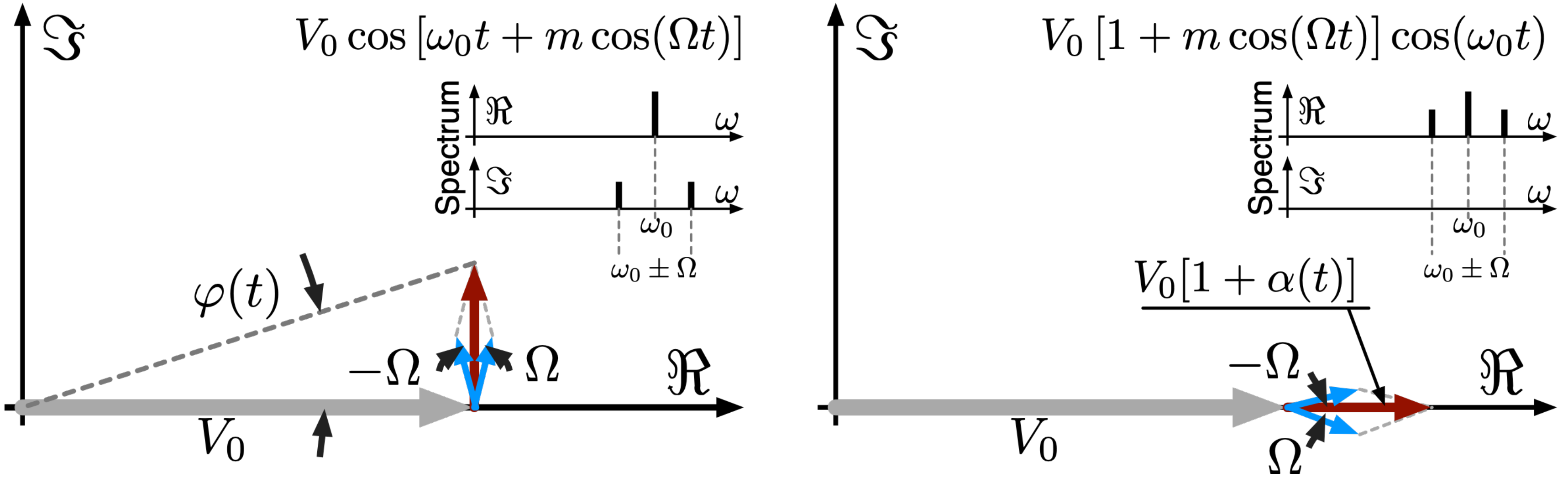

File Modulation-summary

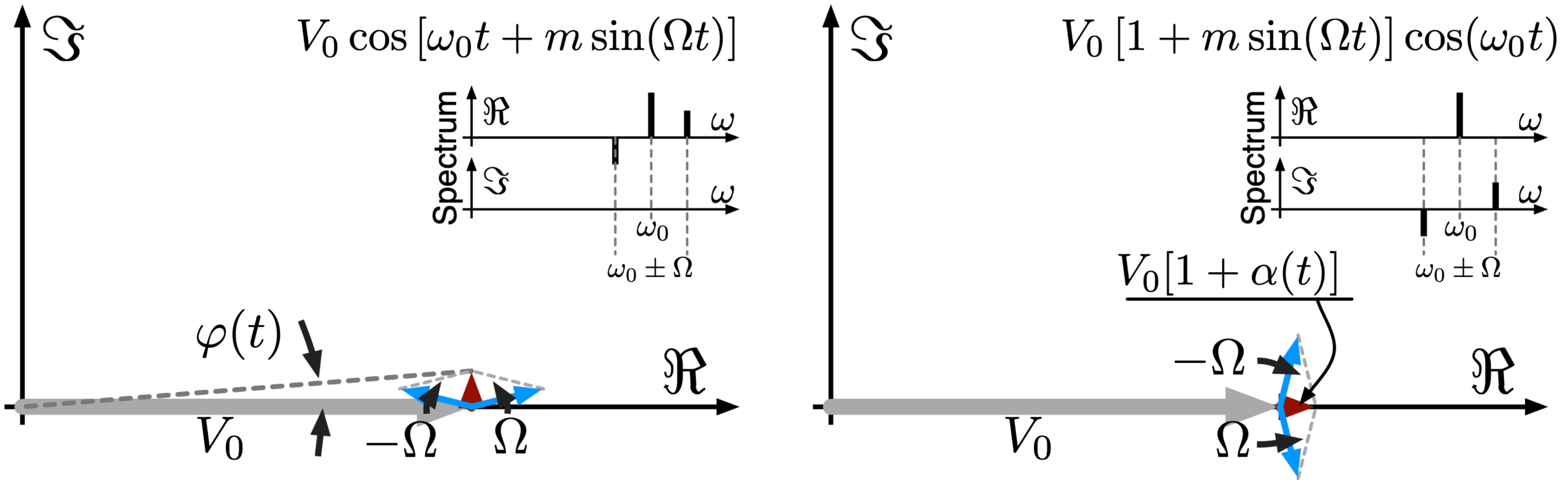

Bandwidth

$\Omega < \omega_0$

random modulation is no exception

Phase modulation – Math

$$v(t) = e^{i(\omega_0 + m \sin \omega_m)t}$$

Phase modulated signal, with modulation index *m*

$$e^{im \sin \theta} = \sum_{n=-\infty}^{\infty} J_n(m)\, e^{in\theta}$$

The full frequency domain representation contains an infinite number of sidebands ruled by the Jacobi–Anger expansion

$$v(t) = e^{i\omega_0 t} + \frac{m}{2} e^{i(\omega_0 + \omega_m)t} - \frac{m}{2} e^{i(\omega_0 - \omega_m)t}$$

For small *m*, the expansion can be truncated to 3 terms, $n = -1 \ldots +1$
Use the asymptotic expansion $J_0(m) \approx 1$, $J_{-1}(m) \approx -m/2$, $J_1(m) \approx m/2$,

Freeze ω_0 —> phase vector representation

$$V(t) = 1 + \frac{m}{2}\left[e^{i\omega_m t} - e^{-i\omega_m t}\right]$$

equivalent to

$$V(t) = 1 + im \sin(\omega_m t)$$

use

$$\sin\theta = \frac{1}{2j}\left(e^{i\theta} - e^{-i\theta}\right)$$

A swinging phase θ is equivalent to a swinging frequency $\Delta f = (1/2\pi)\,(d\theta/dt)$

$$(\Delta f)(t) = m \frac{\omega_m}{2\pi} \cos(\omega_m t) = m f_m \cos(\omega_m t)$$

Quantities Associated to the Clock Signal

Phase-time x(t), and jitter

$$v(t) = V_0\left[1+\alpha(t)\right]\cos\left[2\pi\nu_0 t + \varphi(t)\right] \qquad \mathrm{x}(t) = \frac{\varphi(t)}{2\pi\nu_0}$$

- ITU defines jitter as the variations in the significant instants of a clock or data signal, vs a "perfect" clock
- Jitter —> Usually fast phase changes $f >$ a few tens of Hz
- Wander —> Usually slower phase changes (due to temperature, voltage, etc.)
- Designers first care about consistency of logic functions,
  - First, maximum timing error
  - Sometimes RMS value and probability distribution
- Time and Frequency community focuses on
  - PM noise spectra
  - Delay spectra
  - Two-sample variances (ADEV, TDEV, etc.)

Unlike x(t), the **jitter** includes telecom-oriented industrial standards

Phase time (fluctuation) x(t)

- Let's allow $\varphi(t)$ to exceed $\pm\pi$, and count the no of turns
- This is easily seen by scaling ν down (up) to 1 Hz with a noise-free gear work
- The phase-time fluctuation associated to $\varphi(t)$ is

$$\mathrm{x}(t) = \frac{\varphi(t)}{2\pi\nu}$$

- In frequency synthesis, x(t) is independent of ν
- a constant in noise-free synthesis (likewise, y(t))

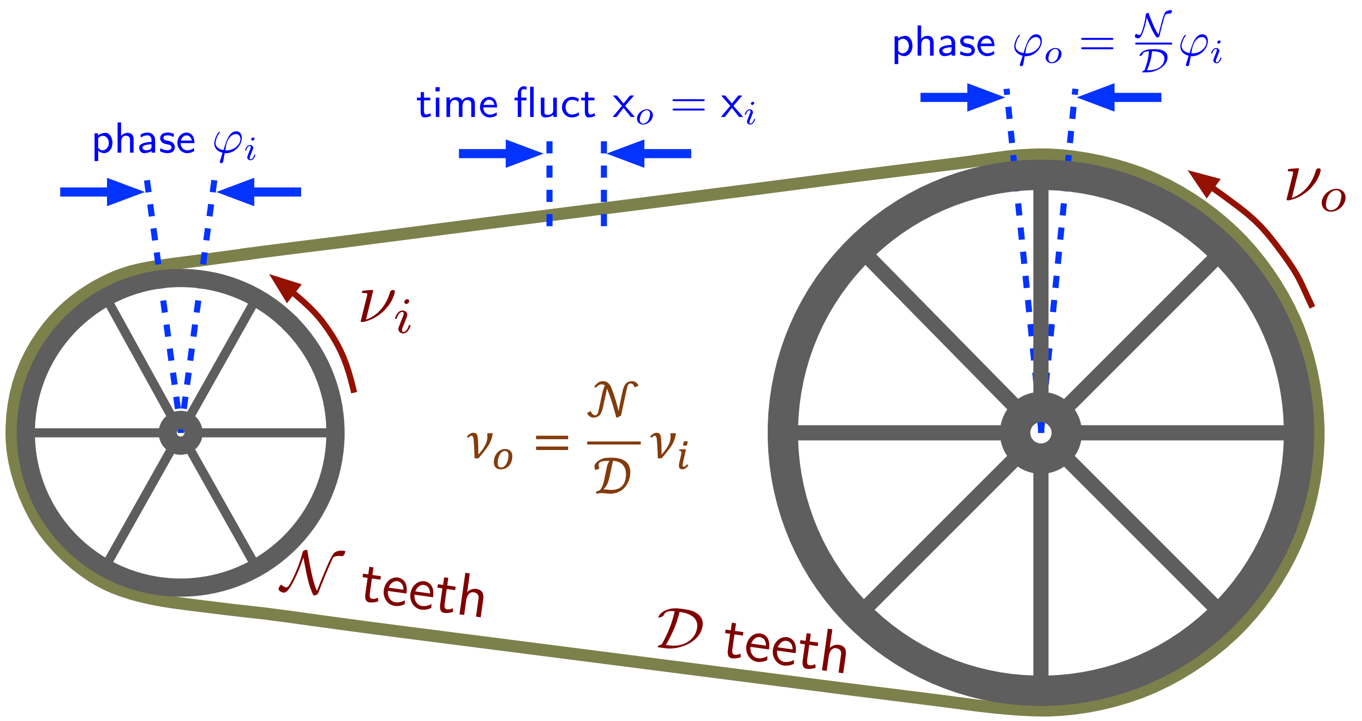

The frequency fluctuation $(\Delta\nu)(t)$

Freeze the random phase, and move the fluctuation to the frequency

$$\varphi(t) = 2\pi \int [\nu(t) - \nu_0] \; dt$$

$$\varphi(t) = 2\pi \int (\Delta\nu)(t) \; dt$$

$$v(t) = V_0 \left[1 + \alpha(t)\right] \cos\left[2\pi\nu_0 t + 2\pi \textstyle\int (\Delta\nu)(t) \; dt\right]$$

carrier frequency

phase fluctuation

The fractional-frequency fluctuation y(t)

$$\mathrm{y}(t) = \frac{(\Delta\nu)(t)}{\nu_0}$$

$$\varphi(t) = 2\pi\nu_0 \int \frac{(\Delta\nu)(t)}{\nu_0}\, dt$$

$$v(t) = V_0\,[1+\alpha(t)]\cos\left[2\pi\nu_0 t + 2\pi\nu_0 \textstyle\int \mathrm{y}(t)\, dt\right]$$

carrier frequency

phase fluctuation

Physical quantities

$$v(t) = V_0\,[1+\alpha(t)]\cos\left[2\pi\nu_0 t + \varphi(t)\right]$$

Allow $\varphi(t)$ to exceed $\pm\pi$ and count the number of turns, so that $\varphi(t)$ describes the clock fluctuation in full

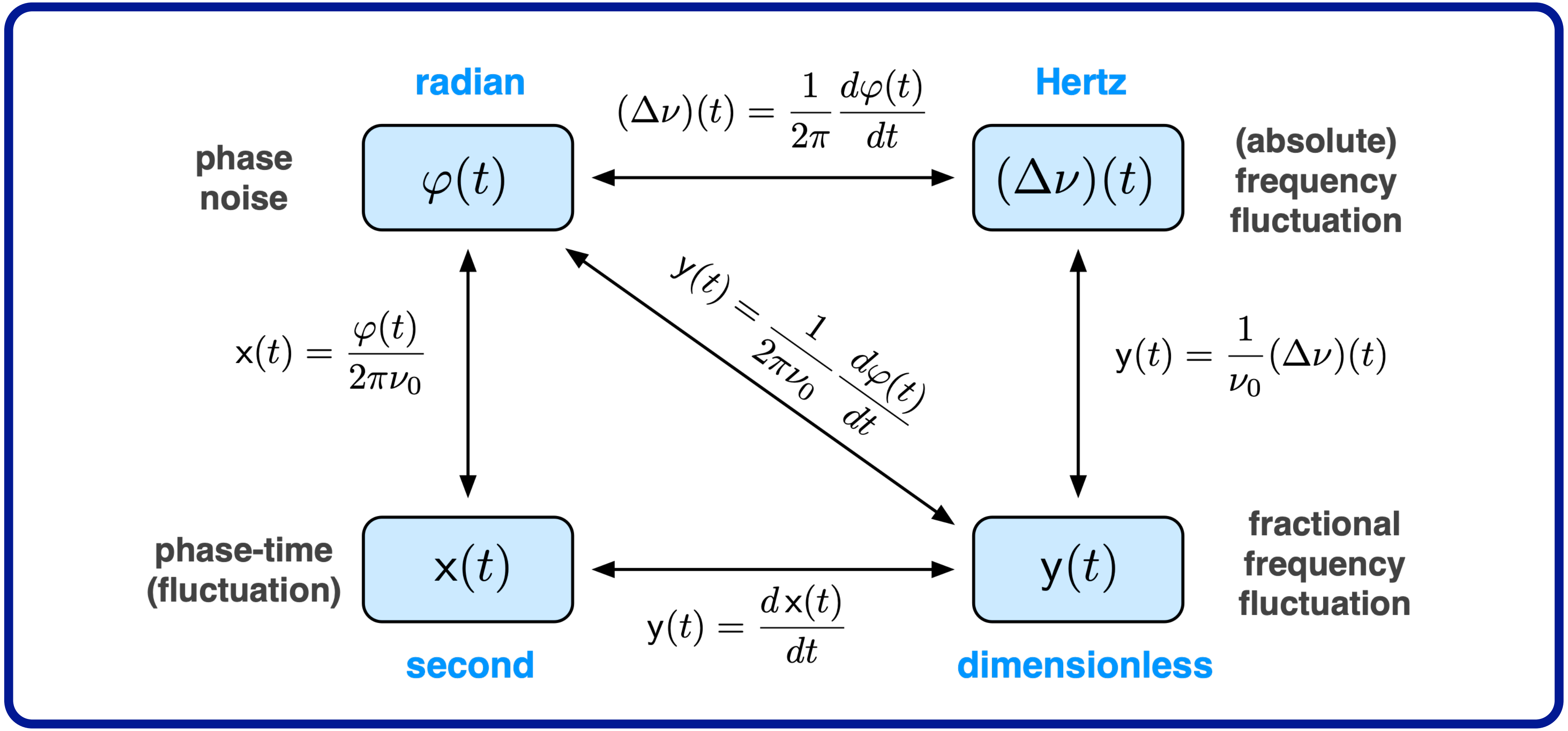

Analogies

- The “error” of a wrist watch is usually expressed in seconds, if not in minutes.
- The frequency of the internal oscillator (5 Hz for the balance wheel, and 2^{15} Hz for the quartz) does not matter.
- In TF, the “time error” is denoted with x(t) [seconds]
- The fractional “error” of an instrument or of a standard is often expressed in percent (%) or in parts-per-million (ppm).
- This way of expressing the “error” is independent of the value of the measured quantity
- In TF, the “fractional frequency error” is denoted with y(t) [dimensionless]

A Useful notation

boldface notation	
total = nominal + fluctuation	
$\boldsymbol{\varphi}(t) = 2\pi\nu_0 t + \varphi(t)$	phase
$\boldsymbol{\nu}(t) = \nu_0 + (\Delta\nu)(t)$	frequency
$\mathbf{x}(t) = t + \mathrm{x}(t)$	time
$\mathbf{y}(t) = 1 + \mathrm{y}(t)$	fractional frequency

Noise Spectra

$S_\varphi(f)$ and $\mathcal{L}(f)$

Power Spectral Density (PSD)

Definition of PSD

$$S(f) = \mathcal{F}\{\mathcal{C}(\tau)\}$$

$\mathcal{C}(\tau)$ is the autocovariance

$\mathcal{F}\{\,\}$ is the Fourier Transform

Match SI units

- $\varphi(t)$ –> rad
- $S_\varphi(f)$ –> $\mathrm{rad}^2/\mathrm{Hz}$
- Log scale –> $\mathrm{dBrad}^2/\mathrm{Hz}$

Thermal limit $S_\varphi = kT_{eq}/P_0$

Power P_0, thermal energy kT_{eq}

Practical estimation

$$S_\varphi(f) = \frac{2}{T}\langle \Phi_T(f)\Phi_T^*(f)\rangle_m$$

- Based on WK theorem
- Single-sided $S(f)$, $f > 0$
- Fourier transform Φ_T of the digitized and truncated φ
- Average on m realizations

The quantity $\mathcal{L}(f)$

Why changing symbol after changing the unit?

$$\mathcal{L}(f) = \frac{1}{2}S_\varphi(f) \qquad \text{IEEE Std 1139}$$

- Always in log scale using $10\log_{10}(\mathcal{L})$
- Non-SI unit $\mathrm{dBc/Hz}$
- Literally, "c" is a square angle, $\mathrm{c} = 2\ \mathrm{rad}^2$

Obsolete definition of $\mathcal{L}(f)$

$$\mathcal{L}(f) = \frac{\text{SSB power in 1 Hz BW}}{\text{carrier power}}$$

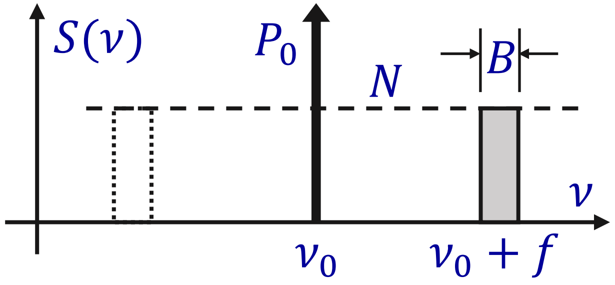

Always given in $\mathrm{dBc/Hz}$ using $10\log_{10}(\mathcal{L})$
dBc means dB below the carrier

Experimentally incorrect

Instruments measure φ, not N/P_0

Unsuitable to low f or to large noise

At sufficiently low f, it happens that
$10\log_{10}\mathcal{L}(f) > 0\ \mathrm{dB}$ –> Denominator nulls

Incorrect way to assess PM noise

$$\mathcal{L} = N/P_0$$

- Pure PM noise

$$S_\varphi(f) = 2N/P_0$$

- Equal amount of AM and PM noise

$$S_\varphi(f) = N/P_0$$

- Pure AM noise

$$S_\varphi(f) = 0$$

Misleading

- Intended to describe PM noise, but the definition does not match
- Non-SI unit $\mathrm{dBc/Hz}$
- A lot of confusion comes from $\mathcal{L}(f)$

Additive phase and amplitude noise

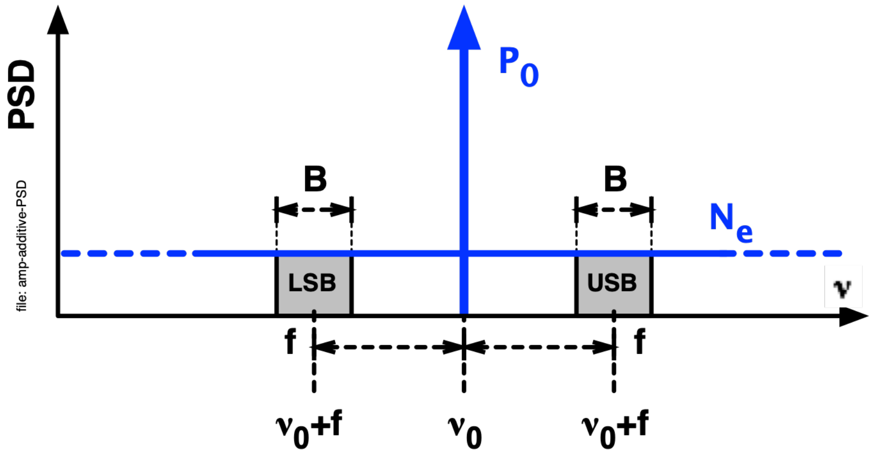

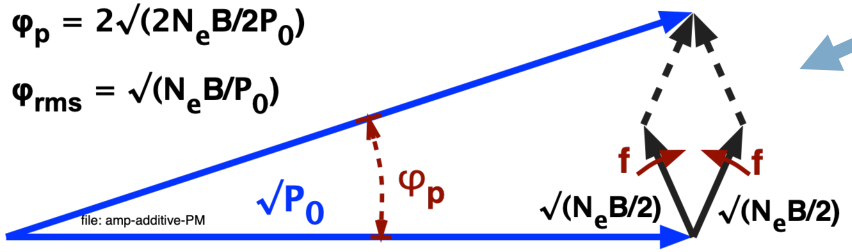

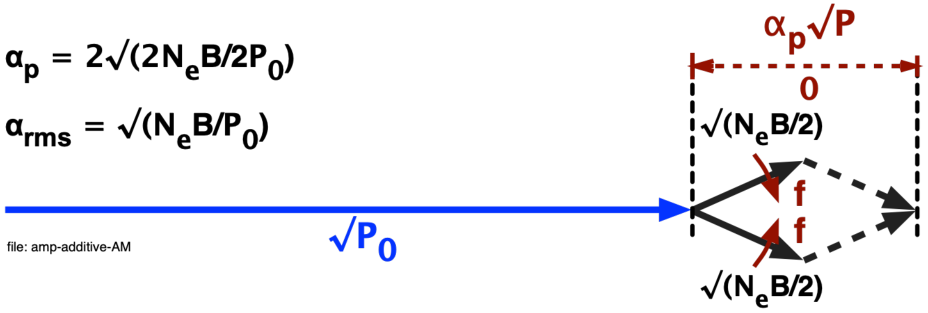

Noise is equally split between AM and PM

PM (rms)

$$v_{\text{usb}}(t) = i\sqrt{N_eB/2}\,e^{i2\pi ft}$$

$$v_{\text{lsb}}(t) = -i\sqrt{N_eB/2}\,e^{-i2\pi ft}$$

AM (rms)

$$v_{\text{usb}}(t) = \sqrt{N_eB/2}\,e^{i2\pi ft}$$

$$v_{\text{lsb}}(t) = \sqrt{N_eB/2}\,e^{-i2\pi ft}$$

Normalize on B

$$S_\varphi(f) = \frac{N_e}{P_0}\,, \qquad S_\alpha(f) = \frac{N_e}{P_0}$$

The polynomial law – or power law

Laurent polynomials –> generalized polynomials which include negative exponents

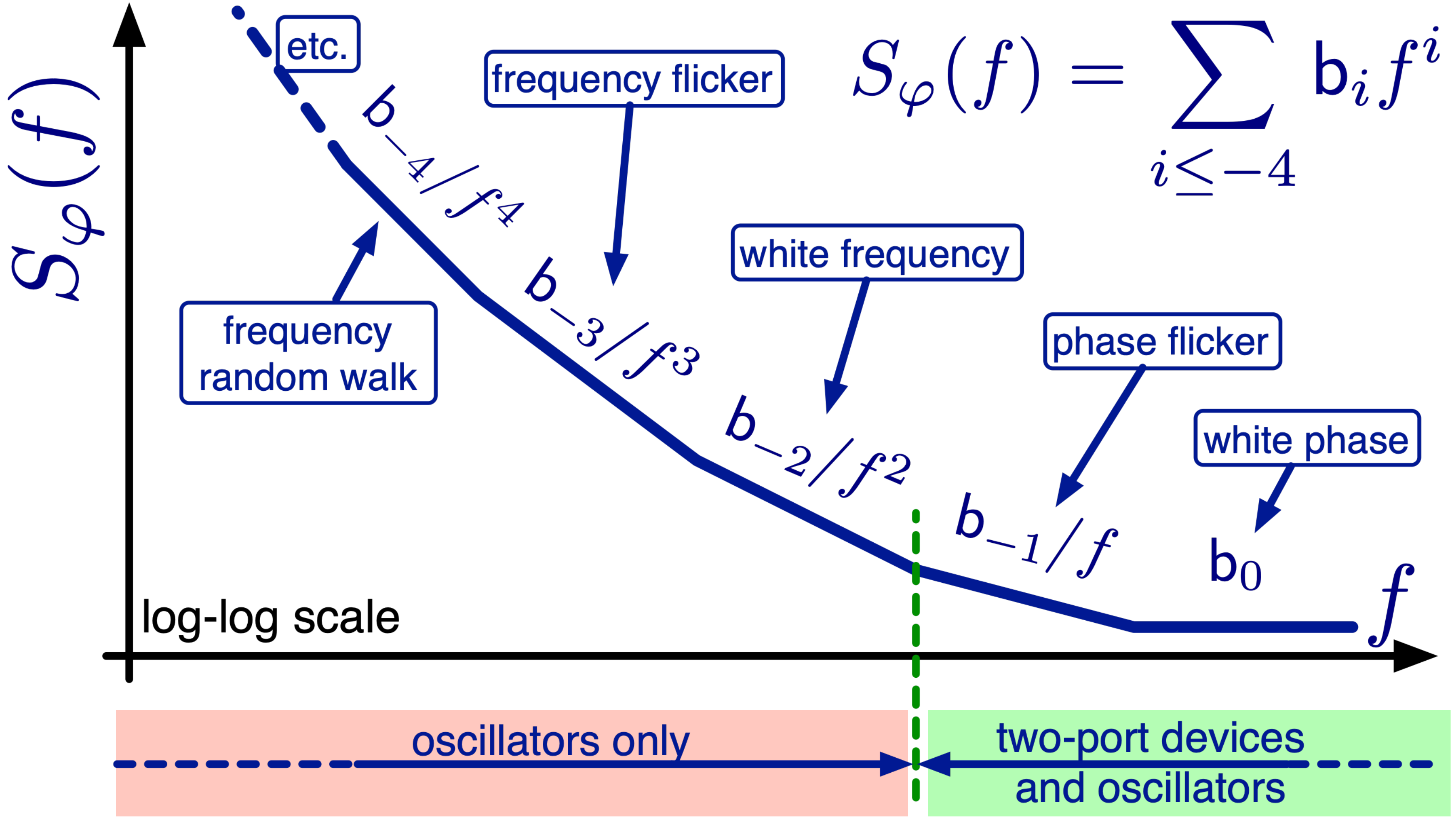

$$S_\varphi(f) = \sum_{i \le -4}^{0} \mathsf{b}_i f^i$$

Amplitude noise

- Not allowed to diverge
- Only white and flicker al low f
- Locally, $1/f^2$ in oscillators

Physical quantities

Rules

$$\frac{d}{dt} \leftrightarrow i\omega$$

$$S_a(\omega) = \mathbb{E}\{A(\omega)A^*(\omega)\}$$

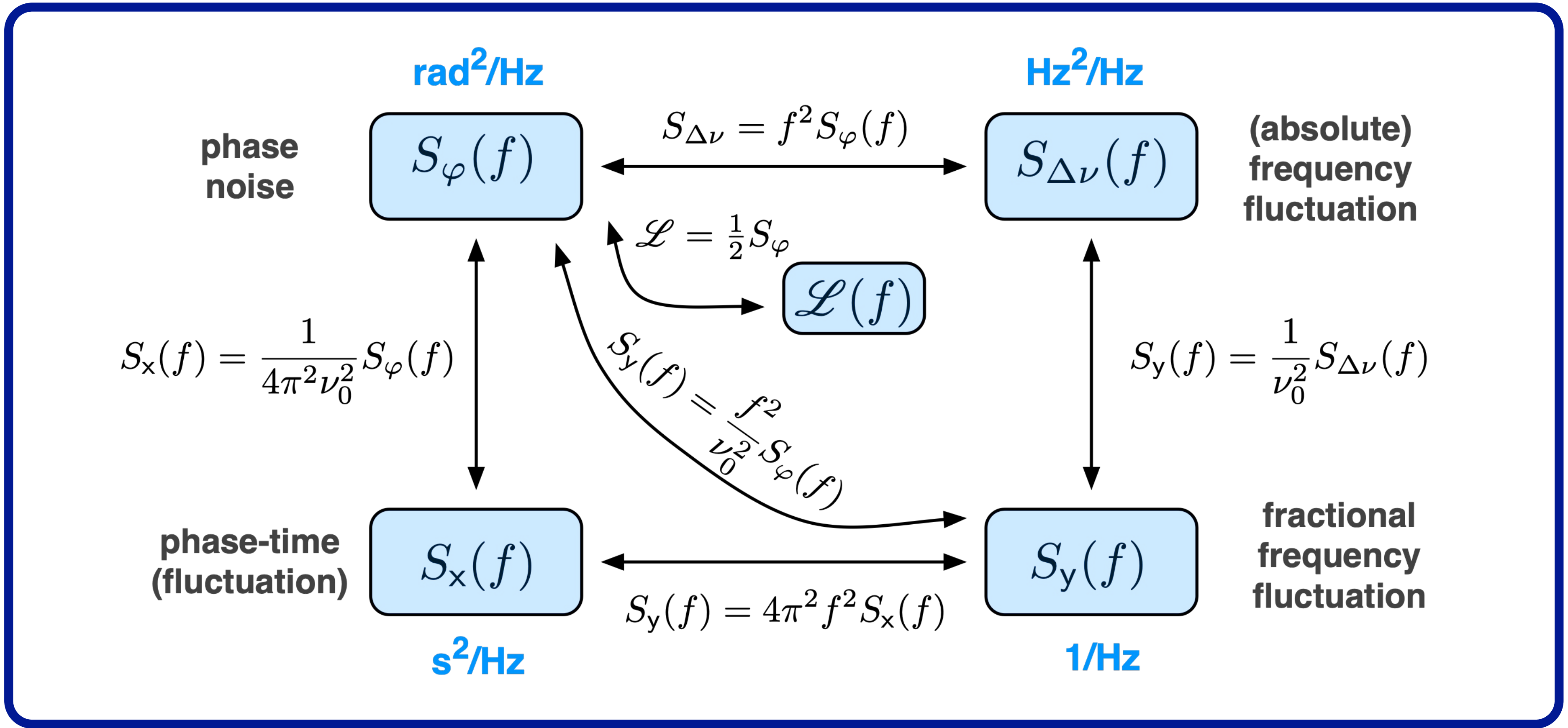

Maximum time fluctuation

- Convert phase noise PSD into time-fluctuation PSD
- Integrate over the suitable bandwidth
- Bandwidth:
  - lower limit is set by the “size” of the system
  - upper limit is set by the circuit bandwidth

The family of Allan variances

$$\sigma_y^2(\tau) = \mathbb{E}\left\{\frac{1}{2}\left[\overline{y}_2 - \overline{y}_1\right]^2\right\}$$

Variance

Experimental

$$\sigma^2 = \frac{1}{n-1}\sum_{i=1}^{n}(y_i - \mu)^2$$

$$\mu = \frac{1}{n}\sum_{i=1}^{n} y_i$$

May depend on n

Mathematical

$$\sigma^2 = \mathbb{E}\{(y_i - \mu)^2\}$$

$$\mu = \mathbb{E}\{y\}$$

Exists under conditions

Try yourself with $y = at$

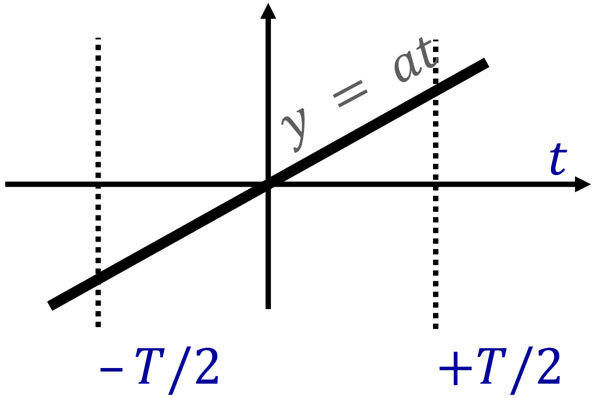

- Take n samples spaced by T_0
- Experimental $\sigma^2 \propto T^2$, depends on n
- The expectation does not exist, unless we fix T

Path to the Allan variance

Problem

The experimental variance

$$\sigma^2 = \frac{1}{n-1}\sum_{i=1}^{n}(y_i-\mu)^2$$

depends on n, and the expectation does not exist

$$\mathbb{E}\left\{\frac{1}{n-1}\sum_{i=1}^{n}(y_i-\mu)^2\right\} \nexists$$

??

Solution

Set $n = 2$

$$\sigma^2 = \frac{1}{2}(y_2-y_1)^2$$

Fix the poor confidence by averaging on *m* realizations

$$\langle\sigma^2\rangle_m = \frac{1}{2m}\sum_{i=1}^{n}(y_2-y_1)^2$$

The average converges to the expectation

$$\sigma^2 = \mathbb{E}\{(y_2-\mu)^2\}$$

Notice that y is still an unspecified quantity

Don't get confused by the factor $1/2$

Experimental variance

$$\sigma^2 = \frac{1}{n-1}\sum_{i=1}^{n}(y_i - \mu)^2$$

set $n = 2$, and expand

boring, trivial algebra

$$\begin{aligned}
\sigma^2 &= (y_2 - \mu)^2 + (y_1 - \mu)^2 \\
&= \left(y_2 - \tfrac{1}{2}[y_2 + y_1]\right)^2 + \left(y_1 - \tfrac{1}{2}[y_2 + y_1]\right)^2 \\
&= \tfrac{1}{4}\left(y_2^2 - 2y_2y_1 + y_1^2\right)^2 + \tfrac{1}{4}\left(y_2^2 - 2y_2y_1 + y_1^2\right)^2 \\
&= \tfrac{1}{2}\left(y_2^2 - 2y_2y_1 + y_1^2\right)^2
\end{aligned}$$

Two-sample variance

$$\sigma^2 = \frac{1}{2}(y_2 - y_1)^2$$

Time-frequency uncertainty theorem

$$D_t = \int_{-\infty}^{\infty} t^2 \left|x(t)\right|^2 \; dt$$

$$D_f = \int_{-\infty}^{\infty} f^2 \left|X(f)\right|^2 \; df$$

integration time τ

Misplaced slide,
it should be shown later

$$D_t \, D_f \geq 1$$

Fast data acquisition
Plenty of data in a short experiment

$$T \gg \tau$$

Fourier analysis

PSD

Fancy variances

Long run behavior of clocks
Few of data in a long experiment

$$T > \tau$$ little margin

Highest τ for a given T
Available data stream –> T

AVAR

Formal definition of the Allan variance

let

$$\bar{y} = \frac{1}{\tau}\int_{t_0}^{t_0+\tau} y(t)\,dt$$

$$\bar{y} = \frac{1}{\tau}\int_{t_0}^{t_0+\tau} y(t)\,dt$$

definition (AVAR)

$$\sigma_y^2(\tau) = \mathbb{E}\left\{\frac{1}{2}\left[\bar{y}_2 - \bar{y}_1\right]^2\right\}$$

same as the experimental variance with $n = 2$, the smallest possible

$$\sigma_y^2(\tau) = \mathbb{E}\left\{\frac{1}{2}\left[\frac{x_2 - 2x_1 + x_0}{\tau}\right]^2\right\}$$

expands as

$$\sigma_y^2(\tau) = \mathbb{E}\left\{\frac{1}{2}\left[\frac{1}{\tau}\int_{\tau}^{2\tau} y(t)\,dt - \frac{1}{\tau}\int_{0}^{\tau} y(t)\,dt\right]^2\right\}$$

Evaluating, replace the expectation with the average on *m* samples

$$\sigma_y^2(\tau) = \frac{1}{m}\sum_{k=0}^{m-1}\frac{1}{2}\left[\bar{y}_{k+1} - \bar{y}_k\right]^2$$

A modern approach

Definition

$$\sigma_y^2(\tau) = \frac{1}{2}\left[\bar{y}_2 - \bar{y}_1\right]^2$$

Use the average or the expectation

Weighted Average

$$\bar{y} = \int_{-\infty}^{\infty} y(t)w(t)dt$$

- It's all about averaging
- Uniform —> AVAR
- Triangle —> MVAR
  constant term of the least-square fit of phase data
- Parabolic —> PVAR
  slope term of the least-square fit of phase data
- Other options are possible

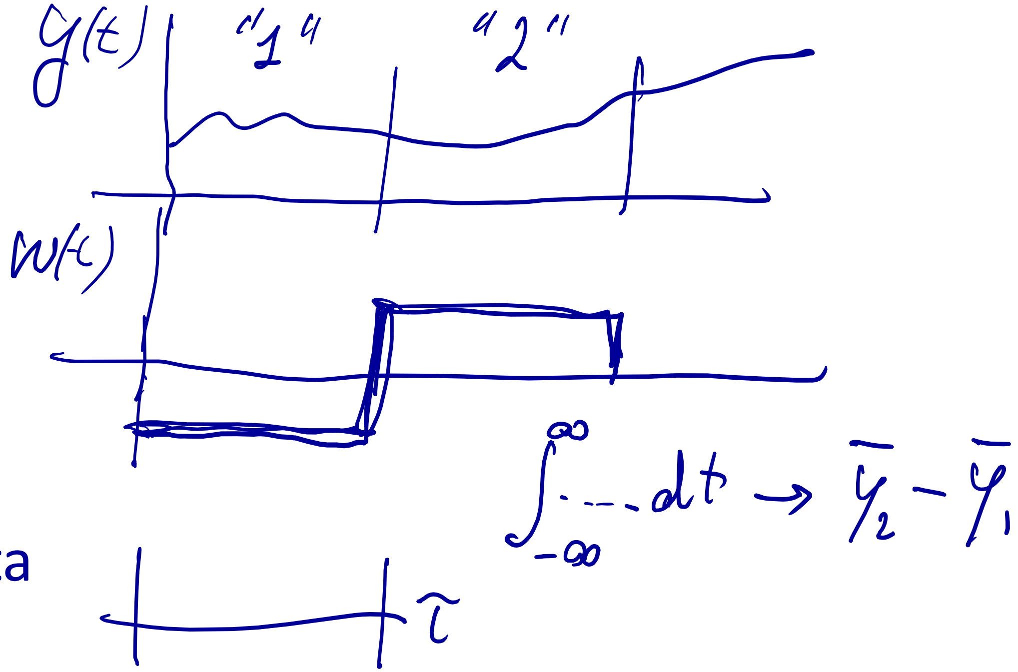

Lecture 7
Scientific Instruments & Oscillators

Lectures for PhD Students and Young Scientists

Enrico Rubiola

CNRS FEMTO-ST Institute, Besancon, France

INRiM, Torino, Italy

Contents

- Counters (Π, Λ and Ω)
- Allan variances
- The measurement of phase noise

ORCID 0000-0002-5364-1835

home page http://rubiola.org

Weighted average

Bare mean

$$\bar{y} = \frac{1}{\tau}\int_0^\tau y(t)dt$$

Use the average or the expectation

Weighted Average

$$\bar{y} = \int_{-\infty}^{\infty} y(t)w(t)dt$$

Normalization $\int_{-\infty}^{\infty} w(t)dt = 1$

There are many options for the weight function $w(t)$

Π (uniform) average

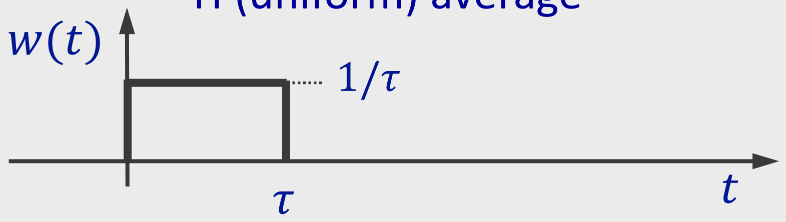

Λ (triangular) average

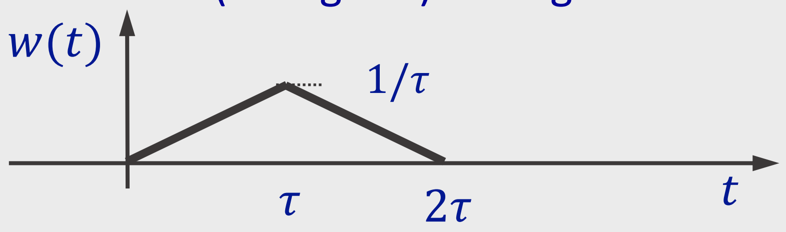

...etc.

Π (classical) counter

E. Rubiola, RSI 76(5) 054703, May 2005

E. Rubiola, Fig.2

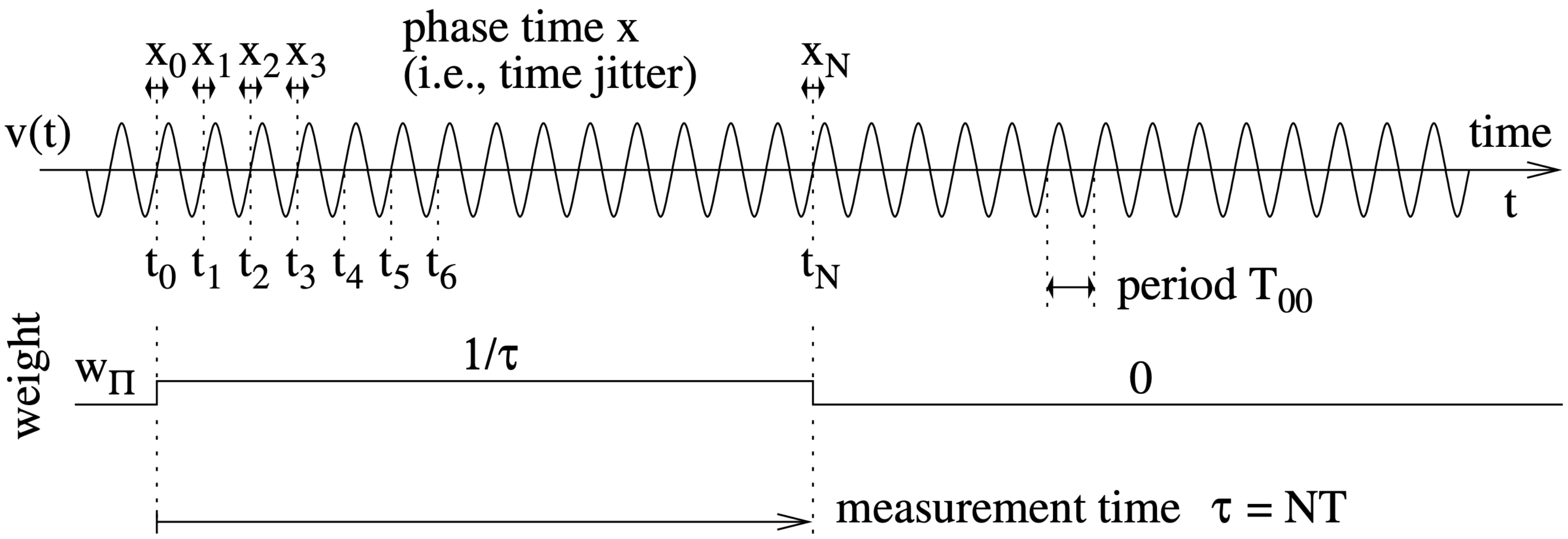

the measure is a scalar product

$$\mathbb{E}\{\nu\} = \int_{-\infty}^{+\infty} \nu(t) w_\Pi(t)\, dt$$ Π estimator

$$w_\Pi(t) = \begin{cases} 1/\tau & 0 < t < \tau \\ 0 & \text{elsewhere} \end{cases}$$ weight

$$\int_{-\infty}^{+\infty} w_\Pi(t)\, dt = 1$$ normalization

variance

$$\sigma_y^2 = \frac{2\sigma_x^2}{\tau^2}$$ classical variance

Λ Counter

E. Rubiola, RSI 76(5) 054703, May 2005

E. Rubiola, Fig.3

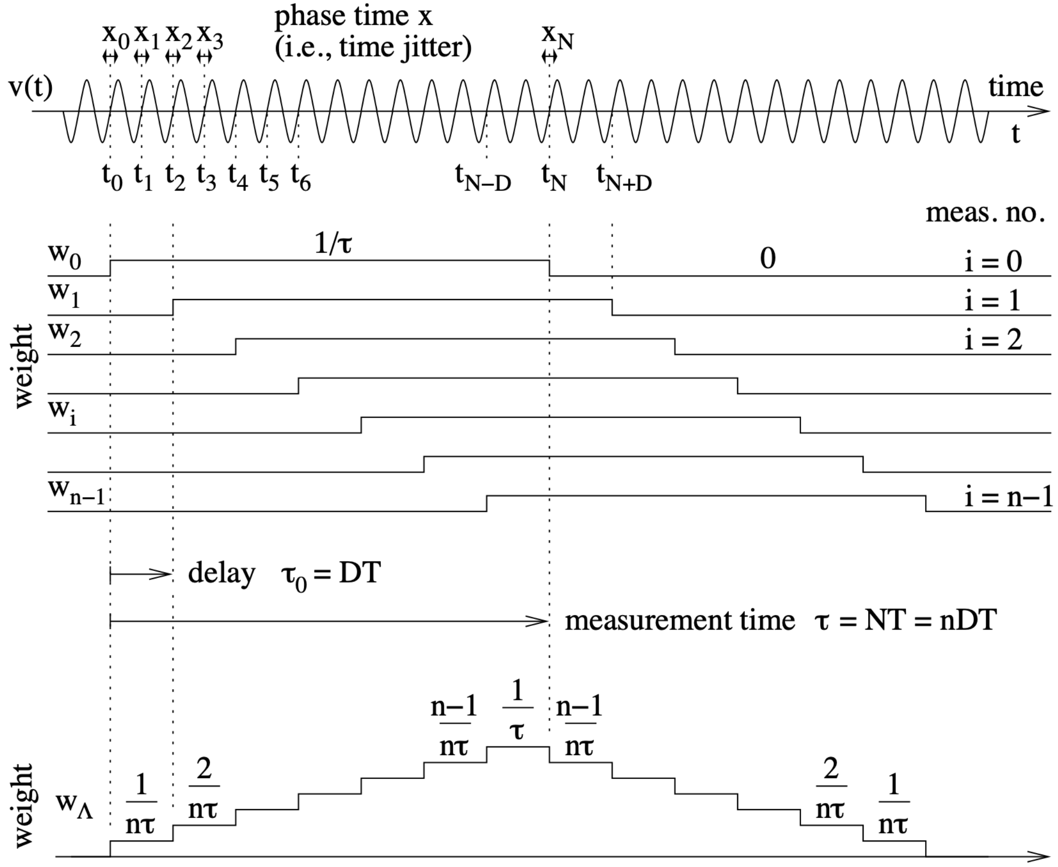

$$\mathbb{E}\{\nu\} = \frac{1}{n}\sum_{i=0}^{n-1} \overline{\nu}_i \qquad \overline{\nu}_i = N/\tau_i$$

Λ estimator

$$\mathbb{E}\{\nu\} = \int_{-\infty}^{+\infty} \nu(t) w_\Lambda(t)\, dt$$

weight

$$w_\Lambda(t) = \begin{cases} t/\tau & 0 < t < \tau \\ 2 - t/\tau & \tau < t < 2\tau \\ 0 & \text{elsewhere} \end{cases}$$

normalization

$$\int_{-\infty}^{+\infty} w_\Lambda(t)\, dt = 1$$

limit t_0 -> 0 of the weight function

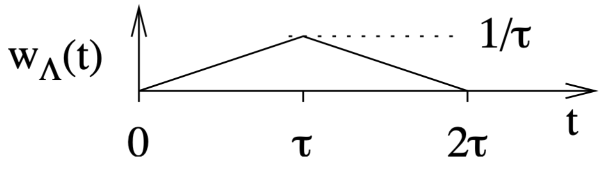

white noise: the autocorrelation function is a narrow pulse, about the inverse of the bandwidth

the variance is divided by n

$$\sigma_y^2 = \frac{1}{n}\,\frac{2\sigma_x^2}{\tau^2}$$

classical variance

Ω (linear-regression) counter

E. Rubiola & al, IEEE Transact. UFFC 63(7) pp.961–969, July 2016

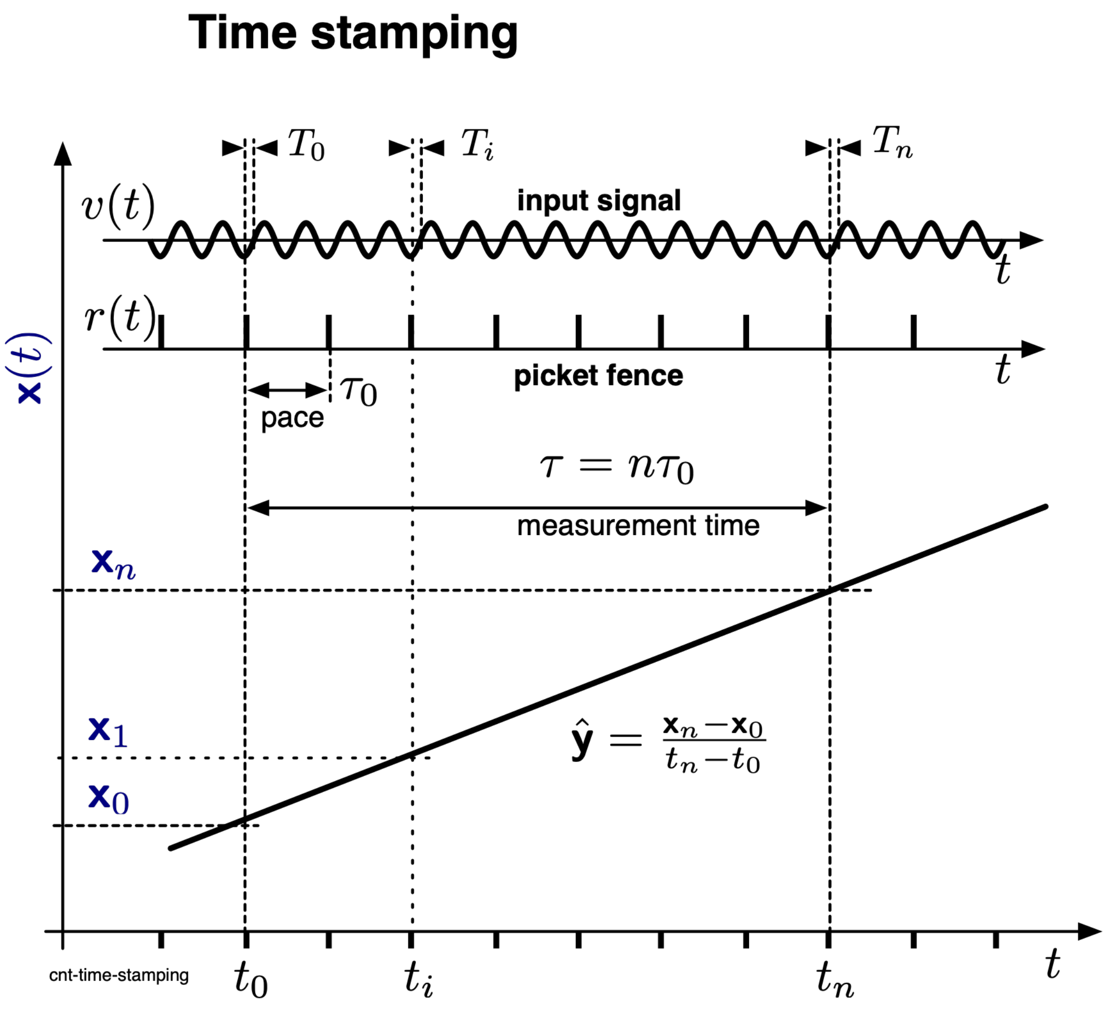

$\mathbf{x}(t) = t + \mathrm{x}(t)$ phase time

$\mathbf{y}(t) = 1 + \mathrm{y}(t)$ fractional frequency

$\mathrm{x}(t) = \varphi(t)/2\pi\nu_0$ fluctuation

$\mathbf{y}(t) = \dot{\mathbf{x}}(t)$

y is estimated with a linear regression on the **x** series

$$\hat{\mathbf{y}} = \frac{\sum_i \left(\mathbf{x}_i - \langle \mathbf{x} \rangle, t_i - \langle t \rangle\right)}{\sum_i \left(t_i - \langle t \rangle\right)^2}.$$

Linear regression on a sequence of time stamps provides accurate estimation of frequency and best rejection of white PM noise

Generalized Allan variance

Allan variance

$$\sigma_y^2(\tau) = \mathbb{E}\left\{\frac{1}{2}\left[\overline{y}_2 - \overline{y}_1\right]^2\right\}$$

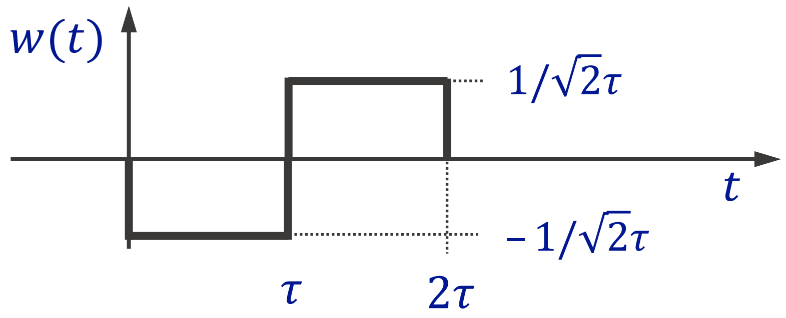

Generalized Allan variance

$$\sigma_y^2(\tau) = \mathbb{E}\left\{\int_{-\infty}^{\infty}[y(t)w(t)]^2\ dt\right\}$$

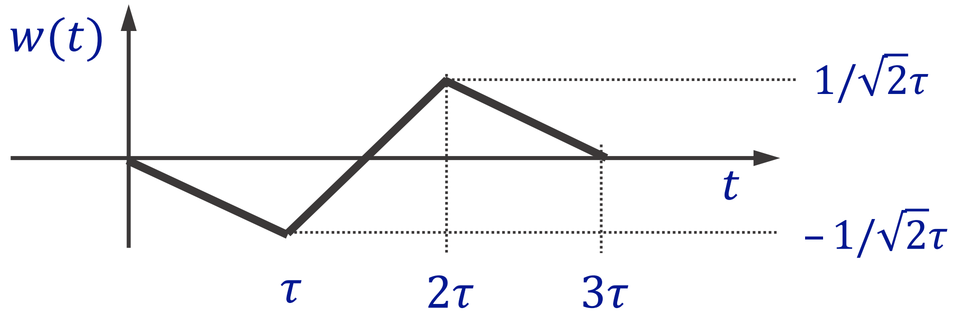

Π Estimator —> Allan Variance

given a series of contiguous non-overlapped measures

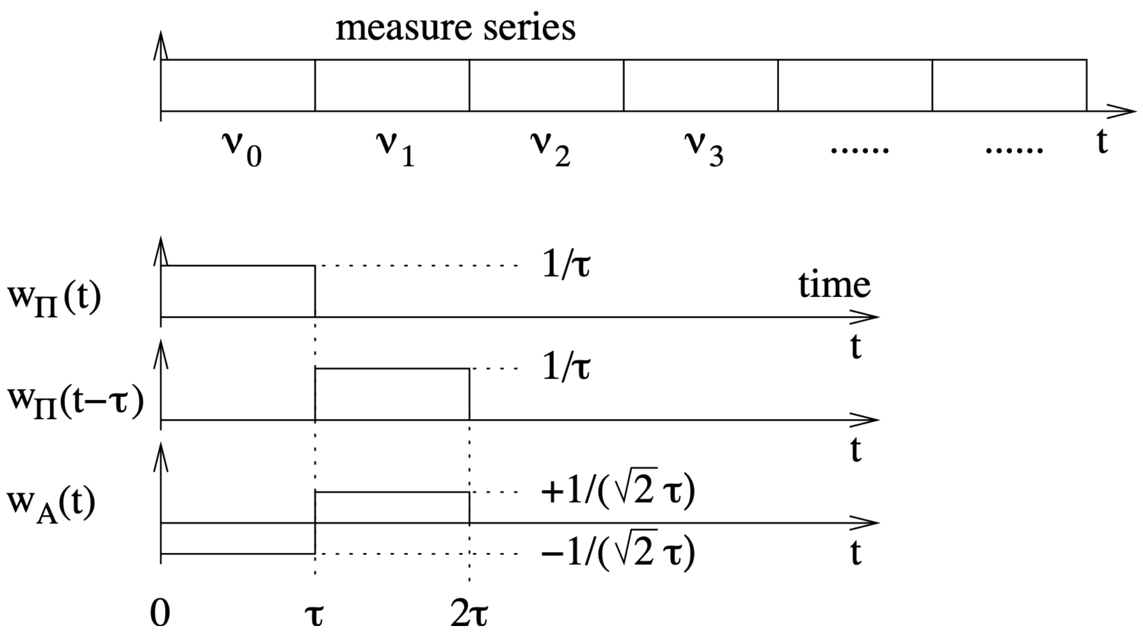

the Allan variance is easily evaluated

$$\sigma_y^2(\tau) = \mathbb{E}\left\{\frac{1}{2}\left[\overline{y}_{k+1} - \overline{y}_k\right]^2\right\}$$

Modified Allan variance

definition

$$\operatorname{mod}\sigma_y^2(\tau) = \mathbb{E}\left\{\frac{1}{2}\left[\frac{1}{n}\sum_{i=0}^{n-1}\left(\frac{1}{\tau}\int_{(i+n)\tau_0}^{(i+2n)\tau_0} y(t)\,dt - \frac{1}{\tau}\int_{i\tau_0}^{(i+n)\tau_0} y(t)\,dt\right)\right]^2\right\}$$

with $\tau = n\tau_0$.

wavelet-like variance

$$\operatorname{mod}\sigma_y^2(\tau) = \mathbb{E}\left\{\left[\int_{-\infty}^{+\infty} y(t)\,w_M(t)\,dt\right]^2\right\}$$

$$w_M = \begin{cases} -\frac{1}{\sqrt{2}\tau^2}t & 0 < t < \tau \\ \frac{1}{\sqrt{2}\tau^2}(2t-3) & \tau < t < 2\tau \\ -\frac{1}{\sqrt{2}\tau^2}(t-3) & 2\tau < t < 3\tau \\ 0 & \text{elsewhere} \end{cases}$$

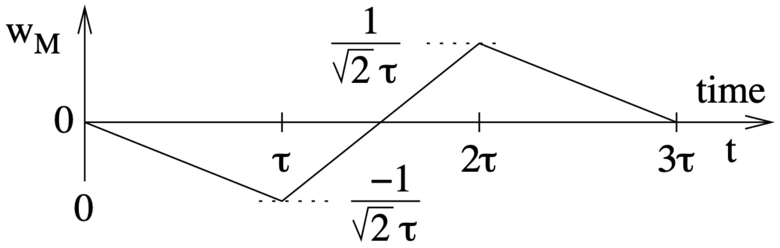

energy

$$E\{w_M\} = \int_{-\infty}^{+\infty} w_M^2(t)\,dt = \frac{1}{2\tau}$$

compare the energy

$$E\{w_M\} = \frac{1}{2}\,E\{w_A\}$$

this explains why the mod Allan variance is always lower than the Allan variance

Overlapped Λ estimator —> MVAR

by feeding a series of L-estimates of frequency in the formula of the Allan variance

$$\sigma_y^2(\tau) = \mathbb{E}\left\{\frac{1}{2}\left[\overline{y}_{k+1} - \overline{y}_k\right]^2\right\}$$

as they were P-estimates

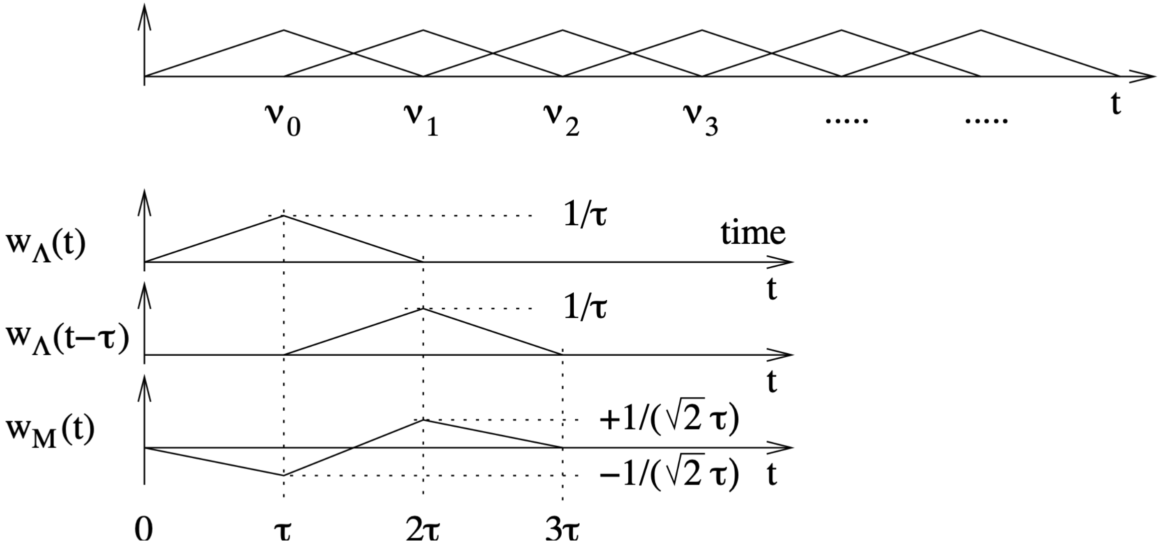

one gets exactly the modified Allan variance!

$$\mathrm{mod}\,\sigma_y^2(\tau) = \mathbb{E}\left\{\frac{1}{2}\left[\frac{1}{n}\sum_{i=0}^{n-1}\left(\frac{1}{\tau}\int_{(i+n)\tau_0}^{(i+2n)\tau_0} y(t)\,dt - \frac{1}{\tau}\int_{i\tau_0}^{(i+n)\tau_0} y(t)\,dt\right)\right]^2\right\}$$

with $\tau = n\tau_0$.

MVAR by-2 decimation rule

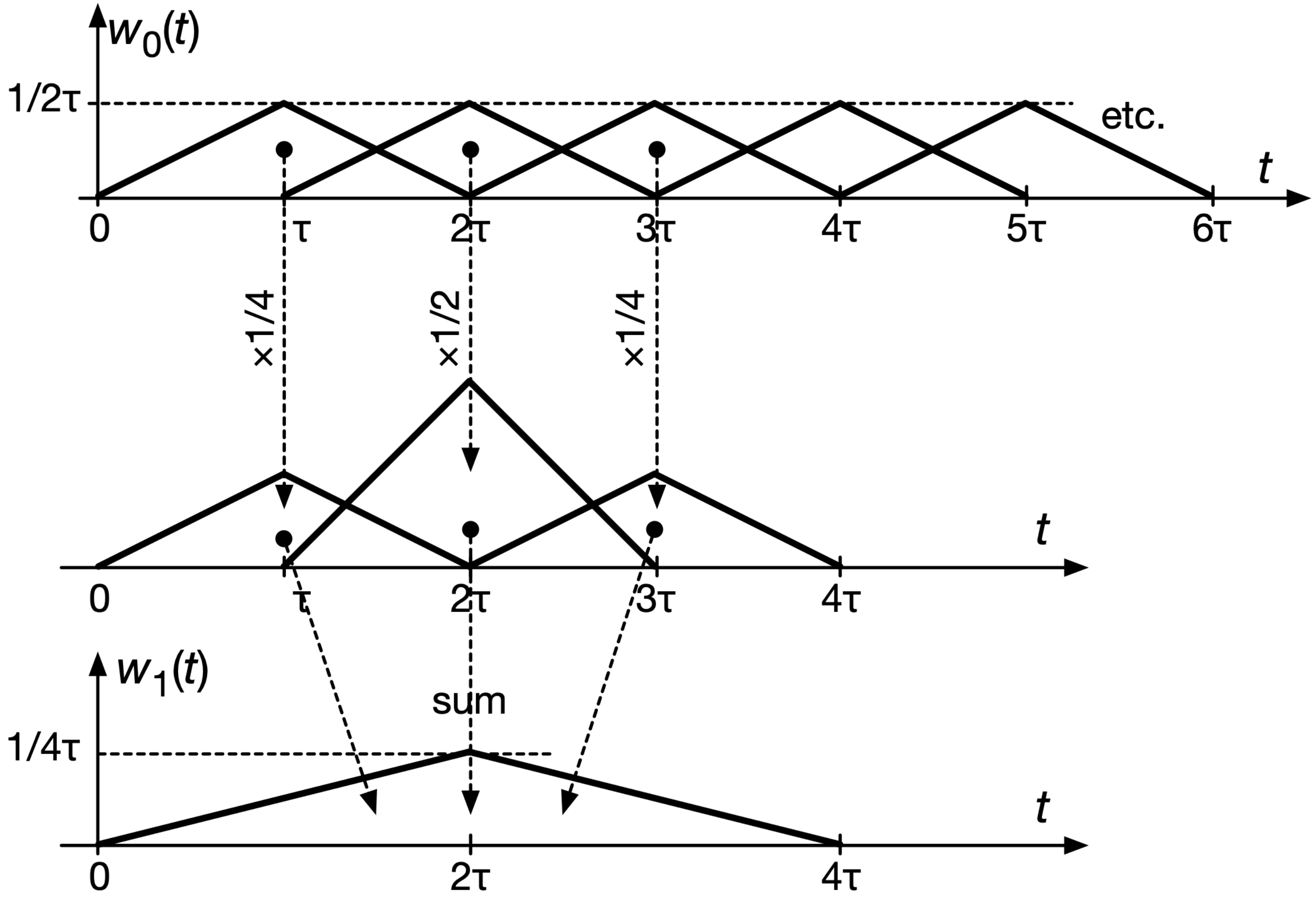

Wavelet interpretation

A wavelet is a unit shock

Zero average

$$\int_{-\infty}^{\infty} w(t)\, dt = 0$$

Energy equal one

$$\int_{-\infty}^{\infty} |w(t)|^2\, dt = 1$$

Nonzero activity limited to the [–*T*/2,*T*/2] interval

$$\int_{-T/2}^{T/2} |w(t)|^2\, dt = 1 - \epsilon$$

D. B. Percival DB, A. T. Walden AT, Wavelet methods for time series analysis, Cambridge 2000, ISBN 0-521-64068-7

Wavelet interpretation

wavelet-like variance

$$\sigma_y^2(\tau) = \mathbb{E}\left\{\left[\int_{-\infty}^{+\infty} y(t)\, w_A(t)\, dt\right]^2\right\}$$

$$w_A = \begin{cases} -\frac{1}{\sqrt{2\tau}} & 0 < t < \tau \\ \frac{1}{\sqrt{2\tau}} & \tau < t < 2\tau \\ 0 & \text{elsewhere} \end{cases}$$

weight (wavelet-like) function

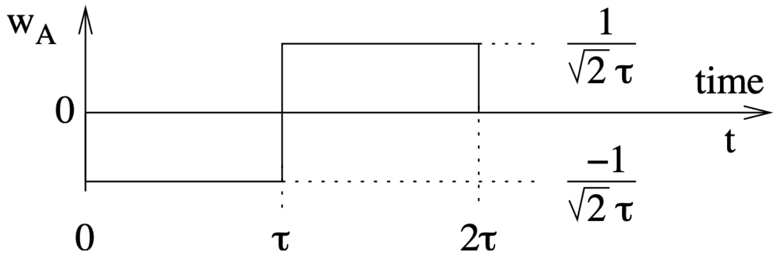

energy

$$E\{w_A\} = \int_{-\infty}^{\infty} w_A^2(t)\, dt = \frac{1}{\tau}$$

the Allan variance differs from a wavelet variance in the normalization on power, instead of on energy

Statistical interpretation

Follows immediately from the derivation / definition

the expectation

$$\mathbb{E}\left\{\left[\bar{\mathrm{y}} - \mathbb{E}\left\{\bar{\mathrm{y}}\right\}\right]^2\right\}$$

does not exist

$$\sigma_{\mathrm{y}}^2(\tau) = \frac{1}{n-1}\sum_{k=0}^{n-1}\left[\bar{\mathrm{y}}_k - \mu\right]^2$$

depends on *n*

Use the smallest *n*, and take the expectation

definition (AVAR)

$$\sigma_{\mathrm{y}}^2(\tau) = \mathbb{E}\left\{\frac{1}{2}\left[\bar{\mathrm{y}}_2 - \bar{\mathrm{y}}_1\right]^2\right\}$$

In practice, replace the expectation with the average

Filter interpretation

The impulse response of the measurement (same as w_A) approximates a half-octave bandpass filter centered at f tau ≈ 0.45

$$S_y(f) \rightarrow \boxed{|H(f)|^2} \rightarrow \boxed{\int_{-\infty}^{\infty} \ldots dt} \rightarrow \sigma_y^2(\tau)$$

impulse response $h_A(t) = w_A(t)$

$$\sigma_y^2(\tau) = \int_0^\infty S^I(f)\,|H_A(f)|^2\,df$$

$$|H_A(f)|^2 = 2\,\frac{\sin^4(\pi f \tau)}{(\pi f \tau)^2}$$

energy

$$E\{h_A\} = \int_{-\infty}^{\infty} h_A^2(t)\,dt = \frac{1}{\tau}$$

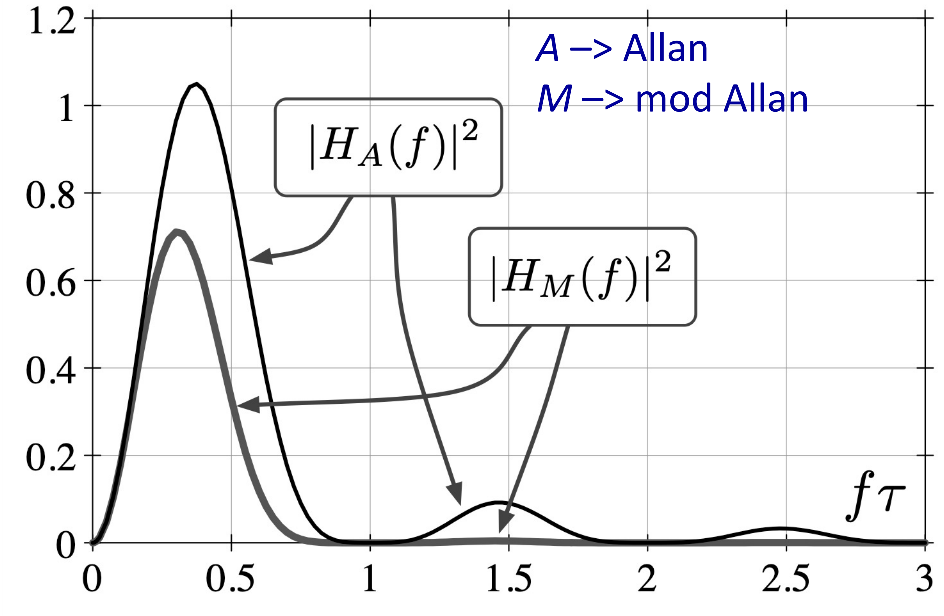

Transfer function $|H_A(f)|^2$

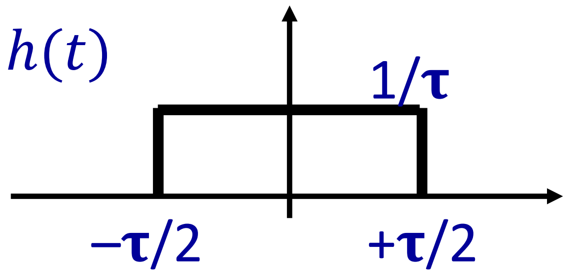

$$H(f) = \frac{\sin(\pi\tau f)}{\pi\tau f}$$

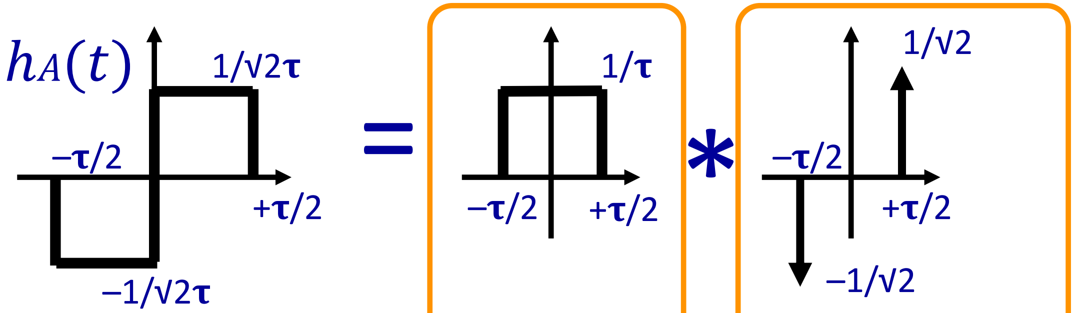

$$|H_A(f)|^2 = 2\frac{\sin^4(\pi\tau f)}{(\pi\tau f)^2}$$

$$H_A(f) = \frac{\sin(\pi\tau f)}{\pi\tau f} \quad \frac{\sqrt{2}}{i}\sin(\pi\tau f) = \frac{\sqrt{2}}{i}\frac{\sin^2(\pi\tau f)}{\pi\tau f}$$

* Convolution operator

Transfer function $|H_M(f)|^2$

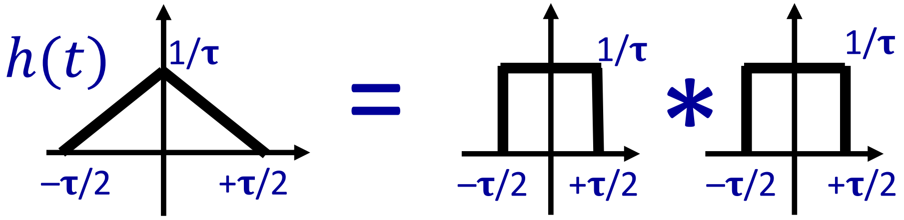

$$\frac{\sin(\pi\tau f)}{\pi\tau f} \quad \frac{\sin(\pi\tau f)}{\pi\tau f}$$

$$H(f) = \frac{\sin^2(\pi\tau f)}{(\pi\tau f)^2}$$

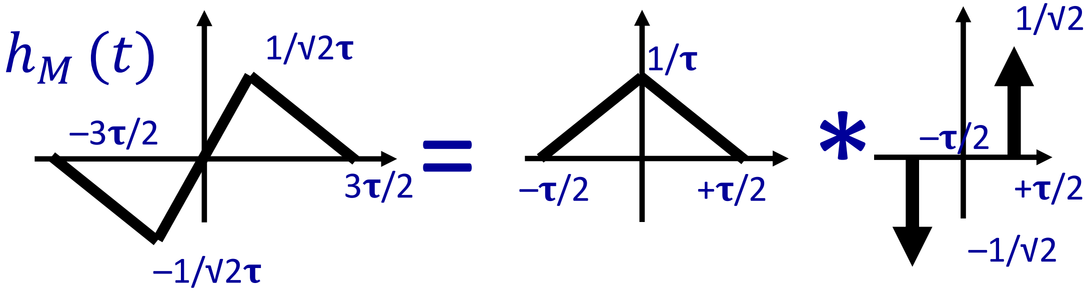

$$|H_M(f)|^2 = 2\frac{\sin^6(\pi\tau f)}{(\pi\tau f)^4}$$

$$H_M(f) = \frac{\sin^2(\pi\tau f)}{(\pi\tau f)^2}\;\frac{\sqrt{2}}{i}\sin(\pi\tau f) = \frac{\sqrt{2}}{i}\frac{\sin^3(\pi\tau f)}{(\pi\tau f)^2}$$

* Convolution operator

Phase noise to AVAR conversion

$$v(t) = V_p\,[1+\alpha(t)]\cos\left[2\pi\nu_0 t + \varphi(t)\right]$$

Phase noise

$$S_\varphi(f) = 2\,\mathbb{E}\left\{\Phi(f)\Phi^*(f)\right\},\ f>0 \quad \text{(expectation)}$$

$$S_\varphi(f) \approx \tfrac{2}{T}\left\langle\Phi(f)\Phi^*(f)\right\rangle_m,\ f>0 \quad \text{(average)}$$

$$\mathrm{y}(t) = \frac{\dot\varphi(t)}{2\pi\nu_0} \quad\Rightarrow\quad S_\mathrm{y}(f) = \frac{f^2}{\nu_0^2}S_\varphi(f)$$

Allan variance
(two-sample wavelet-like variance)

$$\sigma^2_\mathrm{y}(\tau) = \mathbb{E}\left\{\frac{1}{2}\left[\overline{\mathrm{y}}_2 - \overline{\mathrm{y}}_1\right]^2\right\}$$

approaches a half-octave bandpass filter (for white noise), hence it converges even with processes steeper than 1/f

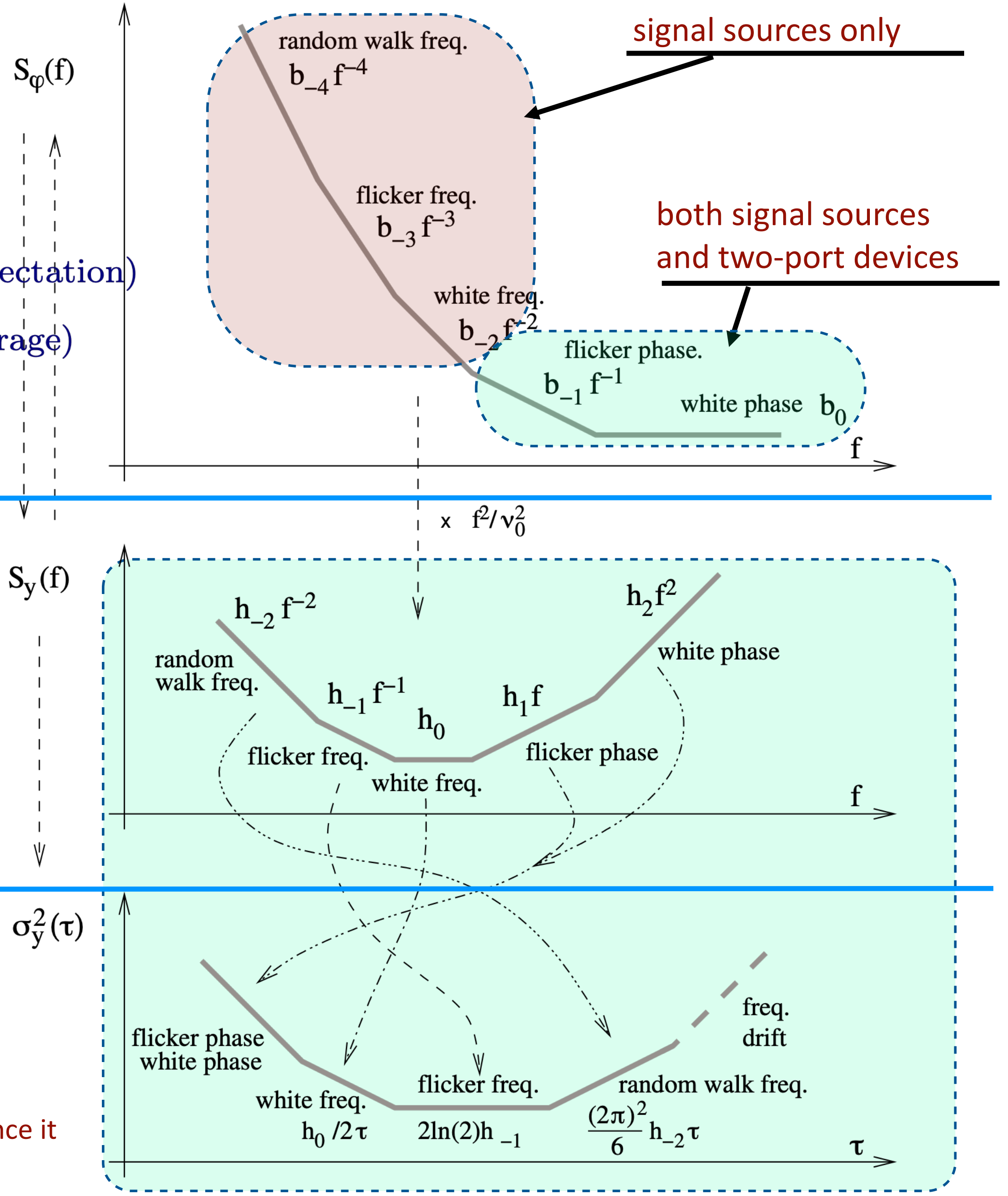

noise type	$S_y(f)$	AVAR ${}^{A}\sigma_y^2(\tau)$	MVAR ${}^{M}\sigma_y^2(\tau)$	HVAR ${}^{H}\sigma_y^2(\tau)$	PVAR ${}^{P}\sigma_y^2(\tau)$	TVAR ${}^{T}\sigma_x^2(\tau)$
Blue PM	$h_3 f^3$	$\frac{3 f_H^2}{8\pi^2}\frac{h_3}{\tau^2}$ $0.0380\ f_H h_3/\tau^2$	$\frac{10\gamma+\ln 48+10\ln(\pi f_H\tau)}{16\pi^4}\frac{h_3}{\tau^4}$ $\frac{[10\gamma+\ln 48+10\ln\pi]}{16\pi^4}=0.0135$	$\frac{5 f_H^2}{18\pi^2}\frac{h_3}{\tau^2}$ $0.0281\ f_H h_3/\tau^2$	$\frac{9[\gamma+\ln(4\pi f_H\tau)]}{4\pi^4}\frac{h_3}{\tau^4}$ $\frac{9[\gamma+\ln(4\pi)]}{4\pi^4}=0.0718$	$\frac{10\gamma+\ln 48+10\ln(\pi f_H\tau)}{48\pi^4}\frac{h_3}{\tau^2}$ $\frac{10\gamma+\ln 48+10\ln\pi}{48\pi^2}=0.00451$
White PM	$h_2 f^2$	$\frac{3 f_H}{4\pi^2}\frac{h_2}{\tau^2}$ $0.0760\ f_H h_2/\tau^2$	$\frac{3}{8\pi^2}\frac{h_2}{\tau^3}$ $0.0380\ h_2/\tau^3$	$\frac{5 f_H}{9\pi^2}\frac{h_2}{\tau^2}$ $0.0563\ f_H h_2/\tau^2$	$\frac{3}{2\pi^2}\frac{h_2}{\tau^3}$ $0.152\ h_2/\tau^3$	$\frac{1}{8\pi^2}\frac{h_2}{\tau}$ $0.0127\ h_2/\tau$
Flicker PM	$h_1 f$	$\frac{3\gamma-\ln 2+3\ln(2\pi f_H\tau)}{4\pi^2}\frac{h_1}{\tau^2}$ $[3\gamma-\ln 2+3\ln 2\pi]/4\pi^2=0.166$	$\frac{(24\ln 2-9\ln 3)}{8\pi^2}\frac{h_1}{\tau^2}$ $0.0855\ h_1/\tau^2$	$\simeq\frac{5[\gamma+\ln(\sqrt[10]{48}\,\pi f_H\tau)]}{9\pi^2}\frac{h_1}{\tau^2}$ $5[\gamma+\ln(\sqrt[10]{48}\,\pi)]/9\pi^2=0.119$	$\frac{3\,[\ln(16)-1]}{2\pi^2}\frac{h_1}{\tau^2}$ $0.269\ h_1/\tau^2$	$\frac{(8\ln 2-3\ln 3)}{8\pi^2}h_1$ $0.0285\ h_1$
White FM	h_0	$\frac{1}{2}\frac{h_0}{\tau}$	$\frac{1}{4}\frac{h_0}{\tau}$	$\frac{1}{3}\frac{h_0}{\tau}$	$\frac{3}{5}\frac{h_0}{\tau}$	$\frac{1}{12}h_0\tau$
Flicker FM	$h_{-1}f^{-1}$	$2\ln(2)\ h_{-1}$ $1.39\ h_{-1}$	$\frac{27\ln 3-32\ln 2}{8}h_{-1}$ $0.935\ h_{-1}$	$\frac{8\ln 2-3\ln 3}{3}h_{-1}$ $0.750\ h_{-1}$	$\frac{2\,[7-\ln(16)]}{5}h_{-1}$ $1.69\ h_{-1}$	$\frac{27\ln 3-32\ln 2}{24}h_{-1}\tau^2$ $0.312\ h_{-1}\tau^2$
Random walk FM	$h_{-2}f^{-2}$	$\frac{2\pi^2}{3}h_{-2}\tau$ $6.58\ h_{-2}\tau$	$\frac{11\pi^2}{20}h_{-2}\tau$ $5.43\ h_{-2}\tau$	$\frac{2\pi^2}{9}h_{-2}\tau$ $2.19\ h_{-2}\tau$	$\frac{26\pi^2}{35}h_{-2}\tau$ $7.33\ h_{-2}\tau$	$\frac{11\pi^2}{60}h_{-2}\tau^3$ $1.81\ h_{-2}\tau^3$
Integrated flicker FM	$h_{-3}f^{-3}$	not convergent	not convergent	$\frac{\pi^2[27\ln 3-32\ln 2]}{9}h_{-3}\tau^2$ $8.205\ h_{-3}\tau^2$	not convergent	not convergent
Integrated RW FM	$h_{-4}f^{-4}$	not convergent	not convergent	$\frac{44\pi^2}{90}h_{-4}\tau^3$ $4.825\ h_{-4}\tau^3$	not convergent	not convergent
linear drift D_y		$\frac{1}{2}D_y^2\tau^2$	$\frac{1}{2}D_y^2\tau^2$	0	$\frac{1}{2}D_y^2\tau^2$	$\frac{1}{6}D_y^2\tau^4$
Spectral response $\lvert H(\theta)\rvert^2$, $\theta=\pi f\tau$		$\frac{2\sin^4\theta}{\theta^2}$	$\frac{2\sin^6\theta}{\theta^4}$	$\frac{16\sin^6\theta}{9\,\theta^2}$	$\frac{9\left[2\sin^2\theta-\theta\sin 2\theta\right]^2}{2\,\theta^6}$	$\frac{\tau^2}{3}\,\frac{2\sin^6\theta}{\theta^4}$
$\gamma=0.577$ is the Euler Mascheroni constant. Formulae hold for $\tau\gg f_H/2$ where appropriate, f_H = bandwidth (sharp cutoff filter). MVAR, PVAR and TVAR require $\tau\gg\tau_0$, where τ_0 = sampling interval.						${}^{T}\sigma_x^2(\tau)=\frac{\tau^2}{3}\,{}^{M}\sigma_y^2(\tau)$

The Time-Domain Beat Method

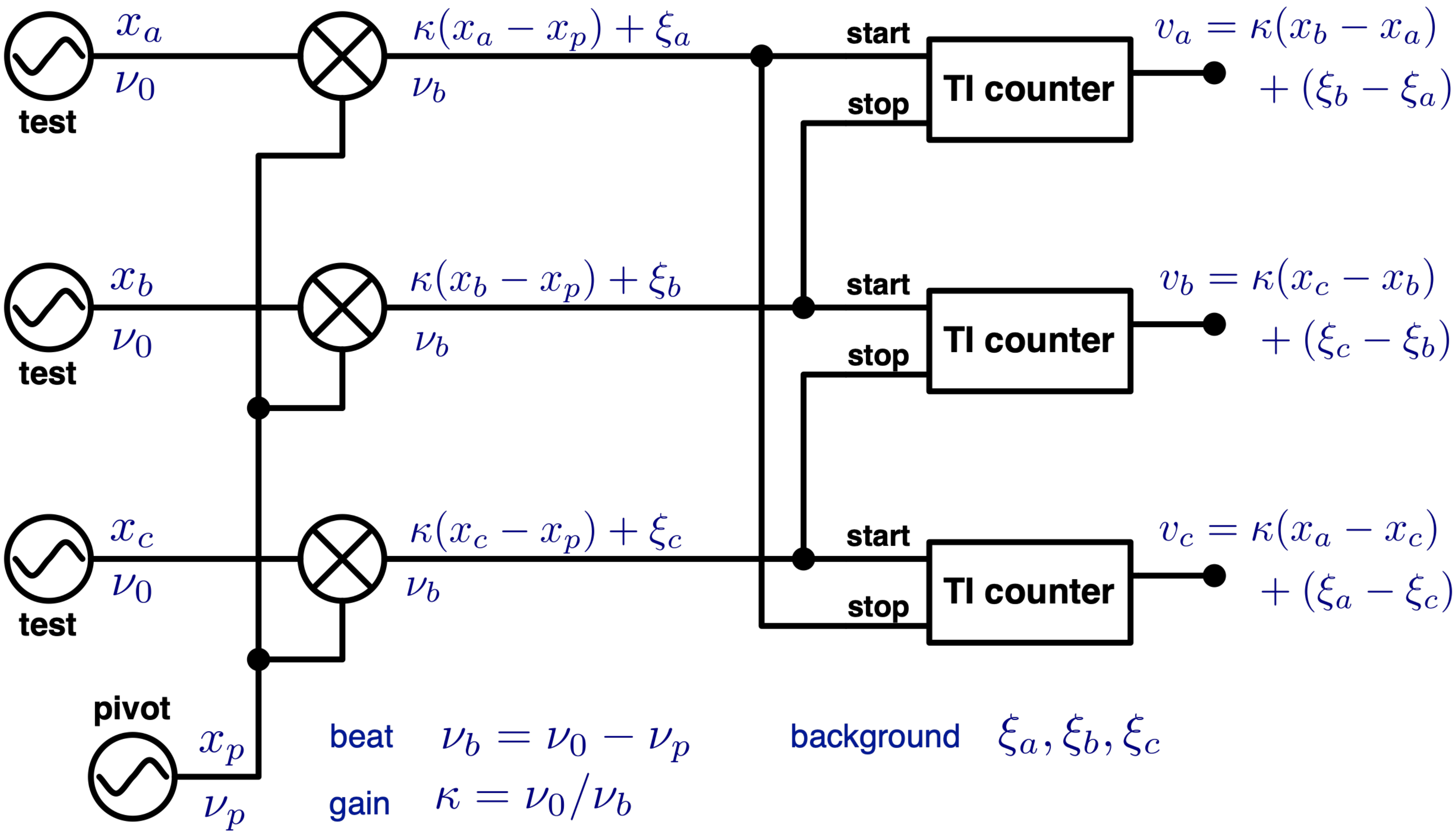

beat $\nu_b = \nu_0 - \nu_p$

gain $\kappa = \nu_0 / \nu_b$

background ξ_a, ξ_b, ξ_c

Some Facts About the Estimation

Dead time

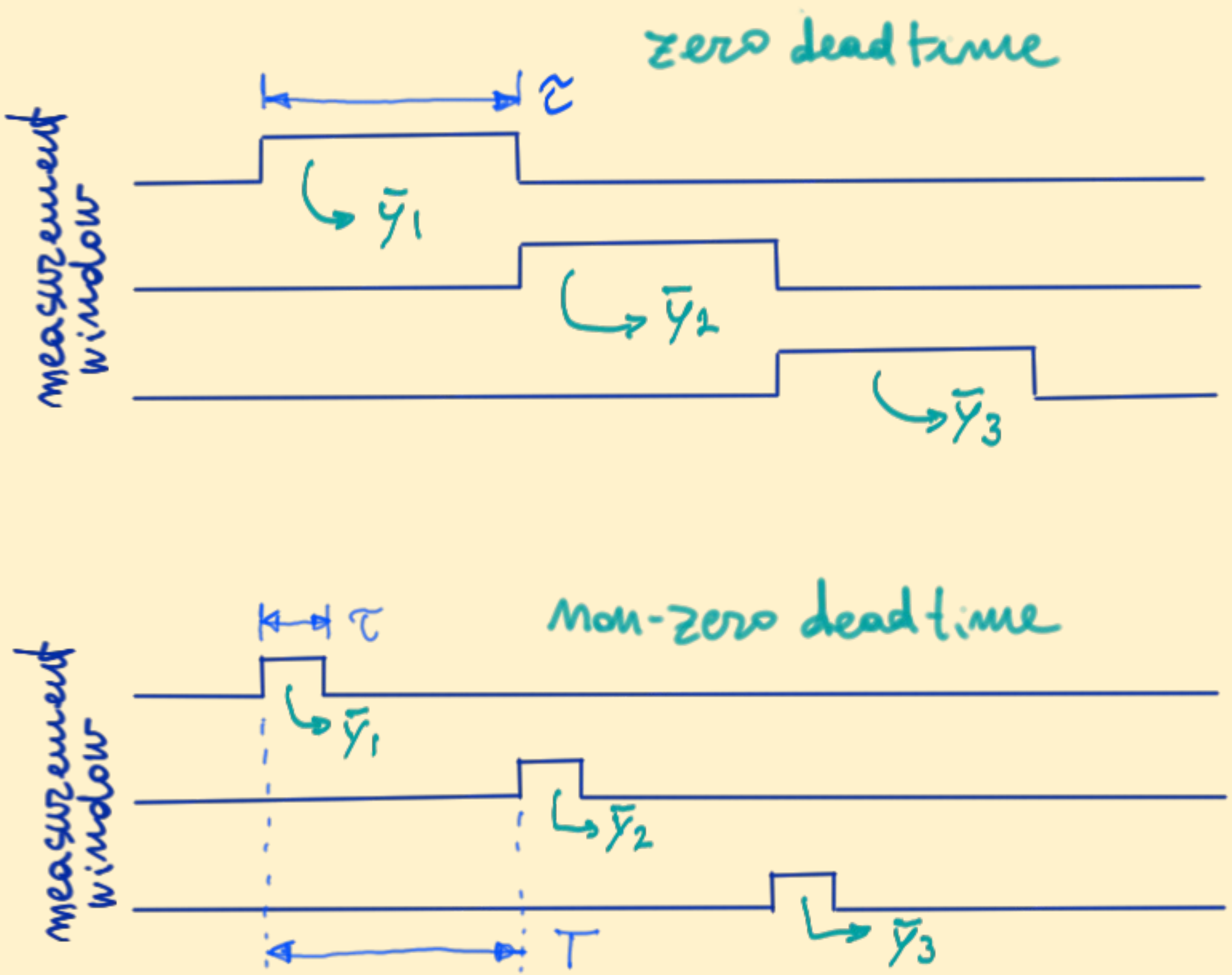
zero dead time
τ
measurement window
$\bar{y}_1$
$\bar{y}_2$
$\bar{y}_3$
non-zero dead time
τ
measurement window
$\bar{y}_1$
$\bar{y}_2$
$\bar{y}_3$
T

Allan variance with or without overlapping

Allan variance with overlapping

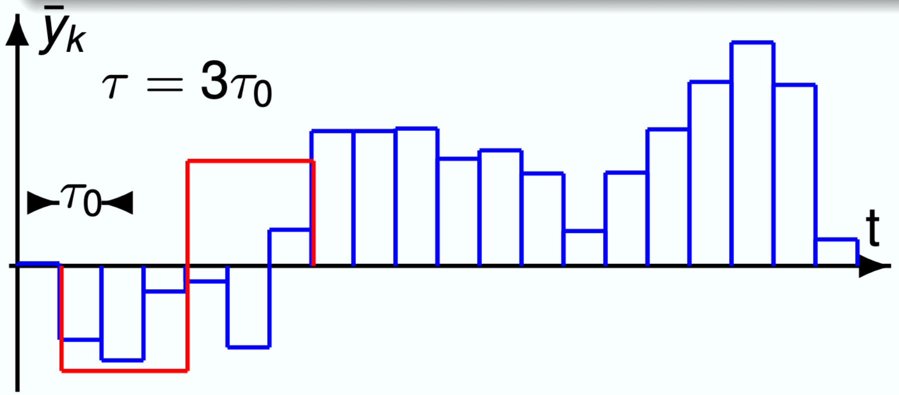

τ_0-steps moving average

Benefits and drawbacks :

- lower dispersion
- more correlated estimates

Allan variance without overlapping

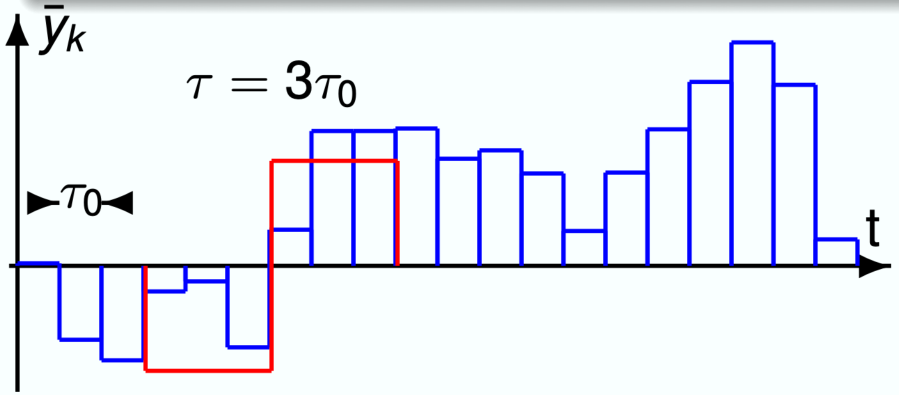

Shifted by τ-steps :
$\tau = 3\tau_0 \Leftrightarrow \bar{Y}_1 = (\bar{y}_1 + \bar{y}_2 + \bar{y}_3)/3$

Benefits and drawbacks :

- less correlated estimates
- higher dispersion

Courtesy of F. Vernotte

Chi-square and Rayleigh distribution

Allan variance: $\sigma_y^2(\tau) = \frac{1}{2}\left\langle (\bar{y}_2 - \bar{y}_1)^2 \right\rangle$

Estimate: $\hat{\sigma}_y^2(\tau) = \frac{1}{2N}\sum_{i=1}^{N} (\bar{y}_2 - \bar{y}_1)^2$

- $\bar{y}_2 - \bar{y}_1$: Gaussian centered values
- $(\bar{y}_2 - \bar{y}_1)^2$: χ_1^2 distribution
- $\frac{1}{2N}\sum_{i=1}^{N} (\bar{y}_2 - \bar{y}_1)^2$: χ_N^2 distribution

Allan deviation: $\sigma_y(\tau) = \sqrt{\frac{1}{2}\left\langle (\bar{y}_2 - \bar{y}_1)^2 \right\rangle}$

Estimate: $\hat{\sigma}_y(\tau) = \sqrt{\frac{1}{2N}\sum_{i=1}^{N} (\bar{y}_2 - \bar{y}_1)^2} \quad \Rightarrow \chi_N$ distributed (Rayleigh)

***N* is the Equivalent Degrees of Freedom (EDF)**

Courtesy of F. Vernotte

Reminder about the Equivalent Degrees of Freedom

Meaning of the EDF

$\mathrm{Mean}(\chi^2_\nu) = \nu$ and $\mathrm{Variance}(\chi^2_\nu) = 2\nu$

The EDF ν contains the information about the dispersion of the random variable χ^2_ν

Estimation of the EDF

$$\hat{\sigma}^2_y(\tau) = \frac{1}{2N}\sum_{i=1}^{N}(\bar{y}_2 - \bar{y}_1)^2 \quad \Rightarrow \quad \chi^2_N \text{ if } \{\bar{y}_1, \bar{y}_2, \ldots\} \text{ uncorrelated!}$$

False:

- for low frequency noises (flicker and random walk FM)
- with overlapping variances

EDF estimation not included here.
Read the Greenhall article

Algorithm for estimating the EDF

- **C. Greenhall and W. Riley, 2003**, *"Uncertainty of Stability Variances Based on Finite Differences"* (35$^{\text{th}}$ PTTI).
  Used in *Stable 32* as well as in *SigmaTheta*.

Courtesy of F. Vernotte

Bayesian statistics, or the inverse problem

- Simulation (direct problem)
  - Start from true value
  - Add noise
  - Gaussian distribution

- Experiment (inverse problem)
  - Start from experimental data
  - Estimate the measurand
  - χ^2 distribution

Bayes theorem

$$p(\theta|\xi) = \frac{\pi(\theta)p(\xi|\theta)}{\pi(\xi)}$$

posterior PDF $p()$
prior PDF $\pi()$
experimental ξ
unknown “true” θ

Highly specialized topic

Developped (among others) by F. Vernotte, and E. Lantz

Dispersion of Allan variance estimates

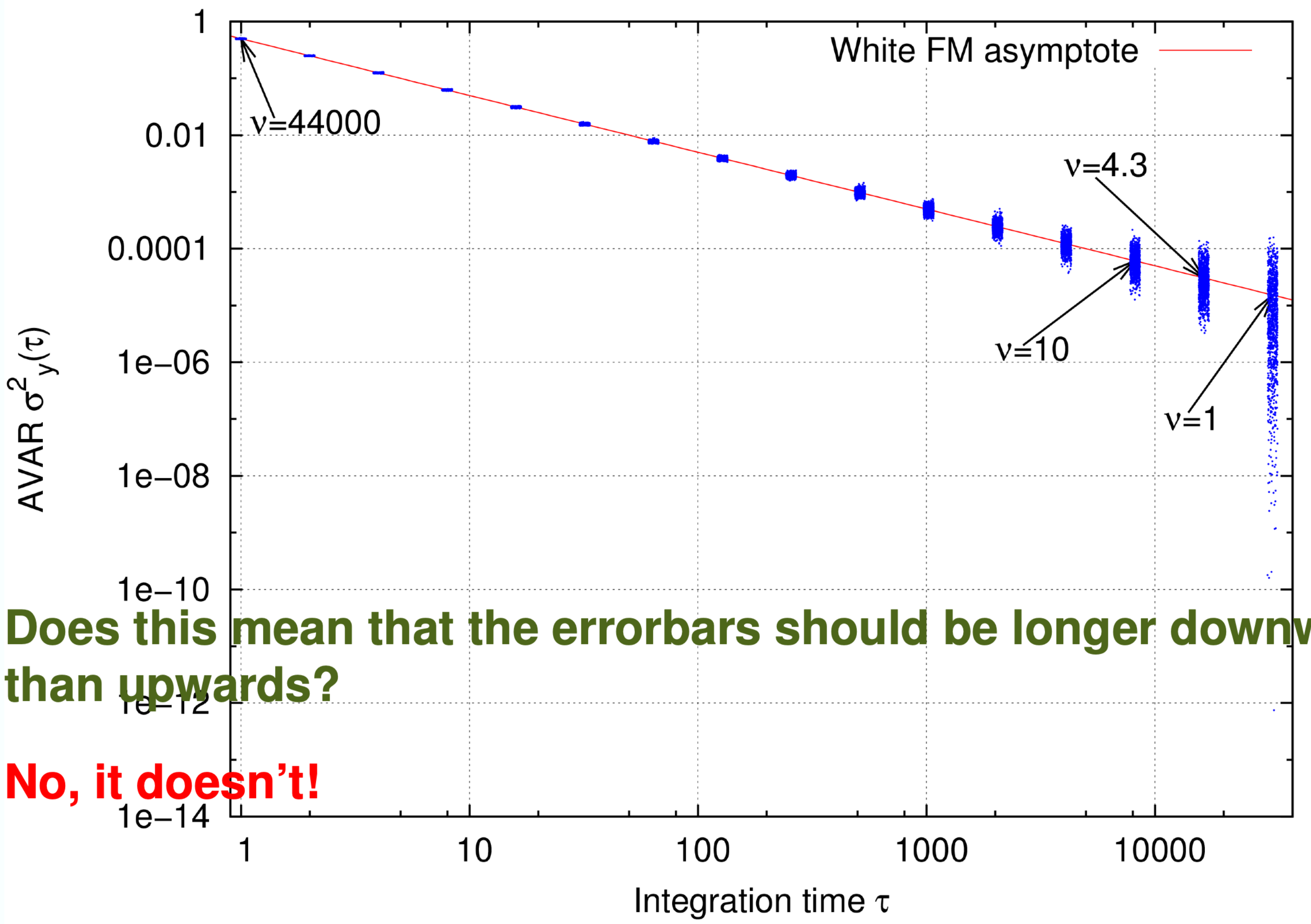

Courtesy of F. Vernotte

Does this mean that the errorbars should be longer downwards than upwards?

No, it doesn't!

Probability density function of a χ_2 distribution

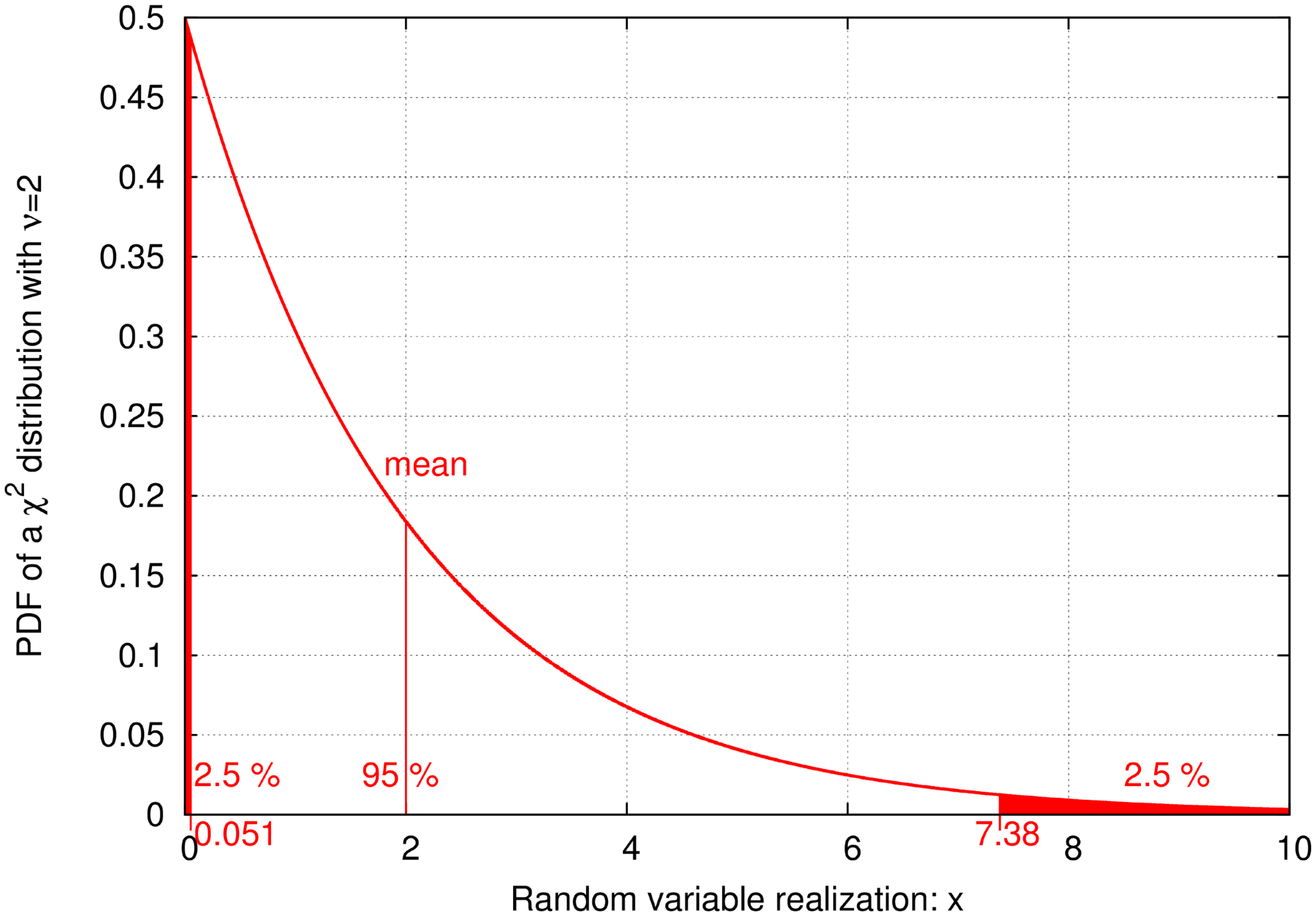

Courtesy of F. Vernotte

Errorbars over Allan variance estimates

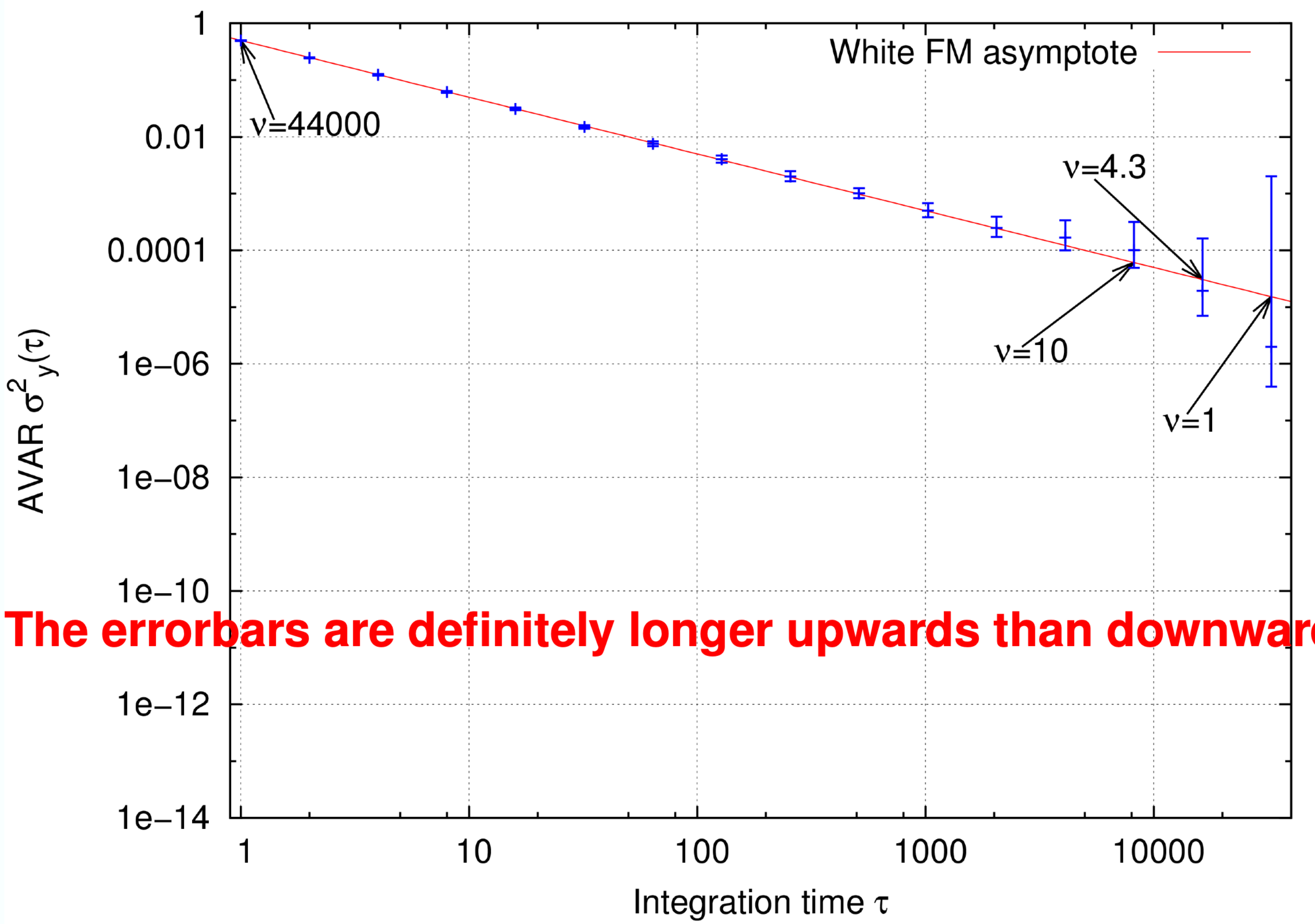

The errorbars are definitely longer upwards than downwards!

Courtesy of F. Vernotte

Other Variances

The most widely used variances

- **The Picinbono variance** (Hadamard):

$$\sigma_p^2(\tau) = \frac{1}{9}\left\langle\left(-\bar{y}_1 + 2\bar{y}_2 - \bar{y}_3\right)^2\right\rangle.$$

$$|H_p(f)|^2 = \frac{16}{9}\frac{\sin^6(\pi\tau f)}{(\pi\tau f)^2}.$$

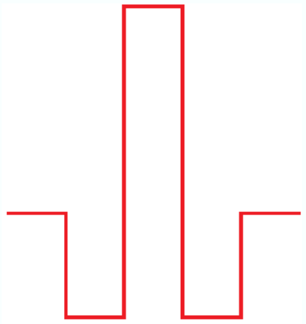

- **The modified Allan variance** (MVAR):

$$\mathrm{Mod}\sigma_y^2(\tau) = \frac{1}{2}\left\langle\left(\frac{1}{n}\sum_{i=1}^{n}\bar{y}_{i+n} - \bar{y}_i\right)^2\right\rangle$$

$$|H_M(f)|^2 = \frac{\sin^6(\pi\tau f)}{(\pi\tau f)^2 n^2 \sin^2(\pi\tau_0 f)}.$$

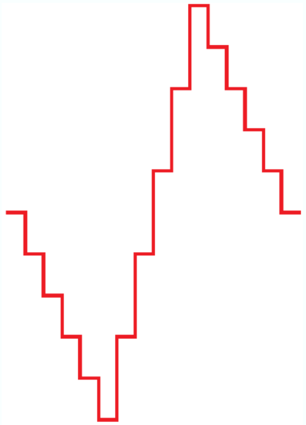

- **The time variance** (TVAR):

$$\sigma_x^2(\tau) = \frac{\tau^2}{3}\mathrm{Mod}\sigma_y^2(\tau).$$

Courtesy of F. Vernotte

Increasing the number of edf: the Total variance

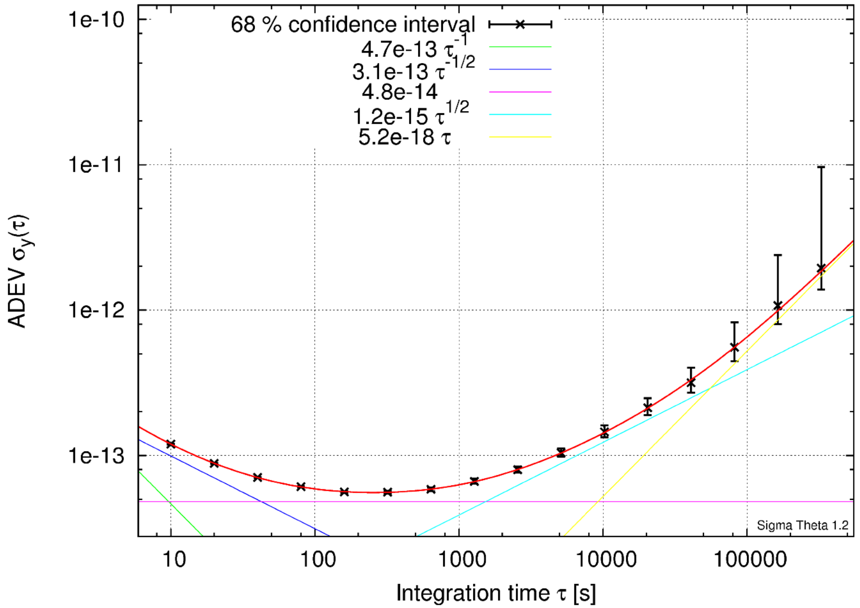

The longer the time duration, the larger the uncertainty.

What about very long term stability ?

In order to improve estimates for very long term, D. Howe developed:

- Total variance: *UFFC-47(5), 1102-1110 (2000)*
- $\widehat{\text{Theo}}$: *Metrologia 43, S322-S331 (2006)*

Courtesy of F. Vernotte

Main idea: circularizing the data sequence

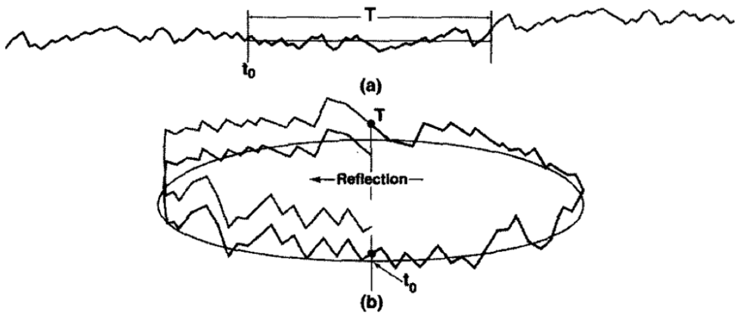

Statistics with Frequency Counters

Experimental Methods

for the measurement of phase noise and frequency stability

Enrico Rubiola

CNRS FEMTO-ST Institute, Besancon, France

INRiM, Torino, Italy

Outline

Saturated mixer
Correlation (dual-channel) measurements
Oscillator phase noise
Photonic techniques
~~Calibration methods~~
Bridge techniques
AM noise
~~Noise in systems~~

home page http://rubiola.org

Measurement – high signal-to-noise ratio

How can we measure a low random signal (noise sidebands)
close to a strong dazzling carrier?

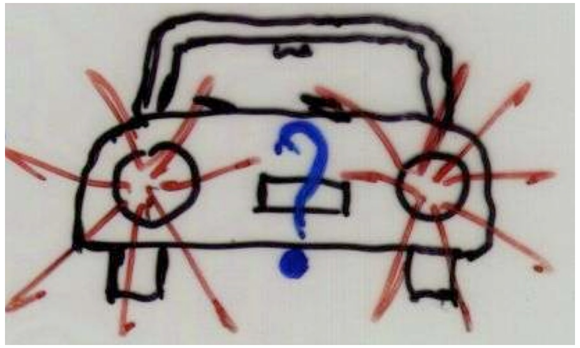

solution(s): suppress the carrier and measure the noise

convolution (low-pass)	$s(t) * h_{lp}(t)$	distorsiometer, audio-frequency instruments
time-domain product	$s(t) \times r(t - T/4)$	traditional instruments for phase-noise measurement (saturated mixer)
vector difference	$s(t) - r(t)$	bridge (interferometric) instruments

PM Noise measurement methods

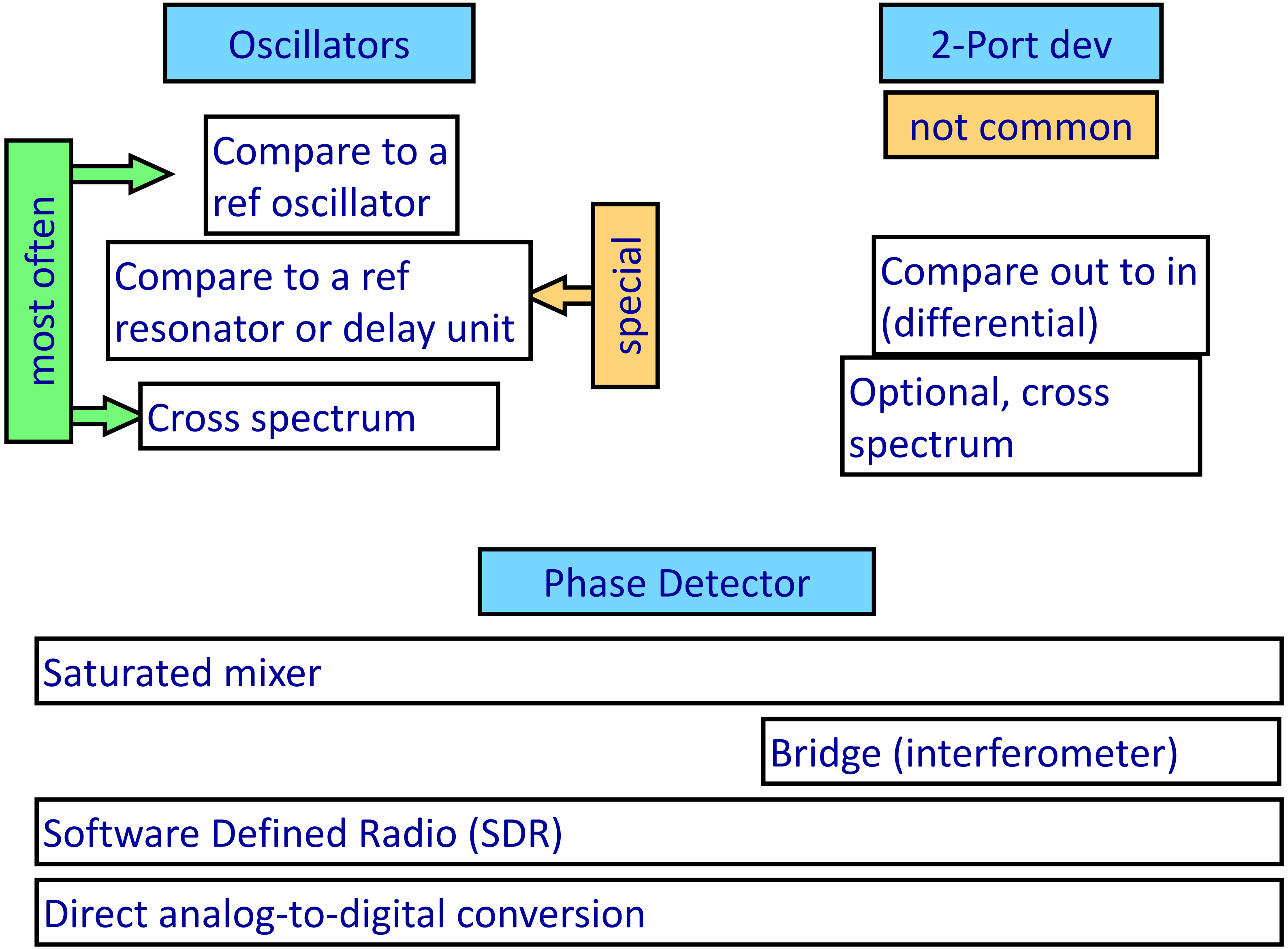

Saturated Mixer

Double-balanced mixer

saturated at both inputs => phase-to-voltage detector

$$v_0(t) = k_\varphi \varphi(t)$$

reference
$\sin(2\pi\nu_0 t)$

signal
$\cos(2\pi\nu_0 t + \varphi)$

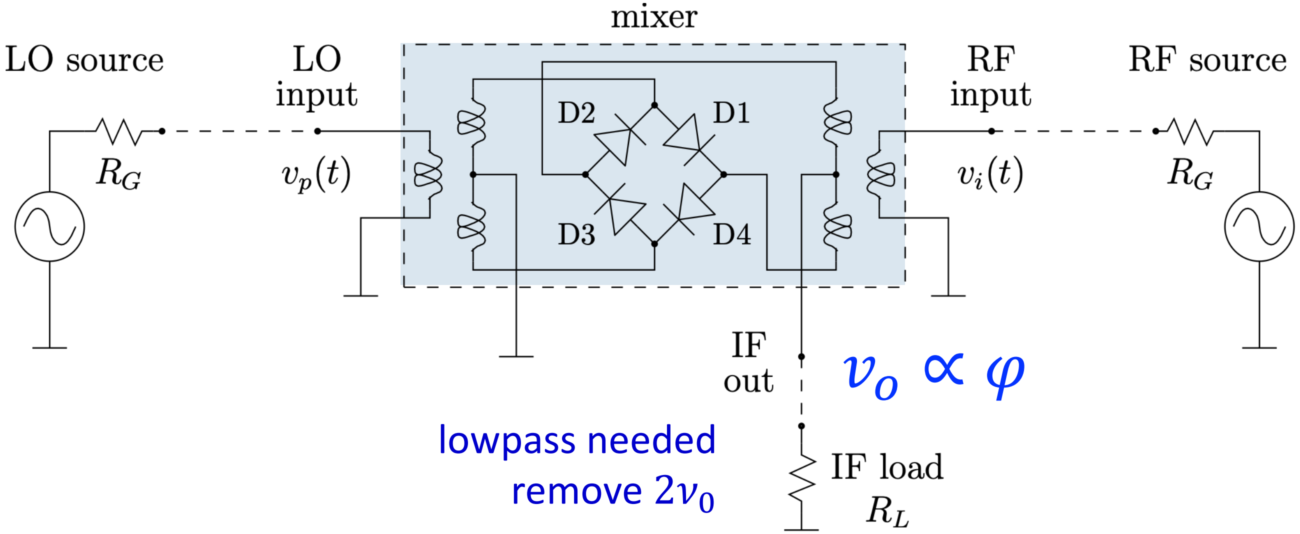

$v_o \propto \varphi$

lowpass needed
remove $2\nu_0$

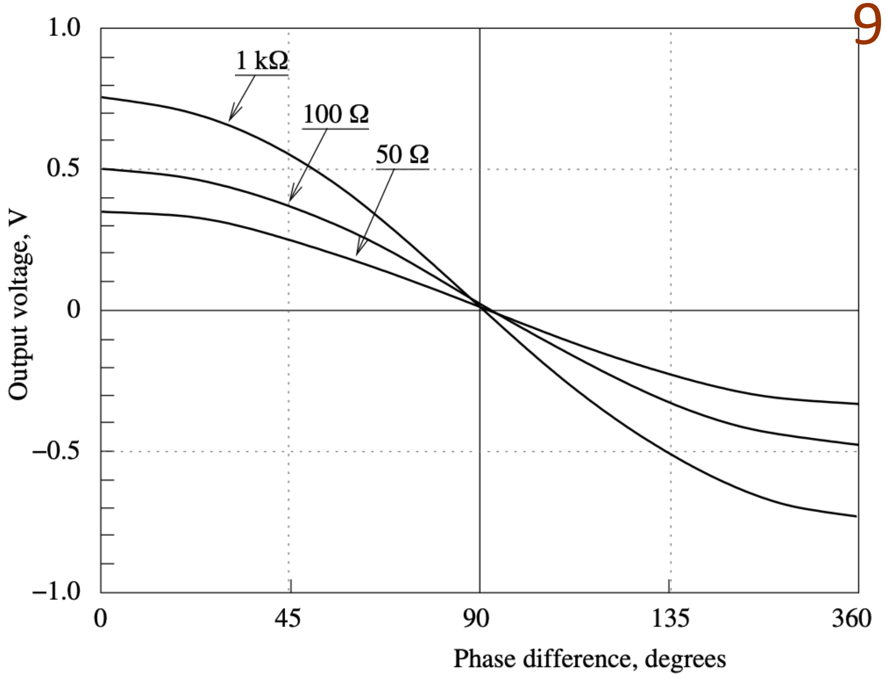

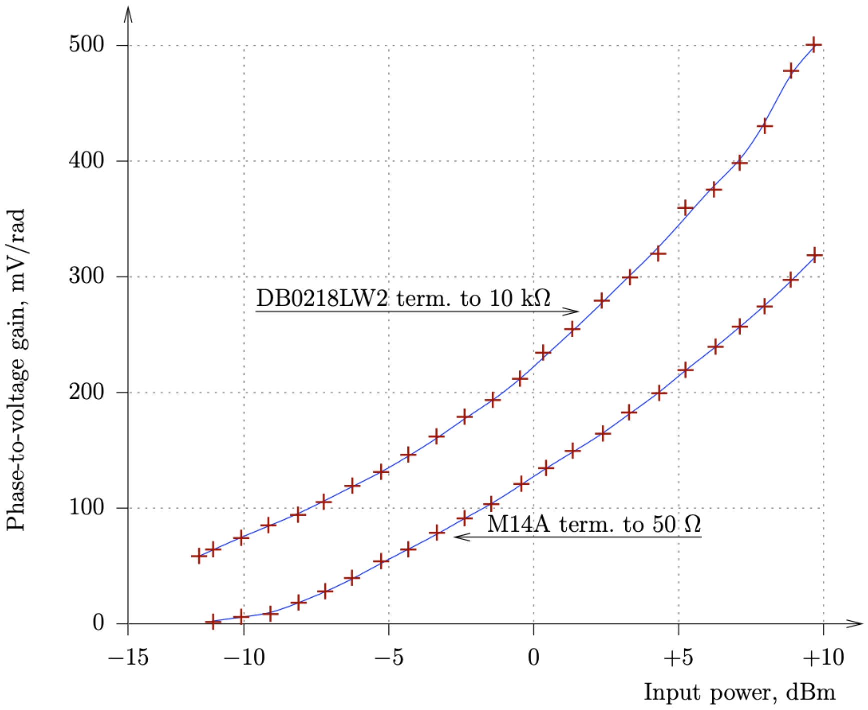

- LO and RF inputs are interchangeable
- Stronger signal –> LO (better isolation)

E. Rubiola, *Tutorial on the double-balanced mixer*, arXiv/physics/0608211

Double-balanced mixer

saturated multiplier
phase-to-voltage detector

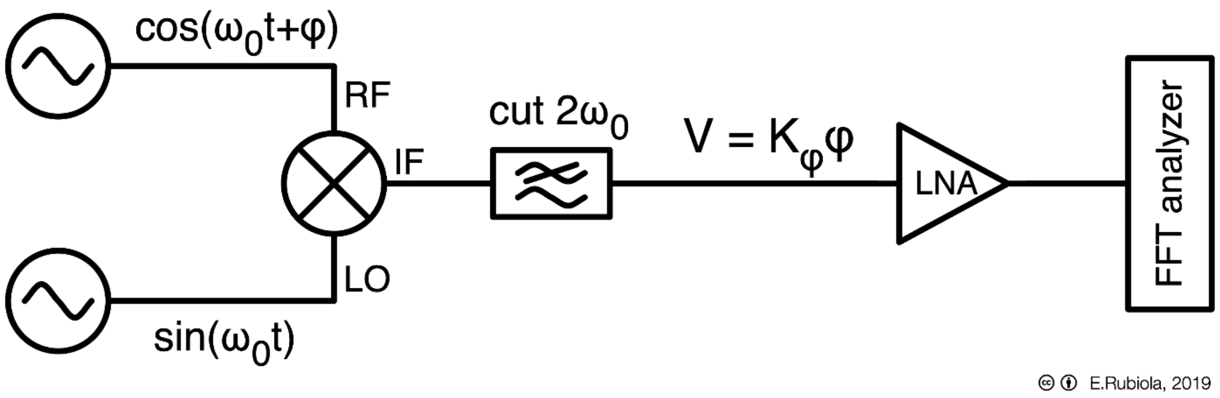

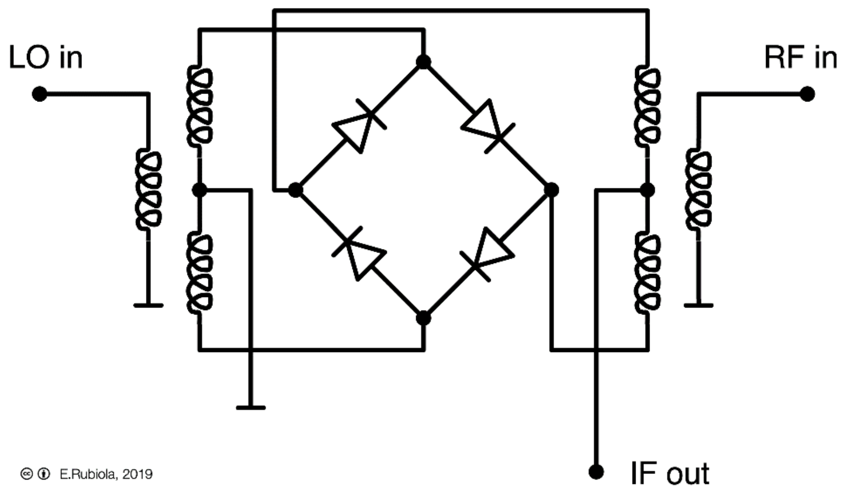

E. Rubiola, *Tutorial on the double-balanced mixer*, arXiv/physics/0608211

U. L. Rohde, E. Rubiola, J. C. Whitaker, Microwave and Wireless Synthesizers, Wiley 2021 (Chapter 2)

Double-balanced mixer

- Power
  - narrow range: ± 5 dB around $P_{\text{nom}} = 7 \dots 10$ dBm
  - $r(t)$ and $s(t)$ should have ≈ same P
- Flicker noise
  - mixer internal diodes
  - typical $S_\varphi = -140$ dBrad^2/Hz at 1 Hz in average-good conditions
- Low gain
  - $k_\varphi \approx 0.2 - 0.3$ V/rad typ, i.e., – 10 to – 14 dBV/rad
- White noise <=> operational amplifier
- Takes in noise <=> power-to-offset conversion
- High sensitivity to 50 Hz magnetic field

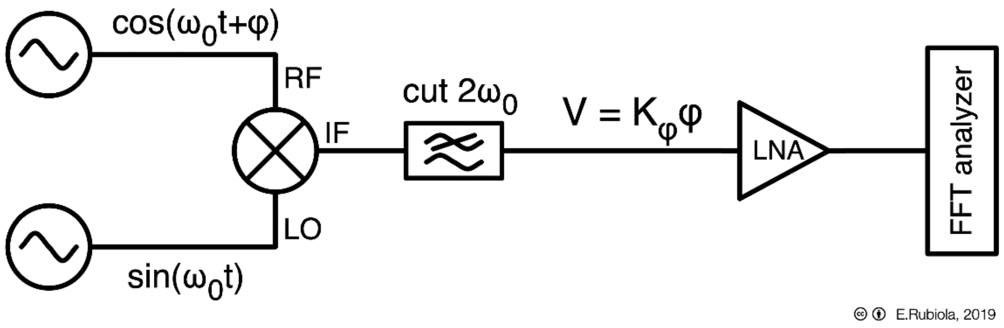

mixer background noise

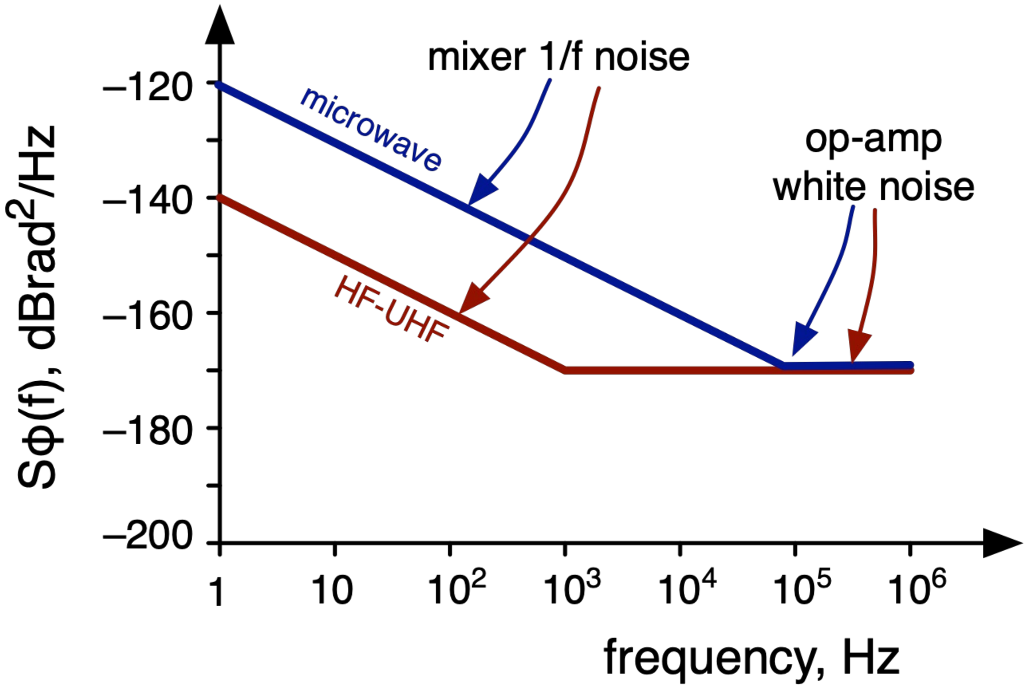

E. Rubiola, Tutorial on the double-balanced mixer, arXiv/physics/0608211, Aug 2006

Mixer's background noise – example

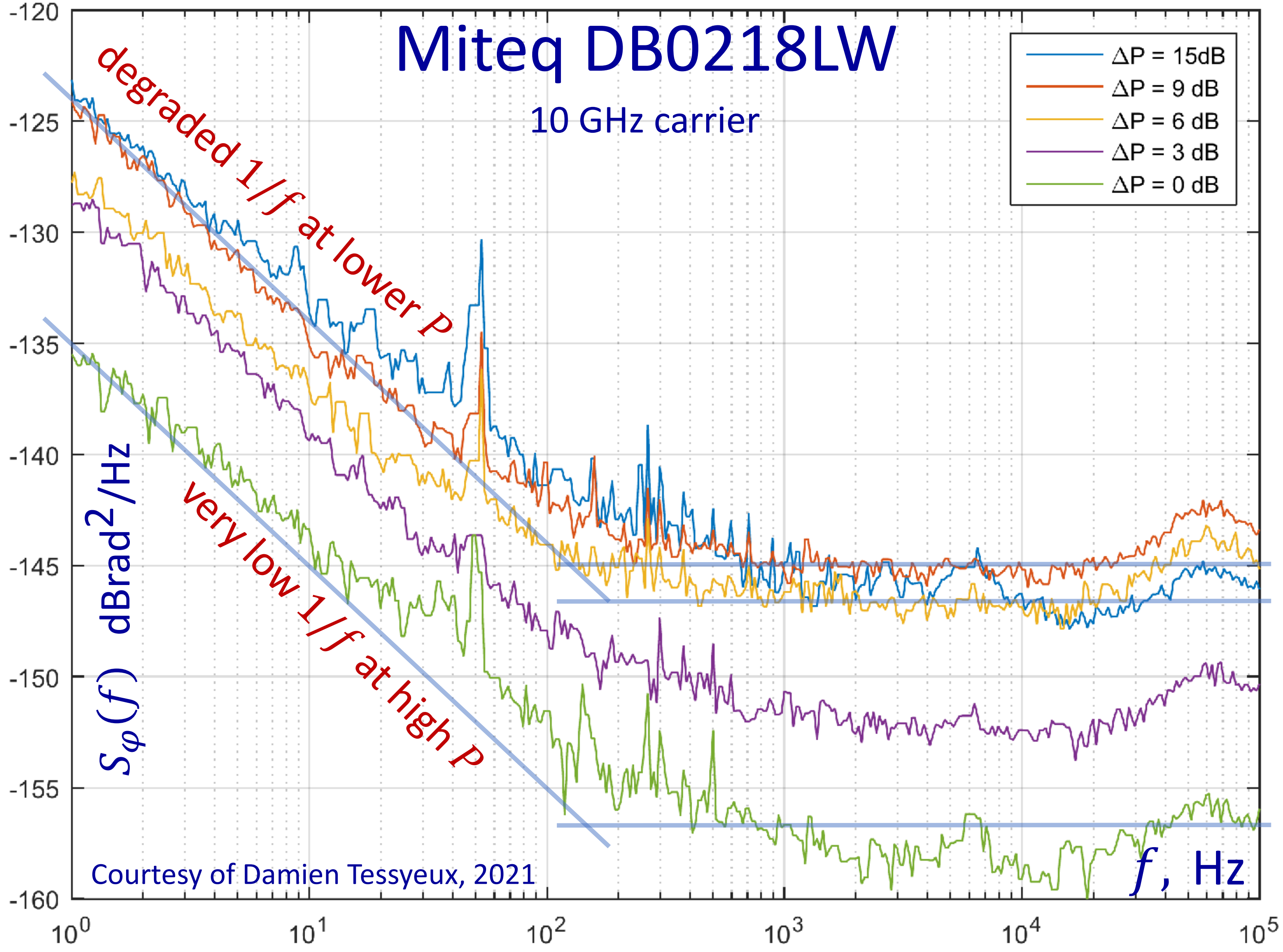

Nominal characteristics

- RF & LO 2–18 GHz
- LO 10 dBm (7–13 dBm)
- RF 1-dB compression +5 dBm
- IF 0–750 MHz (–3 dB)
- Typical loss 6.5 dB (LO 10 dBm)

poor white noise because of low k_φ at low P

white noise limited by the DC amplifier (better amplifiers are available)

The operational amplifier is misused

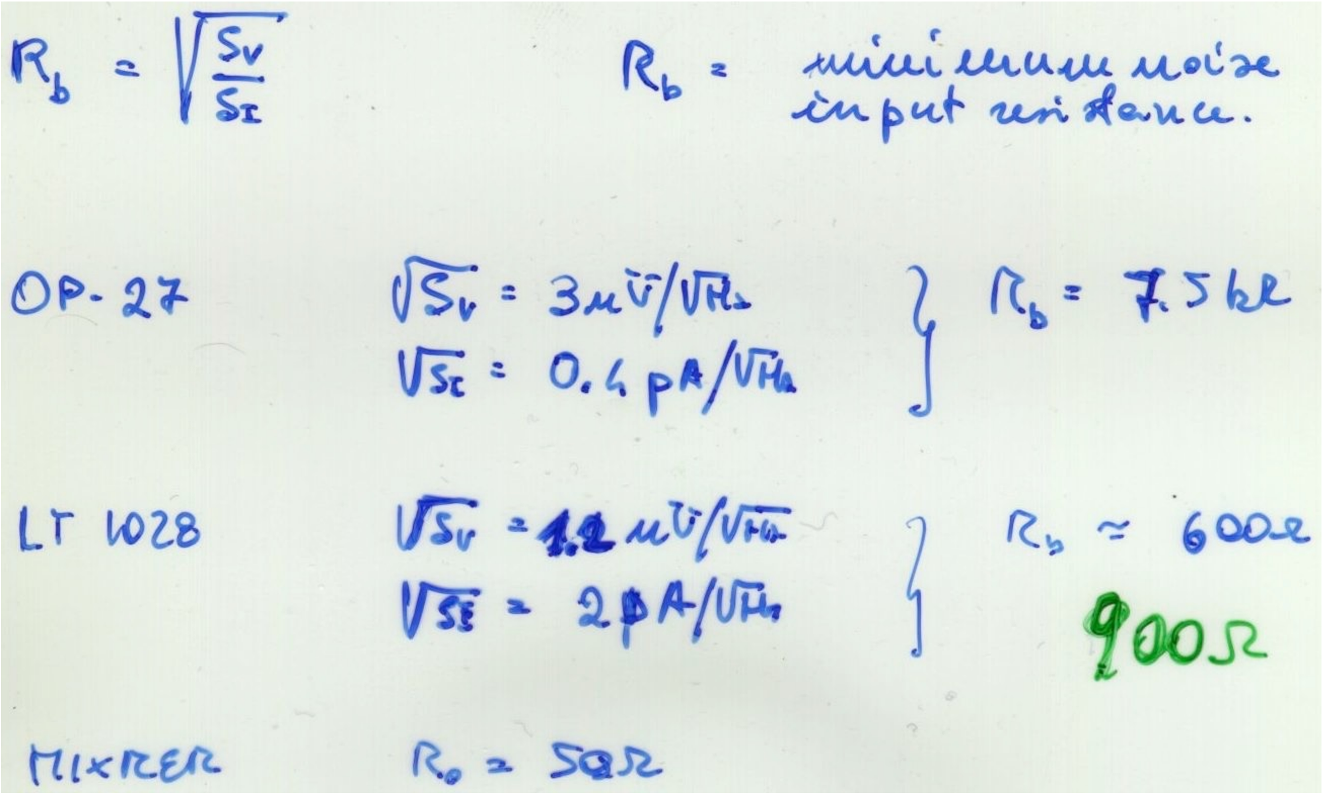

$$R_b = \sqrt{S_V/S_I}$$

OP 27	LT 1028
$e_n = 3\ \mathrm{nV}/\sqrt{\mathrm{Hz}}$	$e_n = 0.85\ \mathrm{nV}/\sqrt{\mathrm{Hz}}$
$i_n = 0.4\ \mathrm{pA}/\sqrt{\mathrm{Hz}}$	$i_n = 1\ \mathrm{pA}/\sqrt{\mathrm{Hz}}$
$R_b = 7.5\ \mathrm{k\Omega}$	$R_b = 850\ \Omega$
$(1.2\times10^{-21}\ \mathrm{W/Hz})$	$(8.5\times10^{-22}\ \mathrm{W/Hz})$

OP27: [3.2 nV/Hz$^{1/2}$] / [0.2 V/rad] = 16 nrad/Hz$^{1/2}$ (–156 dBrad^2/Hz)

LT1028: [1.2 nV/Hz$^{1/2}$] / [0.2 V/rad] = 2.4 nrad/Hz$^{1/2}$ (–164 dBrad^2/Hz)

Warning: if only one arm of the power supply is disconnected, the LT1028 may delivers a current from the input (I killed a $2k mixer in this way!)

You may duplicate the low-noise amplifier designed at the FEMTO-ST

Rubiola, Lardet-Vieudrin, Rev. Scientific Instruments 75(5) pp. 1323-1326, May 2004

Practical issues

All figures from arXiv/physics/0608211

needs a capacitive-input filter to recirculate the $2\omega_0$ output signal

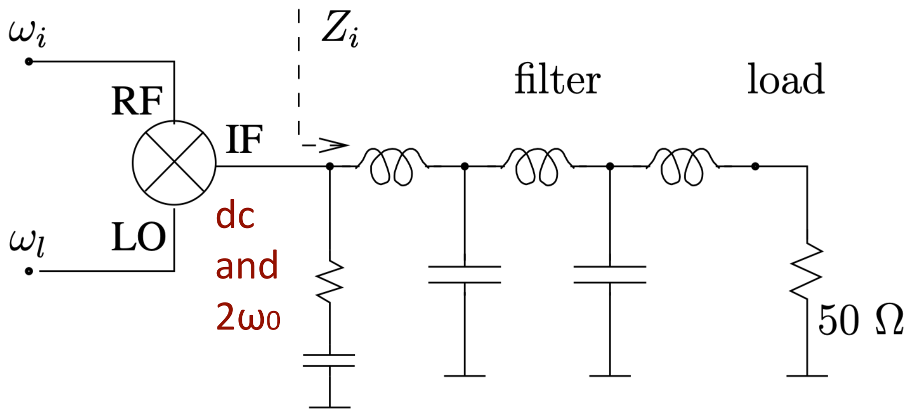

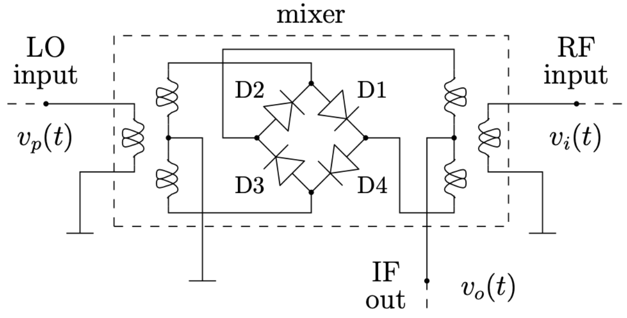

actual phase-to-voltage conversion

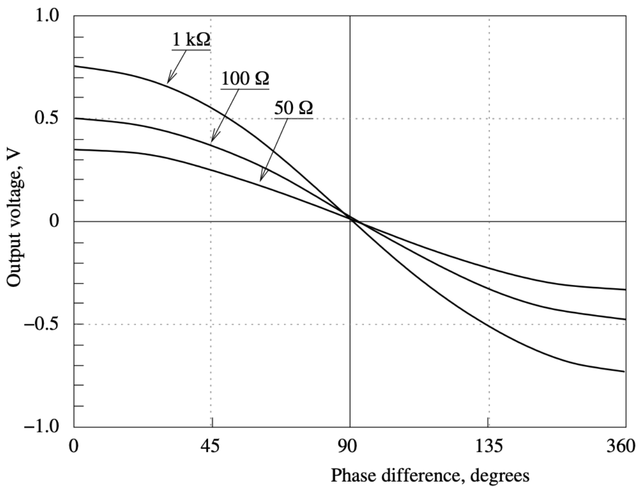

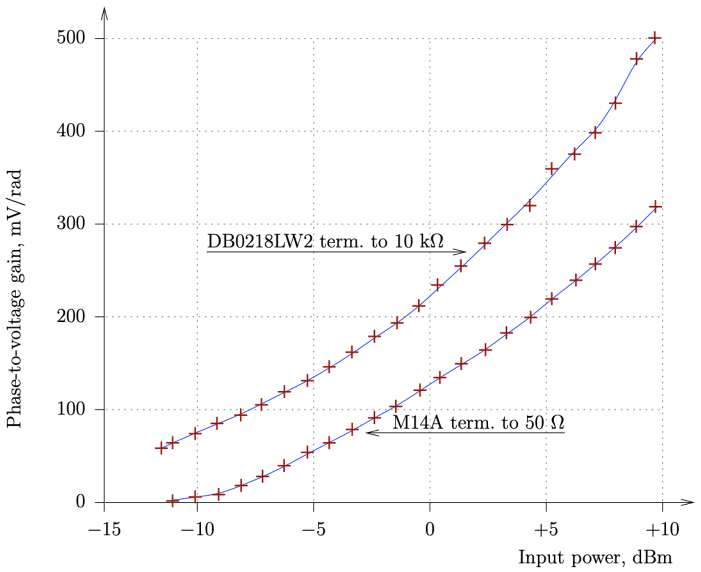

E. Rubiola, *Tutorial on the double-balanced mixer*, arXiv/physics/0608211,

Useful schemes

two-port device under test

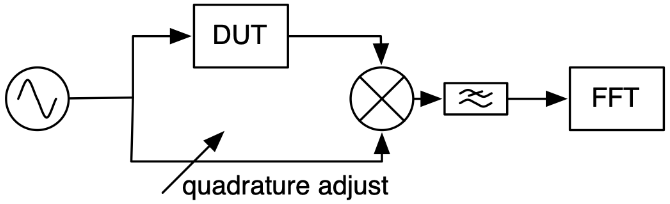

a pair of two-port devices
3 dB improved sensitivity

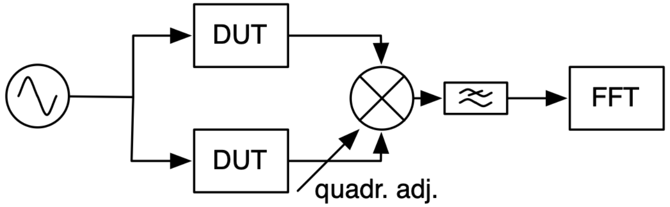

the measurement of an amplifier
needs an attenuator

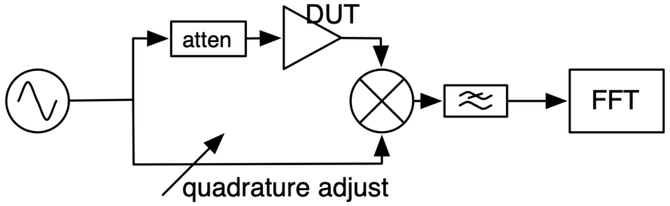

the measurement of a low-power DUT
needs an amplifier, which flickers

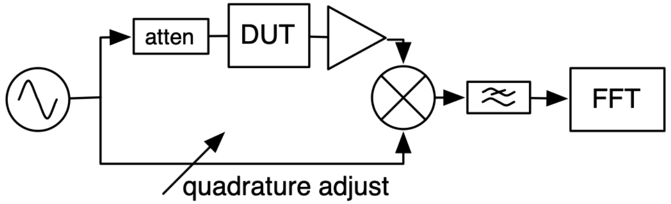

measure two oscillators
best use a tight loop

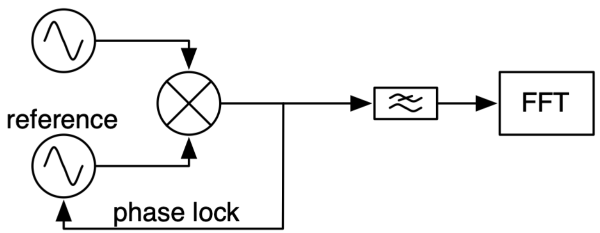

measure an oscillator vs. a resonator

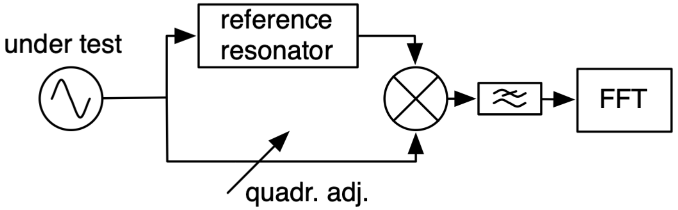

Averaged spectra should be smooth

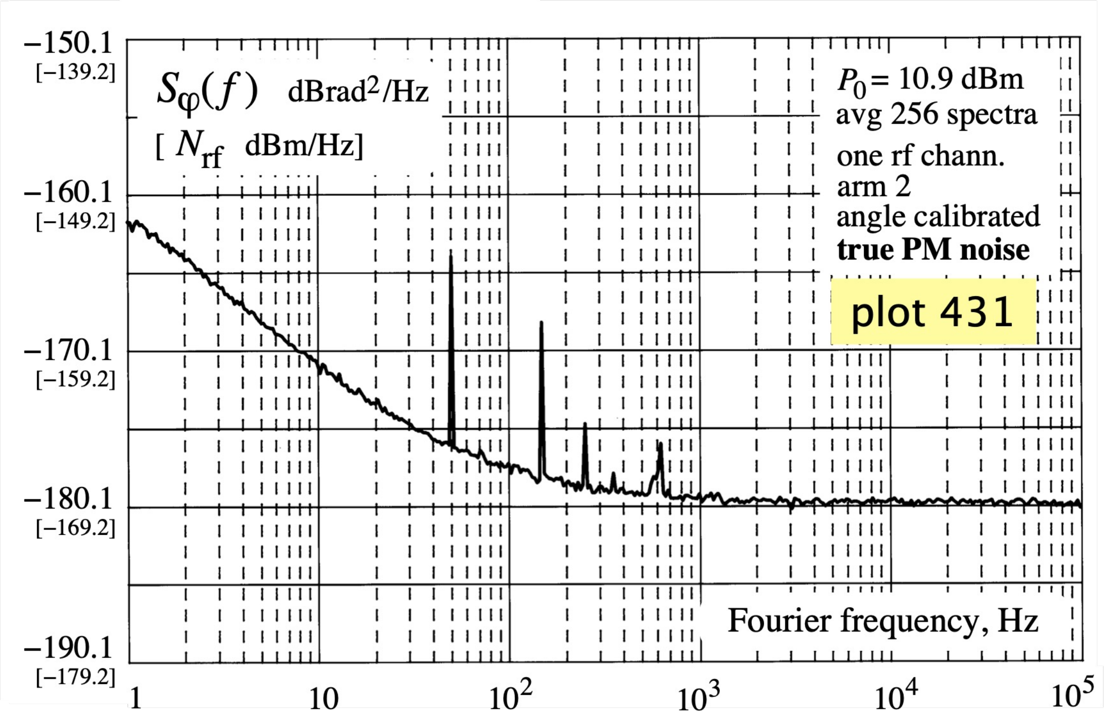

Fig.12(top), from E. Rubiola, V. Giordano, Rev. Sci. Instrum. 73(6) p.2445-2457, June 2002. ©AIP.

Rice representation

$$v(t) = \sum_{n=0}^{\infty} a_n(t)\cos(n\omega_0 t) - b_n(t)\sin(n\omega_0 t)$$

$$S_v(n\omega_0) = \left[a_n^2 + b_n^2\right]/\omega_0$$

$a_n(t)$ and $b_n(t)$ contain the noise in the $\omega_0/2$ band centered at ω_0

stationary & ergodic process (means repeatable and reproducible): the statistics of all $a_n(t)$ and $b_n(t)$ is the same

average on m spectra: confidence of a point improves by $1/m^{1/2}$

interchange ensemble with frequency: smoothness $1/m^{1/2}$

Pollution from power grid

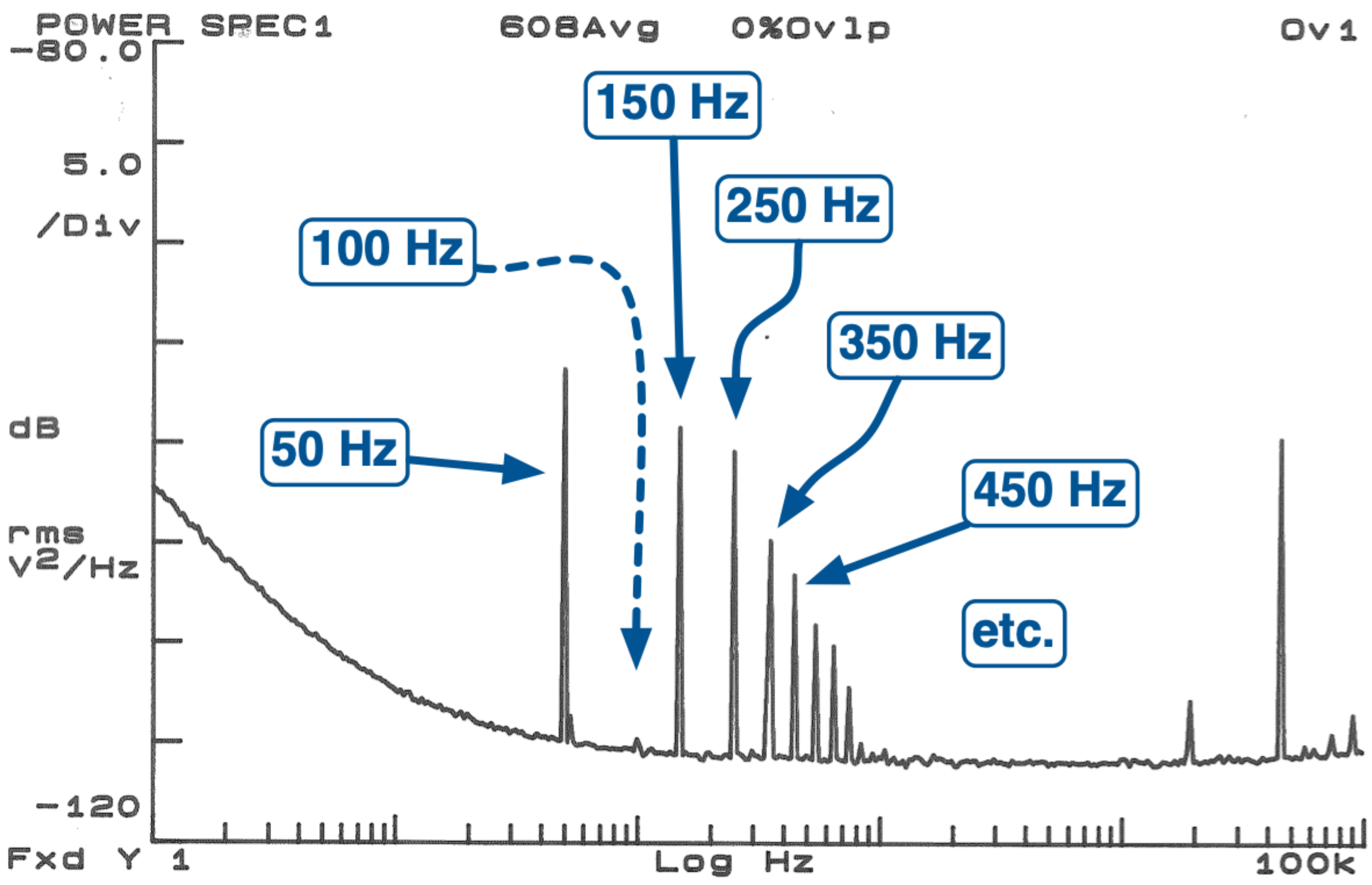

- More visible on components than on oscillators
  - Not hidden by $1/f^2$ and $1/f^3$
- Preference for odd-order harmonics
  - Likely, the signature of the odd symmetry of saturation in transformers iron

Mechanical stability

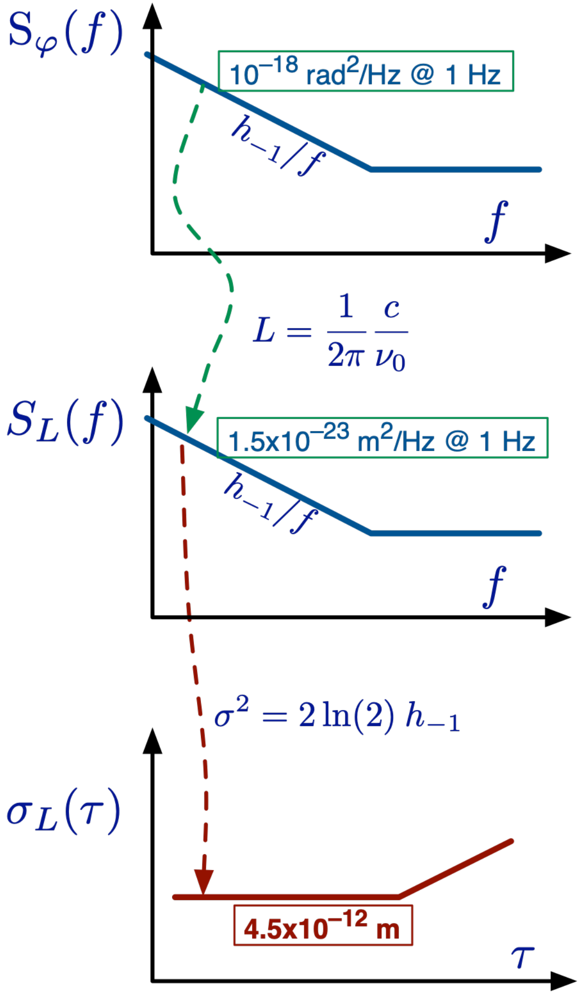

Any phase fluctuation can be converted into length fluctuation

$$L = \frac{\varphi}{2\pi}\frac{c}{\nu_0}$$

b_{-1} = –180 dBrad²/Hz and ν_0 = 10 GHz is equivalent to $S_L = 1.46\text{x}10^{-23}$ m²/Hz at f = 1 Hz

Any flicker spectrum h_{-1}/f can be converted into a flat Allan variance

$$\sigma_L^2 = 2\ln(2)\,h_{-1}$$

A residual flicker of –180 dBrad²/Hz at f = 1 Hz off the 10 GHz carrier is equivalent to

$$\sigma^2 \;=\; 2x10\text{–}\,23\;m^2 \quad \text{—>} \quad \sigma \;=\; 4.5x10\text{–}\,12\;m$$

for reference, the Bohr radius of the H atom is a_0 = 0.529 nm

End of lecture 7

Lecture 8

Scientific Instruments & Oscillators

Lectures for PhD Students and Young Scientists

Enrico Rubiola

CNRS FEMTO-ST Institute, Besancon, France

INRiM, Torino, Italy

Contents

•

ORCID 0000-0002-5364-1835

home page http://rubiola.org

Measurement of Oscillator Phase Noise

Phase Locked Loop (PLL)

The mixer requires signals in quadrature –> phase locking

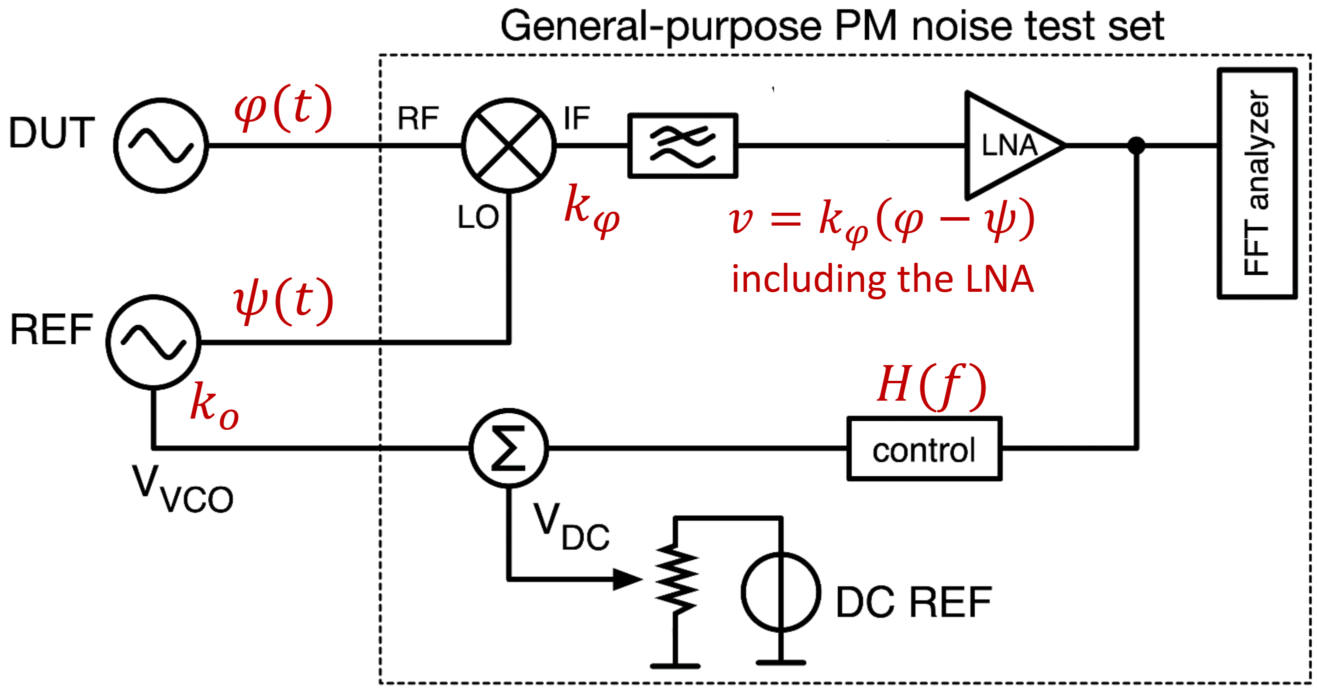

Figure from U. L. Rohde, E. Rubiola, J. C. Whithaker, *Microwave and Wireless Synthesizers*, ISBN 978-1-119-66600-4, ©J.Wiley 2021 (adapted)

Phase tracking –> low-pass filter

$$\frac{S_\varphi(f)}{S_\psi(f)} = \frac{|k_0 k_\varphi H(f)|^2}{4\pi^2 f^2 + |k_0 k_\varphi H(f)|^2}$$

Use the PLL as a high-pass filter

$$\frac{S_v(f)}{S_\varphi(f)} = \frac{k_o^2\, 4\pi^2 f^2}{4\pi^2 f^2 + |k_0 k_\varphi H(f)|^2}$$

Measurement

- Assume $S_\psi \ll S_\varphi$ i.e., noise-free reference oscillator

– or –

- Compare two equal oscillators and divide the spectrum by 2 (take away 3 dB)

The virtues of a fast PLL

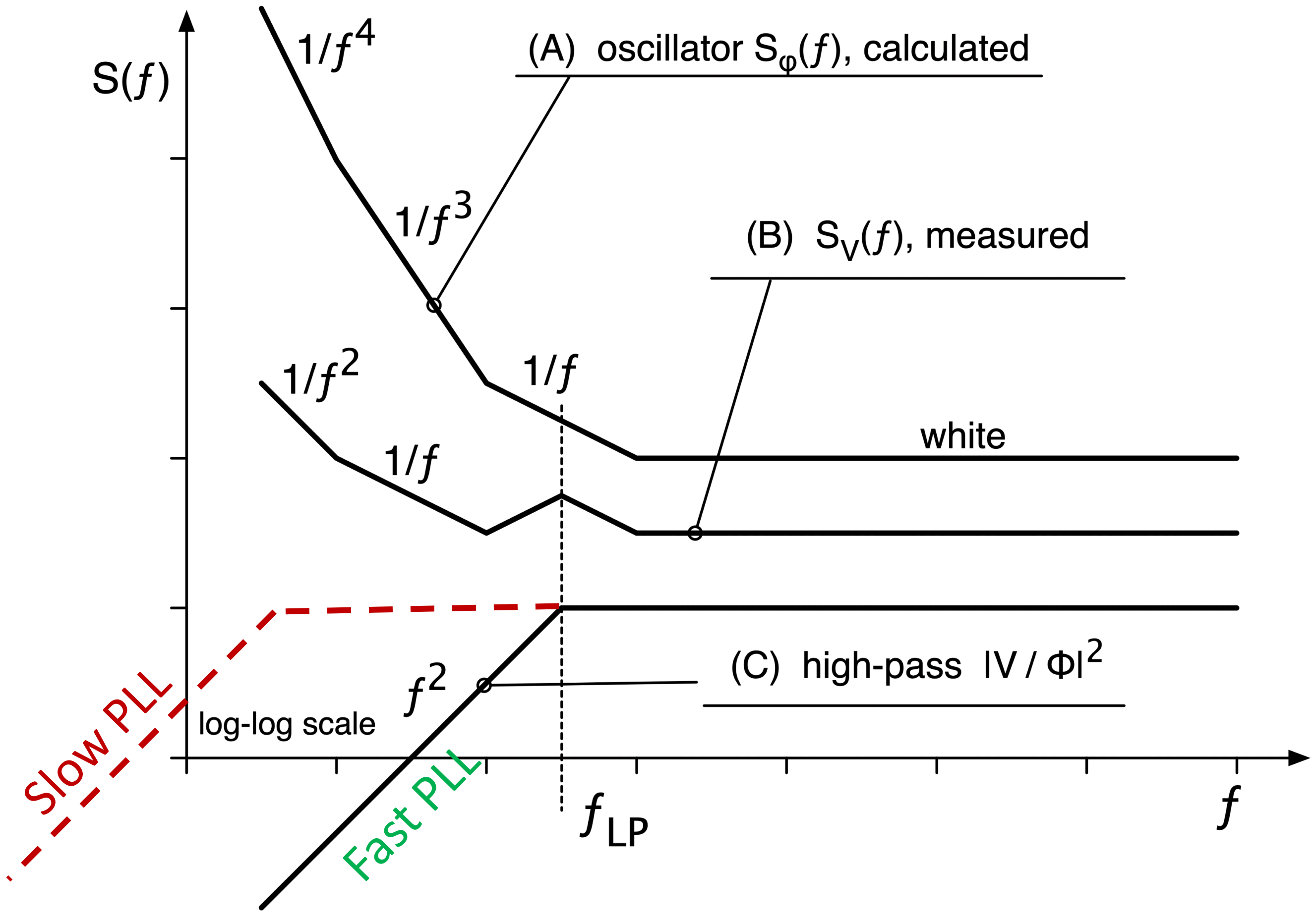

Figure from U. L. Rohde, E. Rubiola, J. C. Whithaker, *Microwave and Wireless Synthesizers*, ISBN 978-1-119-66600-4, ©J.Wiley 2021 (adapted)

Slow PLL

- Large swing at low f
- Large V_{FSR} of the FFT internal ADC
- High quantization noise
- Prone to injection locking

Fast PLL

- High-pass –> lower swing at low f
- Lower quantization noise
- Feedback overrides injection locking

but you have to correct the spectrum for the PLL transfer function

The dual-channel scheme

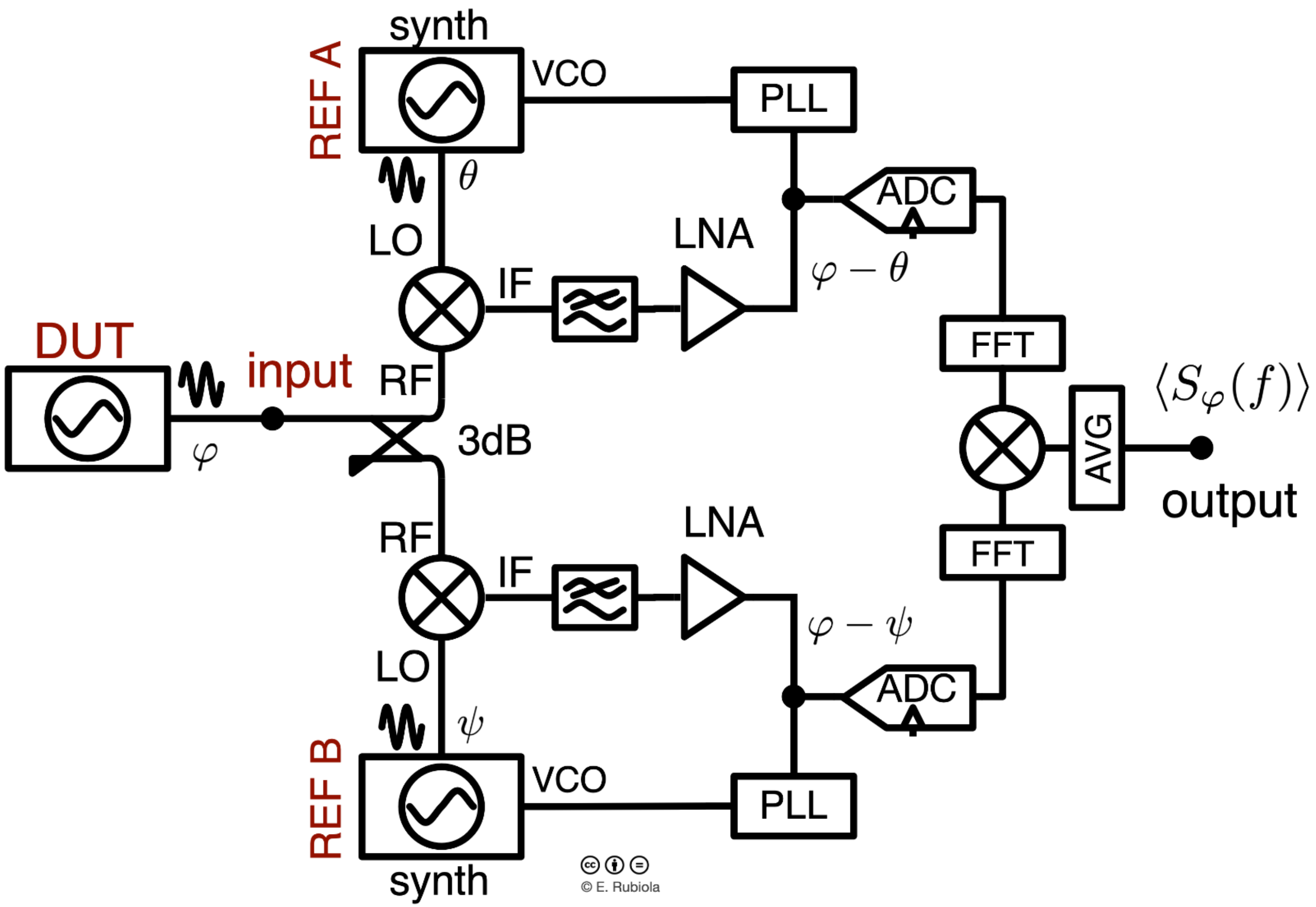

- Double balanced mixer saturated at both inputs
- Inputs in quadrature
- Phase-to-voltage conversion 0.2-0.3 V/rad typ.

- Two statistically independent channels
- Average cross spectrum

$$S_{yx}(f) \to S_{\varphi}(f)$$

- Single-channel noise rejected $\propto 1/\sqrt{m}$ (m is the no of avg), 5 dB per factor-10
- Prone to AM noise of the DUT via power to offset conversion in mixers (mitigated with saturated amplifiers)
- Related commercial instruments
  - Anapico
  - Berkeley Nucleonics Corp
  - Holzworth
  - Keysight
  - NoiseXT / Arcale
  - Wenzel Associates

Measurement of $S\varphi(f)$ with a PLL

- Set the circuit for proper electrical operation
- power level
- lock condition (there is no beat note at the mixer out)
- zero dc error at the mixer output (a small V can be tolerated)
- Choose the appropriate time constant
- Measure the oscillator noise
- At end, measure the background noise

A PLL may not be what it seems

Parasitic locking or coupling of the oscillators may impair the result

BAD SYMPTOMS :

- odd slope S_φ

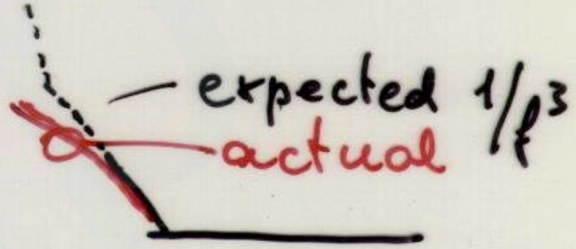

- open-loop waveforms IFout

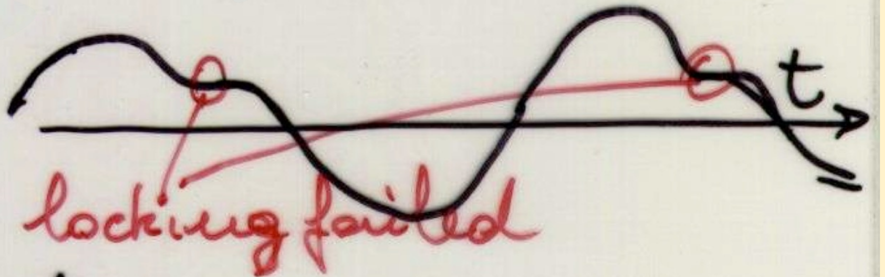

- results (S_φ) depend on the cable length

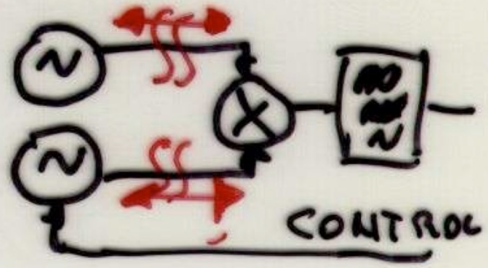

PLL – Two frequencies

The output frequency of the two oscillators is not the same.
A synthesizer (or two synth.) is necessary to match the frequencies

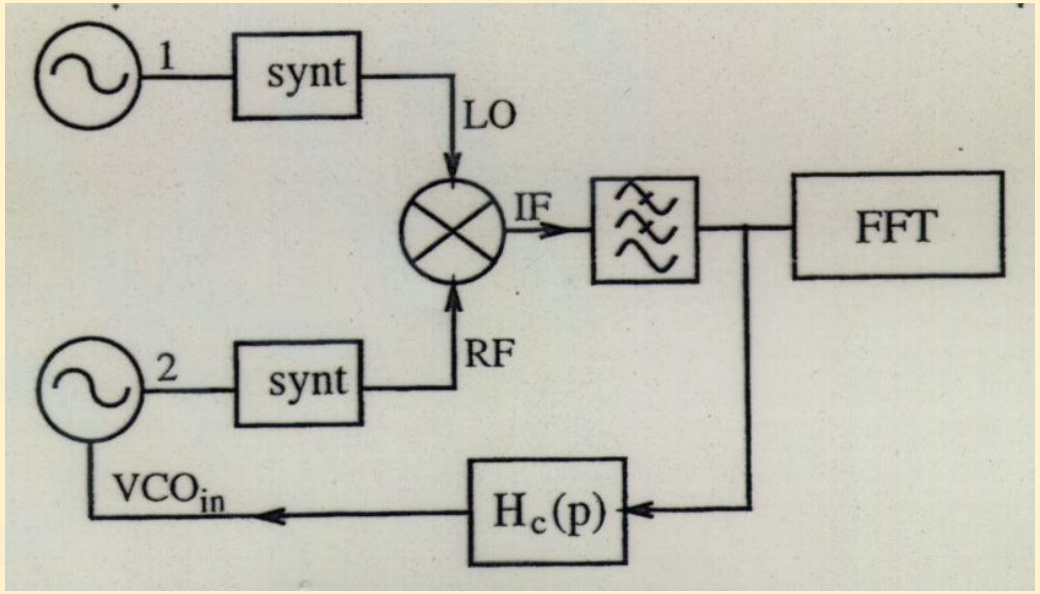

At low Fourier frequencies, the synthesizer noise is lower than the oscillator noise

At higher Fourier frequencies, the white and flicker of phase of the synthesizer may dominate

PLL – microwave oscillators

With low-noise microwave oscillators (like whispering gallery) the noise of a microwave synthesizer at the oscillator output can not be tolerated.

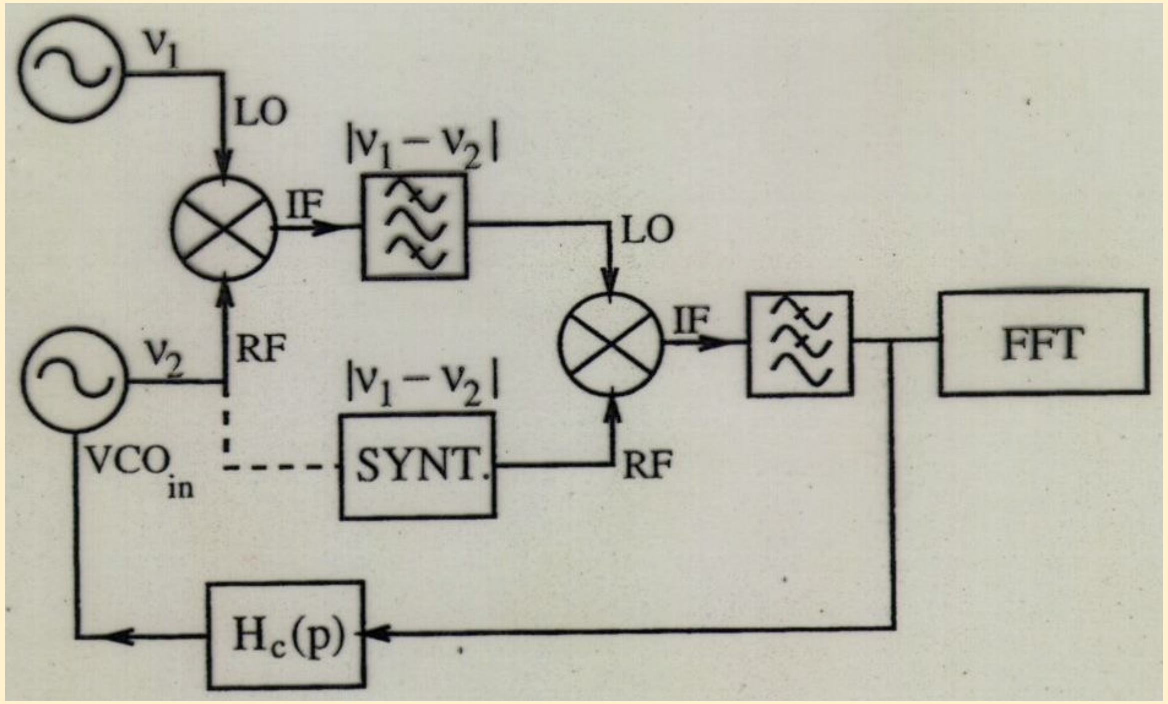

Due to the lower carrier frequency, the noise of a VHF synthesizer is lower than the noise of a microwave synthesizer.

This scheme is useful

- with narrow tuning-range oscillator, which can not work at the same freq.
- to prevent injection locking due to microwave leakage

Design your own instrument

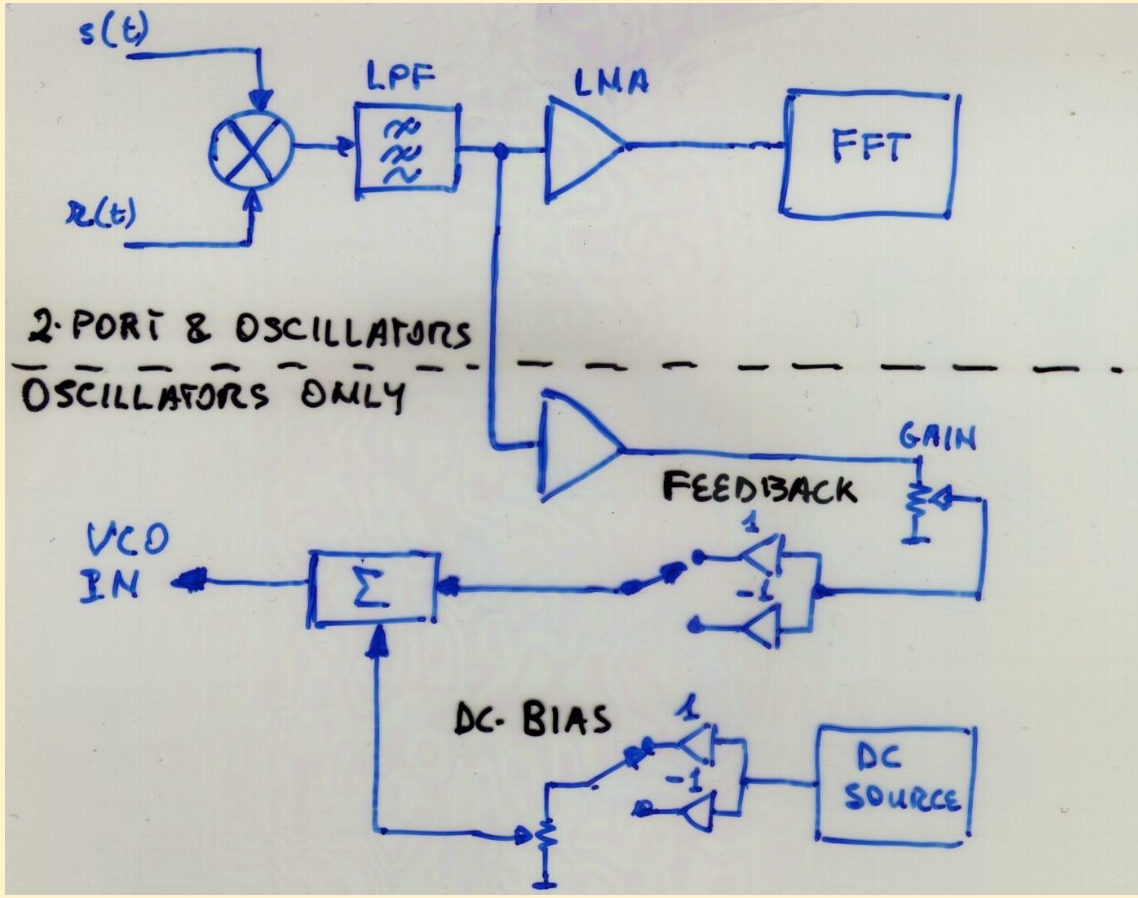

Standard commercial parts:

- double balanced mixer
- low-noise op-amp
- standard low-noise dc components in the feedback path
- commercial FFT analyzer

Afterwards, you will appreciate more the commercial instruments:

– Ergonomics and reliable implementation

– Instruction manual

– Computer interface and software

Frequency discriminator

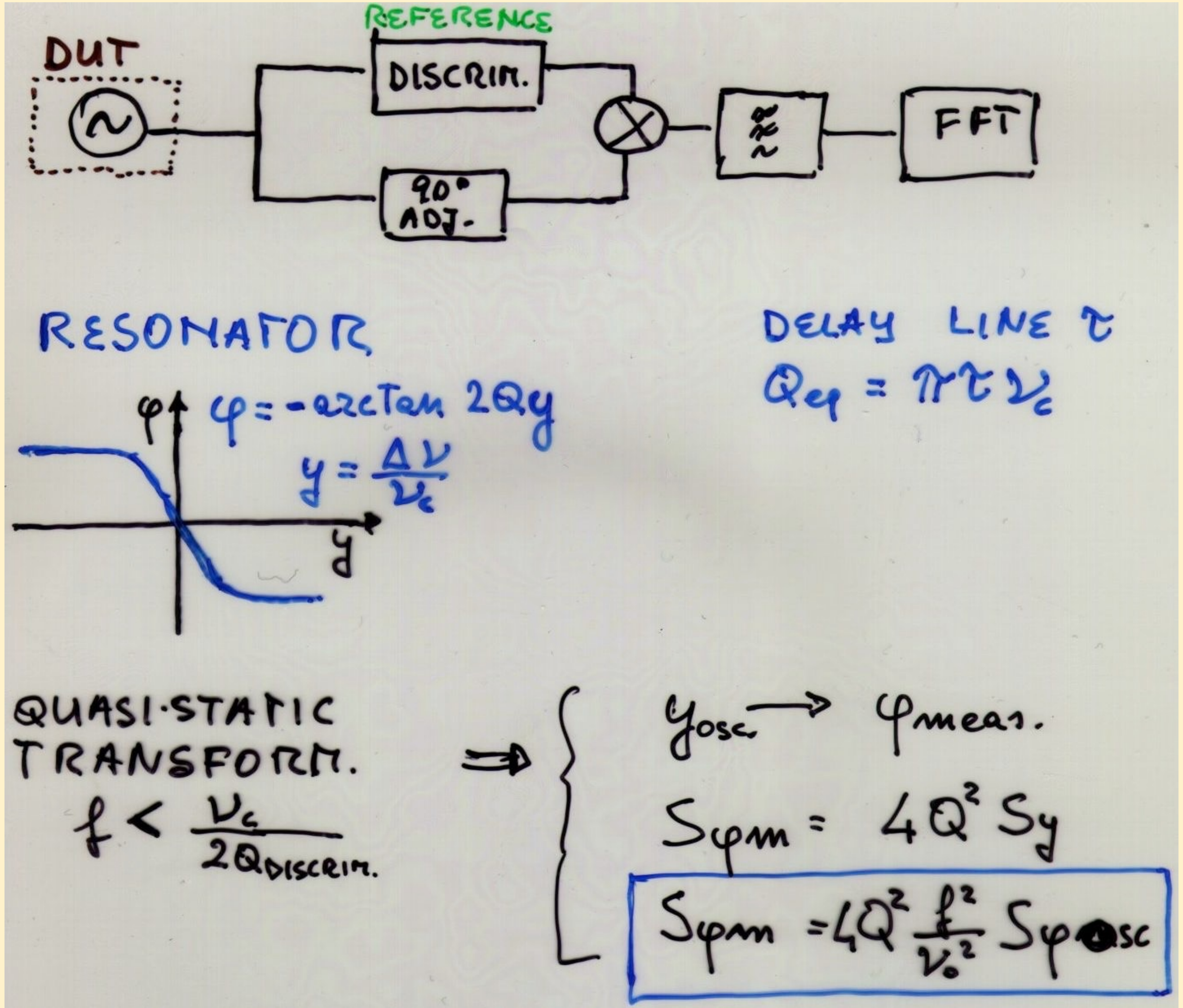

Digital Methods

Digital phase detector

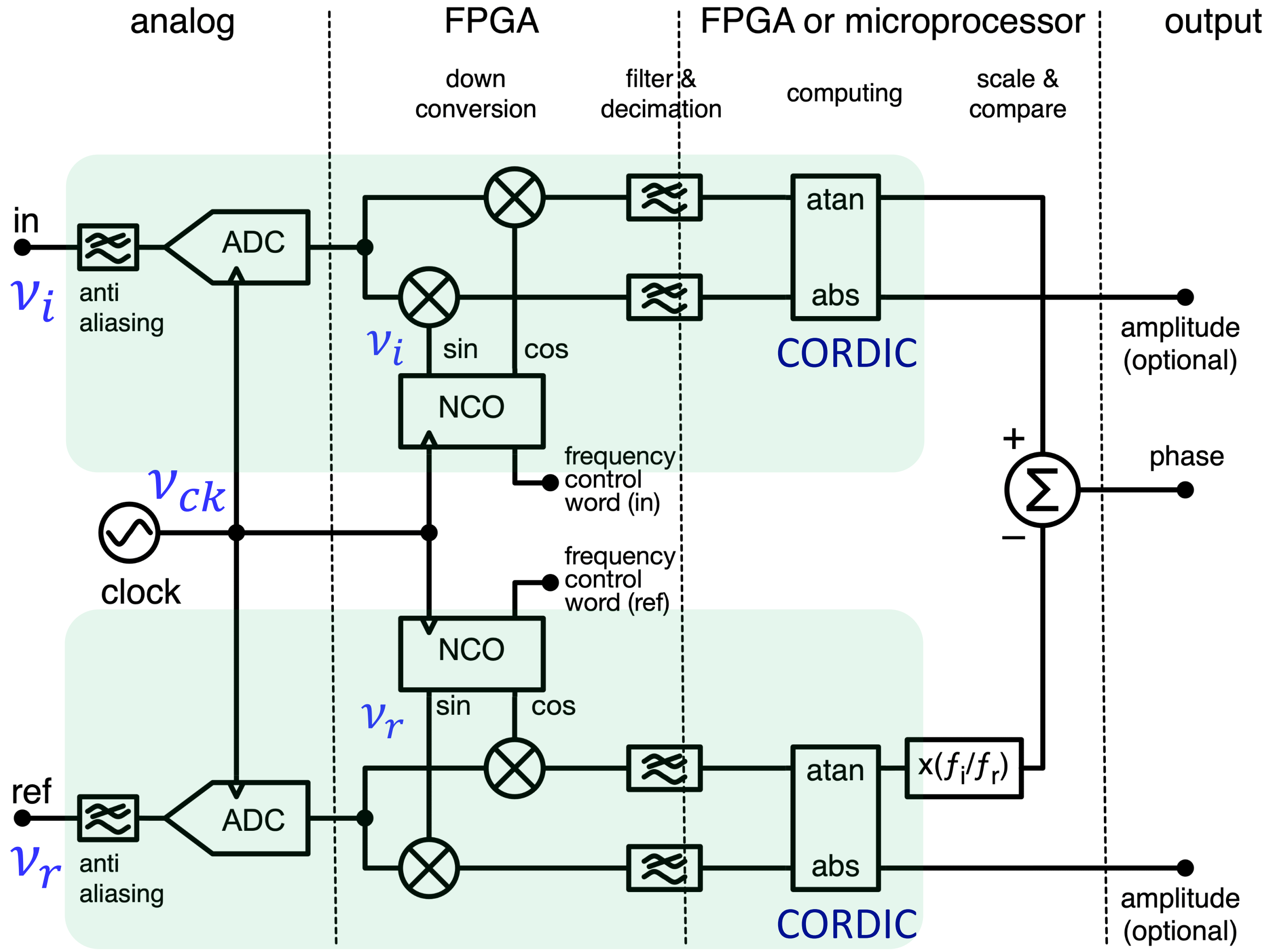

- Software Defined Radio methods
- Technology: ν_{ck} is not free
- The clock cannot be used as the reference
- Two channels are necessary, even if $\nu_i = \nu_r$
- ADCs have poor background noise

- Works with $\nu_i \neq \nu_r$ (interesting applications)
- No problem at large angles, even multiple turns

Figure from U. L. Rohde, E. Rubiola, J. C. Whithaker, *Microwave and Wireless Synthesizers*, ISBN 978-1-119-66600-4, ©J.Wiley 2021 (adapted)

Background noise – Example AD9467 (Alazartech)

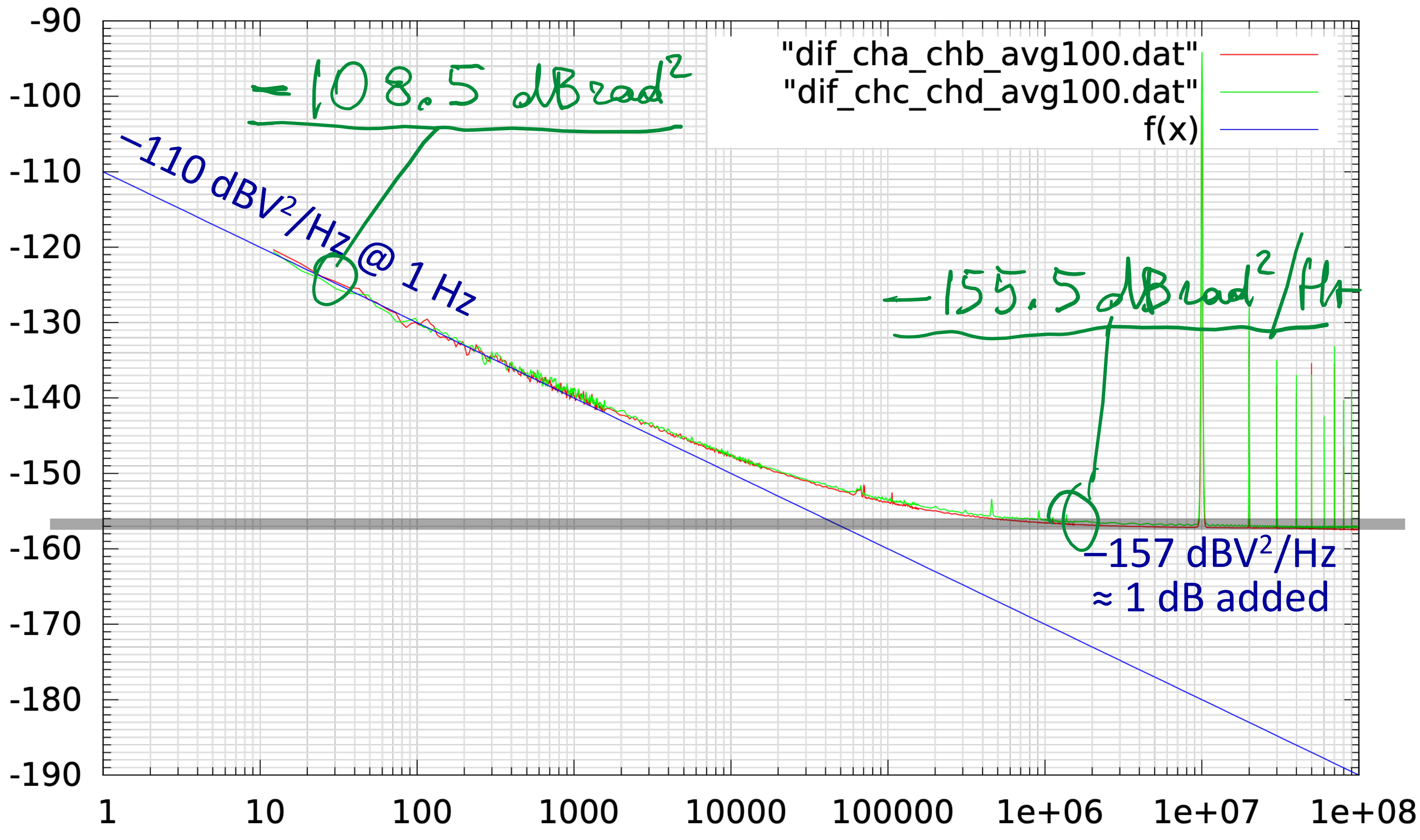

10 MHz, $V_{pp} \approx 0.95\ V_{FSR}$

$V_{FSR} = 2.5\ V_{pp}$
$= 0.88\ V_{rms}$

$0.95 V_{FSR} \rightarrow 0.84\ V_{rms}$
-1.5 dBV

The fully-digital noise analyzer

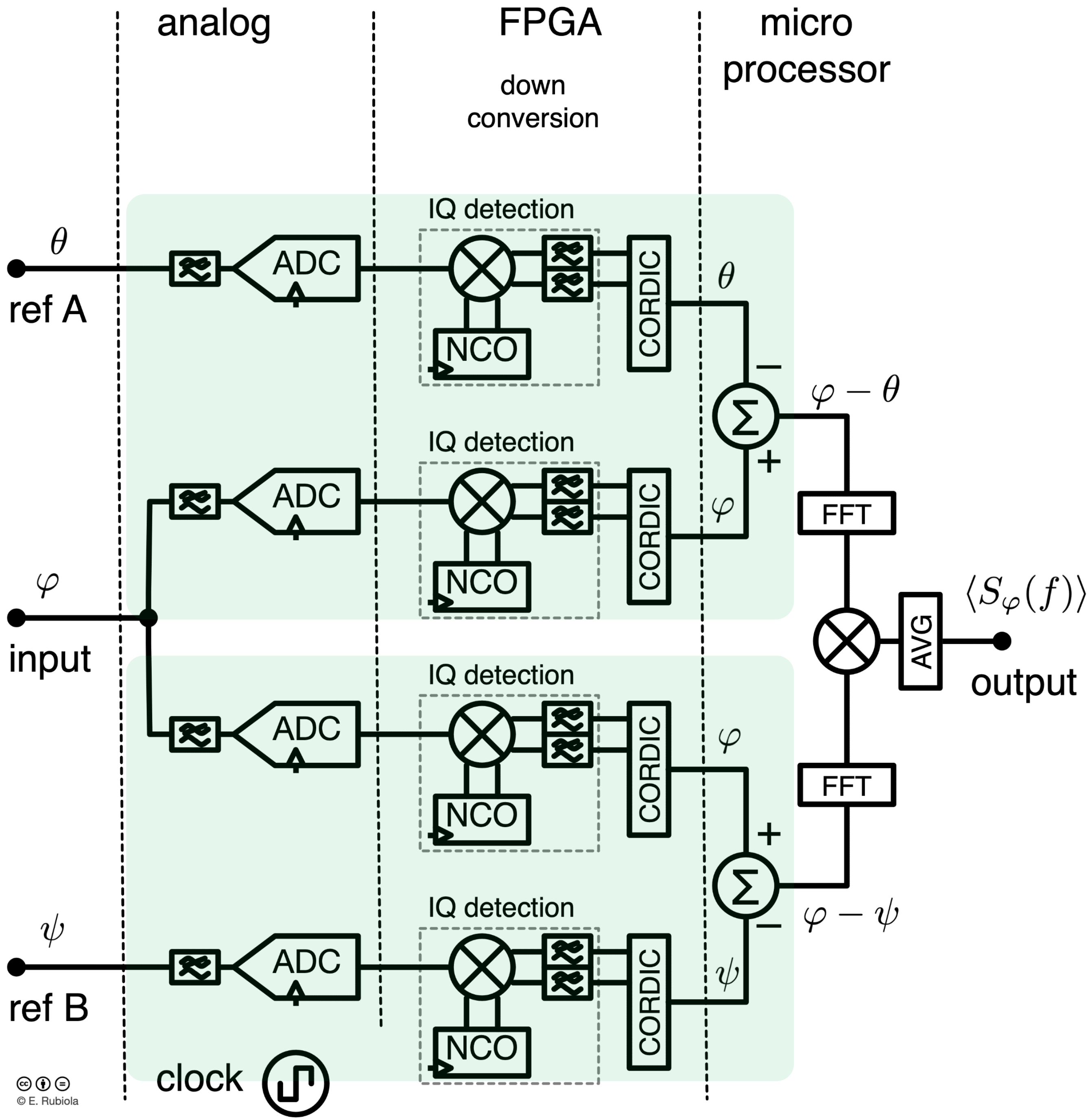

- 4 channels: DUT (2 ch.) and 1 or 2 external references
- Average cross spectrum –> rejection of the background
- 30-200 MHz max (order of)
- Related commercial instruments
  - Arcal / NoiseXT DNA
  - Microchip
    - PhaseStation 53100A (Miles Design & Jackson Labs)
    - 3120A (one ref input)
    - 5120A/5125A (discontinued)

Rohde & Schwarz FSWP8, FSWP26, FSWP50

Architecture

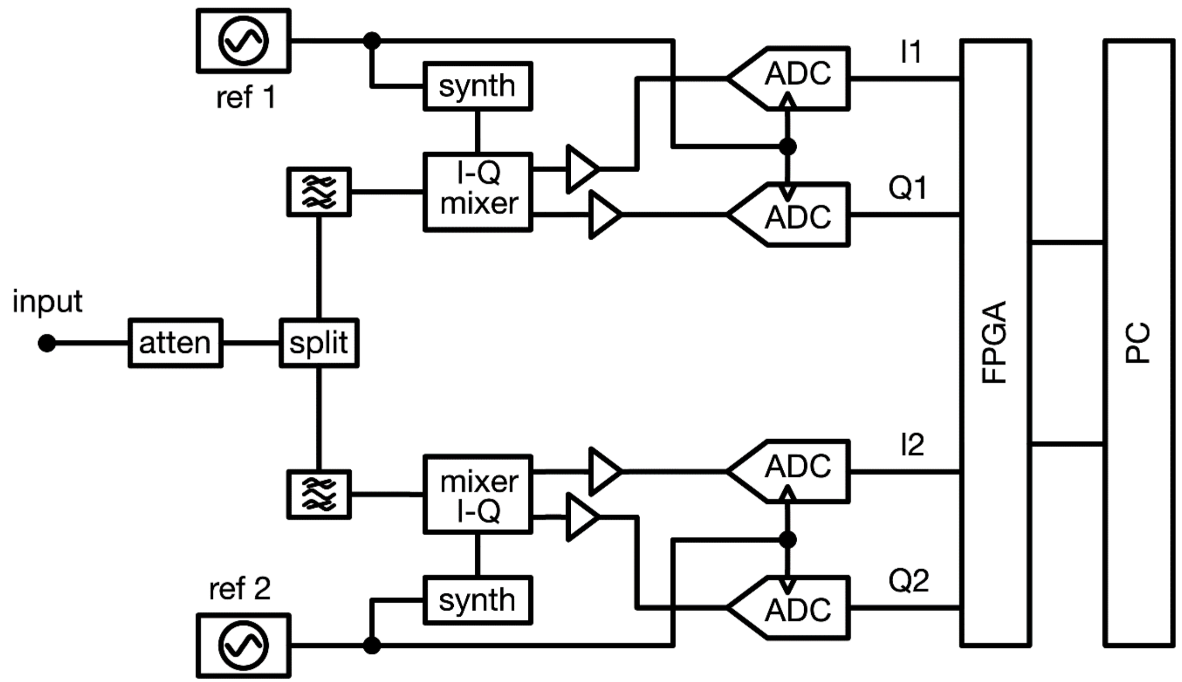

Background Noise at 100 MHz

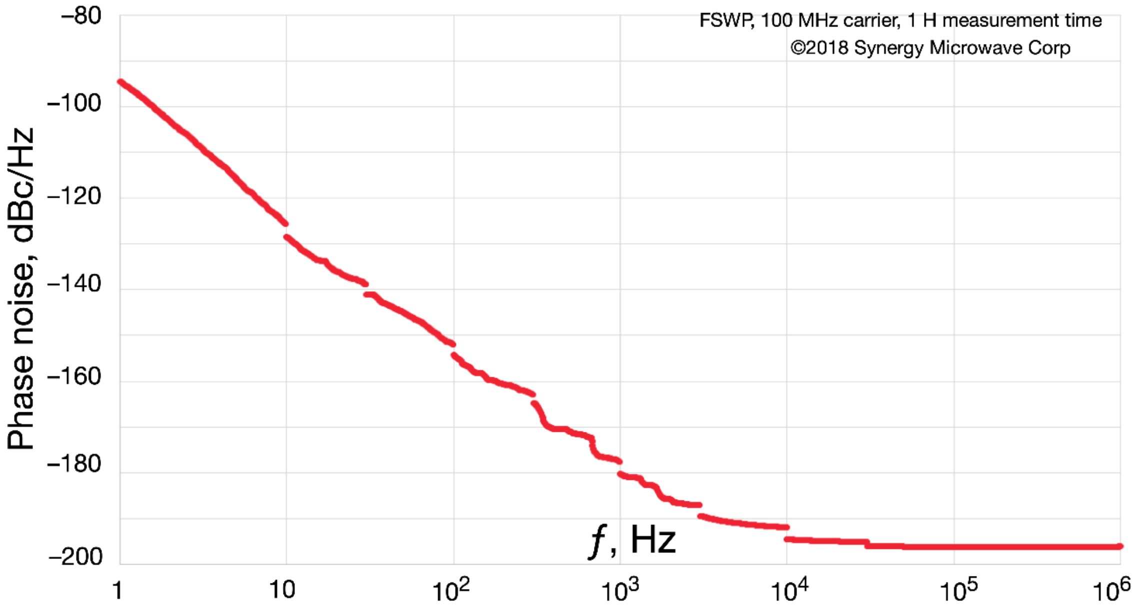

- 4 channels: DUT (2 ch.) and 2 internal references
- Average cross spectrum –> rejection of the background
- Down conversion from 8-50 GHz max to IF conversion
- Powerful, flexible, and expensive all-in-one instrument

Figures from U. L. Rohde, E. Rubiola, J. C. Whithaker, *Microwave and Wireless Synthesizers*, ISBN 978-1-119-66600-4, ©J.Wiley 2021 (adapted)

Noise rejection in logarithmic resolution

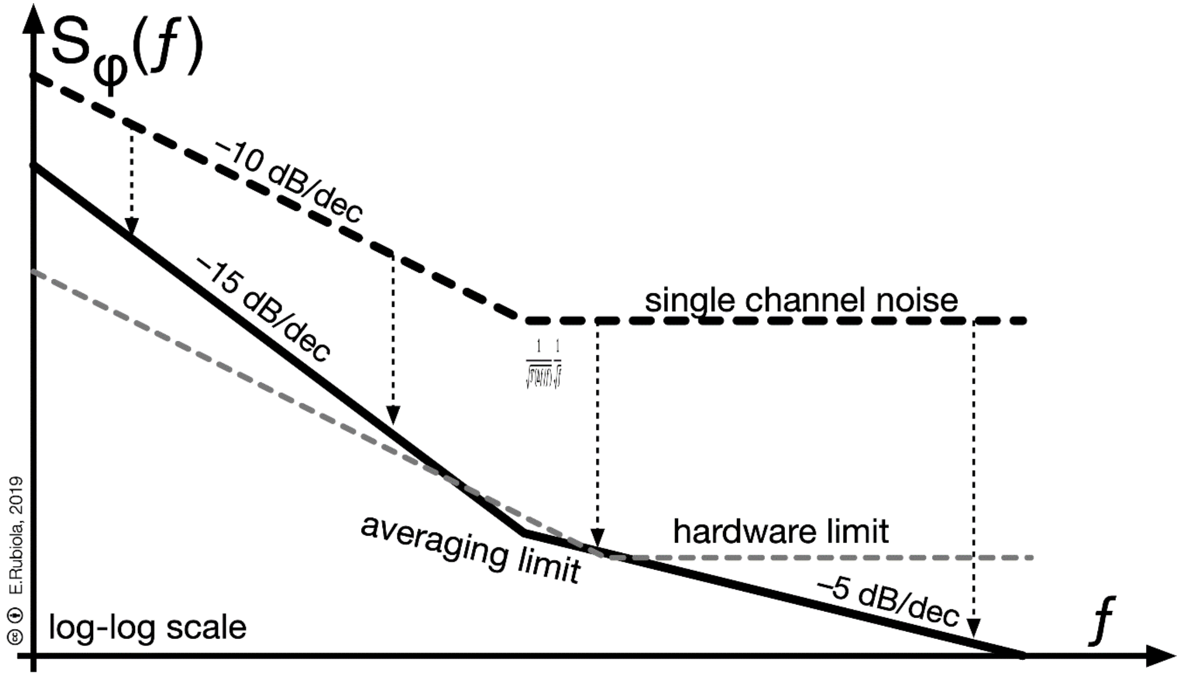

Additional hardware limit applies (input power splitter, AM leakage, crosstalk, etc.)

- Wider RBW (resolution) at higher f
  - Shorter acquisition time T
  - Larger m –> higher noise rejection
- Constant fractional resolution $\mathcal{R} = \Delta f / f$
- μ bins/decade –> resolution
  $$\mathcal{R} = e^{\ln(10)/\mu} - 1$$
- One FFT, time $T = 1/\Delta f = 1/\mathcal{R}f$
- Measurement time $\mathcal{T}$
  $$m = \mathcal{T}/T = \mathcal{T}\mathcal{R}f$$
- Avg limit $S_{\varphi\ BG} = S_{\varphi\ 1ch}/\sqrt{m}$
- Result

$$S_{\varphi\ BG}(f) = \frac{1}{\sqrt{\mathcal{T}\mathcal{R}f}} S_{\varphi\ 1ch}(f)$$

Example – Background of the PhaseStation 53100A

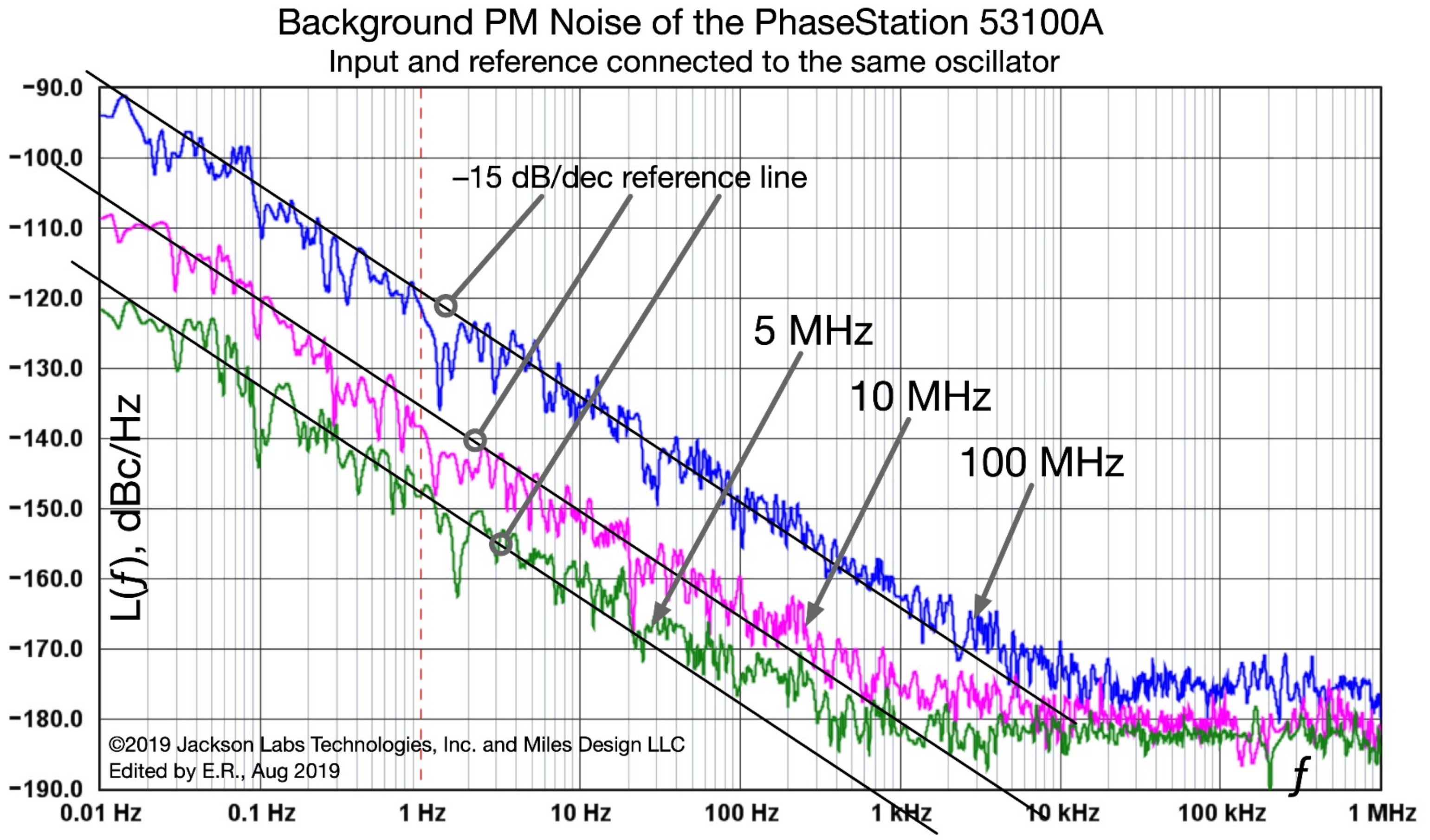

Trace	Input Freq	Input Amplitude	dBc/Hz at 1 Hz	Elapsed	Instrument
100 MHz residual floor	100.0 MHz	11 dBm	−121.1	58m 49s	PhaseStation 53100A
10 MHz residual floor	10.0 MHz	12 dBm	−138.2	33m 5s	PhaseStation 53100A
5 MHz residual floor	5.0 MHz	12 dBm	−148.2	8h	PhaseStation 53100A

- Same oscillator connected to the 4 channels
- Constant $\mathcal{R}$ approximated as bands where $\Delta f = C$
- Flicker –> $1/f\sqrt{f}$, as predicted
- White limited by other phenomena

Figure: Courtesy of John Miles, Miles Design, comments are mine

Limitations of the Cross Spectrum Methods

Anti-correlated noise in power splitters

(Thermometry and Radiometry)

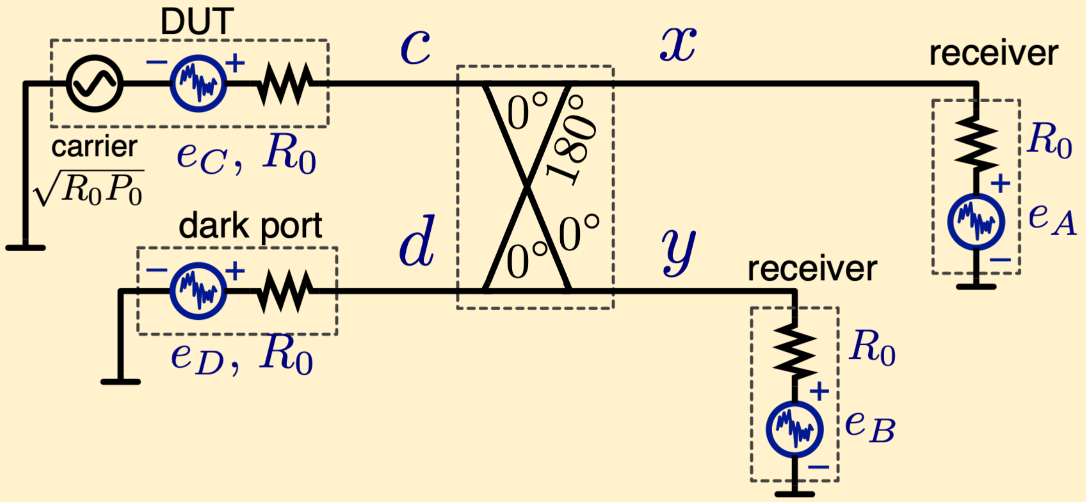

$$x = \frac{1}{2\sqrt{2}}(e_C - e_D) + \tfrac{1}{2}e_A$$

$$y = \frac{1}{2\sqrt{2}}(e_C + e_D) + \tfrac{1}{2}e_B$$

'e' = thermal emf, $\sqrt{4kTR}$

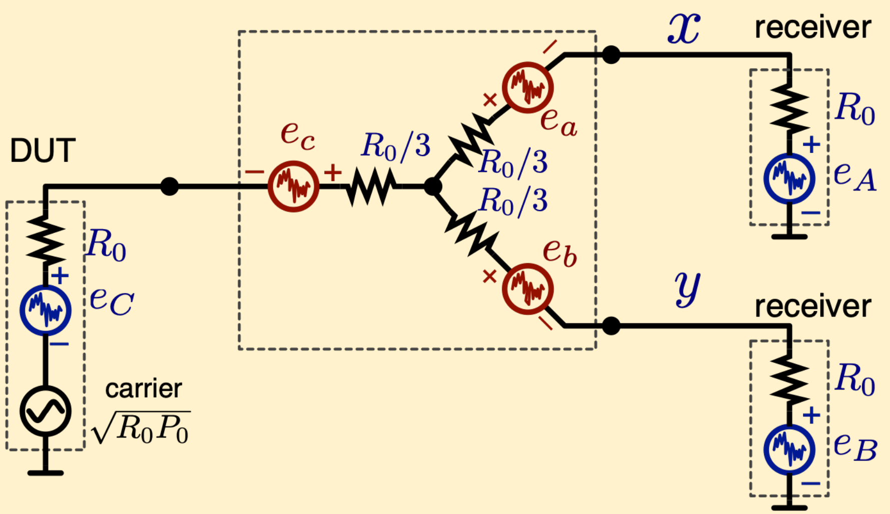

$$x = \tfrac{1}{2}e_A + \tfrac{1}{4}e_B + \tfrac{1}{4}e_C - \tfrac{1}{2}e_a + \tfrac{1}{4}e_b + \tfrac{1}{4}e_c$$

$$y = \tfrac{1}{4}e_A + \tfrac{1}{2}e_B + \tfrac{1}{4}e_C + \tfrac{1}{4}e_a - \tfrac{1}{2}e_b + \tfrac{1}{4}e_c$$

'e' = thermal emf, $\sqrt{4kT/R}$

Anti-correlated noise in power splitters

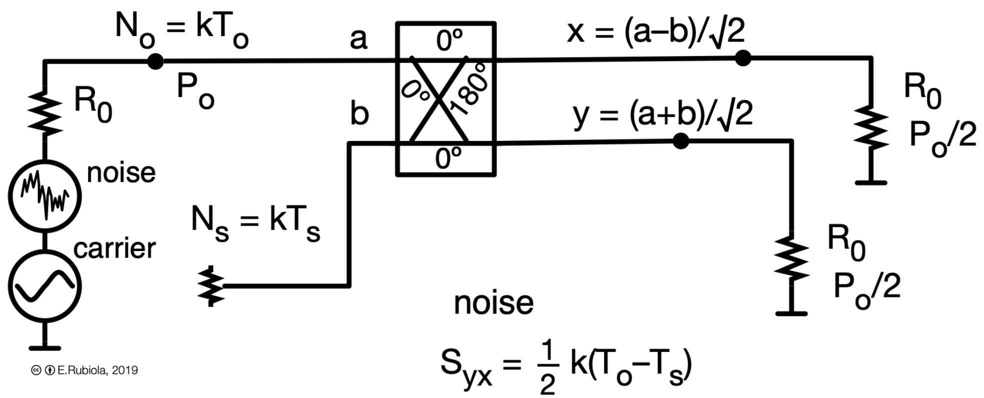

Most instruments

$S_{\varphi\varphi} = k(T_o - T_s) / P_o$

Keysight E5052B

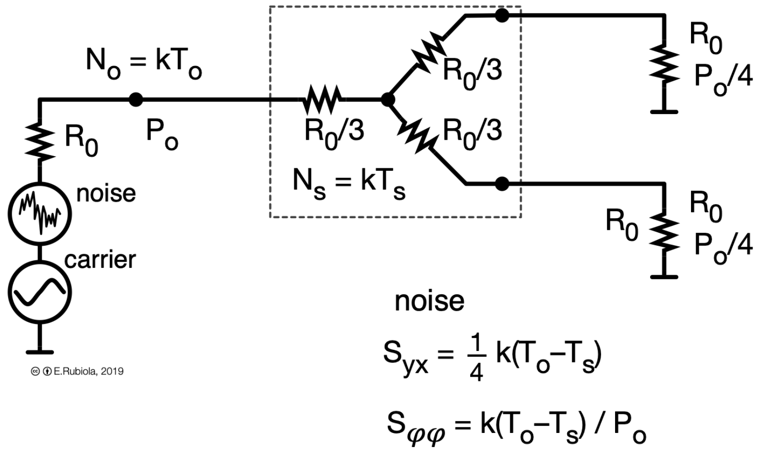

Fig.2 top/bottom, Y. Gruson et al, Metrologia,
27 April 2020, DOI 10.1088/1681-7575/ab8d7b

3 dB (loss-free) power splitter

- Power $P_{out} = P_{osc}/2$
- Correlated noise $-k(T_{osc} - T_{split})/2$

6 dB (resistive) power splitter

- Power $P_{out} = P_{osc}/4$
- Correlated noise $-k(T_{osc} - T_{split})/4$

Displayed noise

$$S_\varphi = \frac{k(T_{osc} - T_{split})}{P_{osc}}$$

Systematic error $\Delta S_\varphi = -kT_{split}/P_{osc} < 0$

A problem with the $|S_{yx}|$ estimator

Most instruments use the estimator

$$S_\varphi(f) = |S_{yx}(f)|$$

- Biased
- Slow, because of noise in $\Im\{S_{yx}(f)\}$
- May hide the anticorrelated artifacts

The best estimator is

$$\widehat{S_\varphi(f)} = \Re\{S_{yx}(f)\}$$

- Fastest
- Unbiased
- Does not hide the anticorrelated artifacts

A weird example

FSWP hacked by A. Roth at the Rohde & Schwarz Research and Development Center in Munich, DE

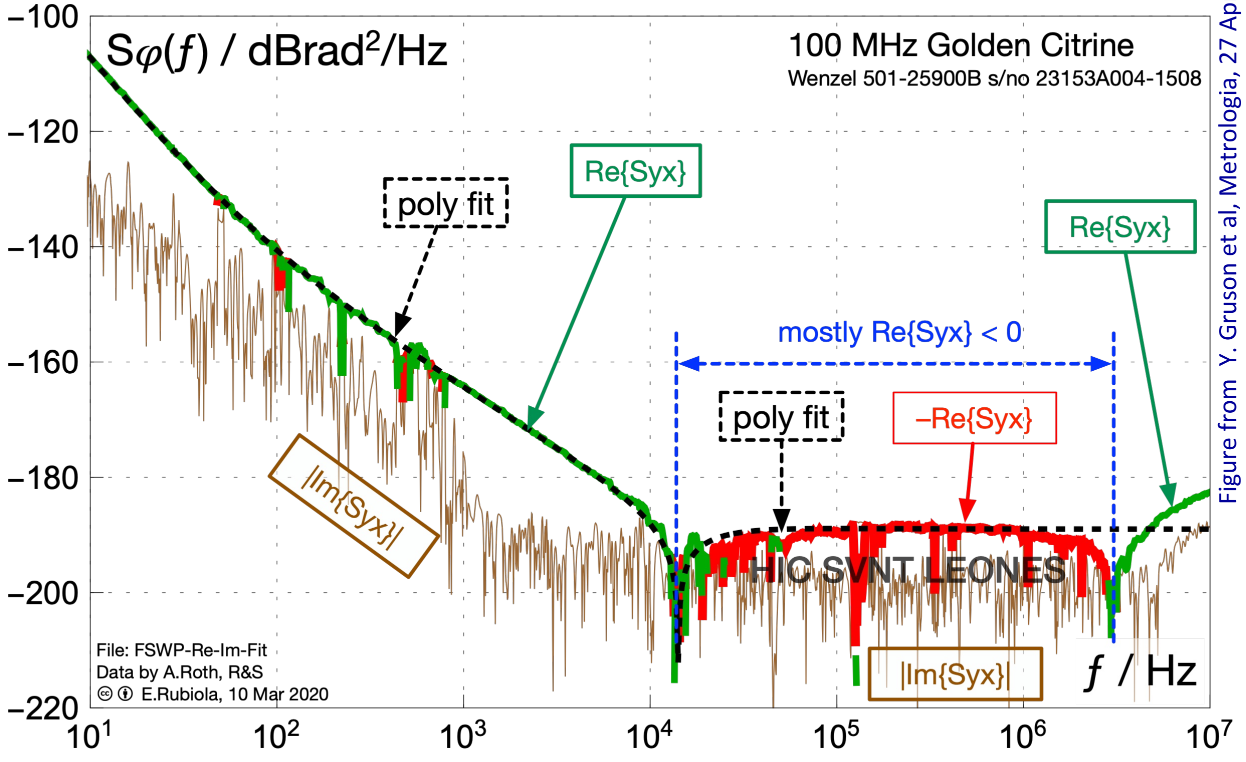

Figure from Y. Gruson et al, Metrologia, 27 April 2020

Read the full article: Y. Gruson et al, Metrologia, 27 April 2020, DOI 10.1088/1681-7575/ab8d7b

The DUT AM noise is correlated

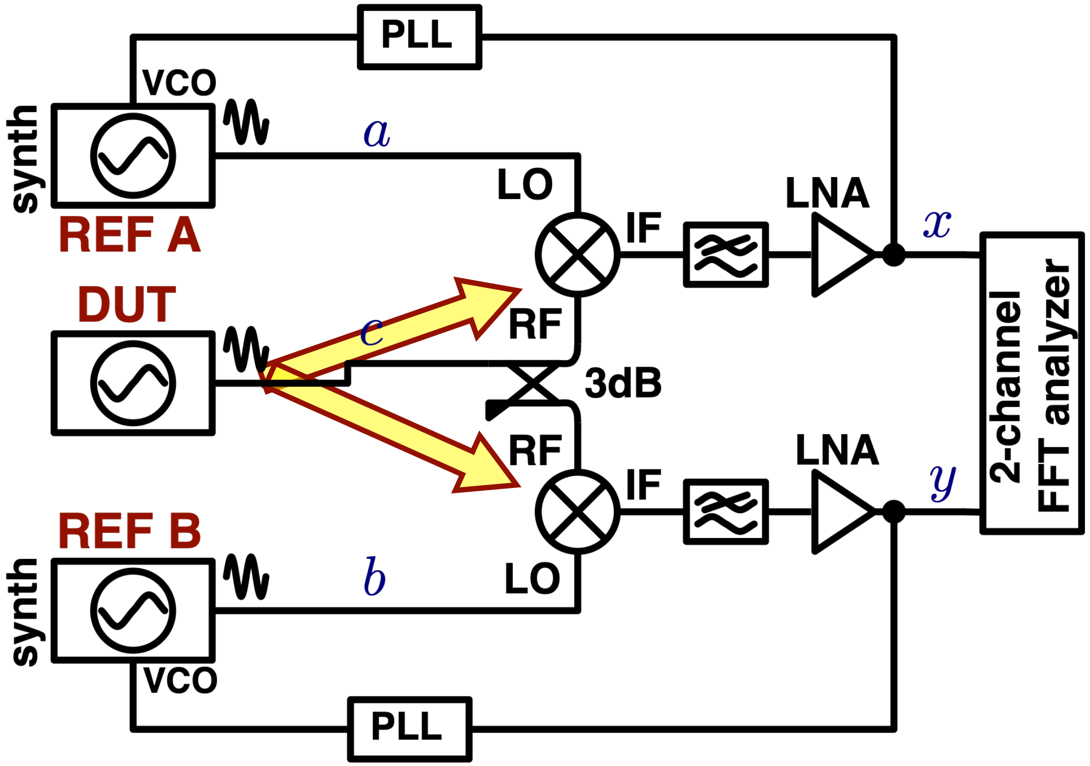

The mixer offset depends on P

$$\Delta P \rightarrow \Delta V_{OS}$$

At the IF output, there is no difference between AM and PM

$$S_\alpha(f) \rightarrow S_v(f)$$

- Unpredictable amount and sign of the correlated term
- Mitigation
  - Saturated amplifiers at the RF inputs
  - But AM/PM conversion in the ampli

E. Rubiola, R. Boudot, IEEE Transact. UFFC 54(5) pp.926-932, May 2007

Common artifacts

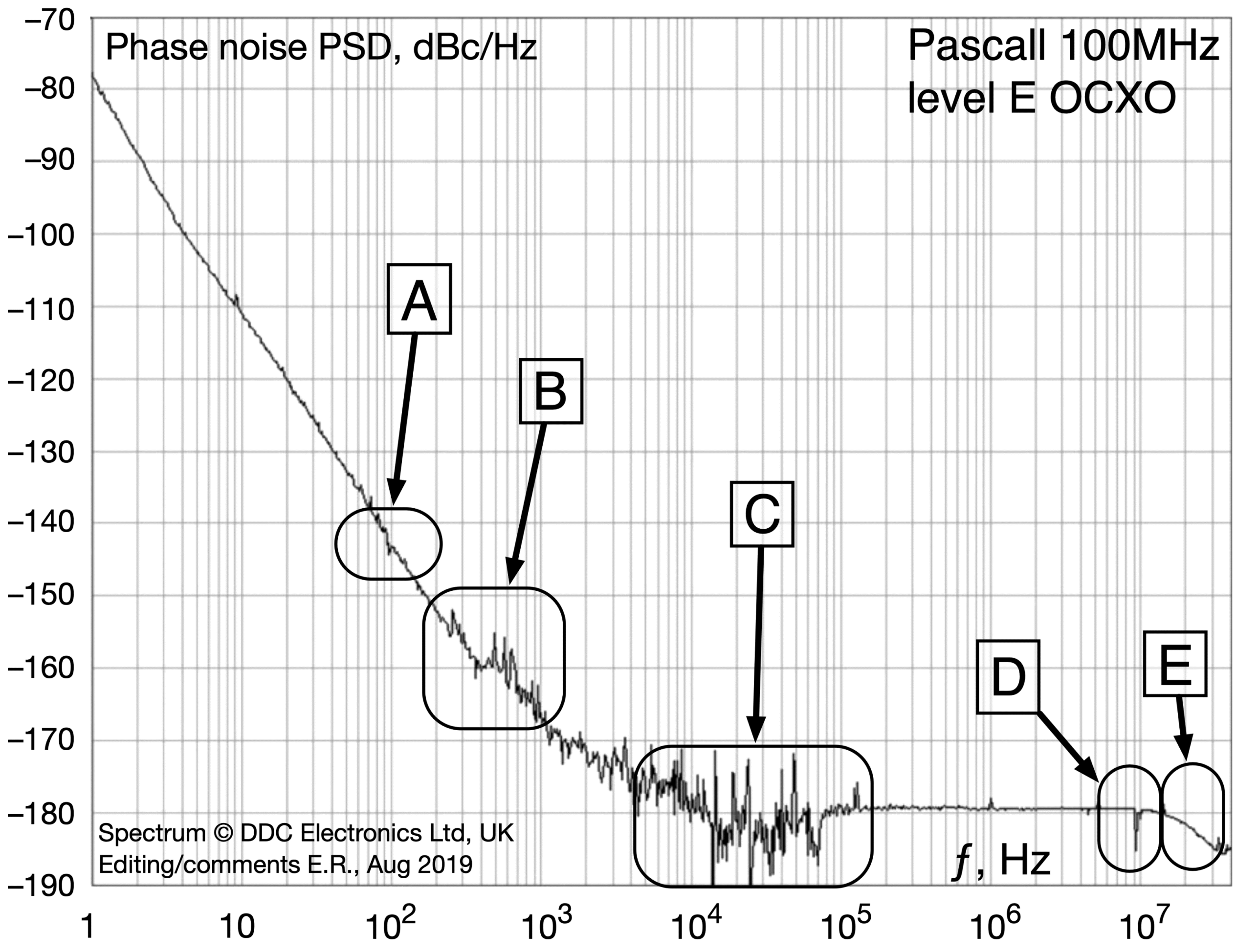

Figure from U. L. Rohde, E. Rubiola, J. C. Whithaker, *Microwave and Wireless Synthesizers*, ISBN 978-1-119-66600-4, ©J.Wiley 2021 (adapted)

My best guesses

A. Discontinuity.
A change in sampling frequency

B. Bump, irregular/noisy plot.
- Spectral leakage
- Correlated effect
- Insufficient averaging

C. Hole, irregular/noisy plot.
- An anti-correlated effect.
- Signature is often seen in the Keysight E5052B

D. Notch. Almost certainly, an anti-correlated spur

E. Filter roll-off (not disturbing)

The 50 Hz and (odd) multiples spurs are not seen. Likely, they are just below the oscillator noise

Too good spectra found online

120 MHz OCXO
P_{out} = 13 dBm
It is unclear if the sample has higher power

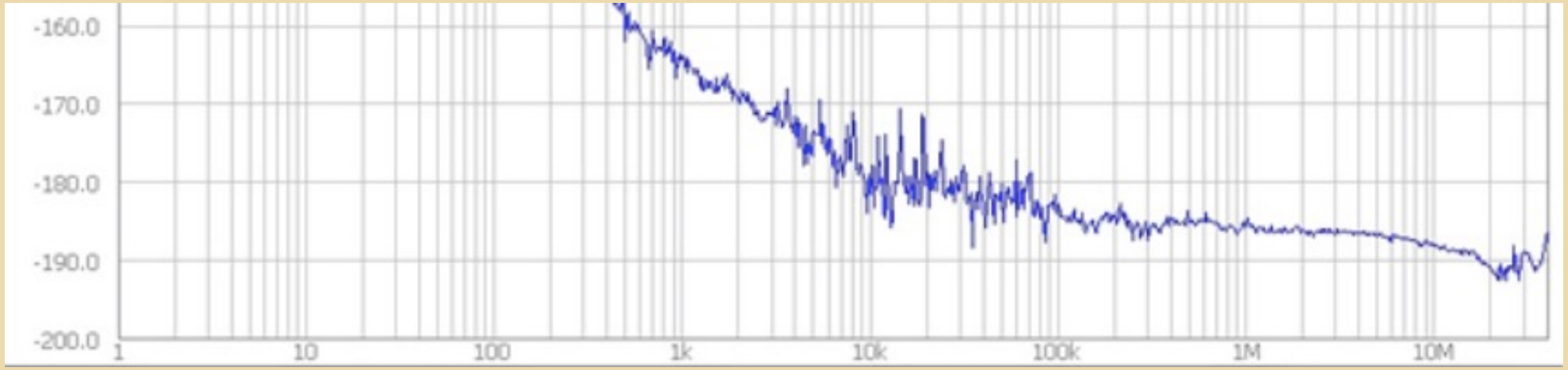

This is an excerpt of a figure, I don't remember where it comes from, apologize

$$S_\varphi(f) = \mathsf{b}_0 = \frac{kT}{P}$$

$$T = \frac{P}{k}\mathsf{b}_0$$

–183 dBrad2/Hz & 20 mW —> T ≈ 725 K
equivalent temperature at the oscillator output
Too low to be correct

Evidence at other frequencies and measurements

Artifacts

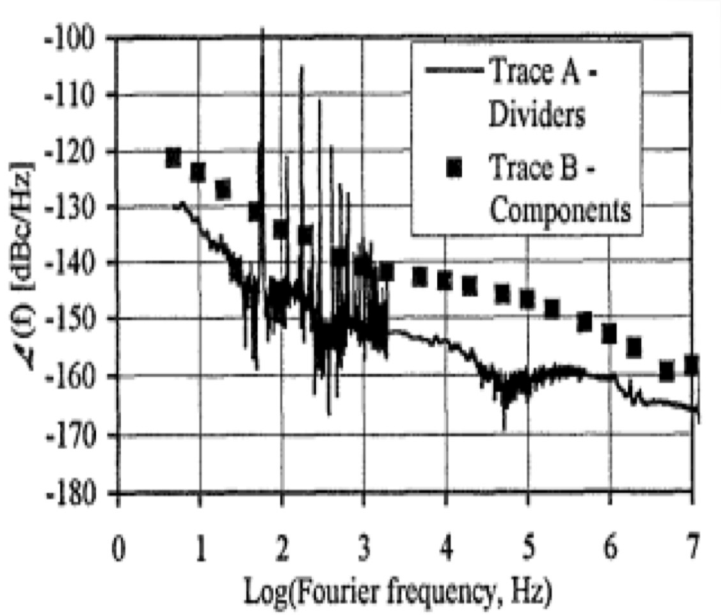

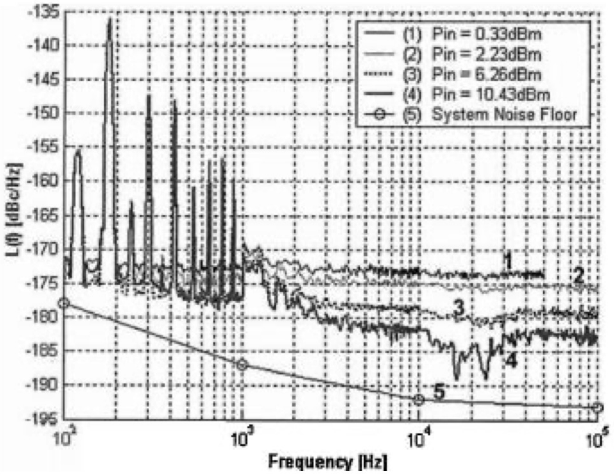

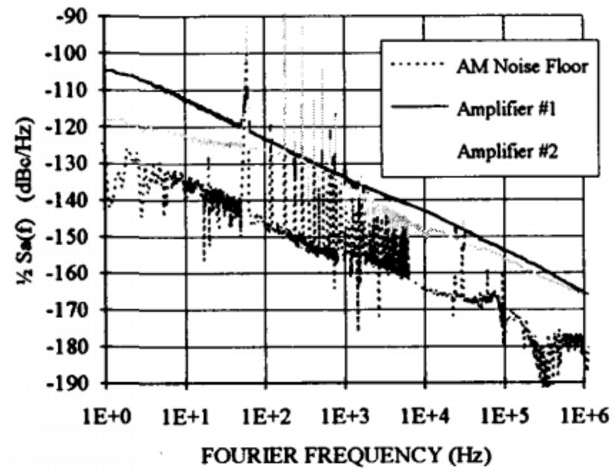

NIST

Courtesy of Craig W. Nelson, NIST

Measurement Results

Phase noise plot on SSA#1

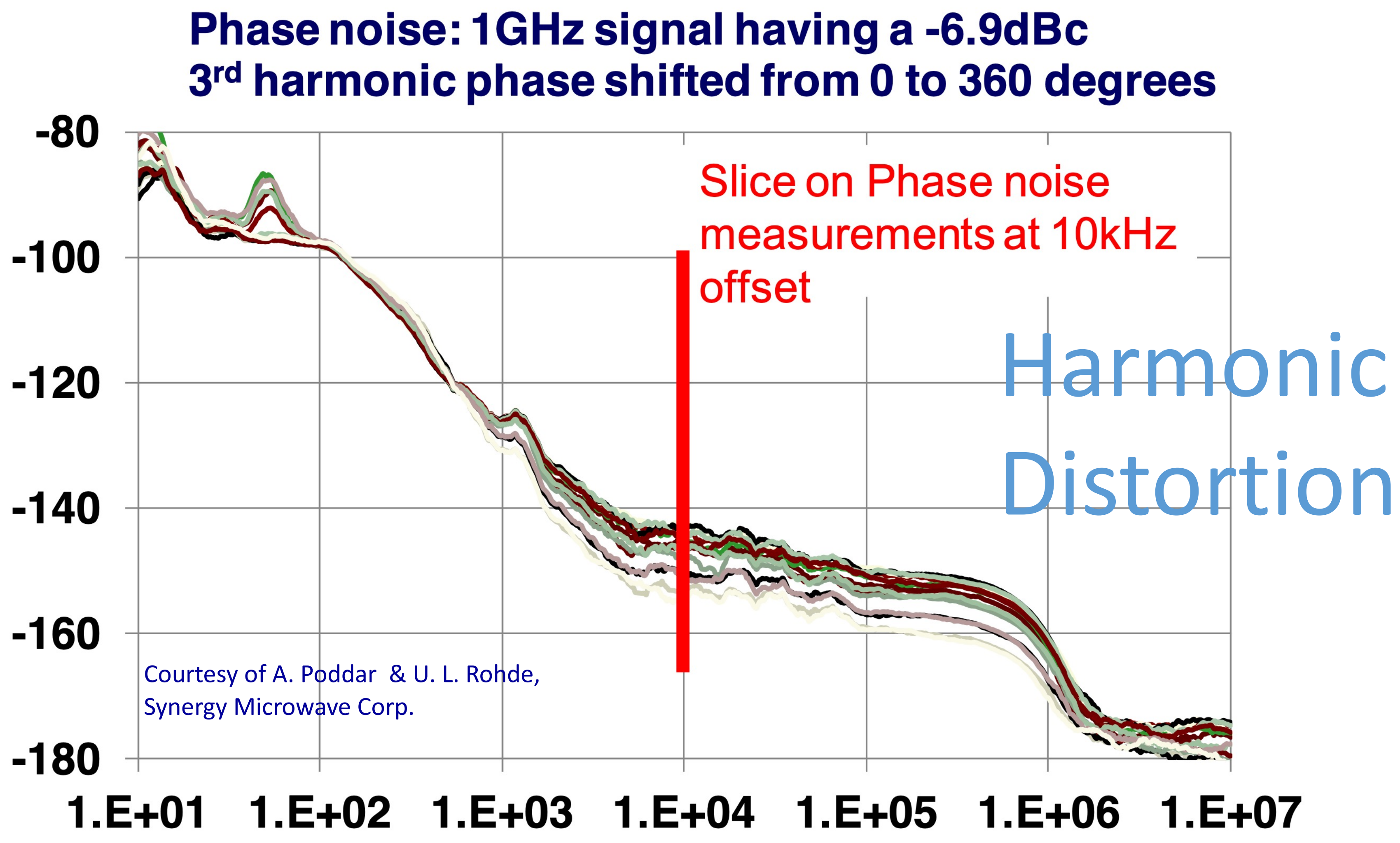

Summary — NIST scheme

- Problems arise when the DUT noise is really low
- Some are understood, others not

- Power splitter temperature —> systematic error
- AM noise —> unpredictable positive/negative error
- Distortion and impedance matching
- ………

Hot (applied) research topic

Calibration – Measurement of of k_φ

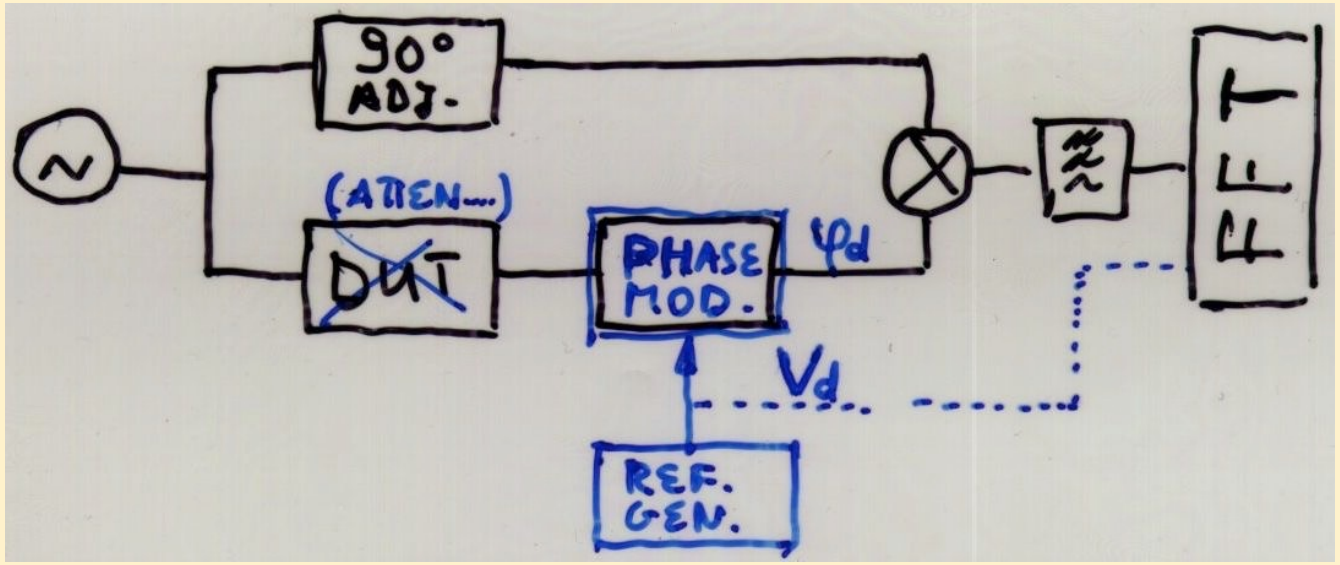

The reference signal can be:

a) a tone:

detect with the FFT,
with a dual-channel FFT, or
with a lock-in

b) random or pseudo random white noise

tone:

$$k_\varphi = \frac{V_m}{k_m V_d}$$

white noise

$$k_\varphi^2 = \frac{S_{Vm}}{k_m^2 S_{Vd}}$$

Some FFTs have a white noise output
Dual-channel FFTs calculate the transfer function $|H(f)|^2 = S_{Vm}/S_{Vd}$

Correlation measurements

Two separate mixers
measure the same DUT.
Only the DUT noise is common

a(t), b(t) –> mixer noise
c(t) –> DUT noise

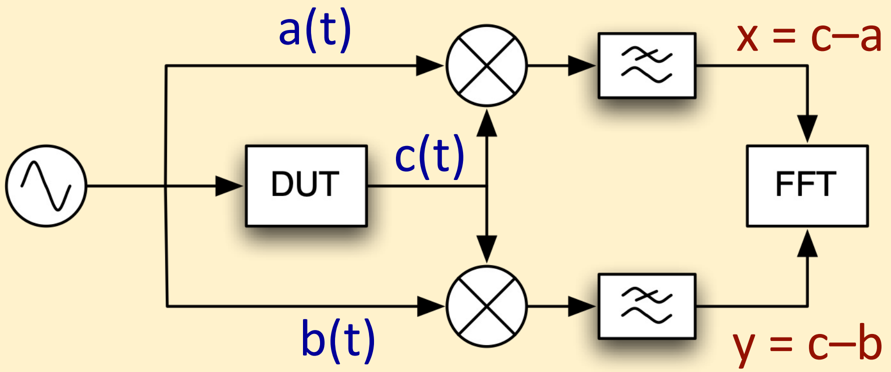

basics of correlation

$$
\begin{aligned}
S_{yx}(f) &= \mathbb{E}\left\{Y(f)X^*(f)\right\} \\
&= \mathbb{E}\left\{(C-A)(C-B)^*\right\} \\
&= \mathbb{E}\left\{CC^* - AC^* - CB^* + AB^*\right\} \\
&= \mathbb{E}\left\{CC^*\right\}
\end{aligned}
$$

0 0 0

$$S_{yx}(f) = S_{cc}(f)$$

in practice, average on m realizations

$$
\begin{aligned}
S_{yx}(f) &= \langle Y(f)X^*(f)\rangle_m \\
&= \langle CC^* - AC^* - CB^* + AB^*\rangle_m \\
&= \langle CC^*\rangle_m + O(1/m)
\end{aligned}
$$

0 as 1/√m

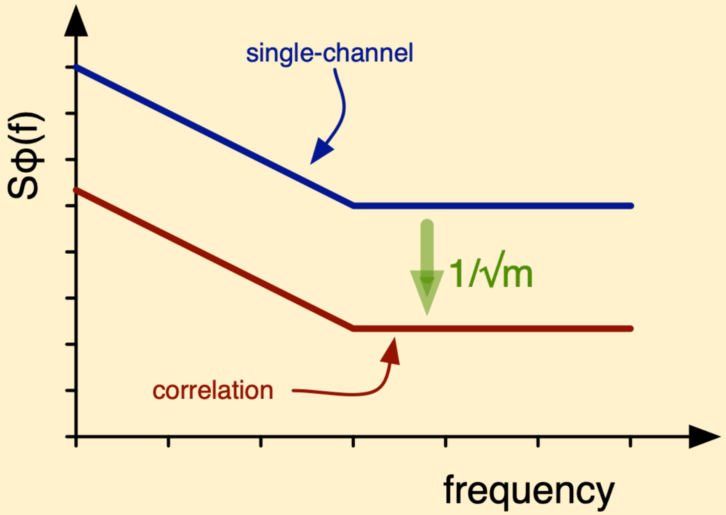

Bridge Techniques

Wheatstone bridge

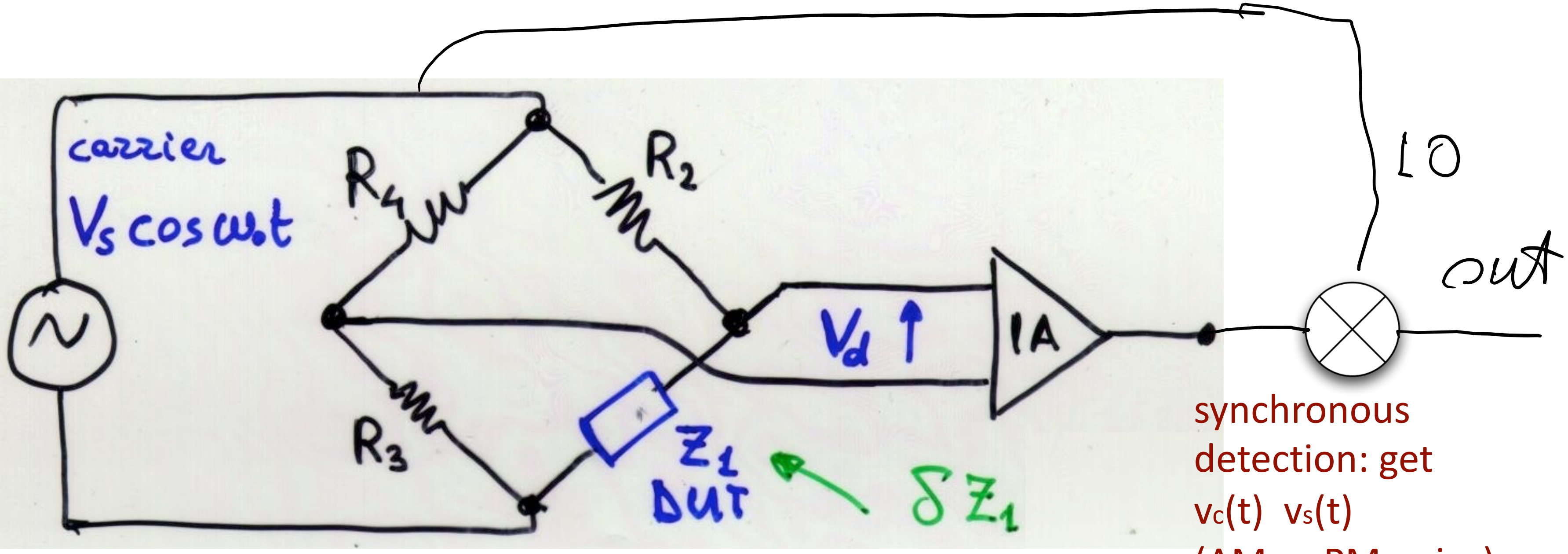

synchronous detection: get $v_c(t)$ $v_s(t)$ (AM or PM noise)

equilibrium: $V_d = 0$ –> carrier suppression

static error δZ_1 –> some residual carrier

real δZ_1 => in-phase residual carrier $V_{re} \cos(\omega_0 t)$

imaginary δZ_1 => quadrature residual carrier $V_{im} \sin(\omega_0 t)$

fluctuating error δZ_1 => noise sidebands

real δZ_1 => AM noise $v_c(t) \cos(\omega_0 t)$

imaginary δZ_1 => PM noise $-v_s(t) \sin(\omega_0 t)$

Bridge AM-PM noise measurement

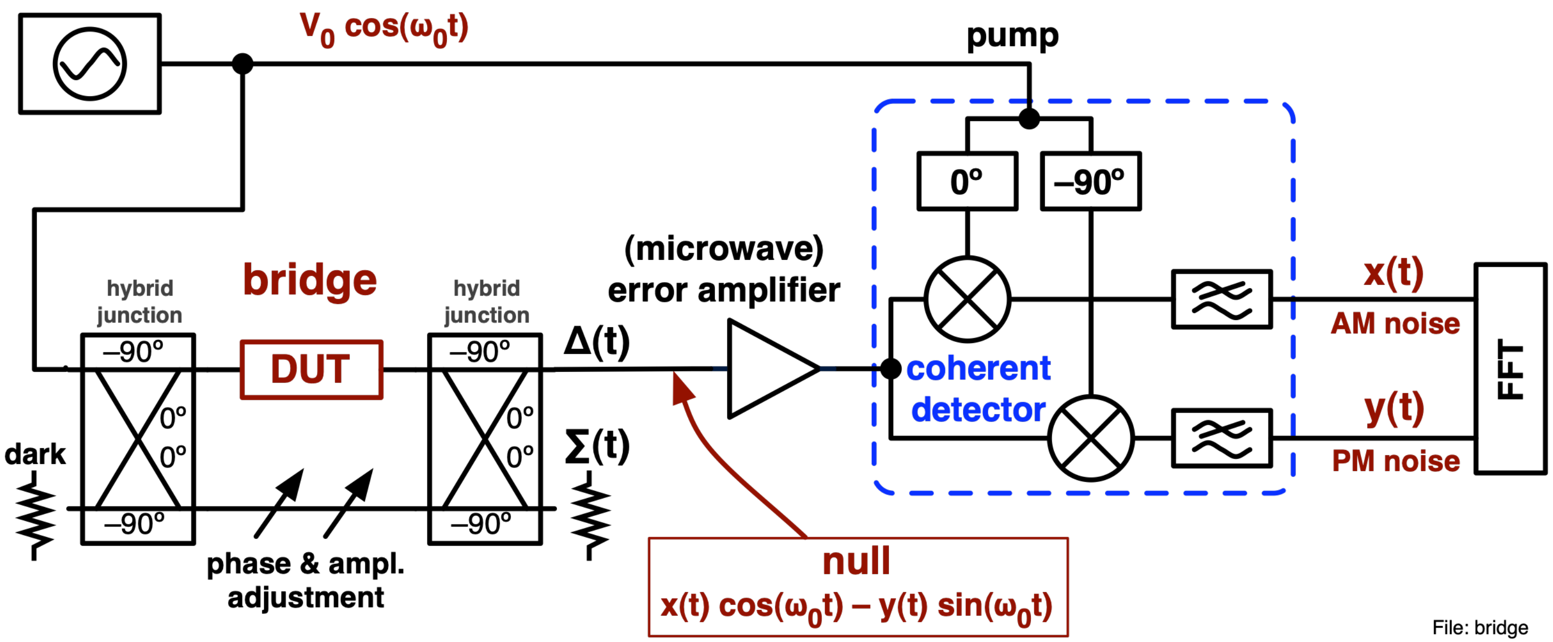

- Bridge => high rejection of the master-oscillator noise
- Amplification and synchronous detection of the noise sidebands
- No carrier => the amplifier can't flicker (no up-conversion of near-dc 1/f)
- High microwave gain before detection => low background
- Low 50-60 Hz residuals because microwave circuits are insensitive to magnetic fields

Bridge – Early ideas

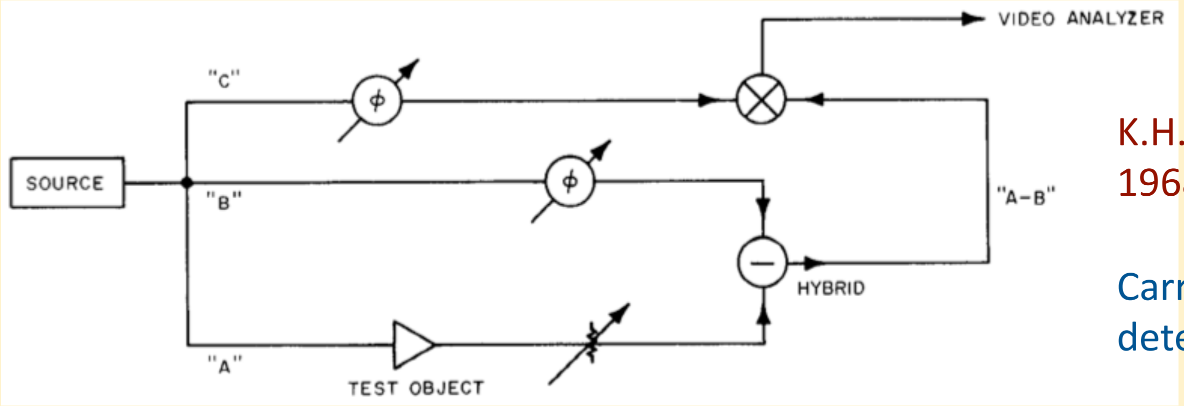

K.H.Sann, IEEE MTT 16(9) p.761-766, sep 1968

Carrier suppression and synchronous detection of the noise sidebands

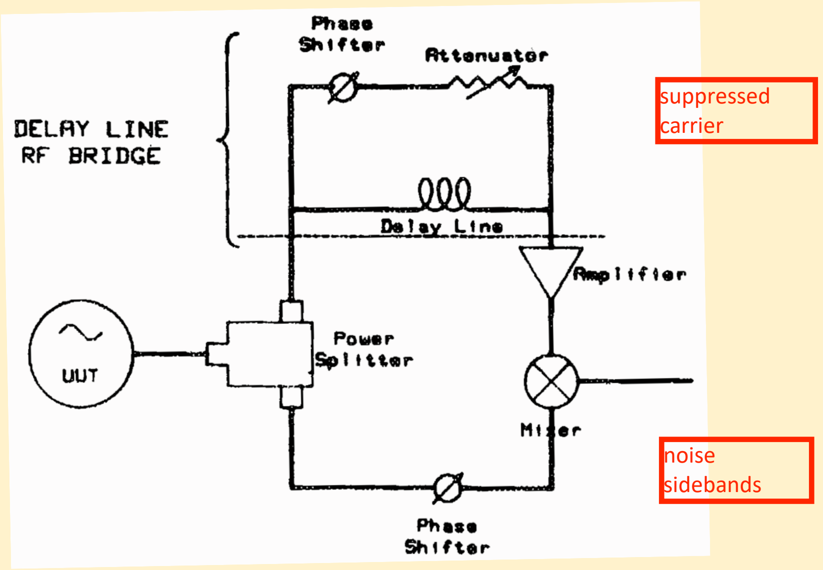

A.L. Lance & al., ISA Transact. 2(4) p.37-84 apr 1982
F. Labaar, Microwaves 21(3) p.65-69, mar 1982

Carrier suppression and amplification of the noise sidebands before synchronous detection

Bridge AM-PM noise measurement

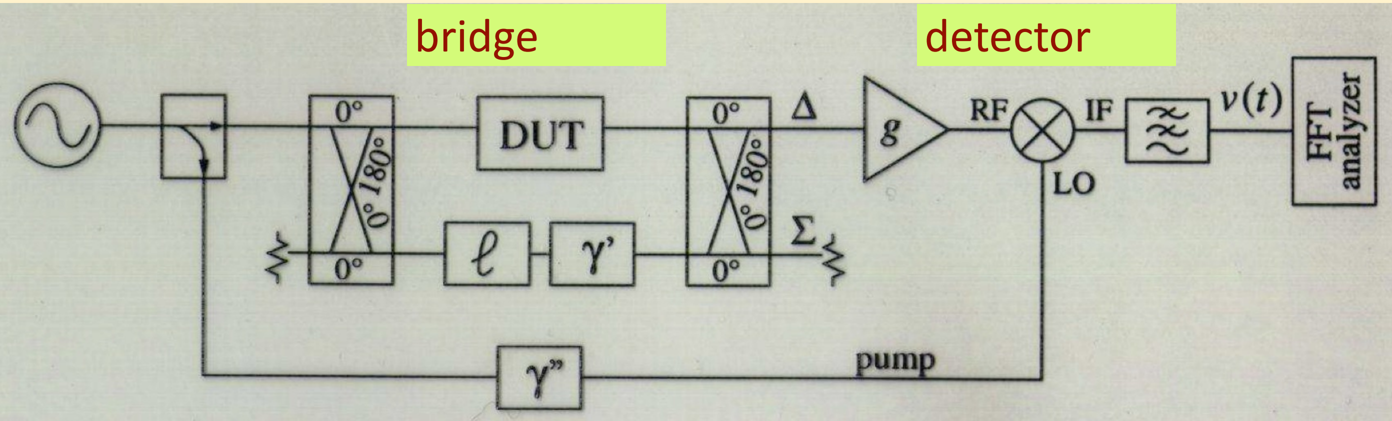

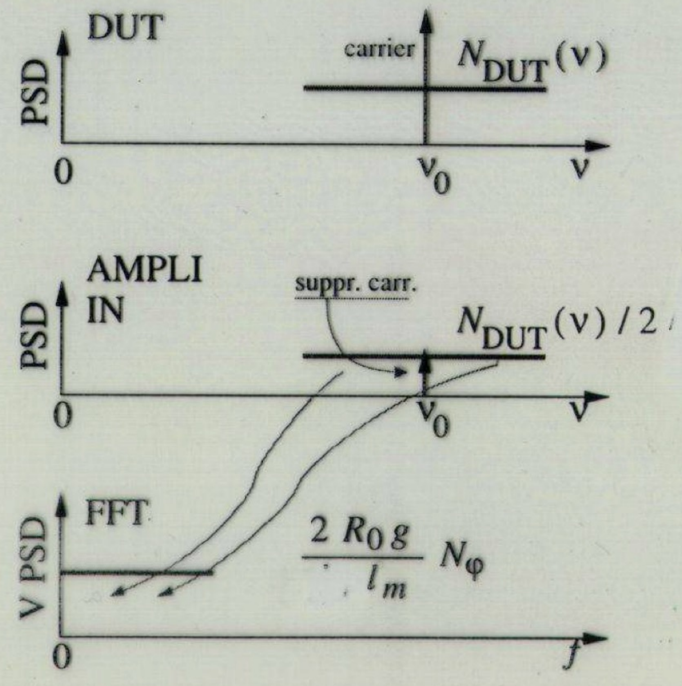

High carrier suppression:

no carrier ⇒ the amplifier can't flicker

High gain:

$$k_\varphi = \frac{v(t)}{\varphi(t)} = \sqrt{\frac{R_0 g P_0}{l_m}} - \text{dissip. losses}$$

Low Noise Floor:

$$S_{\varphi 0} = \frac{2F k_B T_0}{P_0} + \text{dissip. losses}$$

High immunity to 50 Hz B fields

Improved, from RSI **70** 1 pp. 220-225, Jan 1999

and rejection of the master-oscillator noise

yet, difficult for the measurement of oscillators

Build on a commercial instrument

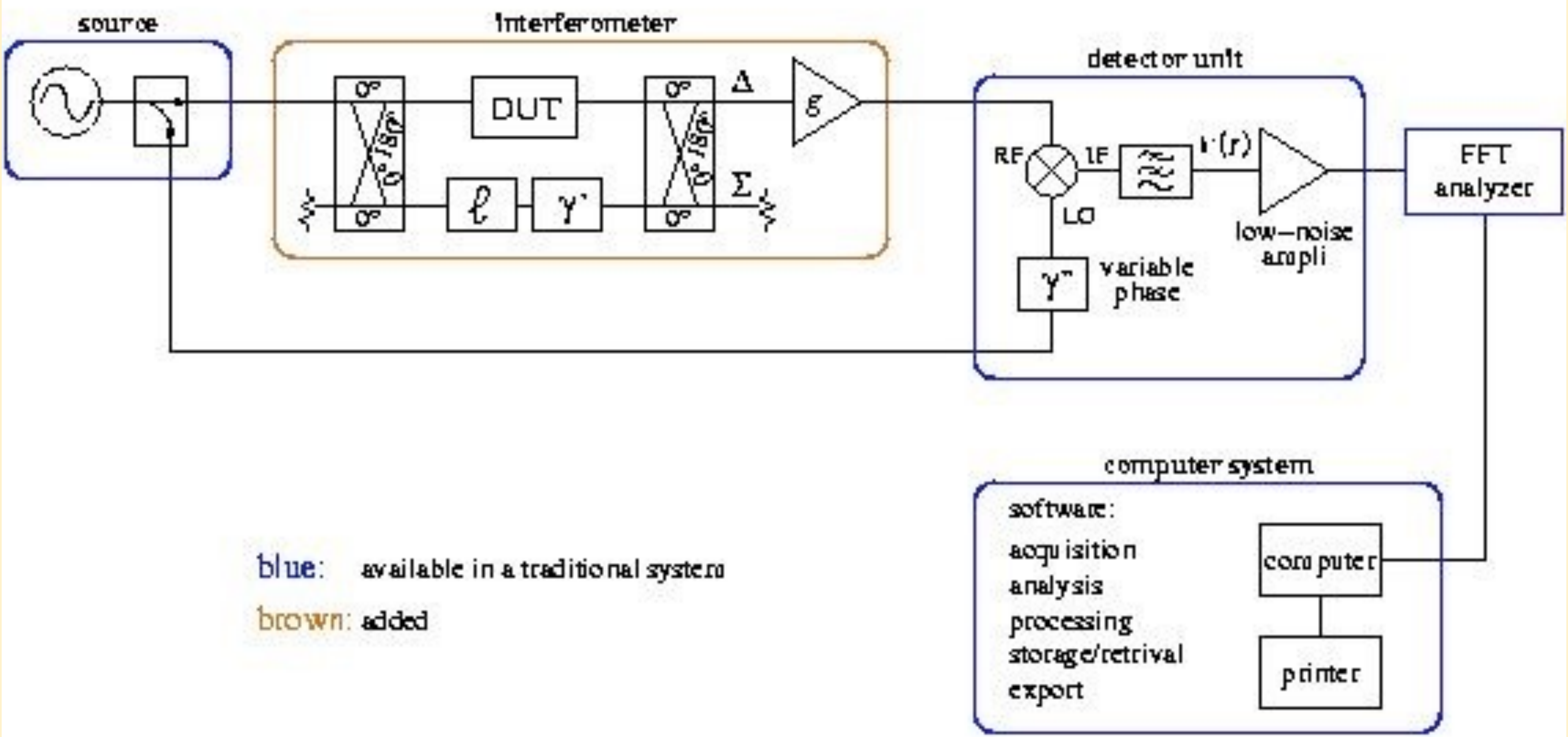

You will appreciate the computer interface and the software ready for use

Origin of flicker in the bridge

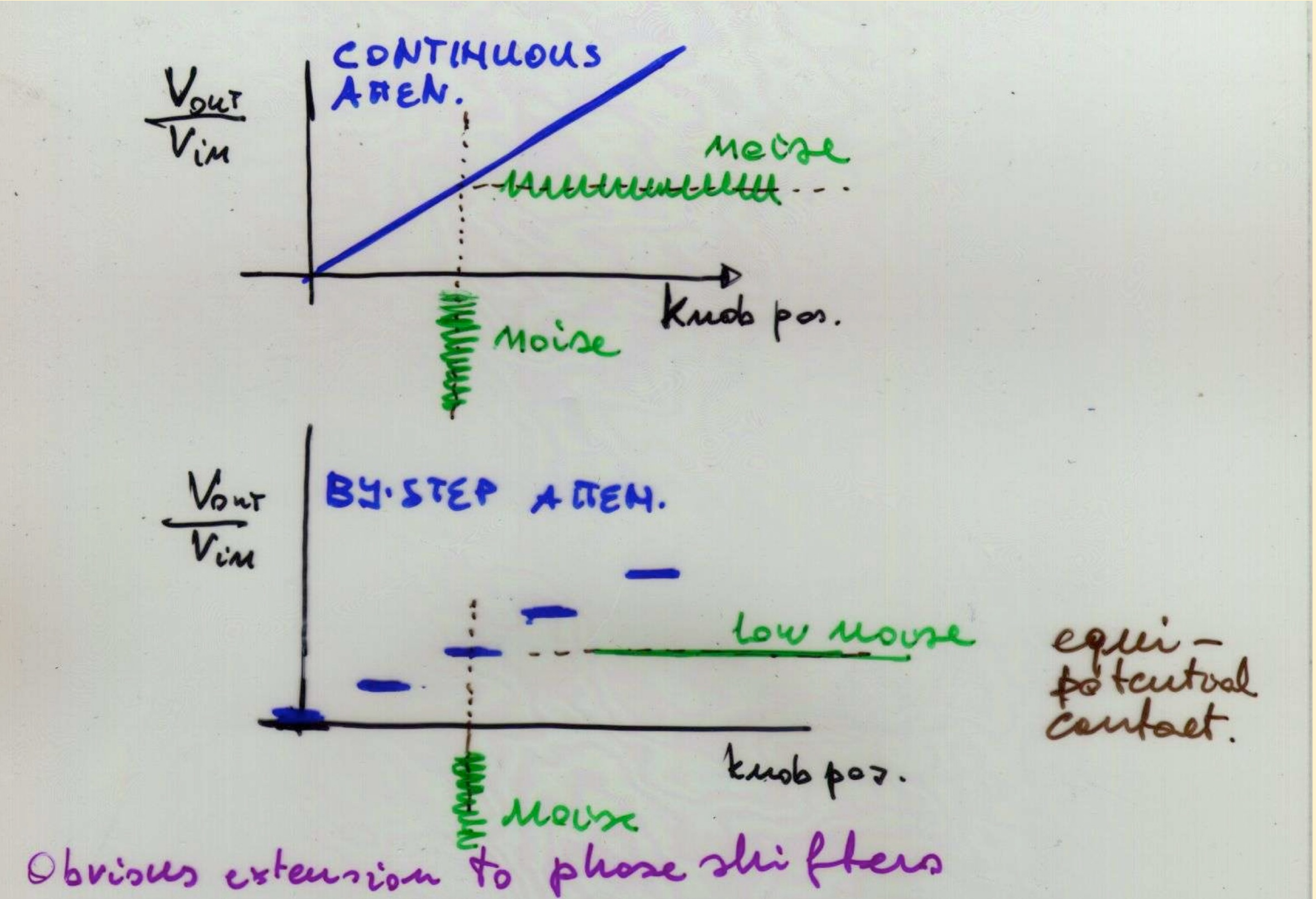

In the early time of electronics, flicker was called “contact noise”

Coarse and fine adjustment

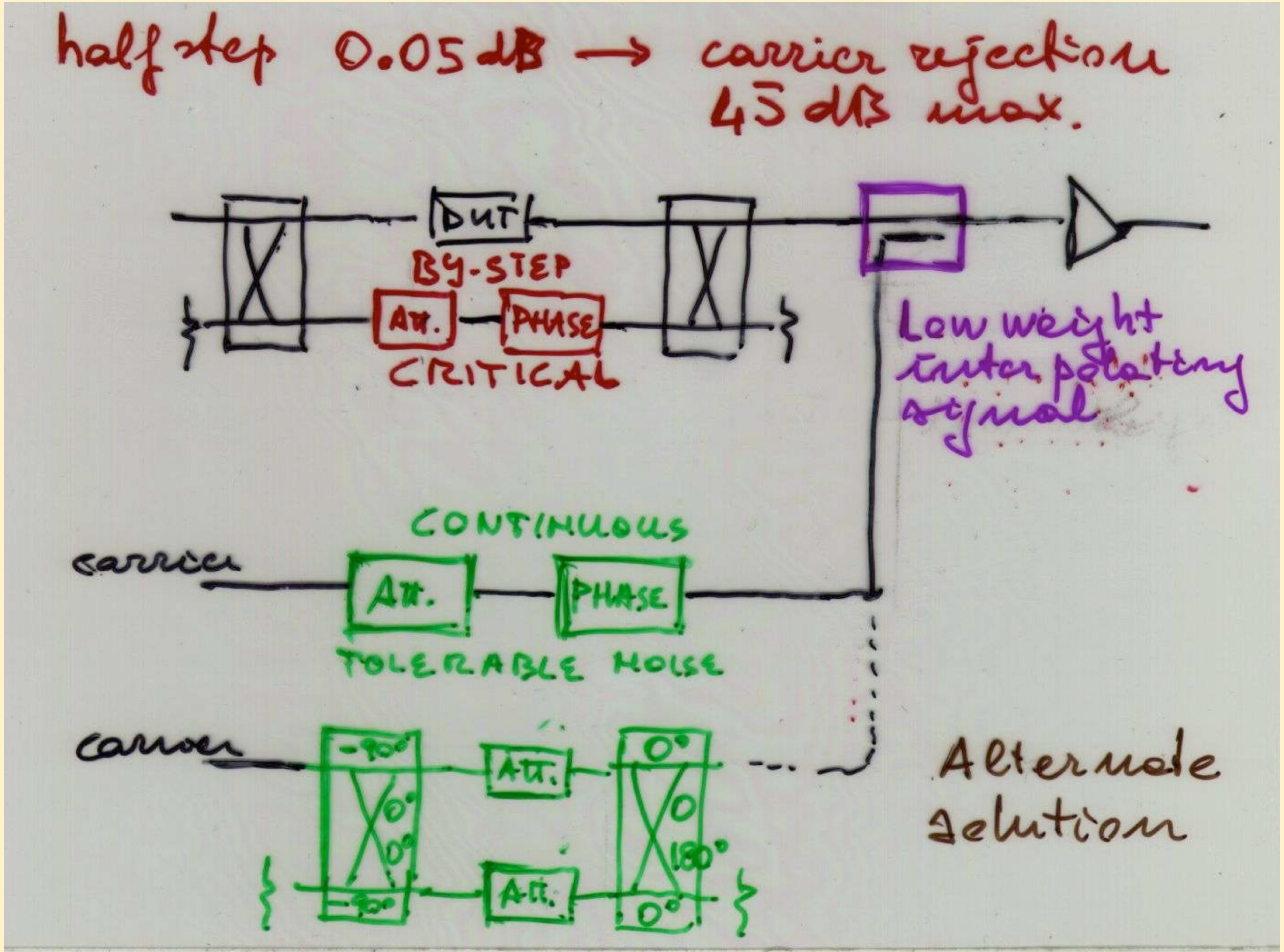

Combine all tricks in one machine

Flicker reduction, correlation, and closed-loop carrier suppression

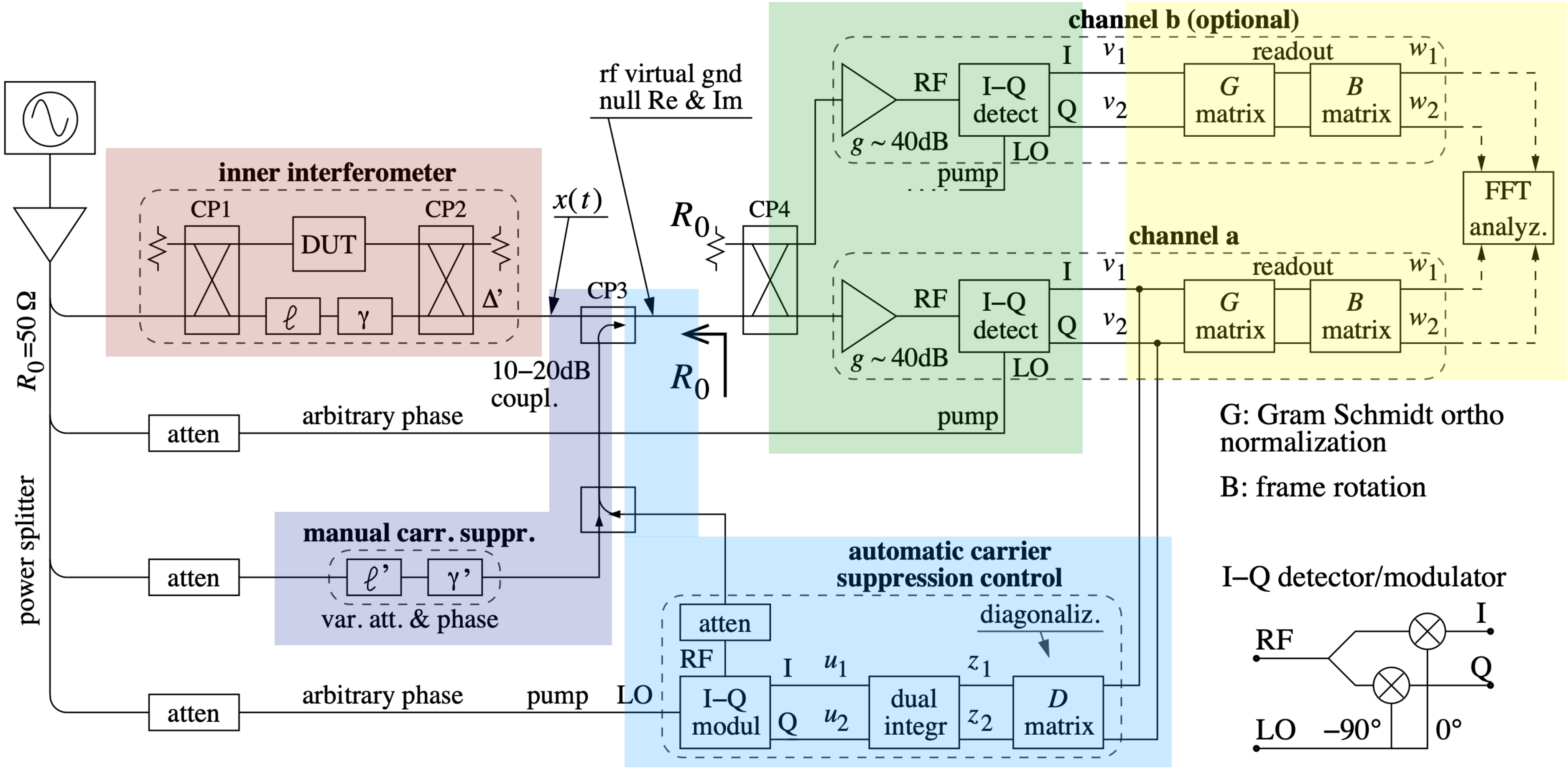

E. Rubiola, V. Giordano, Rev. Scientific Instruments 73(6) pp.2445-2457, June 2002

Example of results

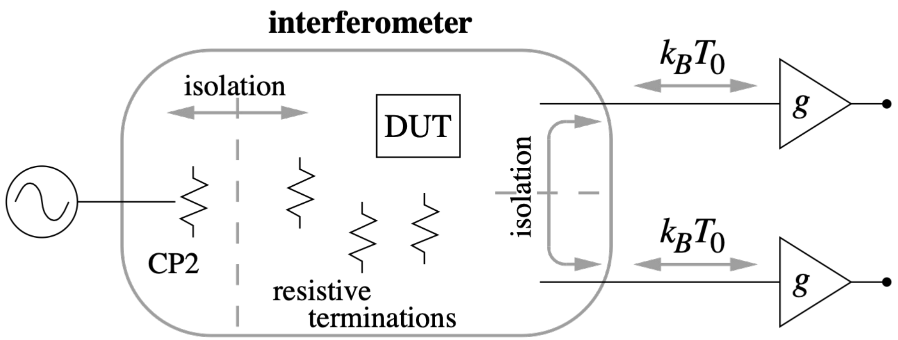

Correlation-and-averaging rejects the thermal noise

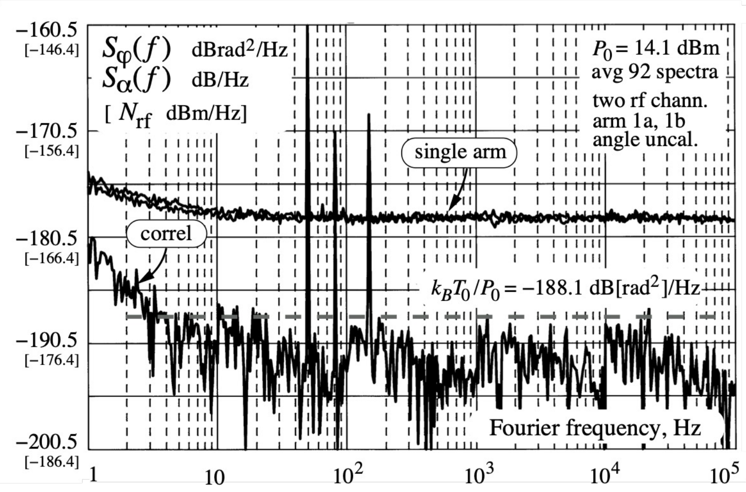

Residual noise of the fixed-value bridge, in the absence of the DUT

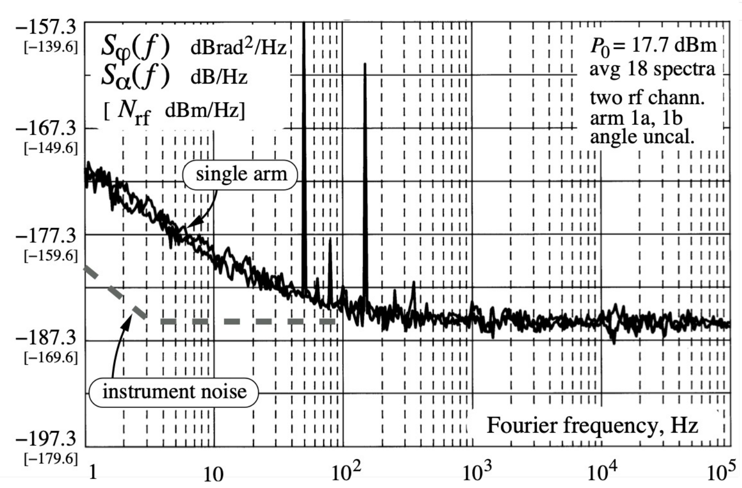

Noise of a pair of HH-109 hybrid couplers measured at 100 MHz

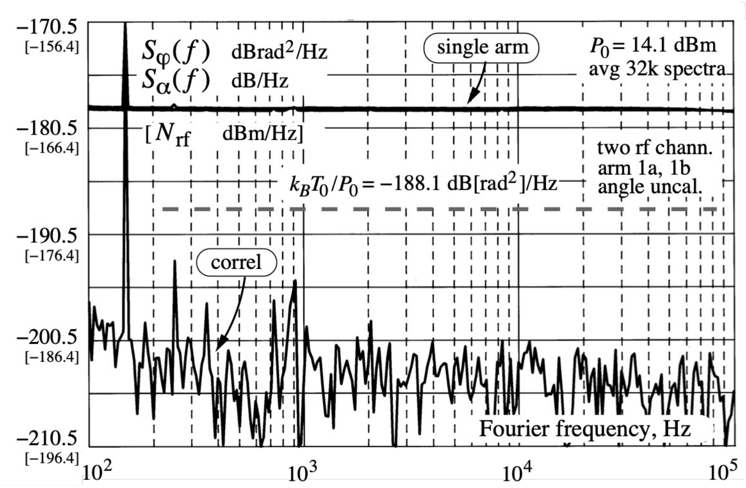

Residual noise of the fixed-value bridge. Same as above, but larger m

Microwave circulator in reverse mode

(for the Pound Scheme)

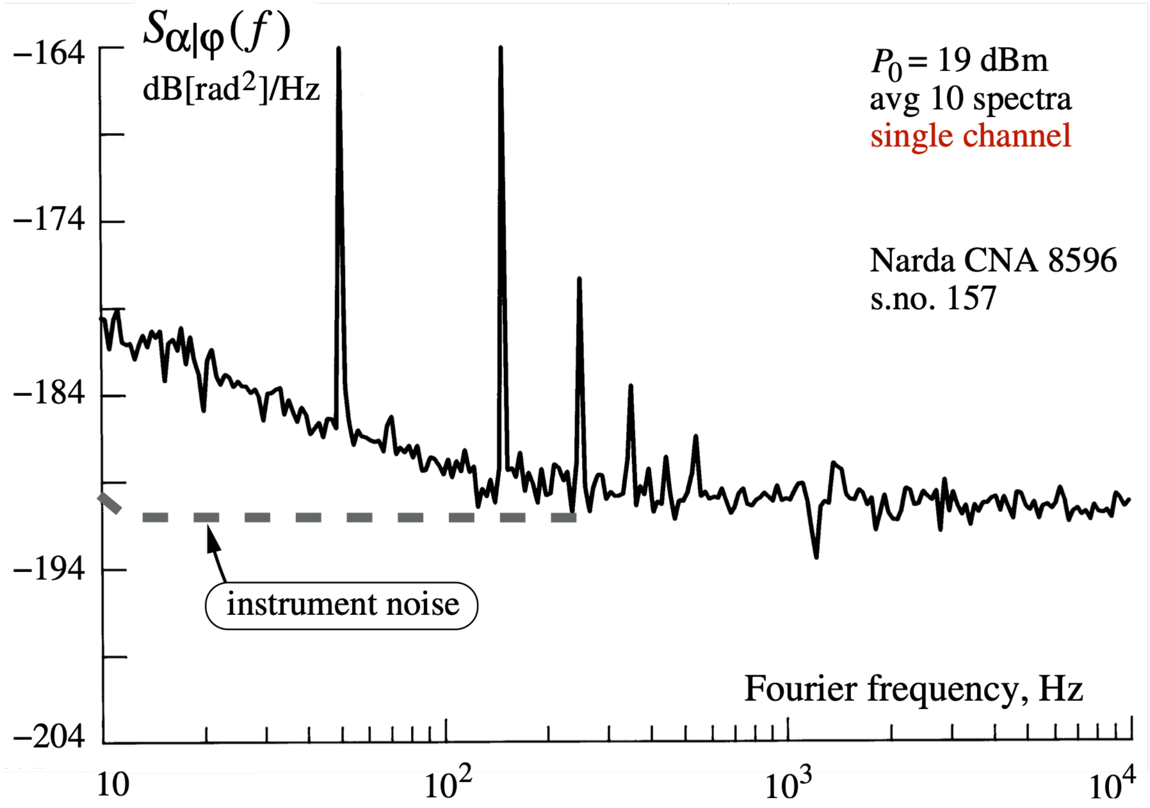

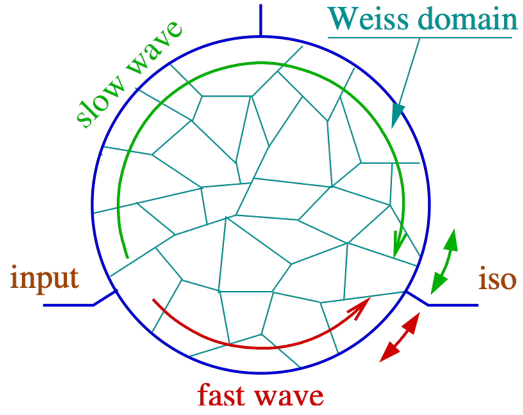

Due to the Larmor precession in the presence of a magnetic field, the speed is gyrotropic.

Isolation is due to the interference between fast and slow wave.

no post-processing is used to hide stray signals, like vibrations or the mains

±45° detection

DUT noise without carrier $n_c(t)\cos\omega_0 t - n_s(t)\sin\omega_0 t$

UP reference $u(t) = V_P\cos(\omega_0 t - \pi/4)$

DOWN reference $d(t) = V_P\cos(\omega_0 t + \pi/4)$

cross spectral density $S_{ud}(f) = \dfrac{1}{2}\left[S_\alpha(f) - S_\varphi(f)\right]$

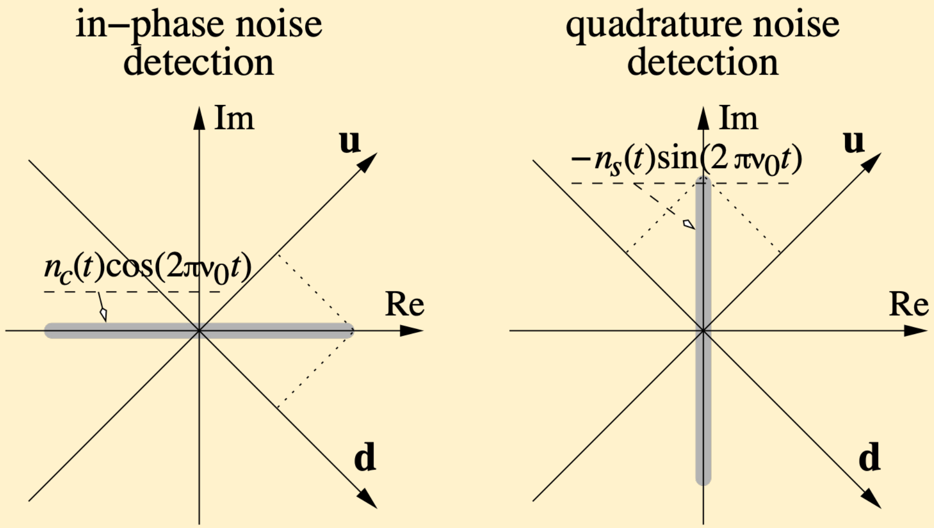

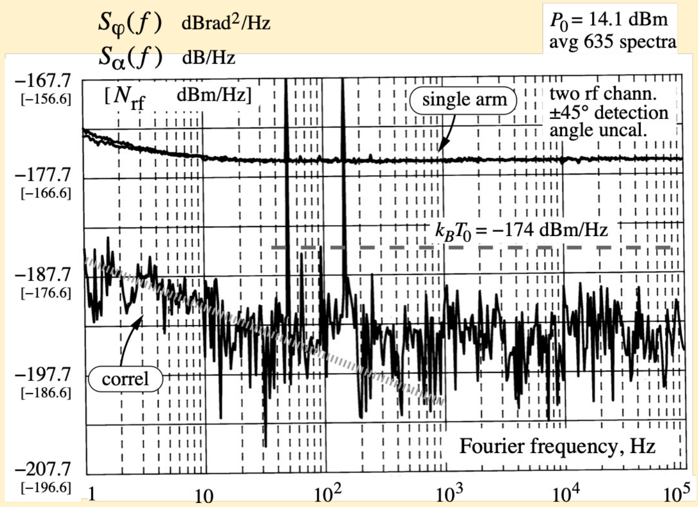

Residual noise, in the absence of the DUT

Smart and nerdy, yet of scarce practical usefulness

First used at 2 kHz to measure electromigration on metals (H. Stoll, MPI)

The complete machine (100 MHz)

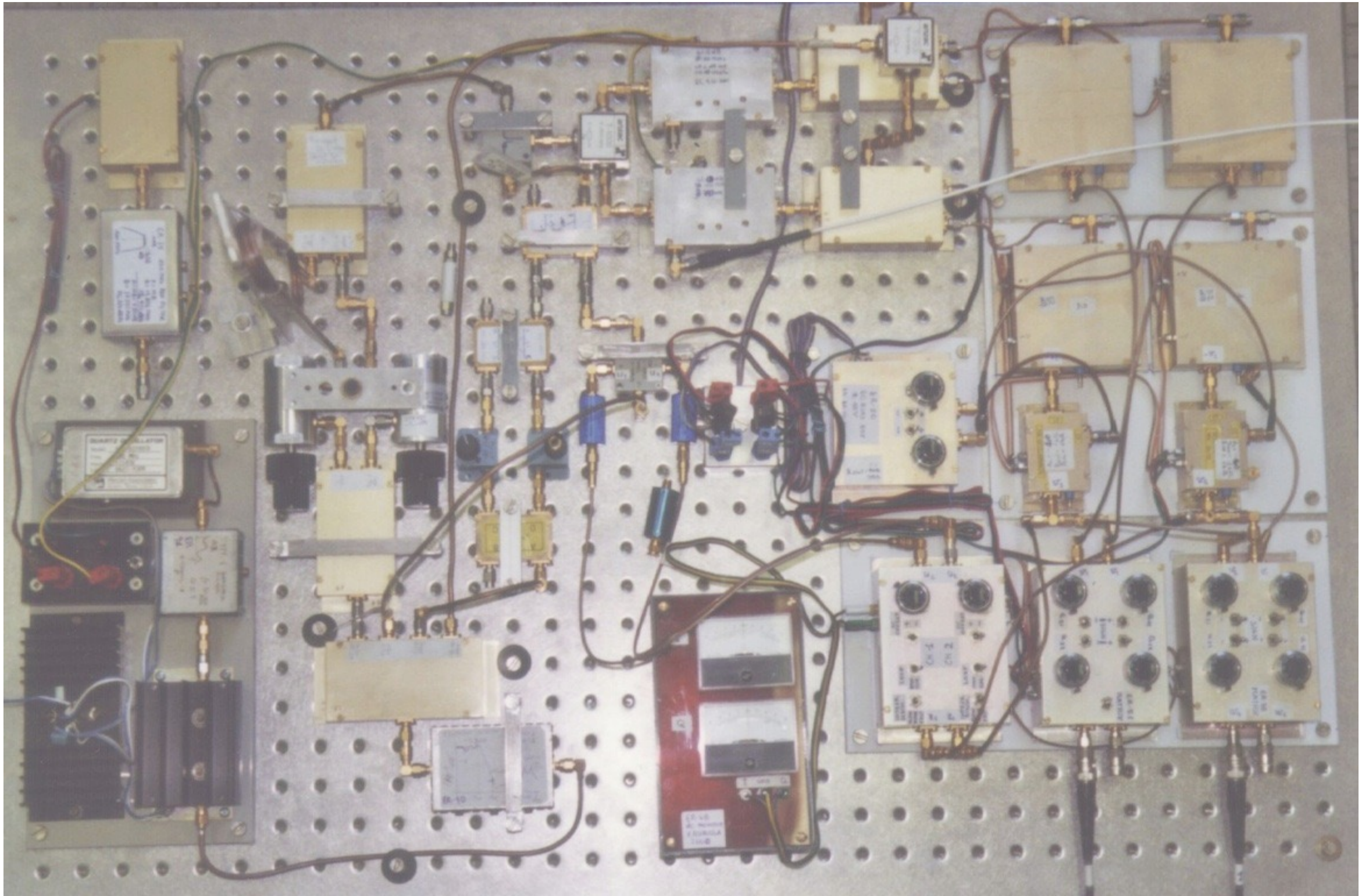

A 9 GHz experiment

(DC circuits not shown)

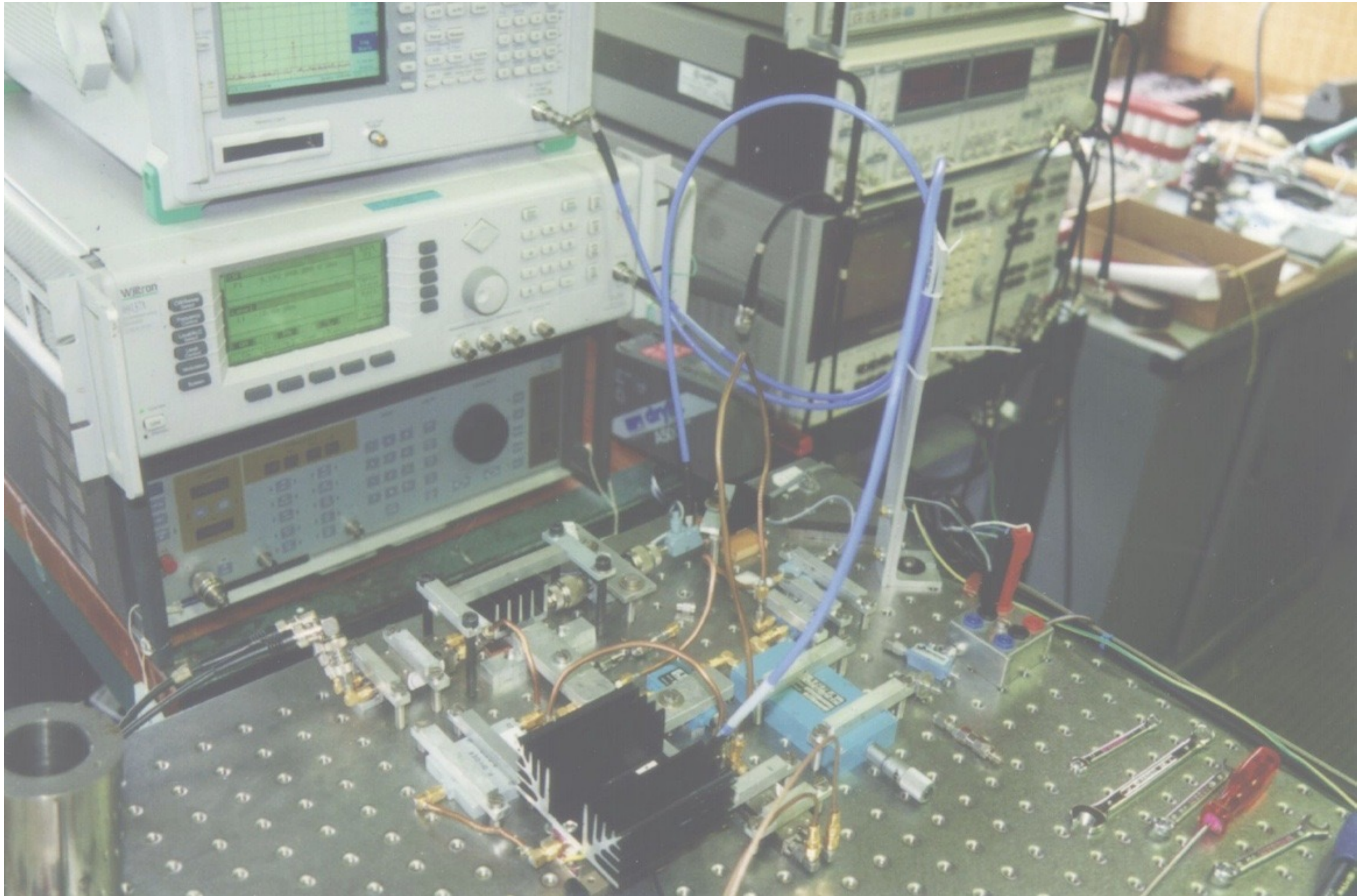

Background Noise

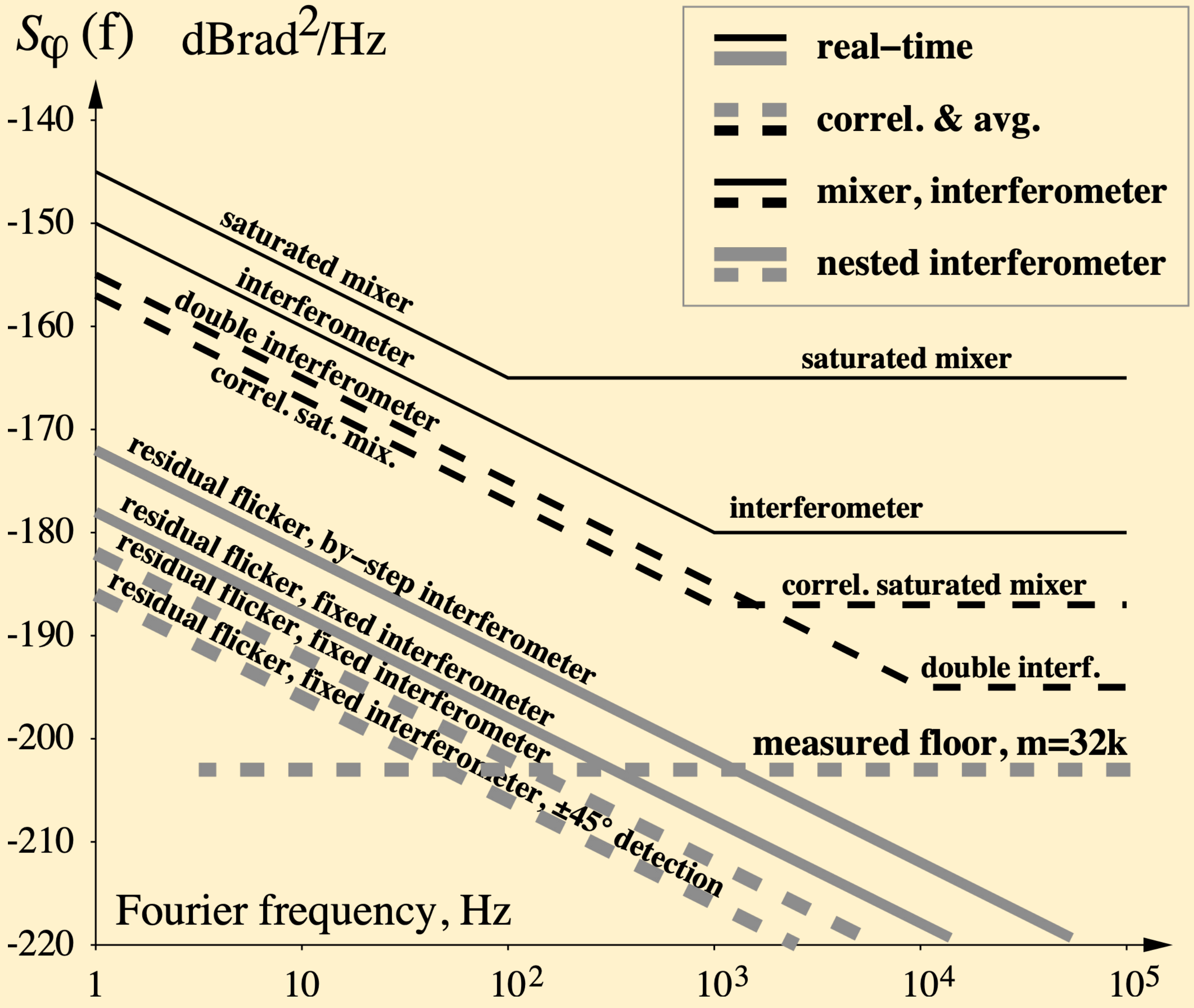

AM Noise

Amplitude noise & laser RIN

AM noise of RF/microwave sources

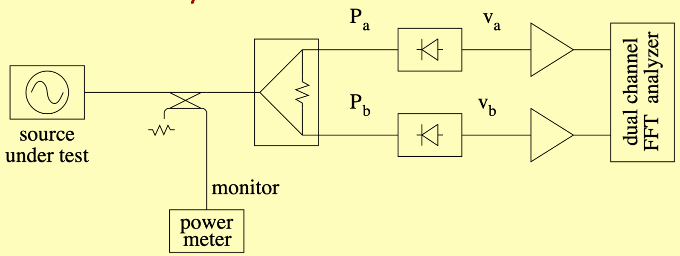

Laser RIN

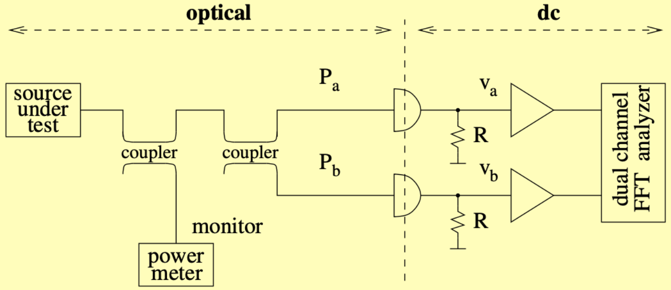

AM noise of photonic RF/microwave sources

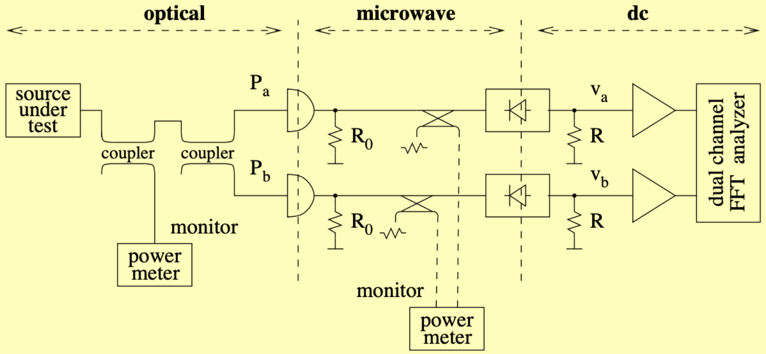

E. Rubiola, the measurement of AM noise, dec 2005
arXiv:physics/0512082v1 [physics.ins-det]

- In PM noise measurements, one can validate the instrument by feeding the same signal into the phase detector
- In AM noise this is not possible without a lower-noise reference
- Provided the crosstalk was measured otherwise, correlation enables to validate the instrument

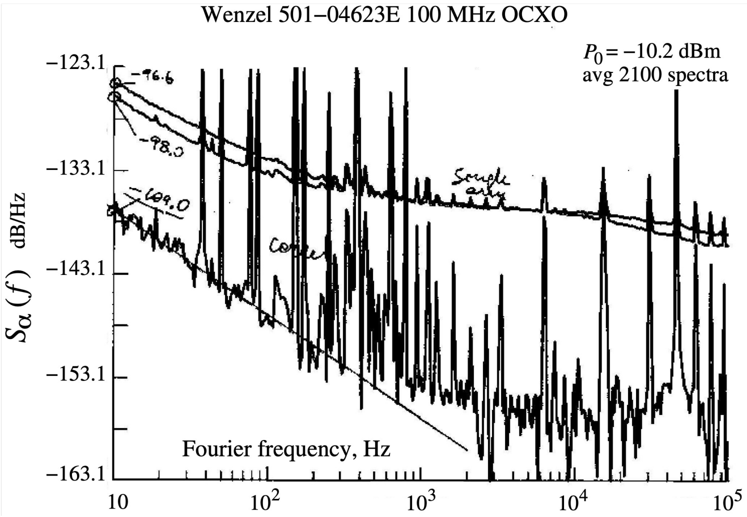

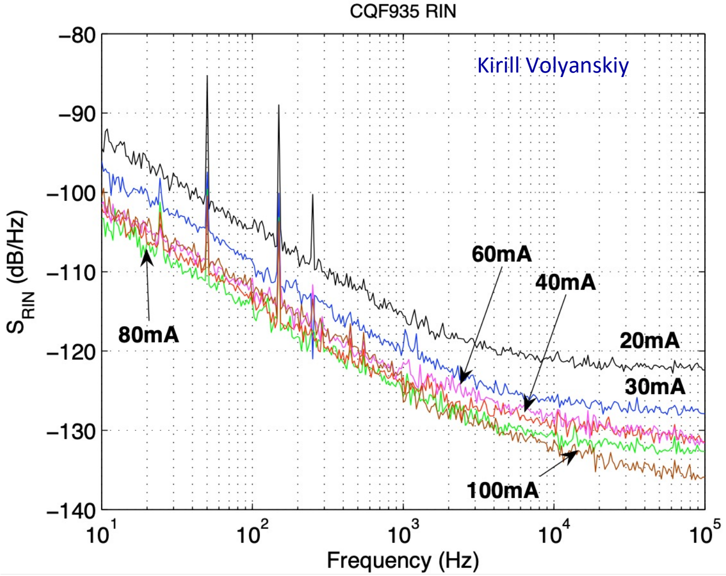

Cross-spectrum method

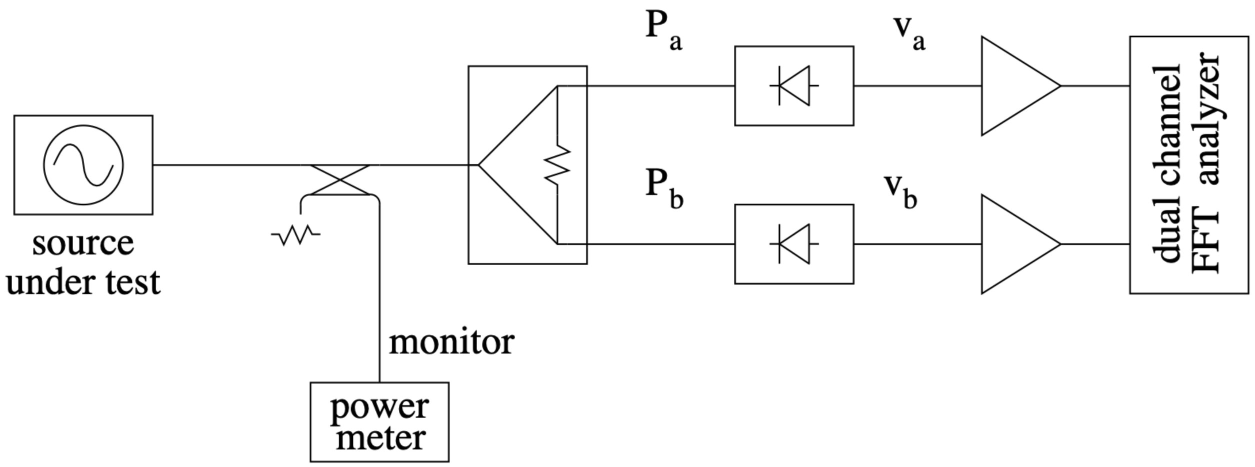

$$v_a(t) = 2k_a P_a \alpha(t) + \text{noise}$$
$$v_b(t) = 2k_a P_b \alpha(t) + \text{noise}$$

The cross spectrum $S_{ba}(f)$ rejects the single-channel noise because the two channels are independent.

$$S_{ba}(f) = \frac{1}{4k_a k_b P_a P_b} S_\alpha(f)$$

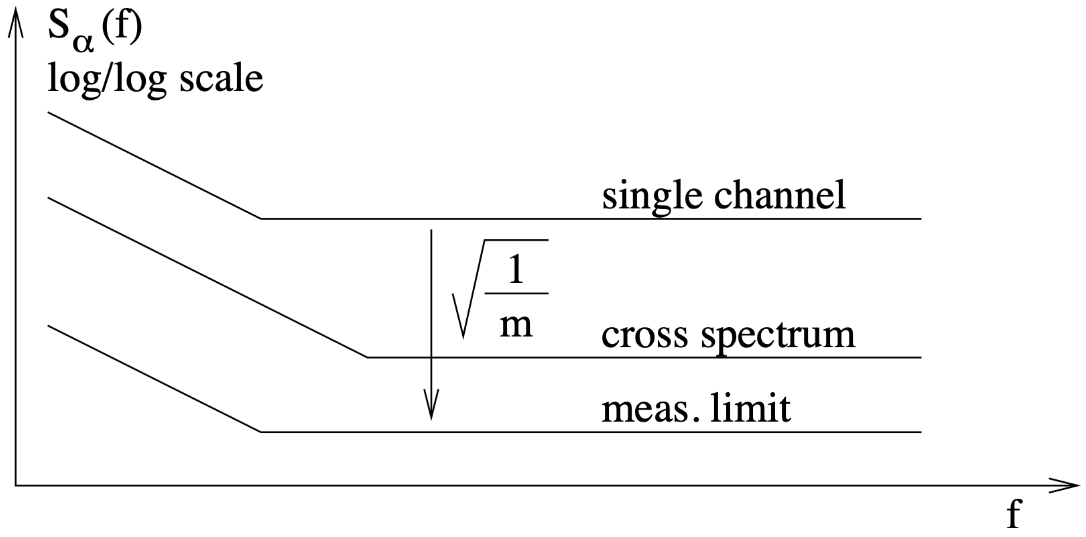

- Averaging on m spectra, the single-channel noise is rejected $\propto 1/\sqrt{m}$
- A cross-spectrum higher than the averaging limit validates the measure
- The knowledge of the single-channel noise is not necessary

Tunnel and Schottky power detectors

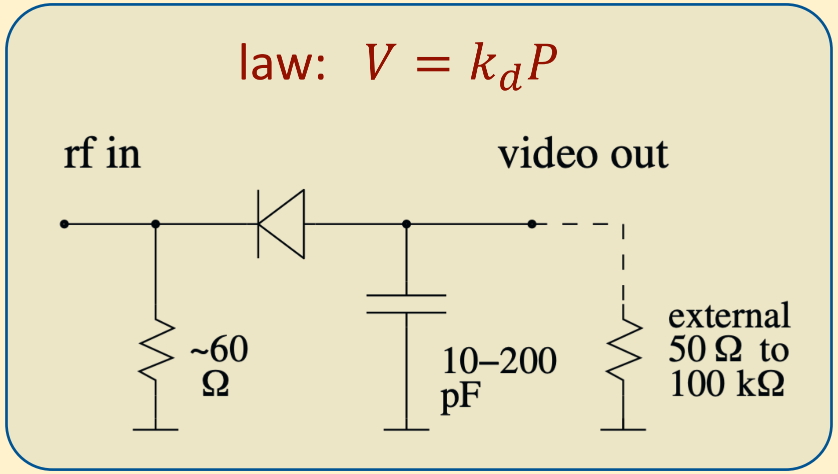

parameter	Schottky	tunnel
input bandwidth	up to 4 decades 10 MHz to 20 GHz	1–3 octaves up to 40 GHz
VSVR max.	1.5:1	3.5:1
max. input power (spec.)	−15 dBm	−15 dBm
absolute max. input power	20 dBm or more	20 dBm
output resistance	1–10 kΩ	50–200 Ω
output capacitance	20–200 pF	10–50 pF
gain	300 V/W	1000 V/W
cryogenic temperature	no	yes
electrically fragile	no	yes

The "tunnel" diode is a backward diode (no negative resistance region)

Measured k_d

load resistance, Ω	detector gain, A^{-1} DZR124AA (Schottky)	detector gain, A^{-1} DT8012 (tunnel)
1×10^2	35	292
3.2×10^2	98	505
1×10^3	217	652
3.2×10^3	374	724
1×10^4	494	750
conditions: power −50 to −20 dBm		

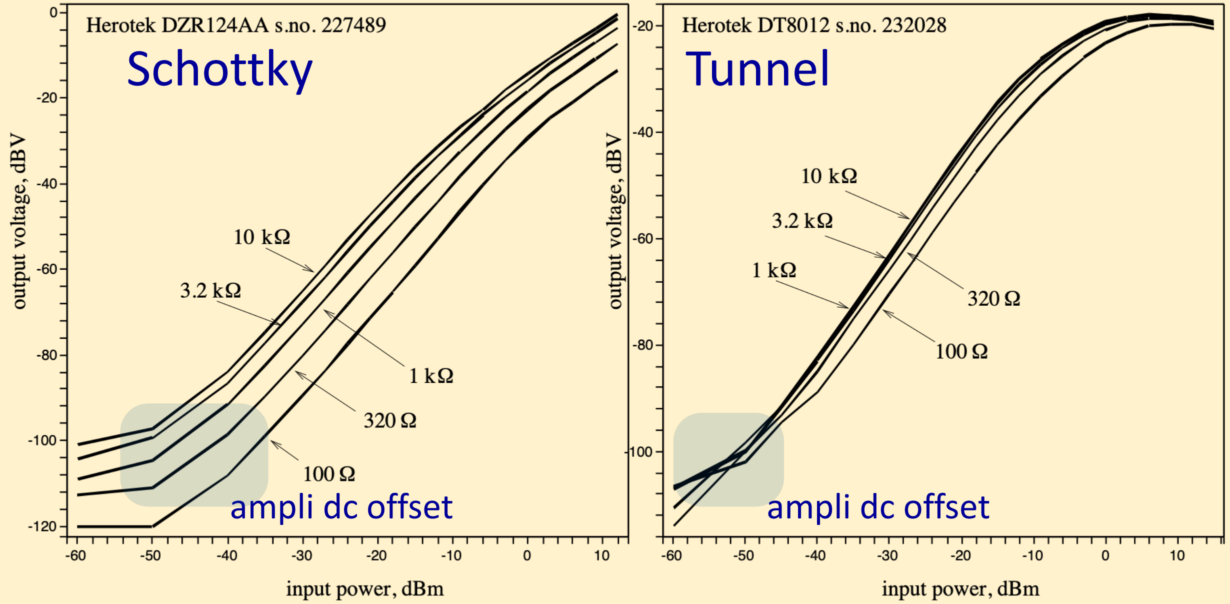

Best SNR at –20 to –15 dBm

Calibration

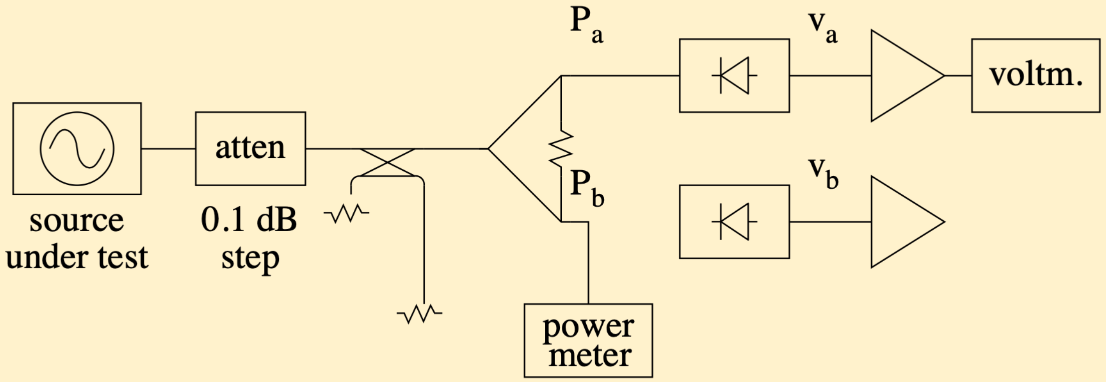

Set a reference $\Delta P_a/P_a$ (0.1 dB) with a by-step attenuator

Measure ΔV_a at the output

$$k_a P_a = \frac{\Delta v_a}{\Delta P/P_a}$$

Repeat interchanging the channels

Note that only the kP product is needed because

$$S_{ba}(f) = \frac{1}{4k_a k_b P_a P_b} S_\alpha(f)$$

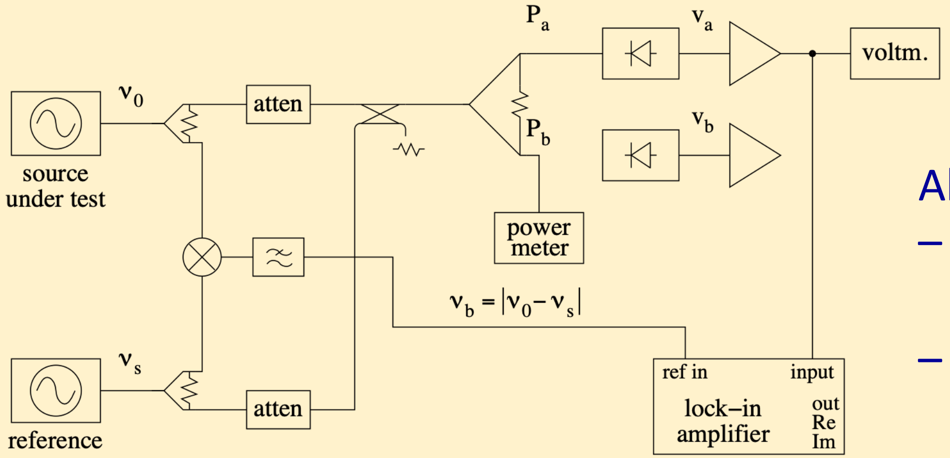

Alternate (and complex) calibration method.

– It exploits the sensitivity and the accuracy of a lock-in amplifier.

– As before, it requires a reference power-ratio

Example of AM noise spectrum

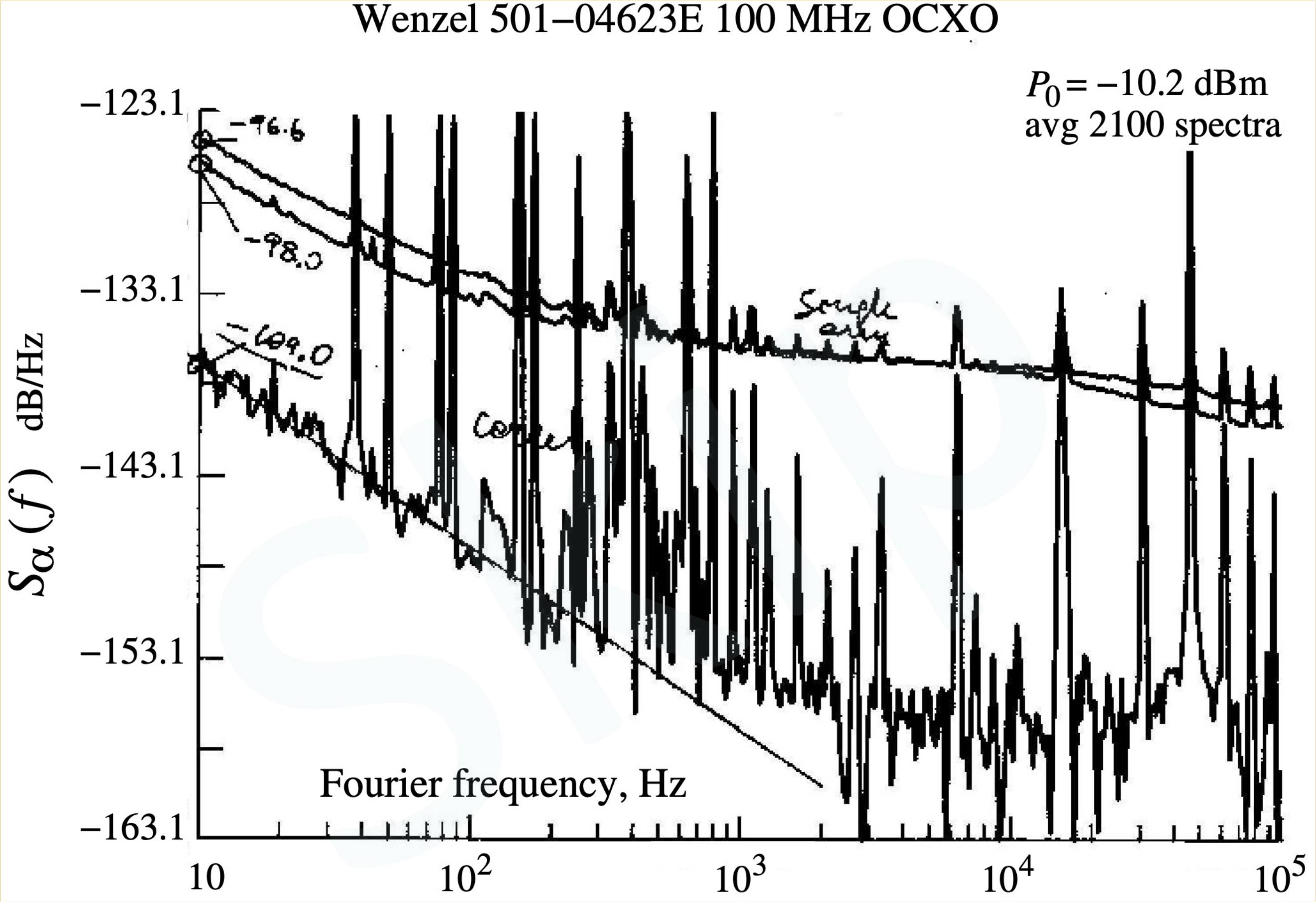

flicker: $h_{-1} = 1.5\times10^{-13}\ \mathrm{Hz}^{-1}\ (-128.2\ \mathrm{dB}) \quad\Rightarrow\quad \sigma_\alpha = 4.6\times10^{-7}$

Single-arm 1/f noise is that of the dc amplifier

(the amplifier is still not optimized)

AM noise of some sources

source	h_{-1} (flicker)		$(\sigma_\alpha)_{\text{floor}}$
Anritsu MG3690A synthesizer (10 GHz)	2.5×10^{-11}	-106.0 dB	5.9×10^{-6}
Marconi synthesizer (5 GHz)	1.1×10^{-12}	-119.6 dB	1.2×10^{-6}
Macom PLX 32-18 0.1 $\rightarrow$ 9.9 GHz multipl.	1.0×10^{-12}	-120.0 dB	1.2×10^{-6}
Omega DRV9R192-105F 9.2 GHz DRO	8.1×10^{-11}	-100.9 dB	1.1×10^{-5}
Narda DBP-0812N733 amplifier (9.9 GHz)	2.9×10^{-11}	-105.4 dB	6.3×10^{-6}
HP 8662A no. 1 synthesizer (100 MHz)	6.8×10^{-13}	-121.7 dB	9.7×10^{-7}
HP 8662A no. 2 synthesizer (100 MHz)	1.3×10^{-12}	-118.8 dB	1.4×10^{-6}
Fluke 6160B synthesizer	1.5×10^{-12}	-118.3 dB	1.5×10^{-6}
Racal Dana 9087B synthesizer (100 MHz)	8.4×10^{-12}	-110.8 dB	3.4×10^{-6}
Wenzel 500-02789D 100 MHz OCXO	4.7×10^{-12}	-113.3 dB	2.6×10^{-6}
Wenzel 501-04623E no. 1 100 MHz OCXO	2.0×10^{-13}	-127.1 dB	5.2×10^{-7}
Wenzel 501-04623E no. 2 100 MHz OCXO	1.5×10^{-13}	-128.2 dB	4.6×10^{-7}

worst

best

Flicker in microwave power detectors

S. Grop, E. Rubiola, Flicker Noise of Microwave Power Detectors, Proc. IFCS-EFTF joint conf. p.40-43, 2009

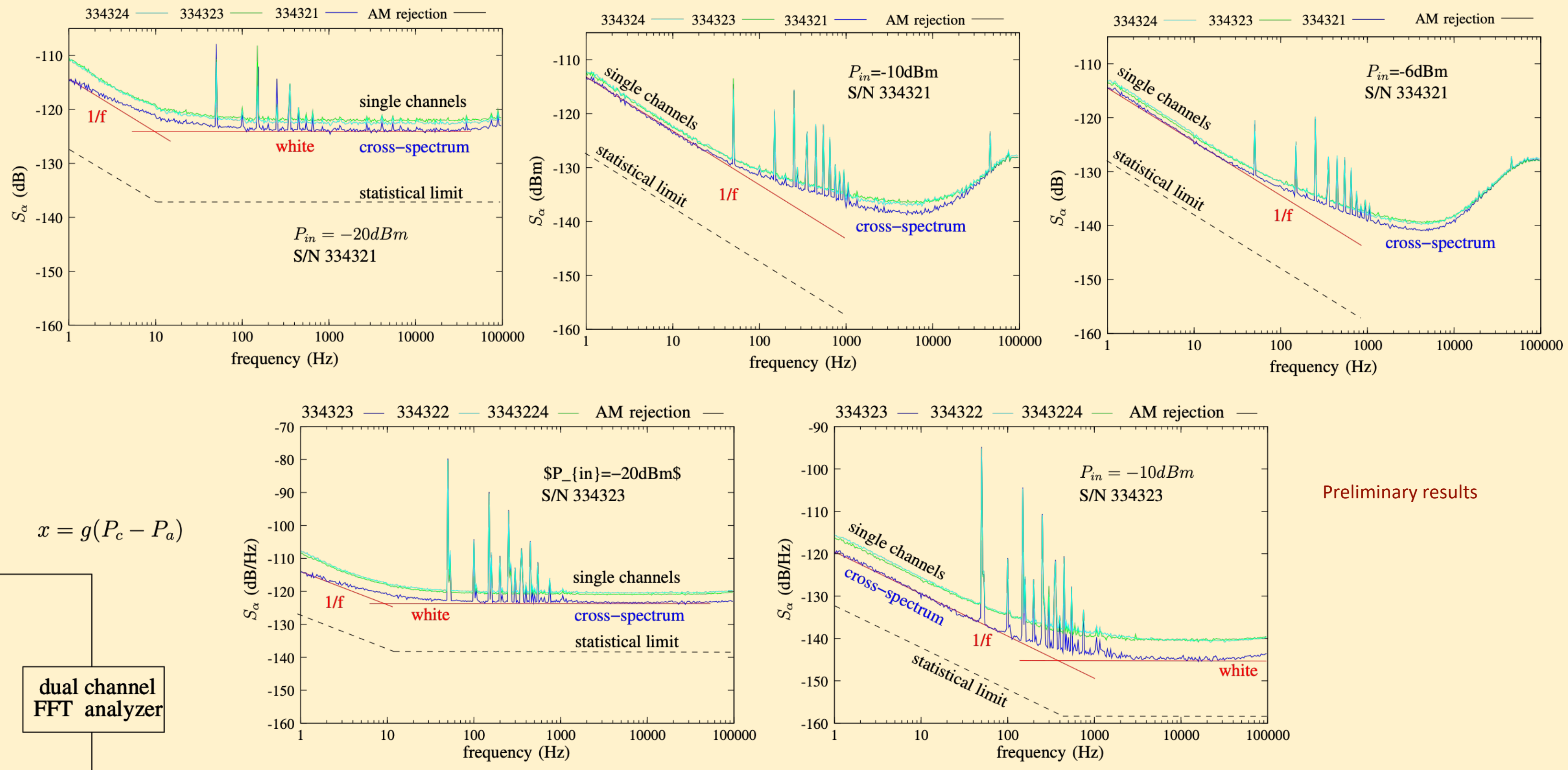

Grop-Rubiola Fig.8 a-e

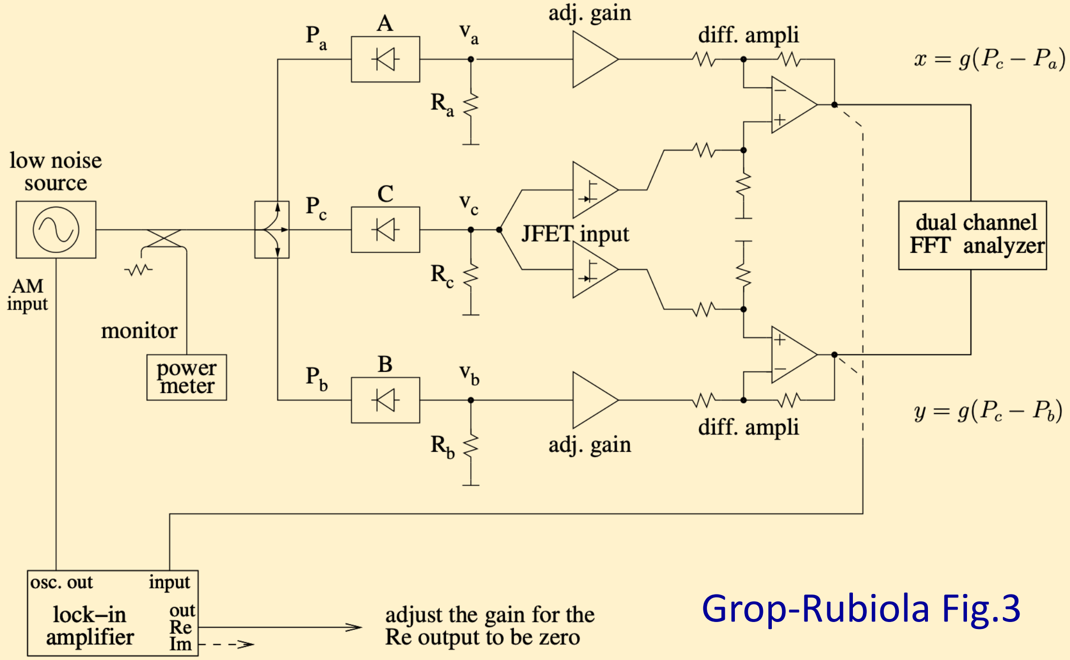

Grop-Rubiola Fig.3

Observed $h_{-1} \approx -150$ dB, similar to the b_{-1} of other diodes (mixer and microwave photodetector)

REVIEW OF SCIENTIFIC INSTRUMENTS **87**, 084702 (2016)

Characterization of zero-bias microwave diode power detectors at cryogenic temperature

Vincent Giordano,[1,a)] Christophe Fluhr,[1] Benoît Dubois,[2] and Enrico Rubiola[1,b)]
[1]*Time and Frequency Department, CNRS FEMTO-ST Institute (UMR 6174), 26 Chemin de l'Epitaphe, 25030 Besançon, France*
[2]*FEMTO Engineering, 32 Avenue de l'Observatoire 25000 Besançon, France*

(Received 5 April 2016; accepted 19 July 2016; published online 23 August 2016)

We present the characterization of commercial tunnel diode low-level microwave power detectors at room and cryogenic temperatures. The sensitivity as well as the output voltage noise of the tunnel diodes is measured as functions of the applied microwave power. We highlight strong variations of the diode characteristics when the applied microwave power is higher than a few microwatts. For a diode operating at 4 K, the differential gain increases from 1000 V/W to about 4500 V/W when the power passes from −30 dBm to −20 dBm. The diode white noise floor is equivalent to a Noise Equivalent Power of 0.8 pW/$\sqrt{\text{Hz}}$ and 8 pW/$\sqrt{\text{Hz}}$ at 4 K and 300 K, respectively. Its flicker noise is equivalent to a relative amplitude noise power spectral density $S_\alpha(1\ \text{Hz}) = -120$ dB/Hz at 4 K. Flicker noise is 10 dB higher at room temperature. *Published by AIP Publishing.* [http://dx.doi.org/10.1063/1.4960087]

Photonic Techniques

The delay-Line as a discriminator

The delay line turns a frequency into a phase

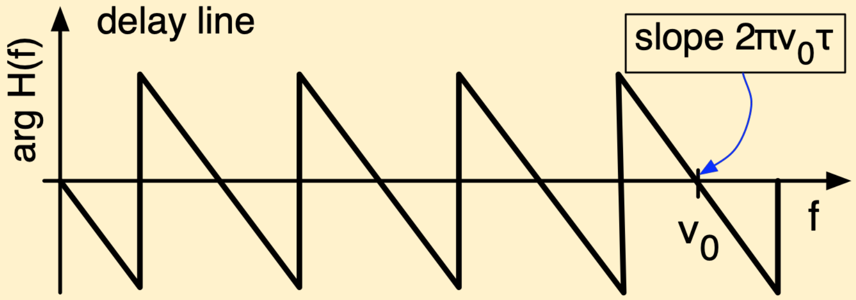

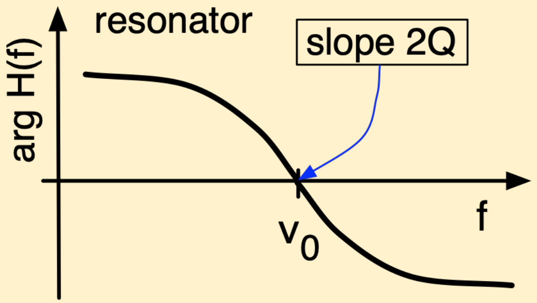

comparing the slope: $$Q_{\mathrm{eq}} = \pi\nu_0\tau$$

- Works at any frequency ν = n/τ, integer τ (the resonator does not)
- S_φ measurement of an oscillator
- Dual-channel S_φ measurement of an oscillator
- Stabilization of an oscillator
- Opto-electronic oscillator

- Coax cable: 50 dB attenuation limits to
  - 950 ns @ 1 GHz (Q=3000) - RG213
  - 300 ns @ 10 GHz (Q=11500) - RG402
- Optical fiber:
  - max delay is not limited by the attenuation
  - 1-100 μs delay is possible ($Q=10^5$–10^7 @ 31 GHz)

Opto-electronic delay line

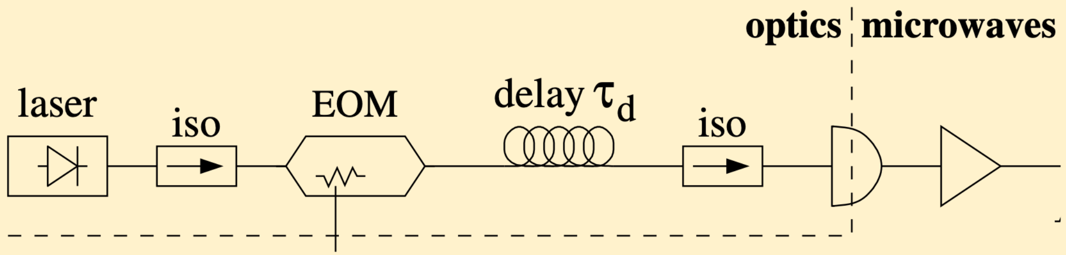

intensity modulation $\quad P(t) = \overline{P}(1 + m\cos\omega_\mu t)$

photocurrent $\quad i(t) = \dfrac{q\eta}{h\nu}\,\overline{P}(1 + m\cos\omega_\mu t)$ $\quad$ shot noise $\quad N_s = 2\dfrac{q^2\eta}{h\nu}\,\overline{P}R_0$

microwave power $\quad \overline{P}_\mu = \dfrac{1}{2}m^2R_0\left(\dfrac{q\eta}{h\nu}\right)^2 P^2$ $\quad$ thermal noise $\quad N_t = FkT_0$

total white noise (shot, thermal)

$$S_{\varphi 0} = \frac{2}{m^2}\left[2\frac{h\nu_\lambda}{\eta}\,\frac{1}{\overline{P}} + \frac{FkT_0}{R_0}\left(\frac{h\nu_\lambda}{q\eta}\right)^2\left(\frac{1}{\overline{P}}\right)^2\right]$$

flicker phase noise

- amplifier GaAs: $b_{-1} \approx -100$ to -110 dBrad^2/Hz, SiGe: $b_{-1} \approx -120$ dBrad^2/Hz
- photodetector $b_{-1} \approx -120$ dBrad^2/Hz [Rubiola & al. MTT/JLT 54(2), feb. 2006
- (mixer $b_{-1} \approx -120$ dBrad^2/Hz)
- the phase flicker coefficient b_{-1} is about independent of power
- in a cascade, $(b_{-1})_{tot}$ adds up, regardless of the device order

optical-fiber phase noise? still an experimental parameter

White noise

intensity modulation $$P(t) = \overline{P}(1 + m\cos\omega_\mu t)$$

photocurrent $$i(t) = \frac{q\eta}{h\nu}\,\overline{P}(1 + m\cos\omega_\mu t)$$

microwave power $$\overline{P}_\mu = \frac{1}{2}\,m^2 R_0 \left(\frac{q\eta}{h\nu}\right)^2 P^2$$

shot noise $$N_s = 2\frac{q^2\eta}{h\nu}\,\overline{P}R_0$$

thermal noise $$N_t = FkT_0$$

shot thermal

total white noise (one detector) $$S_{\varphi 0} = \frac{2}{m^2}\left[2\frac{h\nu_\lambda}{\eta}\,\frac{1}{\overline{P}} + \frac{FkT_0}{R_0}\left(\frac{h\nu_\lambda}{q\eta}\right)^2\left(\frac{1}{\overline{P}}\right)^2\right]$$

total white noise (P/2 each detector) $$S_{\varphi 0} = \frac{16}{m^2}\left[\frac{h\nu_\lambda}{\eta}\,\frac{1}{\overline{P}} + \frac{FkT_0}{R_0}\left(\frac{h\nu_\lambda}{q\eta}\right)^2\left(\frac{1}{\overline{P}}\right)^2\right]$$

Threshold power

$$S_{\varphi 0} = \frac{16}{m^2}\left[\frac{h\nu_\lambda}{\eta}\,\frac{1}{\overline{\overline{P}}} + \frac{FkT_0}{R_0}\left(\frac{h\nu_\lambda}{q\eta}\right)^2\left(\frac{1}{\overline{\overline{P}}}\right)^2\right]$$

holds for two detectors

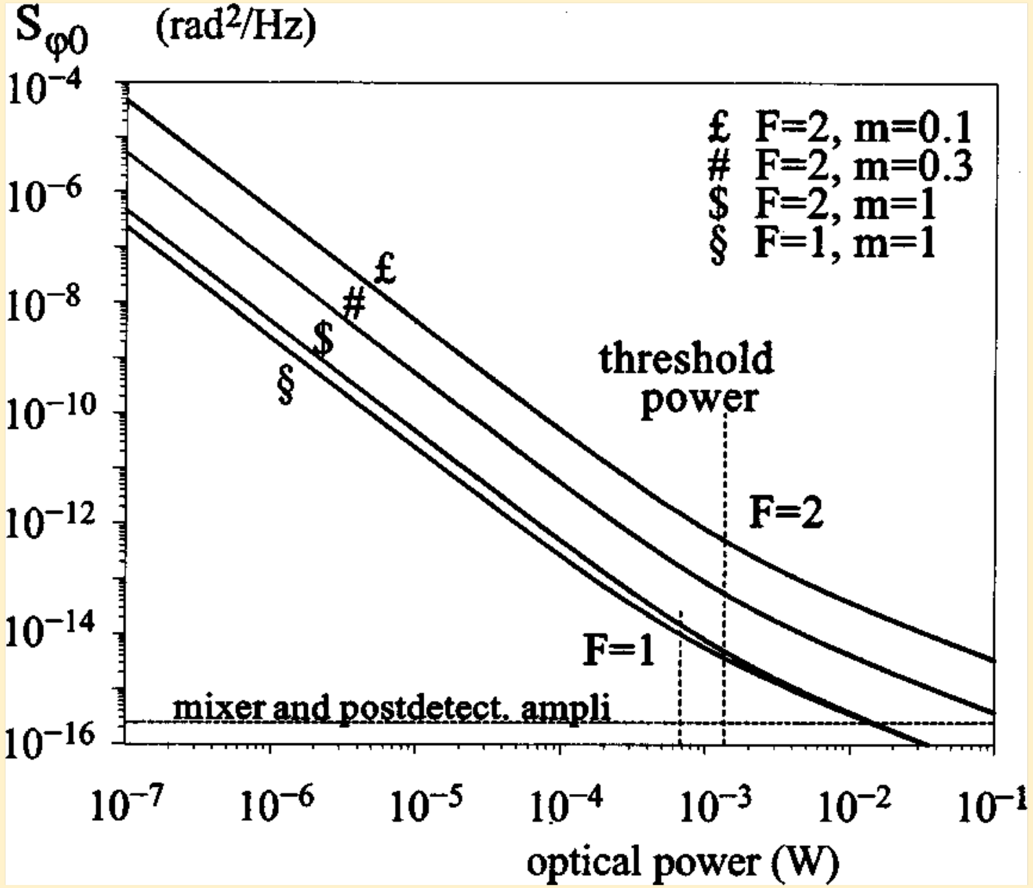

threshold power

$$P_{\lambda,t} = \frac{FkT_0}{R_0}\,\frac{h\nu_\lambda}{q^2\eta}$$

new high-power photodetectors 5-10 mW

Opto-electronic discriminator

Rubiola & al., JOSAB 22(5) p.987–997 (2005) --- Volyanskiy & al., JOSAB 25(12) p.2140–2150 (2008)

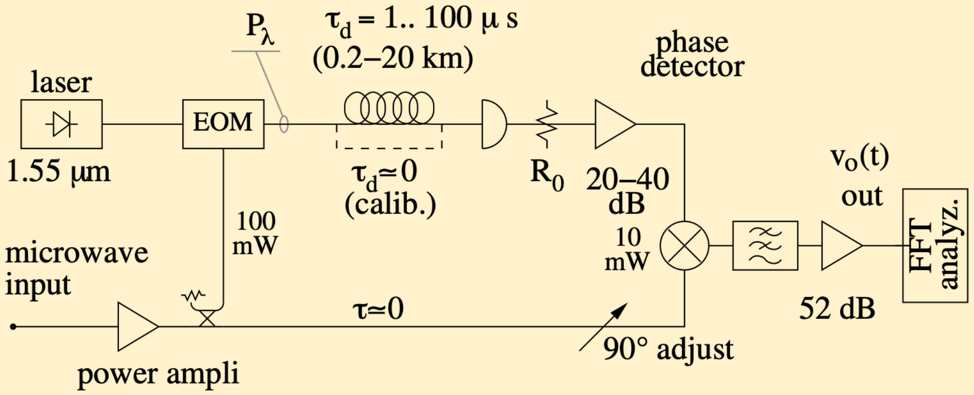

The short arm can be a microwave cable or a photonic channel

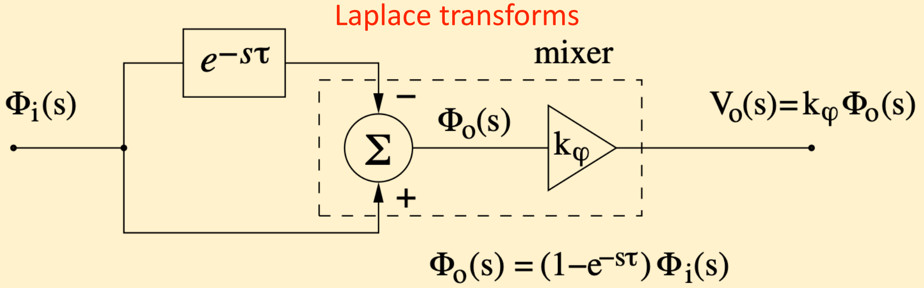

- delay –> frequency-to-phase conversion
- works at any frequency
- long delay (microseconds) is necessary for high sensitivity
- the delay line must be an optical fiber
  fiber: attenuation 0.2 dB/km, thermal coeff. 6.8 10-6/K
  cable: attenuation 0.8 dB/m, thermal coeff. ~ 10-3/K

Laplace transforms

$$\Phi(s) = H_\varphi(s)\Phi_i(s)$$

$$|H_\varphi(f)|^2 = 4\sin^2(\pi f \tau)$$

$$S_y(f) = |H_y(f)|^2\, S_{\varphi\, i}(f)$$

$$|H_y(f)|^2 = \frac{4\nu_0^2}{f^2}\,\sin^2(\pi f \tau)$$

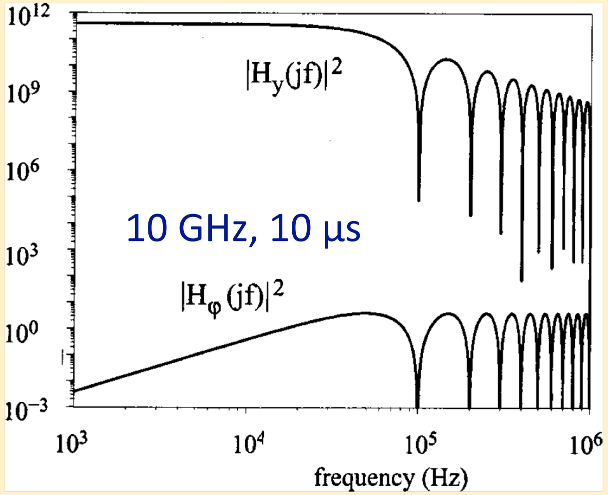

Photodetector $1/f$ noise (1)

Rubiola, Salik, Yu, Maleki, IEEE T MTT 54(2) p.816-820, Feb 2006

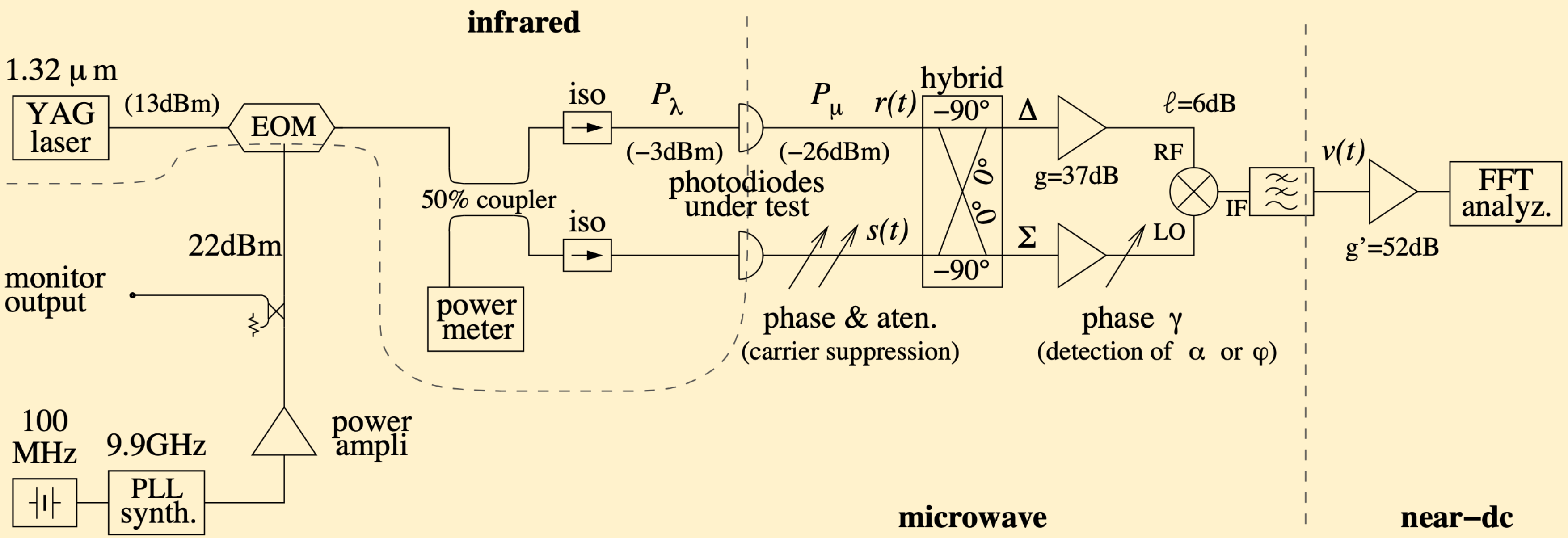

photodiode	$S_\alpha(1\,\text{Hz})$ estimate	$S_\alpha(1\,\text{Hz})$ uncertainty	$S_\varphi(1\,\text{Hz})$ estimate	$S_\varphi(1\,\text{Hz})$ uncertainty
HSD30	−122.7	−7.1 +3.4	−127.6	−8.6 +3.6
DSC30-1K	−119.8	−3.1 +2.4	−120.8	−1.8 +1.7
QDMH3	−114.3	−1.5 +1.4	−120.2	−1.7 +1.6
unit	dB/Hz	dB	dBrad²/Hz	dB

The noise of the ∑ amplifier is not detected [Electron. Lett. 39 19 p. 1389 (2003)]

Photodetector $1/f$ Noise (2)

Rubiola, Salik, Yu, Maleki, MTT 54(2) p.816-820, Feb 2006

- The photodetectors we measured are similar in AM and PM 1/f noise
- The 1/f noise is about -120 dB[rad^2]/Hz
- Other effects are easily mistaken for the photodetector 1/f noise
- Environment and packaging deserve attention in order to take the full benefit from the low noise of the junction

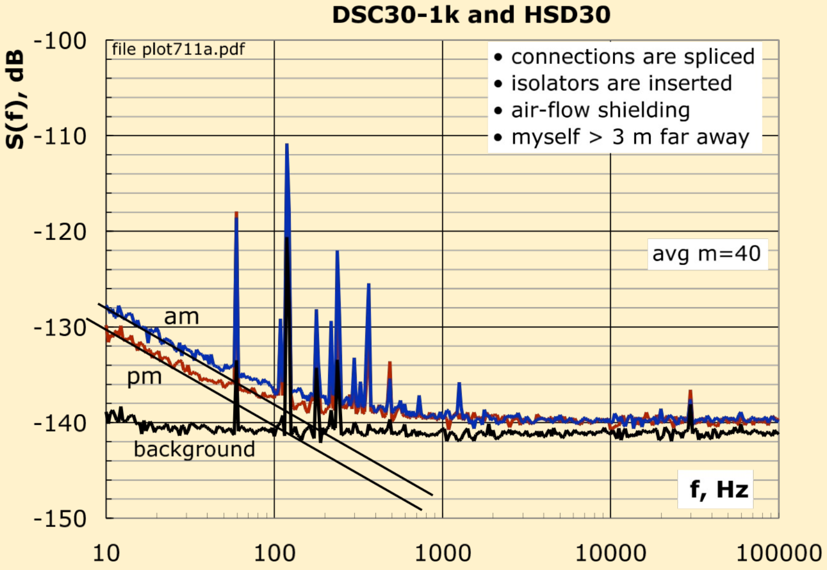

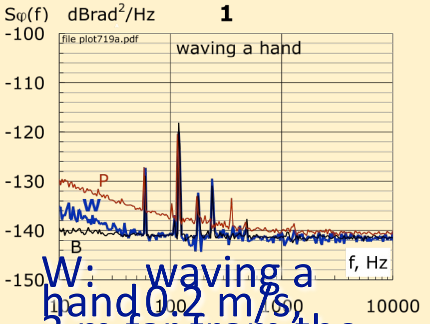

W: waving a hand 0.2 m/s, 3 m far from the system
B: background noise
P: photodiode noise

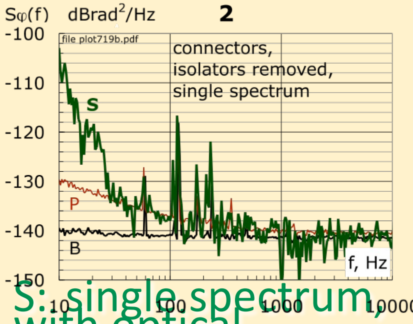

S: single spectrum, with optical connectors and no isolators
B: background noise
P: photodiode noise

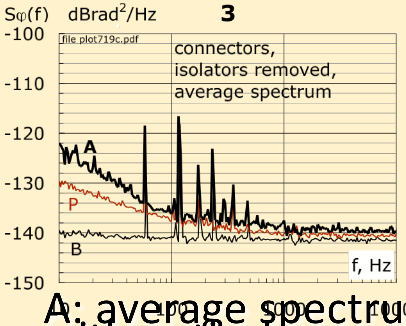

A: average spectrum, with optical connectors and no isolators
B: background noise
P: photodiode noise

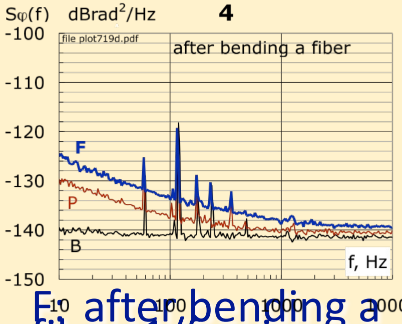

F: after bending a fiber, 1/f noise can increase unpredictably
B: background noise
P: photodiode noise

The effect of AM noise and RIN

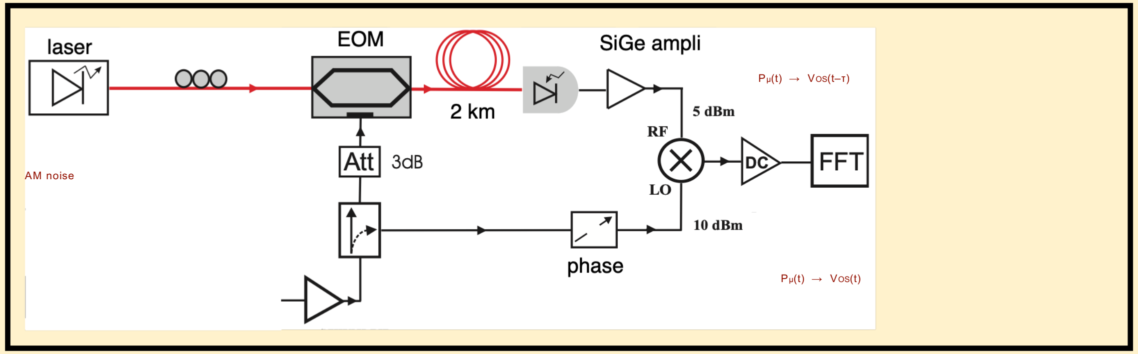

The AM noise turns into Vos fluctuation, which may limit the sensitivity

The delay de-correlates the AM noise. Thus there is no null of sensitivity

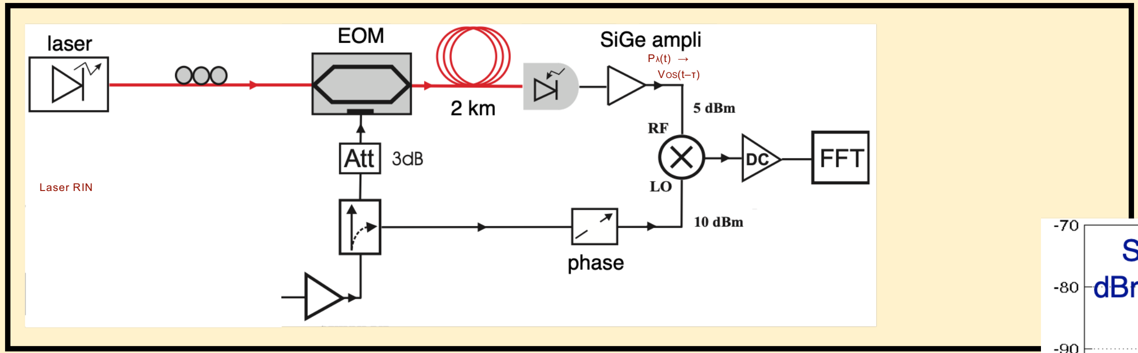

The laser RIN turns into Vos fluctuation, which may limit the sensitivity

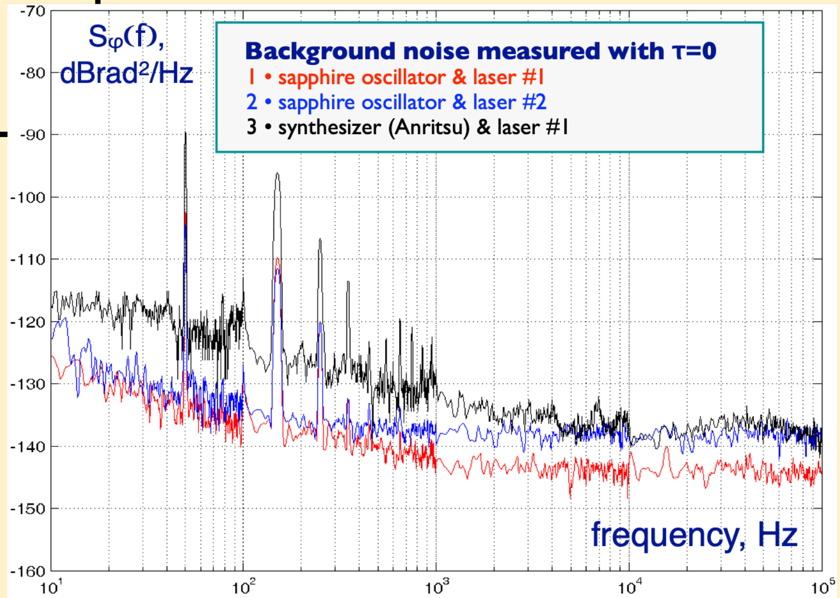

Instrument background measured at zero-length fiber

Lowest AM noise and Lowest RIN give the lowest background noise

Volyanskiy & al., JOSAB (in press).
Also arXiv:0807.3494v1 [physics.optics] July 2008.

Single-channel instrument

Volyanskiy & al., JOSAB 25(12) 2140-2150, Dec.2008. Also arXiv:0807.3494v1 [physics.optics] July 2008.

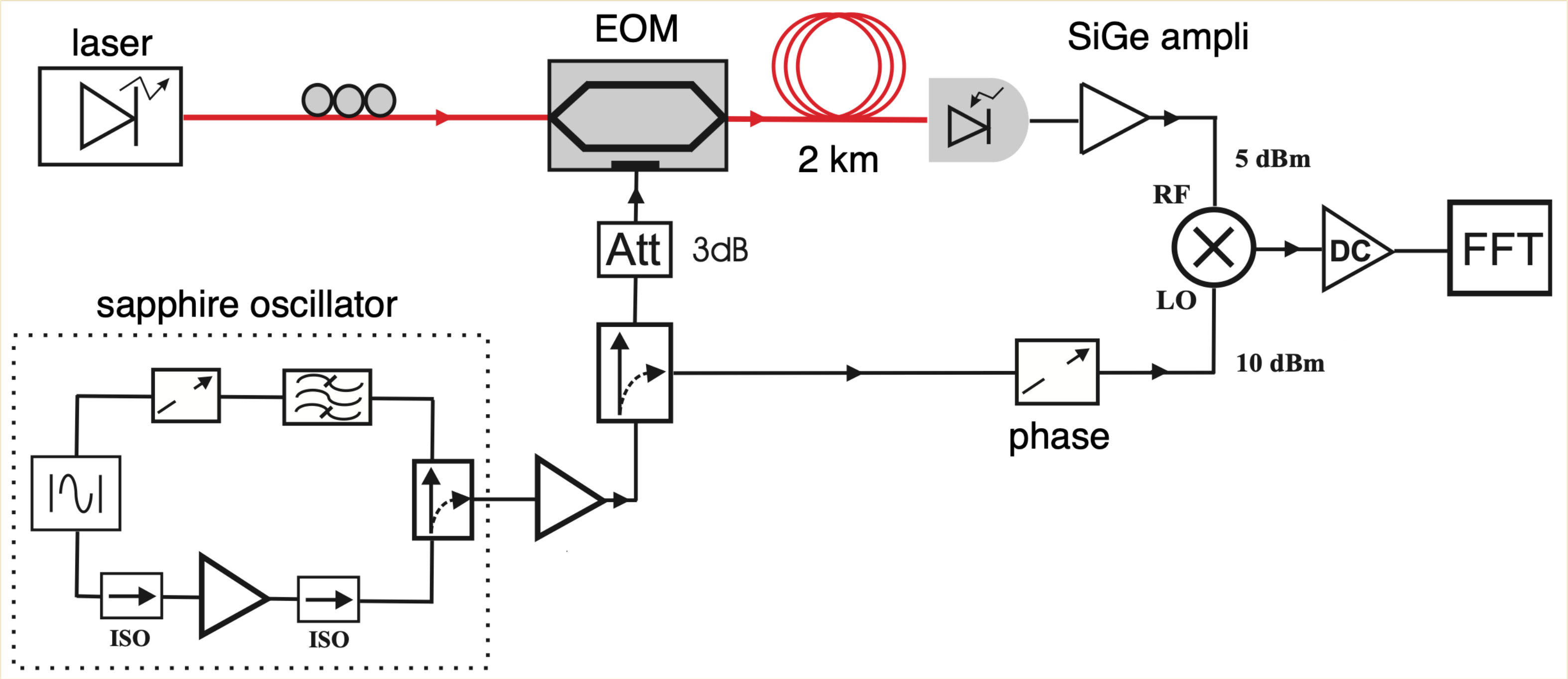

- The laser RIN can limit the instrument sensitivity
- In some cases, the AM noise of the oscillator under test turns into a serious problem (got in trouble with an Anritsu synthesizer)

Measurement of a sapphire oscillator

Volyanskiy & al., JOSAB 25(12) 2140-2150, Dec.2008. Also arXiv:0807.3494v1 [physics.optics] July 2008.

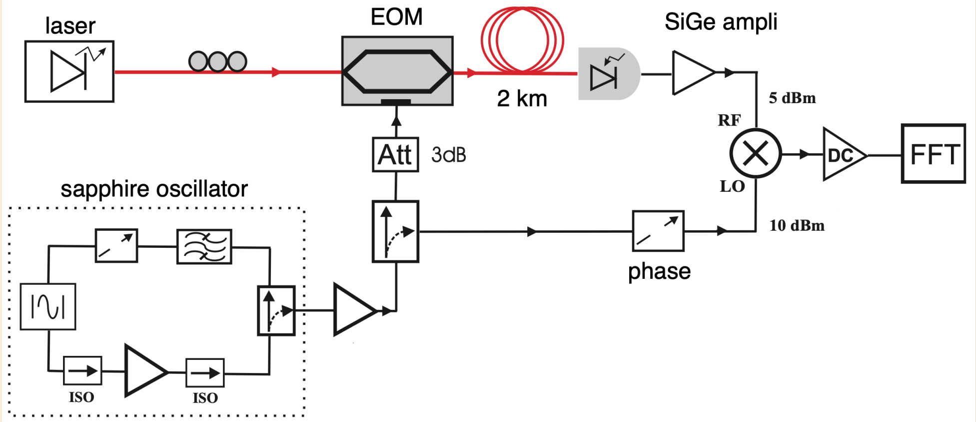

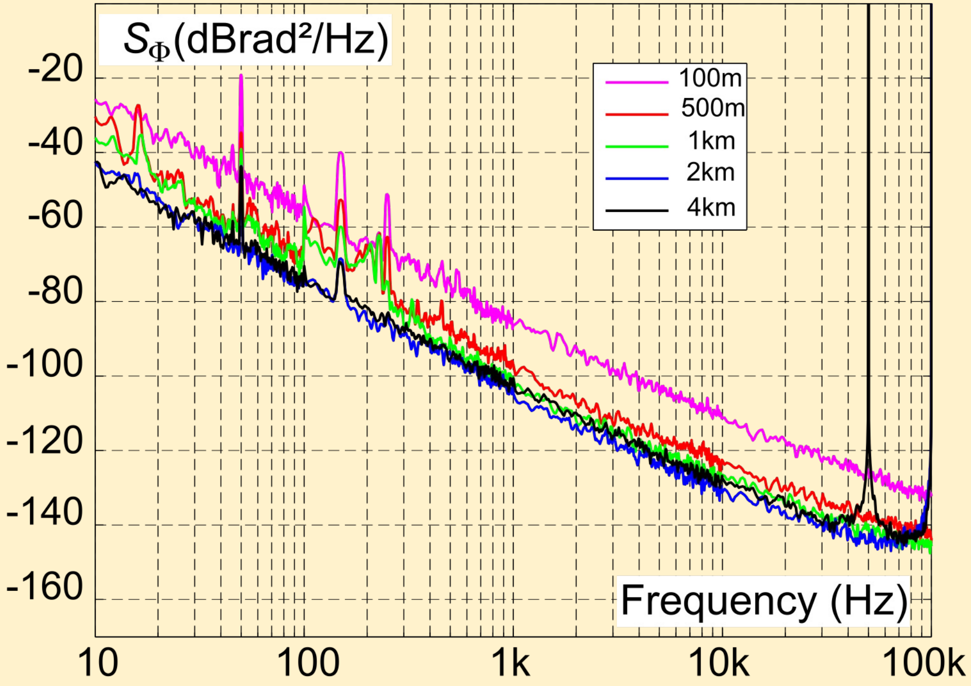

- The instrument noise scales as 1/τ, yet the blue and black plots overlap magenta, red, green => instrument noise
  blue, black => noise of the sapphire oscillator under test
- The 1/ƒ3 phase noise (frequency flicker) outperforms the 10 GHz sapphire oscillator (the lowest-noise microwave oscillator)
- Low AM noise of the oscillator under test is necessary

Measurement of the optical-fiber noise

Volyanskiy & al., JOSAB 25(12) 2140-2150, Dec.2008. Also arXiv:0807.3494v1 [physics.optics] July 2008.

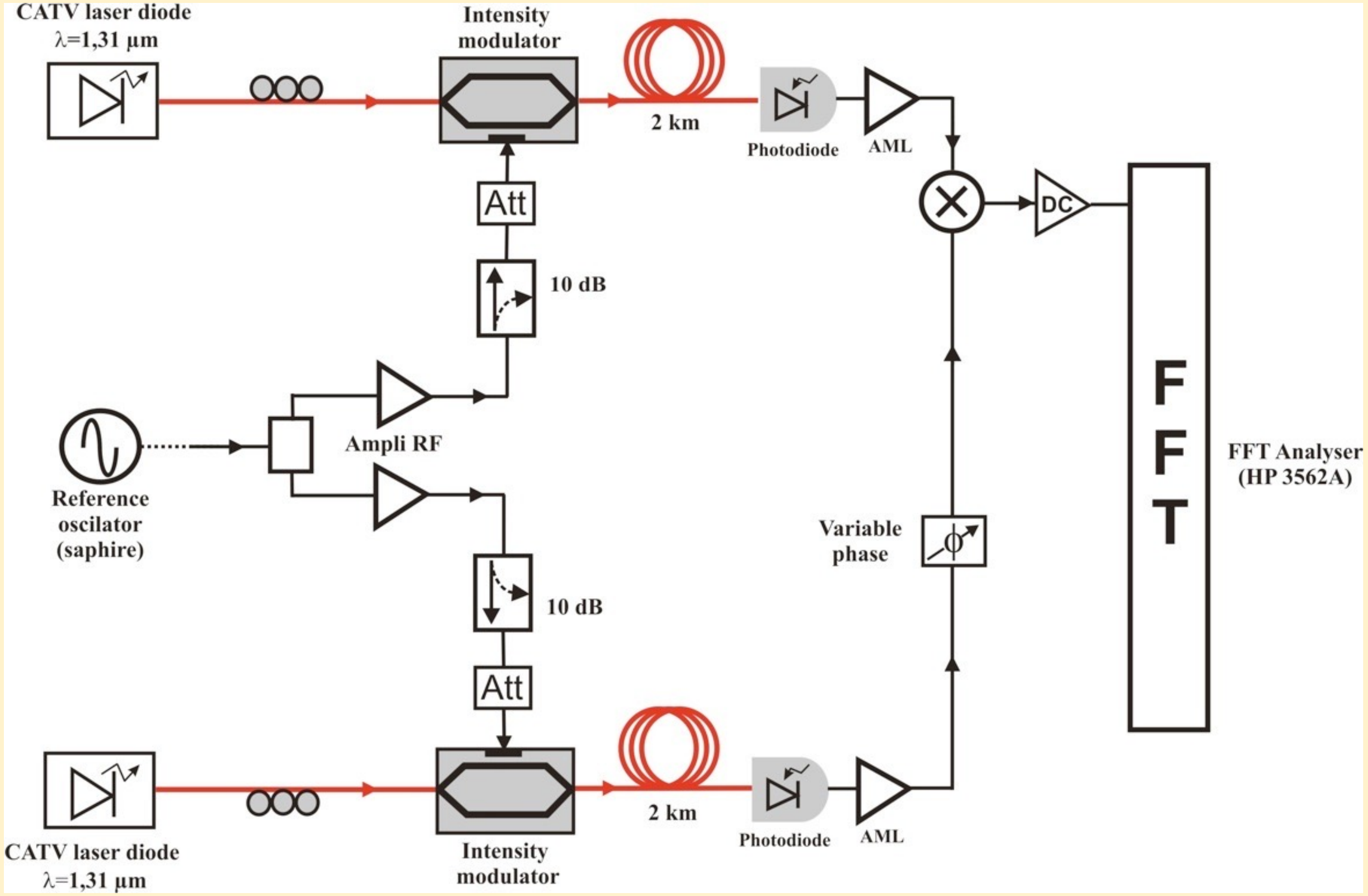

- matching the delays, the oscillator phase noise cancels
- this scheme gives the total noise
  2 × (ampli + fiber + photodiode + ampli) + mixer
  thus it enables only to assess an upper bound of the fiber noise

Measurement of the Optical-Fiber Noise

Volyanskiy & al., JOSAB 25(12) 2140-2150, Dec.2008. Also arXiv:0807.3494v1 [physics.optics] July 2008.

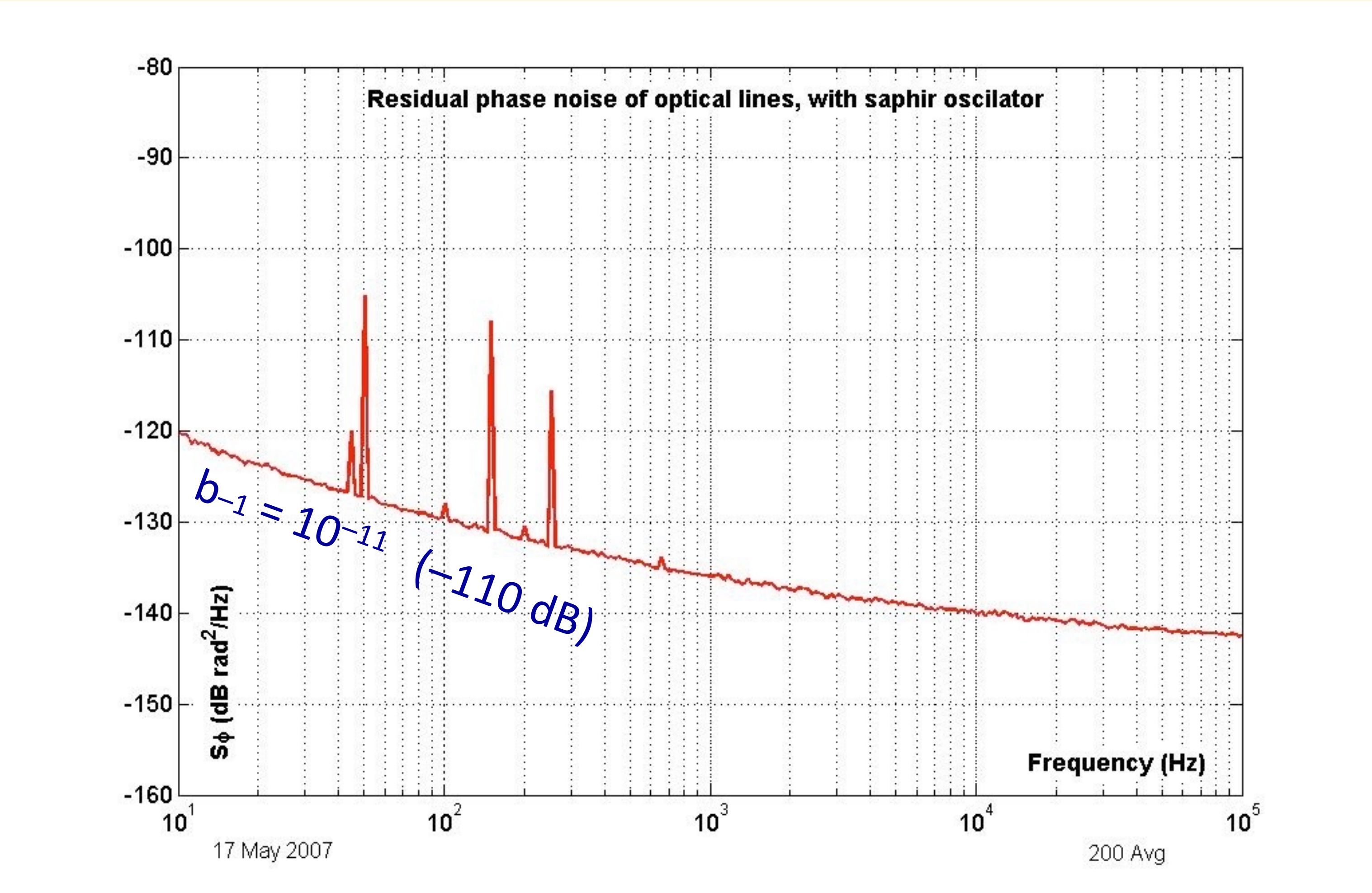

Dual-channel (correlation) measurement

Volyanskiy & al, JOSA B and arXiv:0807.3494v1 [physics.optics] July 2008

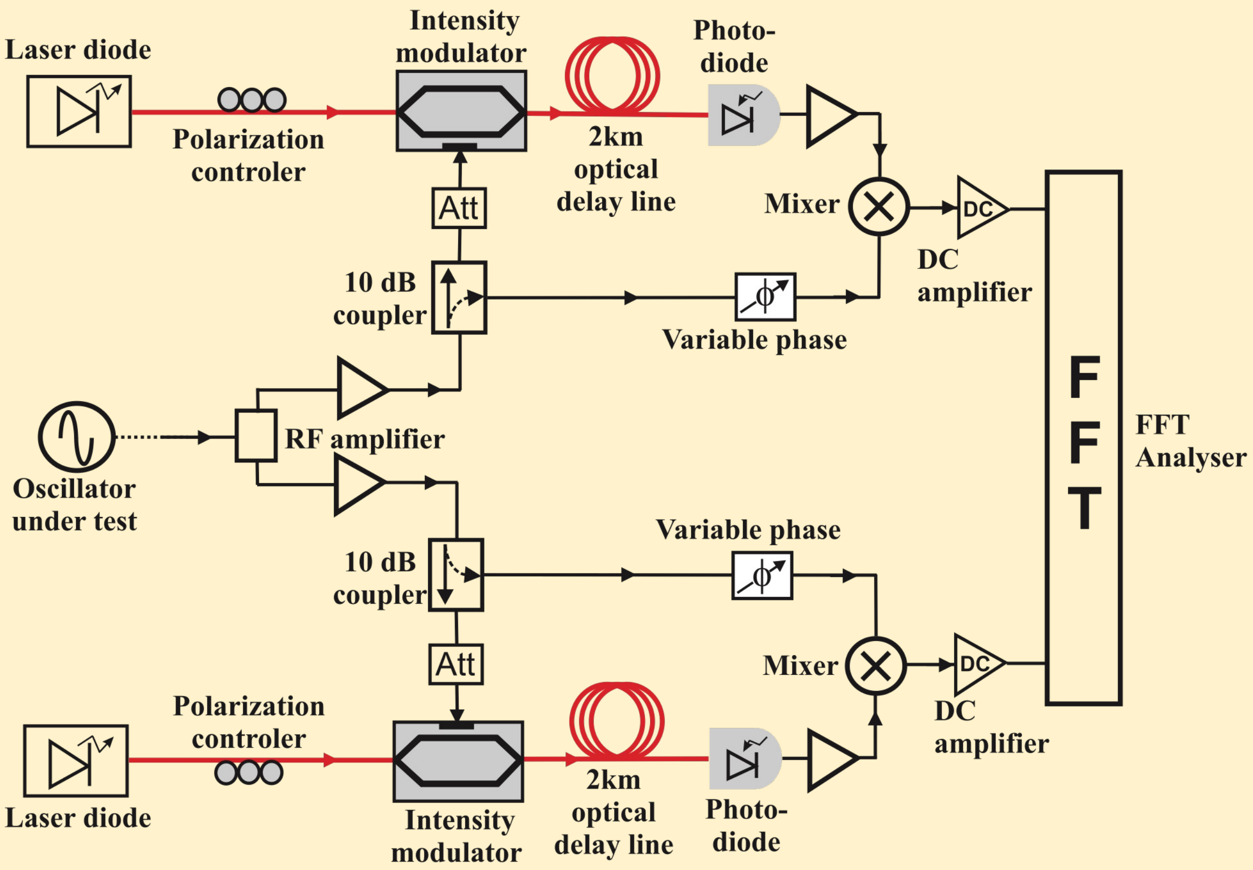

Improvements

- Understanding flicker (photodetectors and amplifiers)
- SiGe technology provides lower 1/f phase noise
- CATV laser diodes exhibit lower AM/FM noise
- Low Vπ EOMs show higher stability because of the lower RF power
- Optical fiber sub-mK temperature controlled

derives from: E. Salik, N. Yu, L. Maleki, E. Rubiola, Proc. Ultrasonics-FCS Joint Conf., Montreal, Aug 2004 p.303-306

Dual-channel (correlation) measurement

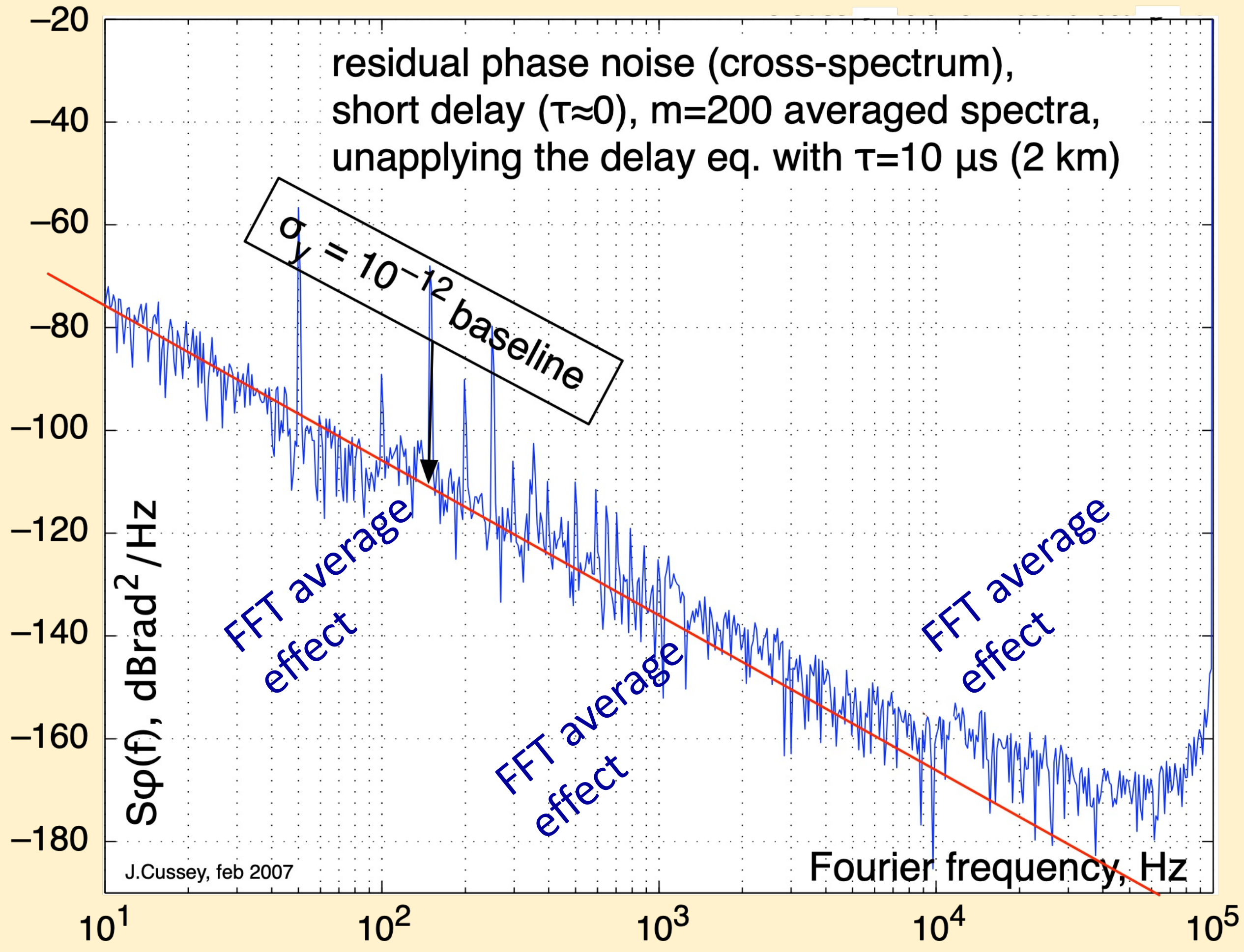

Physical phenomena in optical fibers

Birefringence. Common optical fibers are made of amorphous Ge-doped silica, for an ideal fiber is not expected to be birefringent. Nonetheless, actual fibers show birefringent behavior due to a variety of reasons, namely: core ellipticity, internal defects and forces, external forces (bending, twisting, tension, kinks), external electric and magnetic fields. The overall effect is that light propagates through the fiber core in a non-degenerate, orthogonal pair of axes at different speed. Polarization effects are strongly reduced in polarization maintaining (PM) fibers. In this case, the cladding structure stresses the core in order to increase the difference in refraction index between the two modes.

Polarization mode dispersion (PMD). This effect rises from the random birefringence of the optical fiber. The optical pulse can choose many different paths, for it broadens into a bell-like shape bounded by the propagation times determined by the highest and the lowest refraction index. Polarization vanishes exponentially along the light path. It is to be understood that PMD results from the vector sum over multiple forward paths, for it yields a well-shaped dispersion pattern.

Bragg scattering. In the presence of monocromatic light (usually X-rays), the periodic structure of a crystal turns the randomness of scattering into an interference pattern. This is a weak phenomenon at micron wavelengths because the inter-atom distance is of the order of 0.3--0.5 nm. Bragg scattering is not present in amorphous materials.

Brillouin scattering. In solids, the photon-atom collision involves the emission or the absorption of an acoustic phonon, hence the scattered photons have a wavelength slightly different from incoming photons. An exotic form of Brillouin scattering has been reported in optical fibers, due to a transverse mechanical resonance in the cladding, which stresses the core and originates a noise bump on the region of 200--400 MHz.

Raman scattering. This phenomenon is similar to Rayleigh scattering, but it involves the optical branch of phonons.

Rayleigh scattering. This is random scattering due to molecules in a disordered medium, by which light looses direction and polarization. A small fraction of the light intensity is thereby back-scattered one or more times, for it reaches the fiber end after a stochastic to-and-fro path, which originates phase noise. In SM fibers at 1.55 µm it contributes 0.15 dB/km to the optical loss.

Kerr effect. This effect states that an electric field changes the refraction index. So, the electric field of light modulate the refraction index, which originates the 2nd-order nonlinearity.

Discontinuities. Discontinuities cause the wave to be reflected and/or to change polarization. As the pulse can be split into a pulse train depending on wavelength, this effect can turn into noise.

Group delay dispersion (GVD). There exist dispersion-shifted fibers, that have a minimum GVD at 1550 nm. GVD compensators are also available.

PMD-Kerr compensation. In principle, it is possible that PMD and Kerr effect null one another. This requires to launch the appropriate power into each polarization mode, for two power controllers are needed. Of course, this is incompatible with PM fibers.

Which is the most important effect? In the community of optical communications, PMD is considered the most significant effect. Yet, this is related to the fact that excessive PMD increases the error rate and destroys the eye pattern of a channel. In the case of the photonic oscillator, the signal is a pure sinusoid, with no symbol randomness.

AM-PM Noise in Electronic Devices

Enrico Rubiola

CNRS FEMTO-ST Institute, Besancon, France

INRiM, Torino, Italy

Outline

Introduction

White and flicker noise

(Environment)

Noise in amplifier networks

Low-flicker amplifiers

Experiments

home page http://rubiola.org

Additive vs Parametric Noise

additive noise

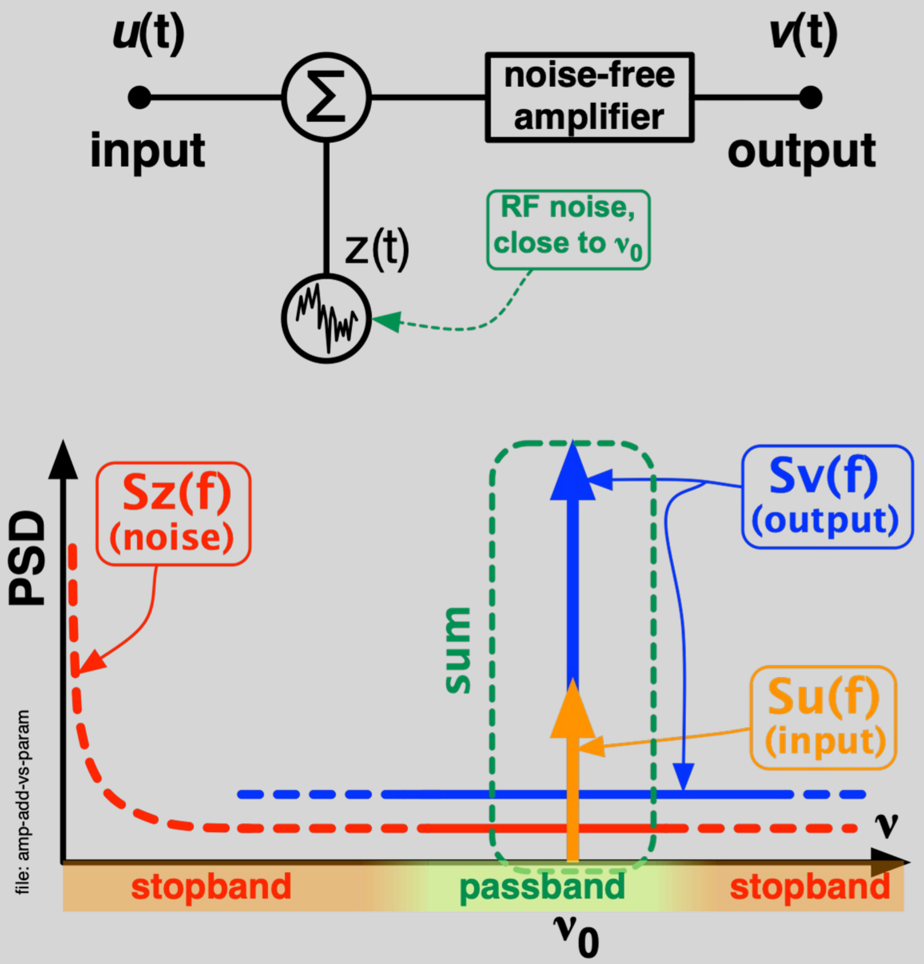

the noise sidebands are independent of the carrier

parametric noise

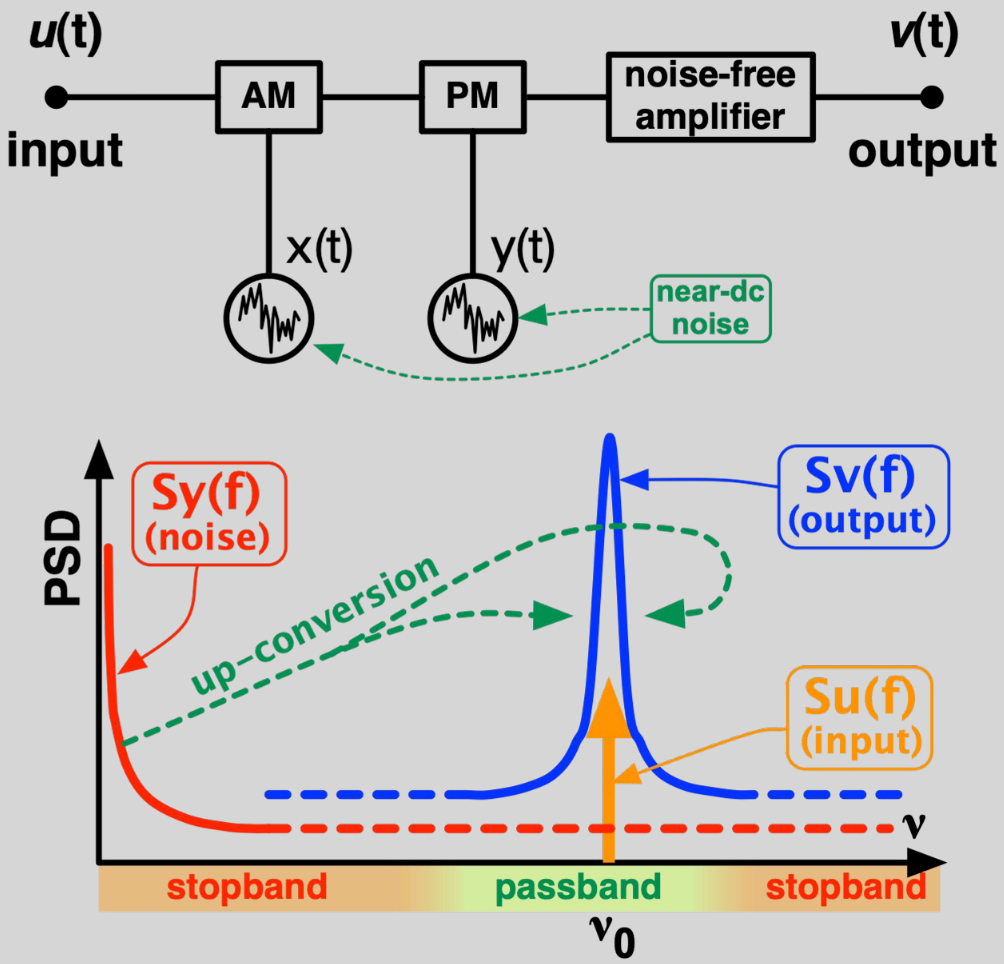

the noise sidebands are proportional to the carrier

AM-PM Noise Types

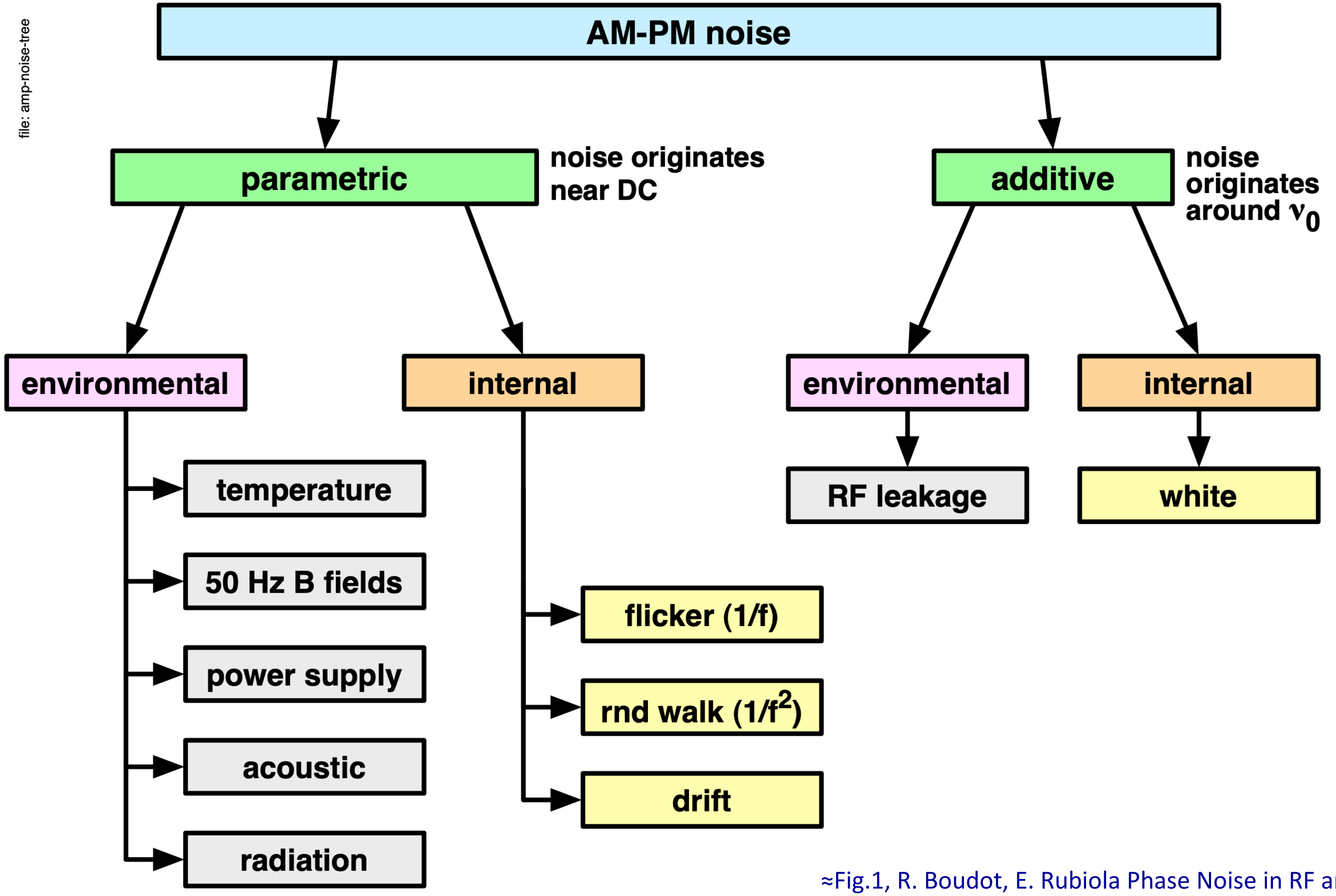

≈Fig.1, R. Boudot, E. Rubiola Phase Noise in RF and Microwave Amplifiers, IEEE T UFFC 59(12) p.613-2628, Dec 2012

Amplifier Flicker Noise

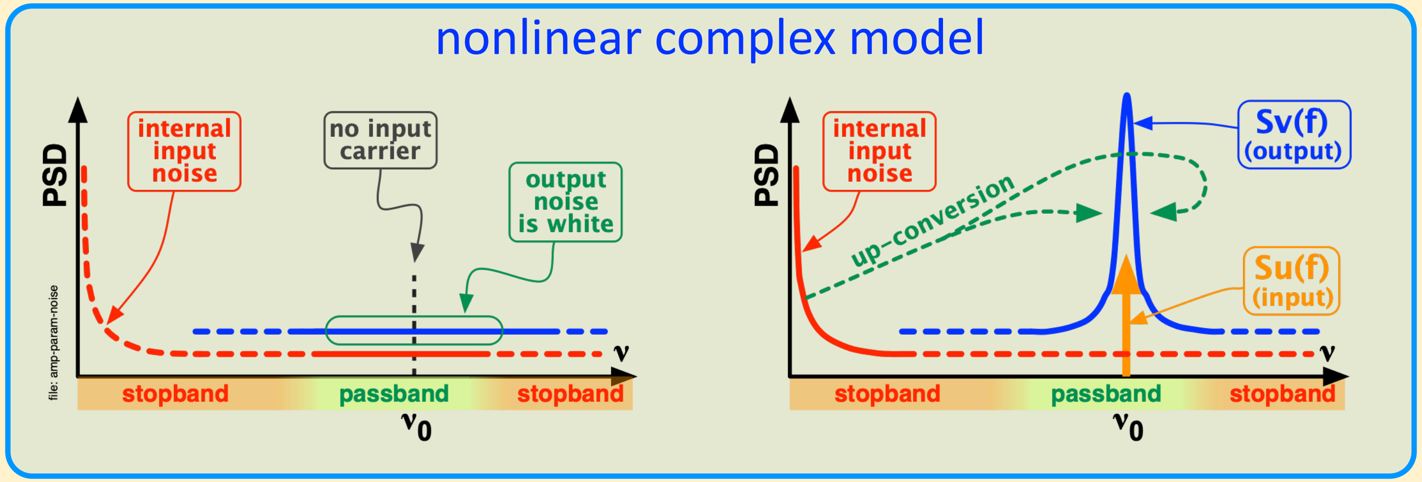

carrier — near-dc noise

$$v_i(t) = V_i\, e^{\imath\omega_0 t} + n'(t) + \imath n''(t)$$

the parametric nature of $1/f$ noise is hidden in n' and n"

substitute (careful, this hides the down-conversion)

$$v_o(t) = a_1 v_i(t) + a_2 v_i^2(t) + \ldots$$

non-linear (parametric) amplifier

expand and select the ω_0 terms

$$v_o(t) = V_i \Big\{ a_1 + 2a_2 \big[n'(t) + \imath n''(t) \big] \Big\} e^{\imath\omega_0 t}$$

The noise sidebands are proportional to the input carrier

get AM and PM noise

$$\alpha(t) = 2\,\frac{a_2}{a_1}\,n'(t) \qquad \varphi(t) = 2\,\frac{a_2}{a_1}\,n''(t)$$

The AM and the PM noise are independent of V_i thus of power

Combining White and Flicker Noise

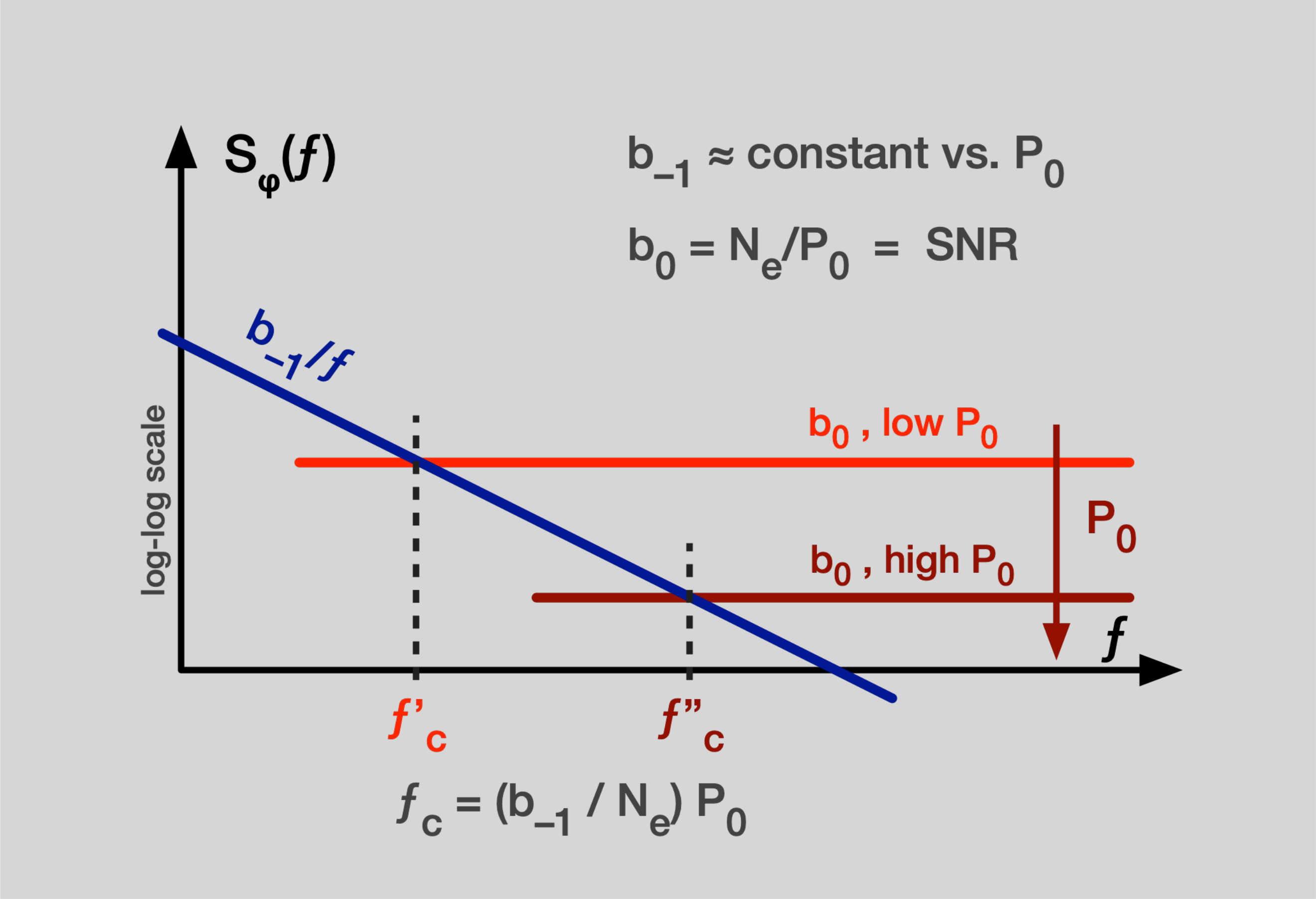

The corner frequency f_c, sometimes specified in data sheets is a misleading parameter because it depends on P_0

Phase Noise vs Power

- The $1/f$ phase noise b_{-1} is about independent of power
- The white noise b_0 scales as the inverse of the power
- The corner frequency is misleading because it depends on power

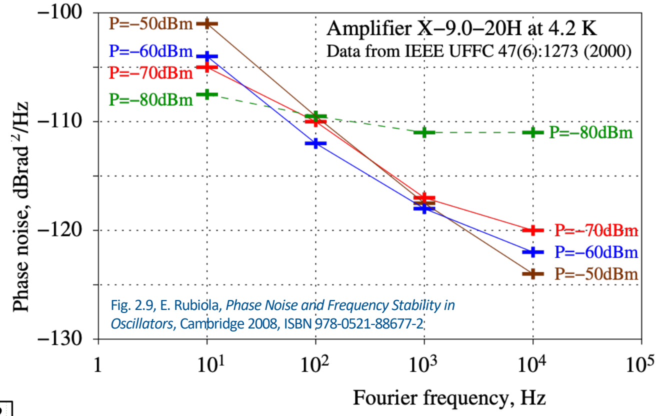

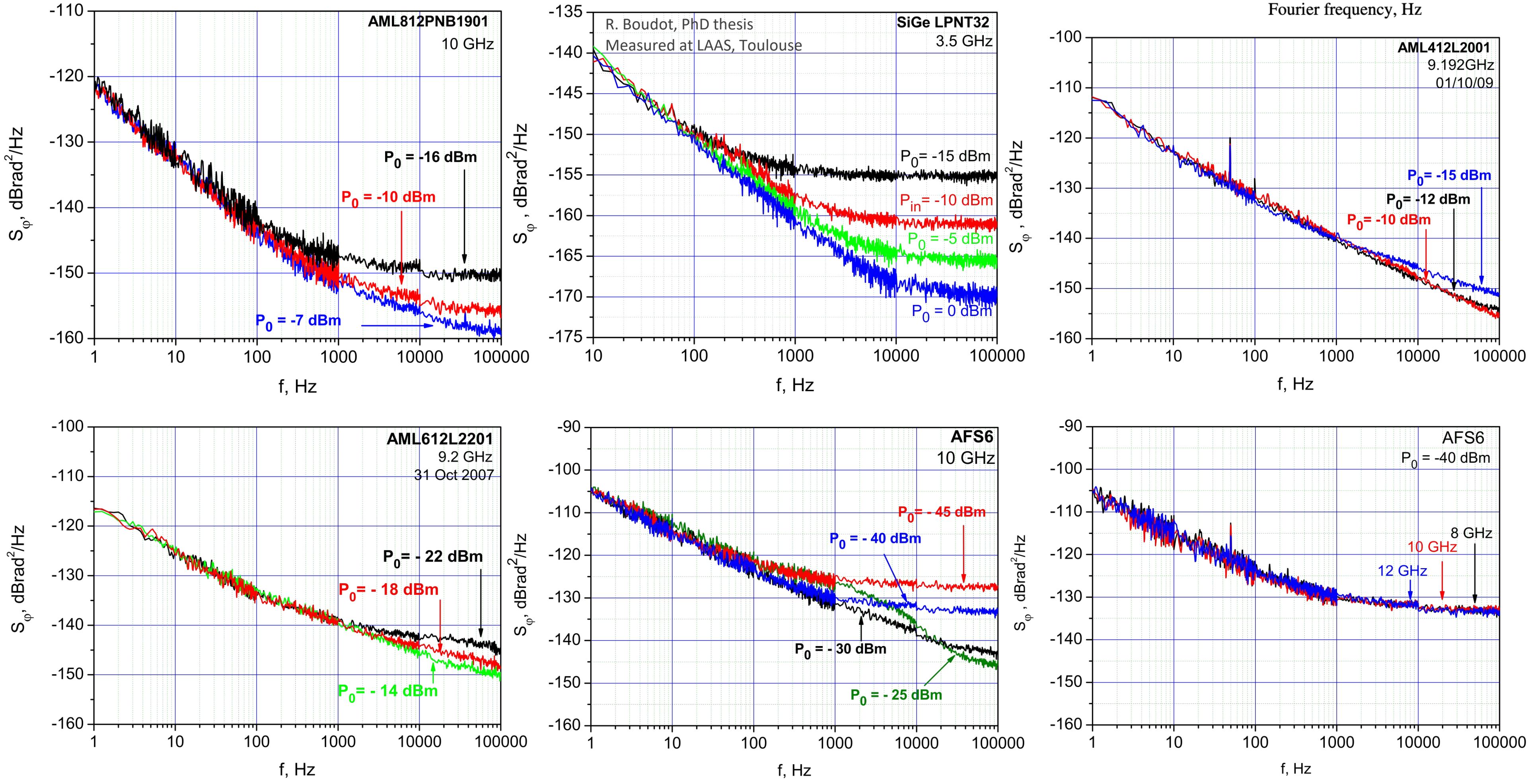

R. Boudot, E. Rubiola Phase Noise in RF and Microwave Amplifiers, IEEE T UFFC 59(12) p.613-2628, Dec 2012 (Fig.6 a-f, rearranged)

Example – Microwave Amplifier

Courtesy of V. Giordano,
FEMTO-ST Institute

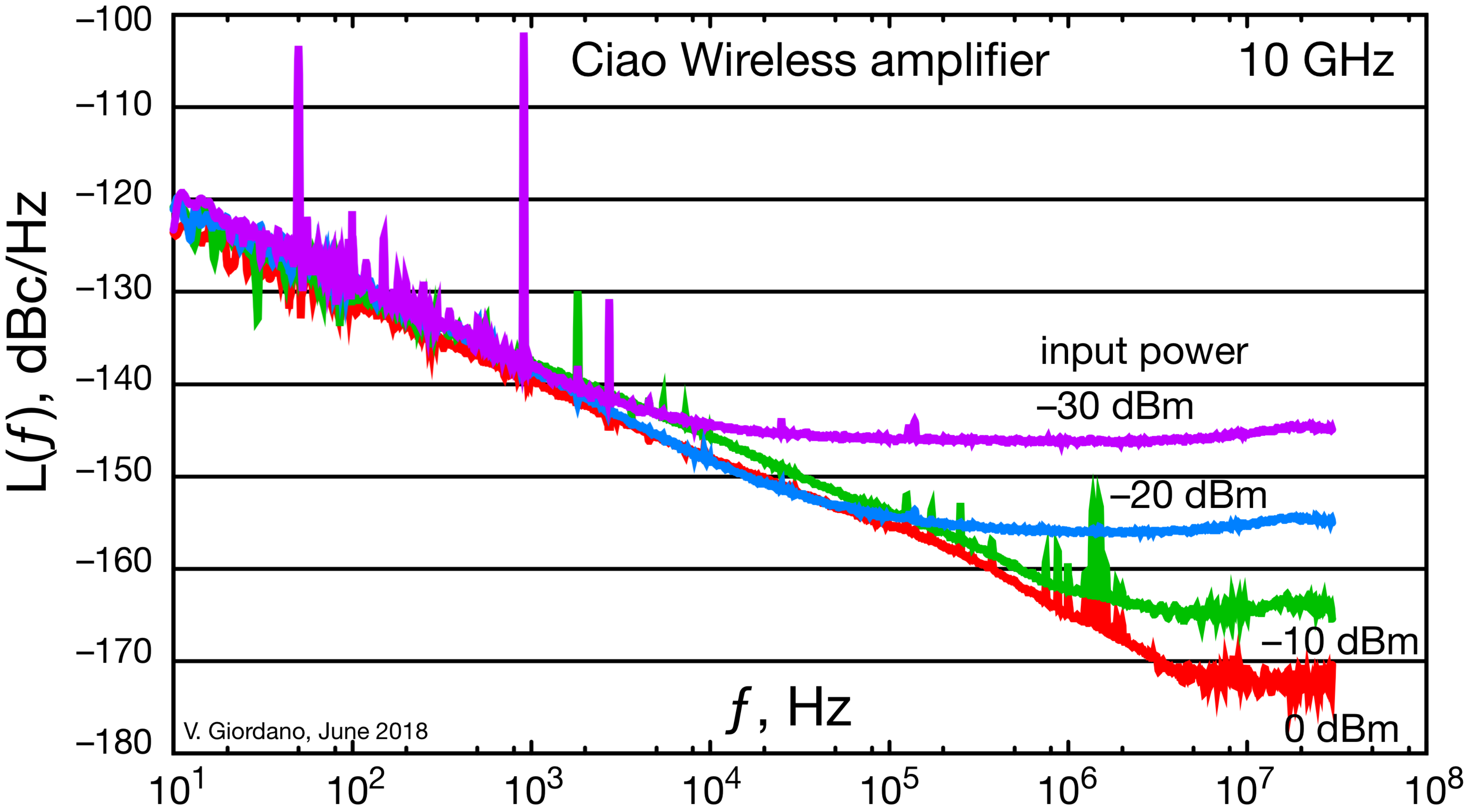

Correlation Between AM and PM Noise

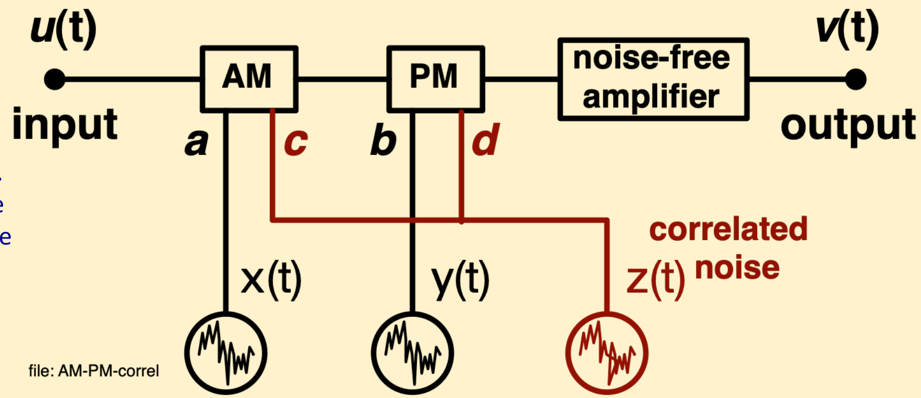

Fig.10, R. Boudot, E. Rubiola Phase Noise in RF and Microwave Amplifiers, IEEE T UFFC 59(12) p.613-2628, Dec 2012

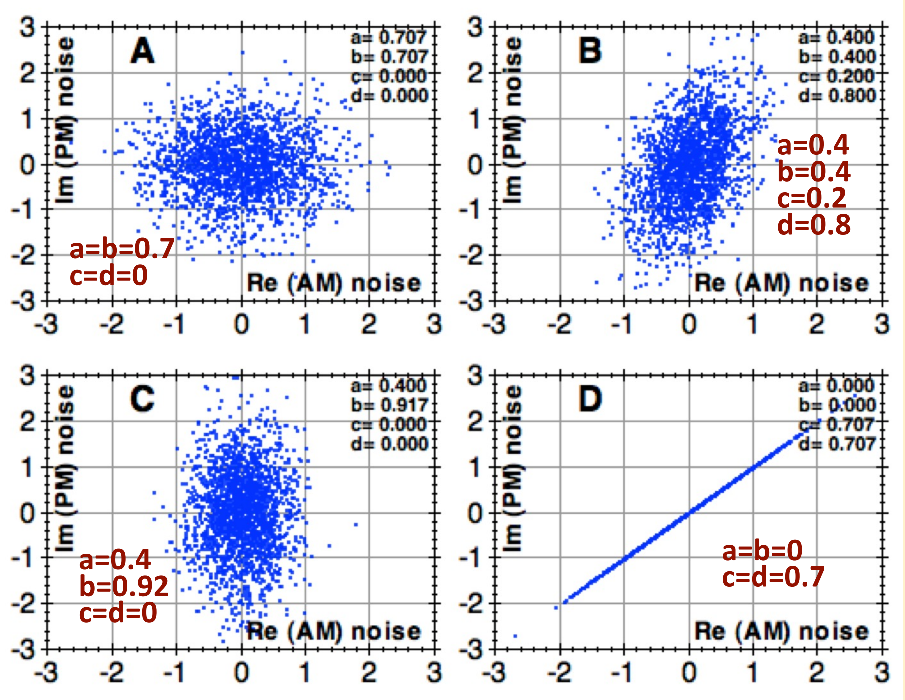

Fig.11, R. Boudot, E. Rubiola Phase Noise in RF and Microwave Amplifiers, IEEE T UFFC 59(12) p.613-2628, Dec 2012

$$a^2 + b^2 + c^2 + d^2 = 1$$

The need for this model comes from the physics of popular amplifiers

- AM and PM fluctuations are correlated because originate from the same near-dc random process
- Bipolar transistor. The fluctuation of the carriers in the base region acts on the base thickness, thus on the gain, and on the capacitance of the reverse-biased base-collector junction.
- Field-effect transistor. The fluctuation of the carriers in the channel acts on the drain-source current, and also on the gate-channel capacitance because the distance between the \`electrodes' is affected by the channel thickness.
- Laser amplifier. The fluctuation of the pump power acts on the density of the excited atoms, and in turn on gain, on maximum power, and on refraction index.

Flicker of Some Amplifiers

Amplifier	Frequency (GHz)	Gain (dB)	$P_{1\,\mathrm{dB}}$ (dBm)	F (dB)	DC bias	b_{-1} (meas.) (dBrad^2/Hz)
AML812PNB1901	8 – 12	22	17	7	15 V, 425 mA	–122
AML412L2001	4 – 12	20	10	2.5	15 V, 100 mA	–112.5
AML612L2201	6 – 12	22	10	2	15 V, 100 mA	–115.5
AML812PNB2401	8 – 12	24	26	7	15 V, 1.1A	–119
AFS6	8 – 12	44	16	1.2	15 V, 171 mA	–105
JS2	8 – 12	17.5	13.5	1.3	15 V, 92 mA	–106
SiGe LPNT32	3.5	13	11	1	2 V, 10 mA	–130
Avantek UTC573	0.01 – 0.5	14.5	13	3.5	15 V, 100 mA	–141.5
Avantek UTO512	0.005–0.5	21	8	2.5	15 V, 23 mA	–137

R. Boudot, E. Rubiola Phase Noise in RF and Microwave Amplifiers,
IEEE T UFFC 59(12) p.613-2628, Dec 2012 (Tab.I, ≠artwork)

Flicker Noise of Components

device	PM b_{-1}	AM h_{-1}	frequency	References and comments
Si bipolar HF-UHF amplifier	–135 … –145		5…1000 MHz	(general experience)
SiGe HBT µwave amplifier	–120 … –130		4…20 GHz	(general experience)
GaAs HBT µwave amplifier	–95 … –110		3…10 GHz	(general experience)
Cr3+ maser amplifier (0.2 cm3)	≈ –160		11 GHz	G.J.Dick, private discussion
HF-UHF double-balanced mixer	–135 … –150		5…1000 MHz	(general experience)
µwave double-balanced mixer	–110 … –125		4…20 GHz	(general experience)
µwave circulator (iso port)	–170	–170	9.1 GHz	Rubiola & al, IEEE T.UFFC 51(8) 957-963 (2004)
µwave isolator (terminated circulator)	–150	–150	≈ 10 GHz	Woode & al, MST 9(9) 1593-9 (1998)
HF-UHF ferrite power splitter	–170	–170	100 MHz	Rubiola, Giordano, RSI 73(6) 2445-2457 (2002)
HF-UHF variab. attenuator (potentiometer)	–150		100 MHz	Rubiola, Giordano, RSI 70(1) 220-225 (1999)
HF-UHF by-step attenuator	–170	–170	100 MHz	Rubiola, Giordano, RSI 73(6) 2445-2457 (2002)
µwave variable attenuator (absorber)	–150		9.1 GHz	Rubiola, Giordano, RSI 70(1) 220-225 (1999)
µwave line stretcher	–150		100 MHz	Rubiola, Giordano, RSI 70(1) 220-225 (1999)
µwave power detector (Schottky)	----	–120	10 GHz	Grop, Rubiola, preliminary (in progress)
µwave photodetector	–120	–120	10 GHz	Rubiola & al, TMTT/JLT 54(2) 816-820 (2006)
2-4 km optical-fiber microwave link	< –110		10 GHz	Volyanskiy & al, JOSAB 25(12) 2140-2150 (2008)

Line Stretcher

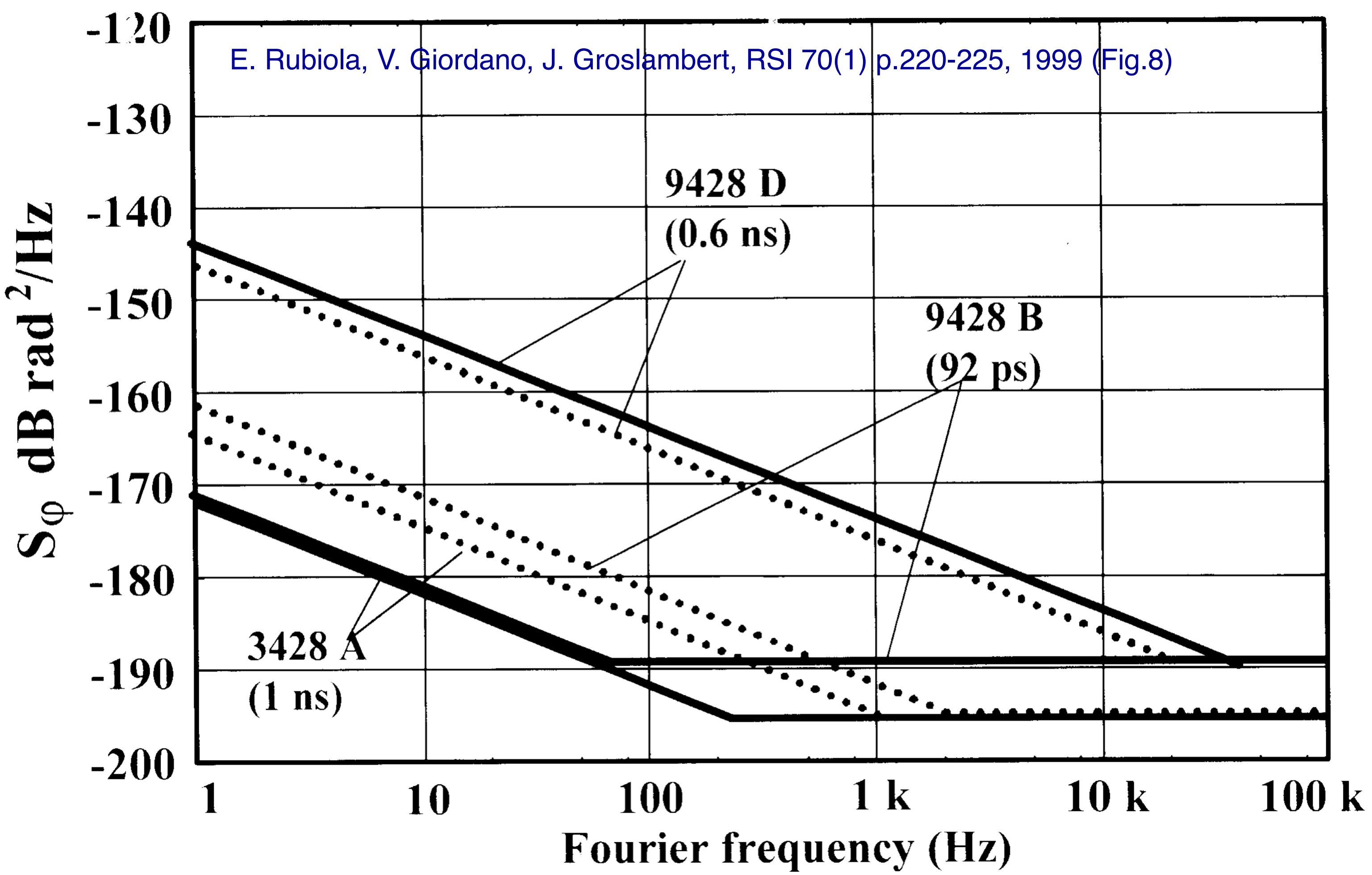

Microwave line stretchers measured at 100 MHz (all devices are manufactured by Arra)

solid line: PM noise,
dotted line: AM noise

Circulators in Isolation Mode

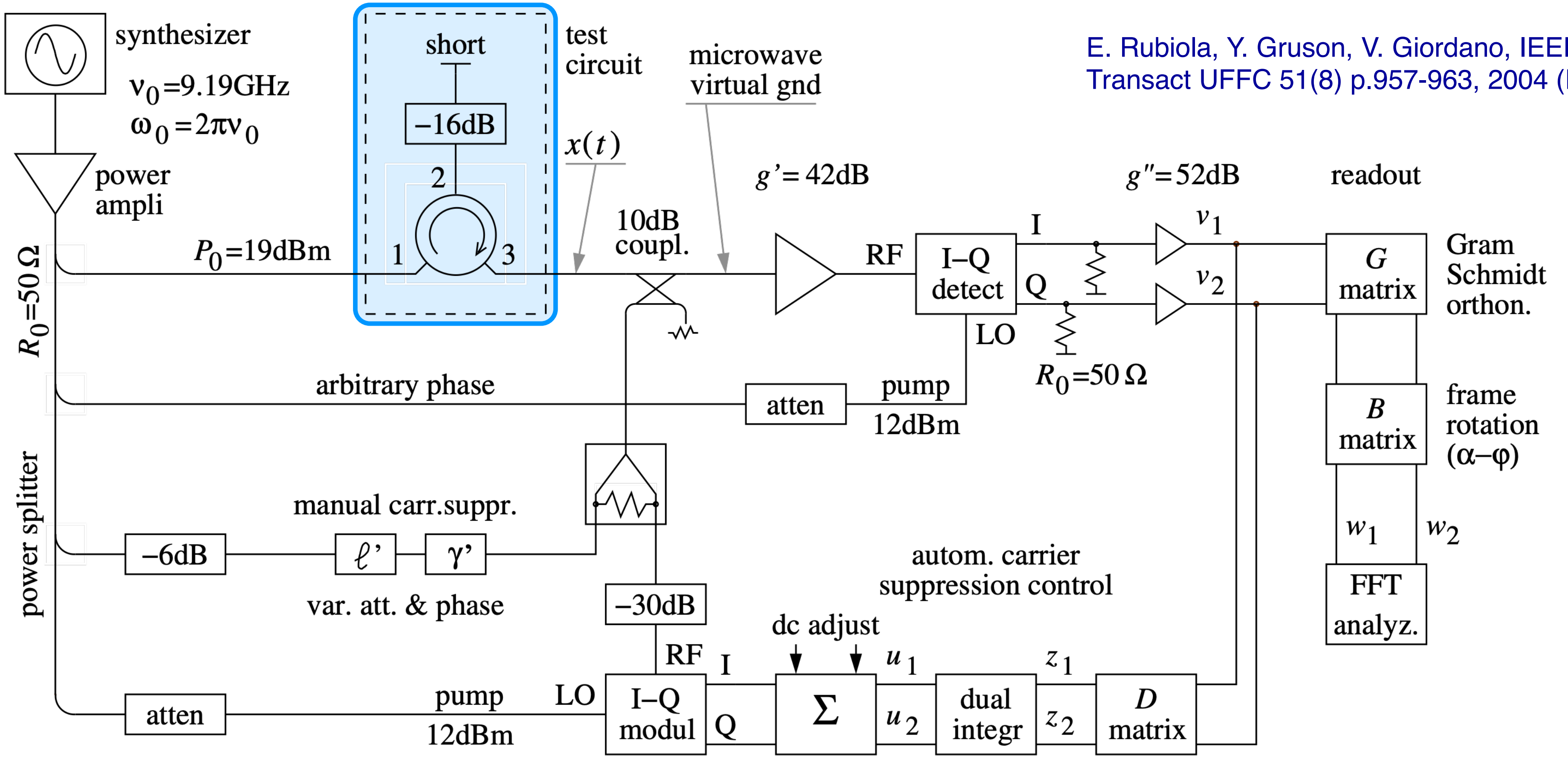

E. Rubiola, Y. Gruson, V. Giordano, IEEE Transact UFFC 51(8) p.957-963, 2004 (Fig.3)

- Destructive interference takes place inside the circulator
- The instruments amplifies and detects the noise sidebands
- The test circuit simulates the insertion in the Pound frequency control

Circulators in Isolation Mode

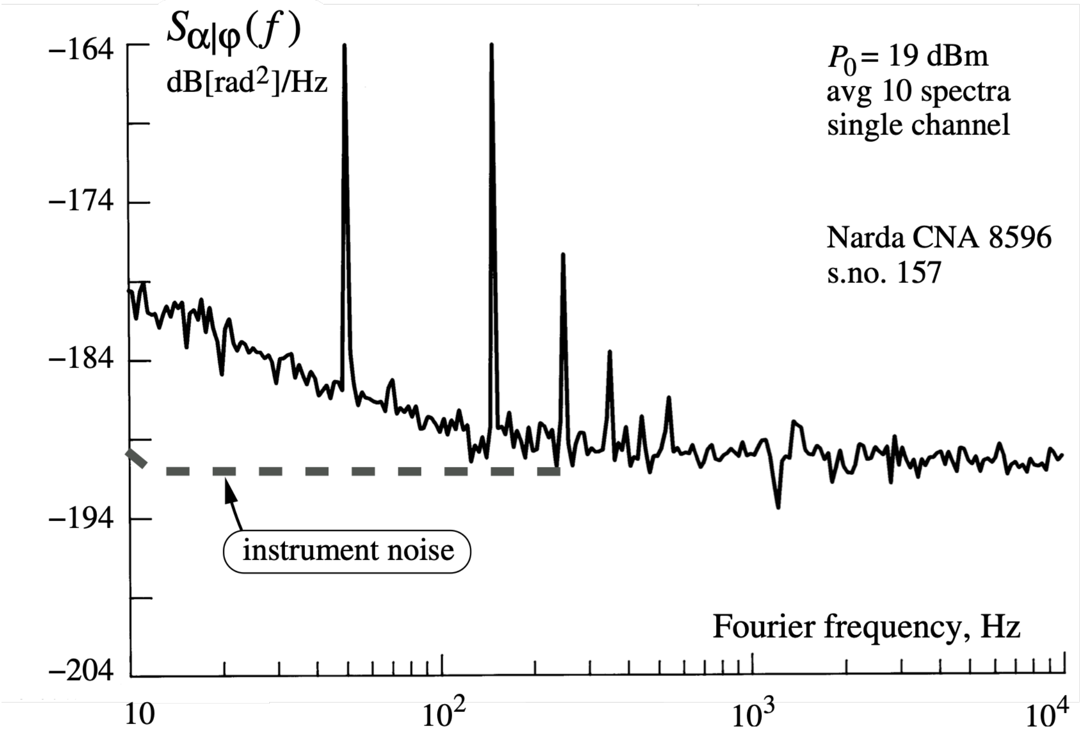

E. Rubiola, Y. Gruson, V. Giordano, IEEE Transact UFFC 51(8) p.957-963, 2004 (Fig.4)

factory and device type	ser. no.	$S_{\alpha\|\varphi}(1\,\text{Hz})$ dB[rad^2]/Hz min.	max.	equivalent stability oscillator $\sigma_y(\tau)$, $\times 10^{-15}$	mechanical $\sigma_l(\tau)$, $\times 10^{-12}$ m
Aercomm J180-124	1320	−165.1	−162.6	22	36
Dorado 4CCC 10-1 ⋆	101	−171.6	−168.0	12	19
Trak C80124/A	E001	−165.9	−160.3	28	47
	E003	−165.7	−164.0	19	31
Narda CNA 8596	157	−170.3	−170.3	9	15
	158	−170.3	−169.1	10	17
Sivers Lab 7041X ‡	625	−176.0	−164.0	n.a.	n.a.
residual instrum. noise		< 180			(4.9)

⋆ designed for cryogenic applications
‡waveguide isolator

E. Rubiola, Y. Gruson, V. Giordano, IEEE Transact UFFC 51(8) p.957-963, 2004 (Tab.I, ≠artwork)

Circulators in Transmission Mode

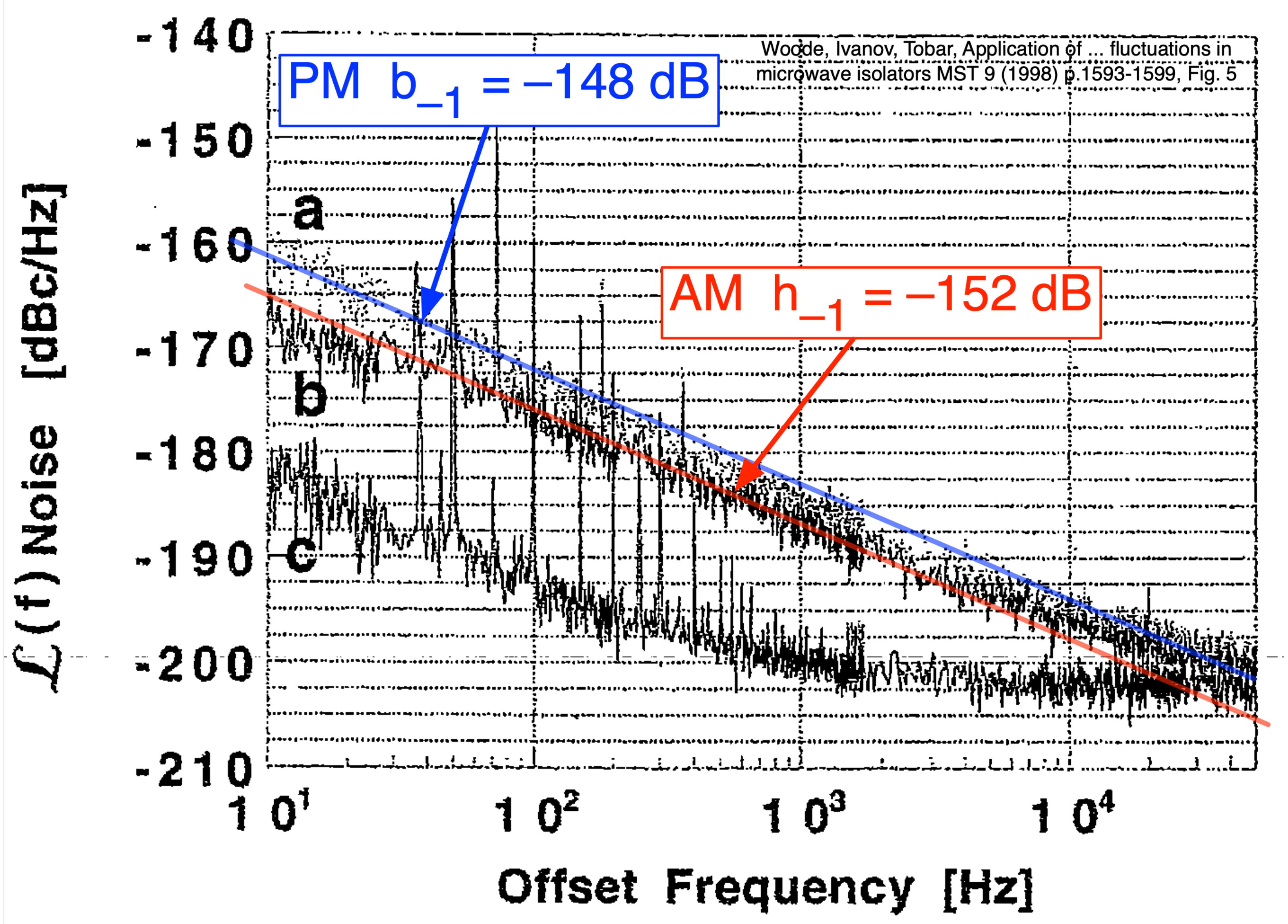

The typical $1/f$ noise b_{-1} is of the order of –150 dB

RA Woode, EN Ivanov, ME Tobar, "Application of The Interferometric Noise Measurement Technique for the Study of Intrinsic Fluctuations in Microwave Isolators," Meas. Sci. Technol., vol. 9, no. 9, pp. 1593-9, 1998 (Fig.5)

There can be a 2-3 dB calibration error on this figure, see my annotations on the scanned article.

VHF Passive Devices

two by-step attenuators

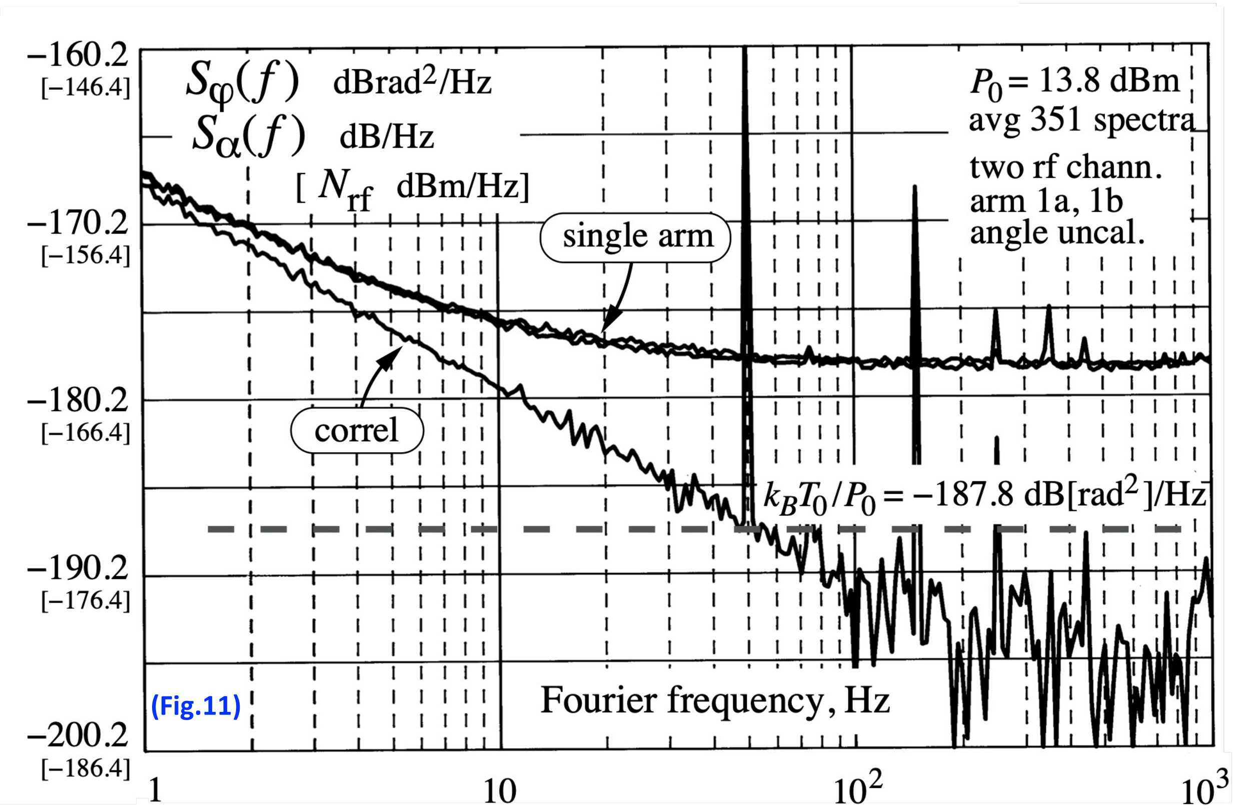

two ferrite hybrid junctions

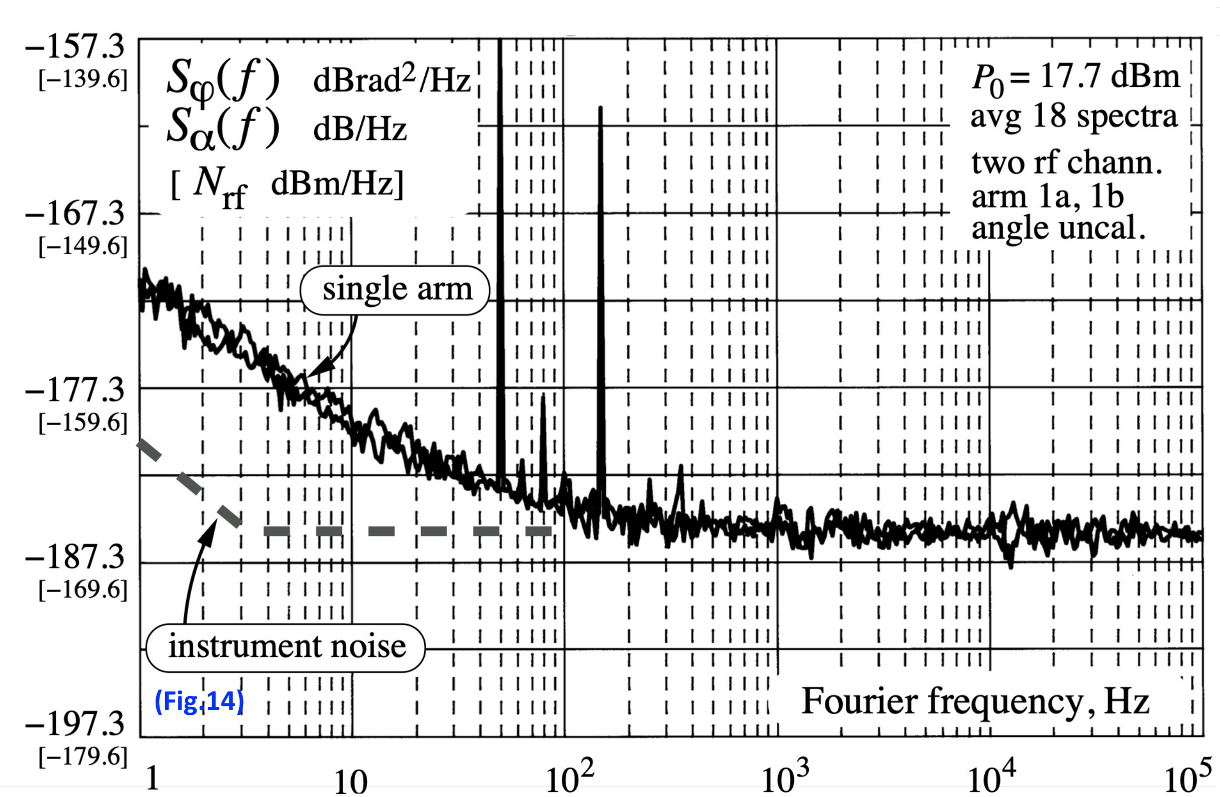

Figs from E. Rubiola, V. Giordano, RSI 73(6) p.2445-2457, 2002

Environmental Effects in RF Amplifiers

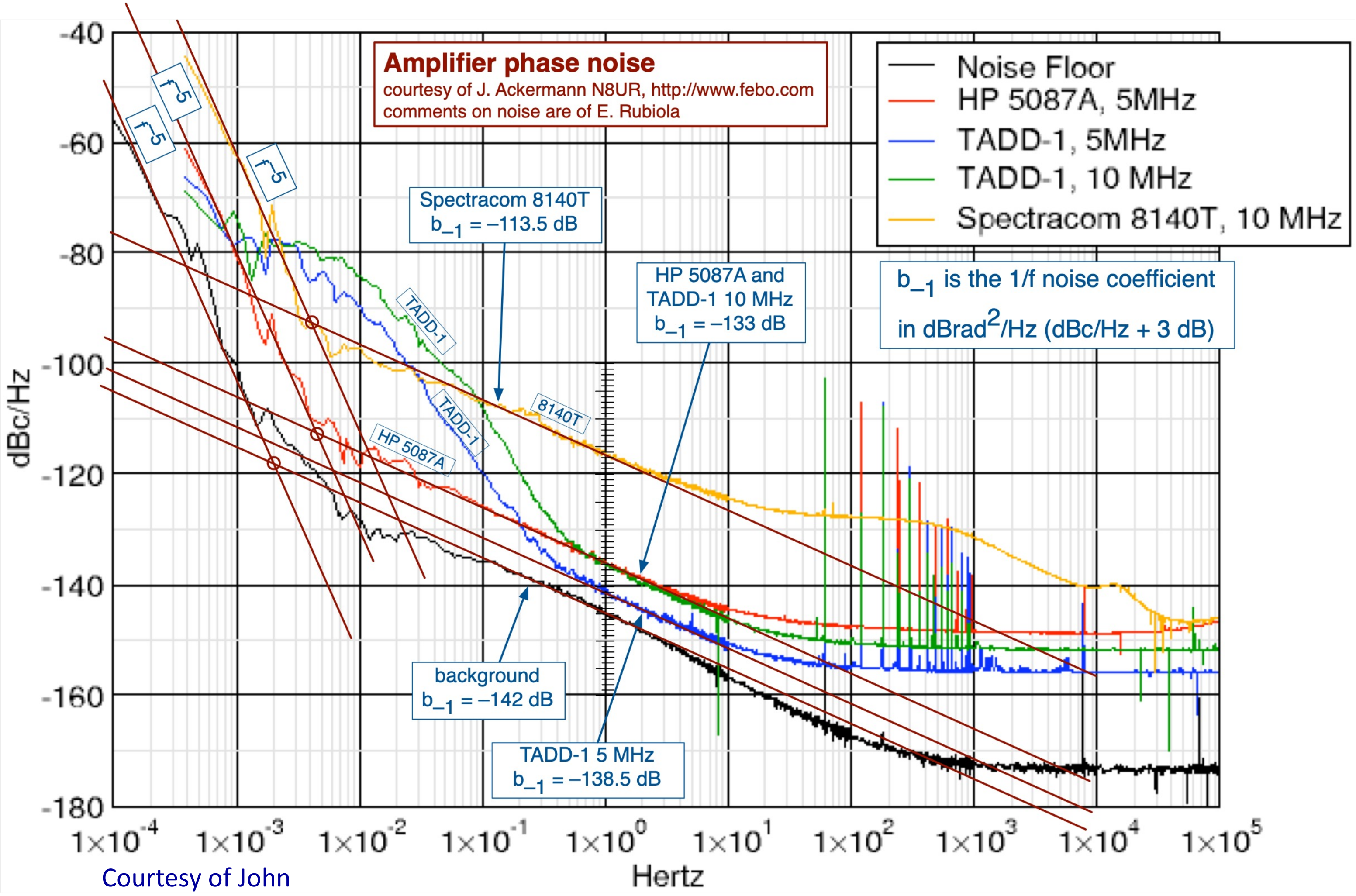

Courtesy of John Ackermann, N8UR

It is experimentally observed that the temperature fluctuations cause a spectrum $S\_\alpha(f)$ or $S_\varphi(f)$ of the $1/f^5$ type

Yet, at lower frequencies the spectrum folds back to $1/f$

Noise in Amplifier Networks

Still not like how this section is organized

White Noise in Cascaded Amplifiers

White noise is chiefly the noise of the first stage

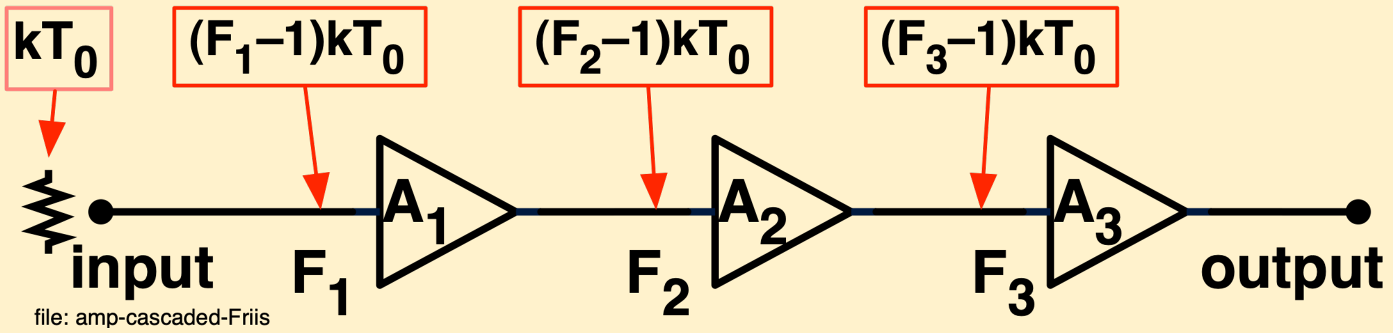

$$N_e = F_1 k T_0 + \frac{(F_2 - 1)kT_0}{A_1^2} + \frac{(F_3 - 1)kT_0}{A_2^2 A_1^2} + \ldots$$

$$F = F_1 + \frac{(F_2 - 1)}{A_1^2} + \frac{(F_3 - 1)}{A_2^2 A_1^2} + \ldots$$

Friis formulae
H. T. Friis, Proc. IRE 32
p.419-422, jul 1944
Noise is chiefly that of the 1st stage

$$b_0 = \frac{FkT_0}{P_0}$$

white
phase noise

$$b_0 = \frac{F_1 k T_0}{P_0} + \frac{(F_2 - 1)kT_0}{A_1^2 P_0} + \frac{(F_3 - 1)kT_0}{A_2^2 A_1^2 P_0} + \ldots$$

Friis formula
for phase noise

Parametric Noise in Cascaded Amplifiers

E. Rubiola, Phase Noise and Frequency Stability in Oscillators, Cambridge 2008, ISBN 978-0521-88677-2

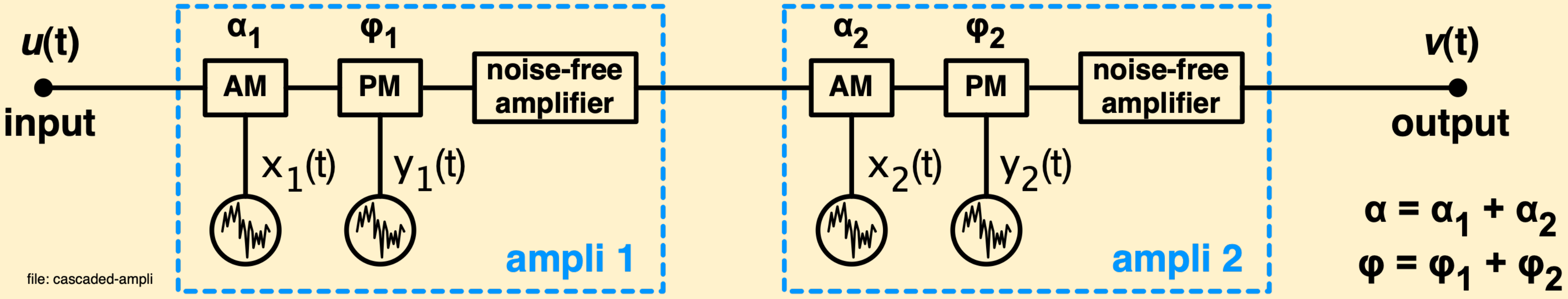

Flicker: the two amplifiers are independent

$$\mathbb{E}\{\alpha^2\} = \mathbb{E}\{\alpha_1^2\} + \mathbb{E}\{\alpha_2^2\} \qquad S_\alpha = S_{\alpha\,1} + S_{\alpha\,2}$$

$$\mathbb{E}\{\varphi^2\} = \mathbb{E}\{\varphi_1^2\} + \mathbb{E}\{\varphi_2^2\} \qquad S_\alpha = S_{\varphi\,1} + S_{\varphi\,2}$$

Environment: a single process drives the two amplifiers

$$\alpha = \alpha_1 + \alpha_2 \qquad \mathbb{E}\{\alpha^2\} = \mathbb{E}\{(\alpha_1 + \alpha_2)^2\}$$

$$\varphi = \varphi_1 + \varphi_2 \qquad \mathbb{E}\{\varphi^2\} = \mathbb{E}\{(\varphi_1 + \varphi_2)^2\}$$

Yet there can be a time constant, not necessarily the same for the two devices

Phase Noise in Cascaded Amplifiers

R. Boudot, E. Rubiola Phase Noise in RF and Microwave Amplifiers, IEEE T UFFC 59(12) p.613-2628, Dec 2012 (Fig.7 a-c, rearranged)

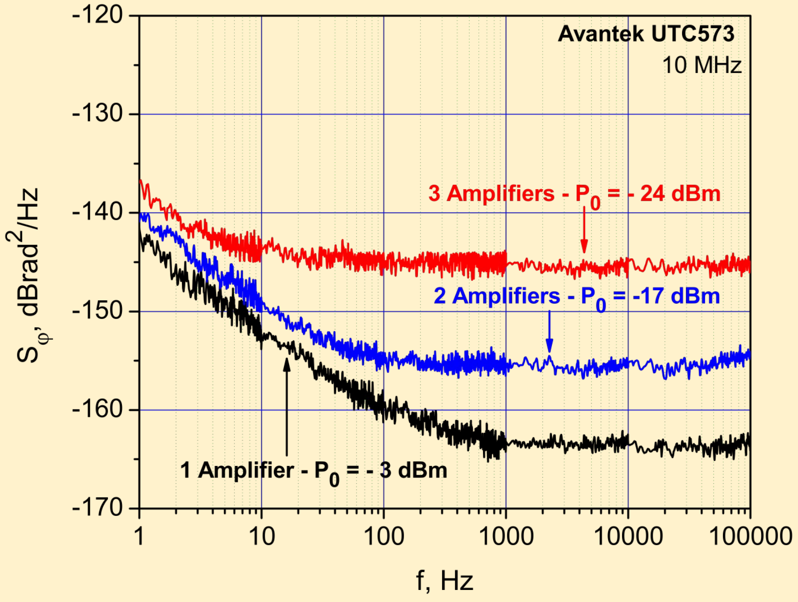

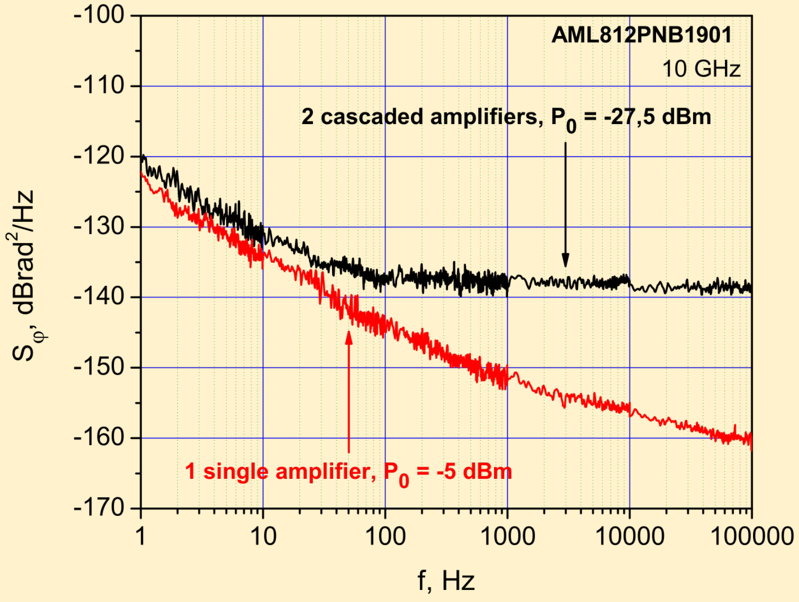

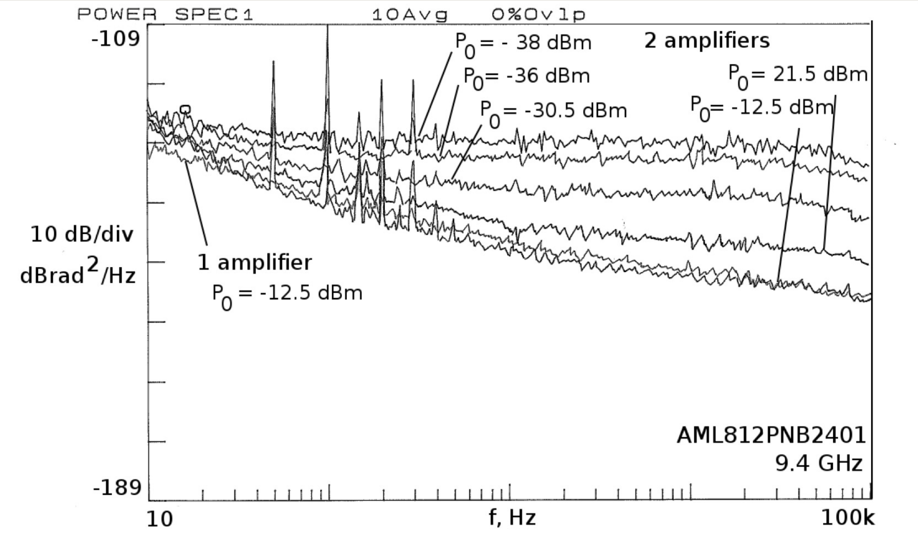

The expected flicker of a cascade increases by:

3 dB, with 2 amplifiers

4.8 dB, with 3 amplifiers

White noise is limited by the (small) input power

Flicker Noise in Parallel Amplifiers

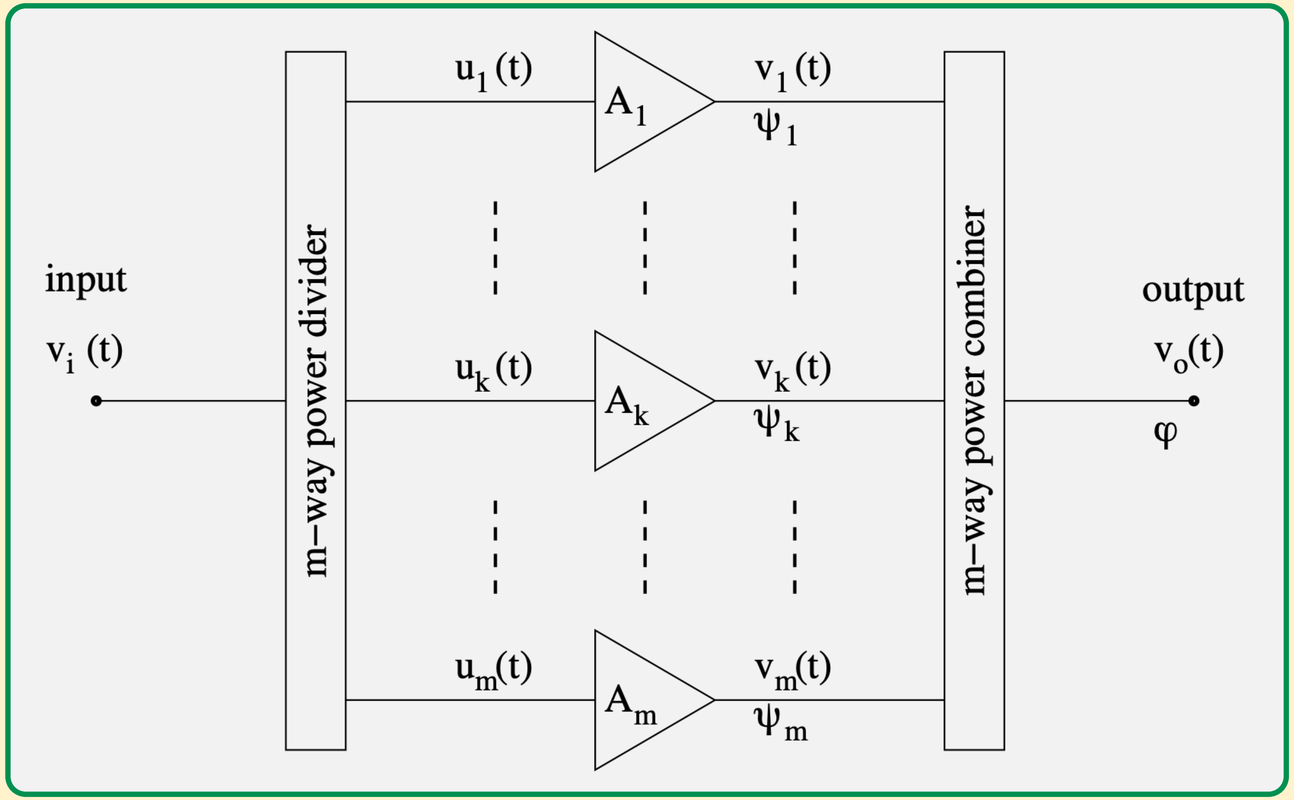

Fig.2.16 from E. Rubiola, *Phase Noise and Frequency Stability in Oscillators*, Cambridge 2008, ISBN 978-0521-88677-2

$$b_{-1} = \frac{1}{m}\left[b_{-1}\right]_{\text{cell}}$$

- The phase flicker coefficient b_{-1} is about independent of power
- The flicker of a branch is not increased by splitting the input power
- At the output,
  - the carrier adds up coherently
  - the phase noise adds up statistically
- Hence, the $1/f$ phase noise is reduced by a factor m
- Only the flicker noise can be reduced in this way

Parallel Amplifiers, Mathematics

$$u_k(t) = \frac{1}{\sqrt{m}} v_i(t) \qquad \text{cell input}$$

$$v_o(t) = \frac{1}{\sqrt{m}} \sum_{k=1}^{m} v_k(t) \qquad \text{main output}$$

$$v_k(t) = \frac{1}{\sqrt{m}} V_i \Big\{ a_1 + 2a_2 \big[n'_k(t) + \imath n''_k(t) \big] \Big\} e^{\imath 2\pi\nu_0 t} \qquad \text{cell} \rightarrow \text{output}$$

$$\psi_k(t) = 2\frac{a_2}{a_1} n''_k(t) \qquad \text{cell}$$

$$\varphi_k(t) = \frac{\frac{1}{m} V_i \, 2a_2 n''_k(t) \, e^{\imath 2\pi\nu_0 t}}{a_1 V_i \, e^{\imath 2\pi\nu_0 t}} = \frac{1}{m} \, 2\frac{a_2}{a_1} \, n''_k(t) \qquad \text{cell} \rightarrow \text{output}$$

$$S_\varphi(f) = \sum_{k=1}^{m} \frac{1}{m^2} \, 4\frac{a_2^2}{a_1^2} \, S_{n''_k}(f) \qquad \sum \text{cells} \rightarrow \text{output}$$

$$S_\varphi(f) = \frac{1}{m} \, 4\frac{a_2^2}{a_1^2} \, S_{n''}(f)$$

$$S_\varphi(f) = \frac{1}{m} \, S_\psi(f) \qquad m \text{ equal cells} \rightarrow \text{output}$$

$$b_{-1} = \frac{1}{m} \, \big[b_{-1} \big]_{\text{cell}}$$

Phase Noise in Parallel Amplifiers

Connecting two amplifier in parallel, a 3 dB reduction of flicker is expected

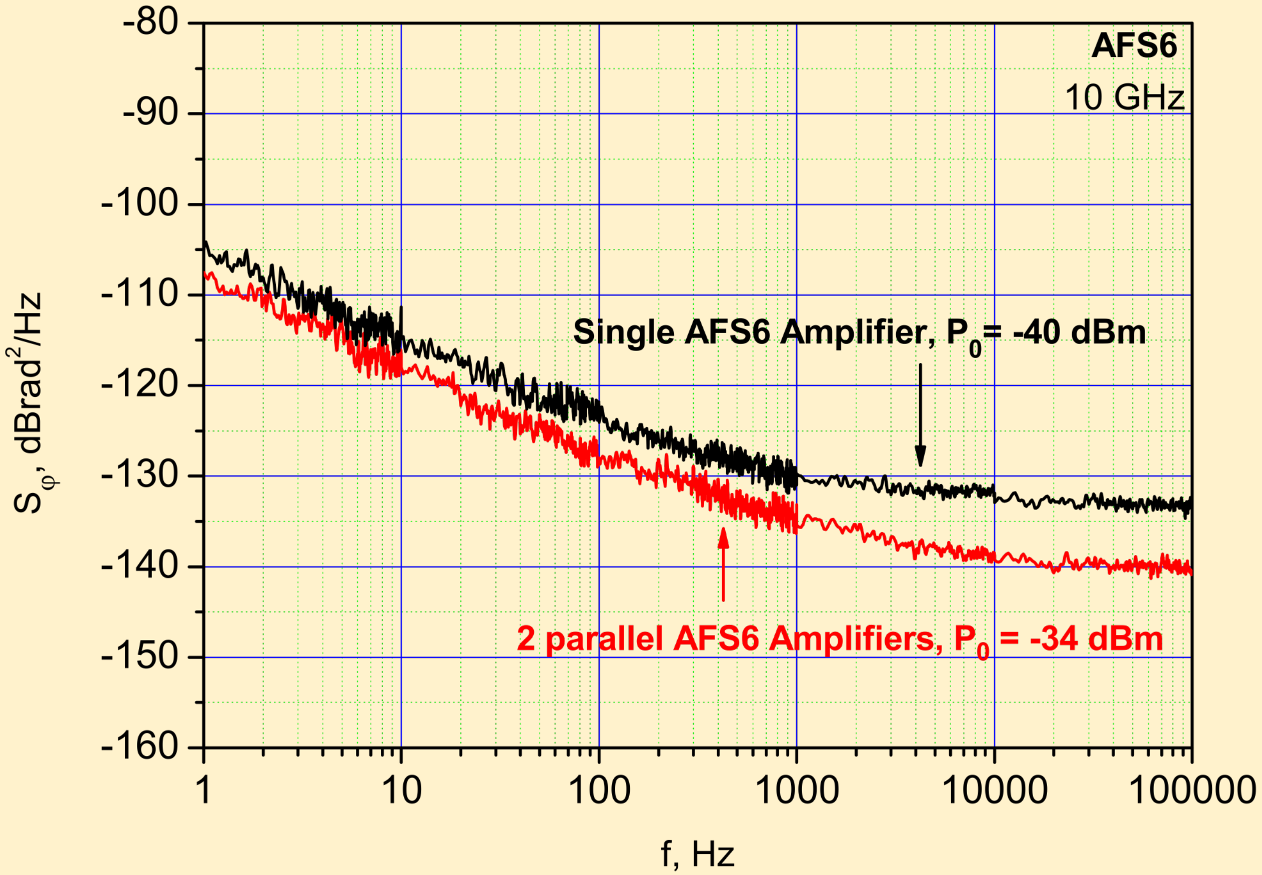

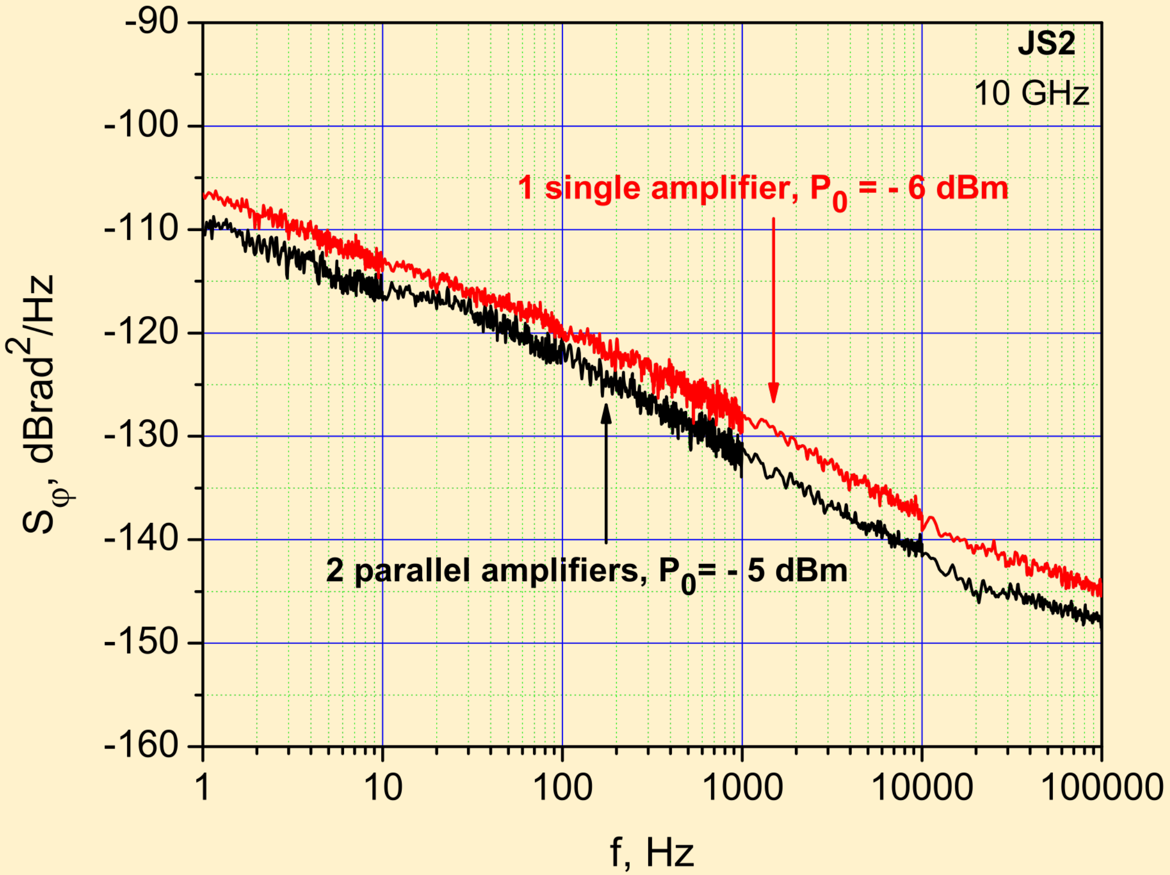

R. Boudot, E. Rubiola Phase Noise in RF and Microwave Amplifiers,
IEEE T UFFC 59(12) p.613-2628, Dec 2012 (Fig.8 a-b, rearranged)

Flicker Noise in Parallel Amplifiers

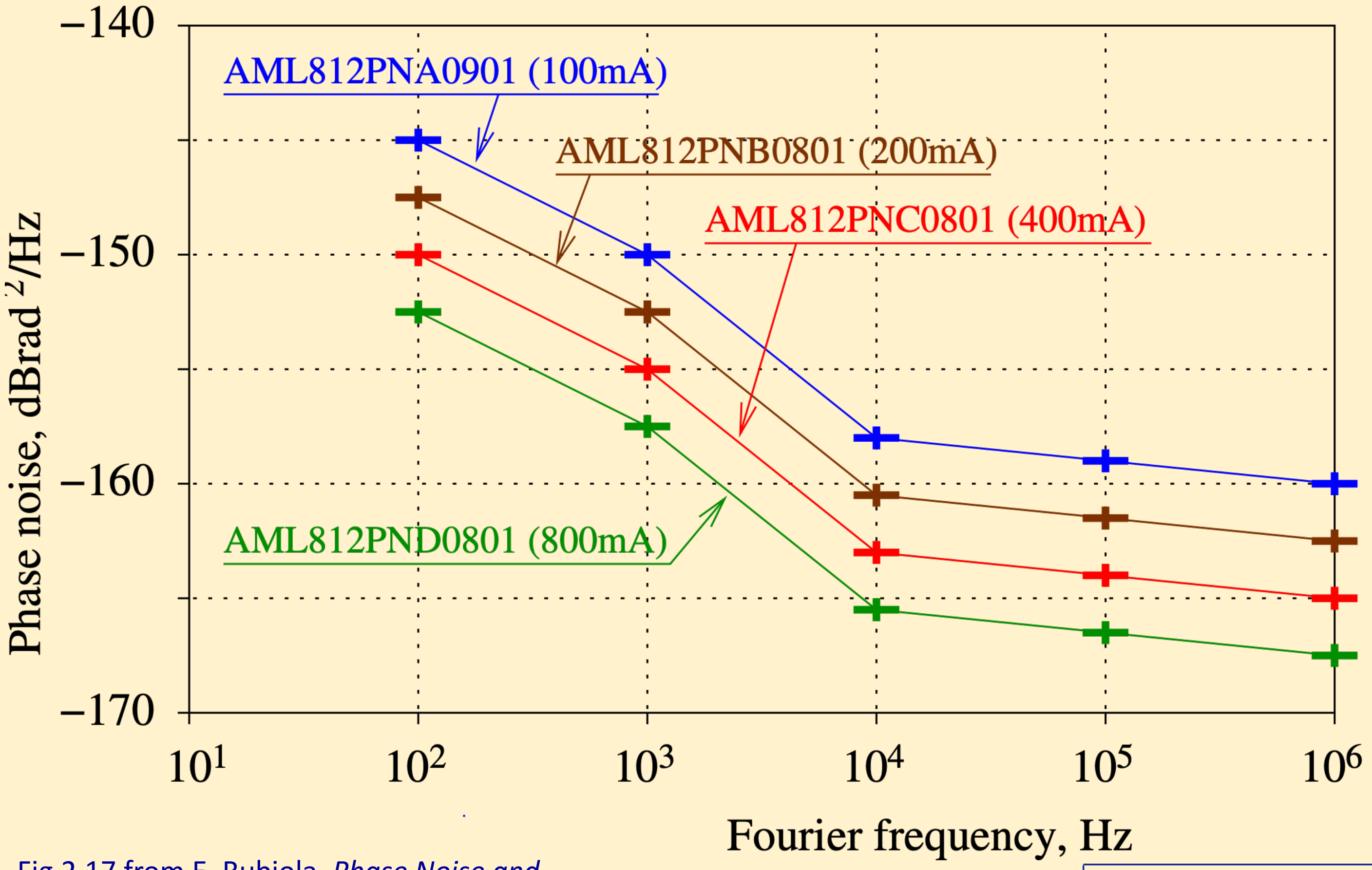

Fig.2.17 from E. Rubiola, *Phase Noise and Frequency Stability in Oscillators*, Cambridge 2008, ISBN 978-0521-88677-2

Specification of low phase-noise amplifiers (AML web page)

amplifier	parameters				phase noise vs. f, Hz			
	gain	F	bias	power	10^2	10^3	10^4	10^5
AML812PNA0901	10	6.0	100	9	−145.0	−150.0	−158.0	−159.0
AML812PNB0801	9	6.5	200	11	−147.5	−152.5	−160.5	−161.5
AML812PNC0801	8	6.5	400	13	−150.0	−155.0	−163.0	−164.0
AML812PND0801	8	6.5	800	15	−152.5	−157.5	−165.5	−166.5
unit	dB	dB	mA	dBm	dBrad^2/Hz			

Volume Law

The volume law results from a gedankenexperiment

- Flicker is of microscopic origin because it has Gaussian PDF (central limit theorem)
- Join the m branches of a parallel device forming a compound
- Phase flicker is proportional to the inverse size of the amplifier active region

- The phase flicker coefficient b_{-1} is about independent of power
- Splitting the signal into branches, at the output,
  - the carrier adds up coherently
  - the phase noise adds up statistically
- Hence, the $1/f$ phase noise is reduced by a factor m
- Only the flicker noise can be reduced in this way

$$b_{-1} = \frac{1}{m}\left[b_{-1}\right]_{\text{cell}}$$

Relevant examples

optical resonator
(50 μm^2) × (π × 5.5 mm)
≈ 1×10^{-12} m^3

sapphire resonator
0.1 × [π × (5/2 cm)^2] × (2.5 cm)
≈ 5×10^{-6} m^3

optical fiber
(10 μm^2) × (2 km)
≈ 2×10^{-7} m^3

5 MHz quartz
0.3 × [π × (1 cm)^2] × (0.1 mm)
≈ 1×10^{-8} m^3

The Error Amplifier

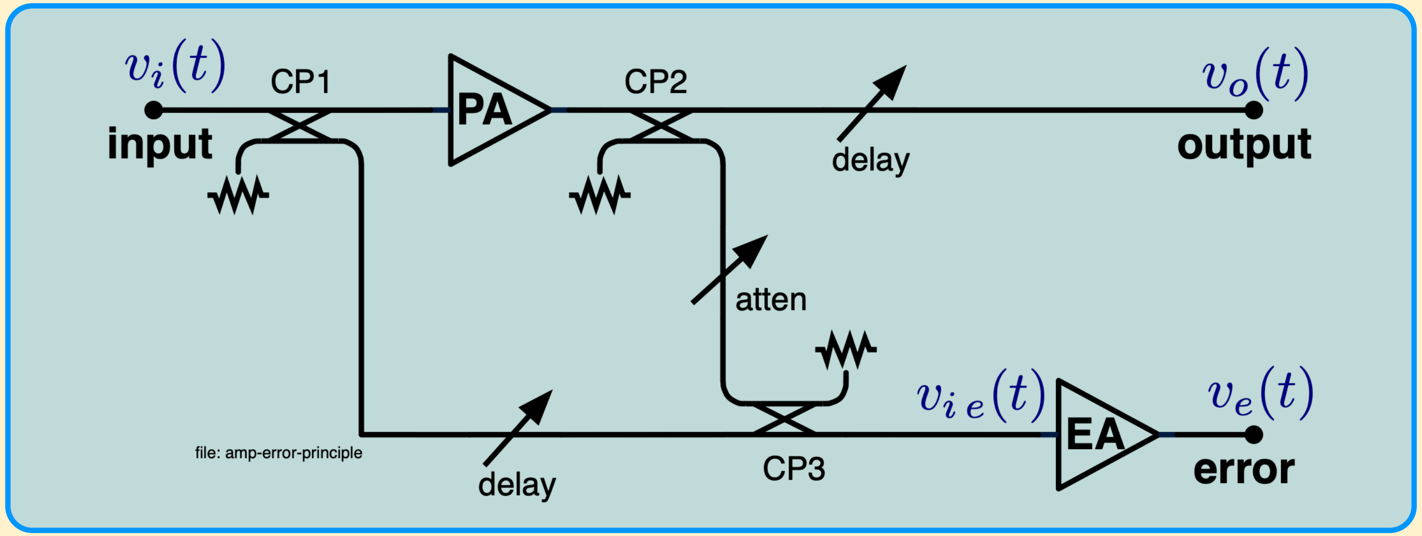

- Use a Power Amplifier (PA) and an Error amplifier (EA)
- The carrier is suppressed (strongly rejected) at the EA input
- Delay matching is needed for wide suppression bandwidth
- Low $1/f$ sidebands at the EA output because there is no carrier
- $v_e(t)$ is proportional to the PA noise sidebands
- Use $v_e(t)$ for the real-time correction of the PA noise
- Feedback or feedforward correction schemes are possible

The Virtues of the Error Amplifier

Assume 3-dB loss-free couplers

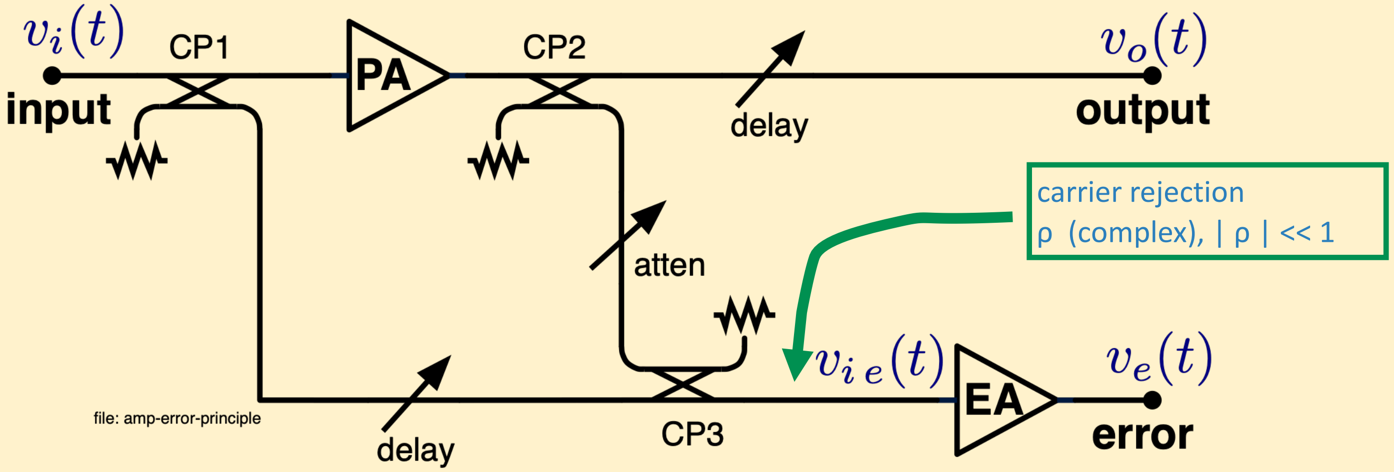

$$(v_{i\,e})_{\mathrm{PA}} = \frac{1}{2} V_i \Big\{ a_1 + a_2 \left[n'(t) + i n''(t) \right] \Big\}_{\mathrm{PA}} e^{i\omega_0 t} \left(\frac{1}{a_1} \right)_{\mathrm{PA}} \qquad \text{PA contrib}$$

$$(v_{i\,e})_{\mathrm{in}} = -\frac{1}{2} V_i \, e^{i\omega_0 t} \, (1 - \rho) \qquad \text{carrier}$$

$$v_{i\,e} = \frac{1}{2} V_i e^{i\omega_0 t} \rho + \frac{1}{2} V_i \Big\{ 2 \frac{a_2}{a_1} \left[n'(t) + i n''(t) \right] \Big\}_{\mathrm{PA}} e^{i\omega_0 t} \qquad \text{EA input}$$

$$v_e = \frac{1}{2} V_i \Big[\rho \{ a_1 \} + \Big\{ 2 a_2 \left[n'(t) + i n''(t) \right] \Big\}_{\mathrm{PA}} + \rho \Big\{ 2 a_2 \left[n'(t) + i n''(t) \right] \Big\}_{\mathrm{EA}} \Big] e^{i\omega_0 t} \qquad \text{error}$$

rejected carrier — PA noise sidebands (useful signal) — rejected EA noise sidebands

Parametric Noise in Regenerative Amplifiers

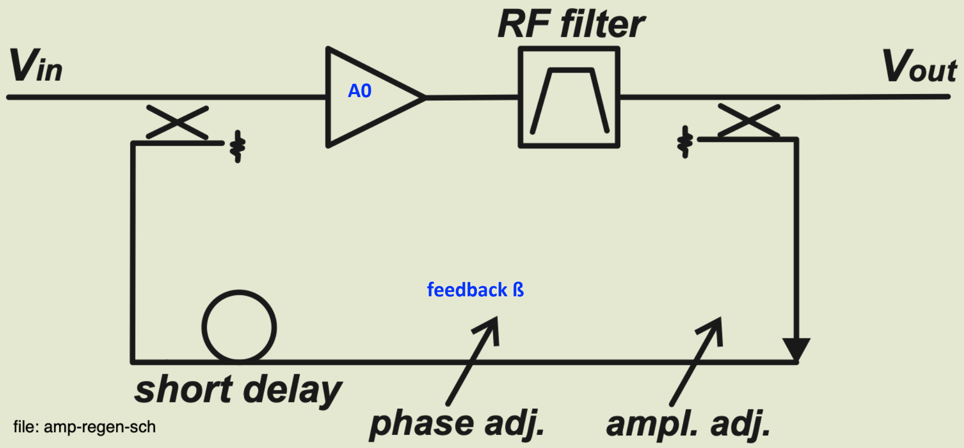

$$A = \frac{A_0}{1 - A_0\beta}$$

$$A = A_0^m \quad \Rightarrow \quad \beta = \frac{A_0^{m-1} - 1}{A_0^m}$$

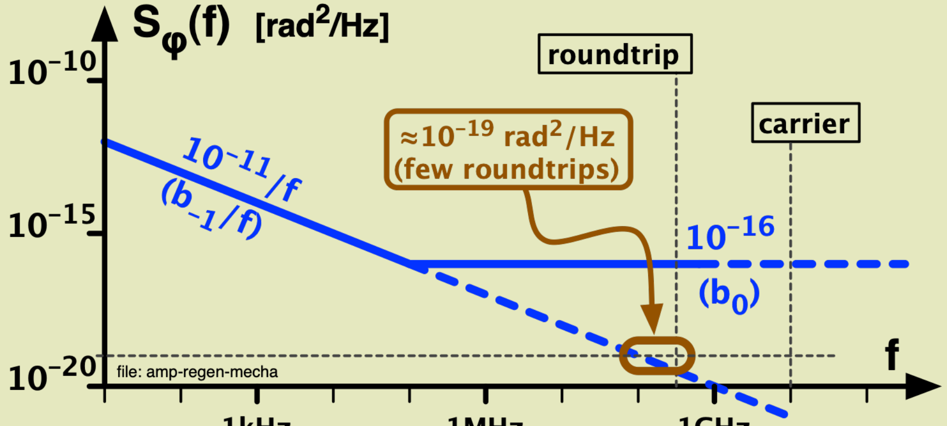

$$A \to \frac{A_0\, e^{i\psi}}{1 - A_0\beta\, e^{i\psi}}$$

$$A = \frac{A_0}{1 - A_0\beta}\left[1 + i\frac{1}{1 - A_0\beta}\,\psi\right] .$$

$$\varphi(t) = \frac{1}{1 - A_0\beta}\,\psi(t)$$

$$(\mathsf{b}_{-1})_{\mathrm{RA}} = \left[\frac{1}{1 - A_0\beta}\right]^2 (\mathsf{b}_{-1})_{\mathrm{ampli}}$$

$$(\mathsf{b}_{-1})_{\mathrm{RA}} = m^2 (\mathsf{b}_{-1})_{\mathrm{ampli}}$$

Phase Noise of a Regenerative Amplifier

The RA replaces the two-stage sustaining amplifier in a Opto-Electronic oscillator

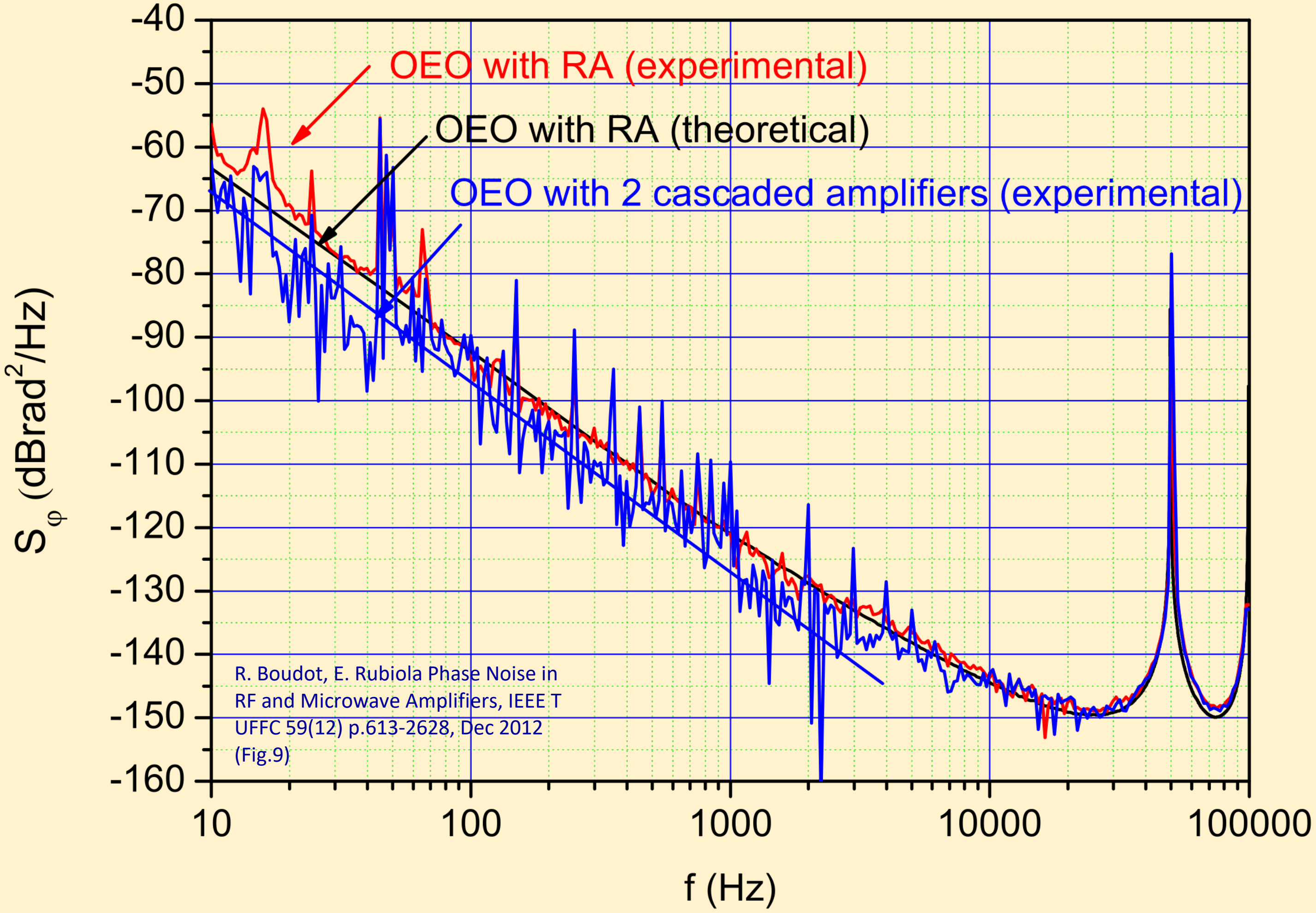

- A RA is set for the gain of two cascaded amplifiers
- As expected, the RA flicker is 3 dB higher than the two amplifiers
- Indirect measurement through the frequency flicker

Low-Flicker RF Amplifiers

Still not like how this section is organized

Conversion (Transposed-Gain) Amplifiers

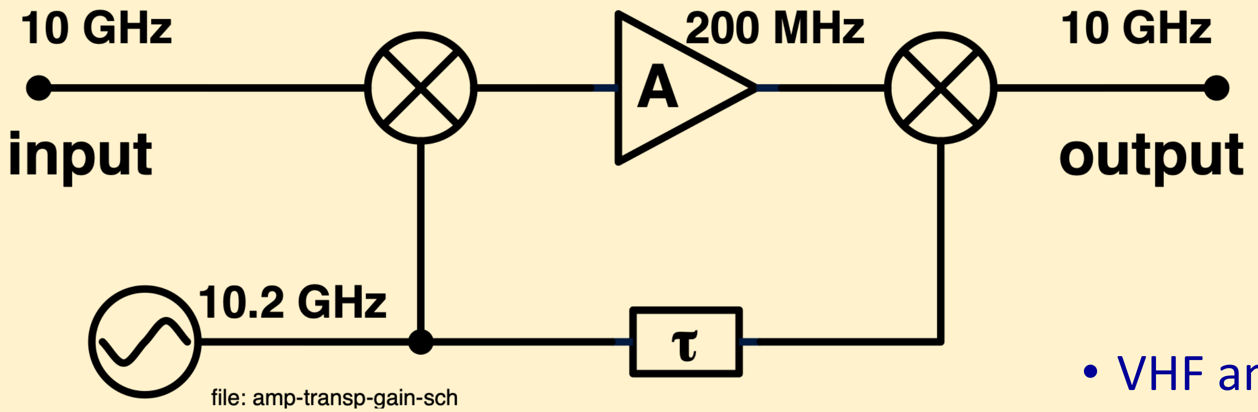

- VHF amplifiers and µwave mixers flicker significantly less than GaAs µwave amplifiers
- Lower flicker is achieved by down-converting to VHF, amplifying, and up-converting back to µwaves
- Can even work close to DC
- For best rejection of the oscillator phase noise, the delay τ compensates for the amplifier group delay
- Made obsolete by the SiGe parallel amplifiers (still useful in higher bands?)

J.K.A. Everard and M.A. Page-Jones, “Ultra Low Noise Microwave Oscillators with Low Residual Flicker Noise”, IEEE International Microwave Symposium, Orlando, Florida, 16–20 May 1995, pp. 693–696

Feedforward Amplifier

- Attenuation and left-hand delay are set for the input signal to be nulled at the input of the Error Amplifier
- The EA amplifies the distortion and the noise of the Power Amplifier
- PA distortion and noise are subtracted by feed-forward subtraction of the EA error signal
- At virtually zero input power, the EA cannot distort and flicker
- For wide-band operation true delay matching is necessary
- Cannot be used in the compression region, otherwise the input-signal nulling does not work
- Originally intended to reduce the distortion of high peak-to-average power ratio of telecom amplifiers. Linear loads (cables and antennas) never push the FFA to the compression region
- For oscillator operation
  - Phase matching is sufficient, instead of true delay matching because of the narrow band
  - Saturation must be ensured by an external circuit

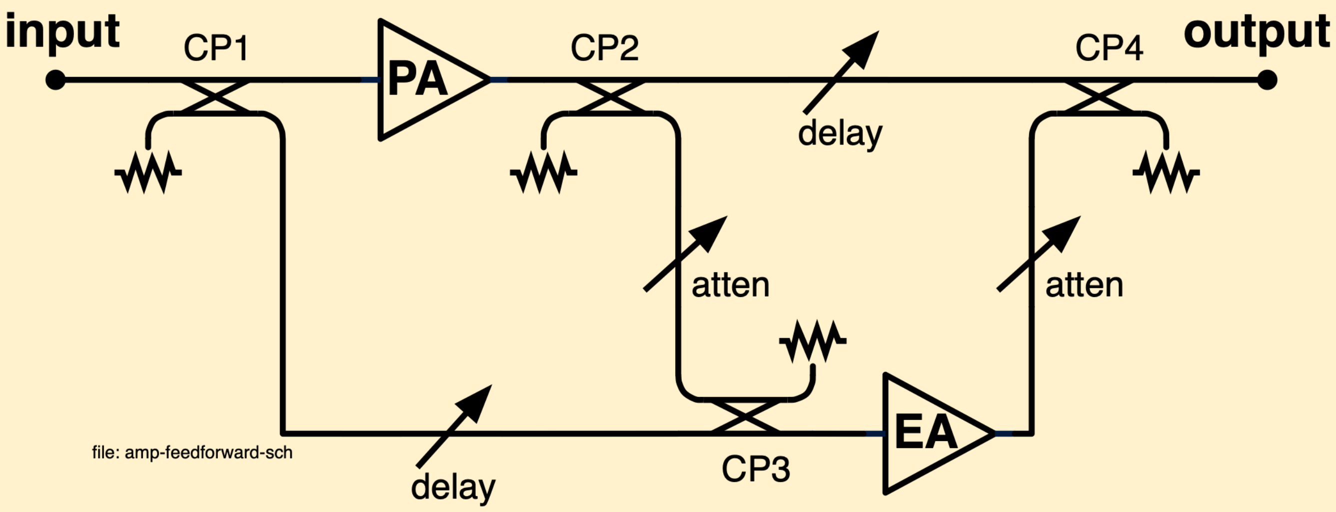

Baseband-Feedback Amplifier

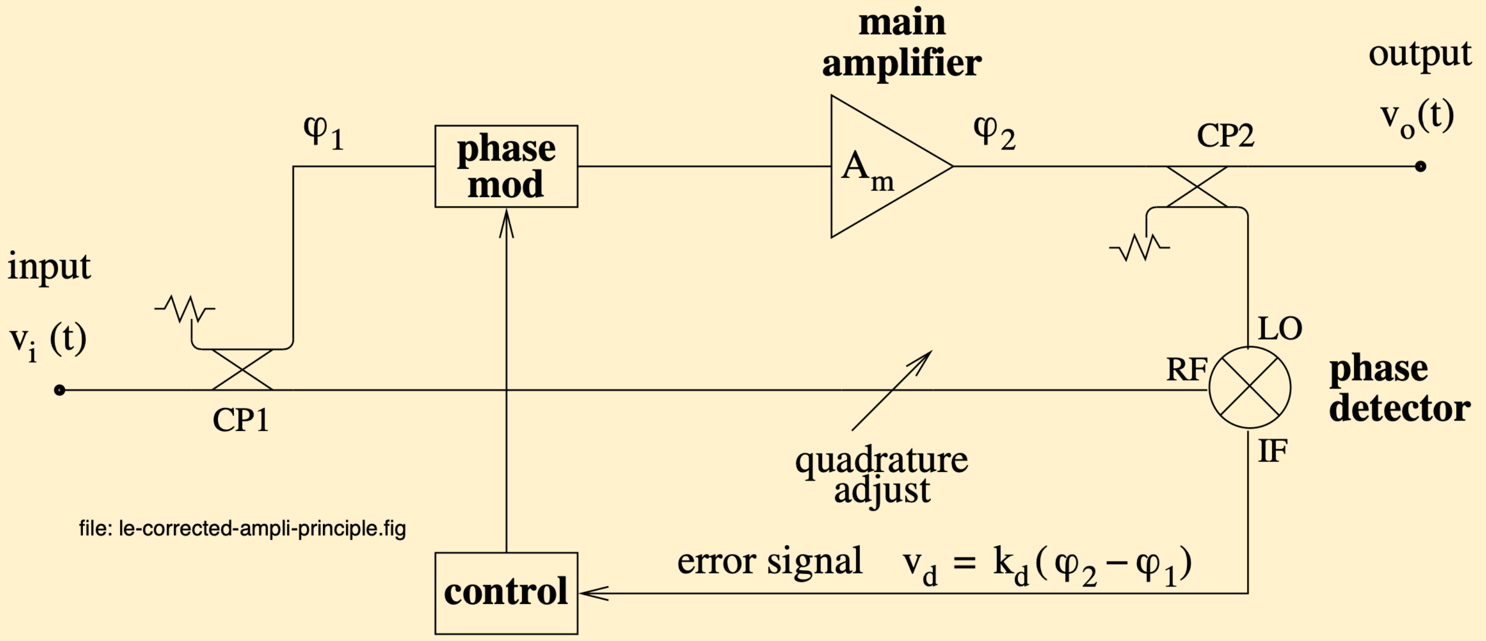

Fig.2.14 from E. Rubiola, *Phase Noise and Frequency Stability in Oscillators*, Cambridge 2008, ISBN 978-0521-88677-2

- The detector measures the phase $\varphi_2 - \varphi_1$ across the main amplifier plus phase modulator
- The control stabilizes

  $$\varphi_2 - \varphi_1 = C$$

  (constant), virtual ground
- The correction of AM noise is also possible in a similar way

Baseband-Feedback Amplifier

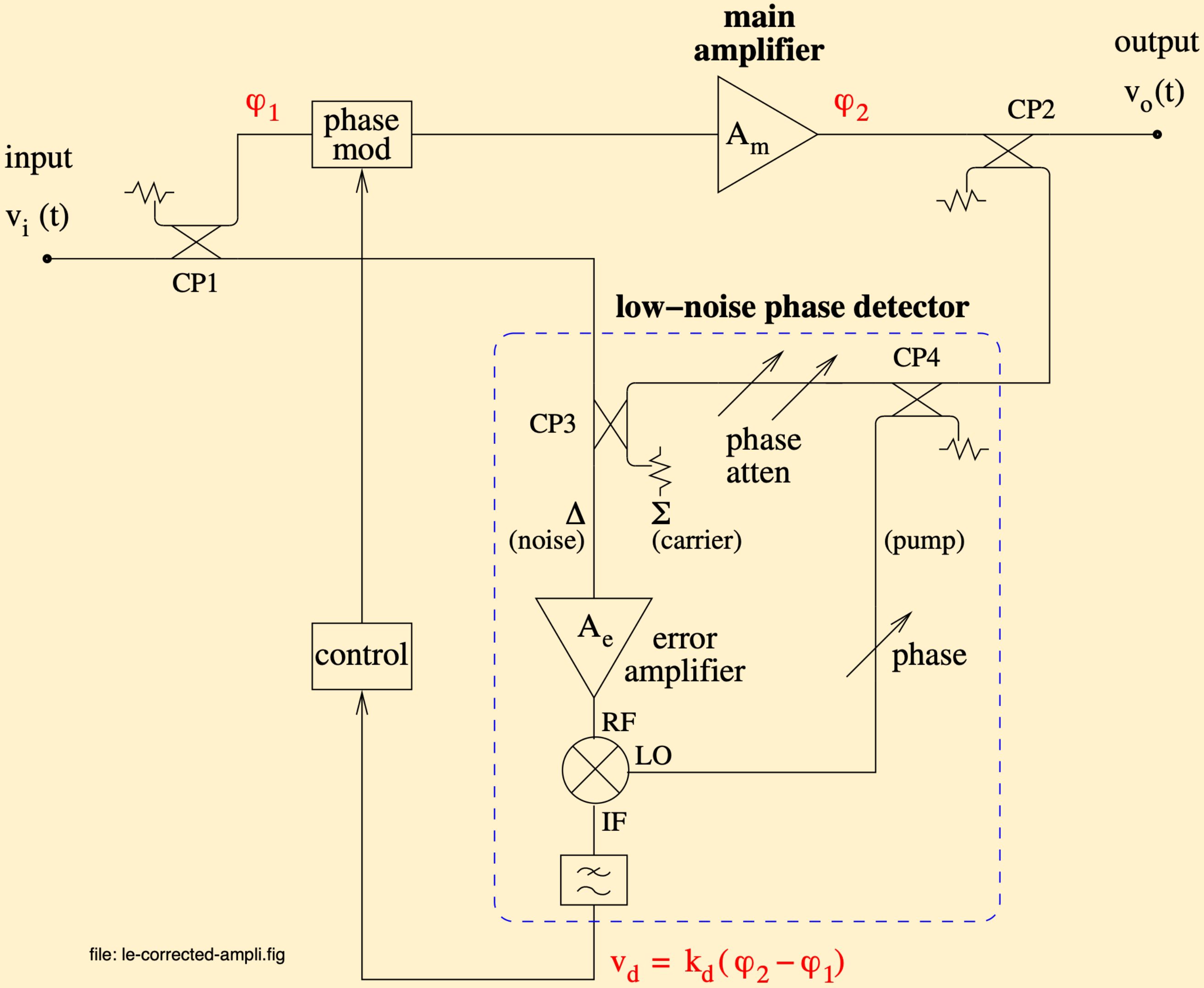

- The detector measures the phase $\varphi_2 - \varphi_1$ across the main amplifier plus phase modulator
- The control stabilizes $\varphi_2 - \varphi_1 = C$ (constant), virtual ground
- Practical implementation with a bridge noise-measurement system
- Notice the use of an error amplifier

Fig.2.15 from E. Rubiola, *Phase Noise and Frequency Stability in Oscillators*, Cambridge 2008, ISBN 978-0521-88677-2

Experiments

Environment

Environmental Effects

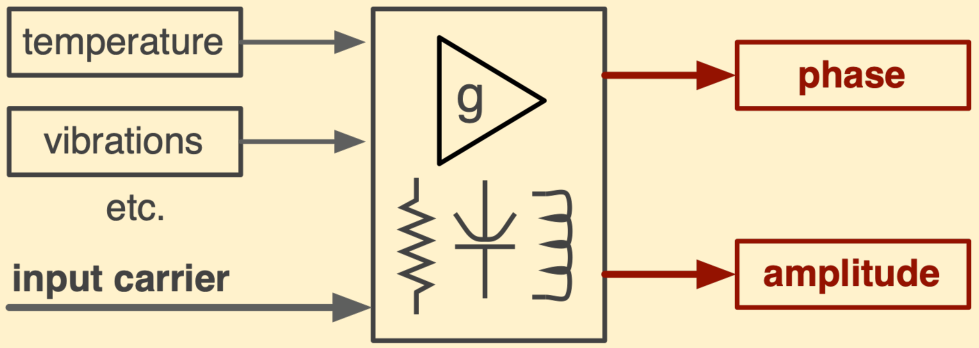

A time constant can be present

- Temperature
- EM interference
  - RF leakage (additive)
  - 50-60 Hz magnetic fields
  - electric fields
- power supply
- acoustic
- radiation

It is experimentally observed that the temperature fluctuations cause a spectrum $S_\alpha(f)$ or $S_\varphi(f)$ of the $1/f^5$ type

Yet, at lower frequencies the spectrum folds back to $1/f$

Random Walk and Drift

- RF amplifier
- µw amplifier
- SiGe amplifier
- RF mixer mixer
- Cr^{3+} µw maser amplifier
- µw mixer
- circulator
- RF variable attenuator (potentiometer)
- RF by-step attenuator
- µw variable attenuator (graphite attenuator)
- variable phase shifter (line stretcher)
- RF ferrite power splitter
- photodetector
- microwave power detector

Radiation

Permanent damage (memory)

Consider skipping

Noise in coaxial cables

Skip this, too tough

- thermal noise (loss)
- acoustical noise
  - piezoelectricity
  - electret effect
- EM noise (leakage)

Phase Noise and Jitter in Digital Electronics

Enrico Rubiola

CNRS FEMTO-ST Institute, Besancon, France

INRiM, Torino, Italy

Outline

home page http://rubiola.org

Acknowledgments

This tutorial gathers a wealth of material developed by

Claudio Calosso, INRIM, Torino, Italy

The Go Digital Team @ FEMTO-ST, Besancon, France
chiefly but not only, Pierre-Yves "PYB" Bourgeois, A. Carolina Cardenas Olaya, Jean-Michel Friedt, Gwenhael "Gwen" Goavec-Merou, Yannick Gruson

…and by myself

Copyright

Caveat

Only a fraction of this can be taught at a 1–2 H session

1 – Basics

Phase Time x(t)

- Let's allow $\varphi(t)$ to exceed $\pm\pi$, and count the no of turns
- This is easily seen by scaling ω down (up) to $\omega = 1$ rad/s using a noise-free gear work
- The phase-time fluctuation associated to $\varphi(t)$ is

$$x(t) = \varphi(t) / \omega_0$$

- $x(t)$ is a normalized quantity, independent of ω_0.

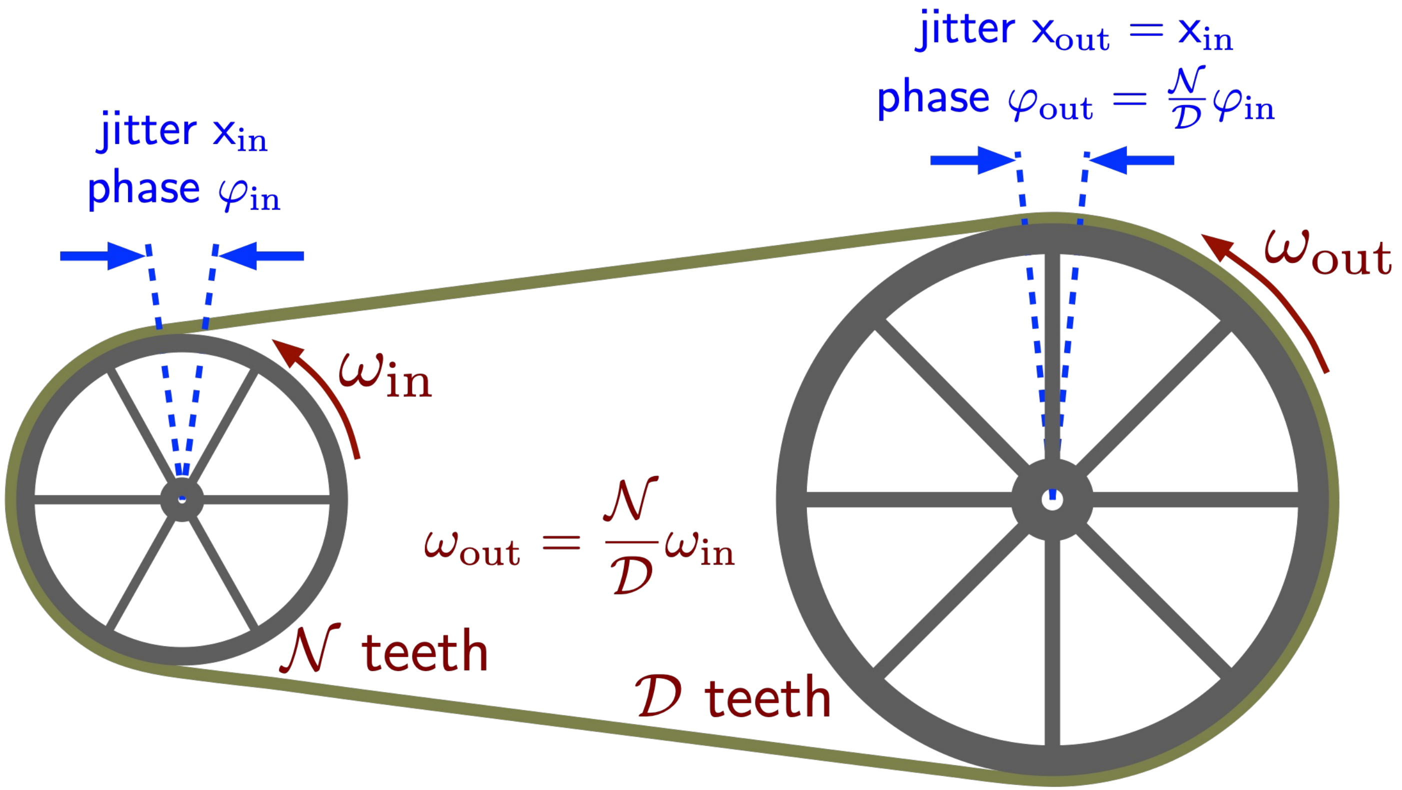

The Polynomial Law

$$v(t) = V_0\,[1+\alpha(t)]\cos\left[2\pi\nu_0 t + \varphi(t)\right]$$

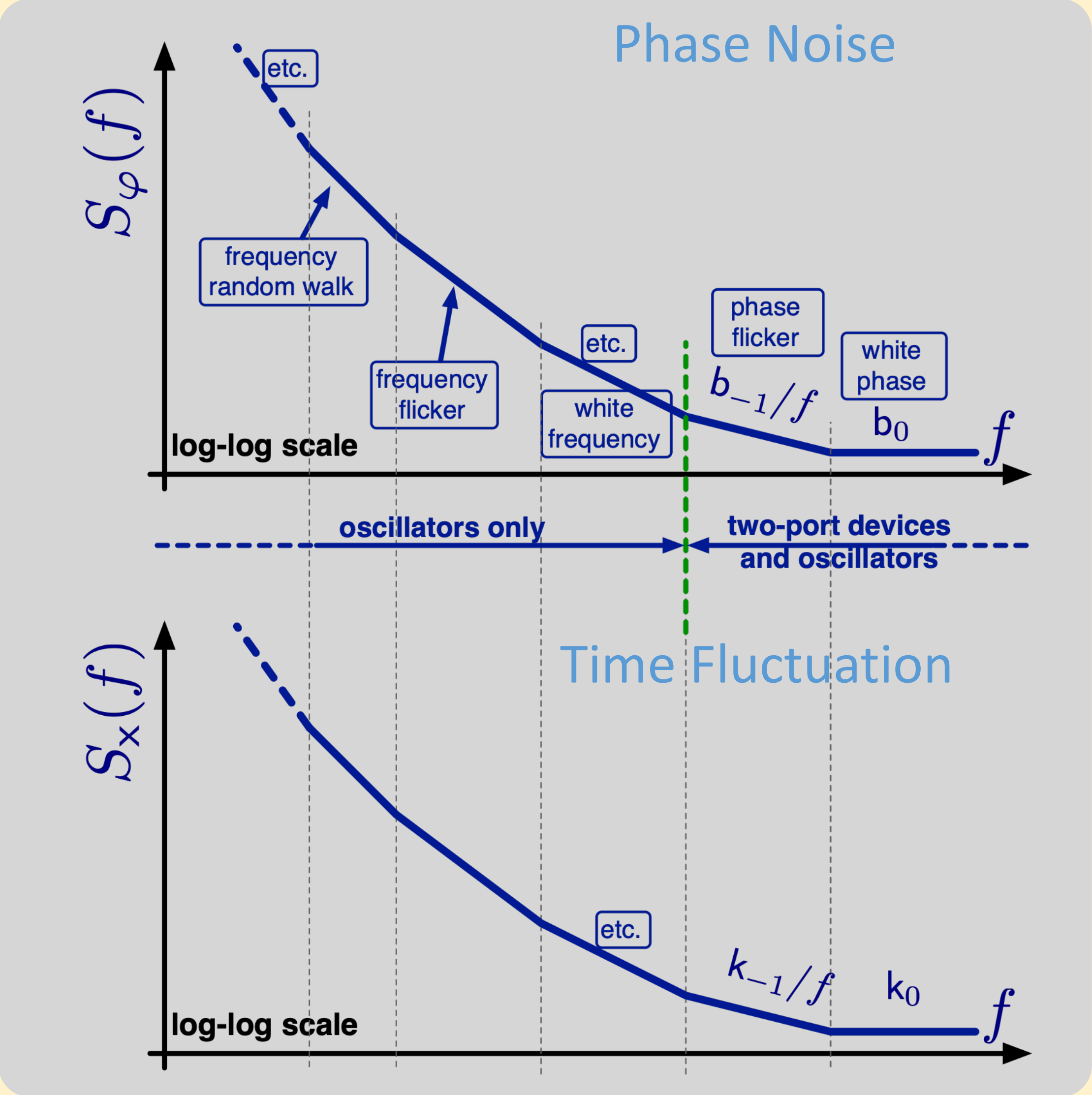

Phase Noise PSD

$$S_\varphi(f) = \sum_{i\le -4}^{0} b_i f^i$$

Phase-time PSD

$$x(t) = \frac{\varphi(t)}{2\pi\nu_0}$$

$$S_x(f) = \sum_{i\le -4}^{0} k_i f^i$$

Fractional Frequency PSD

$$y(t) = \dot{x}(t) = \frac{\dot{\varphi}(t)}{2\pi\nu_0}$$

$$S_y(f) = \sum_{i\le -2}^{2} h_i f^i$$

The Egan Model – Modern View

for phase noise in frequency dividers

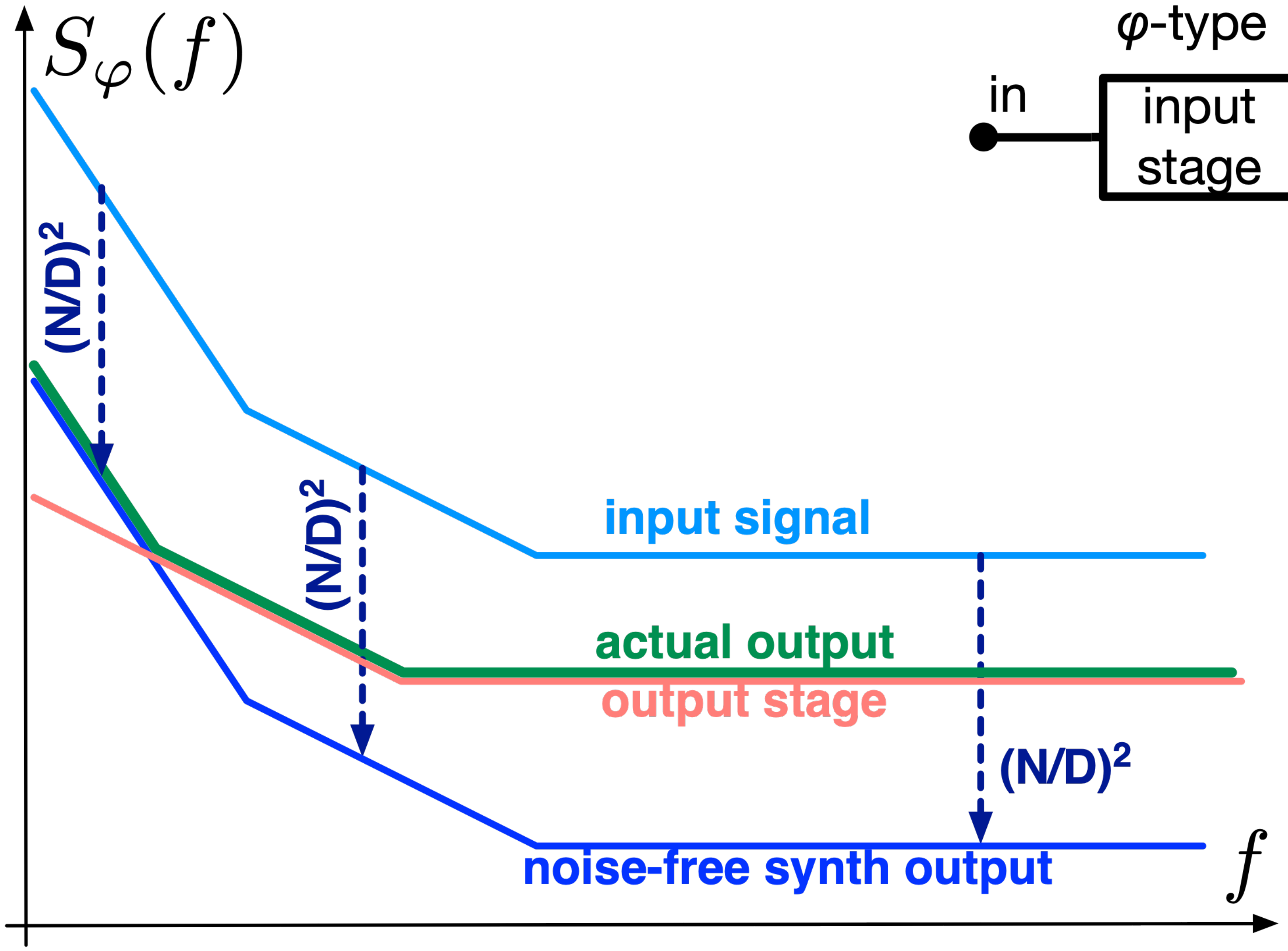

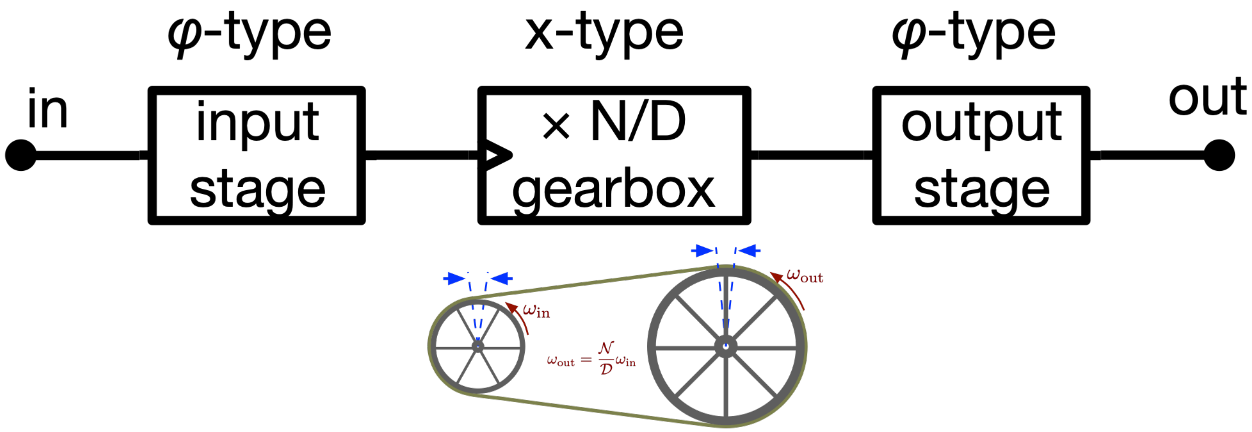

For $N/D \ll 1$, the scaled-down noise hits the output-stage limit

W.F. Egan, Modeling phase noise in frequency dividers, IEEE T UFFC 37(4), July 1990

Phase Noise Sampling

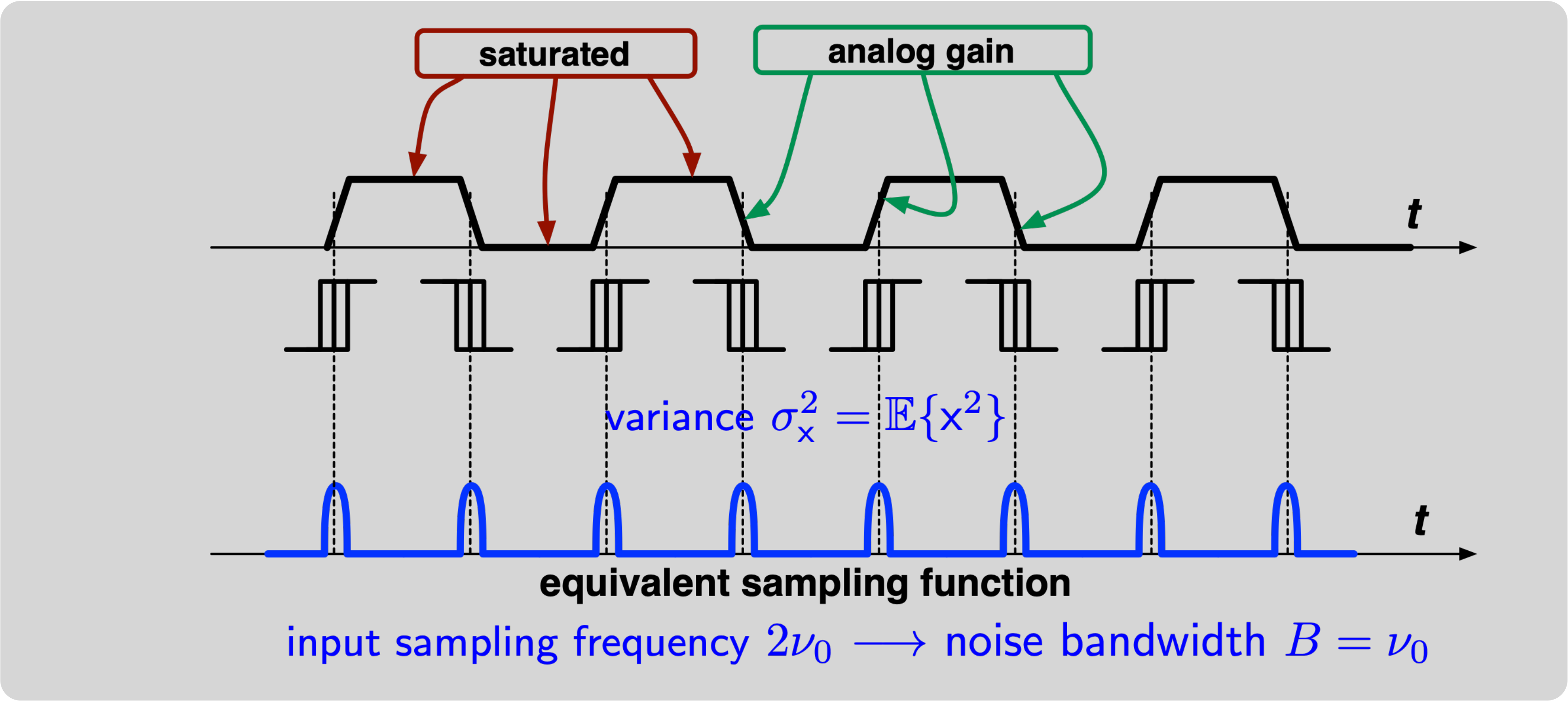

- Sampling occurs at the edges
  - (in some cases, only at rising or falling edges)
- Square wave signals need analog bandwidth at least 3 ν_{max} … 4 ν_{max}
- Aliasing is around the corner

Aliasing Over-Simplified

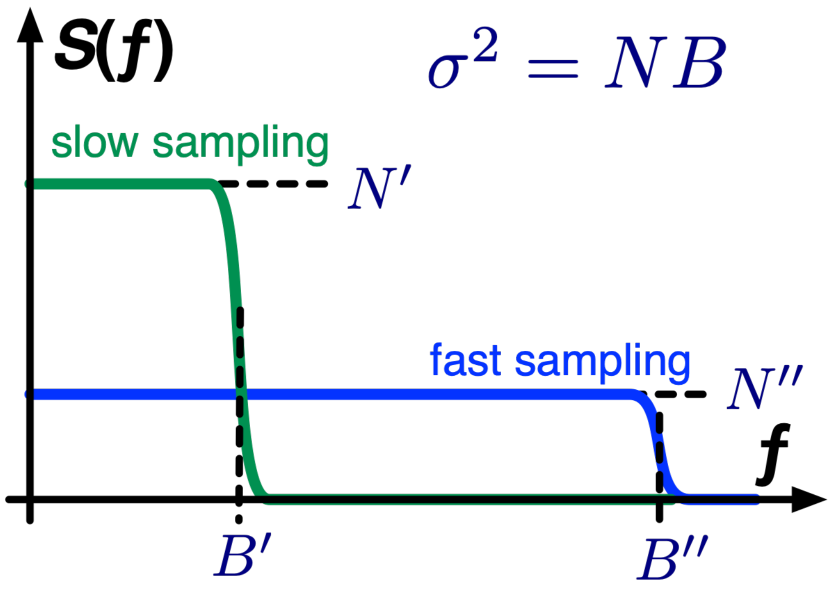

- The Parseval Theorem states that
  the total energy (or power) calculated in the time domain
  and in the frequency domain is the same

$$N'B' = N''B''$$

- Ergodicity allows to
  interchange time domain and statistical ensemble

…and PM noise scales up with the reciprocal of the carrier frequency

Aliasing and 1/f Noise

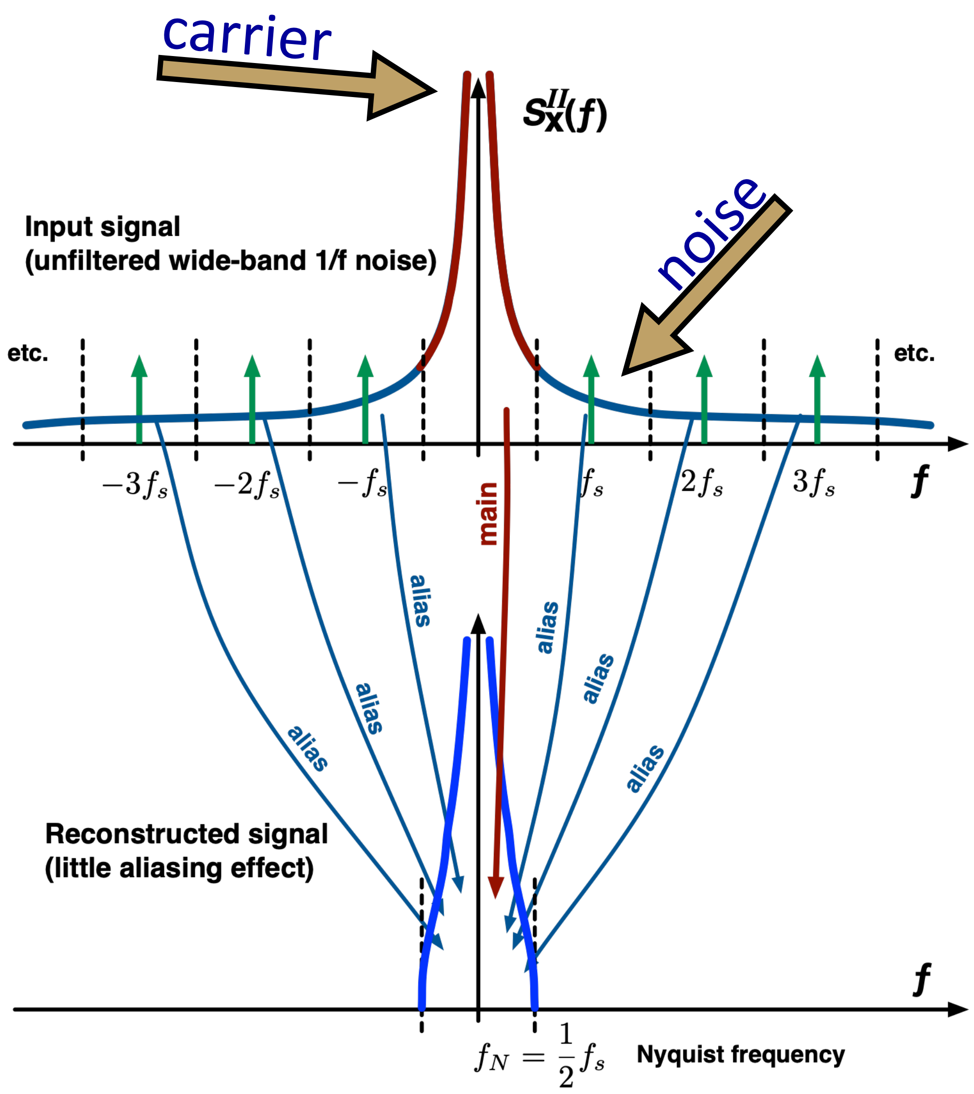

Low power in the high-f aliases

Little or no effect on the noise spectrum

Aliasing of $1/f^2$, $1/f^3$, $1/f^4$… does not strike

2 – FPGAs

Noise Mechanisms

Examples

Additional Facts

FPGA Interconnection Structure

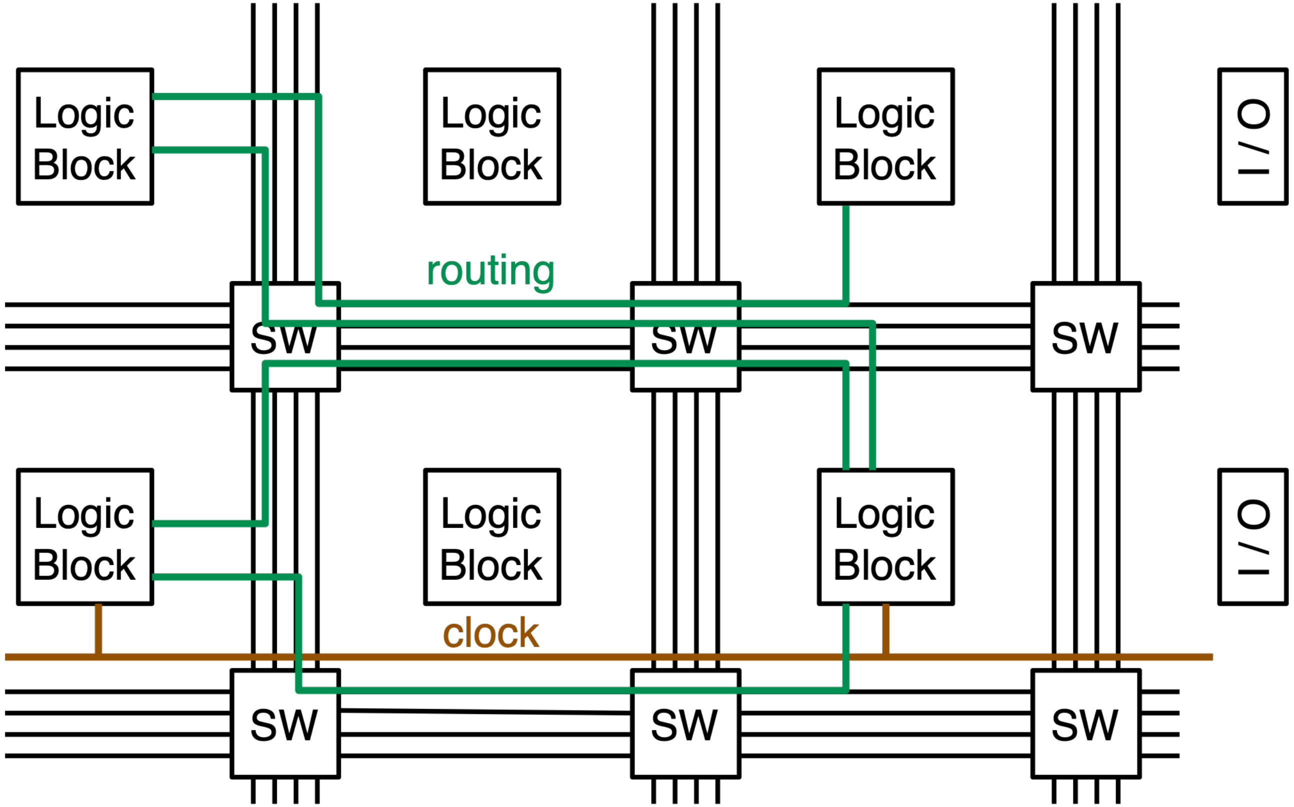

Device dependent blocks

- Input/Output
- RAM
- PLL
- NCO
- …etc.

- Delay & jitter
- General routing through switch points
- Delay & jitter rather uniform in a block
  - Large spread over the interconnect matrix
- Dedicated clock lines managed separately
  - Low and predictable delay & jitter

Output Time Fluctuation

- Output can be synchronized to the clock
- Time fluctuation cannot be smaller than
  - External clock signal
  - Clock input stage
  - Clock distribution
  - Output stage

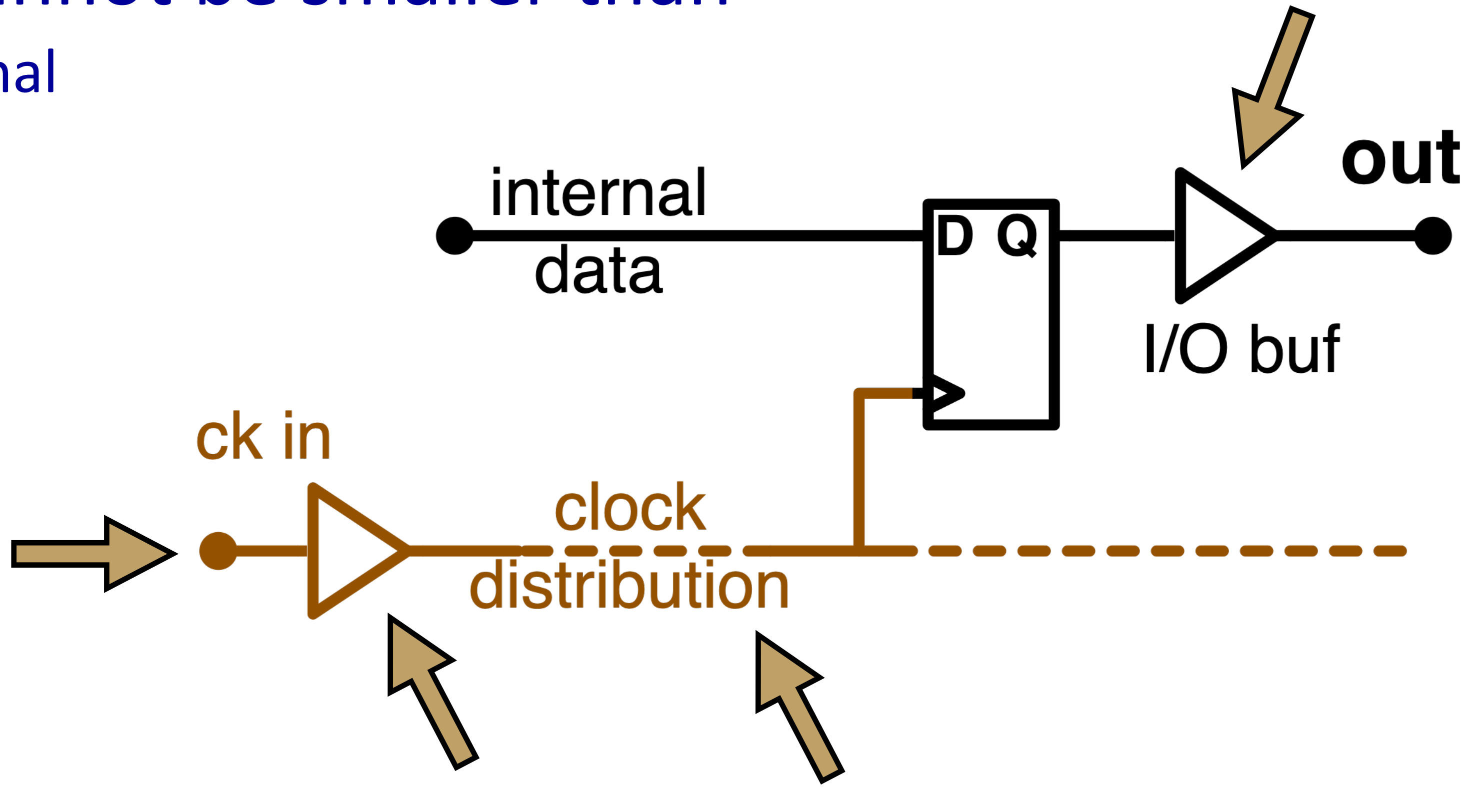

Two Types of Noise Mechanism

- Phase-type noise
- Phase noise $S_\varphi(f)$ is independent of ν_0
- Time fluctuation $S_x(f)$ scales as $1/\nu_0^2$

$$S_x(f) = \frac{1}{4\pi^2\nu_0^2} S_\varphi(f)$$

- Time-type noise
- Time fluctuation $S_x(f)$ is independent of ν_0
- Phase noise $S_\varphi(f)$ scales as ν_0^2

Phase Noise in the Input Stage

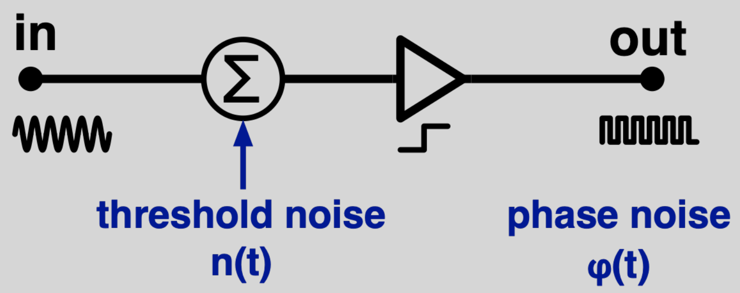

Sinusoid of peak amplitude V_0 results in phase-type noise

$$S_\varphi(f) = \frac{S_n(f)}{V_0^2}$$

constant vs ν_0

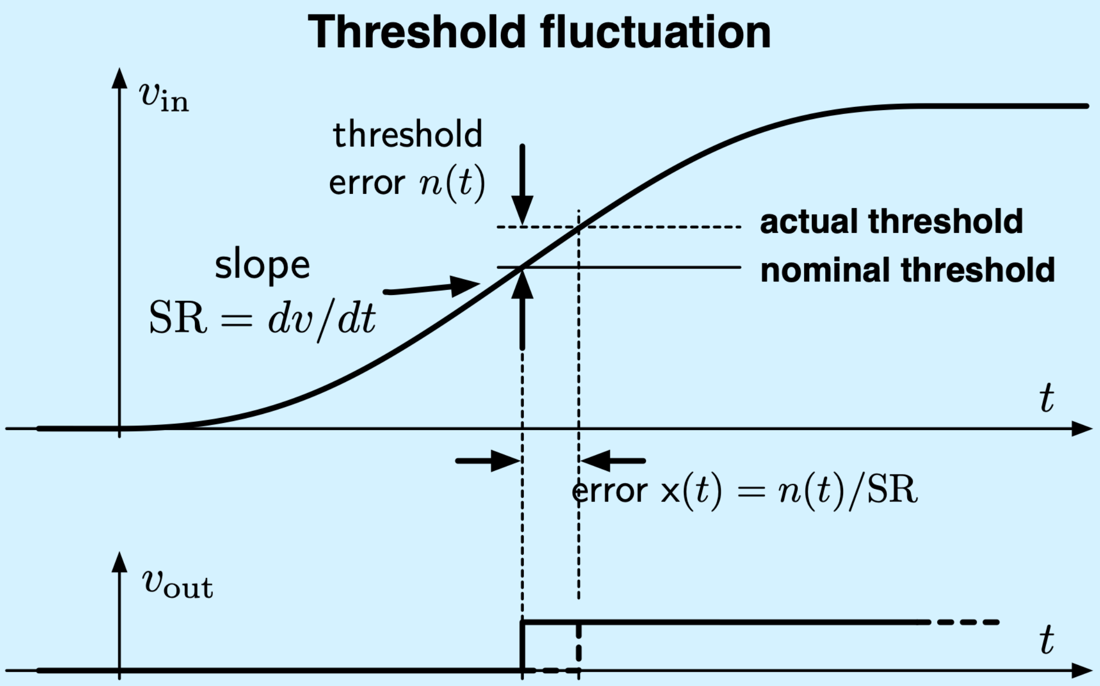

mechanism

$$\mathrm{x}(t) = \frac{n(t)}{(\mathrm{SR})(t)}$$

$$\varphi(t) = \frac{2\pi\nu_0\, n(t)}{(\mathrm{SR})(t)}$$

Phase Noise in the Input Stage

Sinusoidal signal

$$v(t) = V_0\,[1+\alpha(t)]\cos\,[2\pi\nu_0 t + \varphi(t)] \quad \Longrightarrow \quad \mathrm{SR} = 2\pi\nu_0\, V_0$$

$$\mathsf{x}(t) = \frac{n(t)}{\mathrm{SR}} \quad \longrightarrow \quad \mathsf{x}(t) = \frac{1}{2\pi\nu_0}\,\frac{n(t)}{V_0}$$

$$\varphi(t) = \frac{2\pi\nu_0\, n(t)}{\mathrm{SR}} \quad \longrightarrow \quad \varphi(t) = \frac{n(t)}{V_0}$$

phase-type
(**φ**-type)
noise

$$S_\varphi(f) = \frac{S_n(f)}{V_0^2}$$

$$\text{constant vs } \nu_0$$

Phase-Type (φ-type) PM Noise

Aliasing strikes hard on white noise, yet little/not on flicker

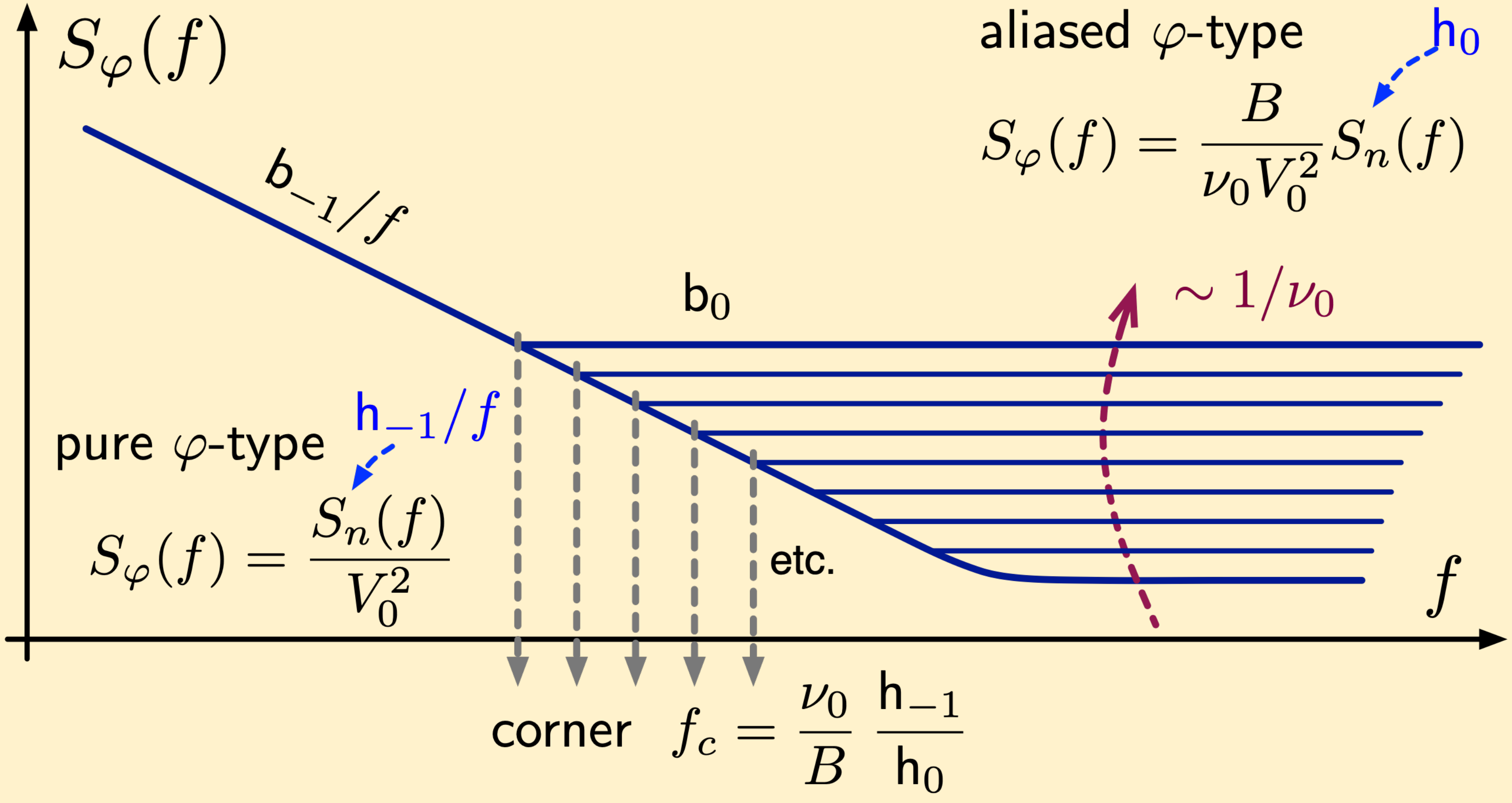

Polynomial law $S_n(f) = \sum h_i f^i$ [do not mistake with $S_y(f)$]

Internal Delay Fluctuation

Time-type (x-type) noise

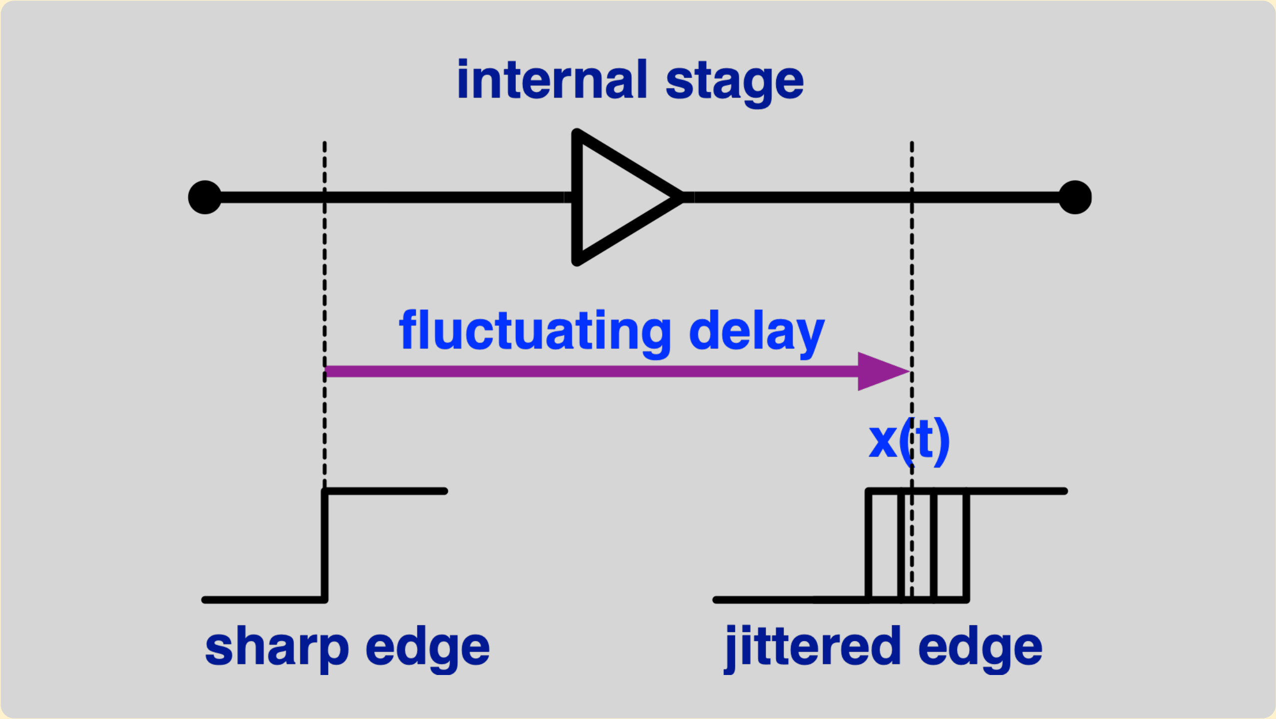

- The internal delay fluctuates by an amount x(t)
- This has nothing to do with threshold and frequency

Time-Type (x-type) Fluctuation

Remember that white noise is subject to aliasing, flicker is not

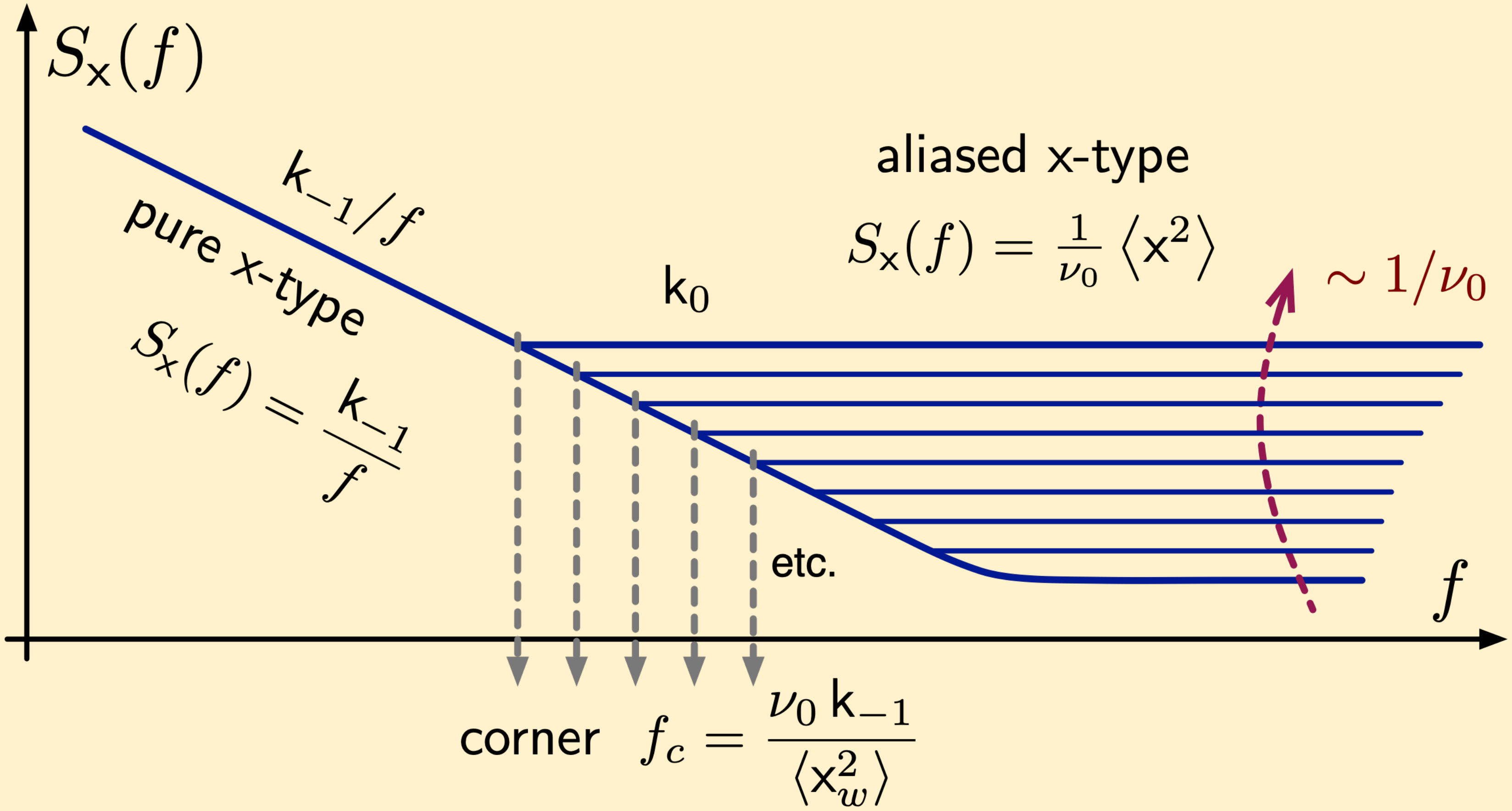

Cyclone III Clock Buffer

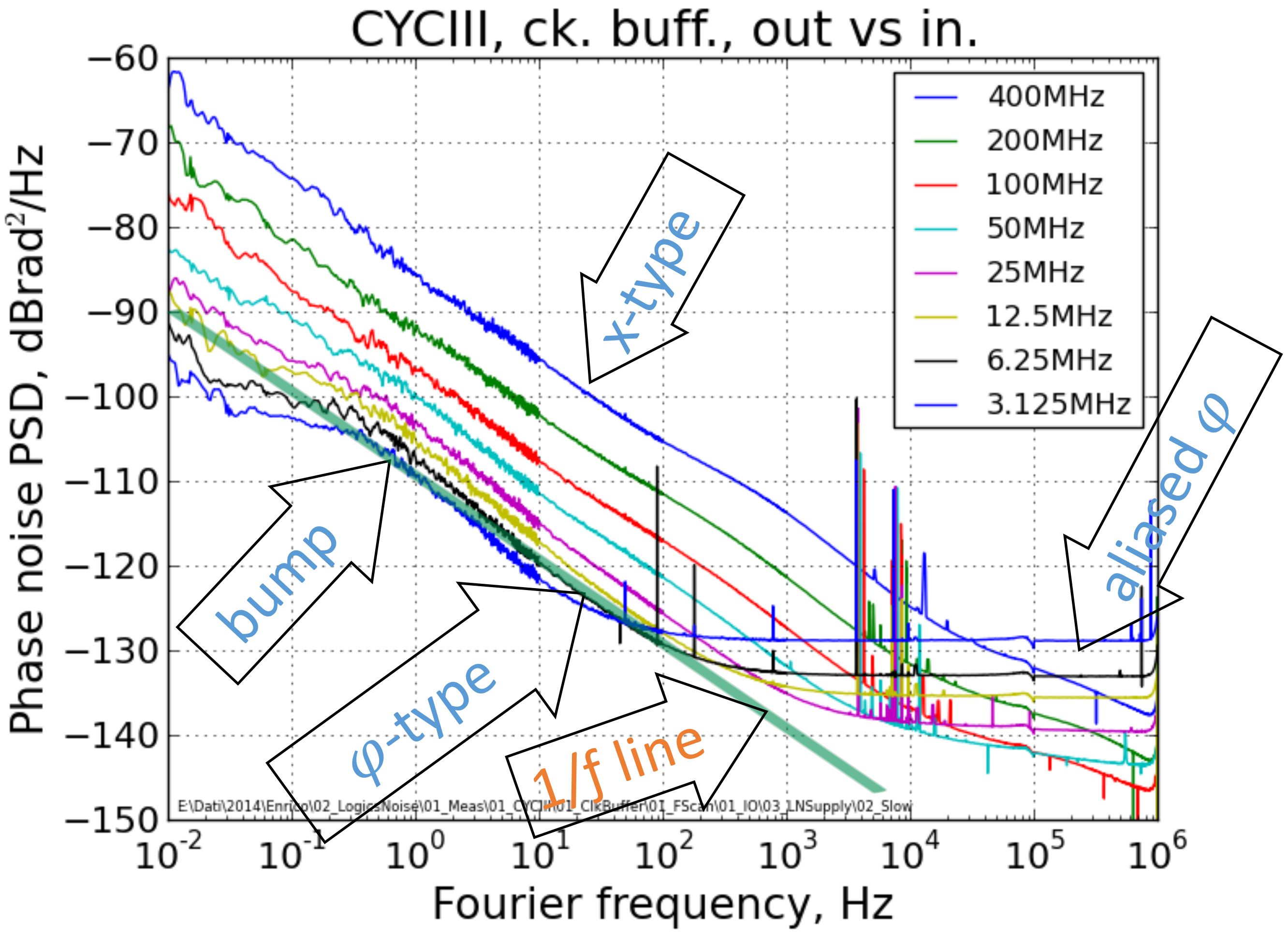

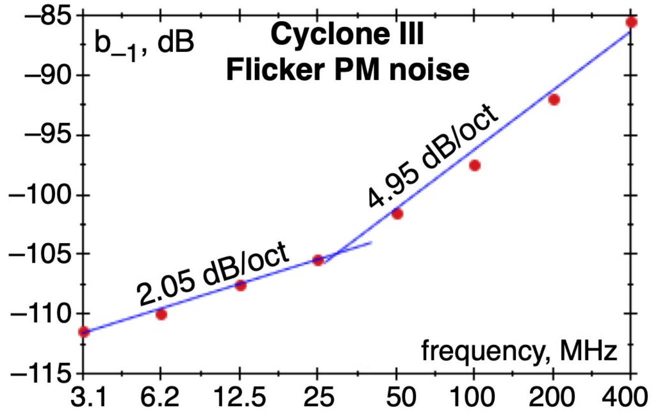

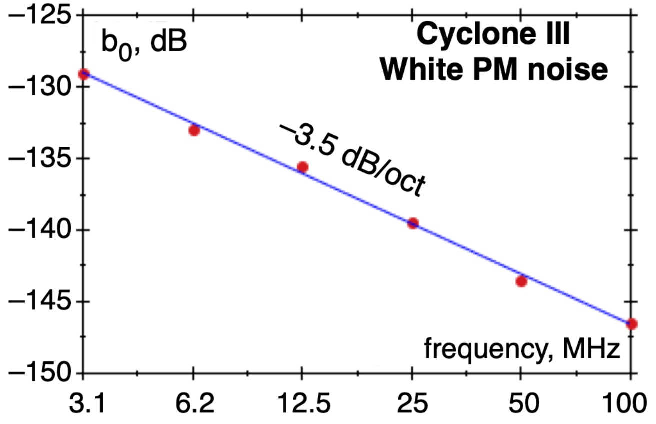

Flicker

- High ν_0 –> x-type: S_φ scales as $\nu_0()$
- Low ν_0 –> φ-type: constant S_φ (but bumps 0.1–10 Hz)

White

- Aliasing at high f and low ν_0

Claudio Calosso wrote (June 26, 2020) Attila ha legato il ginocchio al loop che genera in automatico la soglia.
Se ti ricordi, il controllo aggiustava la tensione di soglia in modo da avere un duty cycle all'uscita
del 50%. Se la soglia fluttua, allora il DC cambia, il controllo se ne accorge e va compensare la variazione della soglia e, di fatto, va a ridurre il rumore residuo del distributore, come dimostrato
dal grafico per frequenze inferiori al ginocchio per 12, 6 e 3 MHz.
Mi aspetto che, aumentando la banda del controllo, il grafico migliori ulteriormente.
Secondo me è una cosa carina, un trucco da tenere presente per le applicazioni dove domina
il rumore della soglia.

Cyclone III Output Buffer

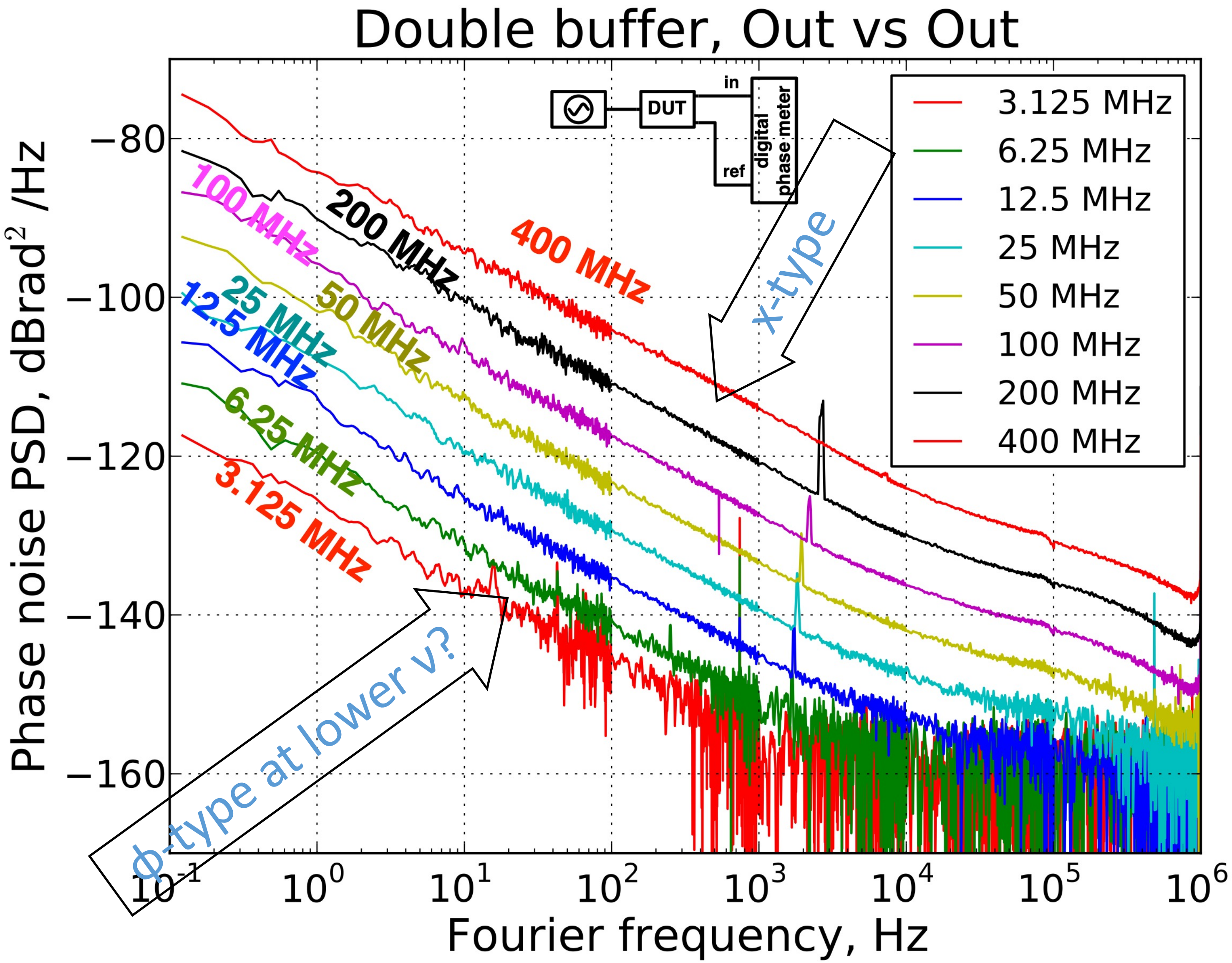

MAX 3000 CPLD [300 nm] (1)

Π divider

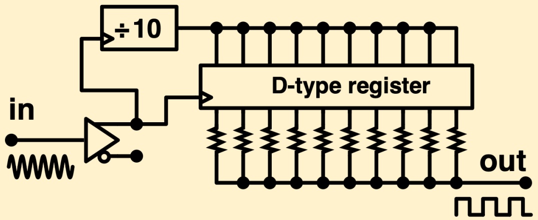

Λ divider

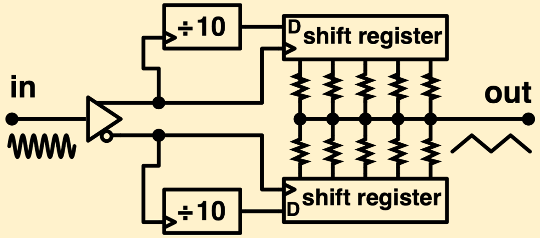

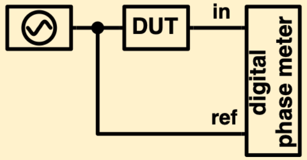

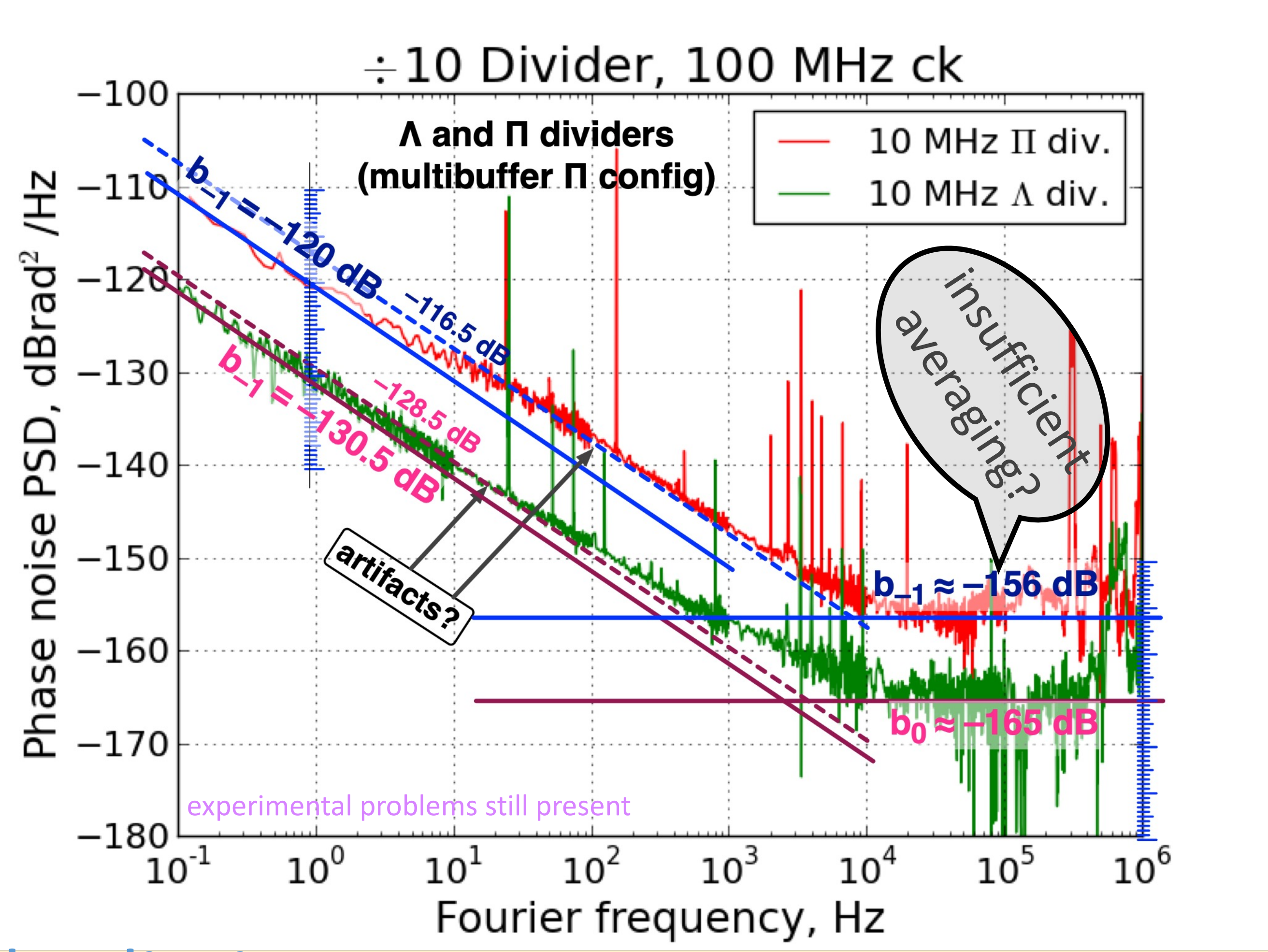

- Flicker region –> Negligible aliasing
  - The Π divider is still not well explained
  - The Λ divider exhibits low 1/ƒ and low white noise

Additional Facts Related to Phase and Noise

Volume Law

Input Chatter

Internal PLL

Thermal Effects

……

The Volume Law

Experiment

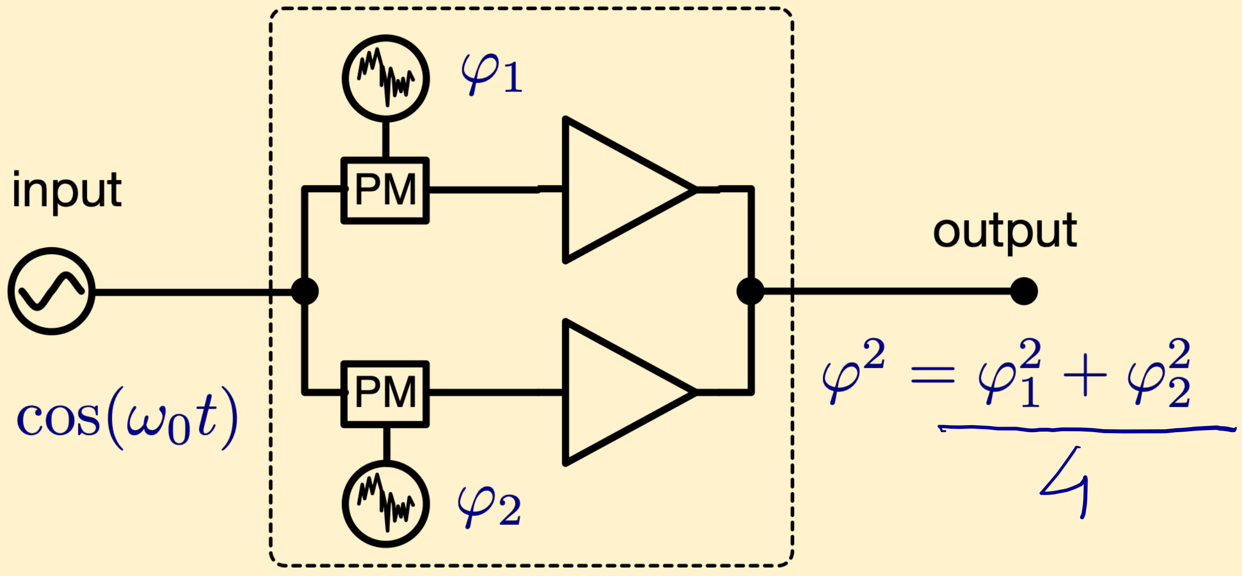

- The 1/ƒ coefficient b–1 is independent of power
- The flicker of a branch does not increase at P/2
- At the output,
  - the carrier adds up coherently
  - the phase noise adds up statistically
- With m branches, the 1/ƒ PM noise is reduced by 1/m
- White noise cannot be reduced in this way

Gedankenexperiment

- Flicker is of microscopic origin because it has Gaussian PDF
- Join the m branches into a compound
- 1/ƒ noise is proportional to 1/V, the volume of the active region

The Volume Law!

All devices used as ÷10 Λ divider at 100 MHz input
(30 MHz with Cyclone and Cyclone II, and results are scaled up as x-type noise)
The Λ divider reduces aliasing (white), thus makes 1/f noise more visible

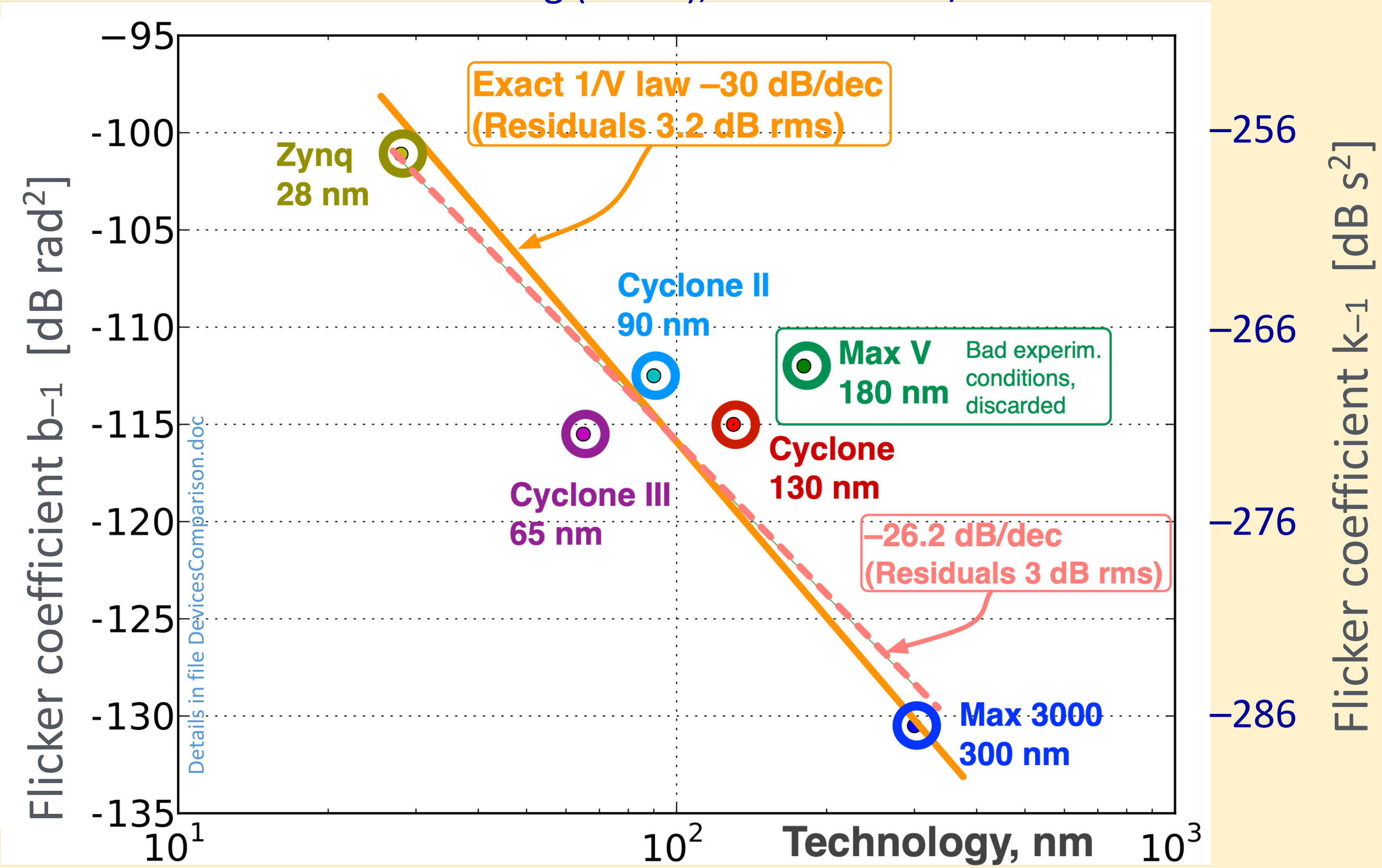

Input Chatter

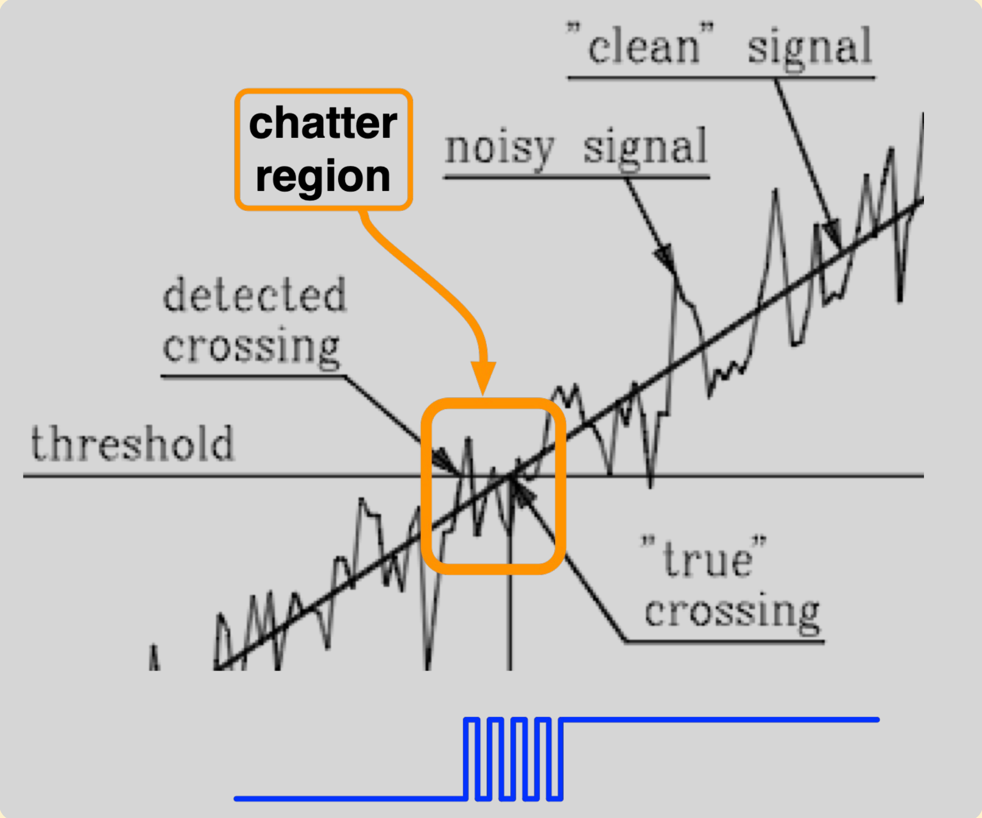

With high-speed devices, chatter can occur at rather high frequencies

Chatter occurs when the RMS Slew Rate of noise exceeds the slew rate of the pure signal

Pure signal

$$v(t) = V_0 \cos(2\pi\nu_0 t)$$

$$\mathrm{SR} = 2\pi\nu_0 V_0$$

Wide band noise

$$\langle \mathrm{SR}^2 \rangle = 4\pi^2 \int_0^B f^2 S_V(f)\, df$$

$$= \frac{4\pi^2}{3}\sigma_V^2 B^2 \quad (\mathrm{rms})$$

Chatter threshold

$$\nu_0^2 = \frac{1}{3}\frac{S_v B^3}{V_0^2}$$

Example

- V_0 = 100 mV peak
- 10 nV/√Hz noise
- 650 MHz max –> 2 GHz noise BW
- Chatter threshold **ν** = 5.2 MHz

Simulation of Chatter

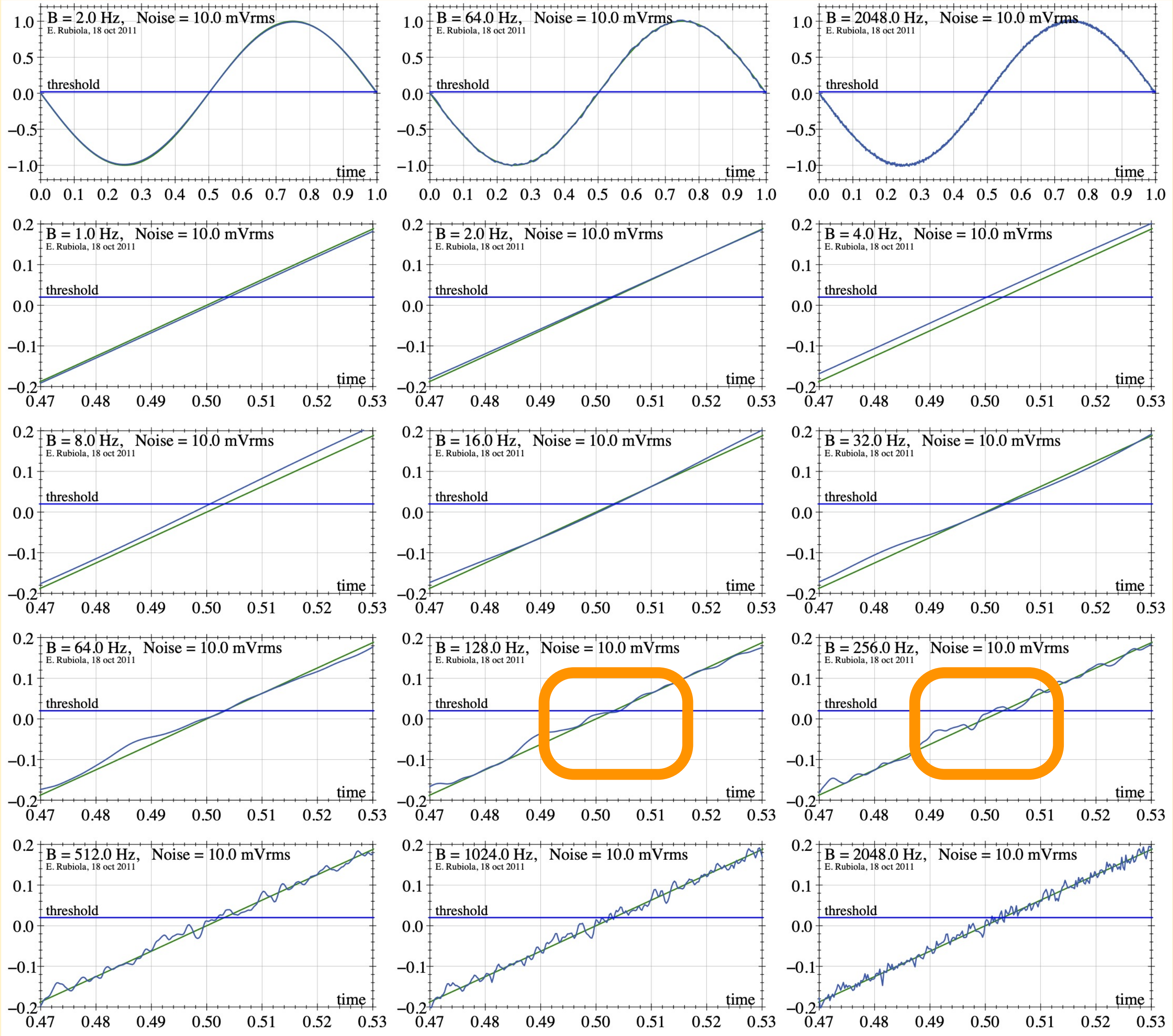

Conditions

ν_0 = 1 Hz,

V_0 = 1 V_{peak}

$\sqrt{\langle v_0^2 \rangle}$ = 10 mV rms noise

Noise BW increases in powers of 2

De-normalize for your needs

Input Chatter – Example

Good agreement with theory

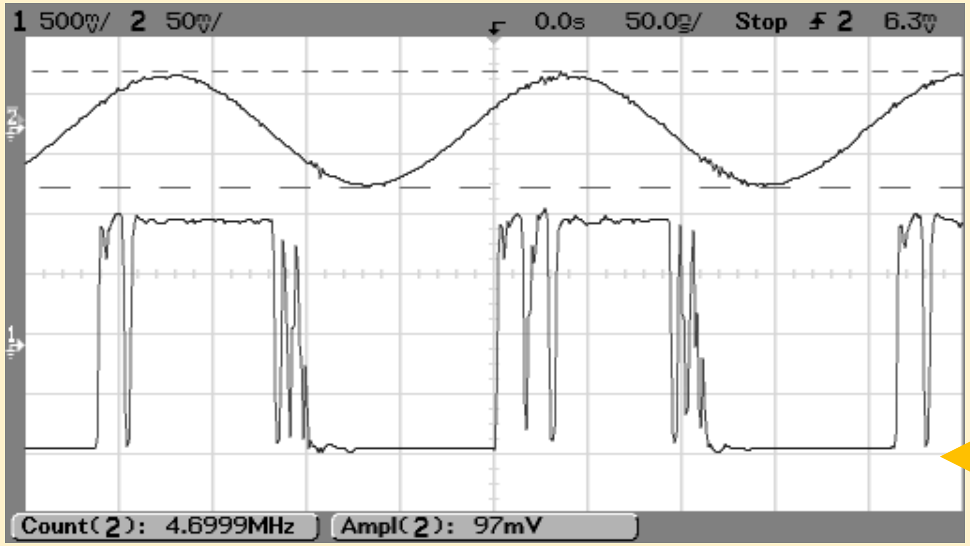

V_0 = 50 mV (100 mV_{pp})

ν_0 = 4.7 MHz

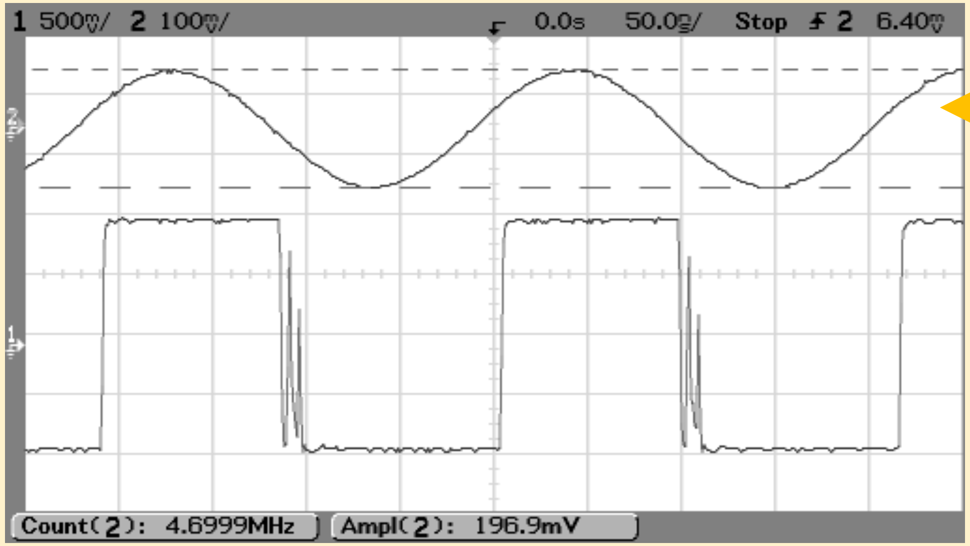

V_0 = 100 mV (200 mV_{pp})

ν_0 = 4.7 MHz

Experiment

- Cyclone III FPGA
- Estimated noise 10 nV/√Hz
- Estimated BW 2 GHz

Asymmetry shows up

Explanation takes a detailed electrical model, which we have not

Cyclone III Internal PLL

A.C. Cárdenas Olaya & al, IEEE Transact. UFFC 66(2) pp.412-416, Feb 2019

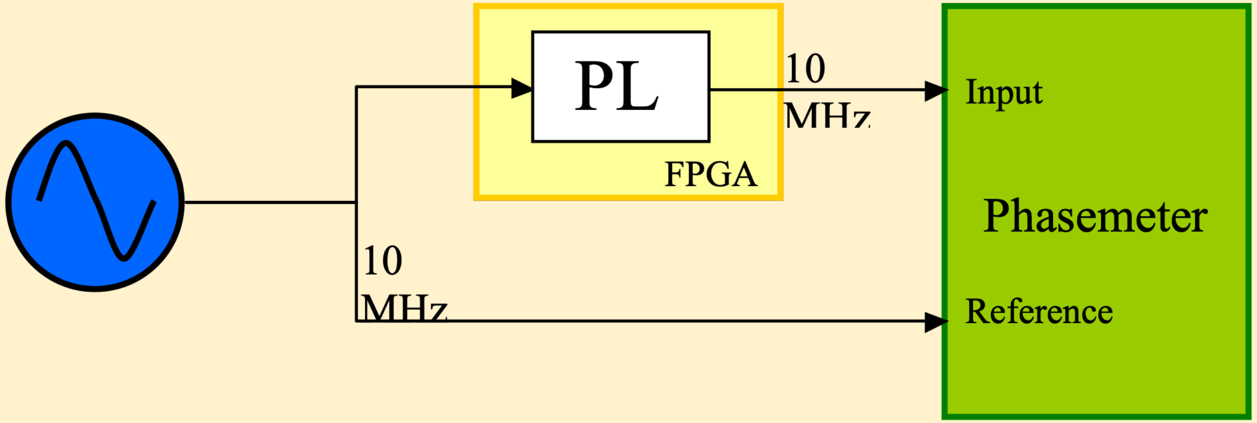

Symmetricom
5120A (30 MHz max)

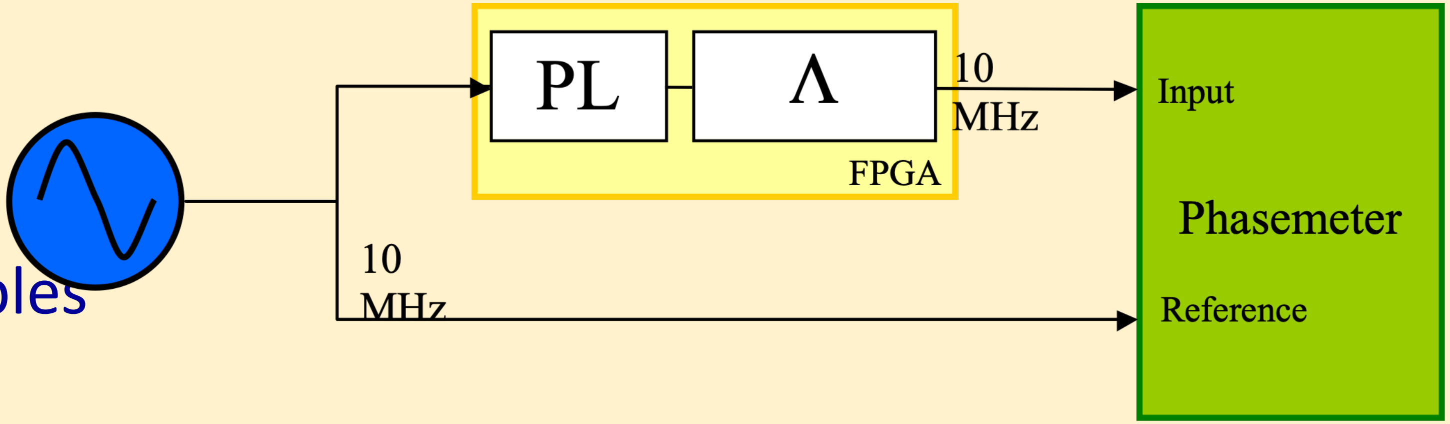

A Λ divider (inside the FPGA) enables the measurement

- The divider noise is low enough
- A trick to work at low frequency

Cyclone III Internal PLL

PLL used as a buffer

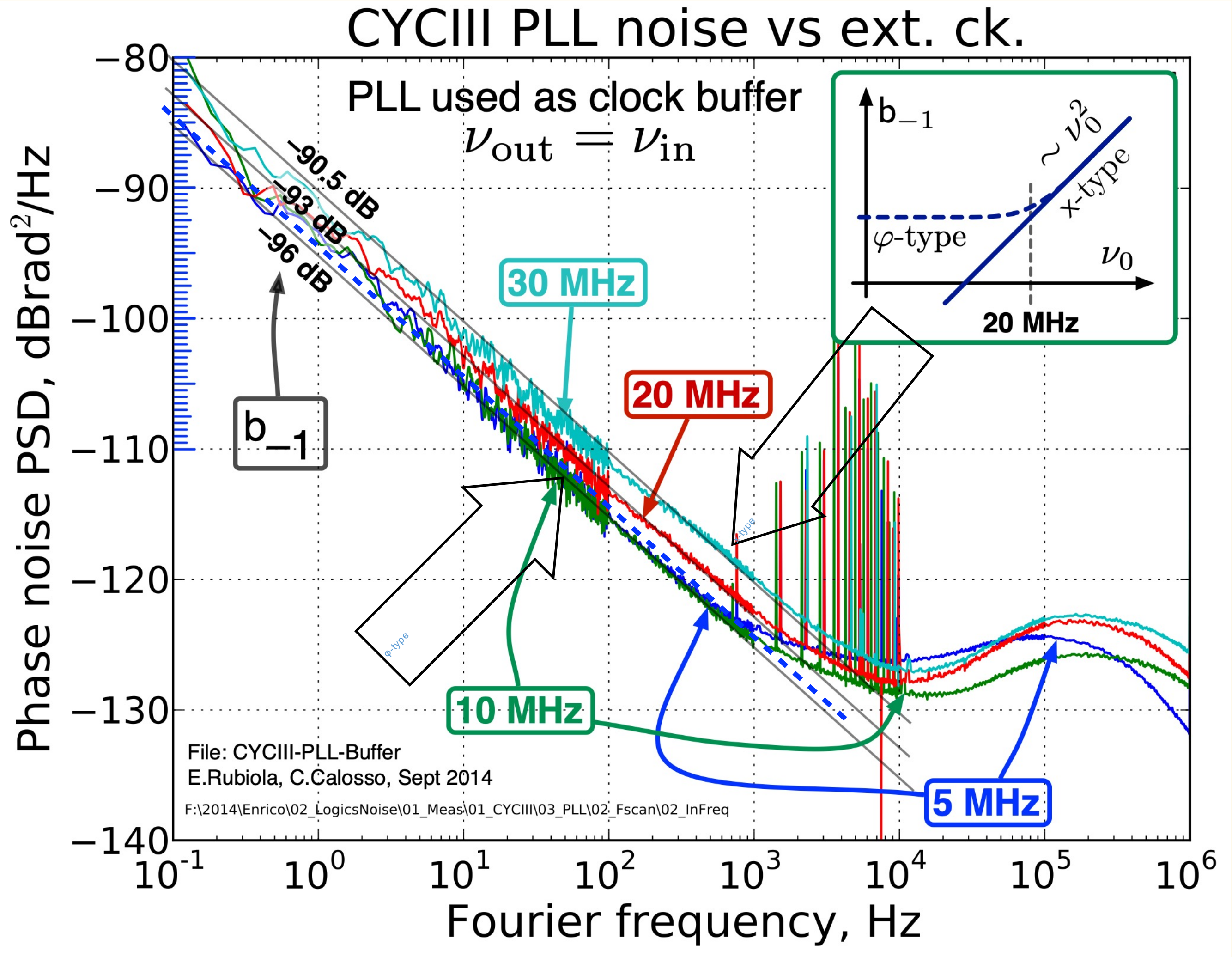

x-type –> analog noise in the phase detector

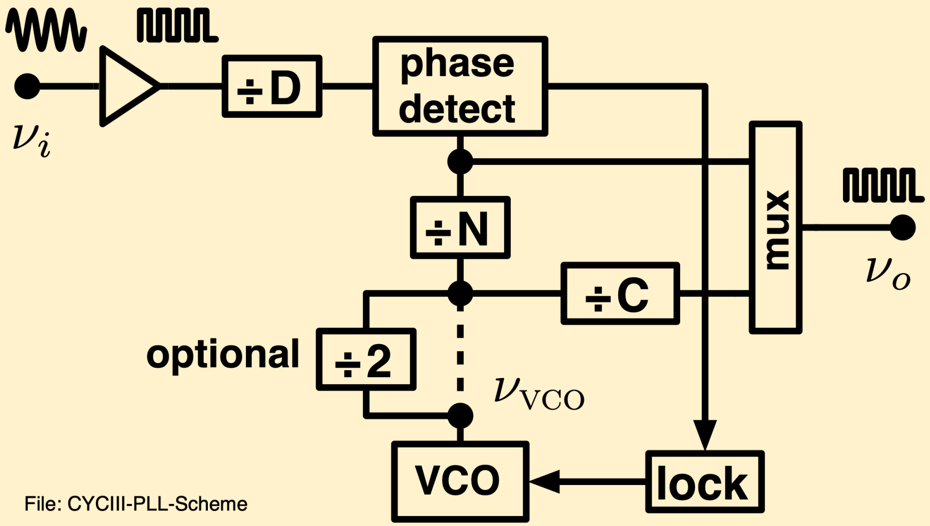

- LC oscillator, 0.6–1.3 GHz, Q≈10
- Optional ÷2 always present
- We set D = 1 (for lowest noise)
- QUARTUS app chooses C and N

Crossover between phi-type and x-type at 20 MHz

Cyclone III Internal PLL

PLL used as a frequency multiplier

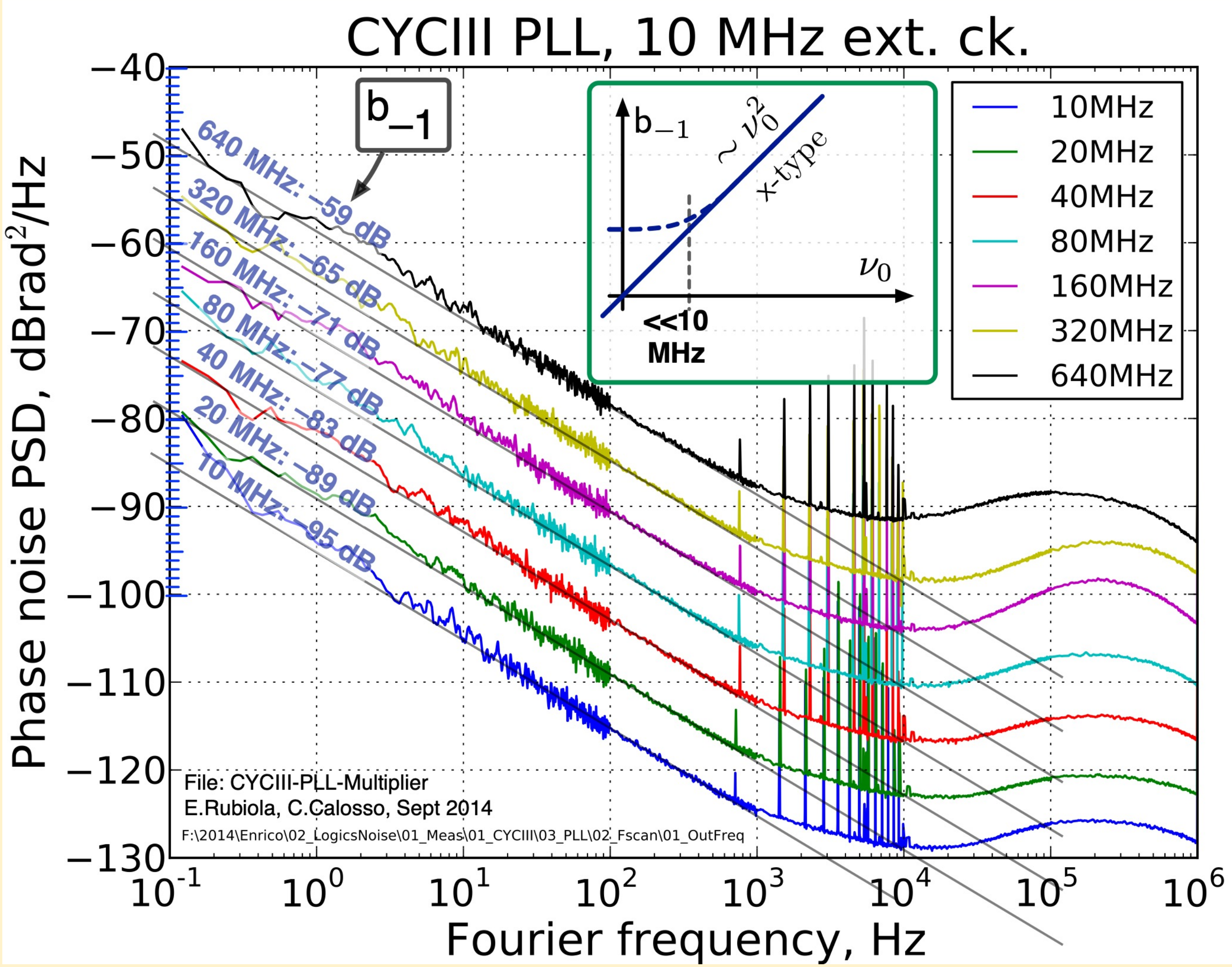

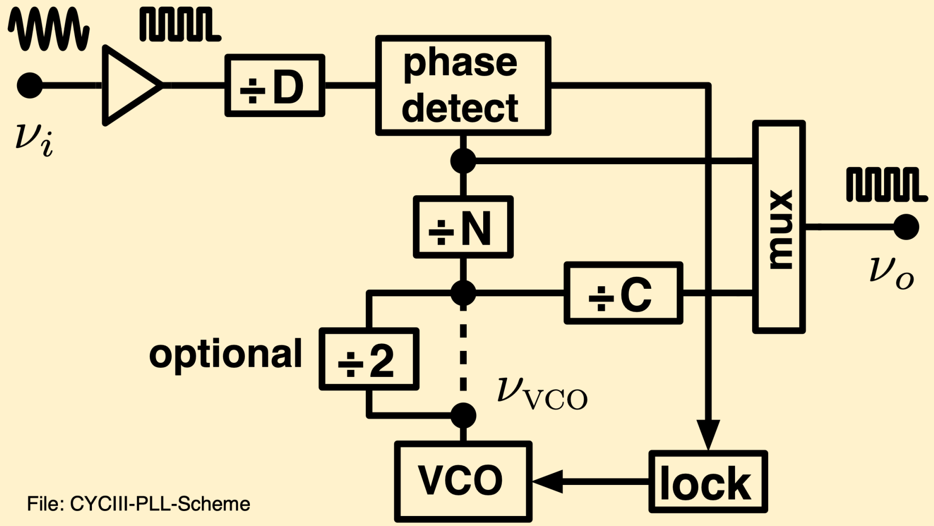

10 MHz input, N x 10 MHz out

- 1/ƒ phase noise is dominant
- Scales as N^2 –> analog noise in the phase detector
- ADEV 1.5x10^{-12} @ 1 s, f_H = 500 Hz

-115 dB + 20 $\log_{10}(\nu_0)$, ν_0 in MHz

Thermal Effects

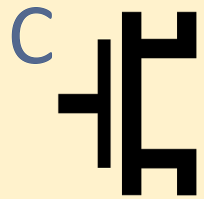

- Principle
  - FPGA dissipation change ΔP by acting on frequency
  - Energy E = CV2 dissipated by the gate capacitor in one cycle
- Conditions
  - Cyclone III used as a clock buffer
  - Environment temperature fluctuations are filtered out with a small blanket (necessary)
  - Two separate measurements (phase meter and counter) –> trusted result

Outcomes

1. Thermal transient, due to the change of the FPGA dissipation
2. Slow thermal drift, due to the environment
3. Overall effect of ΔP

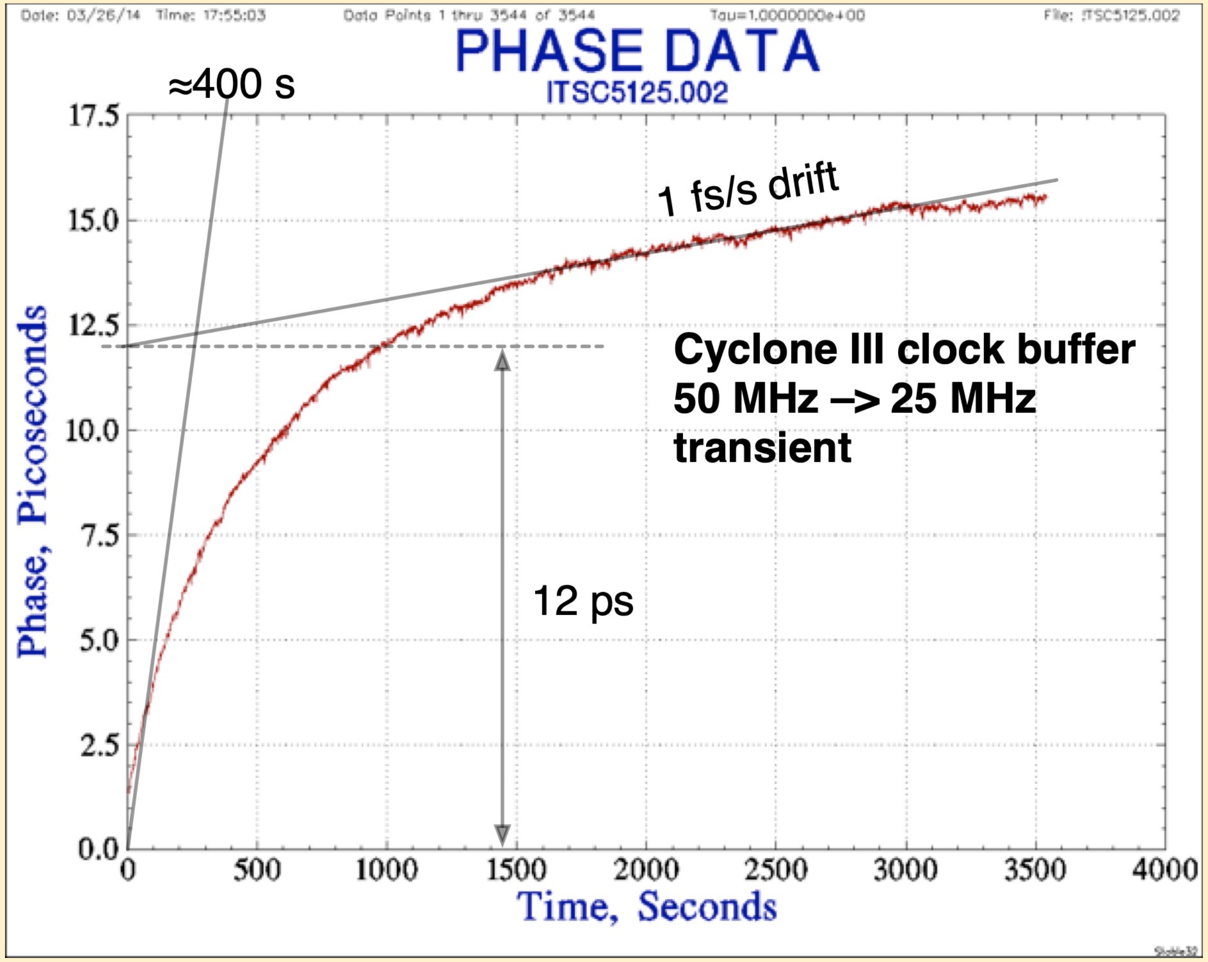

3 – ADCs

Transition Noise Measurement

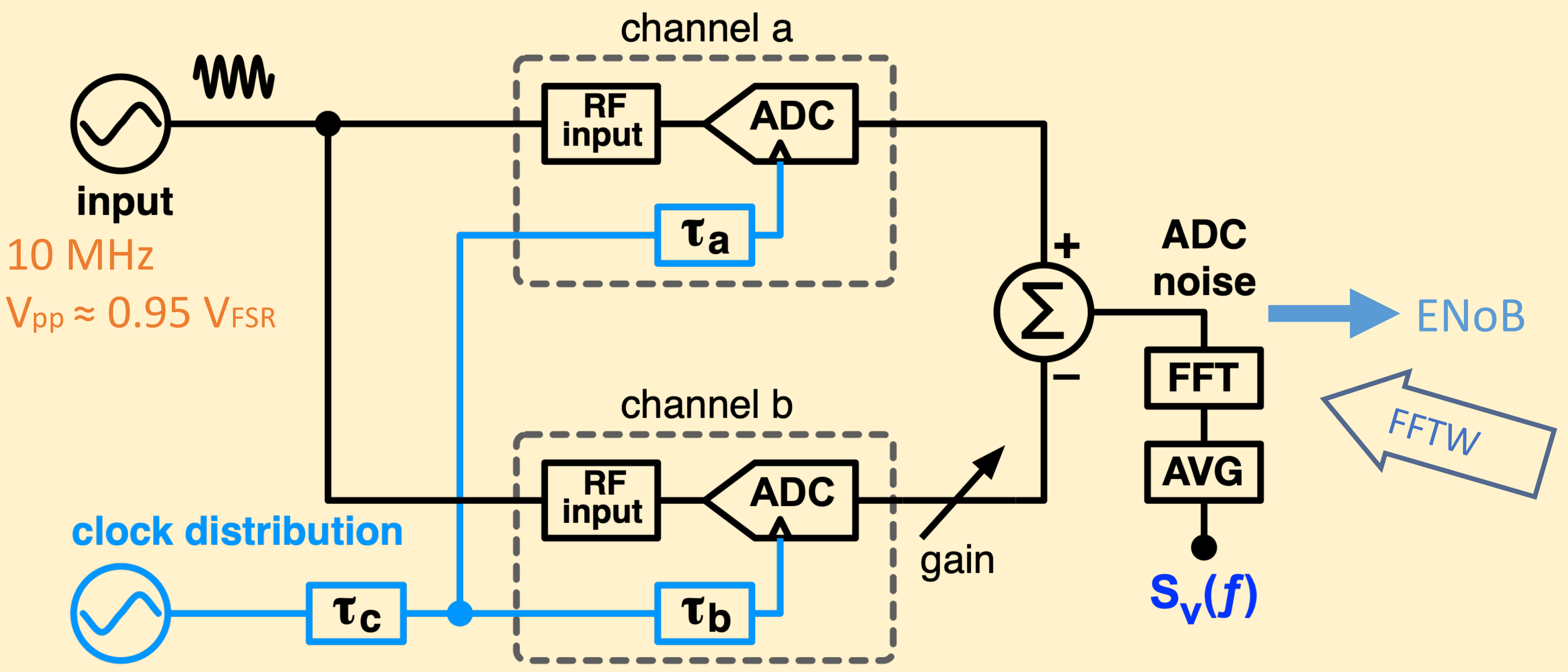

The differential clock jitter introduces additional noise due to the asymmetry between AM and PM

At 10 MHz input, the effect of ≈100 fs jitter does not show up

Background Noise

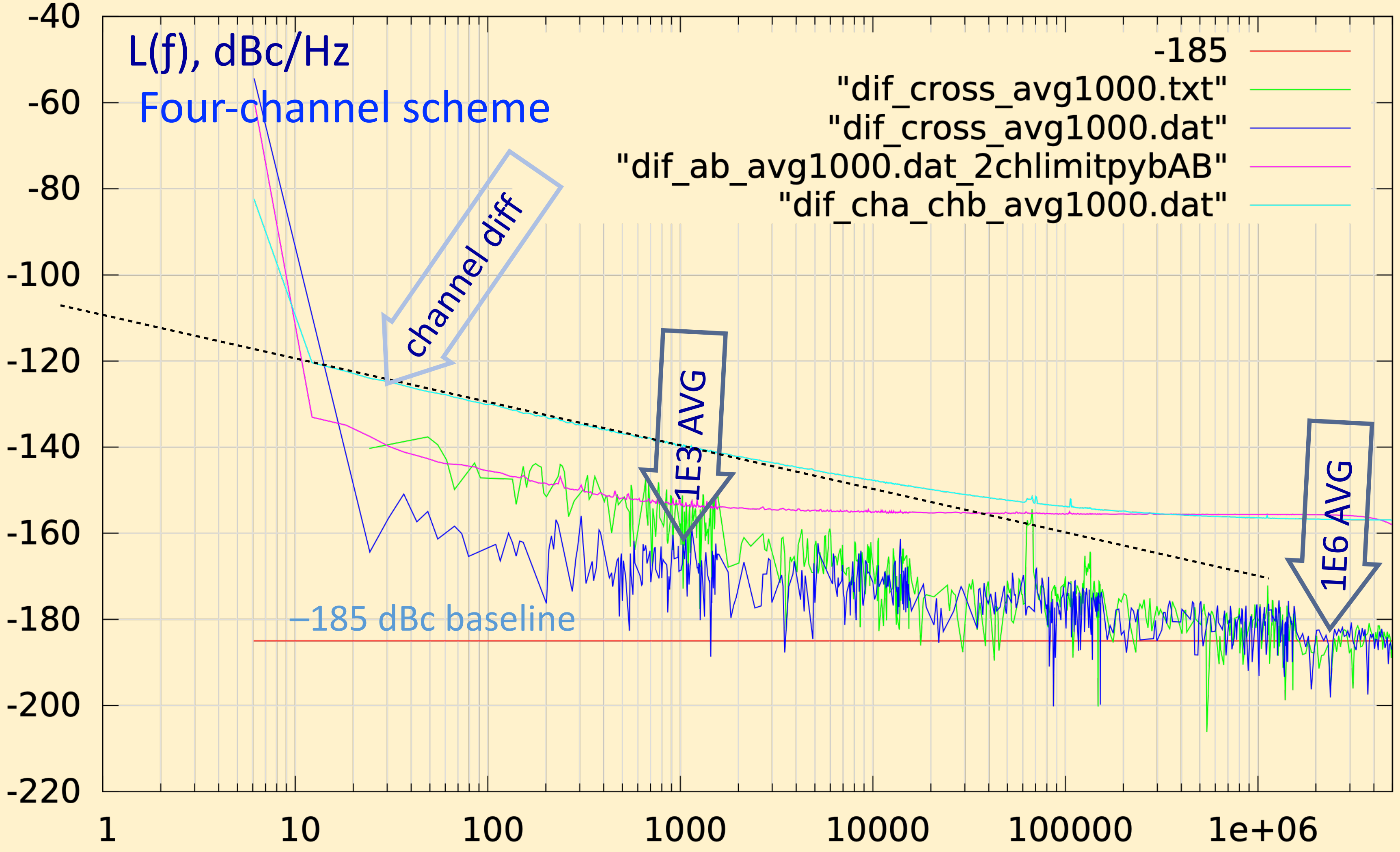

Compared to a Commercial Instrument

– this is done only to make sure that there is no calibration mistake –

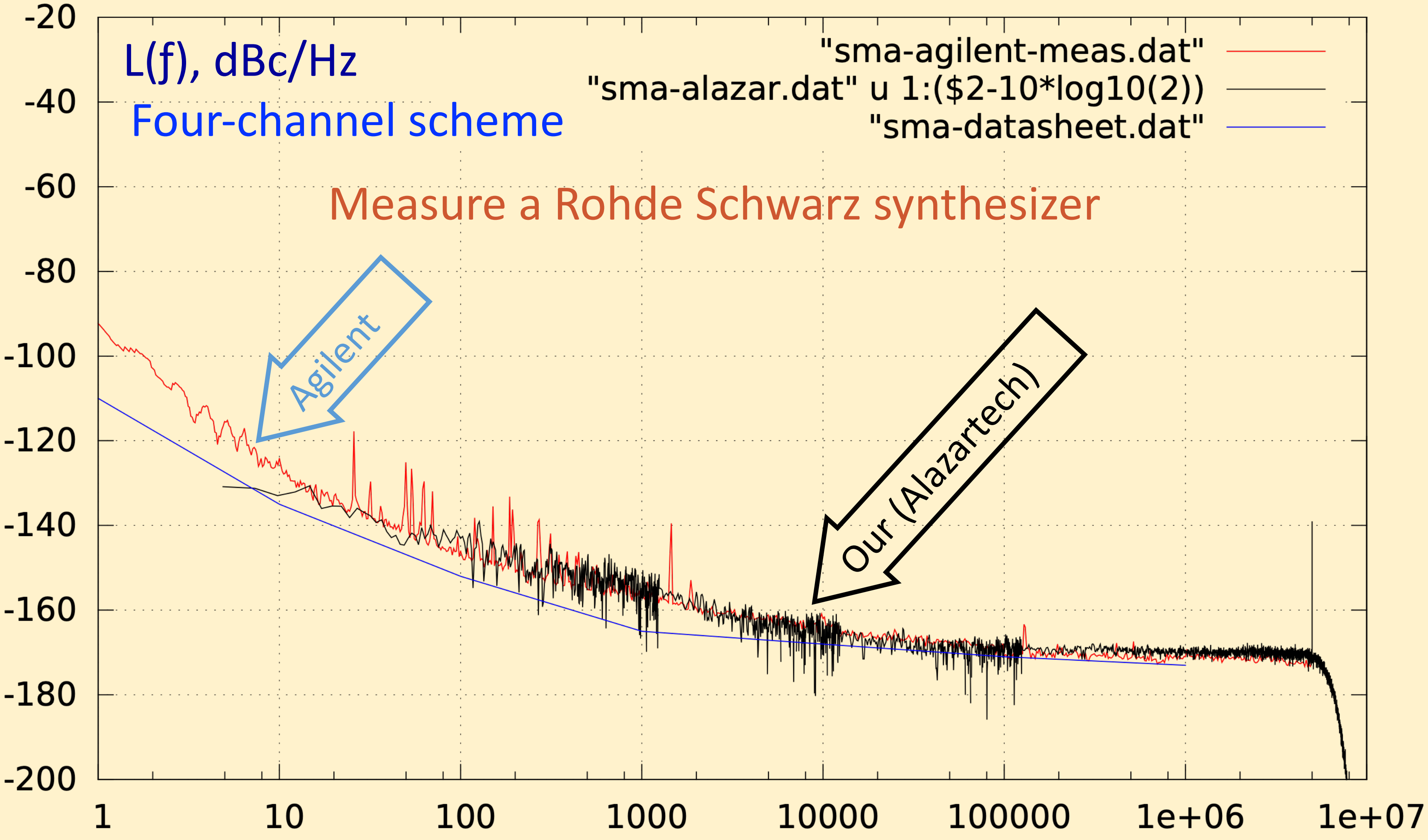

4 – DDSs

Basics

Advanced

Experiments

Basic DDS Scheme

replace θ —> ϕ

integer: $n_k = (n_{k-1} + \mathcal{N}) \bmod \mathcal{D}$

complex: $z_k = z_{k-1} \exp(j\eta)$

phase: $\theta_k = (\theta_{k-1} + \eta) \bmod 2\pi$

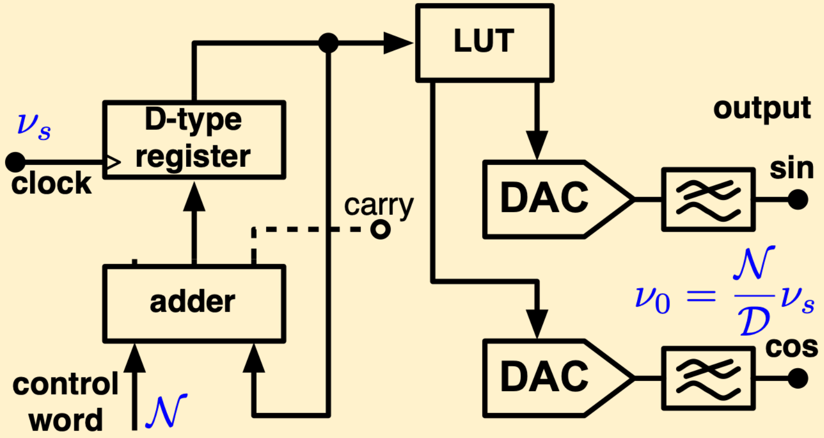

quantity	digital	analog
state variable	n	$\theta = 2\pi \frac{n}{\mathcal{D}}$
assoc. complex		$z = e^{j\theta}$
modulo	$\mathcal{D} = 2^m$	2π
increment	$\mathcal{N}$	$\eta = 2\pi \frac{\mathcal{N}}{\mathcal{D}}$
time	k, $0, 1, 2, \ldots$	$t = k/\nu_s$
clock freq. ν_s	output freq. $\nu_0 = \frac{\mathcal{N}}{\mathcal{D}}\nu_s$	

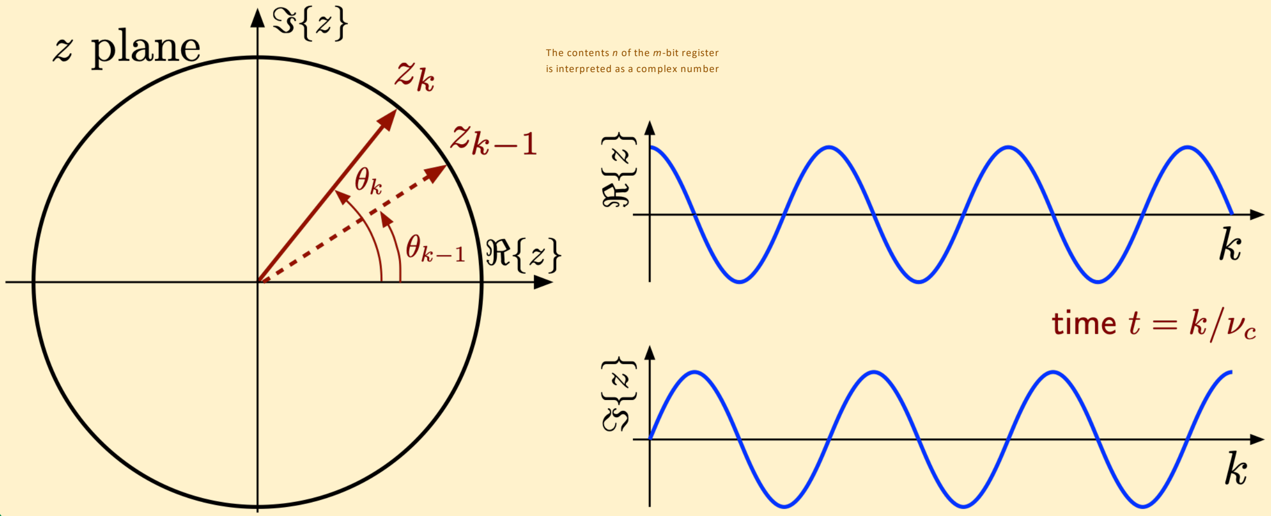

The contents n of the m-bit register is interpreted as a complex number

AD9912, a Fast DDS

48 bit accumulator, 14 bit DAC, 1 GHz clock

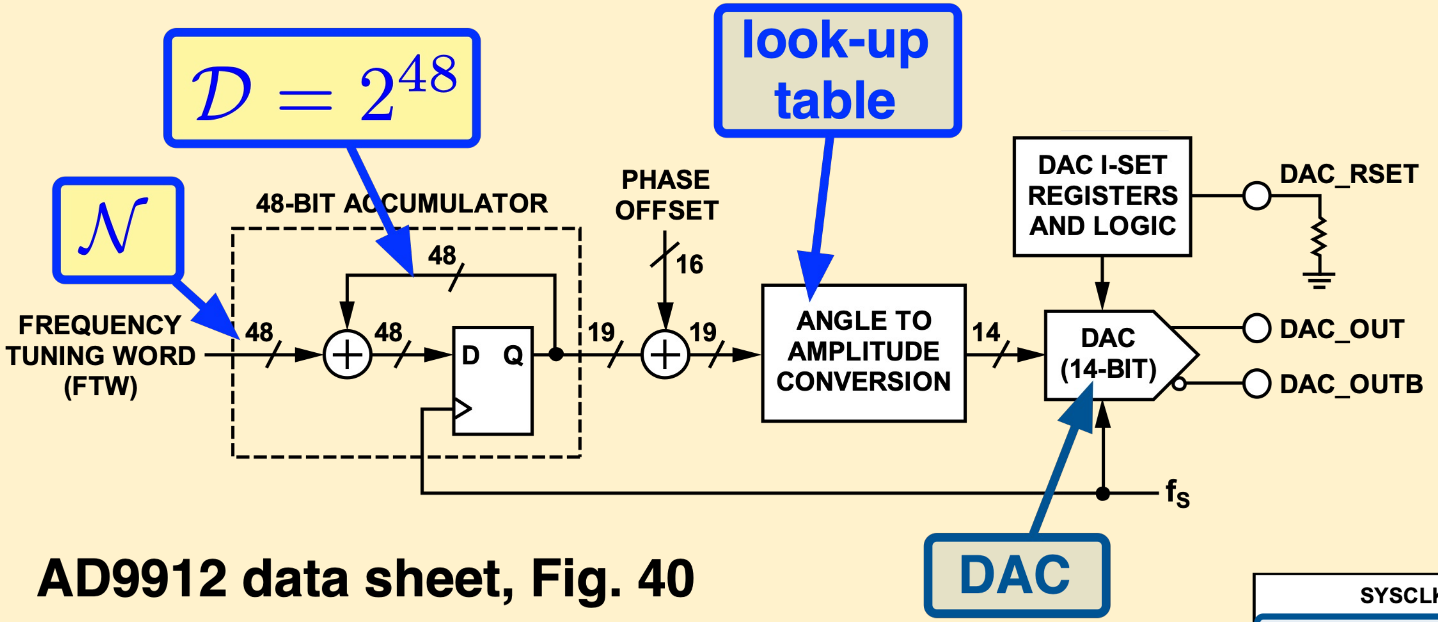

AD9912 data sheet, Fig. 40

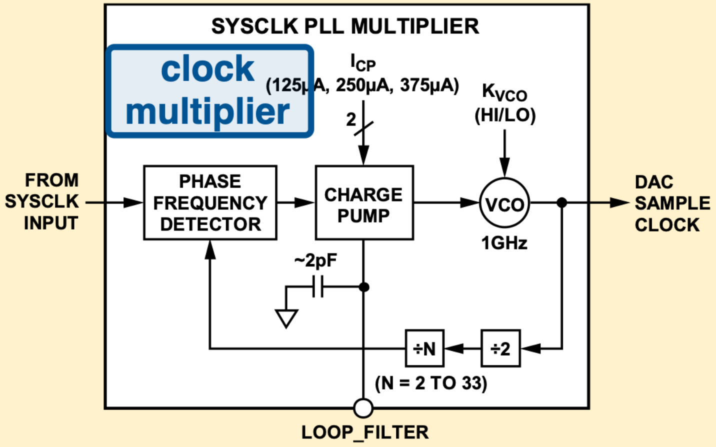

AD9912 data sheet, Fig. 45

State-Variable Truncation

$$n_k = (n_{k-1} + \mathcal{N}) \bmod \mathcal{D}, \quad \mathcal{D} = 2^m$$

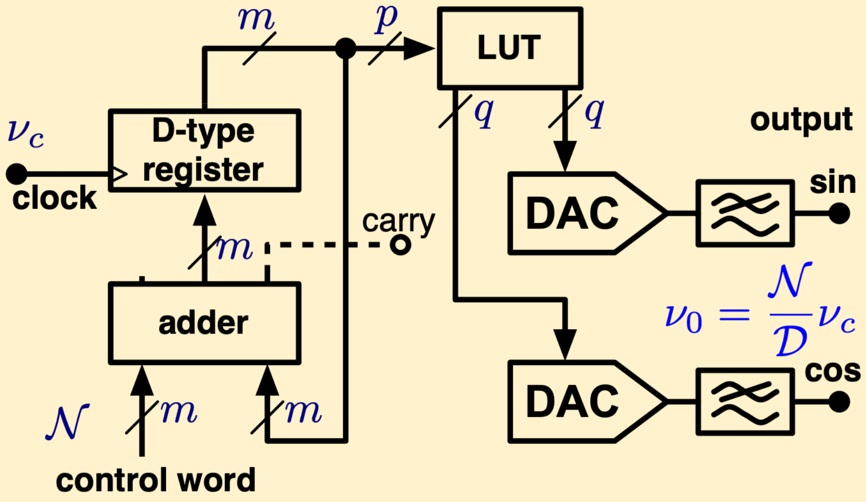

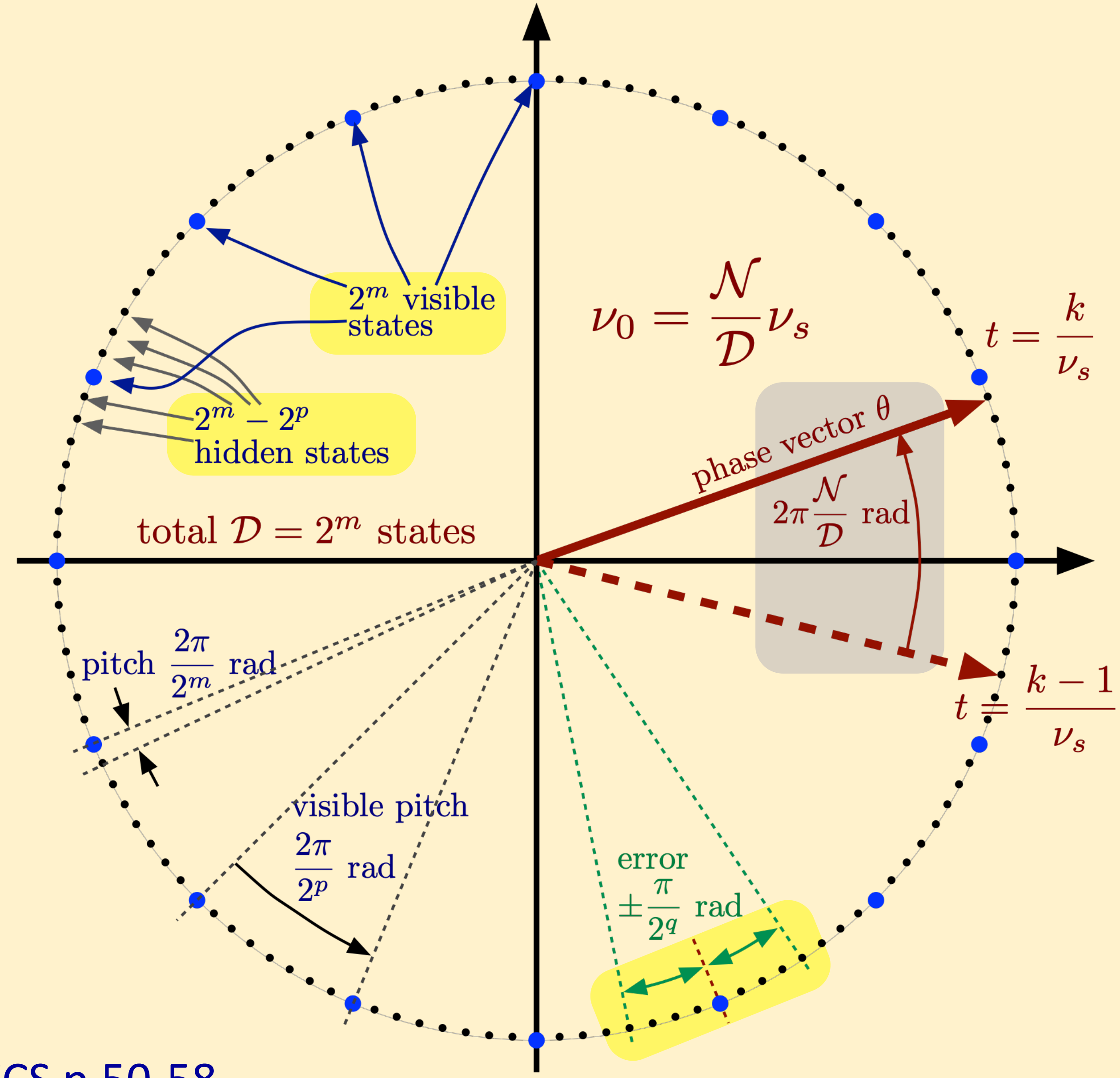

- Only quantization shows up with full m-bit conversion
- Technology –> q max
- Why p > q
- Slow pseudorandom beat, 3d 6h 11m 15s @ 1 GHz, 48 bit

Spurs: Torosyan A, Wilson AN jr, Proc 2005 IFCS p.50-58

Truncation Generates Spurs

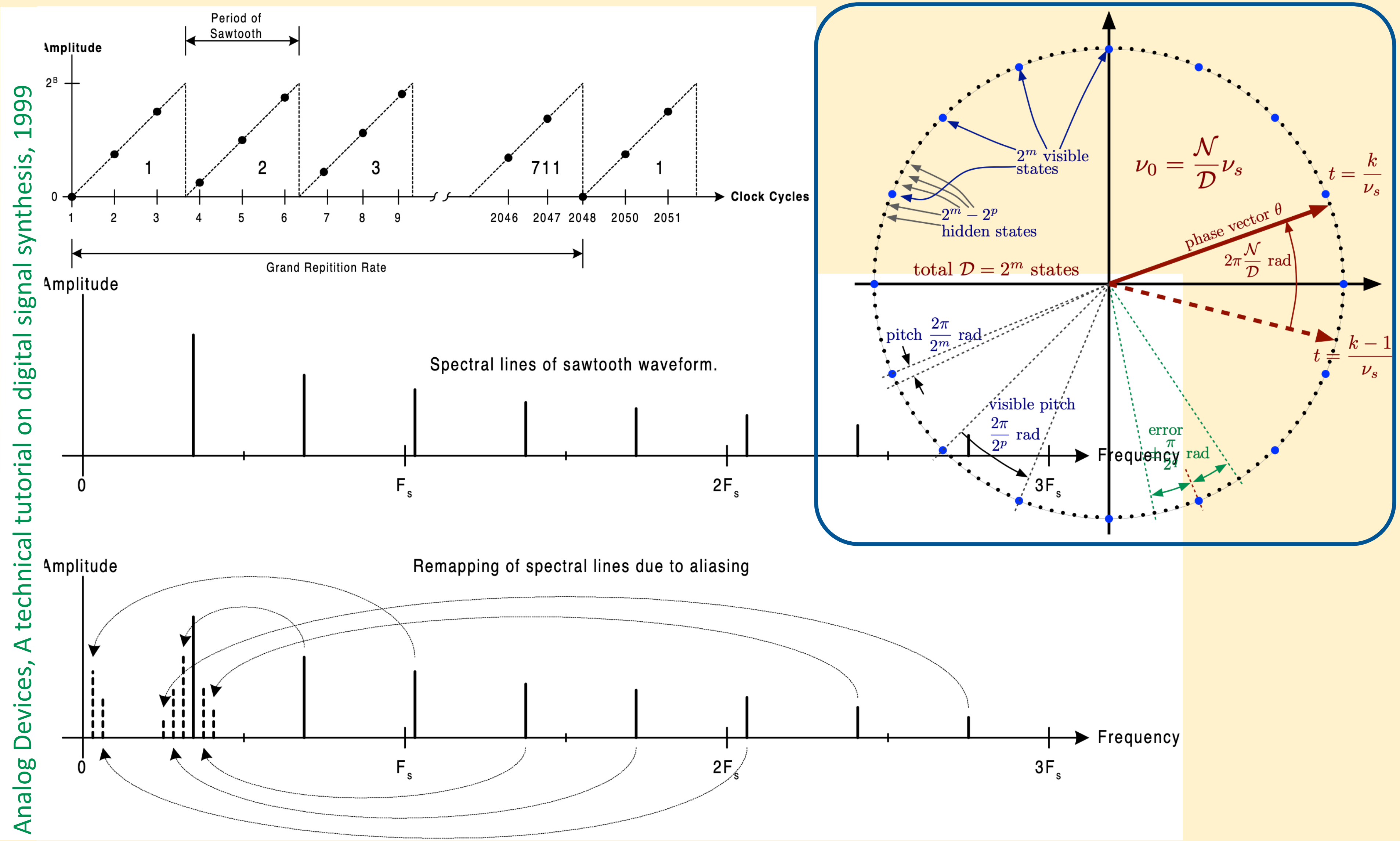

The power of spurs comes at expenses of white noise – yet not as one-to-one

Distortion and Aliasing

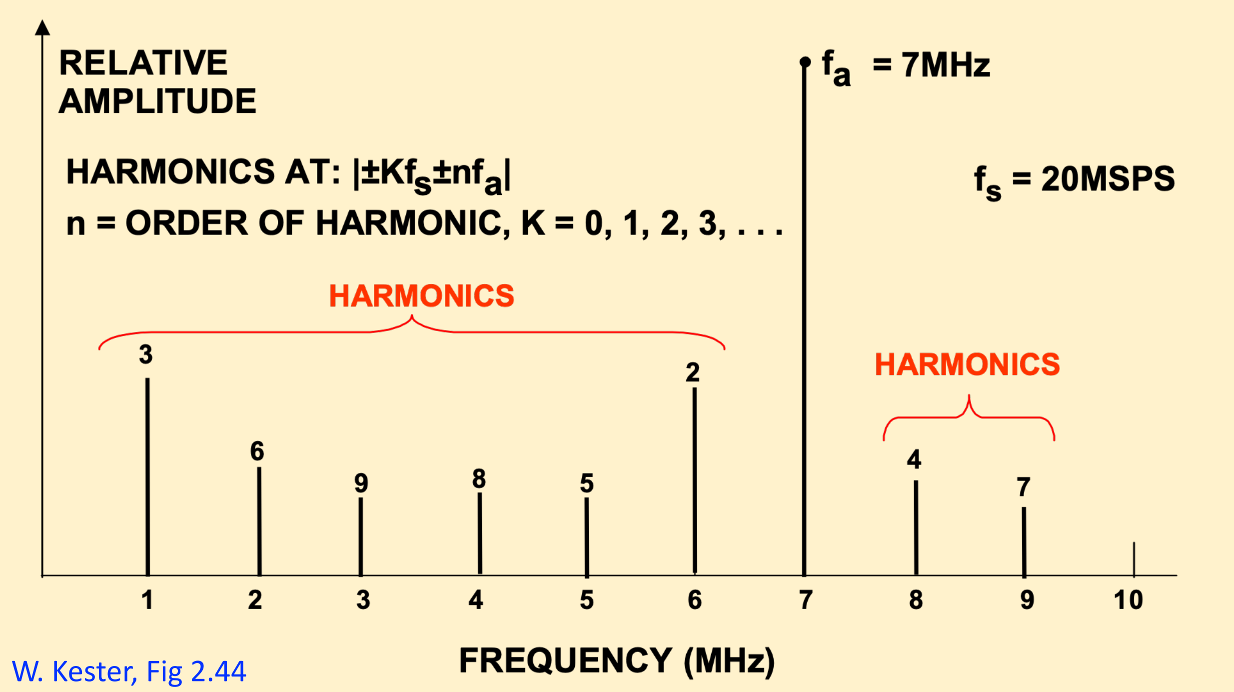

W. Kester, Fig 2.44

Sampling f_s = 20 MHz
Nyquist f_N = 10 MHz
Output f_a = 7 MHz

2nd. 2 x 7 = 14, mirror to 10 —> 6
3rd. 3 x 7 = 21, take away 20 —> 1
4th. 4 x 7 = 28, take away 20 —> 8
5th. 5 x 7 = 35, take away 20 —> 15, mirror to 10 —> 5
6th. 6 x 7 = 42, take away 40 —> 2
7th. 7 x 7 = 49, take away 40 —> 9
8th. 8 x 7 = 56, take away 40 —> 16, mirror to 10 —> 4
9th. 9 x 7 = 63, take away 60 —> 3

W. Kester ed., Analog-Digital Conversion, Analog Devices 2004, ISBN 0-916550-27-3

3.3 V: Lower PM Noise than 1.8 V

Probably related to the cell size and to the dynamic range

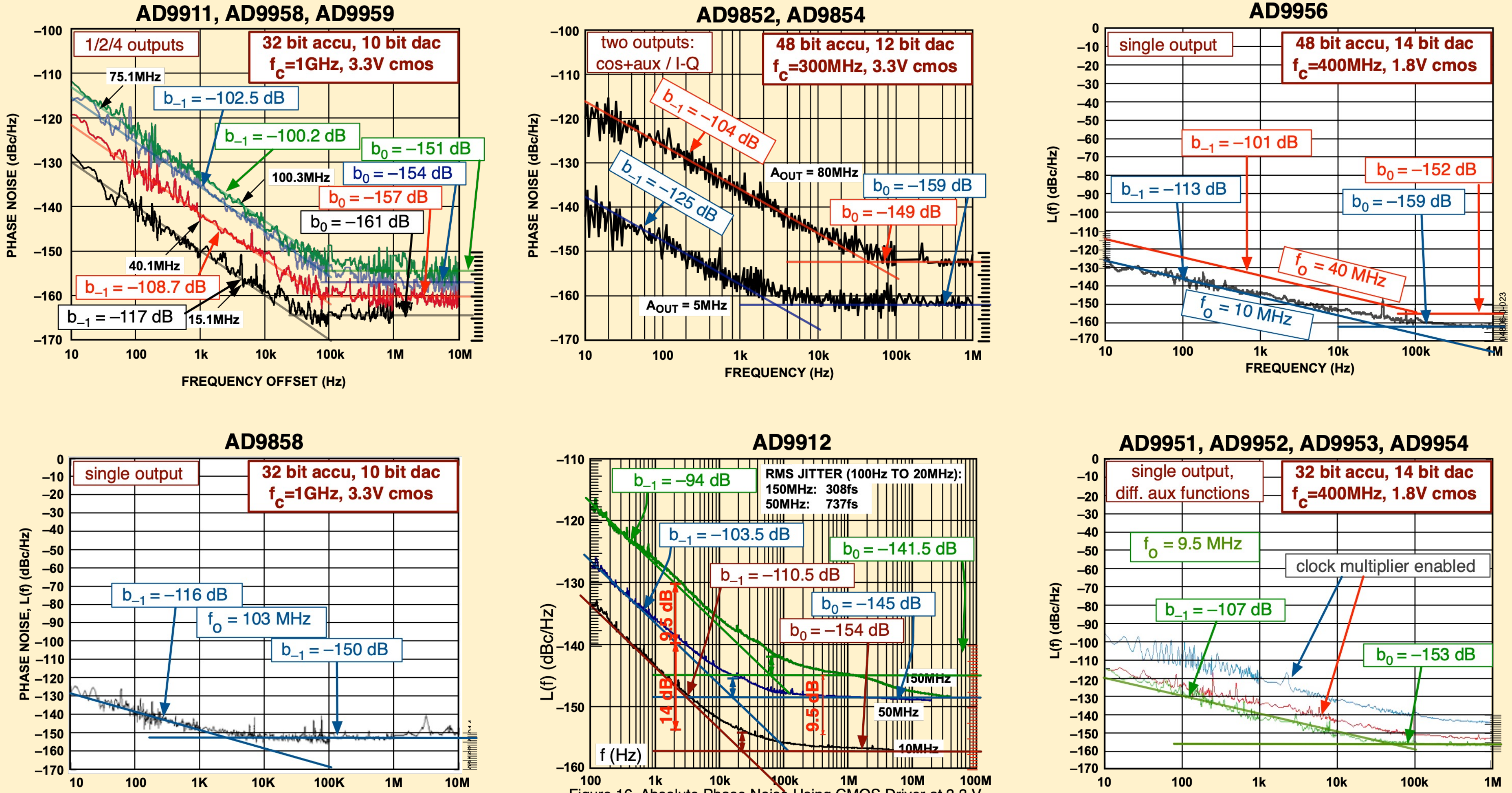

Figure 16. Absolute Phase Noise Using CMOS Driver at 3.3 V, SYSCLK = 1 GHz Wenzel Oscillator (SYSCLK PLL Bypassed) DDS Run at 200 MSPS for 10 MHz

E. Rubiola, Mar 2007 (adapted from the Analog Devices data sheets)

Plots originally used to extract the noise parameters

Experimental Method (PM Noise)

- Pseudorandom noise, slow beat (days)
- The probability that two accumulators are in phase is ≈ 0
- Two separate DDS driven by the same clock have a random and constant delay
- The delay de-correlates the two realizations, which makes the phase measurement possible

Single channel

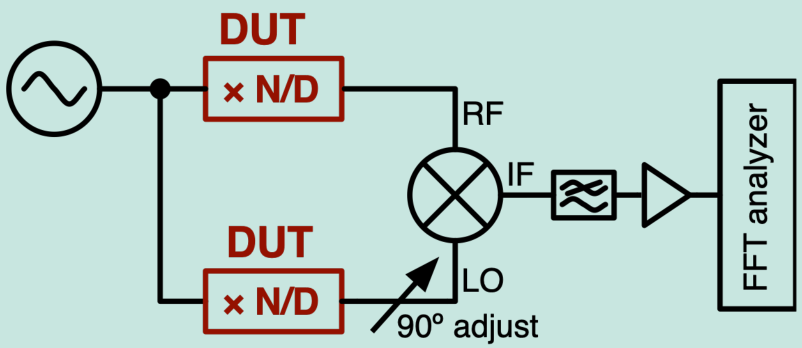

Dual channel

kind of virtual mixer, after (sub)sampling & direct ADC

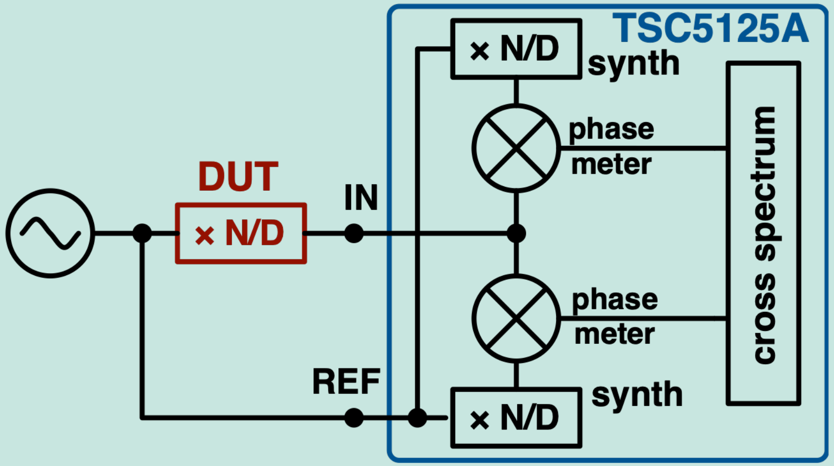

PM Noise vs Output Frequency

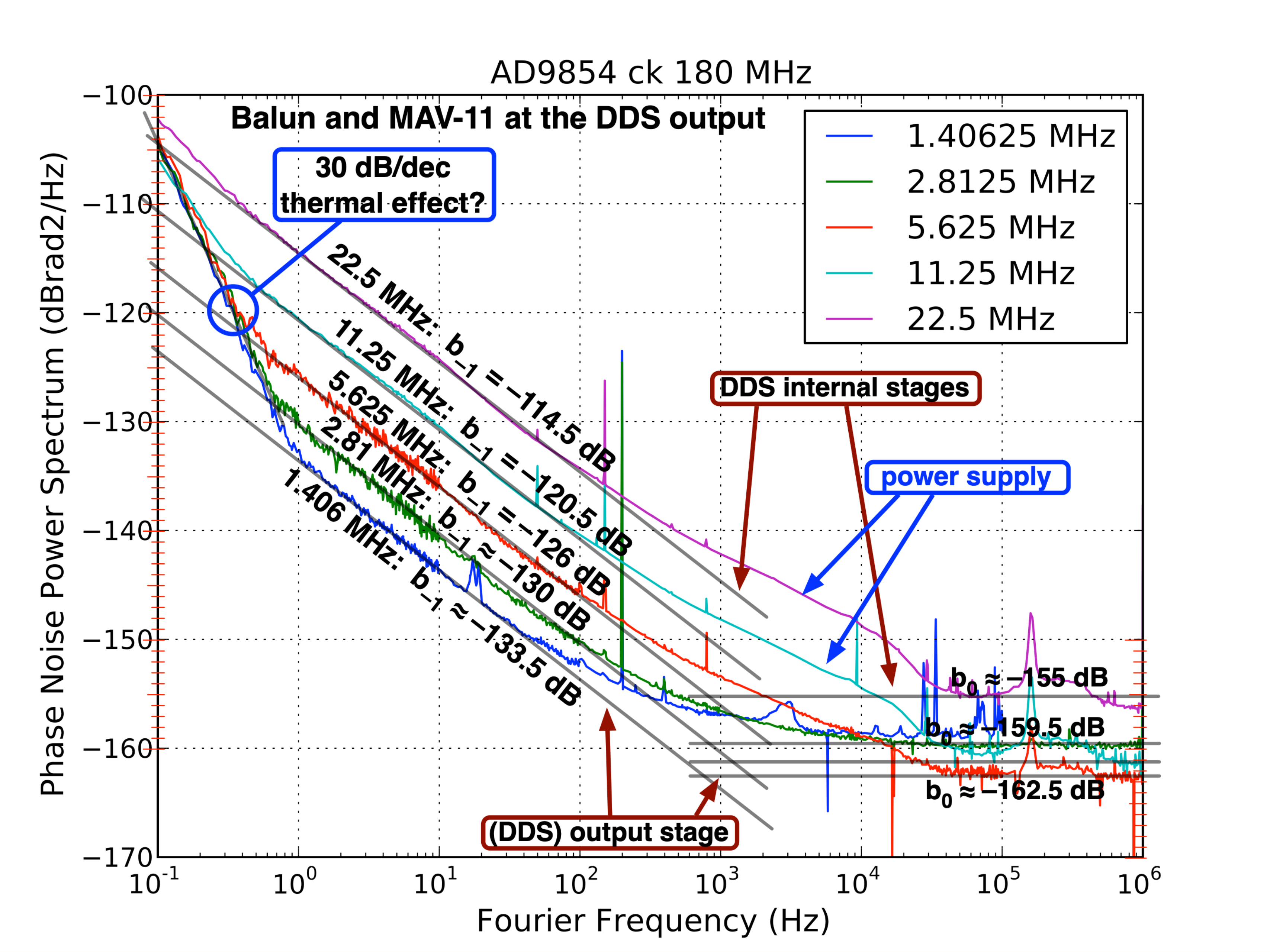

AD9854 Noise

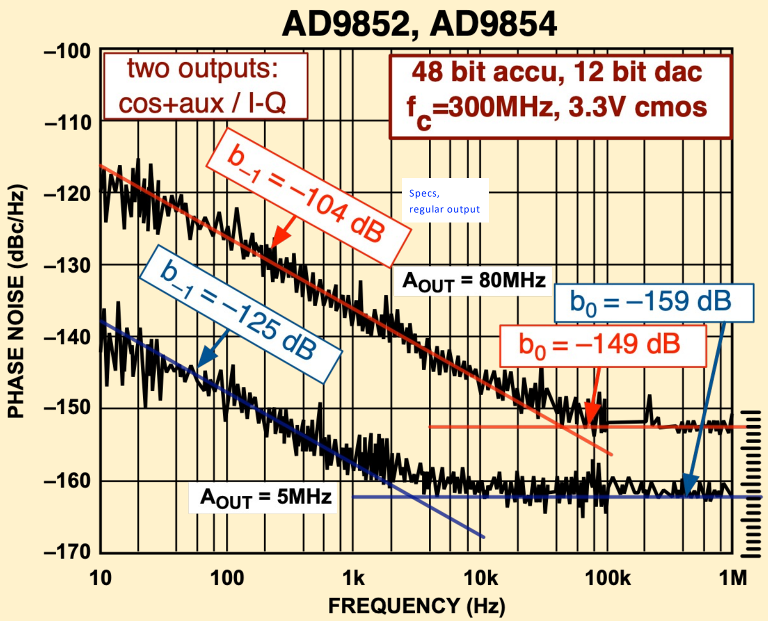

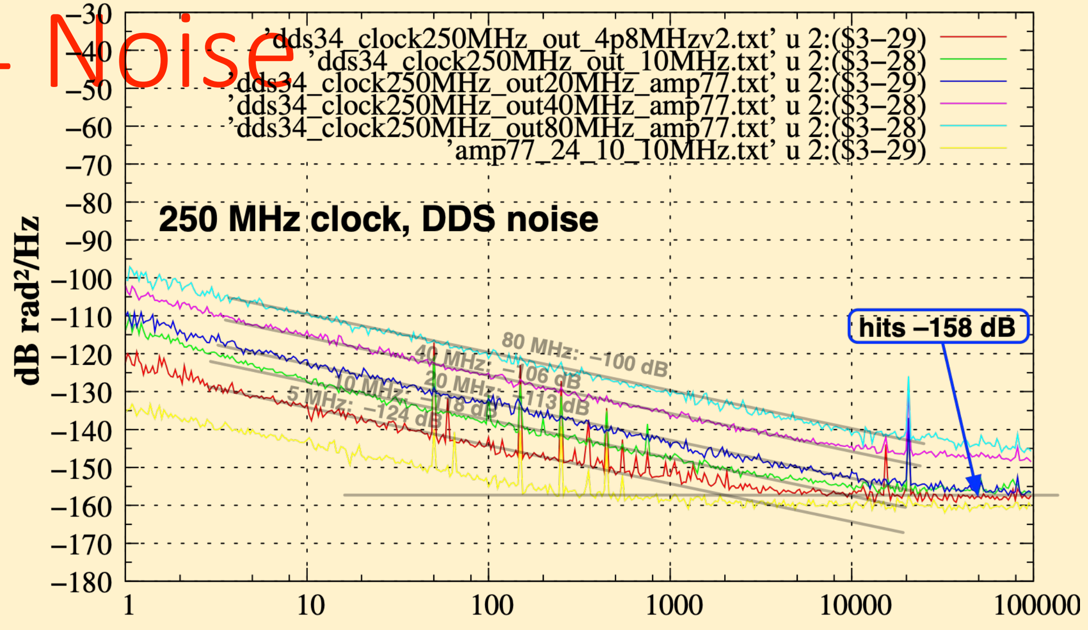

Flicker is in fair agreement

White is made low by spurs

Basic formula for white noise

$$b_0 = \frac{4}{3}\,\frac{1}{2^{2n}\,\nu_s} \quad \text{rad}^2/\text{Hz}$$

who	meas, dB	math, dB	clock, MHz
specs	–159	–155.8	300
YG	–158	–155.0	250
CC	–162.5	–153.6	180

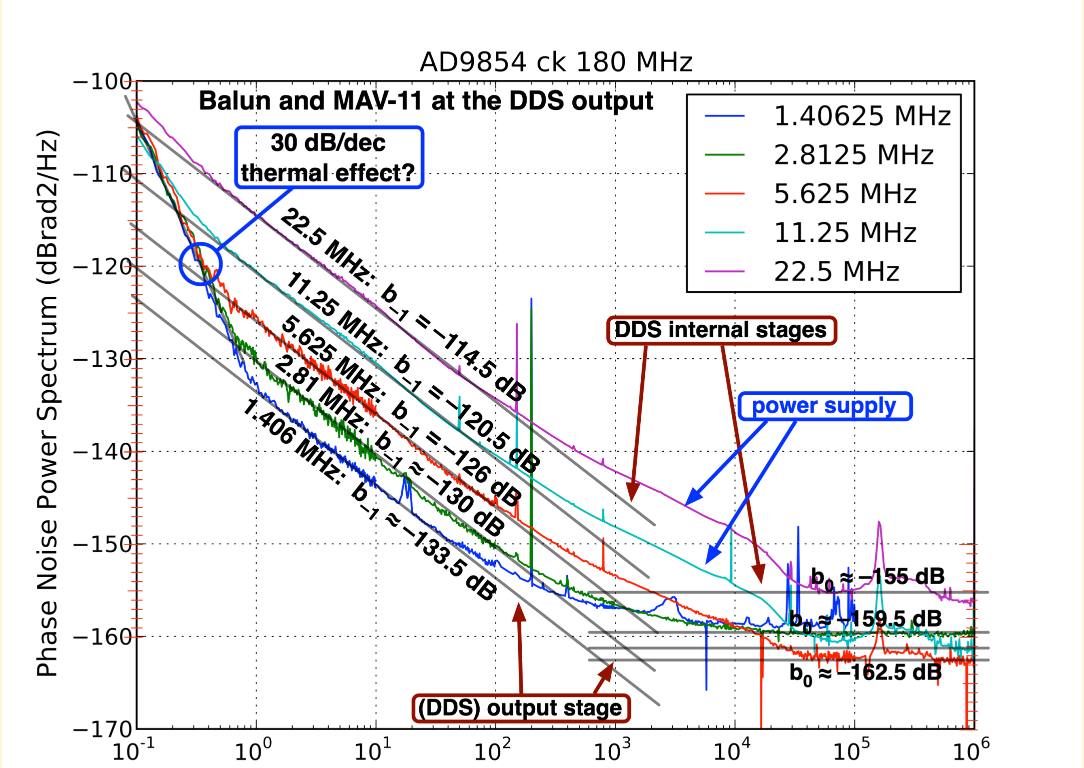

High-Frequency DDSs

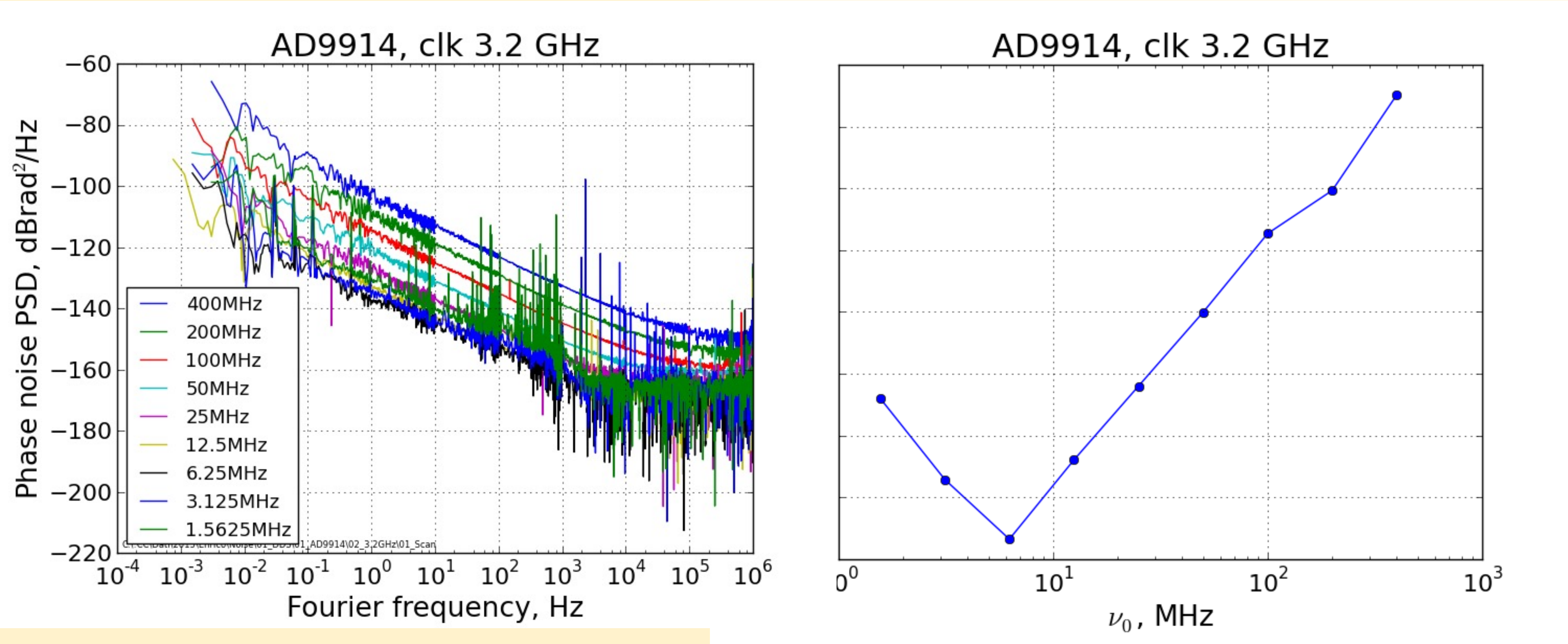

Measured by C. Calosso, INRIM

High-Frequency DDSs

AD9915 12 bit, 2.5 GHz
64 bit accumulator (135 pHz res)

ENOB = 12
$\nu_{ck} = 5$ GHz
$b_0 = -165$ dBrad^2/Hz

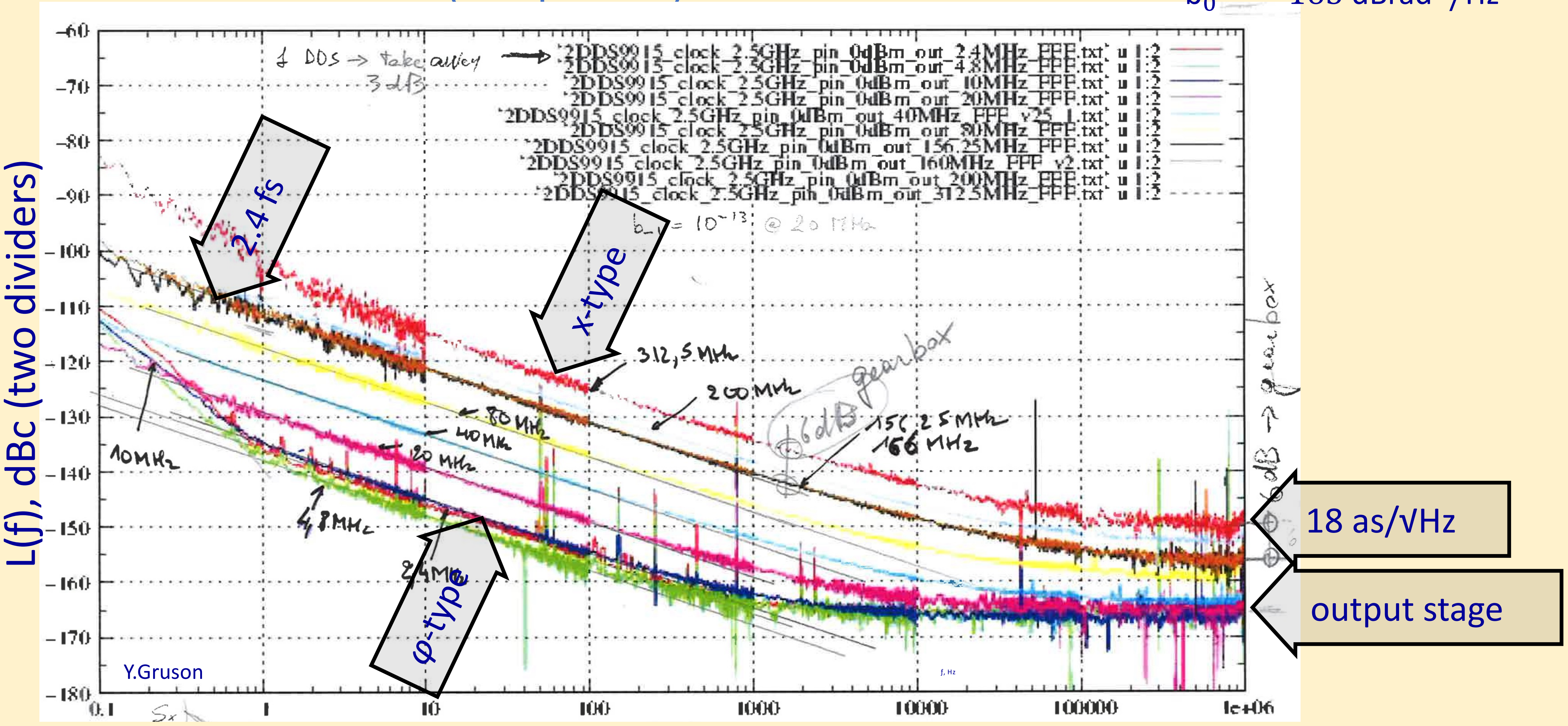

AD 9912 PM Noise

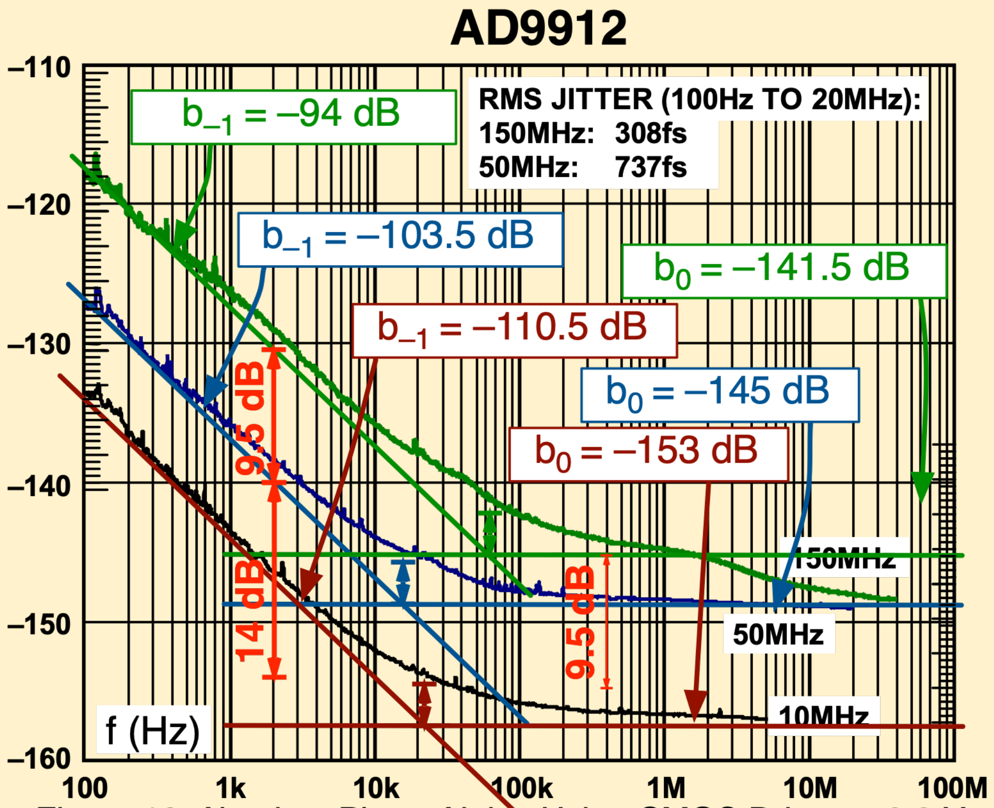

Figure 16. Absolute Phase Noise Using CMOS Driver at 3.3 V, SYSCLK = 1 GHz Wenzel Oscillator (SYSCLK PLL Bypassed) DDS Run at 200 MSPS for 10 MHz

Focus on 1/f only

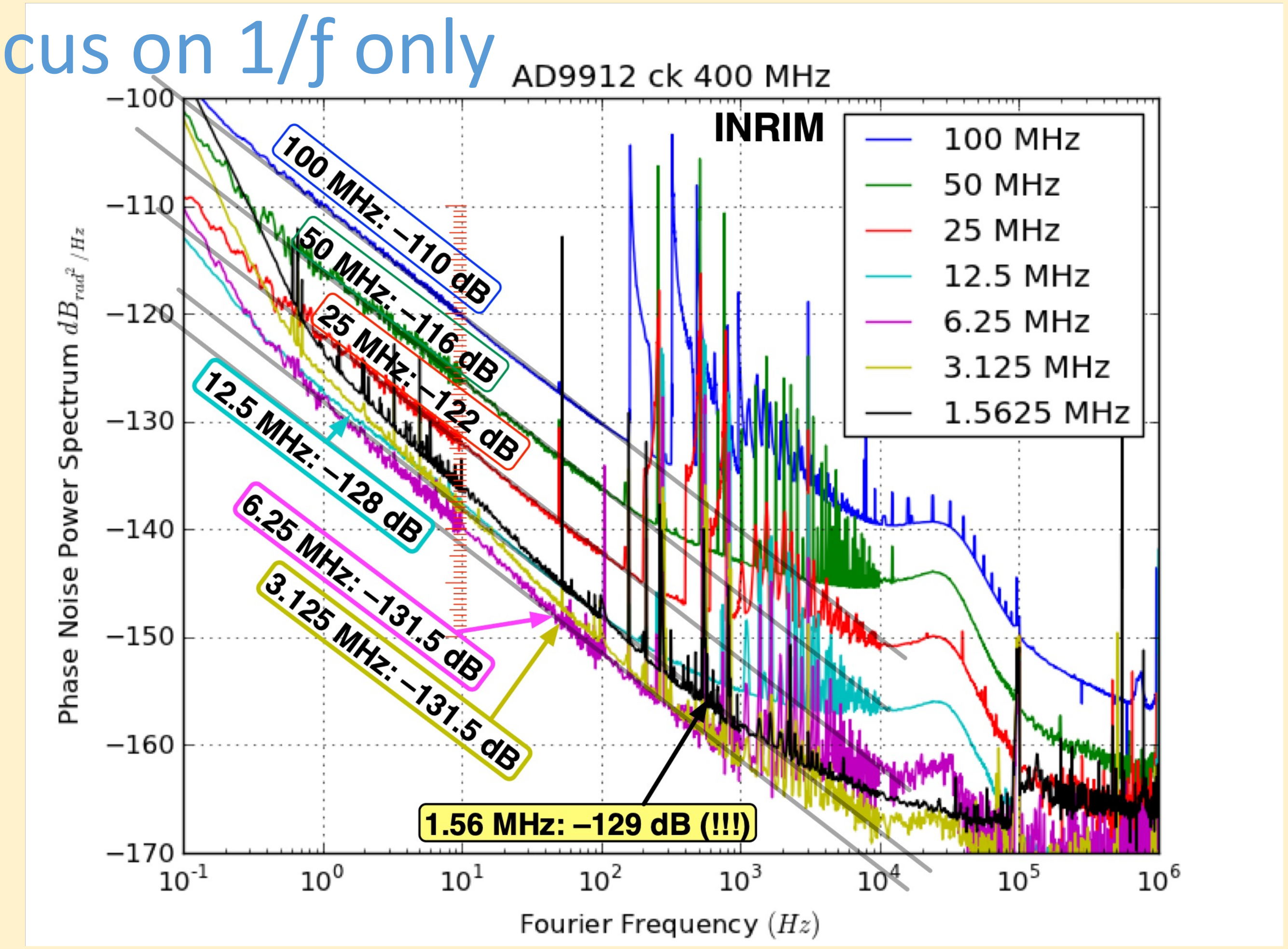

- At 50 MHz and 10/12.5 MHz we get ≈15 dB lower flicker than the data-sheet spectrum
- Experimental conditions unclear in the data sheets

5 — Dividers

Π and Λ Dividers

Microwave Dividers

Aliasing in Π Divider

Regular synchronous divider

The Greek letter Π recalls the square wave Π Π Π Π

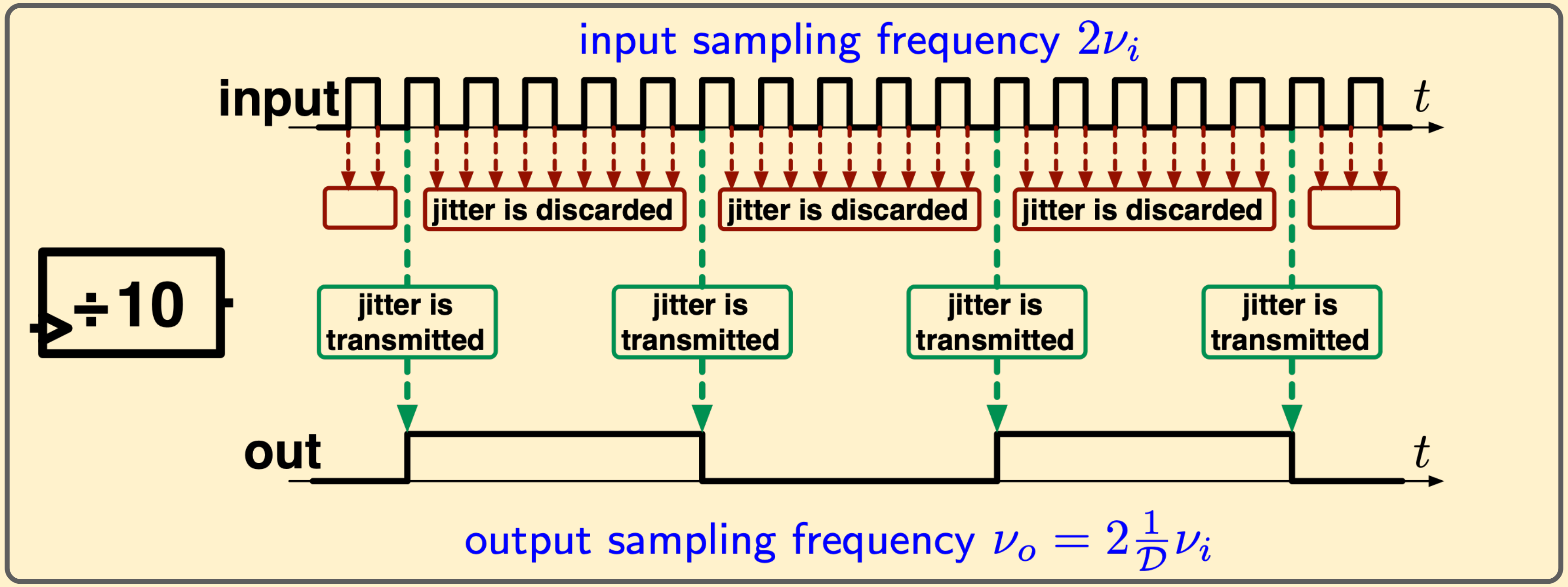

- The gearbox scales $S\varphi$ down by $1/D^2$
- The divider takes 1 edge out of D
  - Raw decimation without low-pass filter
  - Aliasing increases $S\varphi$ by D
- Overall, $S\varphi$ scales down by $1/D$

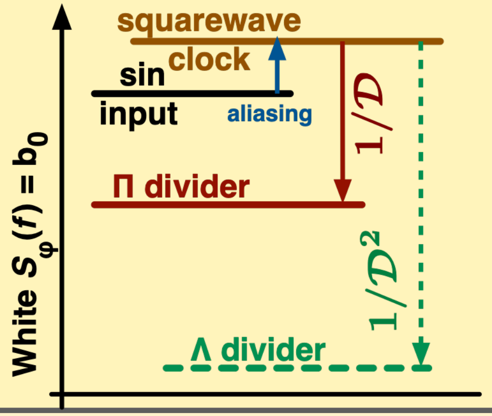

Results – Test on Aliasing

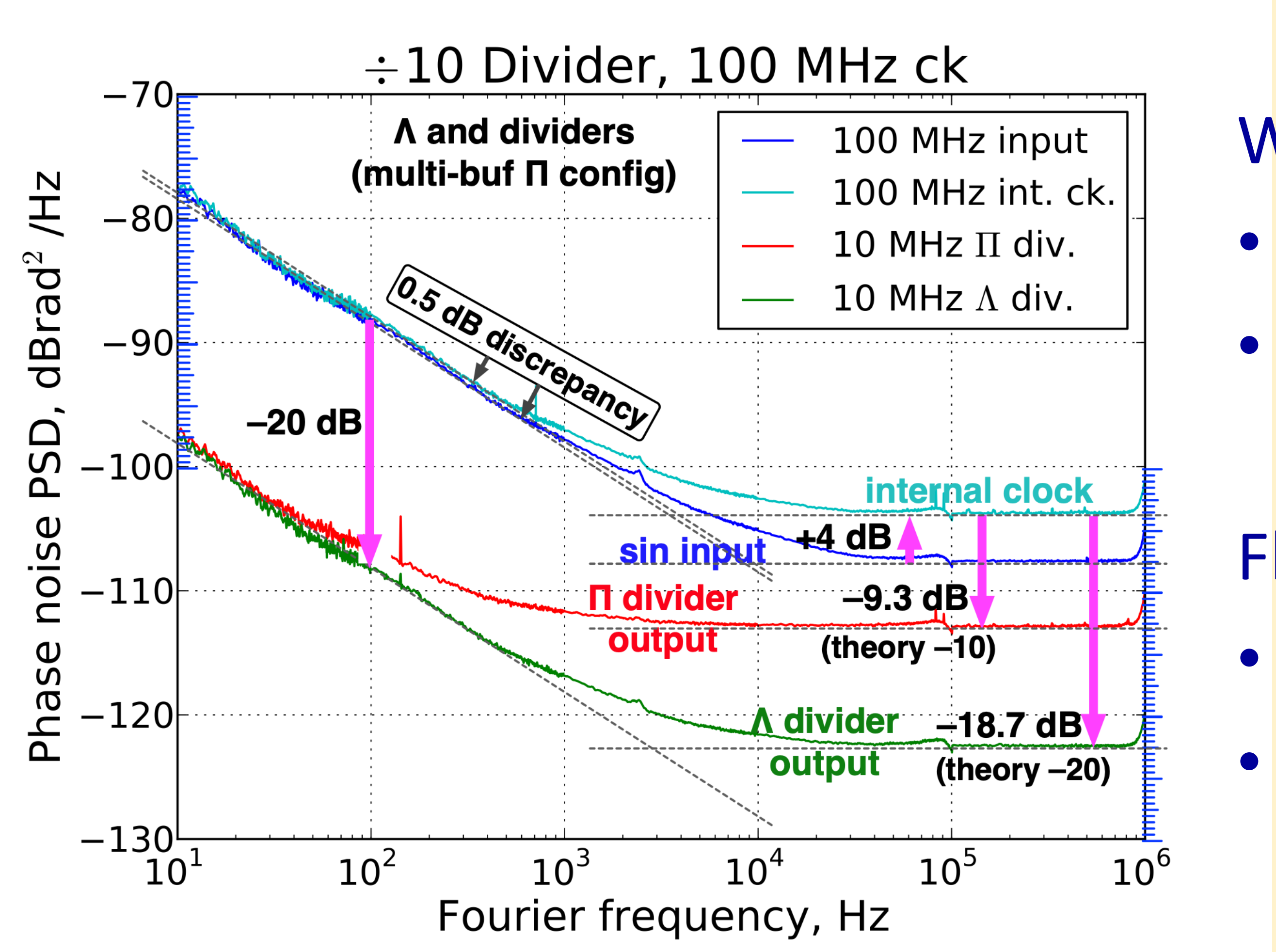

White region

- Aliasing in the front-end –> +4 dB
- 1/D law and 1/D2 law

Flicker region

- Negligible aliasing
- 1/D2 law (–20 dB)

The Λ Divider – Little/No Aliasing

New divider architecture

Series of Greek letters ΛΛΛΛΛ recalls the triangular wave

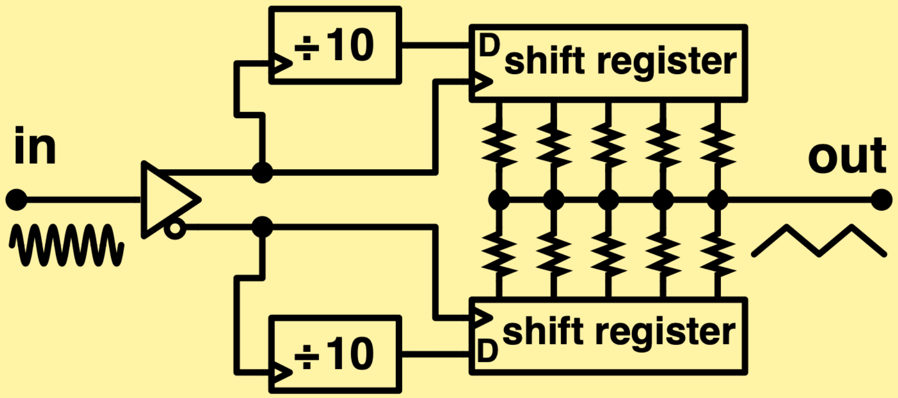

- Gearbox and aliasing –> 1/D law
- Add D independent realizations shifted by 1/2 input clock,
- reduce the phase noise by 1/D,
- … and get back the 1/D2 law

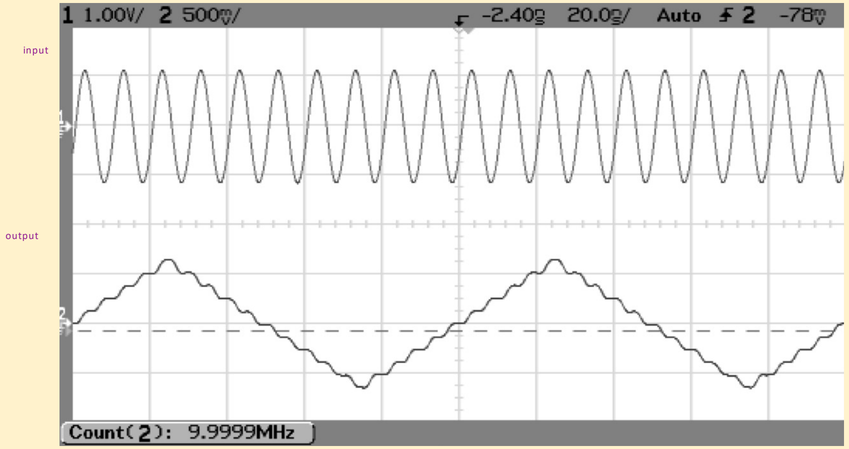

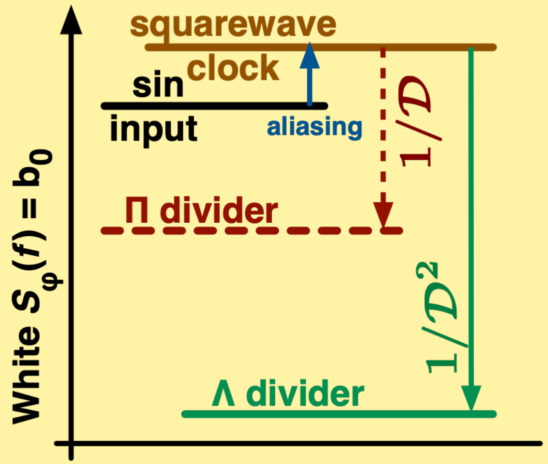

The names Π and Λ derive from the shape of the weight functions in our article on frequency counters

E. Rubiola, On the measurement of frequency … with high-resolution counters, RSI 76 054703, 2005

Phase Noise of Π and Λ Dividers

Multibuffer Π divider

Aliasing is present

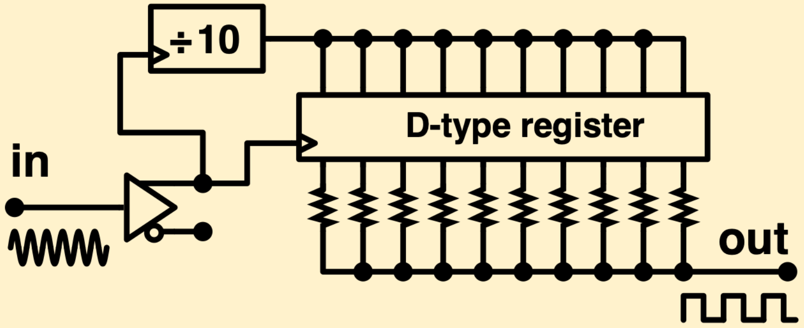

Λ divider

High-f sampling removes aliasing

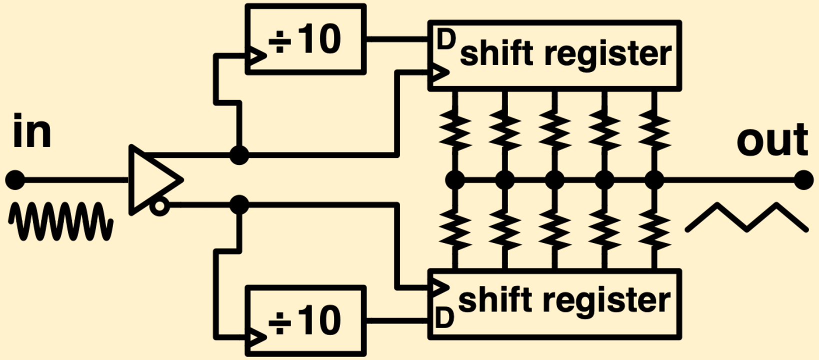

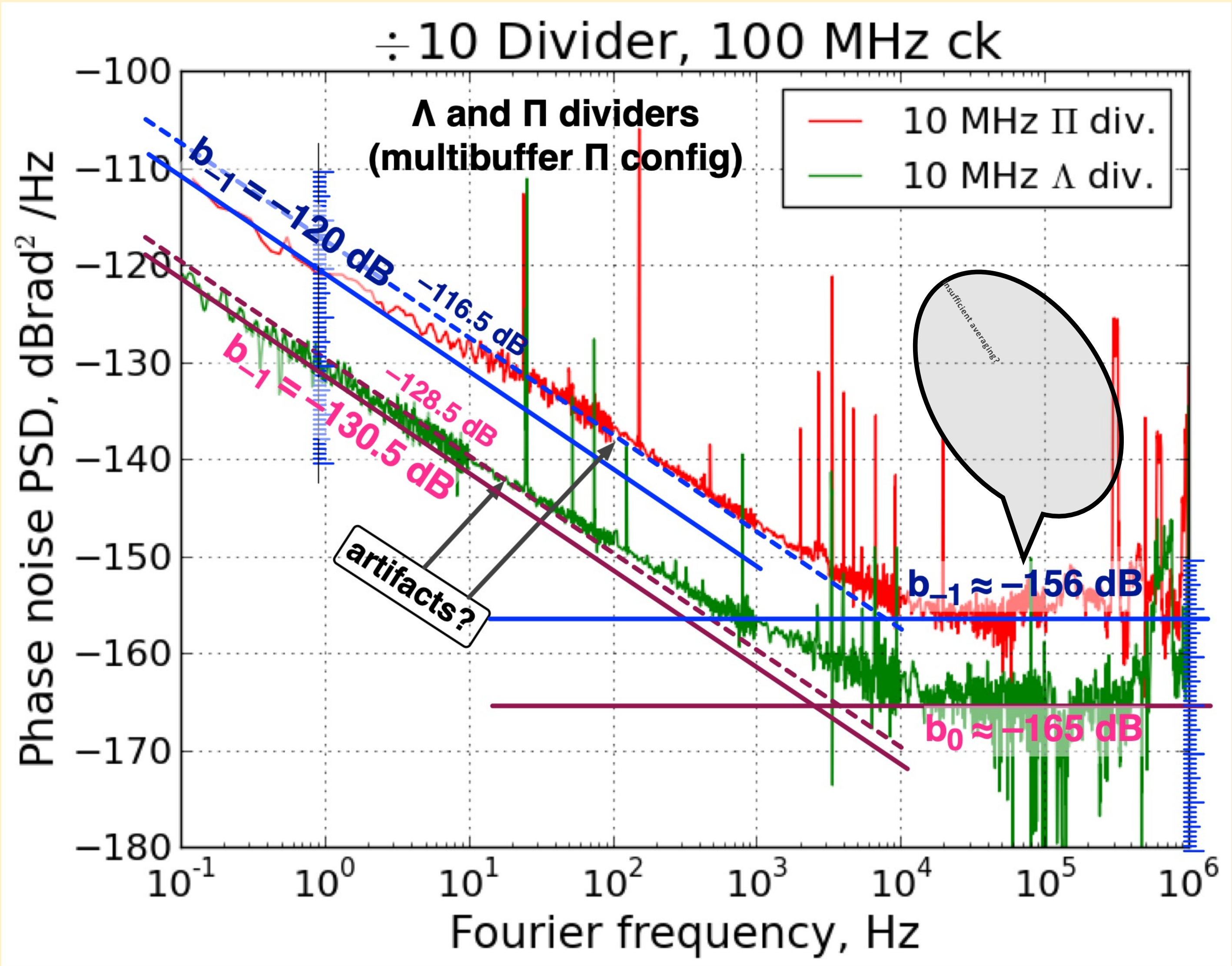

experimental problems still present

The Λ Divider Versus the DDS

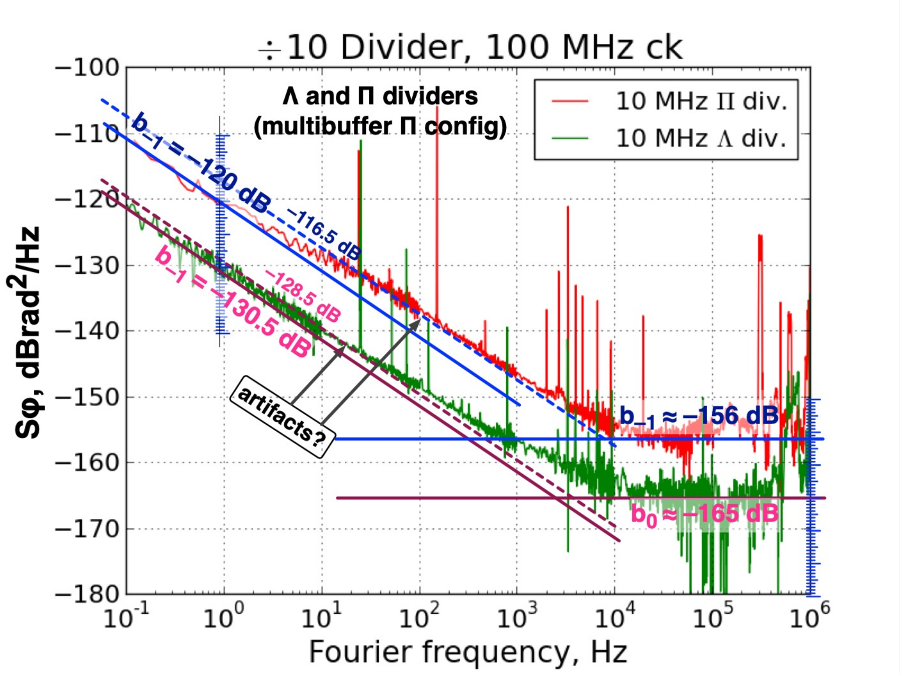

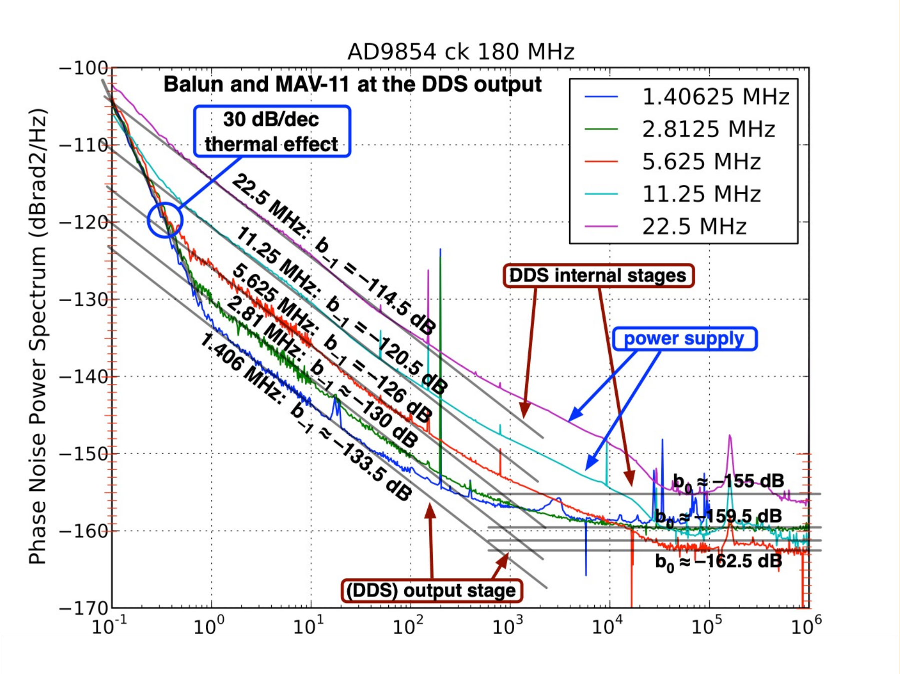

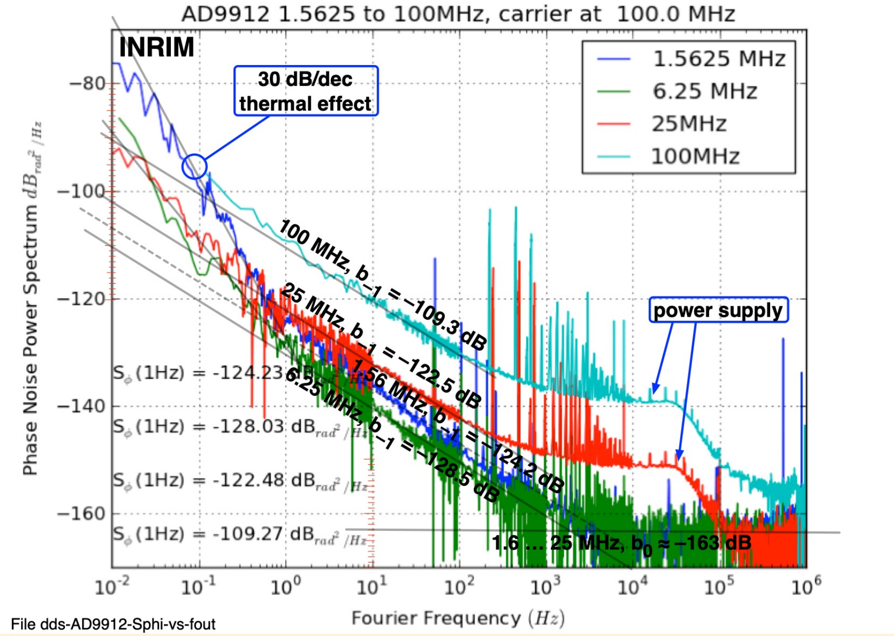

Noise of the Λ divider and two DDSs

noise	Λ div.	AD9854	AD9912
b_0	–165	–160	≈ –163
b_{-1}	–130.5	–121.5	–129 (inferred)
b_{-2}	—	—	–132 plot not shown
b_{-3}	—	–134	(seen at lower ν_0)

Suggested Reading

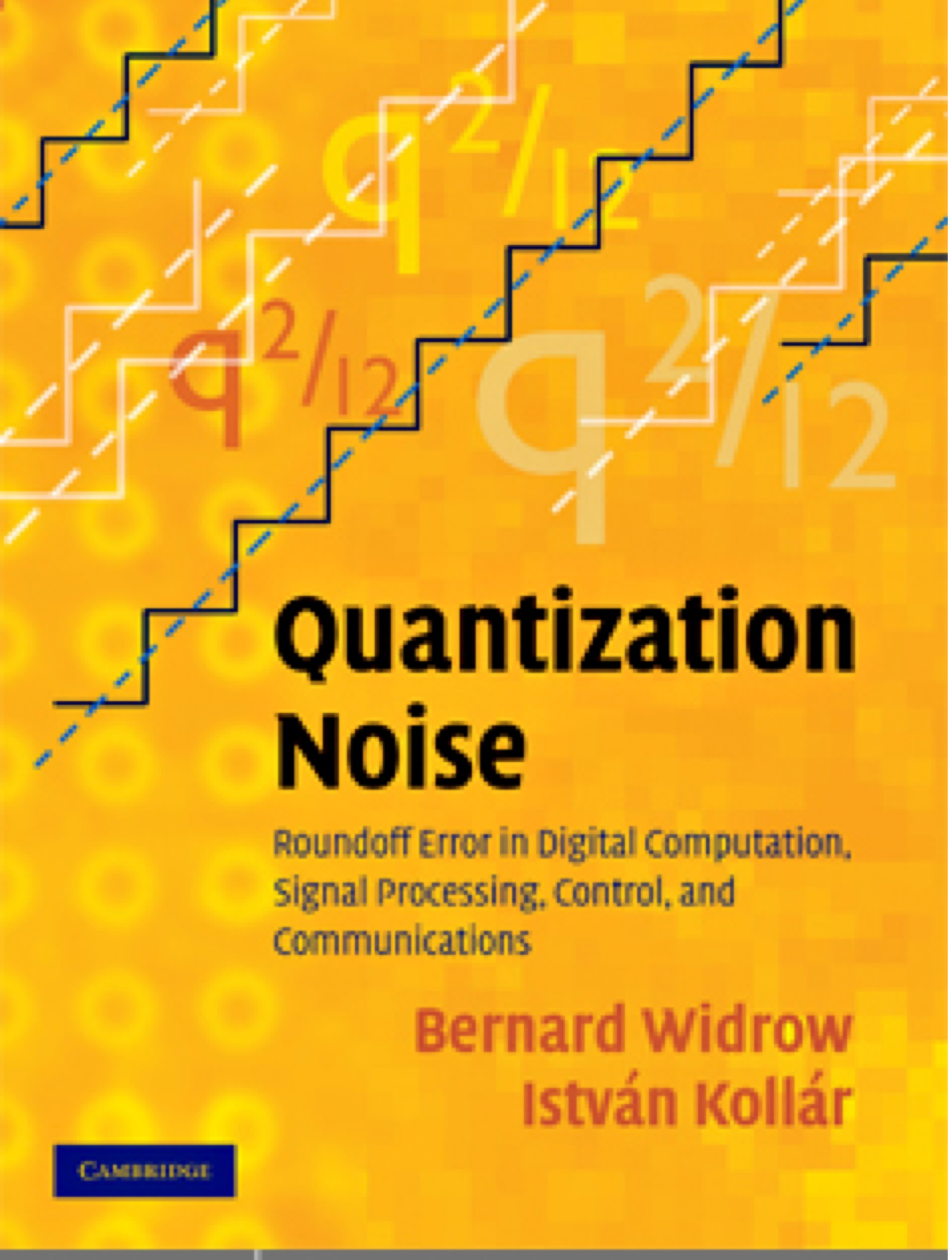

Bernard Widrow,
Istvan Kollar

Quantization Noise

Cambridge 2008
ISBN 978-0-511-40990-5

- Chapter 15: Roundoff noise in FIR digital filters and in FFT calculations
- Appendix G: Quantization of a sinusoidal input

Suggested Reading

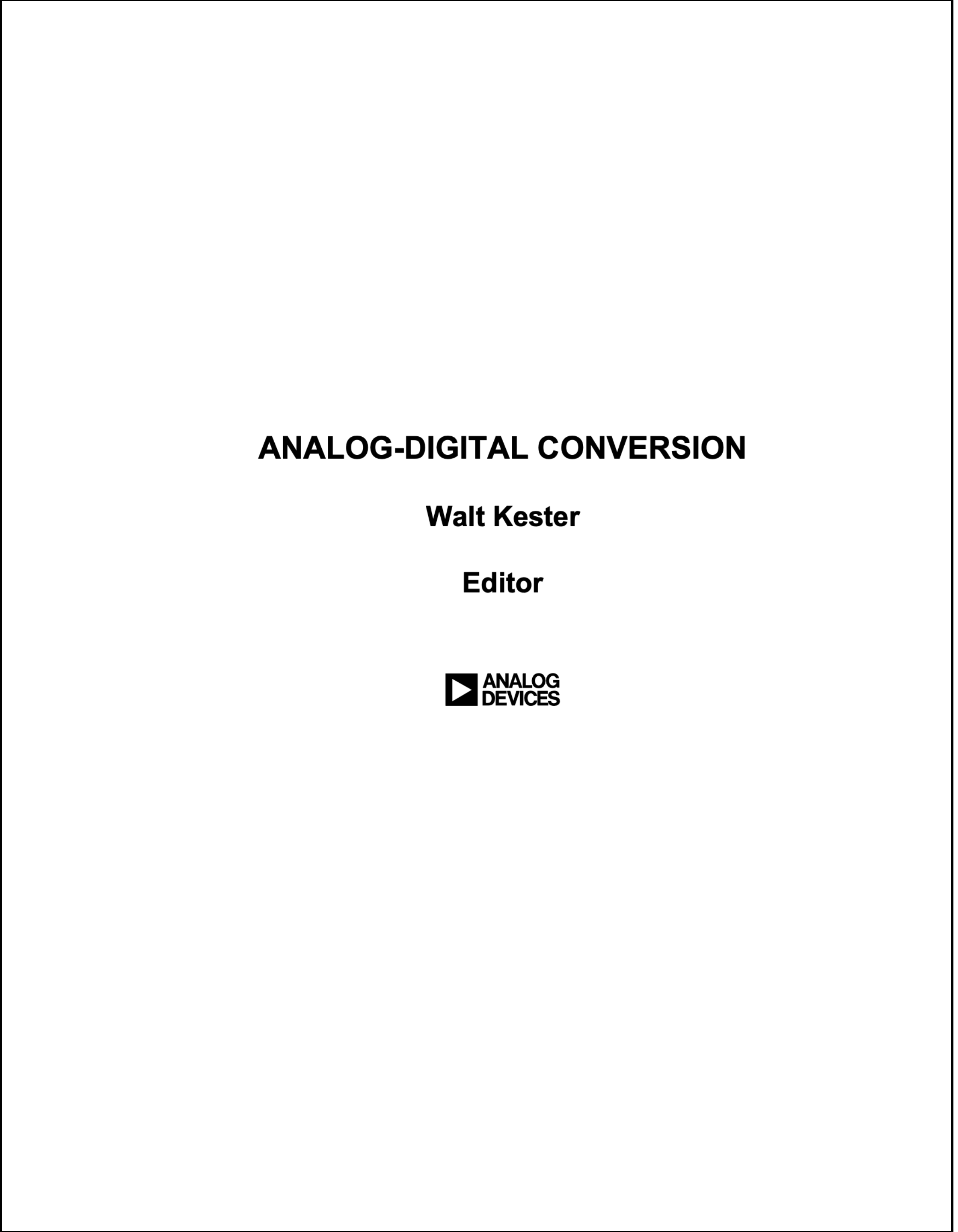
ANALOG-DIGITAL CONVERSION

Walt Kester

Editor

ANALOG DEVICES

Walt Kester (editor)

Analog-Digital Conversion

Analog Devices 2004

ISBN 0-916550-27-3

Suggested Reading

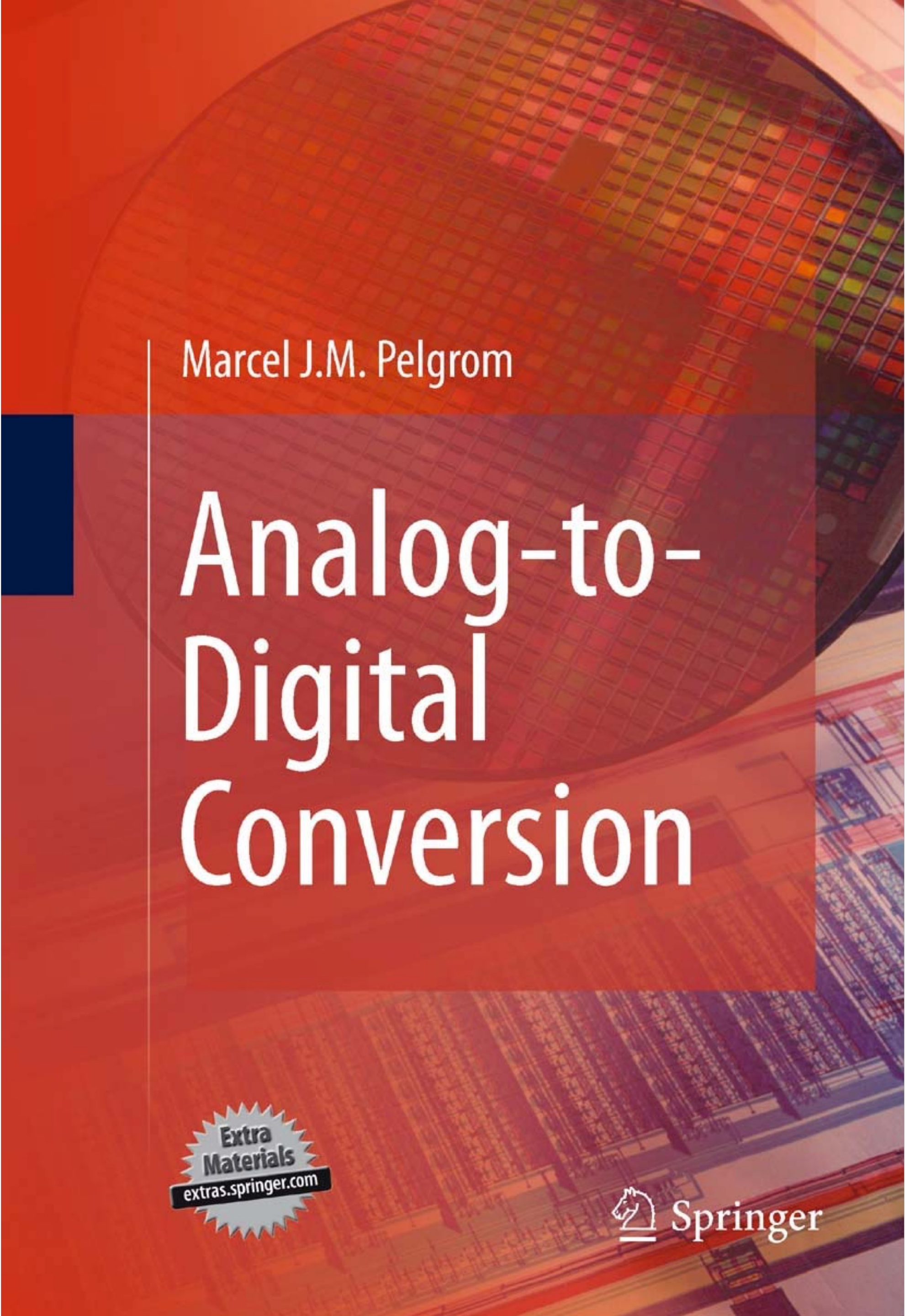

Marcel J. M. Pelgrom

Analog-to-Digital Conversion

Springer 2010
ISBN 978-90-481-8888-8

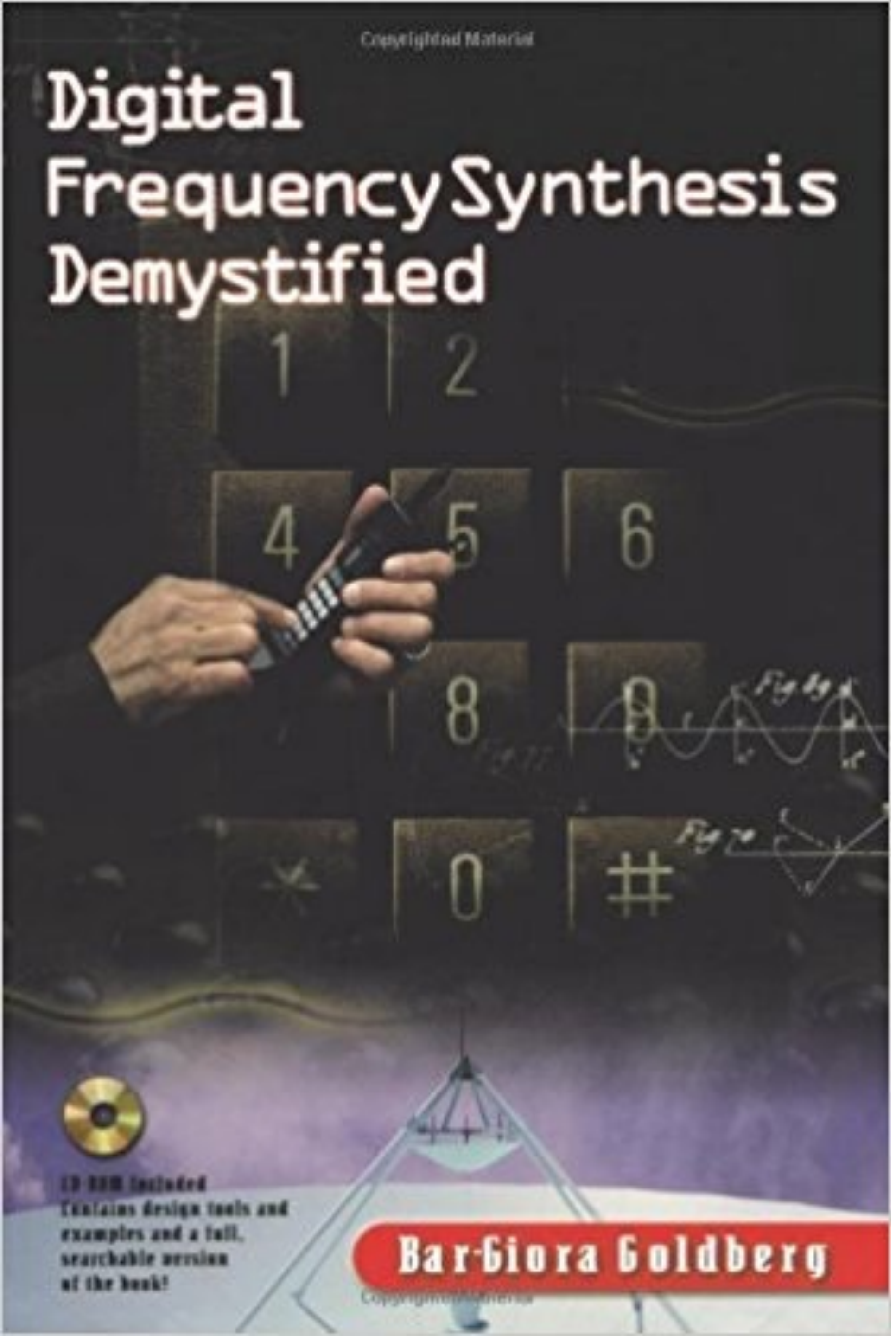

Suggested Reading

Bar-Giora Goldberg

Digital Frequency Synthesis Demystified

Newnes 1999

ISBN 978-1-878707-47-5

Our Articles

- C. E. Calosso, A. C. Cárdenas Olaya E. Rubiola, Phase-Noise and Amplitude-Noise Measurement of DACs and DDSs, IEEE Transact UFFC vol.67 no.2 p.431-439 February 2020
- A. C. Cárdenas Olaya, C. E. Calosso, J.-M. Friedt, S. Micalizio, E. Rubiola, "Phase Noise and Frequency Stability of the Red-Pitaya Internal PLL," IEEE Transact. UFFC vol.66 no.2 p.412-416, Feb 2019
- C. E. Calosso, F. Vernotte, V. Giordano, C. Fluhr, B. Dubois, E. Rubiola Frequency Stability Measurement of Cryogenic Sapphire Oscillators with a Multichannel Tracking DDS and the Two-Sample Covariance, IEEE Transact. UFFC vol.66 no.3 p.616-623, March 2019.
- A. C. Cardenas-Olaya, E. Rubiola, J.-M. Friedt, P.-Y. Bourgeois, M. Ortolano, S. Micalizio, and C. E. Calosso Noise characterization of analog to digital converters for amplitude and phase noise measurements, Rev. Scientific Instruments 88, 065108, June 2017.
- C. E. Calosso, Y. Gruson, E. Rubiola, "Phase noise and amplitude noise in DDS," Proc IFCS p.777-782, May 2012
- C. E. Calosso, E. Rubiola, "The Sampling Theorem in Pi and Lambda Digital Frequency Dividers," Proc IEEE IFCS p.960-962, 2013
- A. C. Cardenas Olaya, E. Rubiola, J.-M. Freidt, P.-Y. Bourgeois, M. Ortolano, S. Micalizio, C. E. Calosso, "Noise characterization of analog to digital converters for amplitude and phase noise measurements," Rev Sci Instrum 88, 065108, June 2017

End of lecture 8

Lecture 9

Scientific Instruments & Oscillators

Lectures for PhD Students and Young Scientists

Enrico Rubiola

CNRS FEMTO-ST Institute, Besancon, France

INRiM, Torino, Italy

Contents

- The Leeson Effect

ORCID 0000-0002-5364-1835

home page http://rubiola.org

The Leeson Effect

Enrico Rubiola
CNRS FEMTO-ST Institute, Besancon, France
INRiM, Torino, Italy

Outline

The original is in a separate file

home page http://rubiola.org

Lecture 9

Scientific Instruments & Oscillators

Lectures for PhD Students and Young Scientists

Enrico Rubiola

CNRS FEMTO-ST Institute, Besancon, France

INRiM, Torino, Italy

Contents

- The Leeson Effect

ORCID 0000-0002-5364-1835

home page http://rubiola.org

The Reference Book for this Lecture

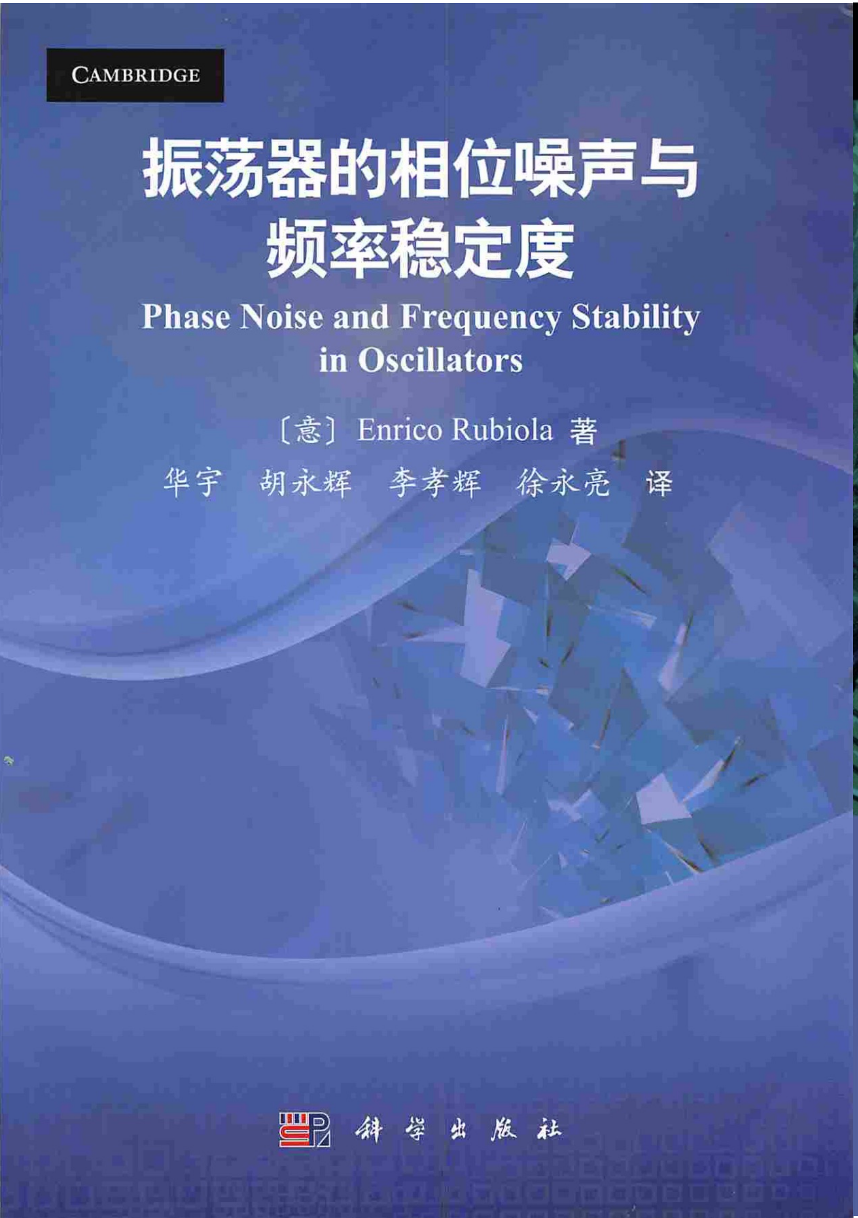

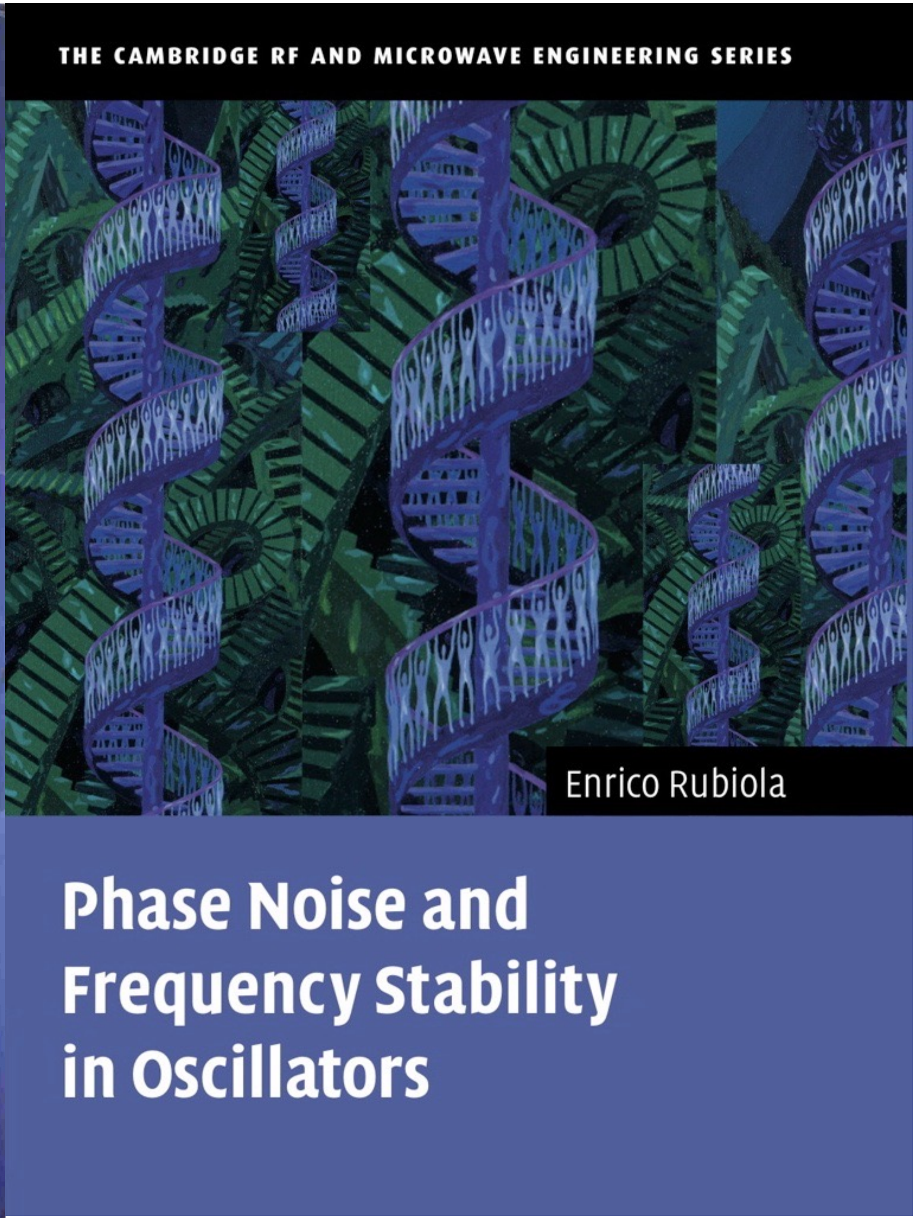

Contents

- Forewords (L. Maleki, D. B. Leeson)
- Phase noise and frequency stability
- Phase noise in semiconductors & amplifiers
- Heuristic approach to the Leeson effect
- Phase noise and feedback theory
- Noise in delay-line oscillators and lasers
- Oscillator hacking
- Appendix

Cambridge University Press, 2008-2012,
ISBN 978-0-521-88677-2, 978-0-521-15328-7,
978-1-139-23940-0

Simplified Chinese, 2014, ISBN 978-7-03-041231-7

The Leeson effect in a nutshell

David B. Leeson, Proc. IEEE 54(2) p.329, Feb 1966
E. Rubiola, Phase Noise and Frequency Stability in Oscillators, Cambridge 2008, 2012

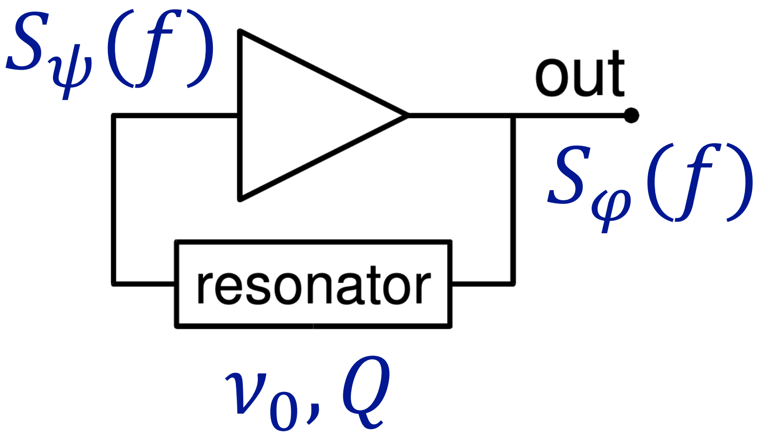

$$S_\varphi(f) = \left[1 + \frac{1}{f^2}\left(\frac{\nu_0}{2Q}\right)^2\right] S_\psi(f)$$

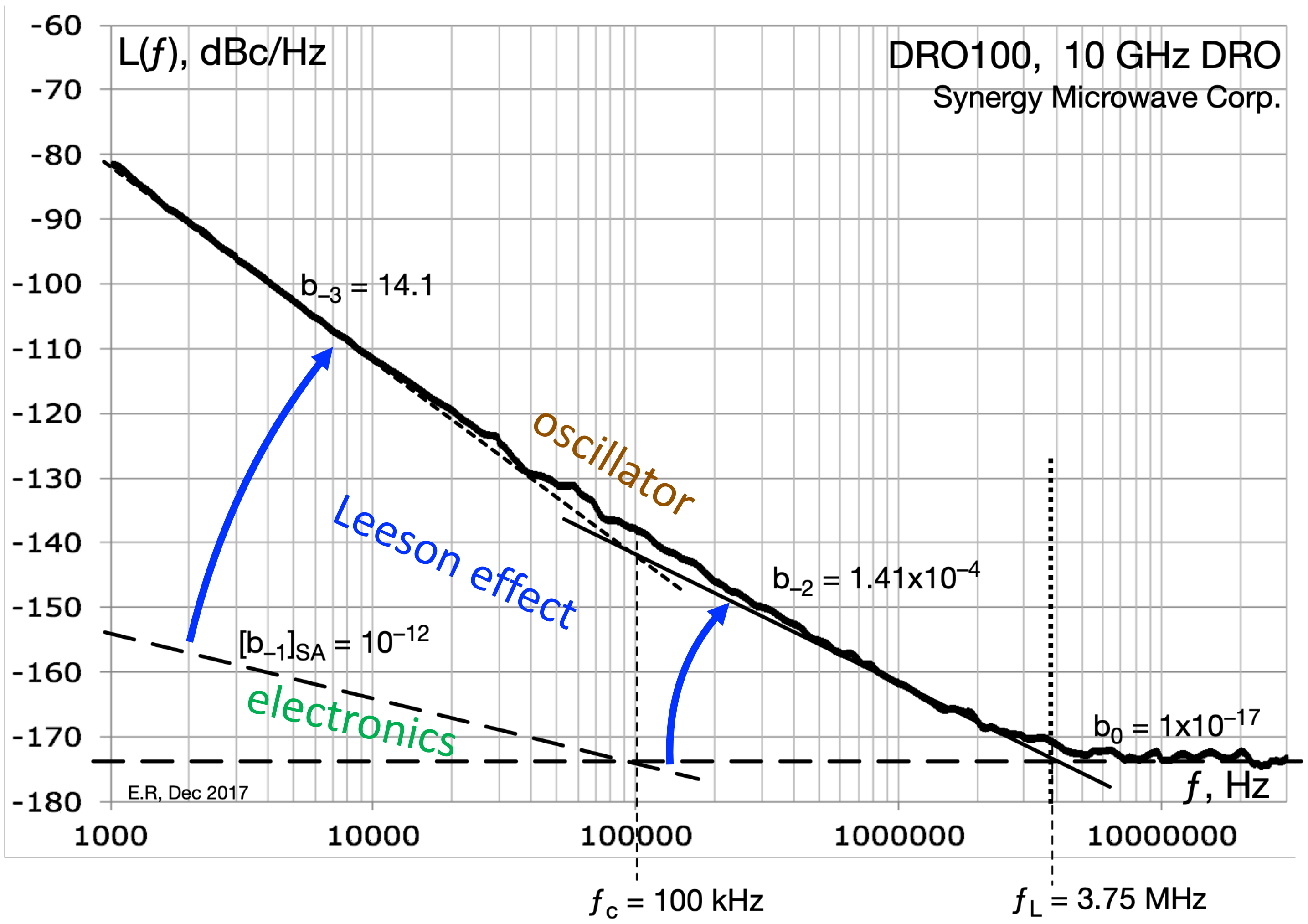

Figure from U. L. Rohde, E. Rubiola, J. C. Whithaker, *Microwave and Wireless Synthesizers*, ISBN 978-1-119-66600-4, ©J.Wiley 2020

Heuristic Explanation of the Leeson Effect

General oscillator model

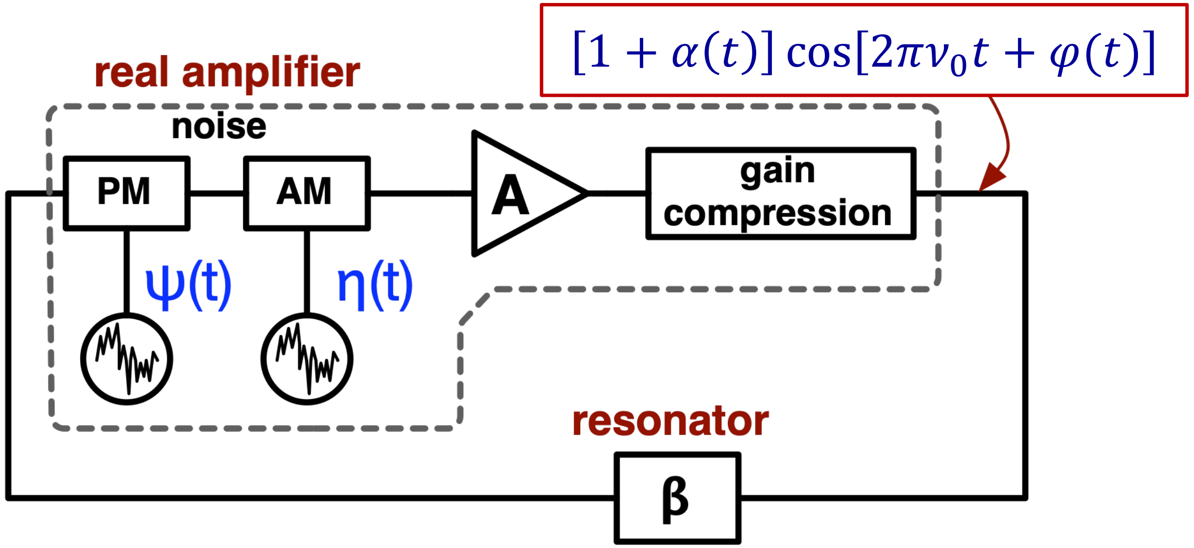

- RLC resonator
- Piezoelectric quartz resonator
- Microwave cavity
- Microwave dielectric resonator
- Fabry-Pérot resonator
- Optomechanic resonator
- Optical fiber
- etc.

Barkhausen condition

$A\beta = 1$ at ν_0

(phase matching)

The Barkhausen condition in practice

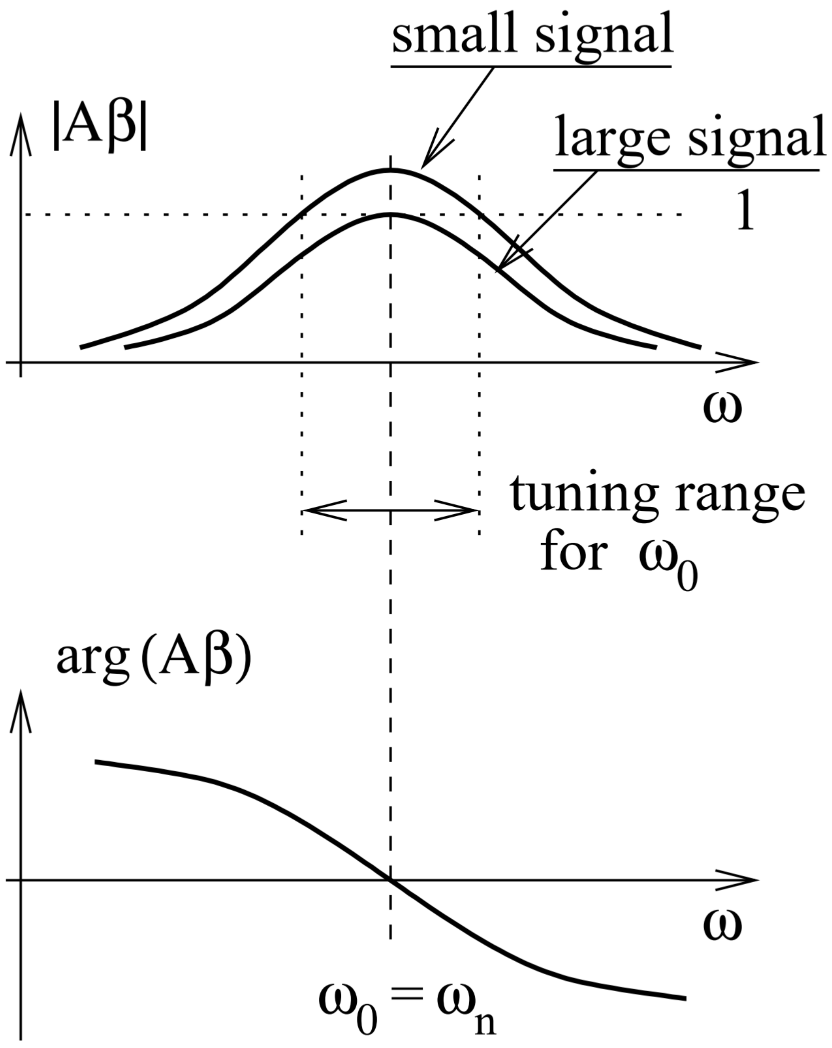

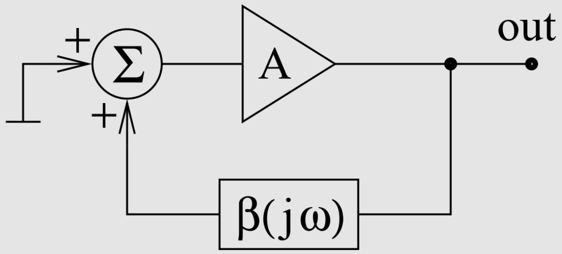

$A\beta = 1$ (complex)
A constant vs ω
$\beta(\omega)$ is the sharp resonance

- $\arg(\beta)$ sets the oscillation frequency
- saturation fixes $|A\beta| = 1$

$$\arg(\beta) = \arctan Q\left(\frac{\omega}{\omega_0} - \frac{\omega_0}{\omega}\right)$$

$$\simeq -2Q\,\frac{\omega - \omega_0}{\omega_0}$$

close to the resonance

Tuning an oscillator

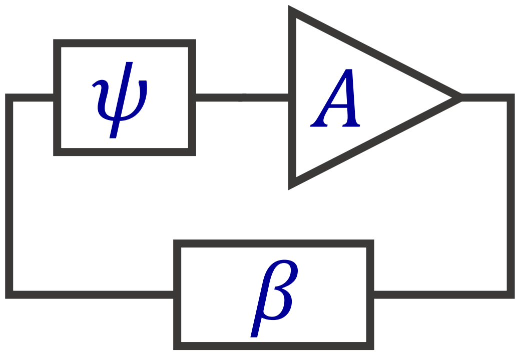

closed loop function

$$H(\nu) = A\beta(\nu)e^{j\psi}$$

$$A(\nu) = \text{const}$$

Phase matching

$$\arg(\beta) + \psi = 0$$

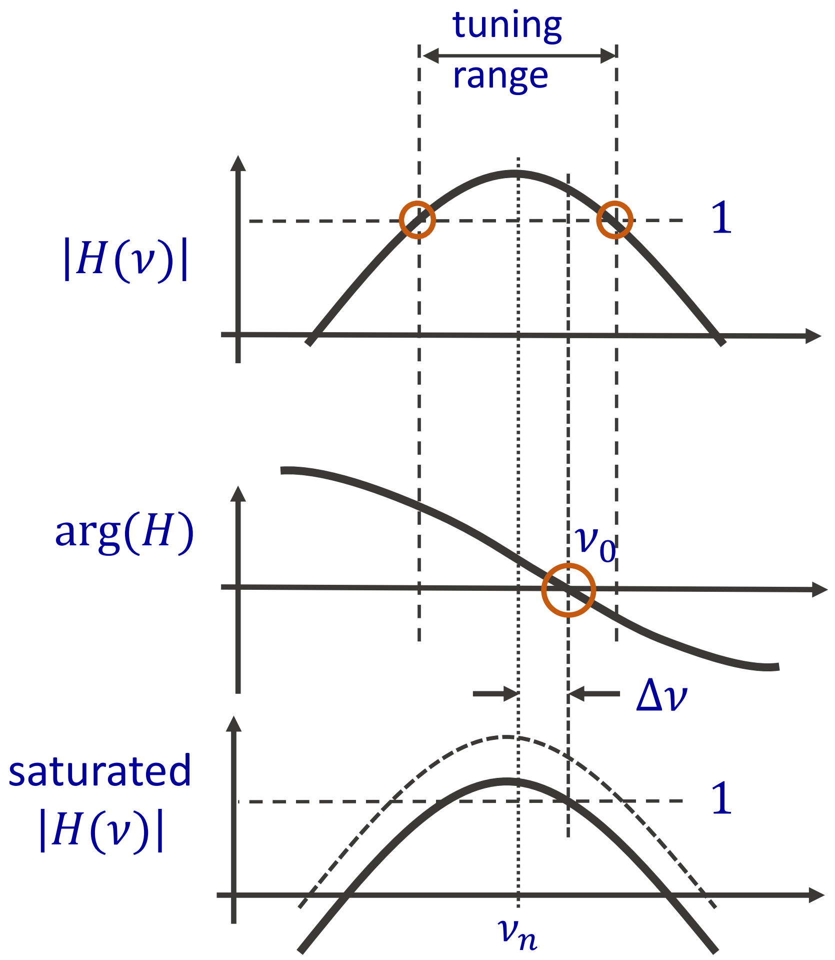

add a phase ψ

Small ψ approximation

$$\psi = 2Q\frac{\Delta\omega}{\omega_0}$$

Tuning

$$\frac{\Delta\nu}{\omega_n} = \frac{\psi}{2Q}$$

Heuristic derivation of the Leeson effect

fast fluctuation: no phase feedback

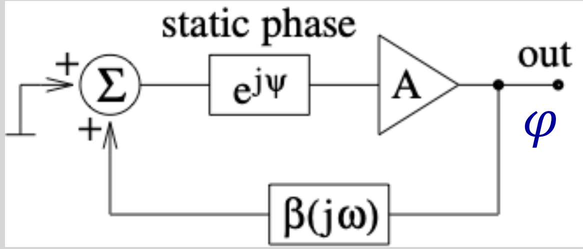

$$\varphi(t) = \psi(t)$$

$$S_\varphi(f) = S_\psi(f)$$

slow fluctuations: $\psi \rightarrow \Delta\nu$ conversion

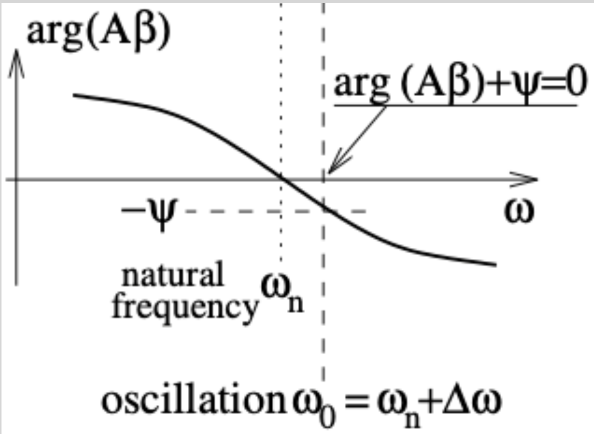

static

$$\Delta\nu = \frac{\nu_0}{2Q}\psi$$

$$S_{\Delta\nu}(f) = \left(\frac{\nu_0}{2Q}\right)^2 S_\psi(f)$$

integral

$$S_\varphi(f) = \frac{1}{f^2}\left(\frac{\nu_0}{2Q}\right)^2 S_\psi(f)$$

fast or slow?

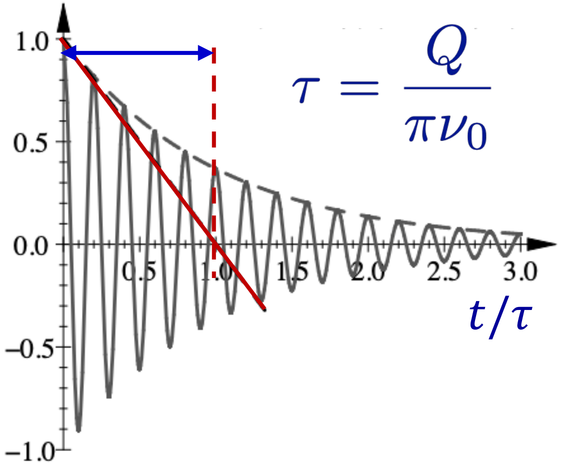

Exact result

$$S_\varphi(f) = \left[1 + \frac{1}{f^2}\left(\frac{\nu_0}{2Q}\right)^2\right] S_\psi(f)$$

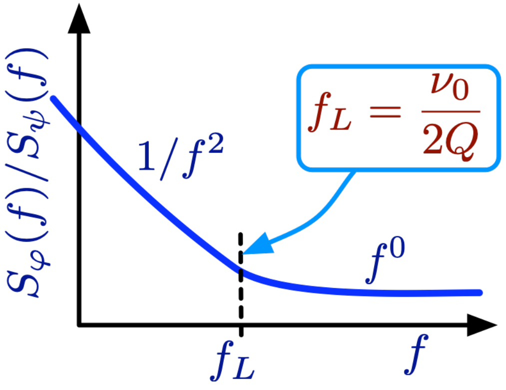

A Method to Sove Phase Noise Problems

Resonator Theory

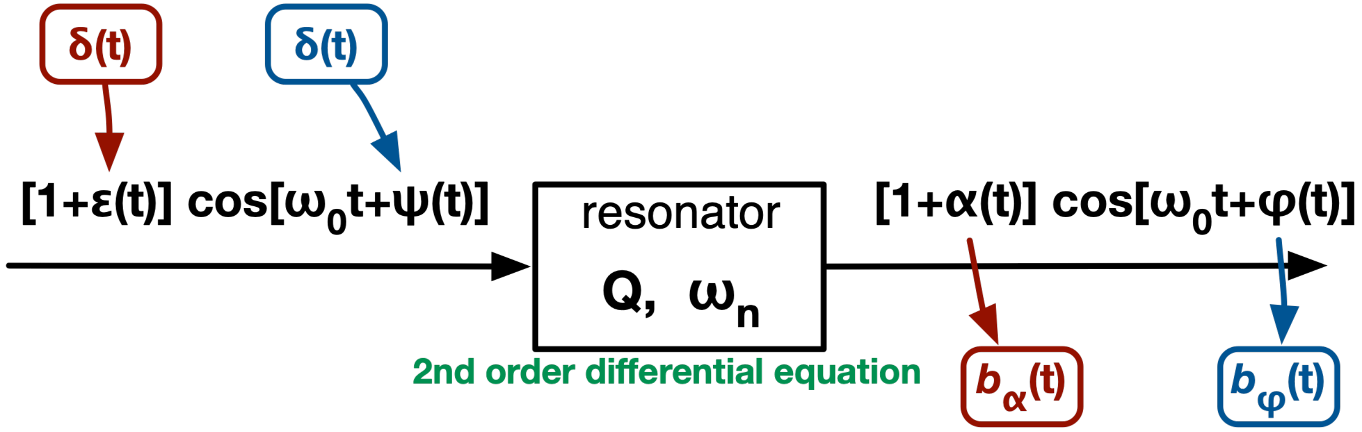

Linear Time-Invariant System

Impulse response and frequency response

in the amplitude-phase space

Linear Time-Invariant (LTI) systems

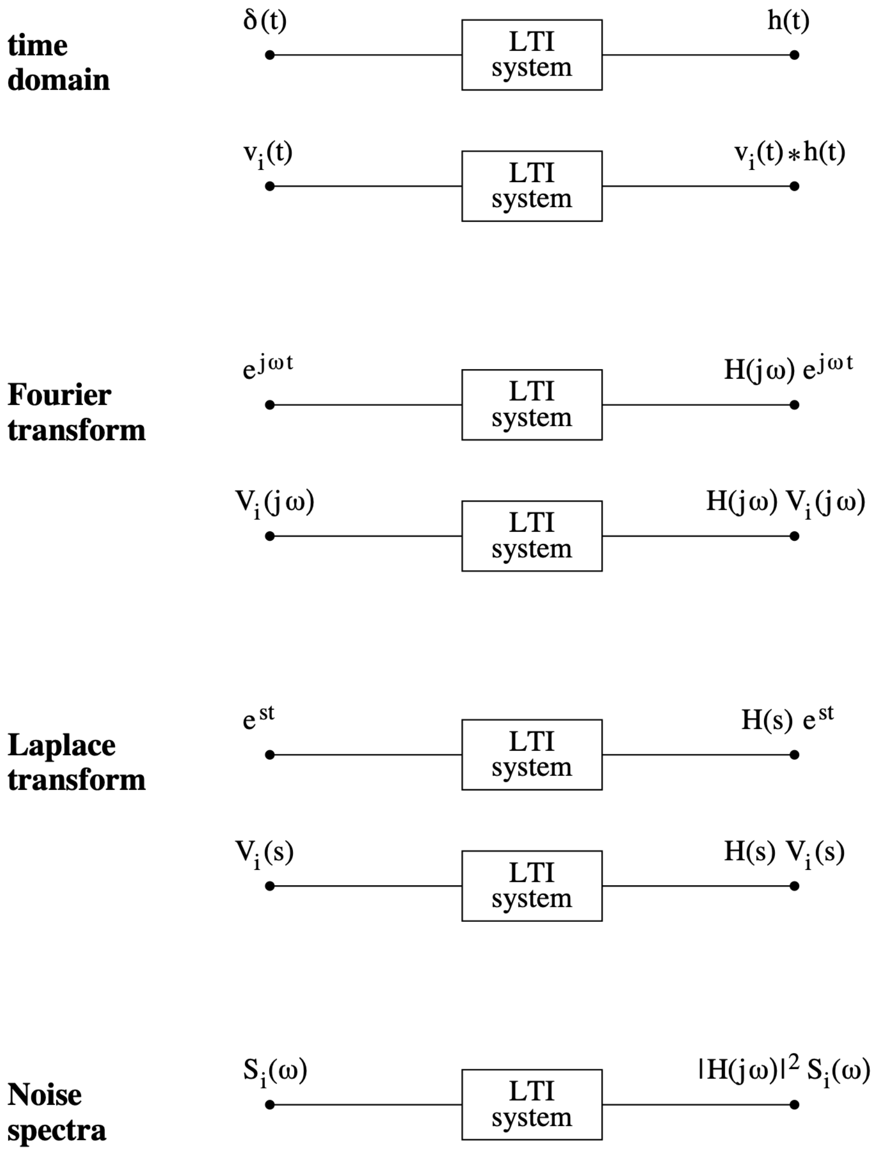

impulse response

response to the generic signal $v_i(t)$

$$H(\omega) = \int_{-\infty}^{\infty} h(t)\, e^{-j\omega t}\, dt$$

$$H(s) = \int_{0}^{\infty} h(t)\, e^{-st}\, dt$$

$H(s)$, $s = \sigma + j\omega$, is the analytic continuation of $H(\omega)$ for causal system, where $h(t) = 0$ for $t < 0$

Time domain

$$\ddot{x} + \frac{\omega_n}{Q}\dot{x} + \omega_n^2 x = \frac{\omega_n}{Q}\dot{v}(t)$$

ω_n natural frequency
Q quality factor
τ relaxation time
$\tau = \frac{2Q}{\omega_n}$
ω_p free-decay pseudofrequency
$\omega_p = \omega_n\sqrt{1 - 1/4Q^2}$

shorthand: $f = \omega/2\pi$

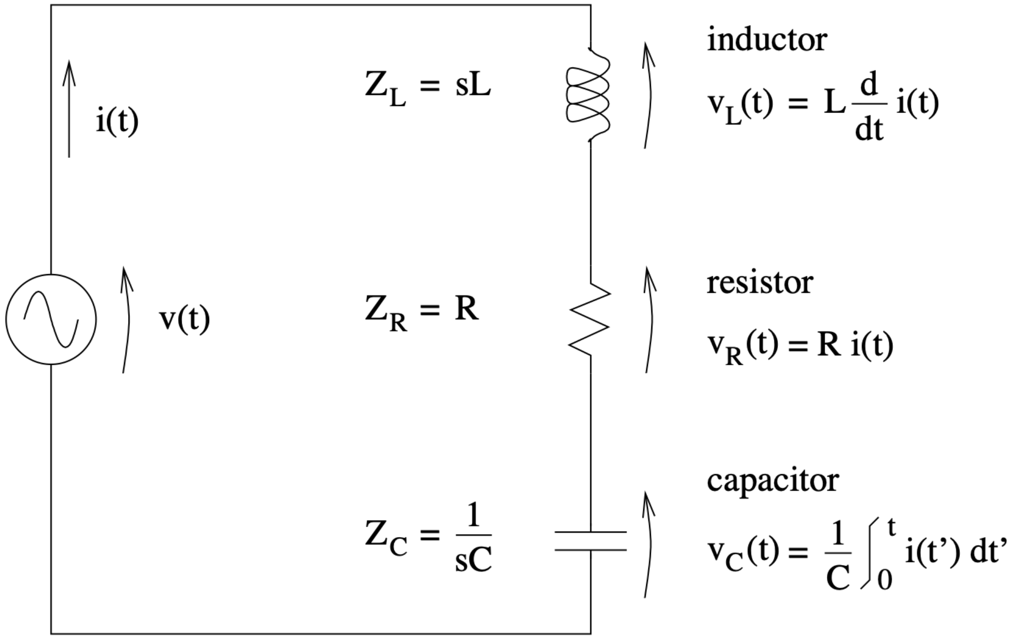

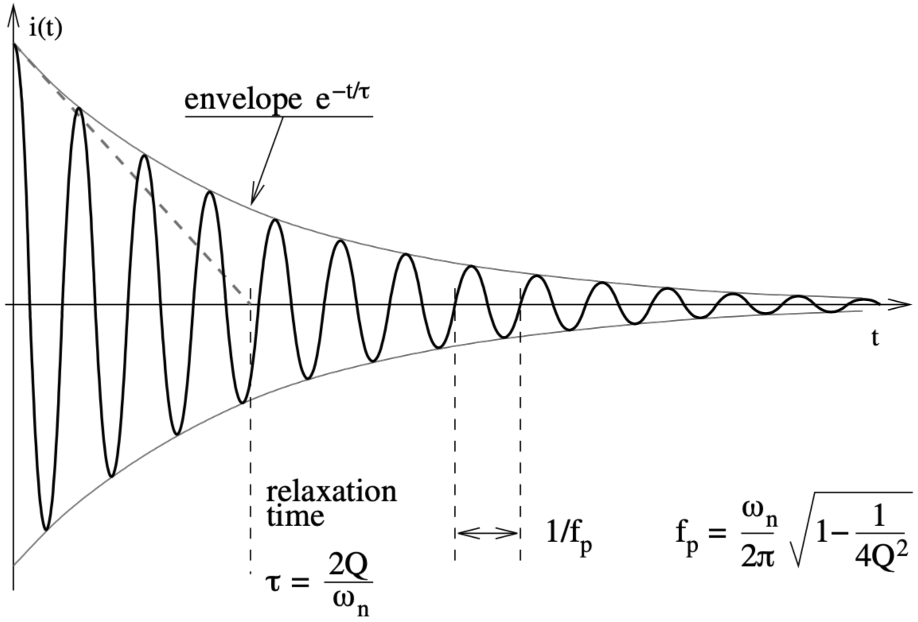

Resonator – Frequency domain

$$\beta(s) = \frac{\omega_n}{Q} \, \frac{s}{s^2 + \frac{\omega_n}{Q} s + \omega_n^2} \qquad s = \sigma + j\omega$$

$$\chi = \frac{\omega}{\omega_n} - \frac{\omega_n}{\omega}$$

$$\beta = \frac{1}{1 + jQ\chi}$$

$$\Re\{\beta\} = \frac{1}{1 + Q^2\chi^2}$$

$$\Im\{\beta\} = \frac{-Q\chi}{1 + Q^2\chi^2}$$

$$|\beta|^2 = \frac{1}{1 + Q^2\chi^2}$$

$$\arg(\beta) = -\arctan(Q\chi)$$

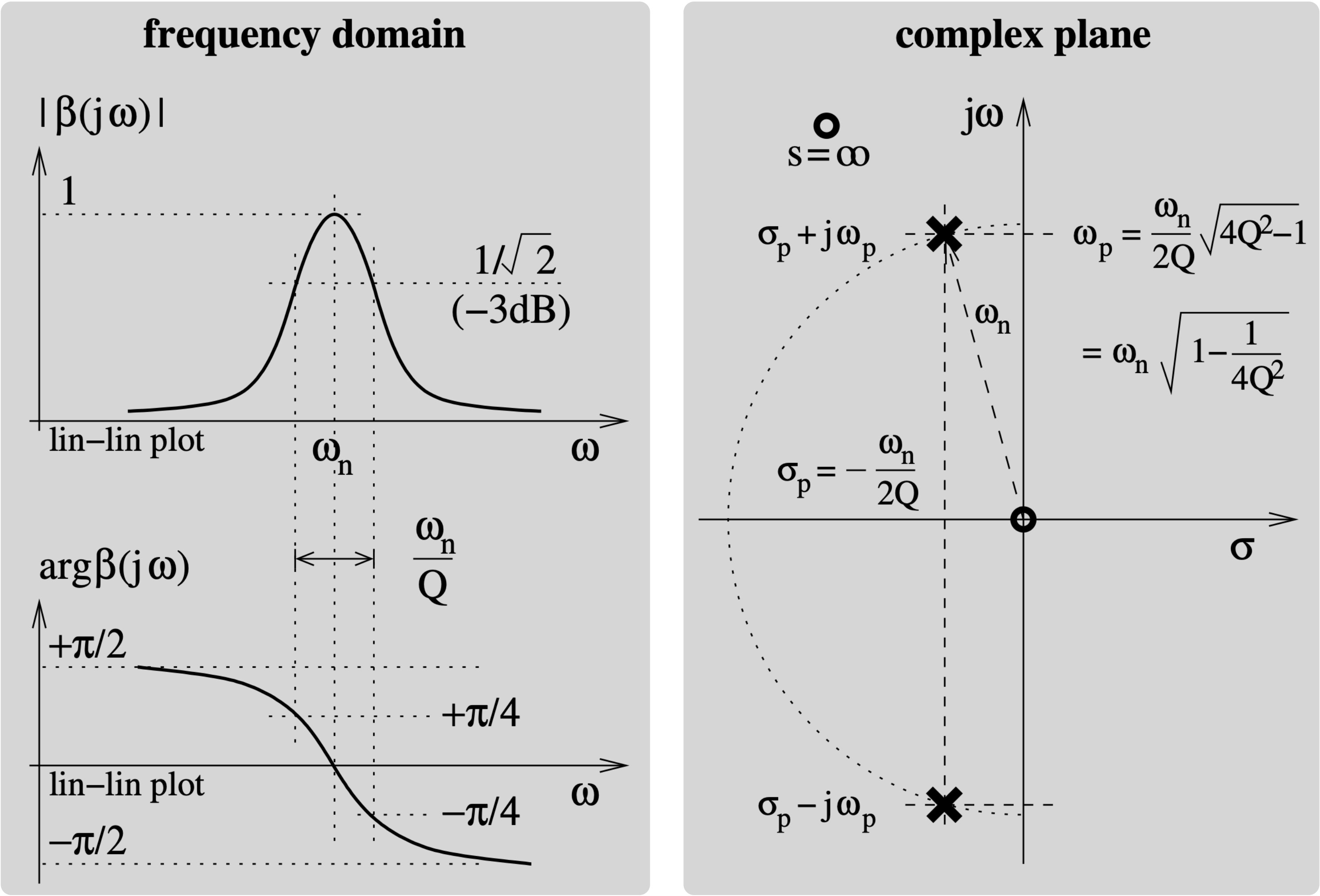

The resonator

$$\ddot{x} + \frac{\omega_n}{Q}\dot{x} + \omega_n^2 x = \frac{\omega_n}{Q}\dot{v}(t)$$

ω_n	natural frequency
Q	quality factor
τ	relaxation time
	$\tau = \frac{2Q}{\omega_n}$
ω_p	free-decay pseudofrequency
	$\omega_p = \omega_n\sqrt{1 - 1/4Q^2}$

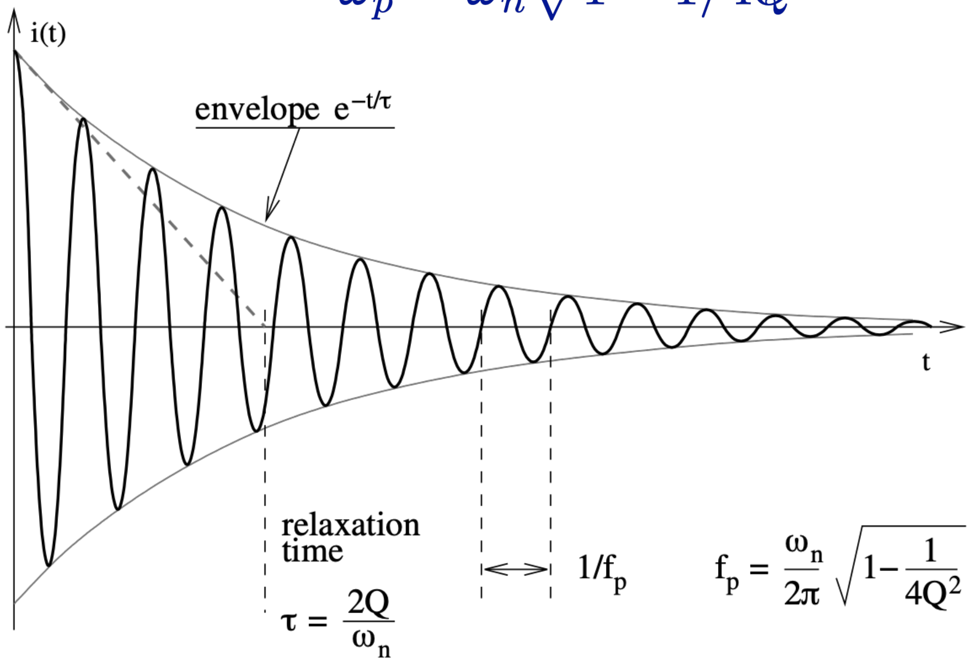

$$\beta(s) = \frac{\omega_n}{Q}\frac{s}{s^2 + \frac{\omega_n}{Q} + \omega_n^2}$$

Laplace $\beta(s) = X(s)/V(s)\,,\quad s = \sigma + j\omega$

frequency domain

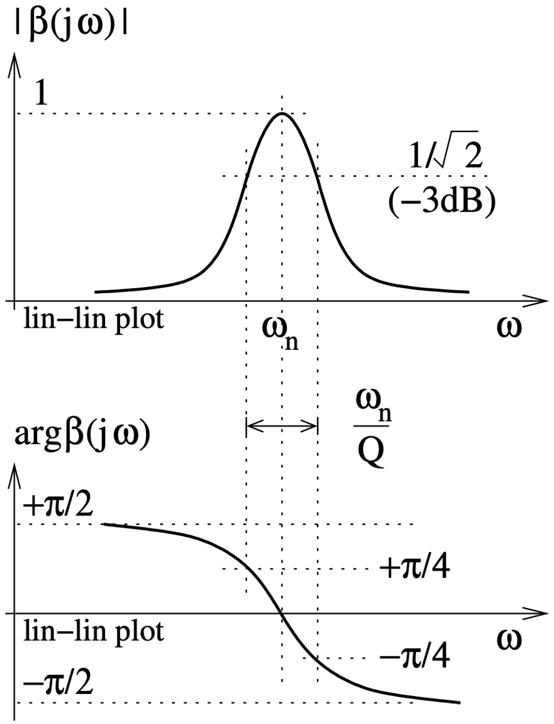

complex plane

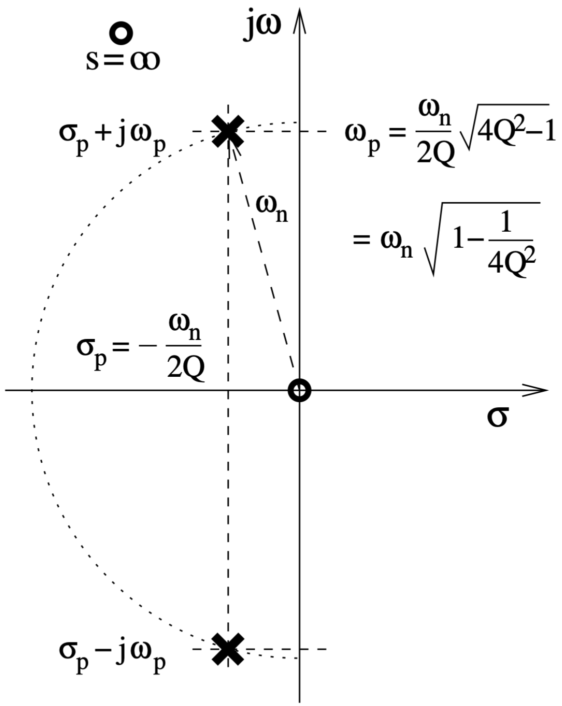

Figures are from E. Rubiola, Phase noise and frequency stability in oscillators, © Cambridge University Press

Laplace-transform patterns

Fundamental theorem of complex algebra: $F(s)$ is completely determined by its roots

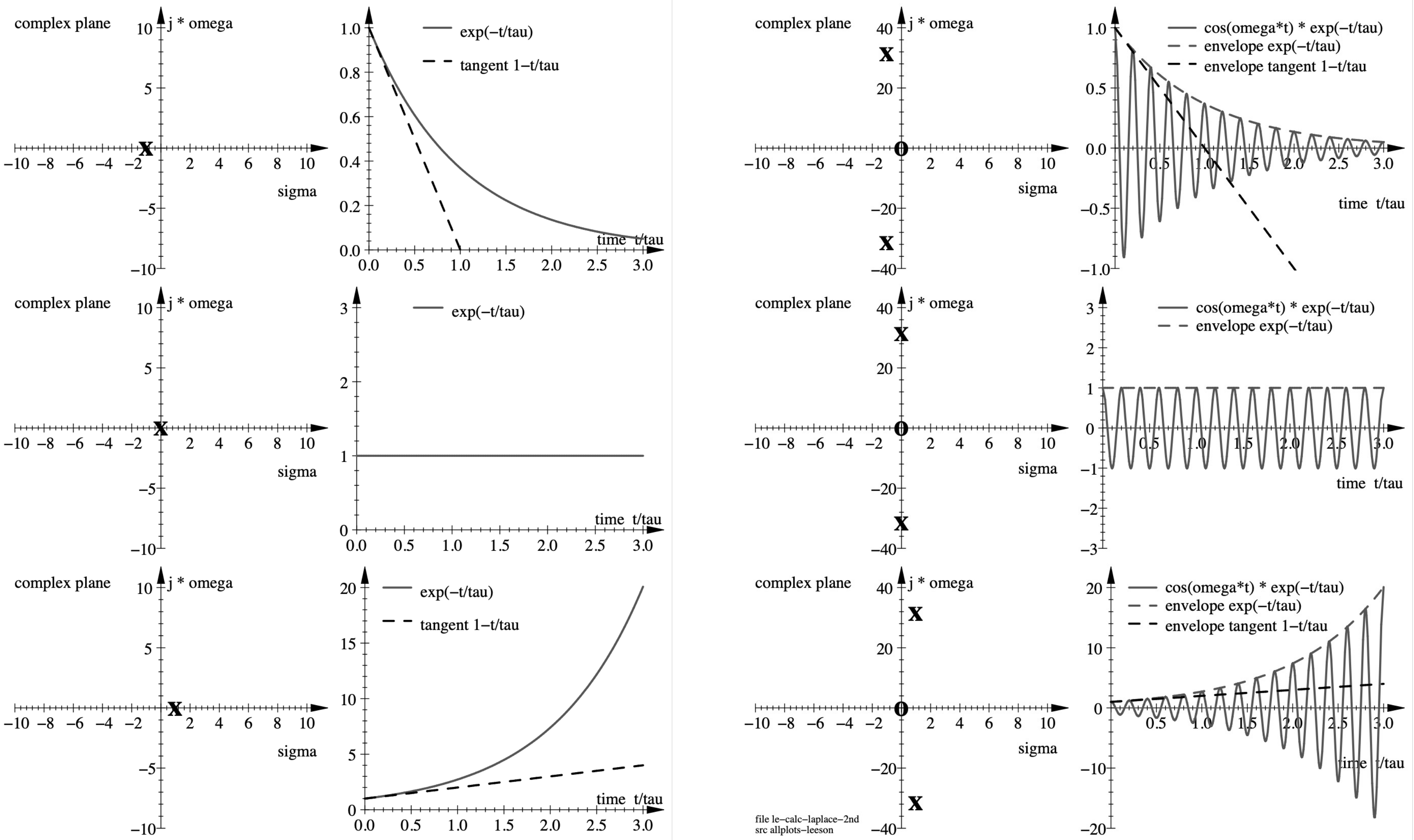

Impulse response of the resonator

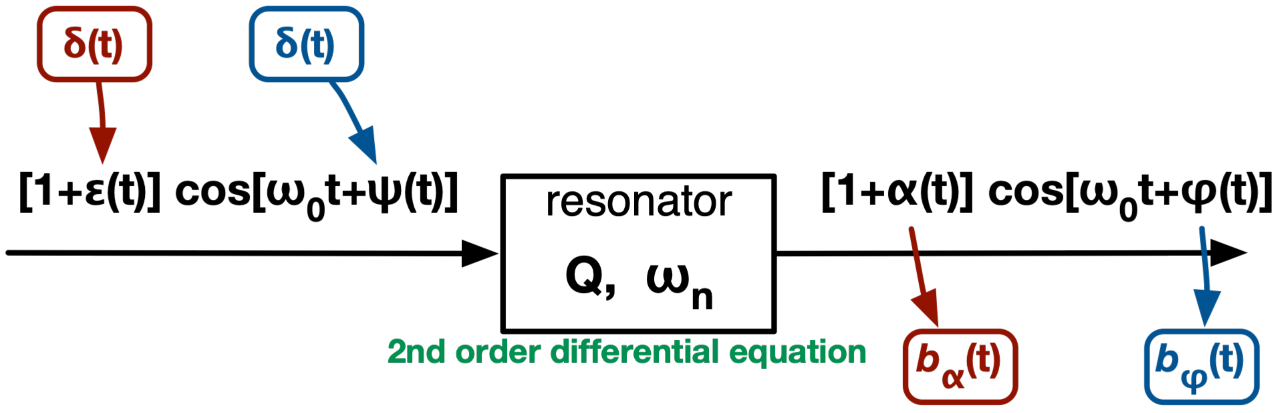

Can't figure out a $\delta(t)$ of phase or amplitude? Use Heaviside (step) $u(t)$ and differentiate

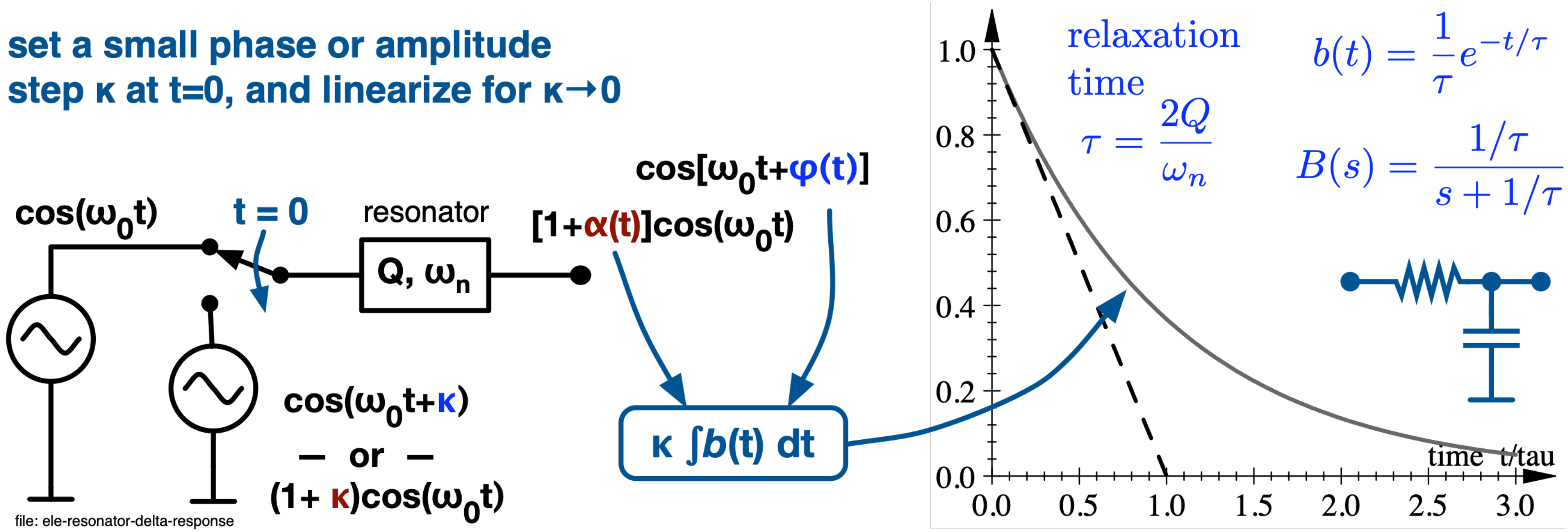

Response to a phase step κ

A phase step is equivalent to switching a sinusoid off at $t = 0$, and switching a shifted sinusoid on at $t = 0$

switched off at $t = 0$ switched on at $t = 0$

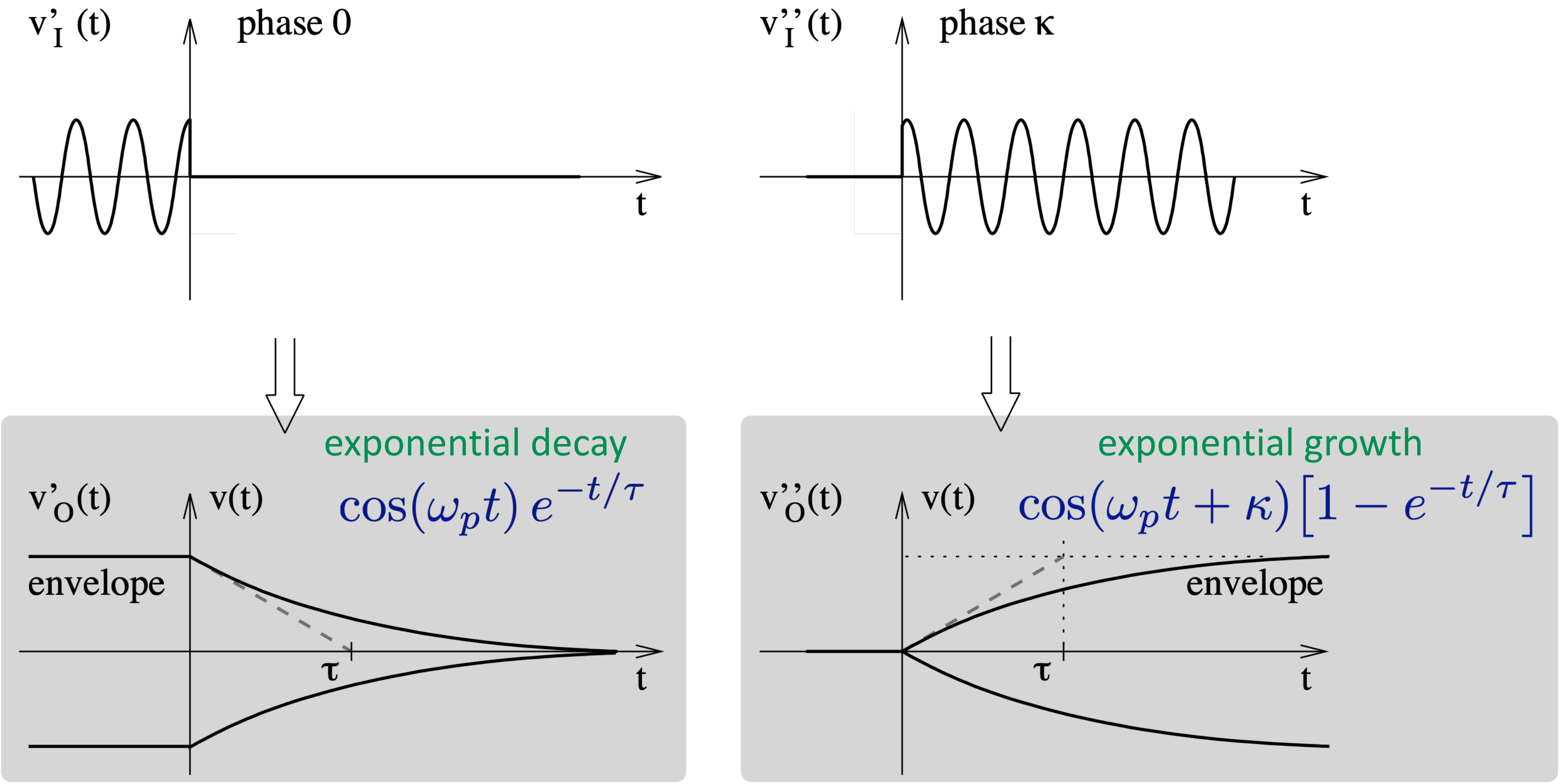

Impulse response, $\omega_0 = \omega_n$

$$v_i(t) = \underbrace{\cos(\omega_0 t)\,\mathrm{u}(-t)}_{\text{switched off at } t=0} + \underbrace{\cos(\omega_0 t + \kappa)\,\mathrm{u}(t)}_{\text{switched on at } t=0}$$

phase step κ at $t = 0$

$$v_o(t) = \cos(\omega_p t)\,e^{-t/\tau} + \cos(\omega_p t + \kappa)\left[1 - e^{-t/\tau}\right] \quad t > 0$$

output

linearize

$$v_o(t) = \cos(\omega_p t) - \kappa\sin(\omega_p t)\left[1 - e^{-t/\tau}\right] \quad \kappa \to 0$$

$$v_o(t) = \cos(\omega_0 t) - \kappa\sin(\omega_0 t)\left[1 - e^{-t/\tau}\right] \quad \omega_p \to \omega_0$$

high Q

$$\mathbf{V_o}(t) = \frac{1}{\sqrt{2}}\left\{1 + j\kappa\left[1 - e^{-t/\tau}\right]\right\}$$

slow-varying phase vector

$$\arctan\left(\frac{\Im\{\mathbf{V_o}(t)\}}{\Re\{\mathbf{V_o}(t)\}}\right) \simeq \kappa\left[1 - e^{-t/\tau}\right]$$

phasor angle

delete κ and differentiate

impulse response

$$\mathrm{b}(t) = \frac{1}{\tau}e^{-s\tau} \quad \leftrightarrow \quad \mathrm{B}(s) = \frac{1/\tau}{s + 1/\tau}$$

Detuned resonator

amplitude
phase

$$\begin{bmatrix}\alpha\\ \varphi\end{bmatrix} = \begin{bmatrix}\mathrm{b}_{\alpha\alpha} & \mathrm{b}_{\alpha\varphi}\\ \mathrm{b}_{\varphi\alpha} & \mathrm{b}_{\varphi\varphi}\end{bmatrix} * \begin{bmatrix}\varepsilon\\ \psi\end{bmatrix} \quad \leftrightarrow \quad \begin{bmatrix}\mathcal{A}\\ \Phi\end{bmatrix} = \begin{bmatrix}\mathrm{B}_{\alpha\alpha} & \mathrm{B}_{\alpha\varphi}\\ \mathrm{B}_{\varphi\alpha} & \mathrm{B}_{\varphi\varphi}\end{bmatrix} \begin{bmatrix}\mathcal{E}\\ \Psi\end{bmatrix}$$

$\Omega = \omega_0 - \omega_n$	detuning
$\beta_0 = \lvert\beta(j\omega_0)\rvert$	modulus
$\theta = \arg(\beta(j\omega_0))$	phase

$$v_i(t) = \underbrace{\frac{1}{\beta_0}\cos(\omega_0 t - \theta)\,\mathfrak{u}(-t)}_{\text{switched off at } t=0} + \underbrace{\frac{1}{\beta_0}\cos(\omega_0 t - \theta + \kappa)\,\mathfrak{u}(t)}_{\text{switched on at } t=0}$$

phase step κ at $t = 0$

$$= \frac{1}{\beta_0}\cos(\omega_0 t - \theta)\,\mathfrak{u}(-t) + \frac{1}{\beta_0}\left[\cos(\omega_0 t - \theta)\cos\kappa - \sin(\omega_0 t - \theta)\sin\kappa\right]\mathfrak{u}(t)$$

$$\simeq \frac{1}{\beta_0}\cos(\omega_0 t - \theta)\,\mathfrak{u}(-t) + \frac{1}{\beta_0}\left[\cos(\omega_0 t - \theta) - \kappa\sin(\omega_0 t - \theta)\right]\mathfrak{u}(t) \qquad \kappa \ll 1.$$

Details

Probe signal, $t \leq 0$

$$v_i(t) = \frac{1}{\beta_0} \cos(\omega_0 t - \theta)$$

where β_0 and θ are chosen for

$$x_o(t) = \cos(\omega_0 t)$$

in stationary conditions

Baseline, $t \leq 0$

$$x_{bl}(t) = \cos(\omega_0 t)$$

Differential equation

$$\ddot{x} + \frac{\omega_n}{Q}\dot{x} + \omega_n^2 x = \frac{\omega_n}{Q}\dot{v}$$

Characteristic equation

$$s^2 + \frac{\omega_n}{Q}s + \omega_n^2 = 0$$

Solutions of the char. eq.

$$s = \sigma_p \pm i\omega_p$$

with

$$\sigma_p = -\frac{\omega_n}{2Q} \quad \omega_p = \frac{\omega_n}{2Q}\sqrt{4Q^2 - 1} \quad \tau = -\frac{1}{\sigma_p} = \frac{2Q}{\omega_n}$$

General solution of the DE

$$x(t) = \mathcal{A}\cos(\omega_p t)e^{-\frac{t}{\tau}} + \mathcal{B}\sin(\omega_p t)\,e^{-\frac{t}{\tau}} + \mathcal{C}\cos(\omega_0 t) + \mathcal{D}\sin(\omega_0 t)$$

The coefficients $\mathcal{A}, \mathcal{B}, \mathcal{C}, \mathcal{D}$ are set by the BCs at $t = 0$ and $t = \infty$

Alternate form of the general solution, make ω_0 explicit using $\omega_p = \omega_0 - \Omega$

$$x(t) = \left[\mathcal{C} + \mathcal{A}\cos(\Omega t)e^{-\frac{t}{\tau}} - \mathcal{B}\sin(\Omega t)\,e^{-\frac{t}{\tau}}\right]\cos(\omega_0 t) + \left[\mathcal{D} + \mathcal{A}\sin(\Omega t)\,e^{-\frac{t}{\tau}} + \mathcal{B}\cos(\Omega t)\,e^{-\frac{t}{\tau}}\right]\sin(\omega_0 t)$$

Define $\Omega = \omega_0 - \omega_p$, where ω_0 is the frequency of the force, and replace $\omega_p = \omega_0 - \Omega$

$$\cos(\omega_p t) = \cos(\Omega t)\cos(\omega_0 t) + \sin(\Omega t)\sin(\omega_0 t)$$

$$\sin(\omega_p t) = -\sin(\Omega t)\cos(\omega_0 t) + \cos(\Omega t)\sin(\omega_0 t)$$

Switch-off transient, $t \geq 0$

$$x_{\text{off}}(t) = \cos(\omega_p t)e^{-\frac{t}{\tau}} = \cos(\Omega t)\,e^{-\frac{t}{\tau}}\cos(\omega_0 t) + \sin(\Omega t)\,e^{-\frac{t}{\tau}}\sin(\omega_0 t)$$

Phase response

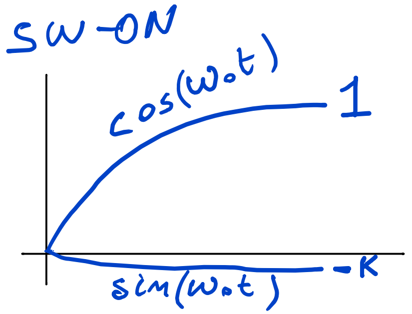

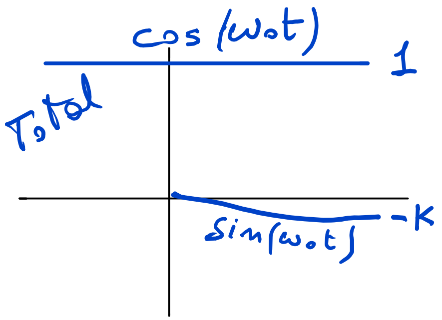

Switch-on transient

$$x_{\mathrm{on}}(t) = \left[\mathcal{C} + \mathcal{A}\cos(\Omega t)e^{-\frac{t}{\tau}} - \mathcal{B}\sin(\Omega t)\,e^{-\frac{t}{\tau}}\right]\cos(\omega_0 t) + \left[\mathcal{D} + \mathcal{A}\sin(\Omega t)\,e^{-\frac{t}{\tau}} + \mathcal{B}\cos(\Omega t)\,e^{-\frac{t}{\tau}}\right]\sin(\omega_0 t)$$

BC

$$t \to \infty \;\Rightarrow\; e^{-t/\tau} \to 0 \qquad \mathcal{C} = 1,\; \mathcal{D} = -\kappa$$

$$t \to 0 \;\Rightarrow\; e^{-t/\tau} \to 1 \qquad \mathcal{C} + \mathcal{A} = 0 \;\Rightarrow\; \mathcal{A} = -1$$

$$\mathcal{D} + \mathcal{B} = 0 \;\Rightarrow\; \mathcal{B} = \kappa$$

$$x_{\mathrm{on}}(t) = \left[1 - \cos(\Omega t)e^{-\frac{t}{\tau}} - \kappa\sin(\Omega t)\,e^{-\frac{t}{\tau}}\right]\cos(\omega_0 t) + \left[-\kappa + \kappa\cos(\Omega t)\,e^{-\frac{t}{\tau}} - \sin(\Omega t)\,e^{-\frac{t}{\tau}}\right]\sin(\omega_0 t)$$

Add switch-off and switch-on transients

$$x_{\mathrm{off}}(t) + x_{\mathrm{on}}(t) = \left[1 - \kappa\sin(\Omega t)\,e^{-\frac{t}{\tau}}\right]\cos(\omega_0 t) - \kappa\left[1 - \cos(\Omega t)\,e^{-\frac{t}{\tau}}\right]\sin(\omega_0 t)$$

Get the effect of the step by subtracting the pre-switch steady state, and deleting κ

$$x_u(t) = \frac{1}{\kappa}\left[x_{\mathrm{off}}(t) + x_{\mathrm{on}}(t) - x_{\mathrm{bl}}(t)\right]$$

$$x_u(t) = \sin(\Omega t)\,e^{-t/\tau}\cos(\omega_0 t) - \left[1 - \cos(\Omega t)\,e^{-t/\tau}\right]\sin(\omega_0 t)$$

Step response

$$\varphi_u = 1 - \cos(\Omega t)\,e^{-t/\tau}$$

$$\alpha_u = -\sin(\Omega t)\,e^{-t/\tau}$$

differentiate →

Impulse response

$$\varphi_\delta = \left[\frac{1}{\tau}\cos(\Omega t) + \Omega\sin(\Omega t)\right]e^{-t/\tau}$$

$$\alpha_\delta = \left[-\Omega\cos(\Omega t) + \frac{1}{\tau}\sin(\Omega t)\right]e^{-t/\tau}$$

Amplitude response

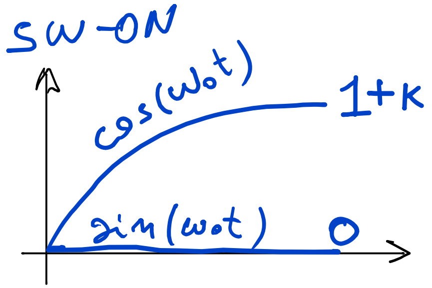

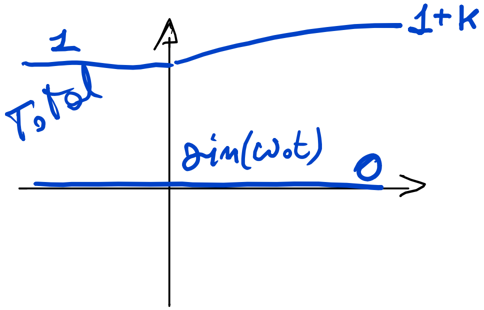

Switch-on transient

$$x_{\text{on}}(t) = \left[\mathcal{C} + \mathcal{A}\cos(\Omega t)e^{-\frac{t}{\tau}} - \mathcal{B}\sin(\Omega t)\, e^{-\frac{t}{\tau}}\right]\cos(\omega_0 t) + \left[\mathcal{D} + \mathcal{A}\sin(\Omega t)\, e^{-\frac{t}{\tau}} + \mathcal{B}\cos(\Omega t)\, e^{-\frac{t}{\tau}}\right]\sin(\omega_0 t)$$

BC

$t \to \infty \;\Rightarrow\; e^{-t/\tau} \to 0$ $\qquad \mathcal{C} = 1 + \kappa,\; \mathcal{D} = 0$

$t \to 0 \;\Rightarrow\; e^{-t/\tau} \to 1$ $\qquad \mathcal{C} + \mathcal{A} = 0 \;\Rightarrow\; \mathcal{A} = -(1+\kappa)$

$\mathcal{D} + \mathcal{B} = 0 \;\Rightarrow\; \mathcal{B} = 0$

$$x_{\text{on}}(t) = \left[(1+\kappa) - (1+\kappa)\cos(\Omega t)e^{-\frac{t}{\tau}}\right]\cos(\omega_0 t) - (1+\kappa)\sin(\Omega t)\, e^{-\frac{t}{\tau}}\sin(\omega_0 t)$$

Add switch-off and switch-on transients

$$x_{\text{off}}(t) + x_{\text{on}}(t) = \left[(1+\kappa) - \kappa\cos(\Omega t)\, e^{-\frac{t}{\tau}}\right]\cos(\omega_0 t) - \kappa\sin(\Omega t)\, e^{-\frac{t}{\tau}}\sin(\omega_0 t)$$

Get the effect of the step by subtracting the pre-switch steady state, and deleting κ

$$x_u(t) = \frac{1}{\kappa}\left[x_{\text{off}}(t) + x_{\text{on}}(t) - x_{\text{bl}}(t)\right]$$

$$x_u(t) = \left[1 - \cos(\Omega t)\, e^{-t/\tau}\right]\cos(\omega_0 t) - \sin(\Omega t)\, e^{-t/\tau}\sin(\omega_0 t)$$

Step response

$$\varphi_u = \sin(\Omega t)\, e^{-t/\tau}$$

$$\alpha_u = 1 - \cos(\Omega t)\, e^{-t/\tau}$$

differentiate →

Impulse response

$$\varphi_\delta = \left[\Omega\cos(\Omega t) - \frac{1}{\tau}\sin(\Omega t)\right]e^{-t/\tau}$$

$$\alpha_\delta = \left[\frac{1}{\tau}\cos(\Omega t) + \Omega\sin(\Omega t)\right]e^{-t/\tau}$$

Impulse response of the detuned resonator

Time domain

$$\begin{bmatrix}\varphi\\ \alpha\end{bmatrix} = \begin{bmatrix}\frac{1}{\tau}\cos(\Omega t) + \Omega\sin(\Omega t) & -\Omega\cos(\Omega t) - \frac{1}{\tau}\sin(\Omega t)\\ \Omega\cos(\Omega t) - \frac{1}{\tau}\sin(\Omega t) & \frac{1}{\tau}\cos(\Omega t) + \Omega\sin(\Omega t)\end{bmatrix} e^{-\frac{t}{\tau}} \begin{bmatrix}\psi\\ \epsilon\end{bmatrix}$$

Laplace Transforms

$$\begin{bmatrix}\Phi\\ \mathrm{A}\end{bmatrix} = \begin{bmatrix}\frac{1}{\tau}\dfrac{s + \frac{1}{\tau} + \tau\Omega^2}{s^2 + \frac{1}{\tau^2} + \frac{2s}{\tau} + \Omega^2} & -\Omega\dfrac{s}{s^2 + \frac{1}{\tau^2} + \frac{2s}{\tau} + \Omega^2}\\ \Omega\dfrac{s}{s^2 + \frac{1}{\tau^2} + \frac{2s}{\tau} + \Omega^2} & \frac{1}{\tau}\dfrac{s + \frac{1}{\tau} + \tau\Omega^2}{s^2 + \frac{1}{\tau^2} + \frac{2s}{\tau} + \Omega^2}\end{bmatrix} \begin{bmatrix}\Psi\\ \mathrm{E}\end{bmatrix}$$

Resonator step and impulse response

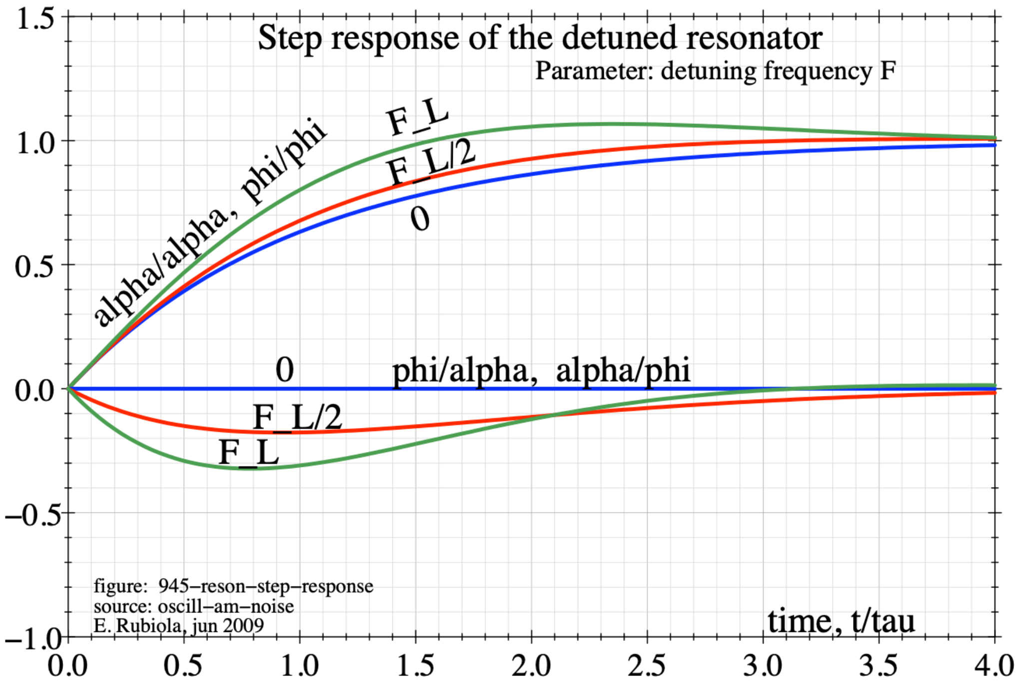

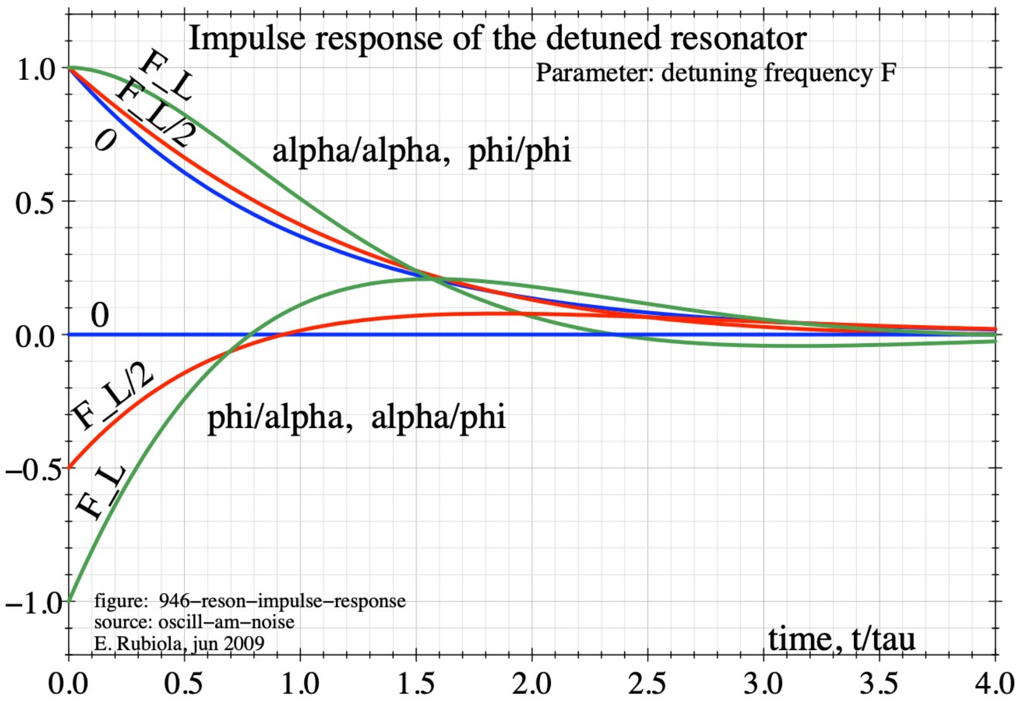

A in one of the coupling terms
may be wrong, double check

Frequency response

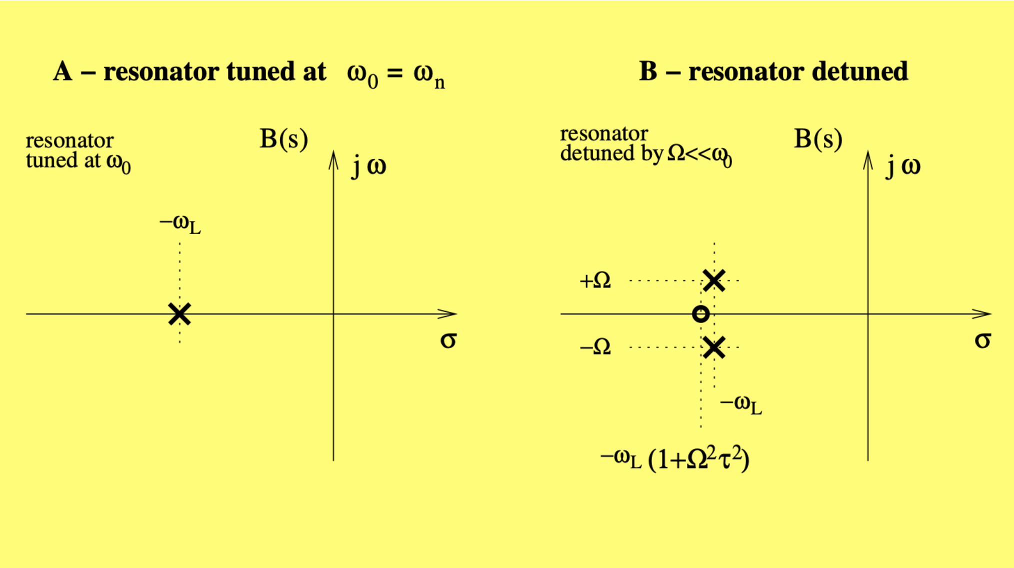

diagonal terms

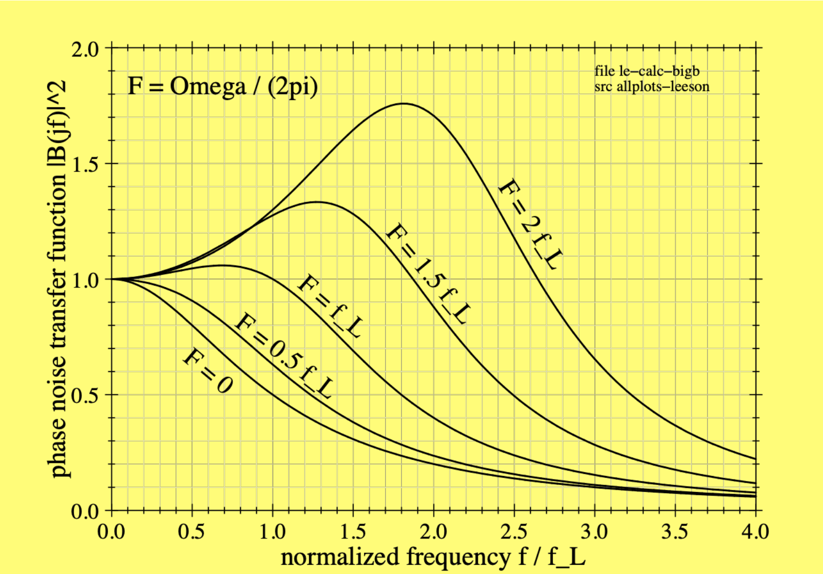

diagonal terms

$$\begin{bmatrix}\Phi\\ \mathrm{A}\end{bmatrix} = \begin{bmatrix} \dfrac{1}{\tau}\,\dfrac{s+\dfrac{1}{\tau}+\tau\Omega^2}{s^2+\dfrac{1}{\tau^2}+\dfrac{2s}{\tau}+\Omega^2} & -\Omega\dfrac{s}{s^2+\dfrac{1}{\tau^2}+\dfrac{2s}{\tau}+\Omega^2} \\ \dfrac{s}{s^2+\dfrac{1}{\tau^2}+\dfrac{2s}{\tau}+\Omega^2} & \dfrac{1}{\tau}\,\dfrac{s+\dfrac{1}{\tau}+\tau\Omega^2}{s^2+\dfrac{1}{\tau^2}+\dfrac{2s}{\tau}+\Omega^2} \end{bmatrix} \begin{bmatrix}\Psi\\ \mathrm{E}\end{bmatrix}$$

Formal Proof for the Leeson Effect

Low-pass representation of AM-PM noise

E. Rubiola, Phase Noise and Frequency Stability in Oscillators, Cambridge 2008–2012

E. Rubiola & R. Brendel, arXiv:1004.5539v1, [physics.ins-det]

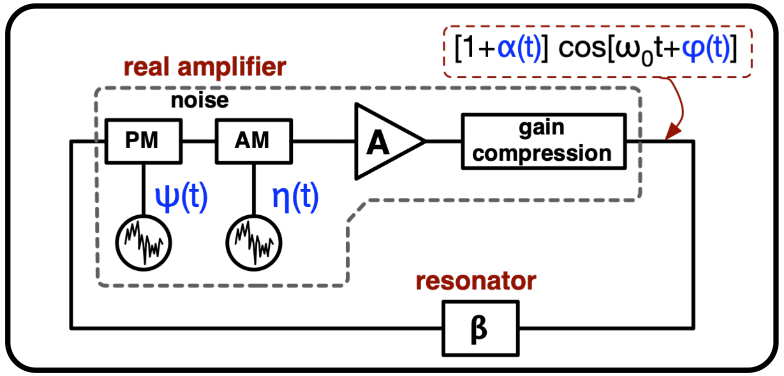

RF, μwaves or optics

The amplifier
– "copies" the input phase to the out
– adds phase noise

low-pass equivalent

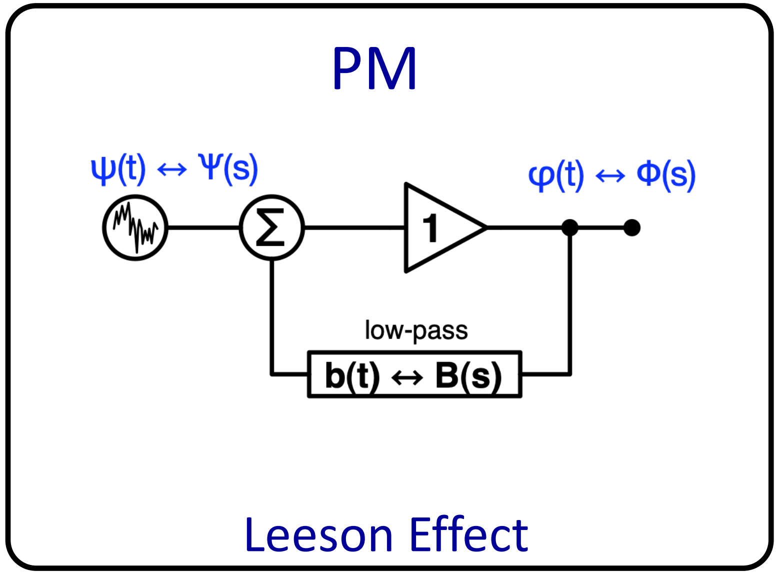

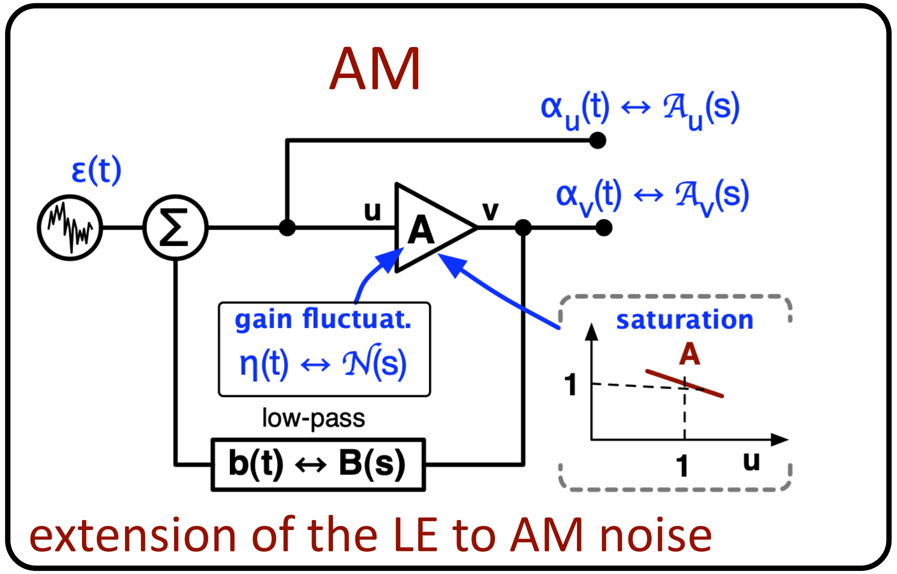

Effect of feedback

Oscillator transfer function (RF)

A – Oscillator transfer function H(s)

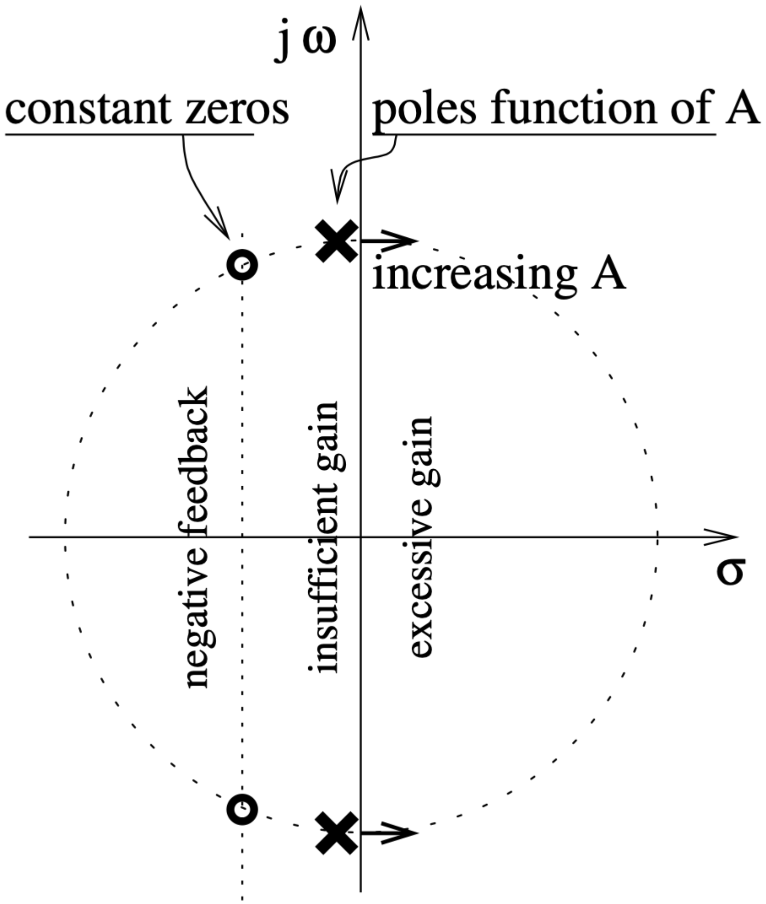

B – Detail of the denominator of H(s)

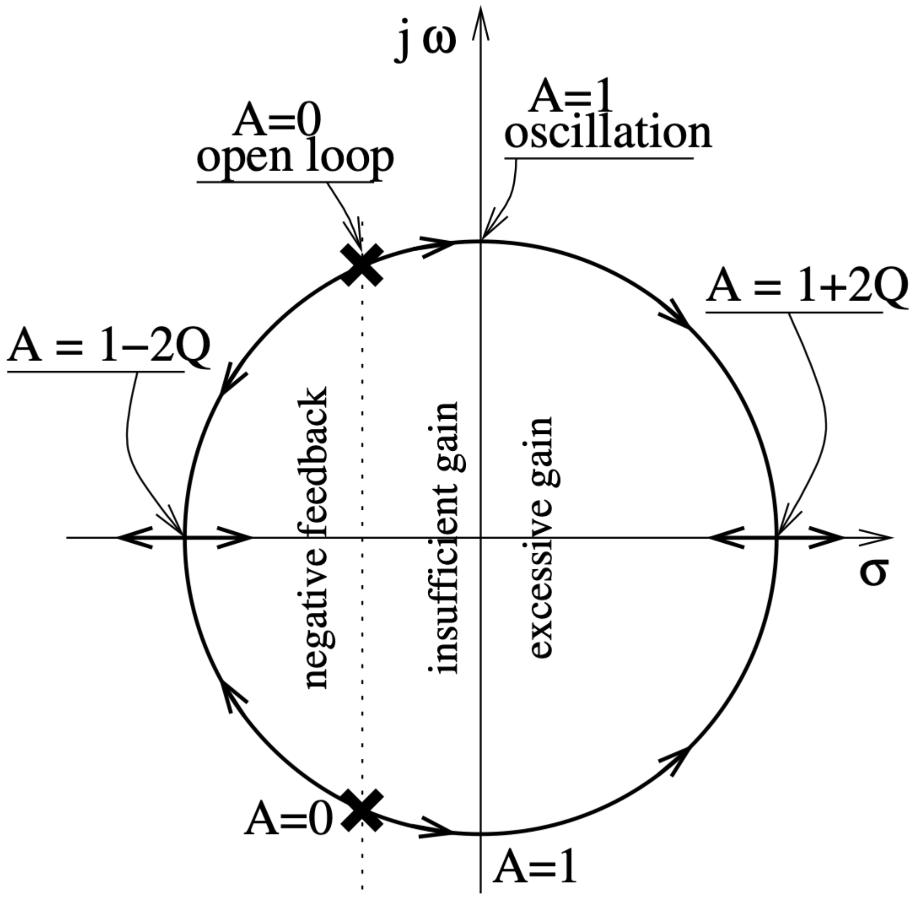

Figures are from E. Rubiola, Phase noise and frequency stability in oscillators, © Cambridge University Press

The Leeson effect

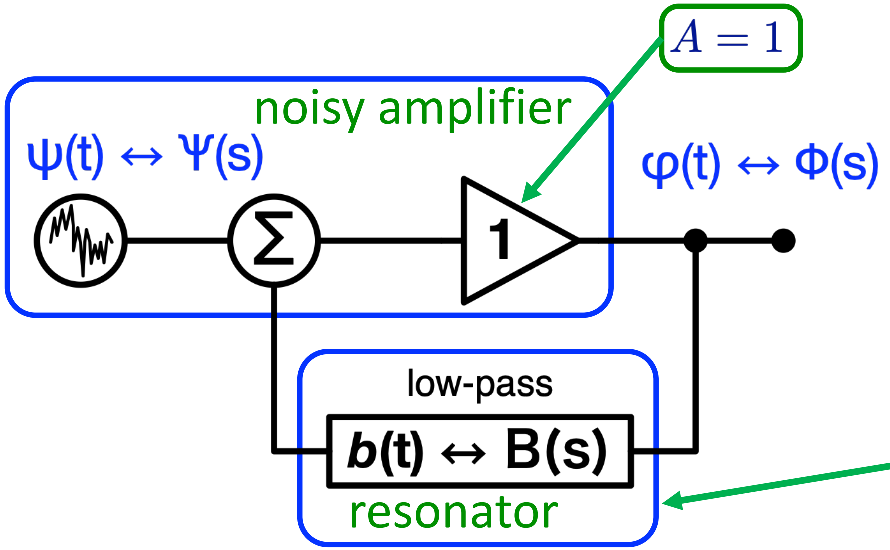

$$B(s) = \frac{1/\tau}{s + 1/\tau}$$

phase-noise transfer function

$\mathrm{H}(s) = \dfrac{\Phi(s)}{\Psi(s)}$	definition
$\mathrm{H}(s) = \dfrac{1}{1 - B(s)}$	general feedback theory
$\mathrm{H}(s) = \dfrac{1 + s\tau}{s\tau}$	Leeson effect

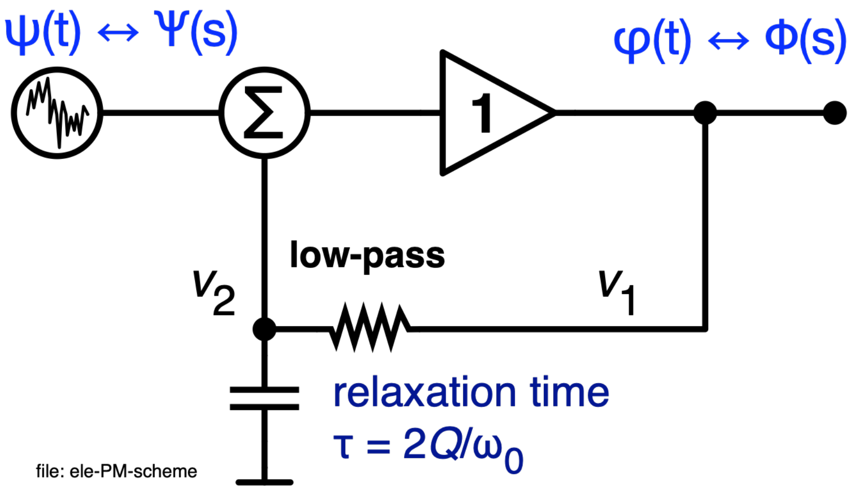

file: ele-PM-scheme

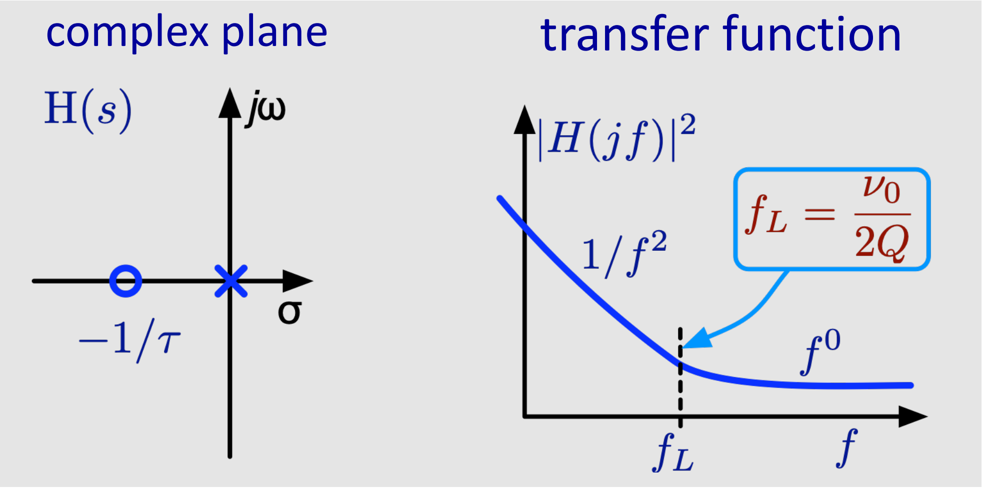

Oscillator with detuned resonator

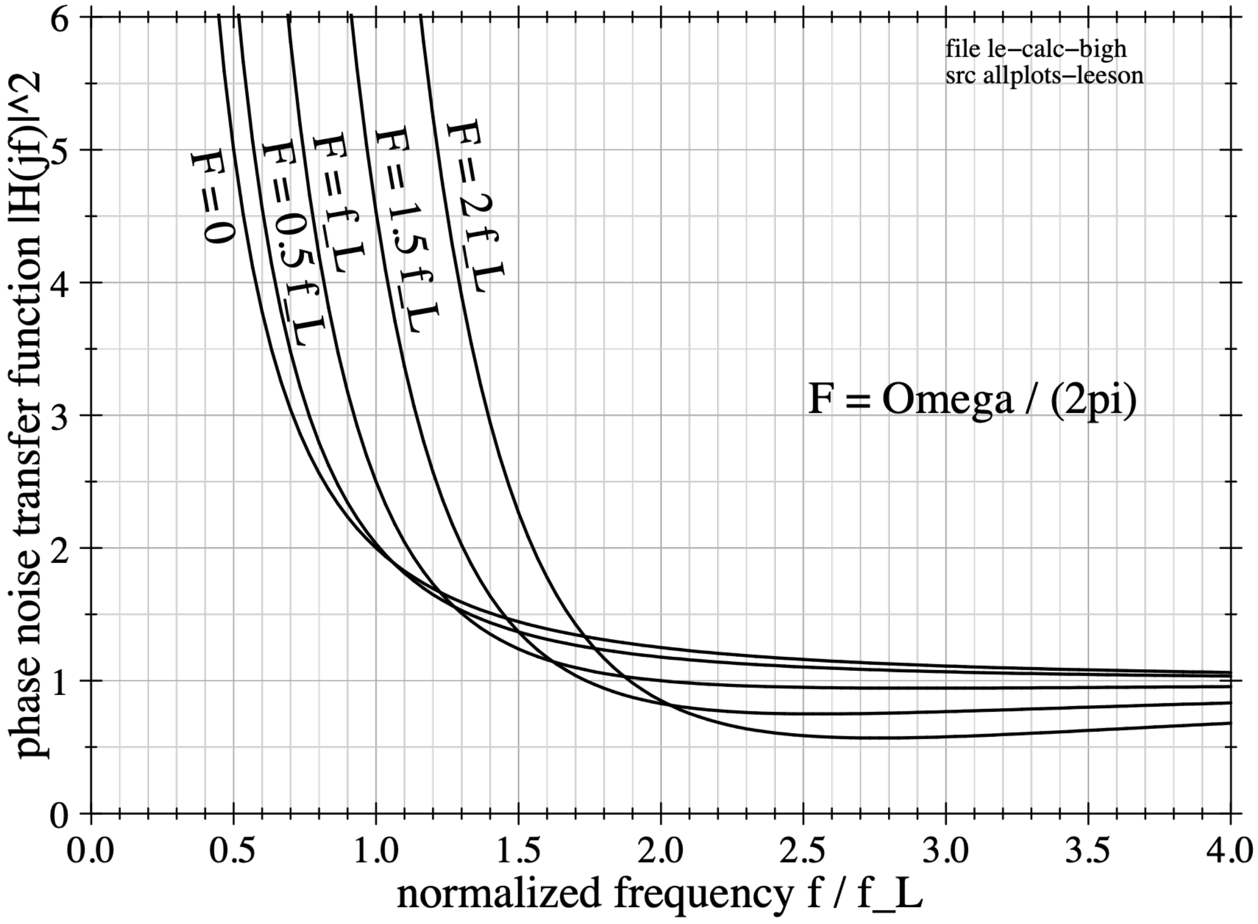

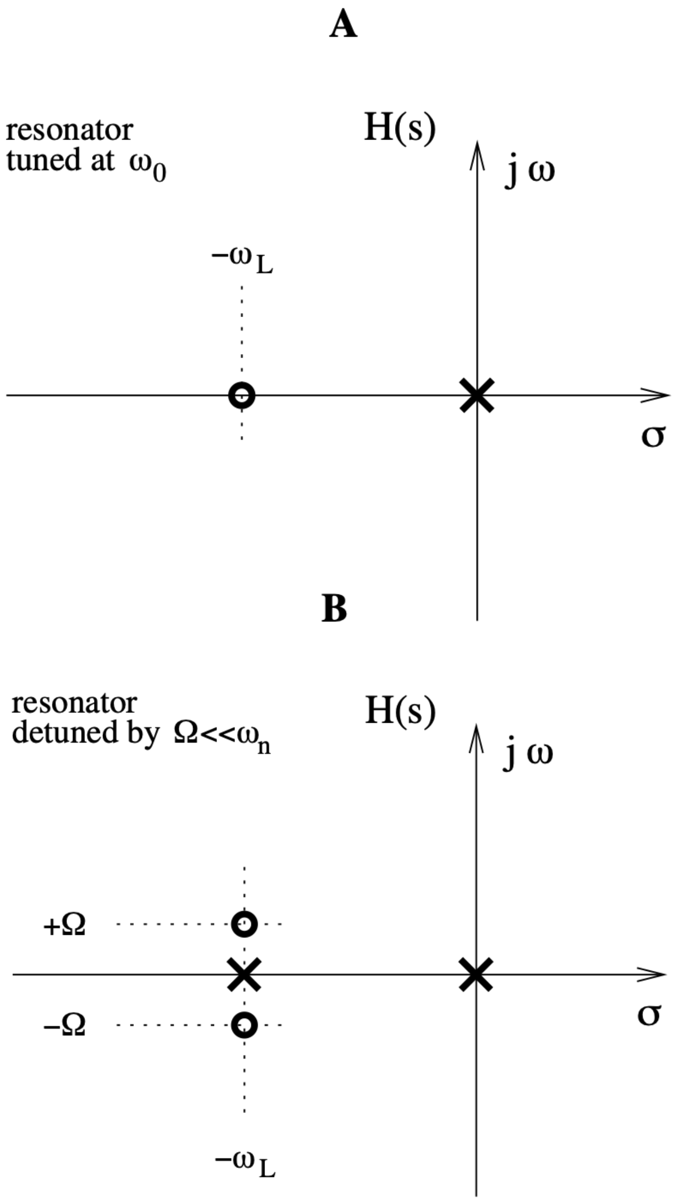

Gain saturation

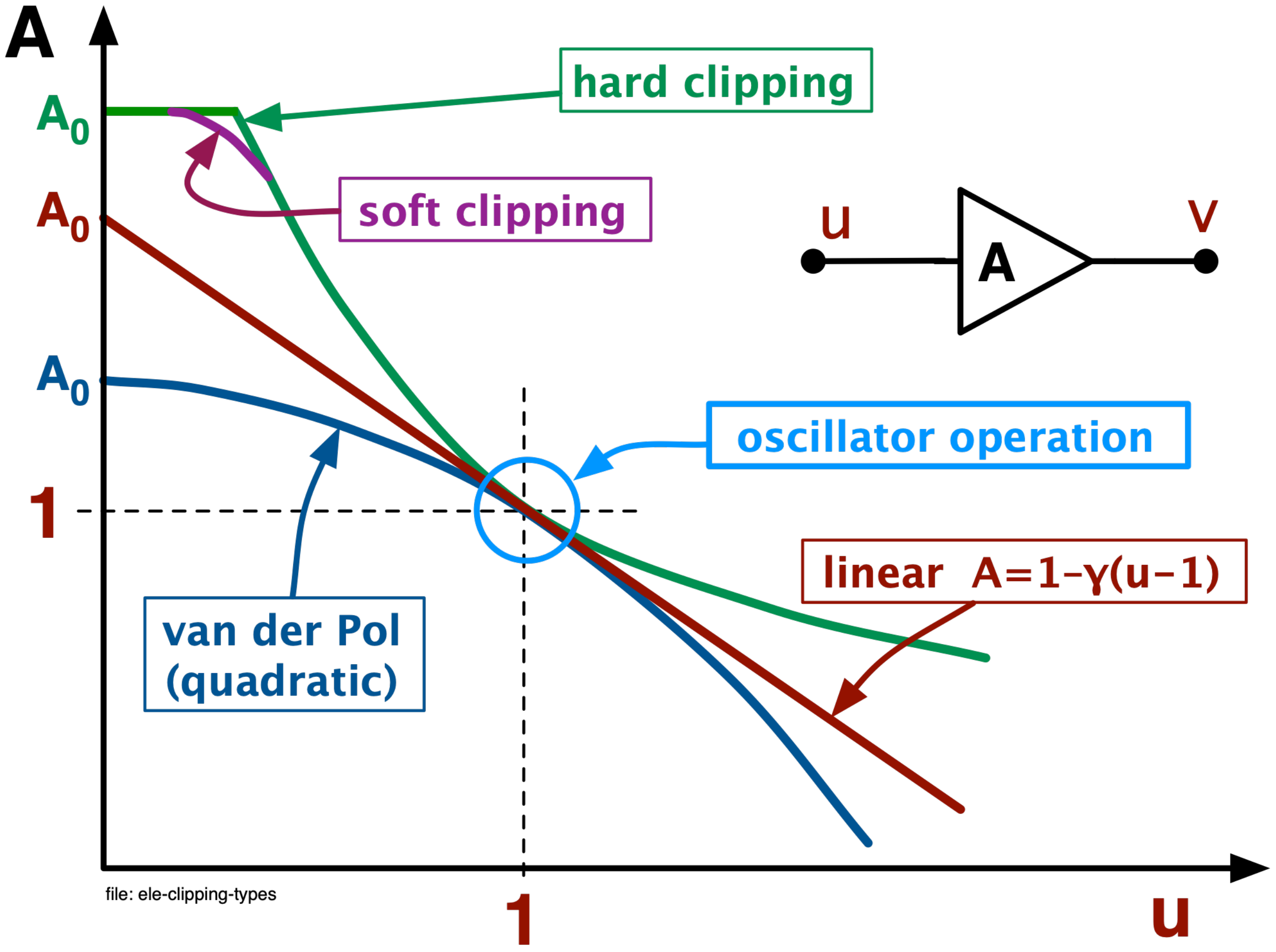

Gain compression is necessary for the oscillation amplitude to be stable

Low-pass model for amplitude (1)

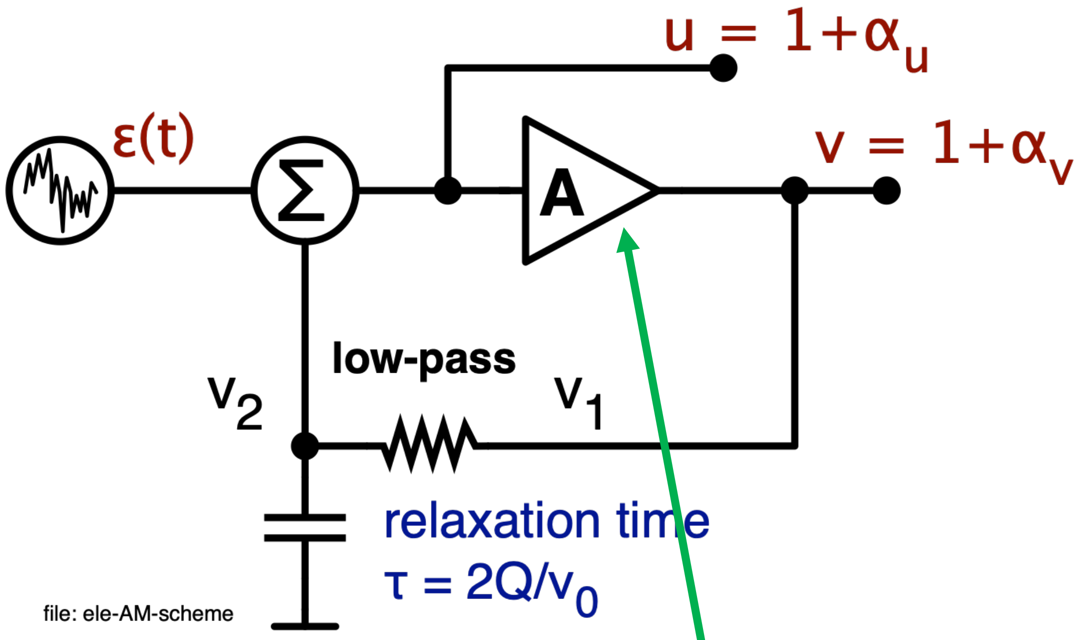

simple feedback theory

$$u = \epsilon + v_2$$

$$v_2 = \frac{1}{\tau}\int (v_1 - v_2)\, dt$$

$$v_2 = u - \epsilon$$

$$v_1 = v = Au$$

$$u = \epsilon + \frac{1}{\tau}\int (A-1)u + \epsilon\, dt$$

differential equation

$$\dot{u} - \frac{1}{\tau}(A-1)\,u = \frac{1}{\tau}\epsilon + \dot{\epsilon}$$

Gain compression is necessary for the oscillation amplitude to be stable

Low-pass model for amplitude (2)

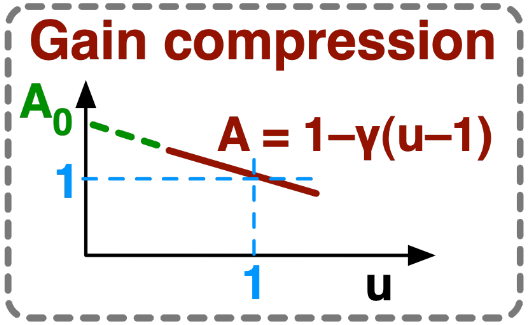

homogeneous differential equation

$$\dot{u} - \frac{1}{\tau}\,(A-1)\,u = 0$$

Three asymptotic cases

At low RF amplitude, let the gain be an arbitrary value denoted with A_0

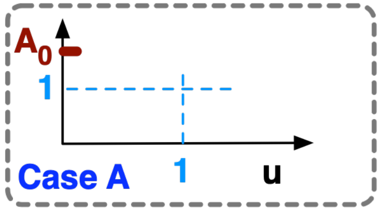

Startup: $u \to 0, \quad A \to A_0 > 1$

$$\dot{u} - \frac{1}{\tau}\,(A_0-1)\,u = 0 \quad \Rightarrow \quad u = C_1 e^{(A_0-1)\,t/\tau}$$

rising exponential

For small fluctuation of the stationary RF amplitude, the gain varies linearly with V

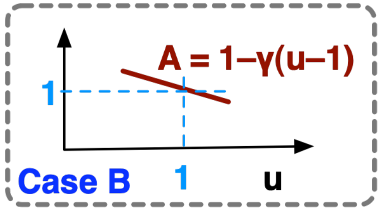

Regime: $u \to 1, \quad A = 1 - \gamma\,(u - 1)$

$$\dot{u} + \frac{\gamma}{\tau}\,(u-1)\,u = 0 \quad \Rightarrow \quad u = C_2 e^{-\gamma\,t/\tau}$$

restoring time constant $\tau_r = \tau/\gamma$

Simplification: the gain varies linearly with V in all the input range

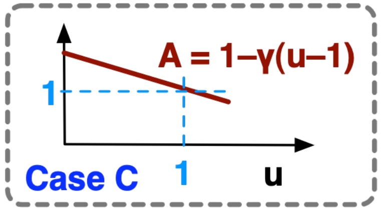

Linear gain: $A = 1 - \gamma\,(u - 1)$

$$u = \frac{1}{\left(\frac{1}{u(0)} - 1\right) e^{-\gamma t/\tau} + 1}$$

Startup – Analysis and simulation

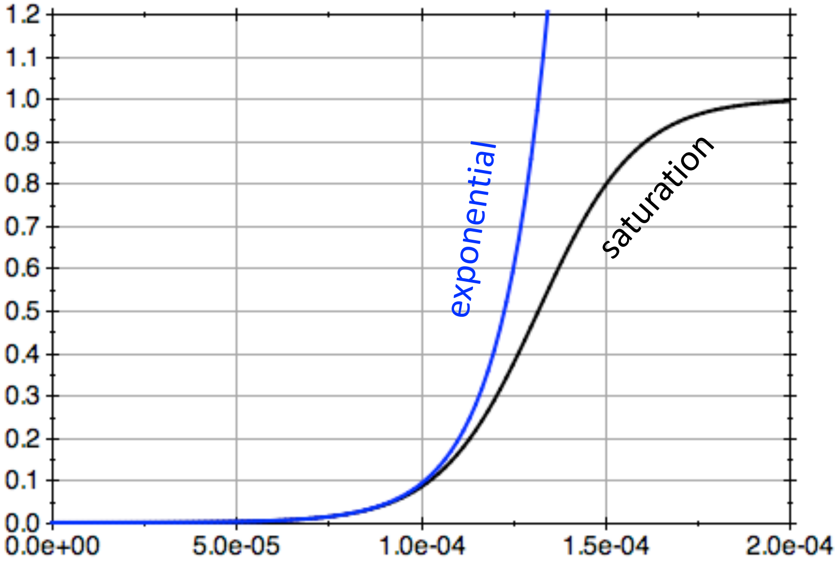

analytical solution,

$$A = 1 - \gamma(u - 1)$$

10 MHz oscillator

$L = 1$ mH

$R = 25\ \Omega$

$Q \approx 503$

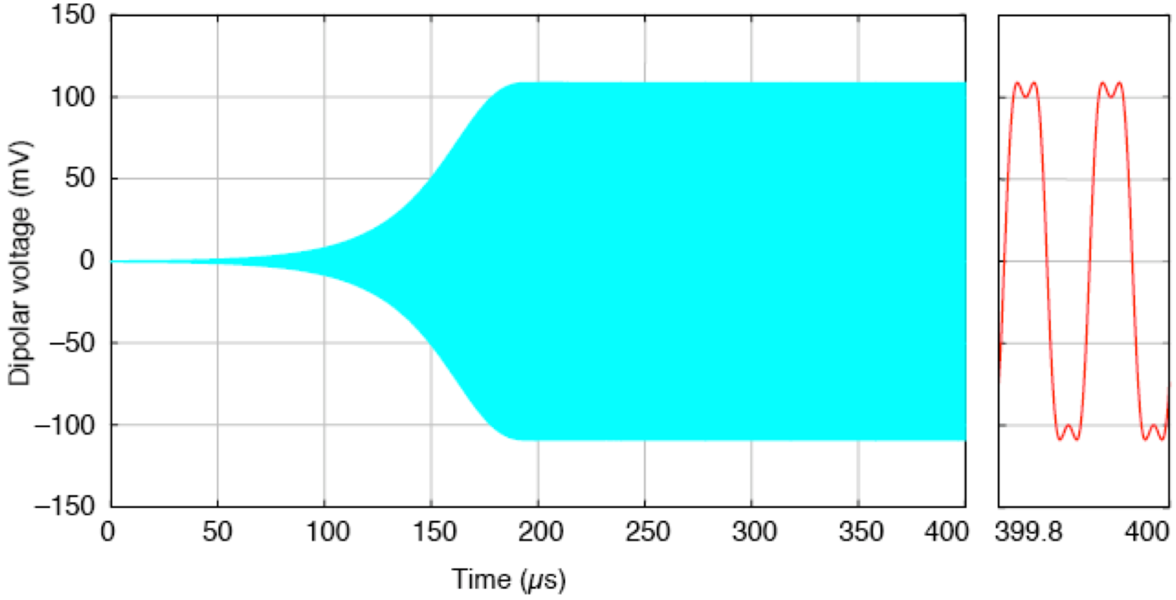

van der Pol oscillator
simulated by Rémi Brendel

Rising exponential.
We find the same time constant – τ/γ

See also Fig.15 of Addouche, Brendel et al., IEEE T UFFC 50(5), May 2003.

Gain fluctuations

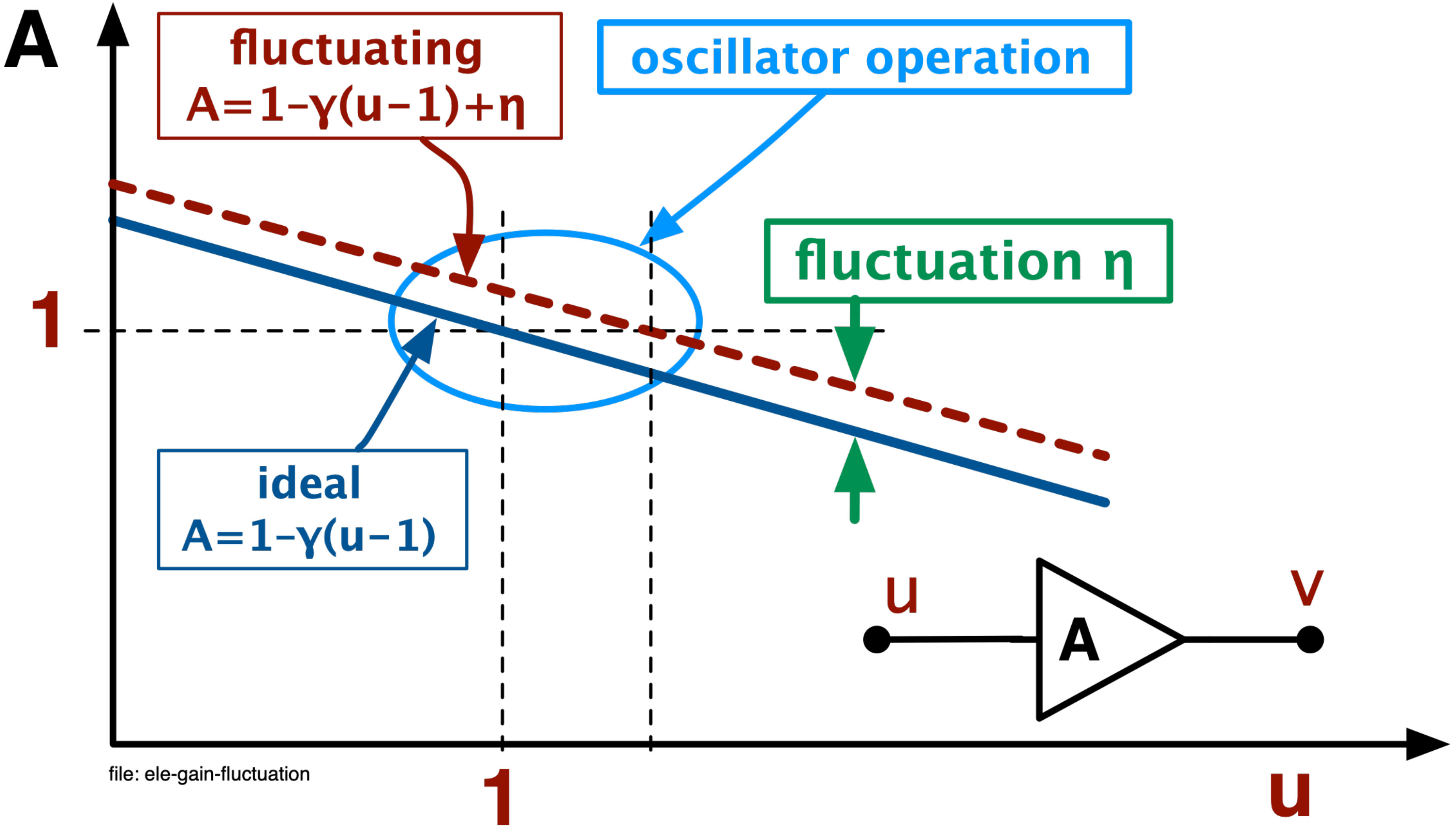

Gain compression is necessary for the oscillation amplitude to be stable

Gain fluctuations – Output is $u(t)$

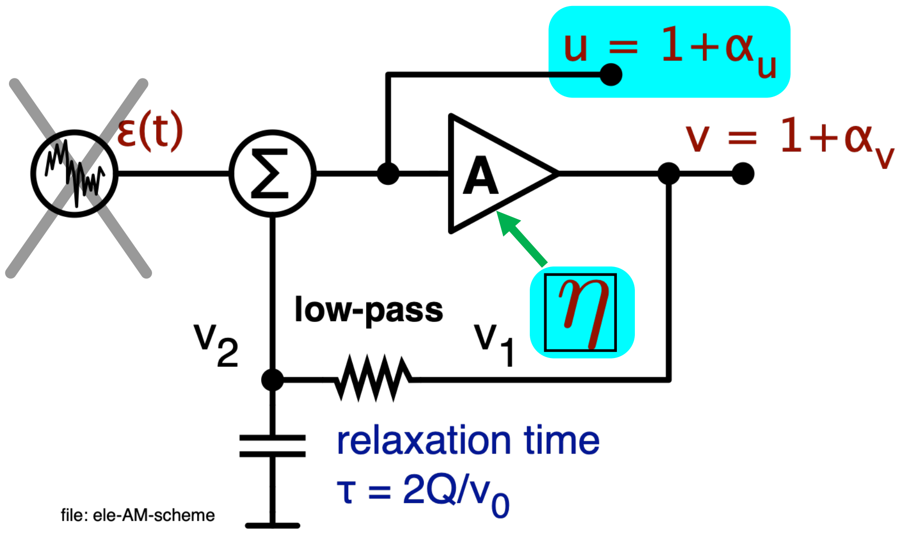

Linearize for low noise and use the Laplace transforms

$$\alpha_u(t) \leftrightarrow \mathcal{A}_u(s) \quad \text{and} \quad \eta(t) \leftrightarrow \mathcal{N}(s)$$

$$\mathrm{H}_u(s) = \frac{\mathcal{A}_u(s)}{\mathcal{N}(s)}$$ definition

$$\mathrm{H}_u(s) = \frac{1/\tau}{s+\gamma/\tau}$$ result

$$\dot{u} = \frac{1}{\tau}(A-1)u$$ non-linear equation

$$A = 1-\gamma(u-1)+\eta$$

$$\dot{u} + \frac{\gamma}{\tau}(u-1)u = \frac{\eta}{\tau}u$$ linearization for low noise

($\dot{u} \to \dot{\alpha}_u$, $(u-1) \to \alpha_u$, $u \to 1$, $u \to 1$)

$$\dot{\alpha}_u + \frac{\gamma}{\tau}\alpha_u = \frac{1}{\tau}\eta$$ linearized equation

$$\left(s+\frac{\gamma}{\tau}\right)\mathcal{A}_u(s) = \frac{1}{\tau}\mathcal{N}(s)$$ Laplace transform

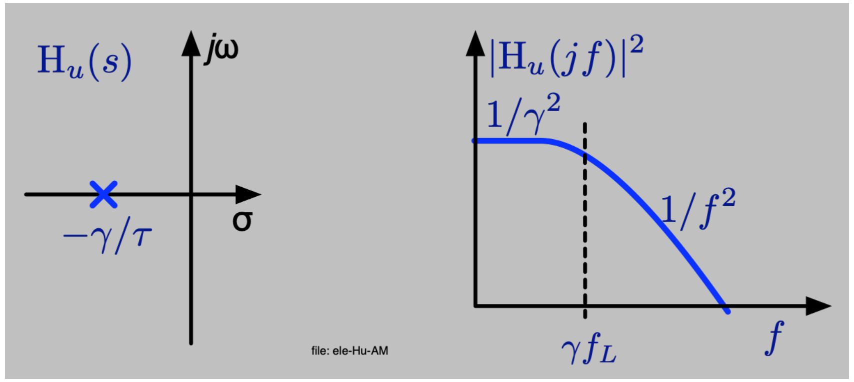

Gain fluctuations – Output is $v(t)$

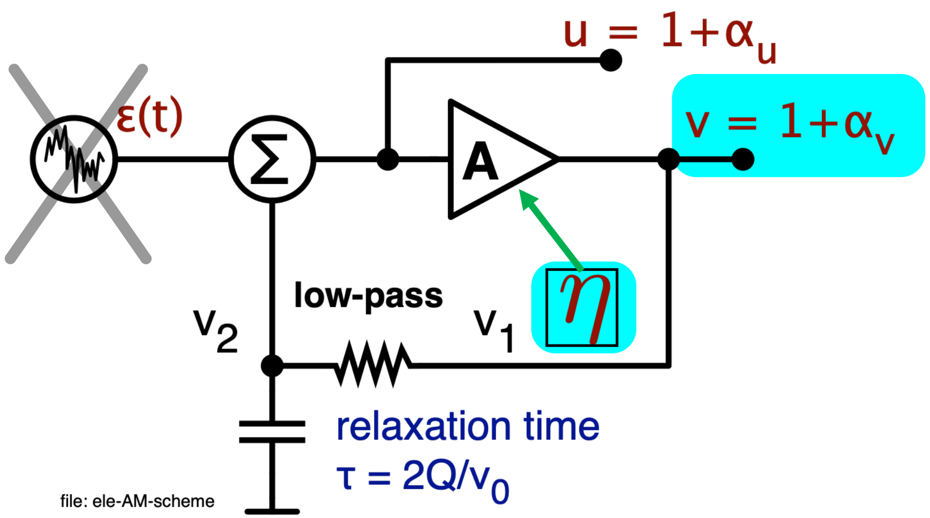

$$\left(s+\frac{\gamma}{\tau}\right)\mathcal{A}_u(s)=\frac{1}{\tau}\mathcal{N}(s)$$ starting equation

$$\mathcal{A}_u(s)=\frac{\mathcal{A}_v(s)-\mathcal{N}(s)}{1-\gamma}$$

$$\left(s+\frac{\gamma}{\tau}\right)\mathcal{A}_v(s)=\left(s+\frac{1}{\tau}\right)\mathcal{N}(s)$$

$$\text{H}(s)=\frac{\mathcal{A}_v(s)}{\mathcal{N}(s)}$$ definition

$$\text{H}(s)=\frac{s+1/\tau}{s+\gamma/\tau}$$ result

boring algebra relates α_v to α_u

$$v=Au$$

$$A=-\gamma(u-1)+1+\eta$$

$$v=[-\gamma(u-1)+1+\eta]\,u$$

$$v=[-\gamma\alpha_u+1+\eta]\;[1+\alpha_u]$$

$$\cancel{1}+\alpha_v=\cancel{1}+\eta-\gamma\alpha_u+\alpha_u-\cancel{\alpha_u\eta}-\cancel{\gamma\alpha_u^2}$$

$$\alpha_v=(1-\gamma)\alpha_u+\eta$$

$$\alpha_u=\frac{\alpha_v-\eta}{1-\gamma}$$

linearization for low noise

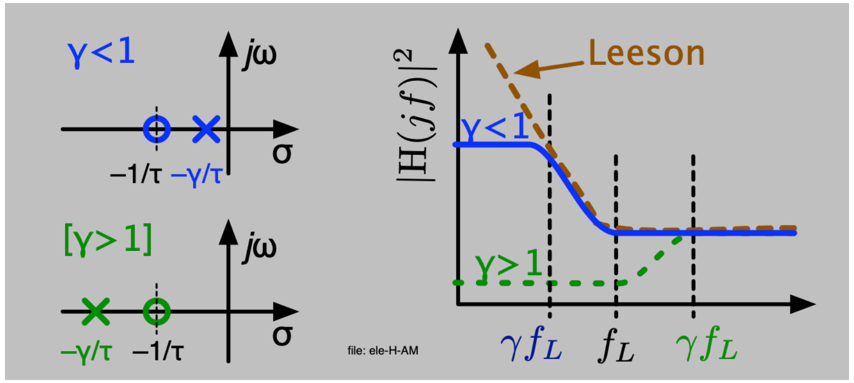

Noise – Output is $u(t)$

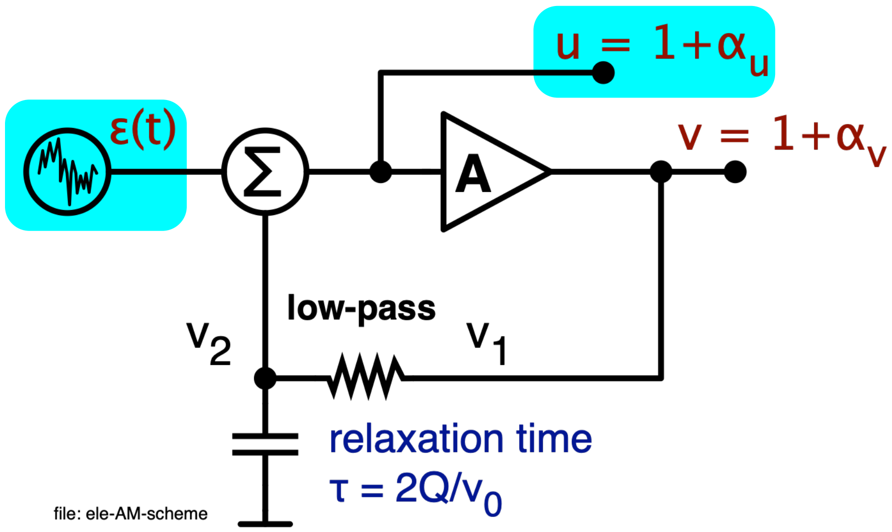

$$\dot{u} = \frac{1}{\tau}(A-1)u + \dot{\epsilon} + \frac{1}{\tau}\epsilon$$ non-linear equation

$$A = 1 - \gamma(u-1)$$

$$\dot{u} + \frac{\gamma}{\tau}(u-1)u = \dot{\epsilon} + \frac{1}{\tau}\epsilon$$ linearization for low noise

($\dot{u} \to \dot{\alpha}_u$, $(u-1) \to \alpha_u$, $u \to 1$)

$$\dot{\alpha}_u + \frac{\gamma}{\tau}\alpha_u = \dot{\epsilon} + \frac{1}{\tau}\epsilon$$ linearized equation

$$\left(s + \frac{\gamma}{\tau}\right) \mathcal{A}_u(s) = \left(s + \frac{1}{\tau}\right) \mathcal{E}(s)$$ Laplace transform

Linearize for low noise and use the Laplace transforms

$$\alpha_u(t) \leftrightarrow \mathcal{A}_u(s) \quad \text{and} \quad \epsilon(t) \leftrightarrow \mathcal{E}(s)$$

$$\mathrm{H}_u(s) = \frac{\mathcal{A}_u(s)}{\mathcal{E}(s)}$$ definition

$$\mathrm{H}_u(s) = \frac{s + 1/\tau}{s + \gamma/\tau}$$ result

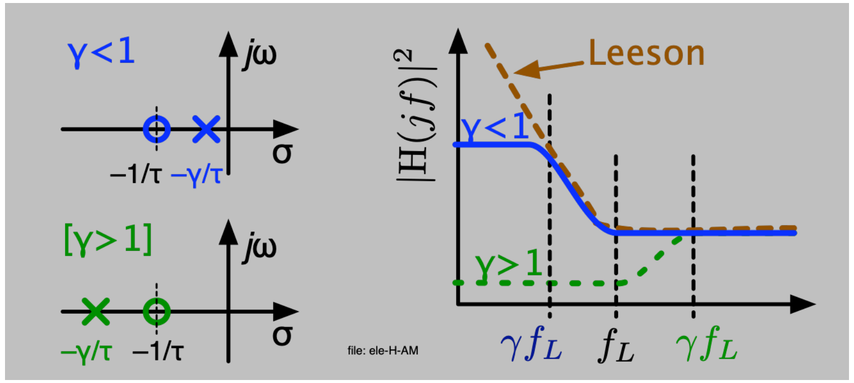

Noise – Output is $u(t)$

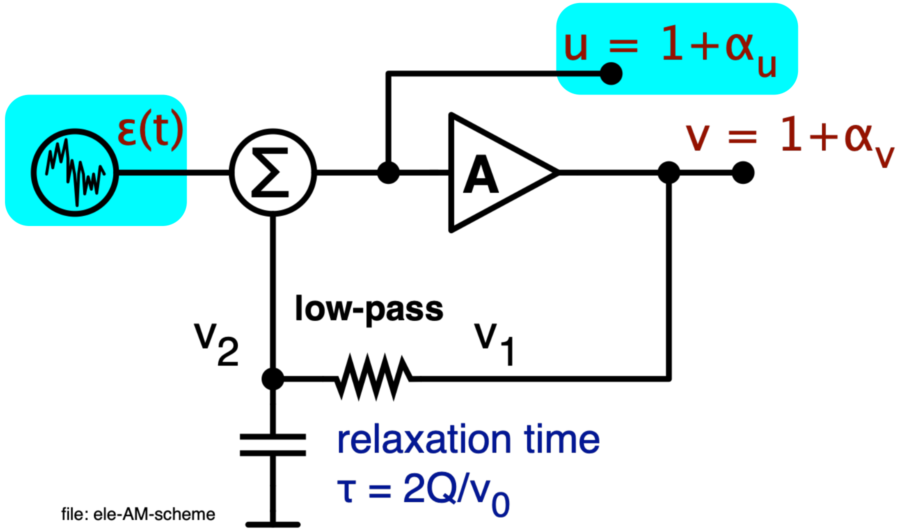

$$\dot{\alpha}_u + \frac{\gamma}{\tau}\alpha_u = \dot{\epsilon} + \frac{1}{\tau}\epsilon$$ linearized equation

$$\alpha_u = \alpha_v/(1-\gamma)$$

$$\frac{1}{1-\gamma}\left(\dot{\alpha}_v + \frac{\gamma}{\tau}\alpha_v\right) = \dot{\epsilon} + \frac{1}{\tau}\epsilon$$

$$\frac{1}{1-\gamma}\left(s + \frac{\gamma}{\tau}\right)\mathcal{A}_v(s) = \left(s + \frac{1}{\tau}\right)\mathcal{E}(s)$$ Laplace transform

$$\mathrm{H}(s) = \frac{\mathcal{A}_v(s)}{\mathcal{E}(s)}$$ definition

$$\mathrm{H}(s) = (1-\gamma)\,\frac{s+1/\tau}{s+\gamma/\tau}$$ result

boring algebra relates α’ to α

$$v = Au$$
$$A = 1 - \gamma(u-1)$$
$$v = [1-\gamma(u-1)]\,u$$
$$1+\alpha_v = [1-\gamma\alpha_u]\,[1+\alpha_u]$$
$$1+\alpha_v = 1+\alpha_u - \gamma\alpha_u - \gamma\alpha_u^2$$ linearization for low noise
$$\alpha_v = (1-\gamma)\alpha_u$$
$$\alpha_u = \frac{\alpha_v}{1-\gamma}$$

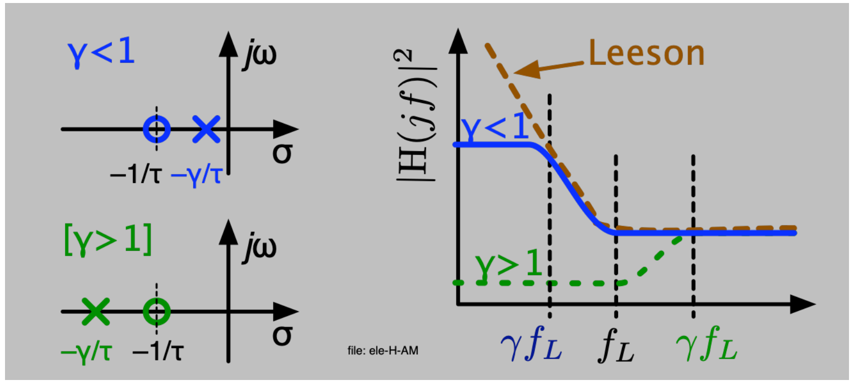

Parametric noise & AM-PM noise coupling

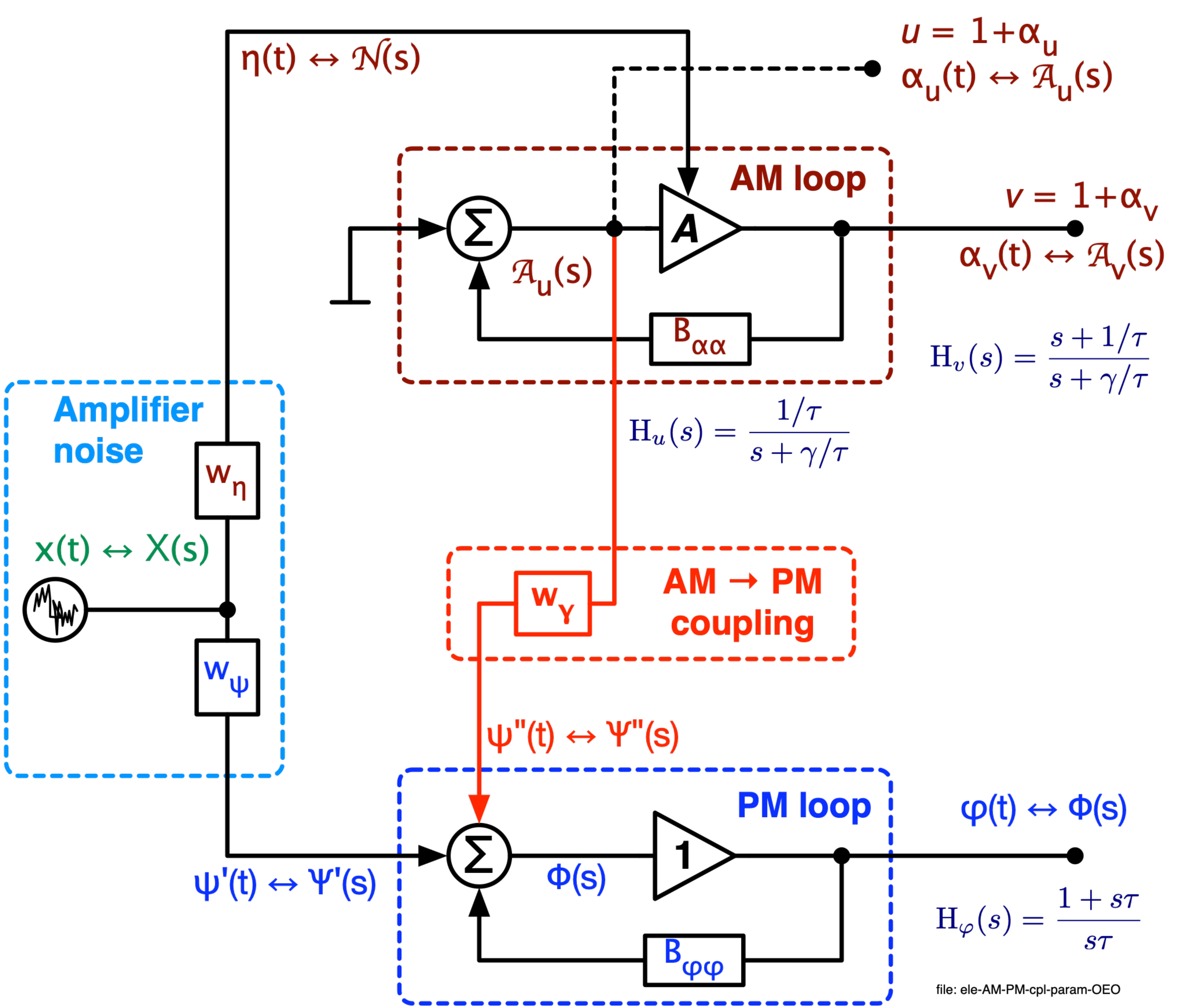

E. Rubiola & R. Brendel, arXiv:1004.5539v1 [physics.ins-det]

Effect of AM-PM noise coupling

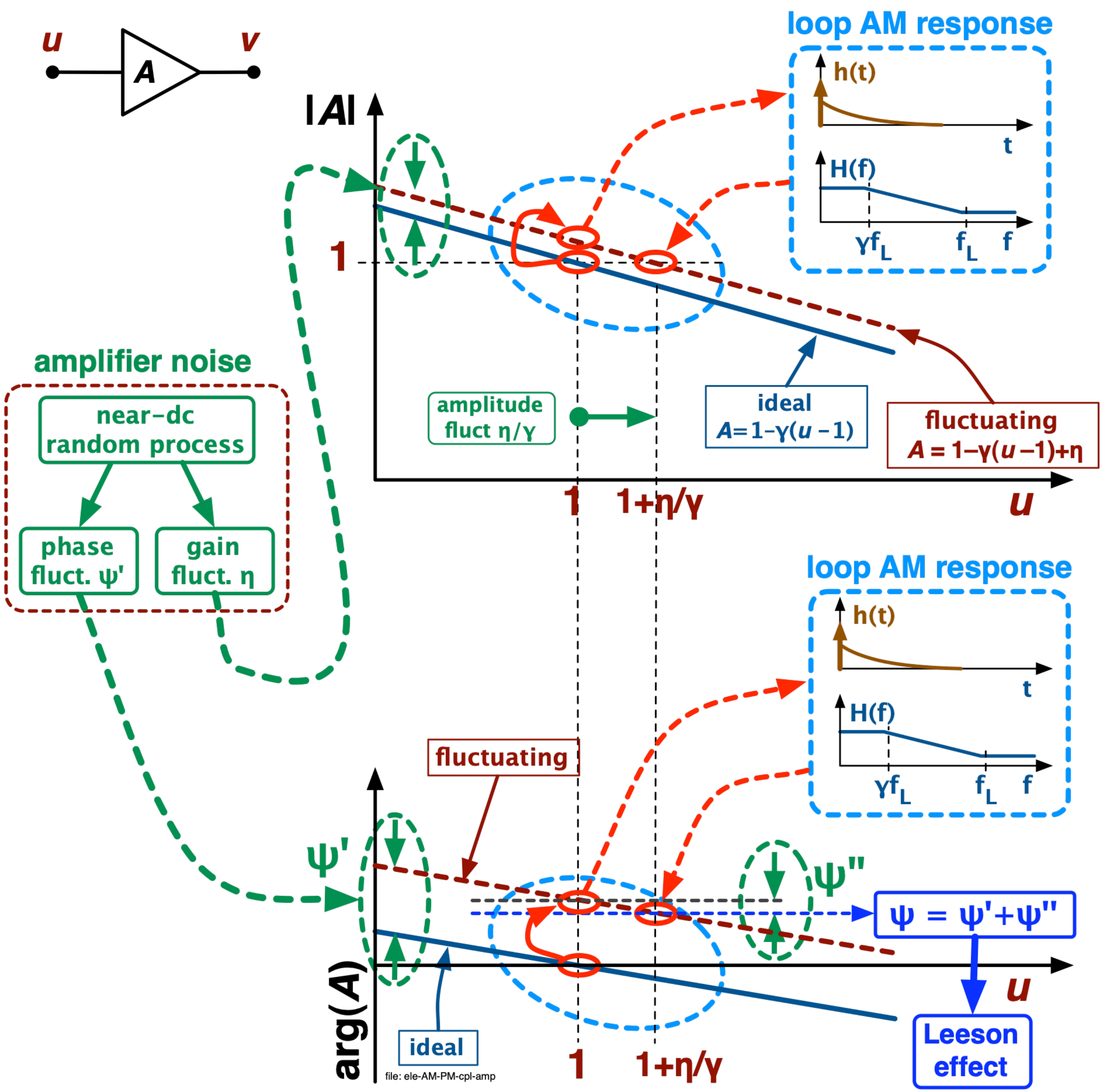

E. Rubiola & R. Brendel, arXiv:1004.5539v1 [physics.ins-det]

Noise transfer function, and spectra

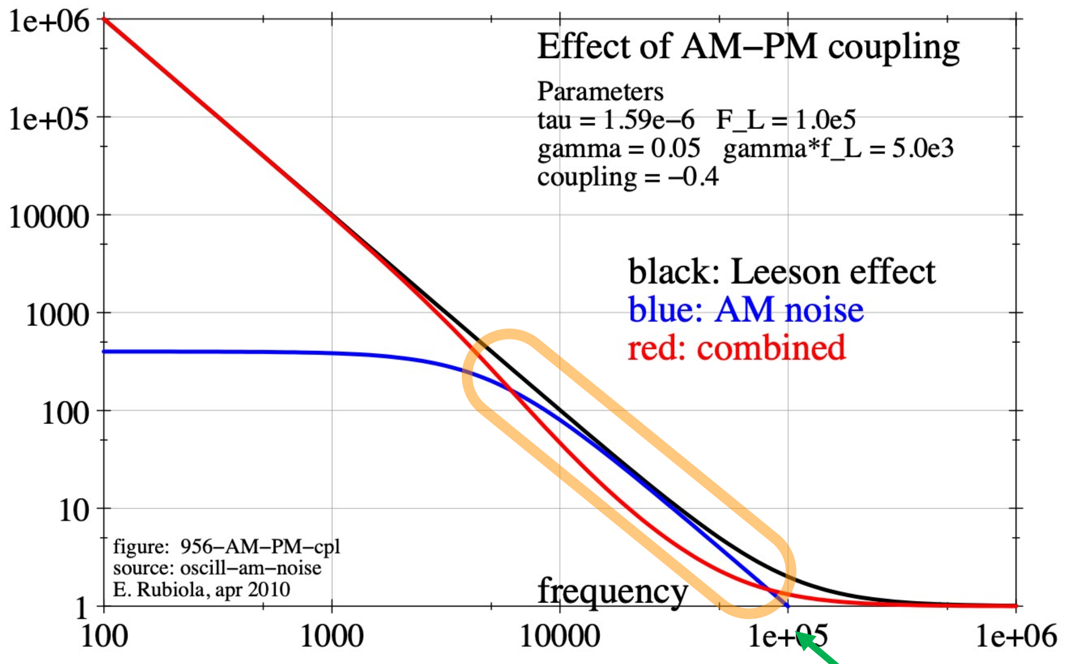

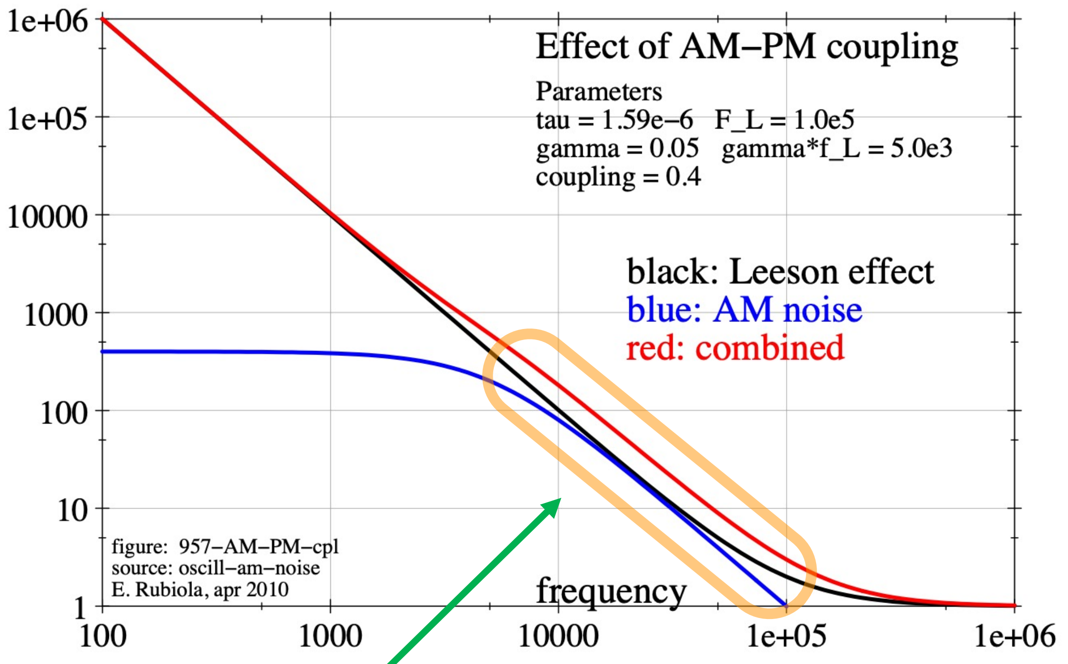

AM-PM coupling shows up here

Notice that the AM-PM coupling can increase or decrease the PM noise

In a real oscillator, flicker noise shows up below some 10 kHz
In the flicker region, all plots are multiplied by $1/f$

Oscillator Hacking

Still not able to hack the Rohde oscillator

Amplifier white and flicker noise

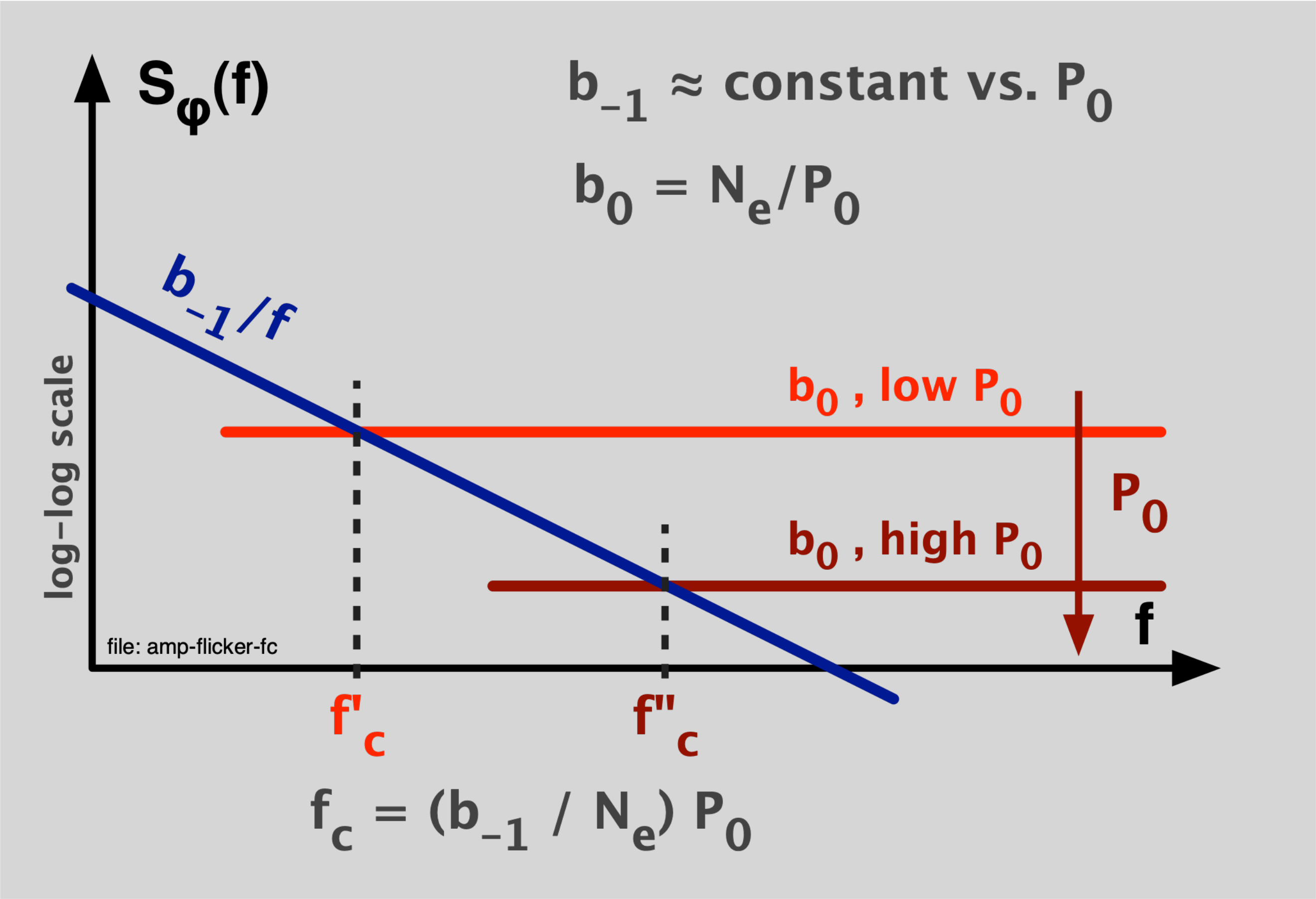

The corner frequency f_c, sometimes specified in data sheets is a misleading parameter because it depends on P_0

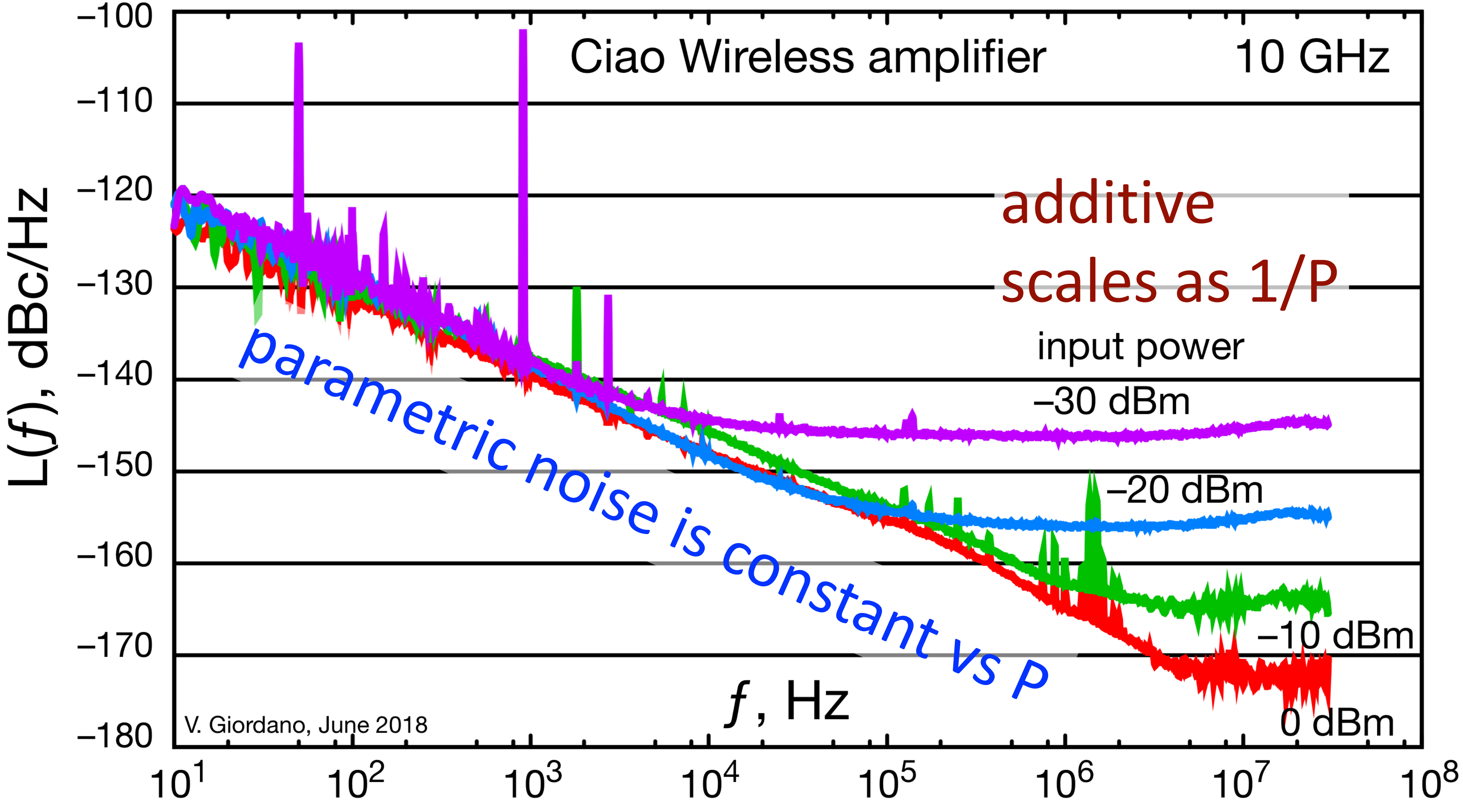

Parametric noise in amplifiers tends to be independent of ν_0

Oscillator noise – Real sustaining amplifier

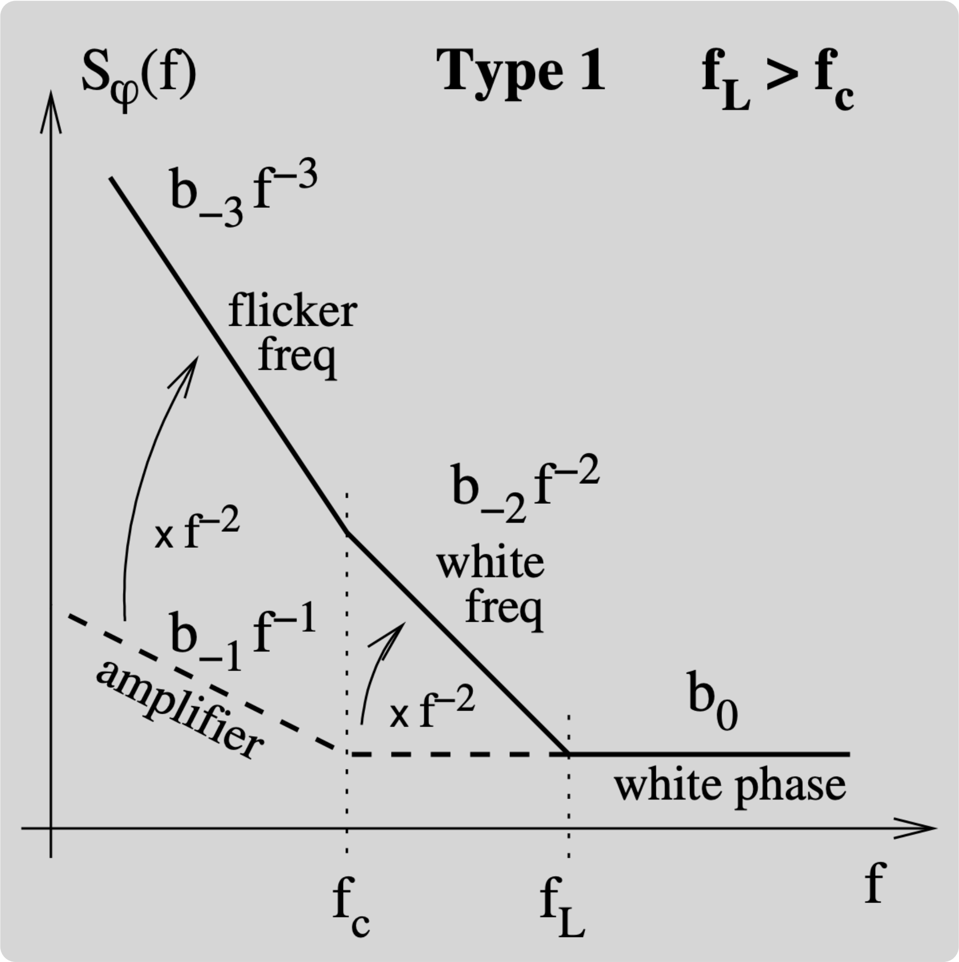

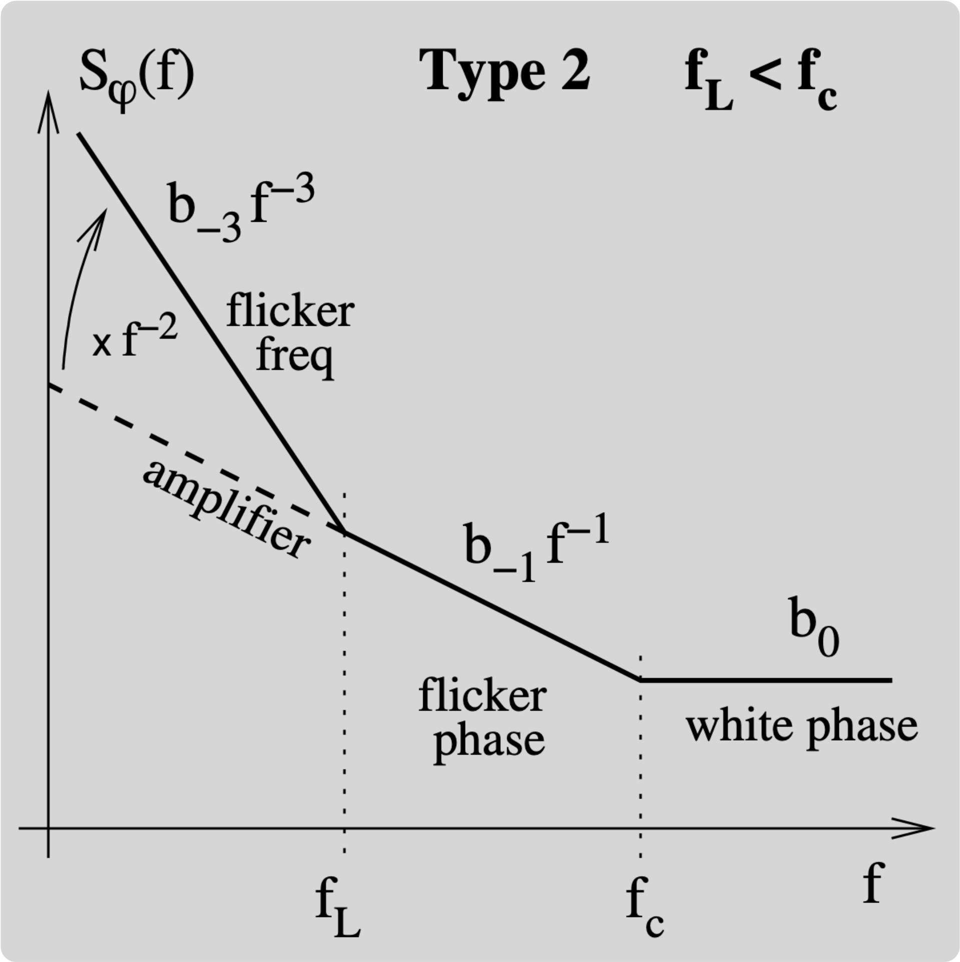

The sustaining-amplifier noise is $S_{\varphi}(f) = \mathrm{b}_0 + \mathrm{b}_{-1}/f$ (white and flicker)

The effect of the output buffer

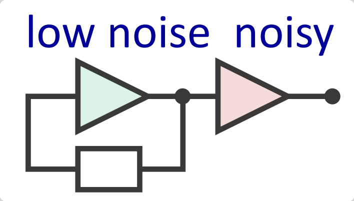

Cascading two amplifiers,
flicker noise adds as

$$S_{\varphi(f)} = [S_\varphi(f)]_1 + [S_\varphi(f)]_2$$

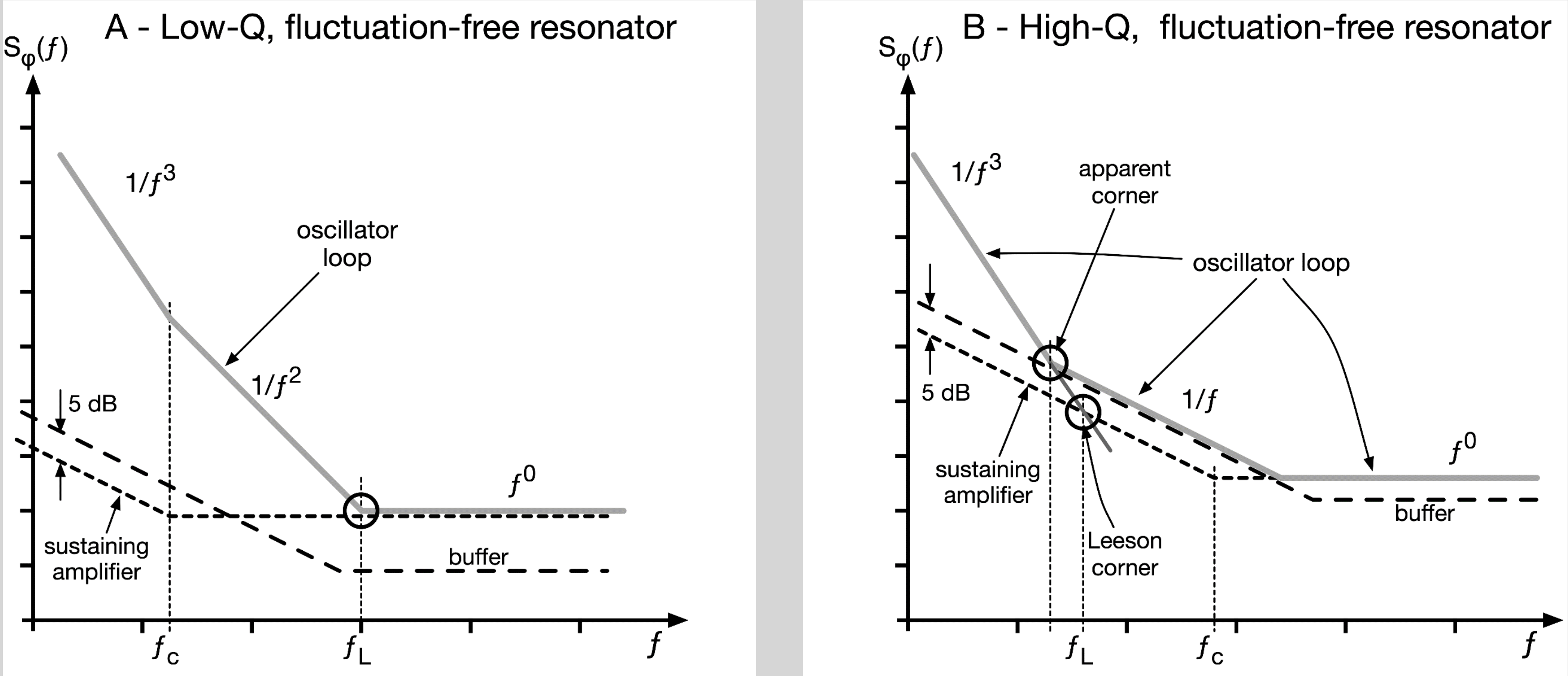

Figure from U. L. Rohde, E. Rubiola, J. C. Whithaker, *Microwave and Wireless Synthesizers*, ISBN 978-1-119-66600-4, ©J.Wiley 2021 (adapted)

The fluctuation of the resonator

- The oscillator tracks the resonator natural frequency, hence its fluctuations
- Phase-to frequency conversion $f^0 \rightarrow 1/f^2$, $1/f \rightarrow 1/f^3$, etc.
- The resonator bandwidth does not apply to the natural-frequency fluctuation. (Tip: an oscillator can be frequency modulated at a rate $\gg f_L$)

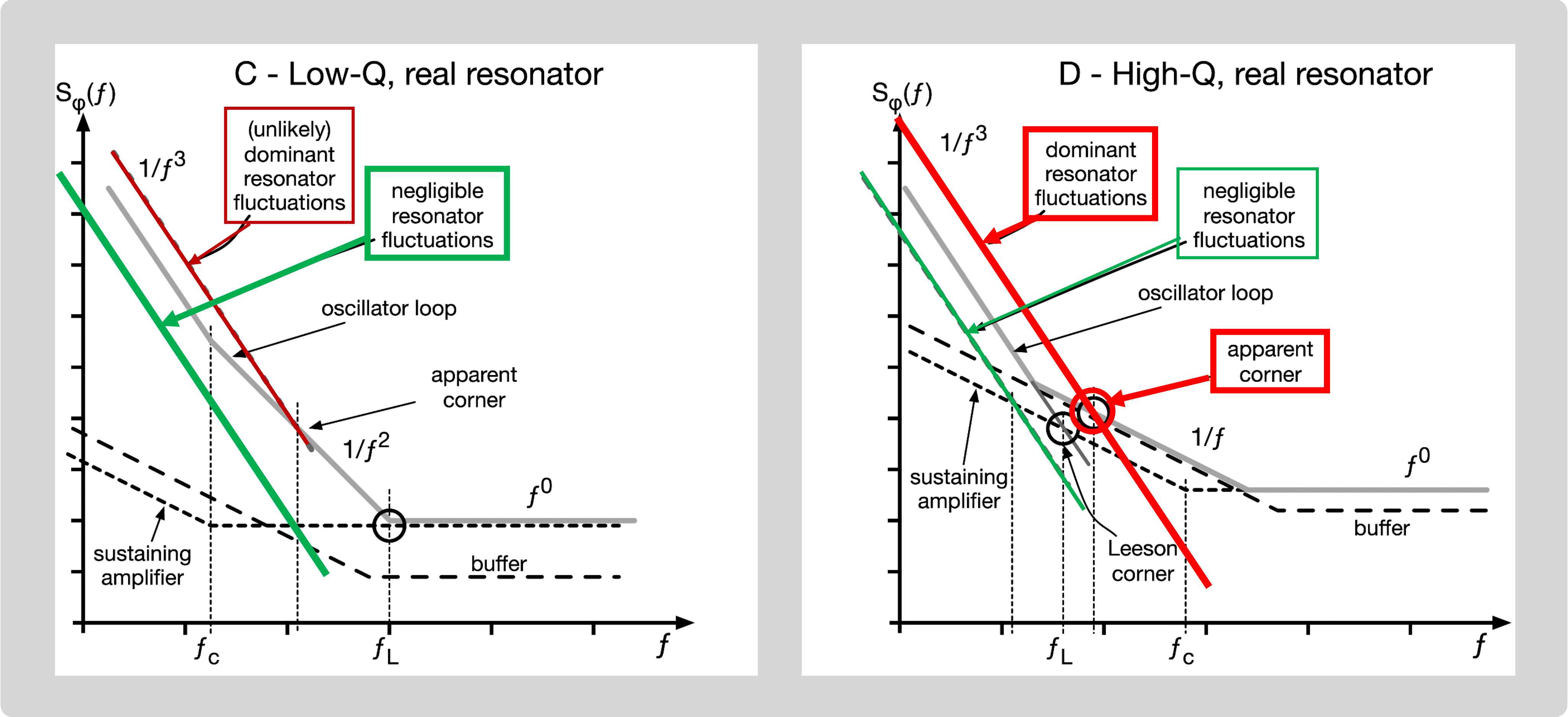

Figure from U. L. Rohde, E. Rubiola, J. C. Whithaker, *Microwave and Wireless Synthesizers*, ISBN 978-1-119-66600-4, ©J.Wiley 2021 (adapted)

Analysis of Commercial Oscillators

The purpose of this section is to help to understand the oscillator inside from the phase noise spectra, plus some technical information. I have chosen some commercial oscillators as an example.

The conclusions about each oscillator represent only my understanding, based on experience and on the data sheets published on the manufacturer web site.

You should be aware that this process of interpretation is not free from errors. My conclusions were not submitted to manufacturers before writing, for their comments could not be included.

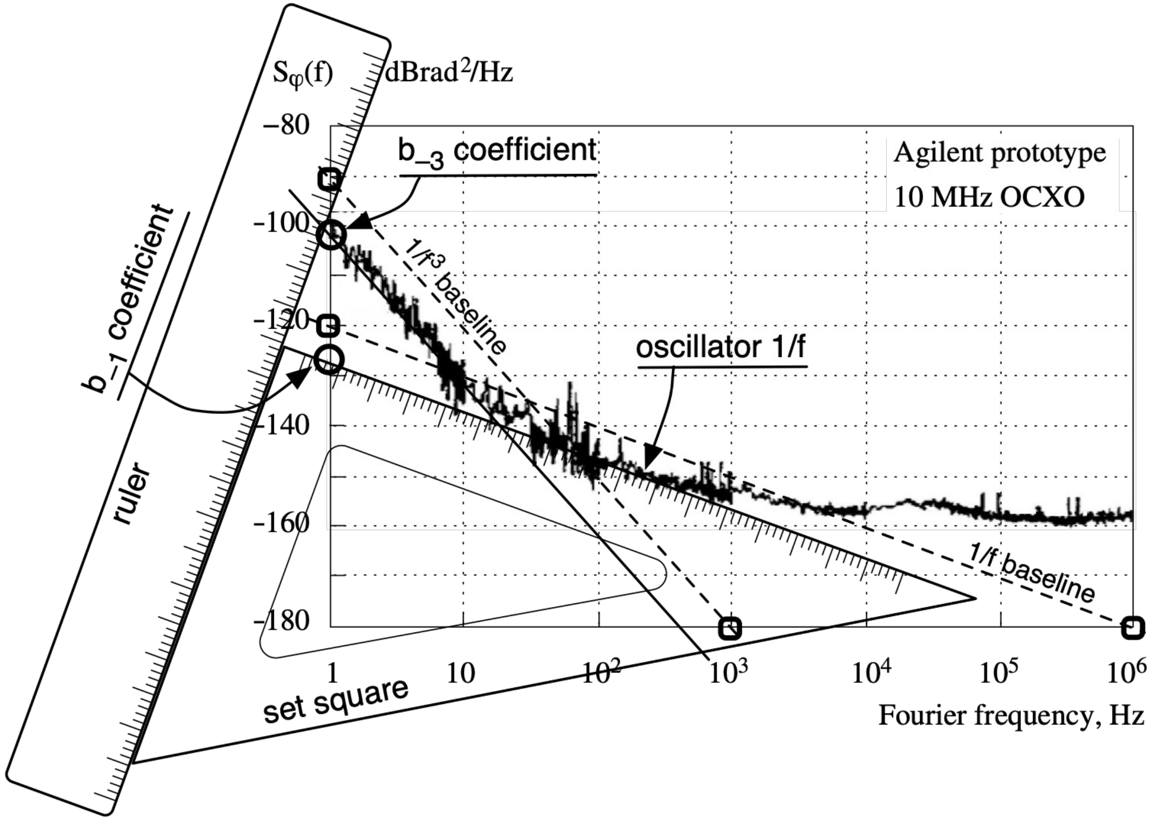

Example – DRO100, Synergy Microwave Corp.

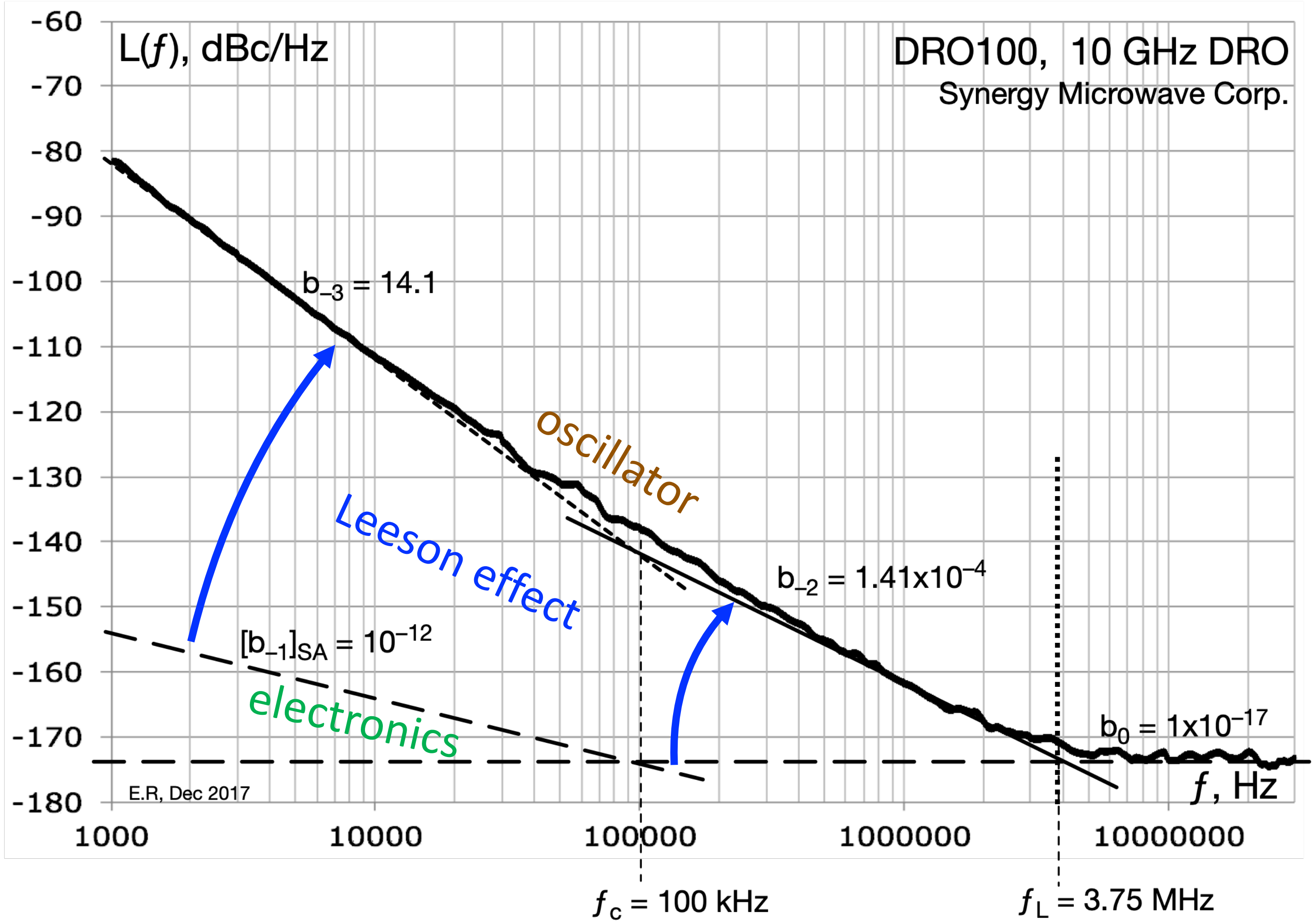

Figure from U. L. Rohde, E. Rubiola, J. C. Whithaker, *Microwave and Wireless Synthesizers*, ISBN 978-1-119-66600-4, ©J.Wiley 2021 (adapted)

1. White PM: $b_0 = 10^{-17}$
- Use $b_0 = FkT/P_0$
- Guess $F = 1.25$ (1 dB)
- Find $P_0 = 520$ µW

2. White FM: $b_{-2} = 1.41\times10^{-4}$
- From $b_{-2}/f^2 = b_0$ find $f_L = 3.75$ MHz
- Use $f_L = \nu_0/2Q$
- Find $Q = 1330$

3. Flicker PM: $b_{-3} = 14.1$
- From $b_{-3}/f^3 = b_{-2}/f^2$ find f_c =100 kHz
- Use $S_\varphi/S_\psi = (f_L/f)^2$ at $f \ll f_L$
- Find $b_{-1} = 10^{-12}$ sustaining amplifier $1/f$

Example – Rakon HSO 14, 5 MHz OCXO

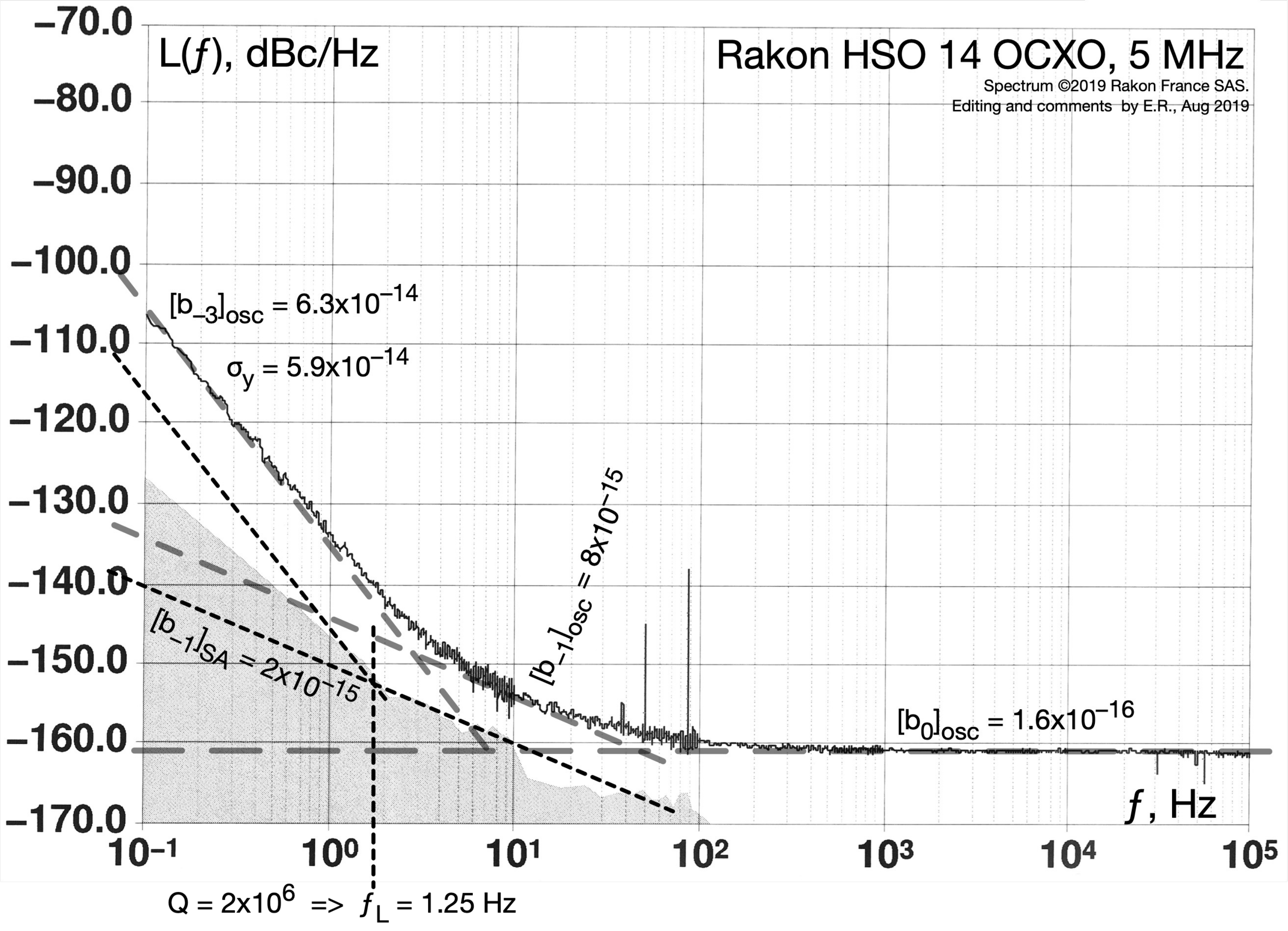

Figure from U. L. Rohde, E. Rubiola, J. C. Whithaker, *Microwave and Wireless Synthesizers*, ISBN 978-1-119-66600-4, ©J.Wiley 2021 (adapted)

1. White PM: $b_0 = 1.6\times10^{-16}$
- Use $b_0 = FkT/P_0$
- Guess $F = 1.25$ (1 dB)
- Find $P_0 = 33\mu W$

2. Flicker PM: $b_{-1} = 8\times10^{-15}$
- Guess $[b_{-1}]_{SA} \approx (1/4)[b_{-1}]_{osc}$
- Find $[b_{-1}]_{SA} = 2\times10^{-15}$ $1/f$ of the sustaining amplifier

3. Flicker FM: $b_{-3} = 6.3\times10^{-14}$
- Guess $Q = 2\times10^6$, premium 5 MHz xtal
- Use $S_\varphi/S_\psi = (f_L/f)^2$ at $f \ll f_L$
- The expected Leeson effect is $[b_{-3}]_{LE} = 2.5\times10^{-15} \ll [b_{-3}]_{osc}$
- Use $S_y(f) = (f^2/\nu_0^2)S_\varphi(f)$
- Find $h_{-1} = 2.52\times10^{-27}$
- Flicker floor: use $\sigma_y^2 = 2\ln(2)\, h_{-1}$
- Find $\sigma_y^2 = 3.5\times10^{-27}$ AVAR $\sigma_y = 5.9\times10^{-14}$ ADEV

Miteq D210B, 10 GHz DRO

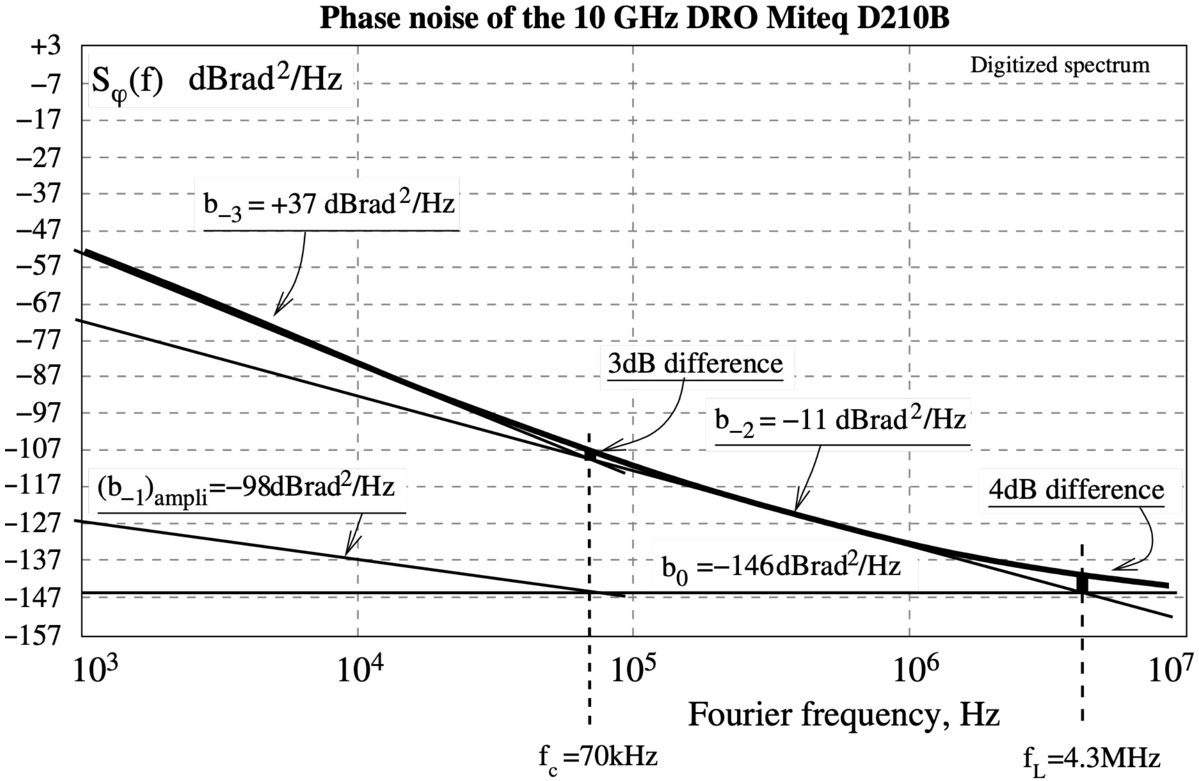

- $kT_0 = 4{\times}10^{-21}$ W/Hz (–174 dBm/Hz)
- floor –146 dBrad2/Hz, guess F = 1.25 (1 dB) => $P_0 = 2$ µW (–27 dBm)
- $f_L = 4.3$ MHz, $f_L = \nu_0/2Q$ => $Q = 1160$
- $f_c = 70$ kHz, $b_{-1}/f = b_0$ =>$b_{-1} = 1.8{\times}10^{-10}$ (–98 dBrad2/Hz) [sust.ampli]
- $h_0 = 7.9{\times}10^{-22}$ and $h_{-1} = 5{\times}10^{-17}$ => $\sigma_y = 2{\times}10^{-11}/\sqrt{\tau} + 8.3{\times}10^{-9}$

Reminder: from the table
$\sigma_y^2(\tau) = h_0/2\tau + 2\ln(2)\,h_{-1}$
$h_0 = b_{-2}/\nu_0^2$
$h_{-1} = b_{-3}/\nu_0^2$

$$b_0 = \frac{FkT_0}{P_0}$$

Poseidon* Scientific Instruments – Shoebox 10 GHz sapphire whispering-gallery oscillator (1)

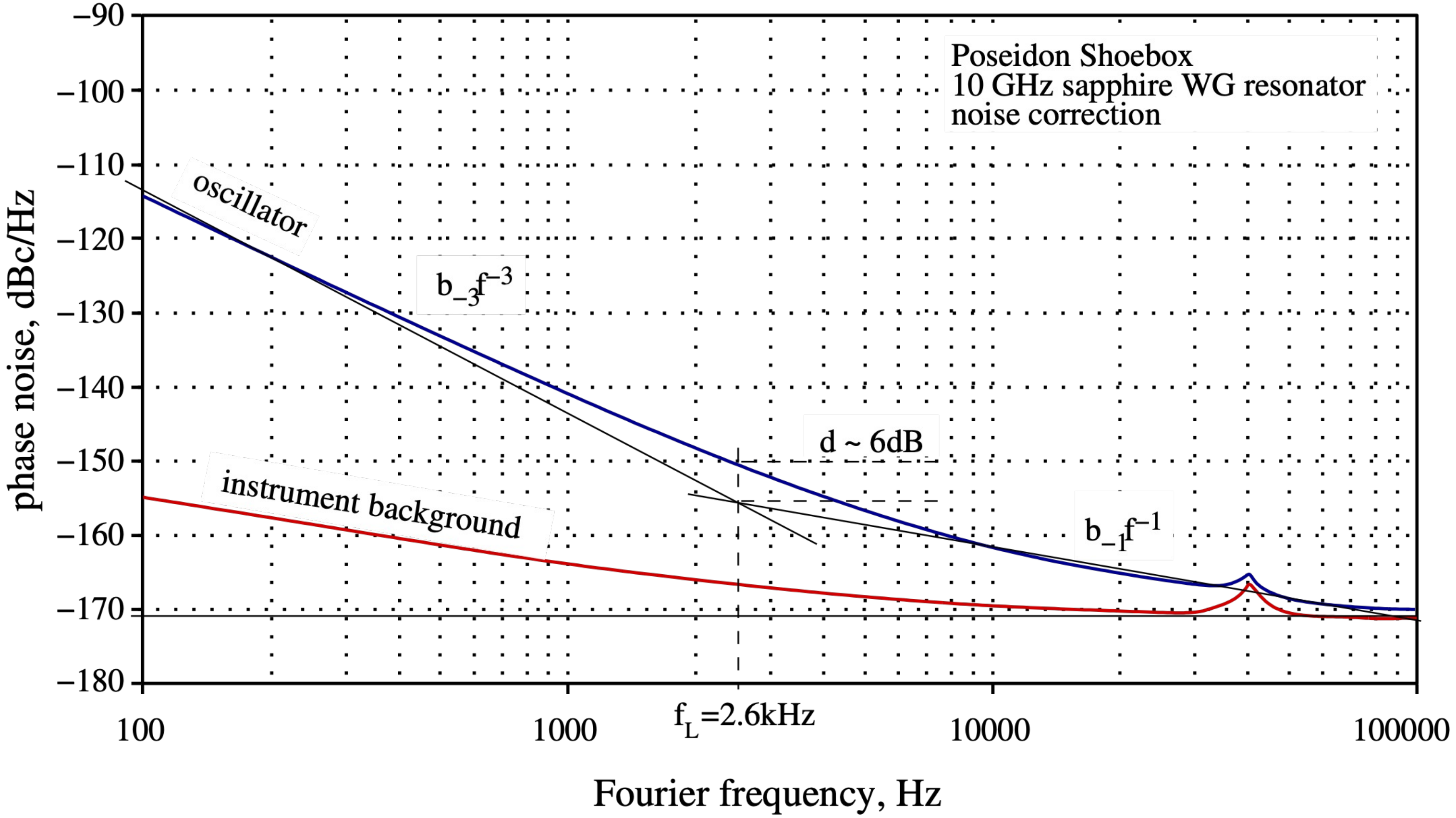

$f_L = \nu_0/2Q = 2.6$ kHz

=> $Q = 1.8\times10^6$

This incompatible with the resonator technology. Typical Q of a sapphire whispering gallery resonator:

2×10^5 @ 295K (room temp), 3×10^7 @ 77K (liquid N), 4×10^9 @ 4K (liquid He).

In addition, d ~ 6 dB does not fit the power-law.

The interpretation shown is wrong, and the Leeson frequency is somewhere else

The spectrum is © Poseidon. The figure is from E. Rubiola, Phase noise and frequency stability in oscillators, © Cambridge University Press

* PSI no longer exists as an independent Company. Now with Raytheon

Poseidon* Scientific Instruments – Shoebox 10 GHz sapphire whispering-gallery oscillator (2)

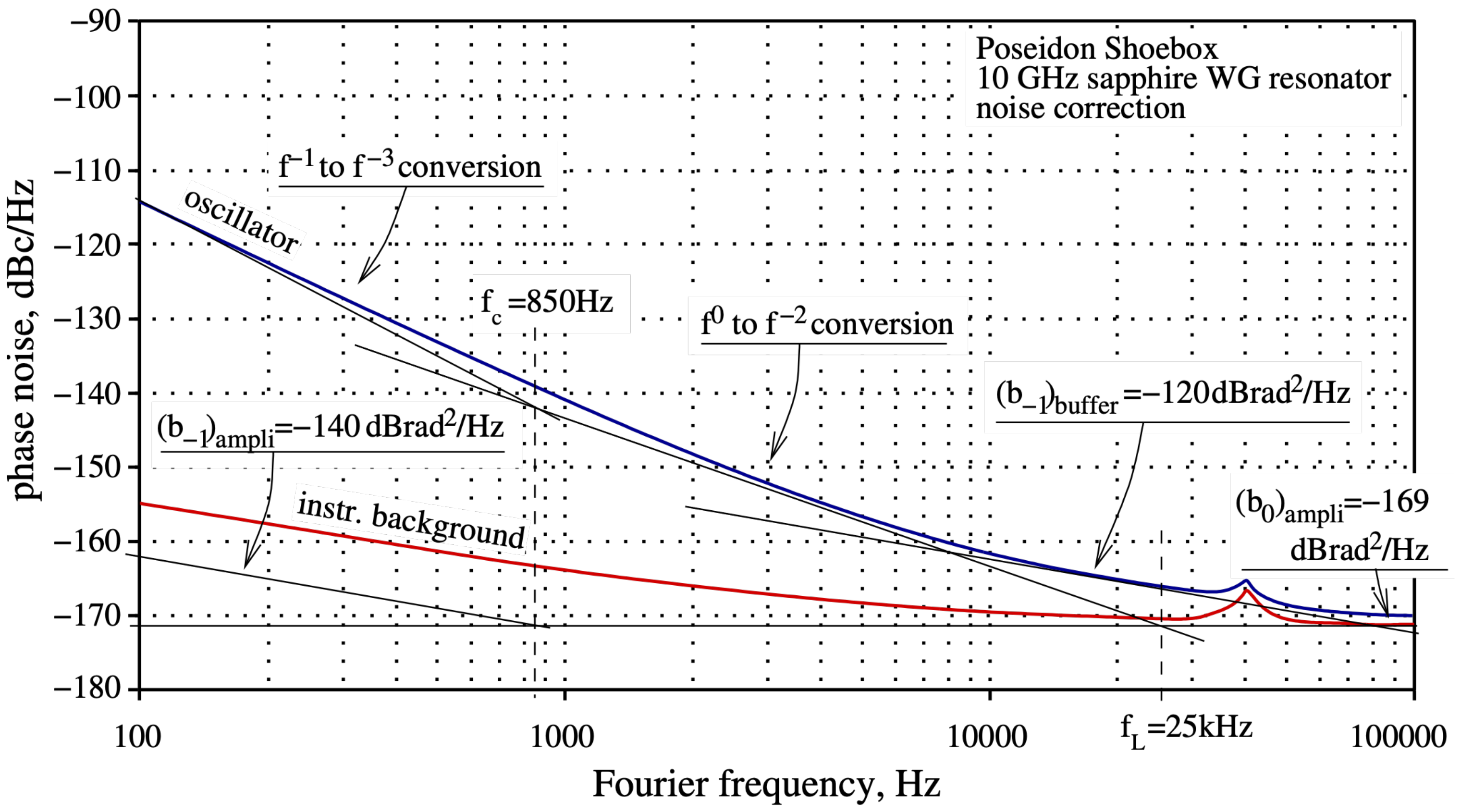

The spectrum is © Poseidon. The figure is from E. Rubiola, Phase noise and frequency stability in oscillators, © Cambridge University Press

The $1/f$ noise of the output buffer is higher than that of the sustaining amplifier (a complex amplifier with interferometric noise reduction / or a Pound control)

In this case both $1/f$ and $1/f^2$ are present

white noise −169 dBrad²/Hz, guess $F = 5$ dB (interferometer) => $P_0 = 0$ dBm
buffer flicker −120 dBrad2/Hz @ 1 Hz
=> good microwave amplifier

$f_L = \nu_0/2Q = 25$ kHz => $Q = 2\times10^5$ (quite reasonable)

$f_c = 850$ Hz => flicker of the interferometric amplifier −139 dBrad²/Hz @ 1 Hz

* PSI no longer exists as an independent Company. Now with Raytheon

Poseidon* Scientific Instruments 10 GHz dielectric resonator oscillator (DRO)

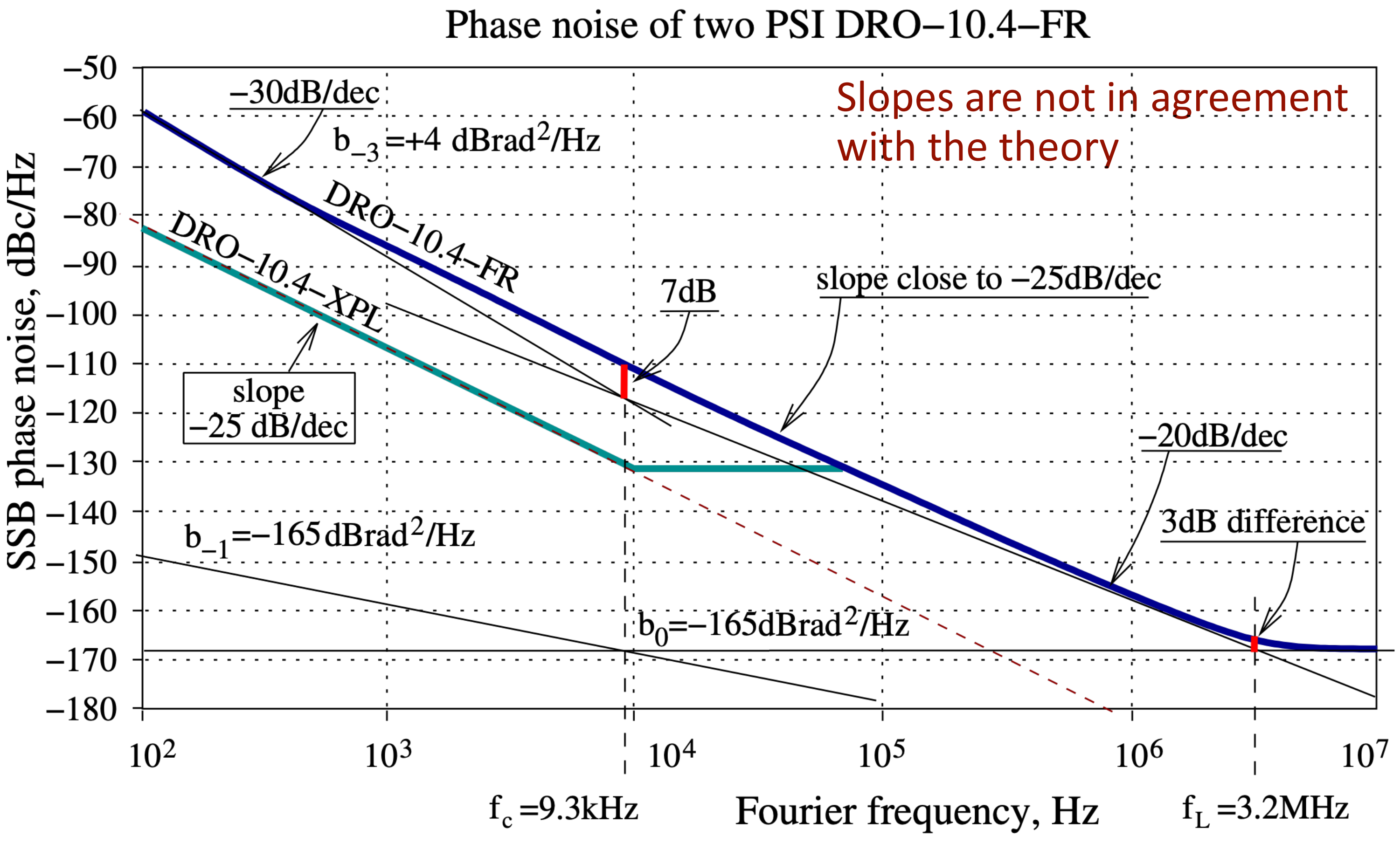

- floor –165 dBrad²/Hz, guess
  $F = 1.25$ (1 dB)
  => $P_0 = 160$ µW (–8 dBm)
- $f_L =$ 3.2 MHz,
  $f_L = \nu_0/2Q$ => $Q = 625$
- $f_c = 9.3$ kHz,
  $b_{-1}/f = b_0$
  => sustaining amplifier
  $b_{-1} = 2.9\times10^{-13}$ (–125 dBrad²/Hz)
  (too low value)

The spectrum is © Poseidon. The figure is from E. Rubiola, Phase noise and frequency stability in oscillators, © Cambridge University Press

* PSI no longer exists as an independent Company. Now with Raytheon

Example – Oscilloquartz 8600 (wrong)

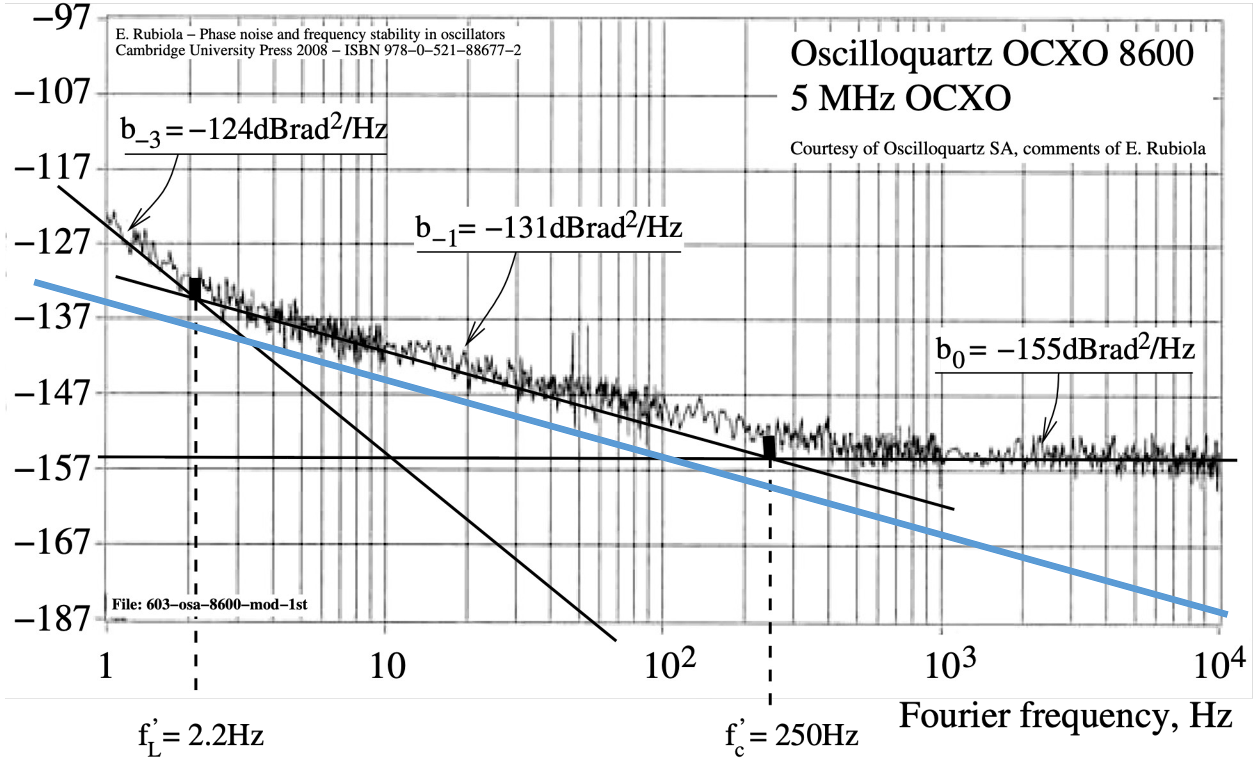

The spectrum is © Oscilloquartz. The figure is from E. Rubiola, Phase noise and frequency stability in oscillators, © Cambridge University Press

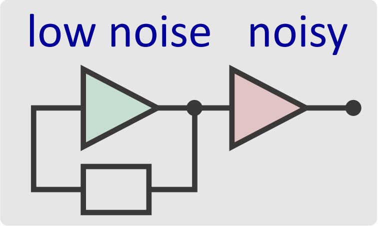

ANALYSIS

1 – floor $S_{\varphi 0}$ = –155 dBrad²/Hz, guess F = 1 dB → P_0 = –18 dBm

2 – ampli flicker S_φ = –132 dBrad²/Hz @ 1 Hz → good RF amplifier

3 – merit factor $Q = \nu_0/2f_L = 5{\cdot}10^6/5 = 10^6$ (seems too low)

4 – take away some flicker for the output buffer:

* flicker in the oscillator core is lower than –132 dBrad²/Hz @ 1 Hz
* f_L is higher than 2.5 Hz
* the resonator Q is lower than 10^6

This is inconsistent with the resonator technology (expect $Q > 10^6$).

The true Leeson frequency is lower than the frequency labeled as f_L

The $1/f^3$ noise is attributed to the fluctuation of the quartz resonant frequency

Example – Oscilloquartz 8600 (trusted)

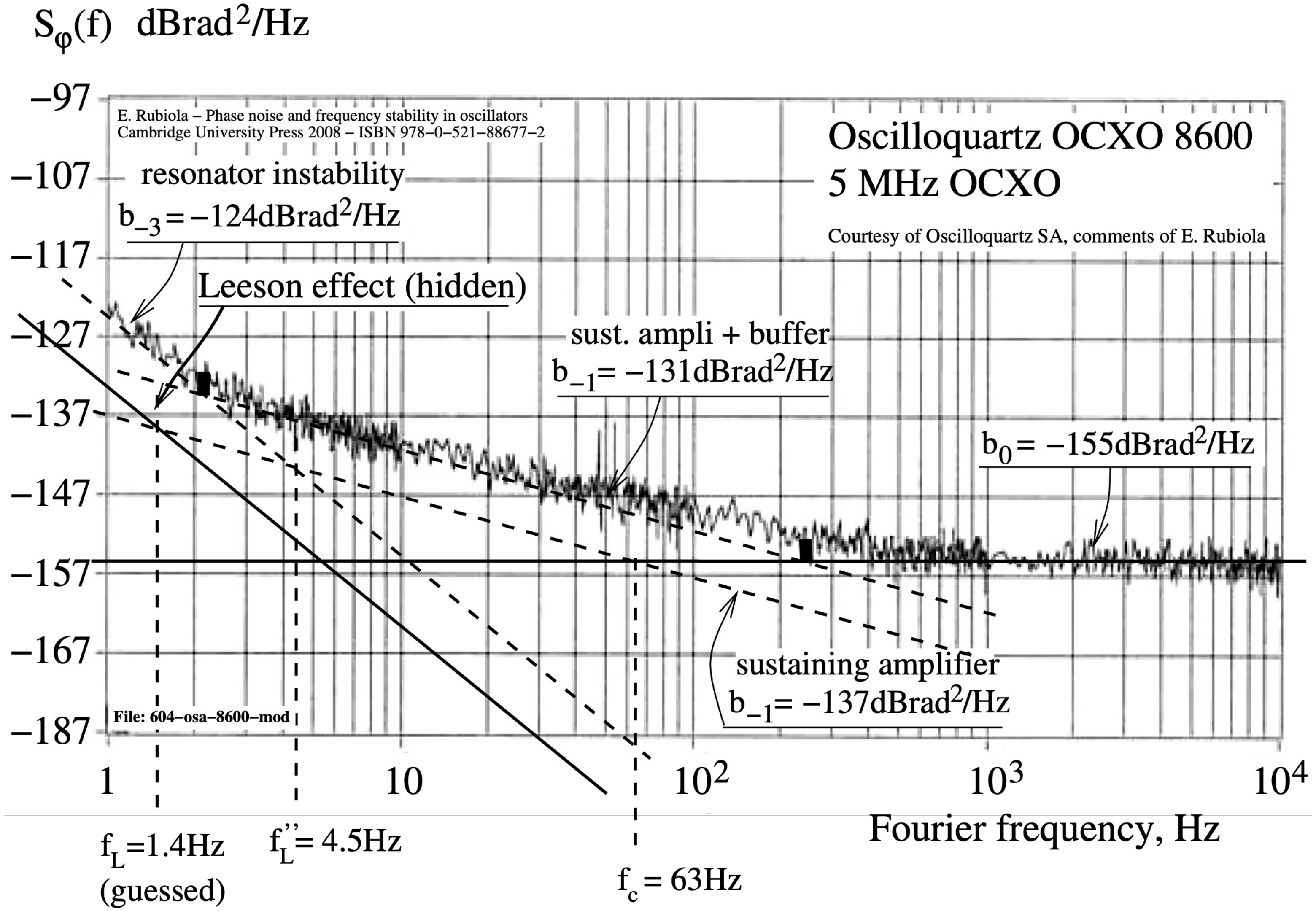

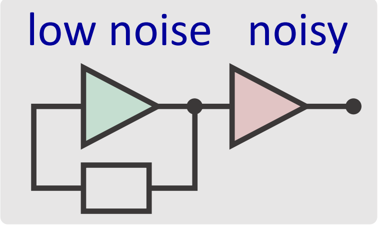

F = 1 dB & b0 => P_0 =– 18 dBm

$(b_{-3})_{osc}$ => $\sigma_y = 1.5\times10^{-13}$, $Q = 5.6\times10^5$ (too low)

Guess

$Q \overset{?}{=} 1.8\times10^6$

=> $\sigma_y = 4.6\times10^{-14}$ Leeson

(too low value!)

Whispering gallery oscillator, liquid-N_2 temperature

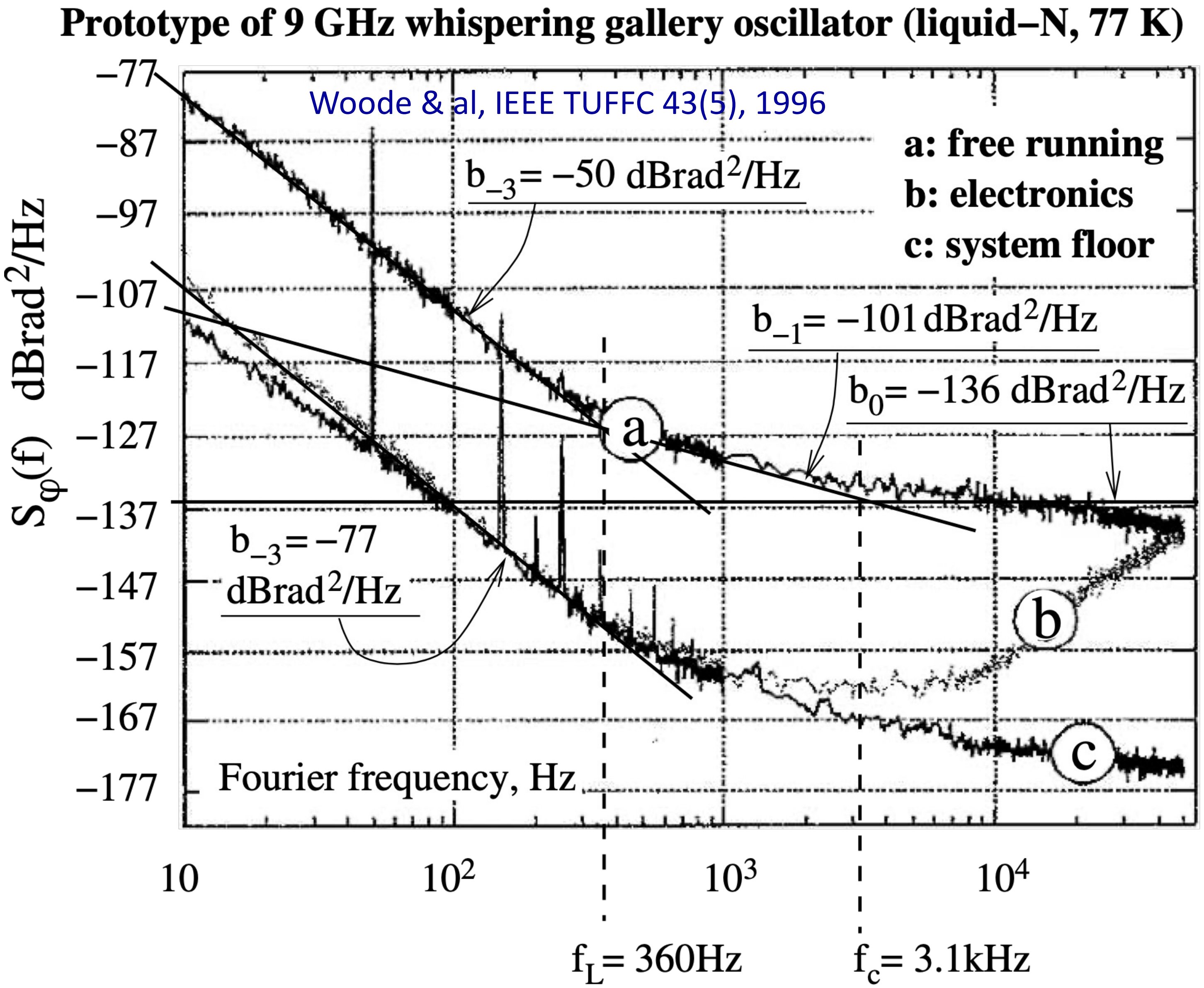

Example – Oscilloquartz 8607

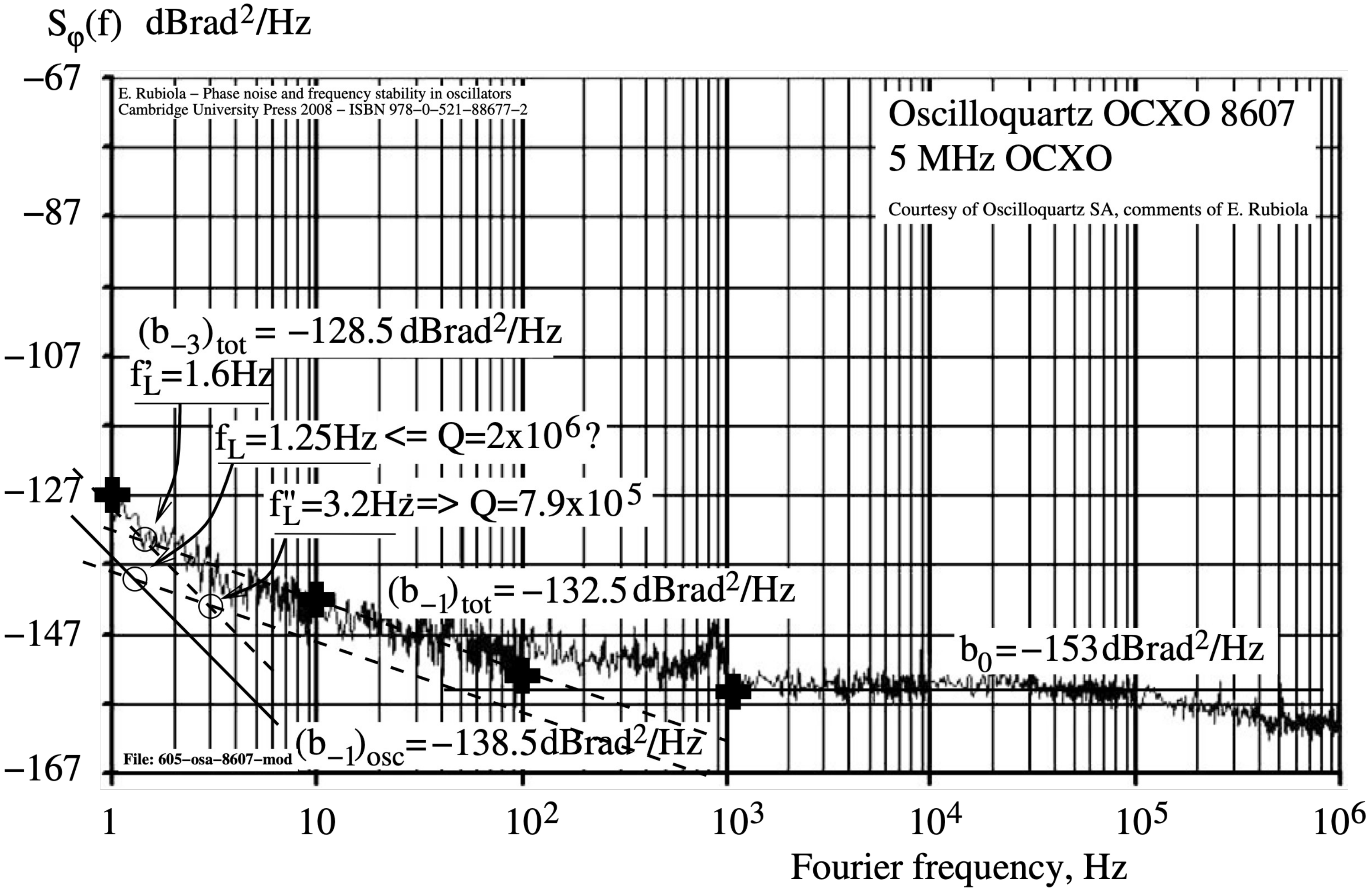

$F = 1$ dB

b_0 => $P_0 = -20$ dBm

$(b_{-3})_{osc}$ => $\sigma_y = 8.8\times10^{-14}$

$Q = 7.8\times10^5$ (too low)

Guess

$Q \overset{?}{=} 2\times106$

$\Rightarrow \sigma_y = 3.5\times10^{-14}$ Leeson

(too low value!)

The spectrum is © Oscilloquartz. The figure is from E. Rubiola, Phase noise and frequency stability in oscillators, © Cambridge University Press

Example – CMAC Pharao

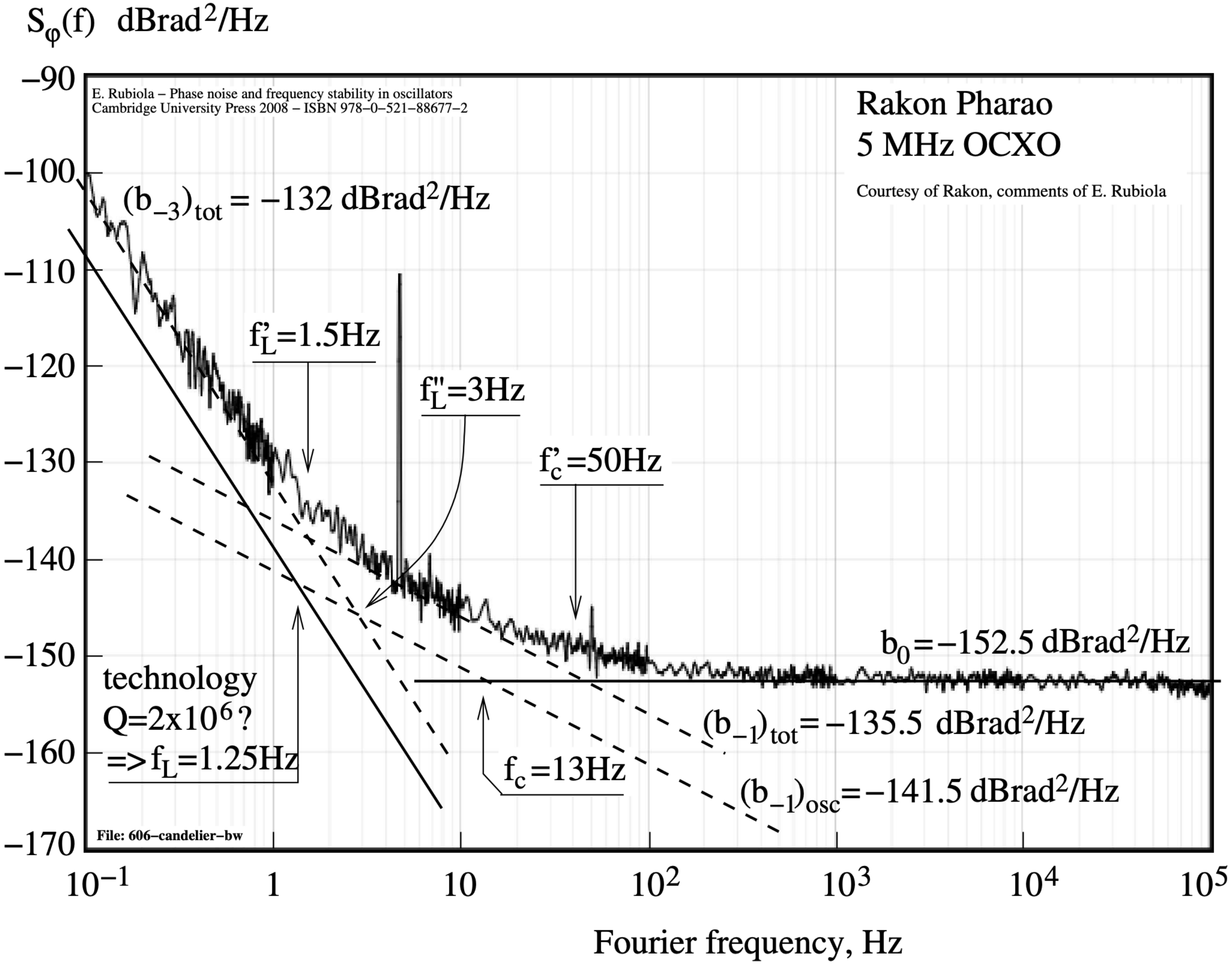

$F = 1$ dB

b_0 => $P_0 =- 20.5$ dBm

$(b_{-3})_{osc}$ => $\sigma_y = 5.9\times10^{-14}$

$Q = 8.4\times10^5$ (too low)

Guess

$Q \overset{?}{=} 2\times106$

$\Rightarrow \sigma_y = 2.5\times10^{-14}$ Leeson

(too low value!)

The spectrum is © Rakon The figure is from E. Rubiola, Phase noise and frequency stability in oscillators, © Cambridge University Press

Example – FEMTO-ST prototype

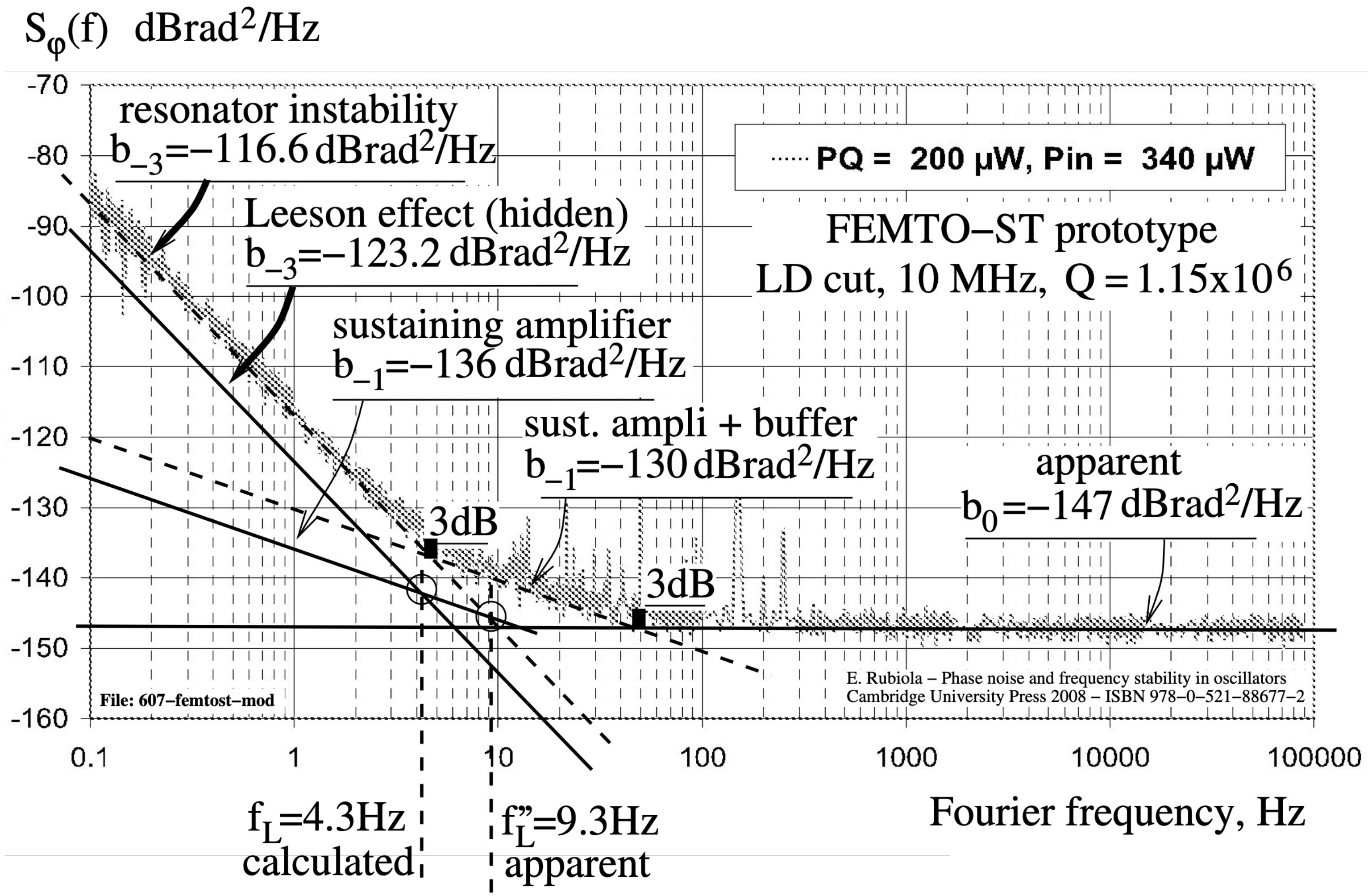

$F = 1$ dB

b_0 => $P_0 = -26$ dBm

$(b_{-3})_{osc}$ => $\sigma_y = 1.7\times10^{-13}$

$Q = 5.4\times10^5$ (too low)

Guess

$Q \stackrel{?}{=} 1.15\times106$

$\Rightarrow \sigma_y = 8.1\times10^{-14}$ Leeson

(too low value!)

Example – Agilent/Keysight 10811

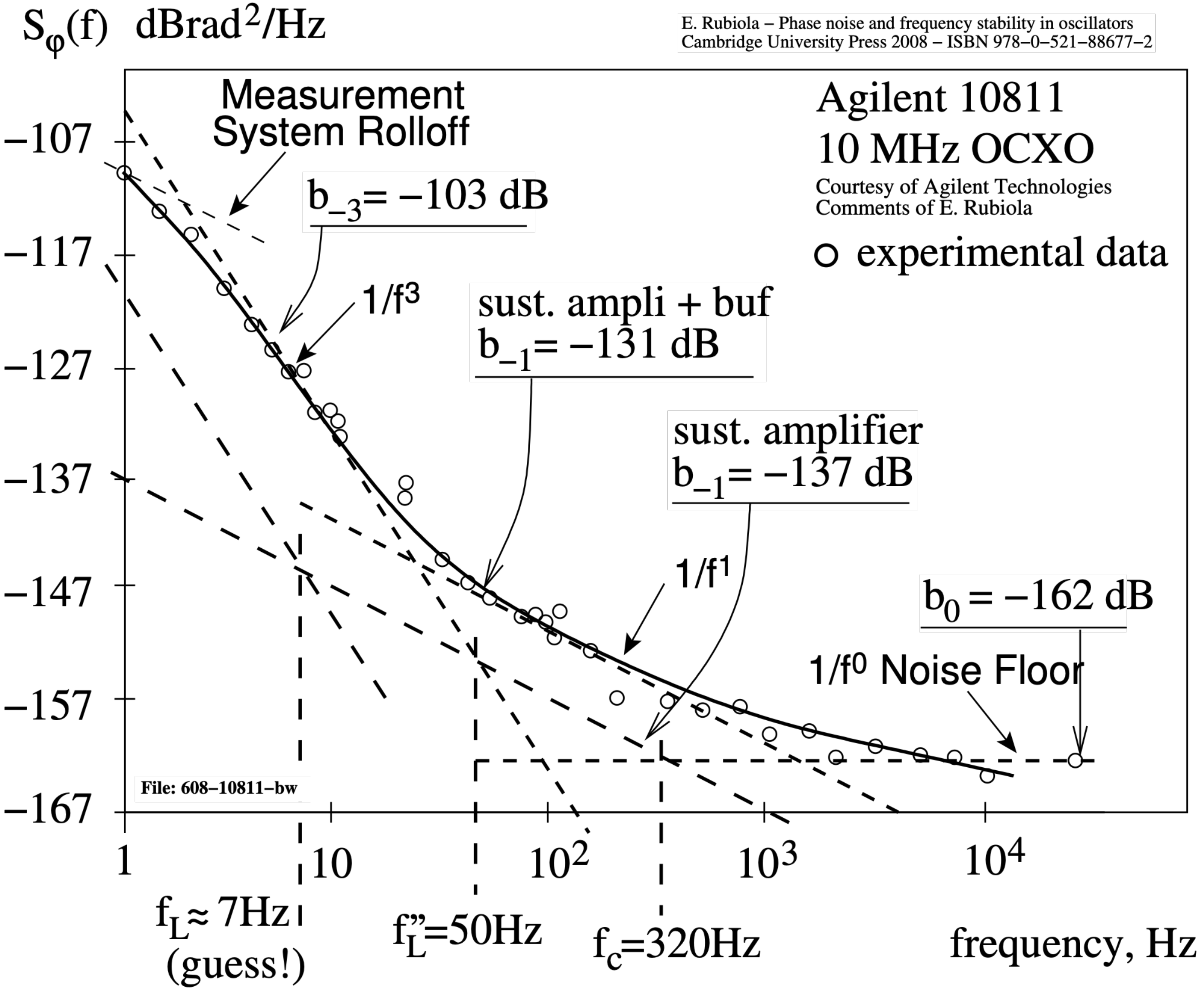

$F = 1$ dB

b_0 => $P_0 = -11$ dBm

$(b_{-3})_{osc}$ => $\sigma_y = 8.3\times10^{-13}$

$Q = 7\times10^5$ (too low)

Guess

$Q \stackrel{?}{=} 7\times105$

$\Rightarrow \sigma_y = 1.2\times10^{-13}$ Leeson

(too low value!)

Caveat – this oscillator may use the carrier extraction from the quartz. If so, our estimation of P_0 is wrong

Example – Agilent (Keysight) prototype

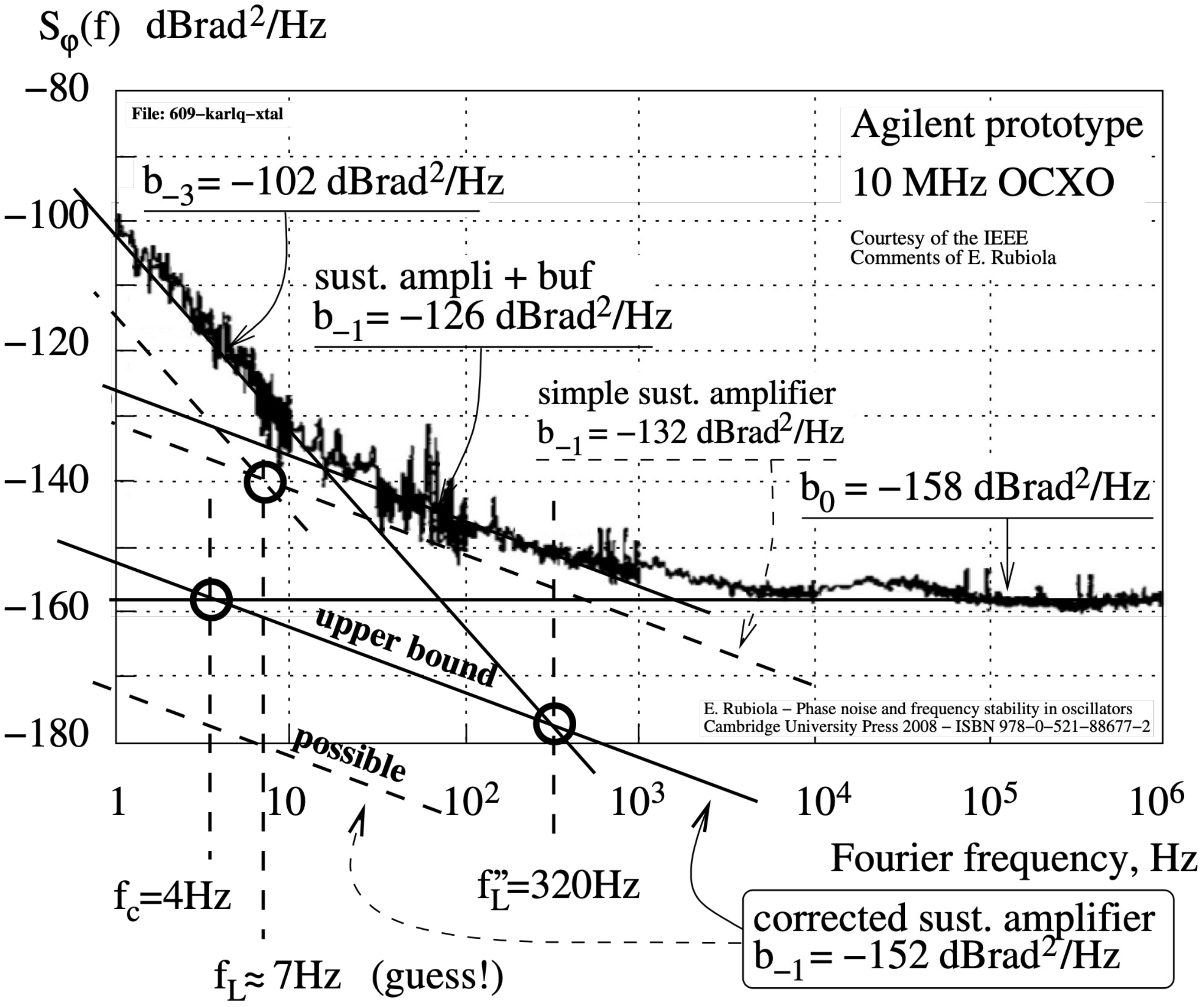

The spectrum is © IEEE. The figure is from E. Rubiola, Phase noise and frequency stability in oscillators, © Cambridge University Press

Interpretation of $S_\varphi(f)$ [1]

Only quartz-crystal oscillators

E. Rubiola – Phase noise and frequency stability in oscillators
Cambridge University Press 2008 – ISBN 978–0–521–88677–2

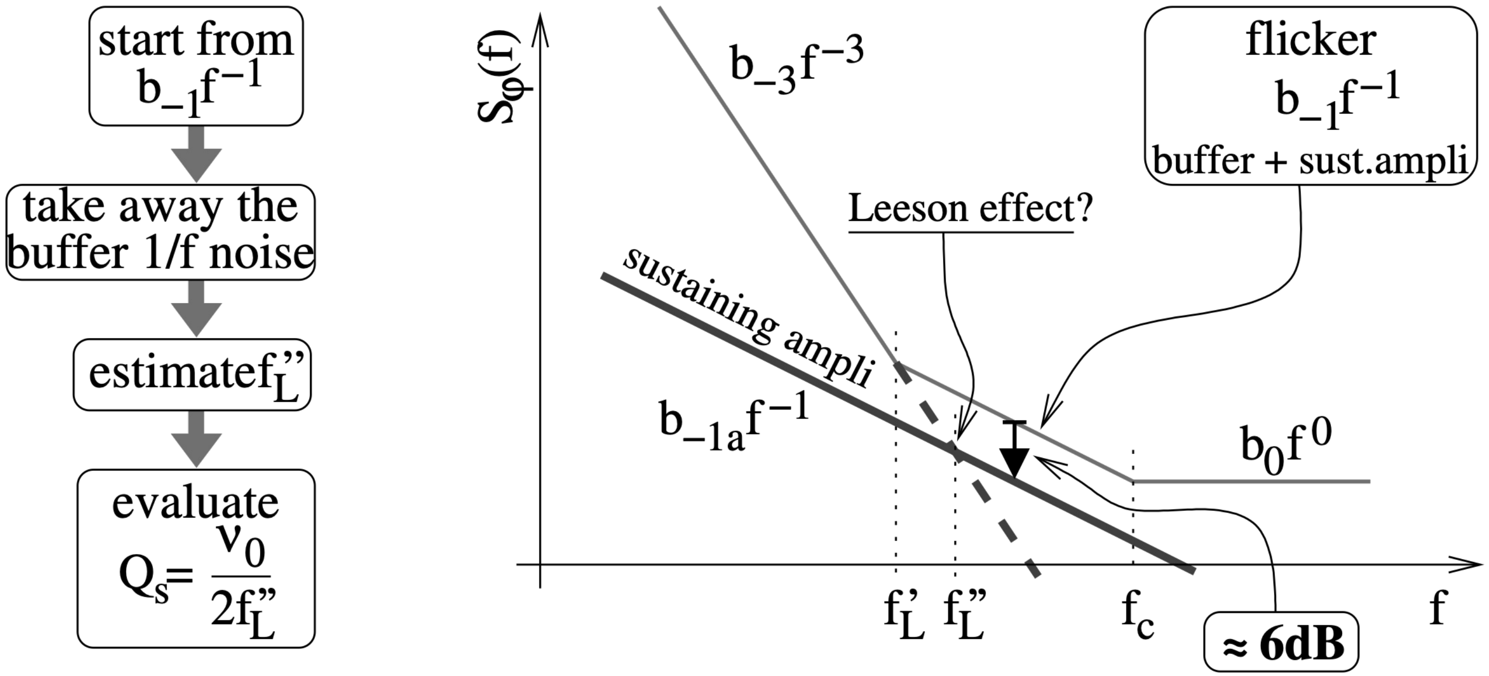

File: 602a–xtal–interpretation

Figures are from E. Rubiola, Phase noise and frequency stability in oscillators, © Cambridge University Press

2–3 buffer stages => the sustaining amplifier contributes ≲ 25% of the total 1/f noise

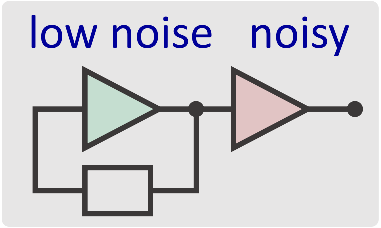

Sanity check:
– power P_0 at amplifier input
– Allan deviation σ_y (floor)

Interpretation of $S_\varphi(f)$ [2]

Only quartz-crystal oscillators

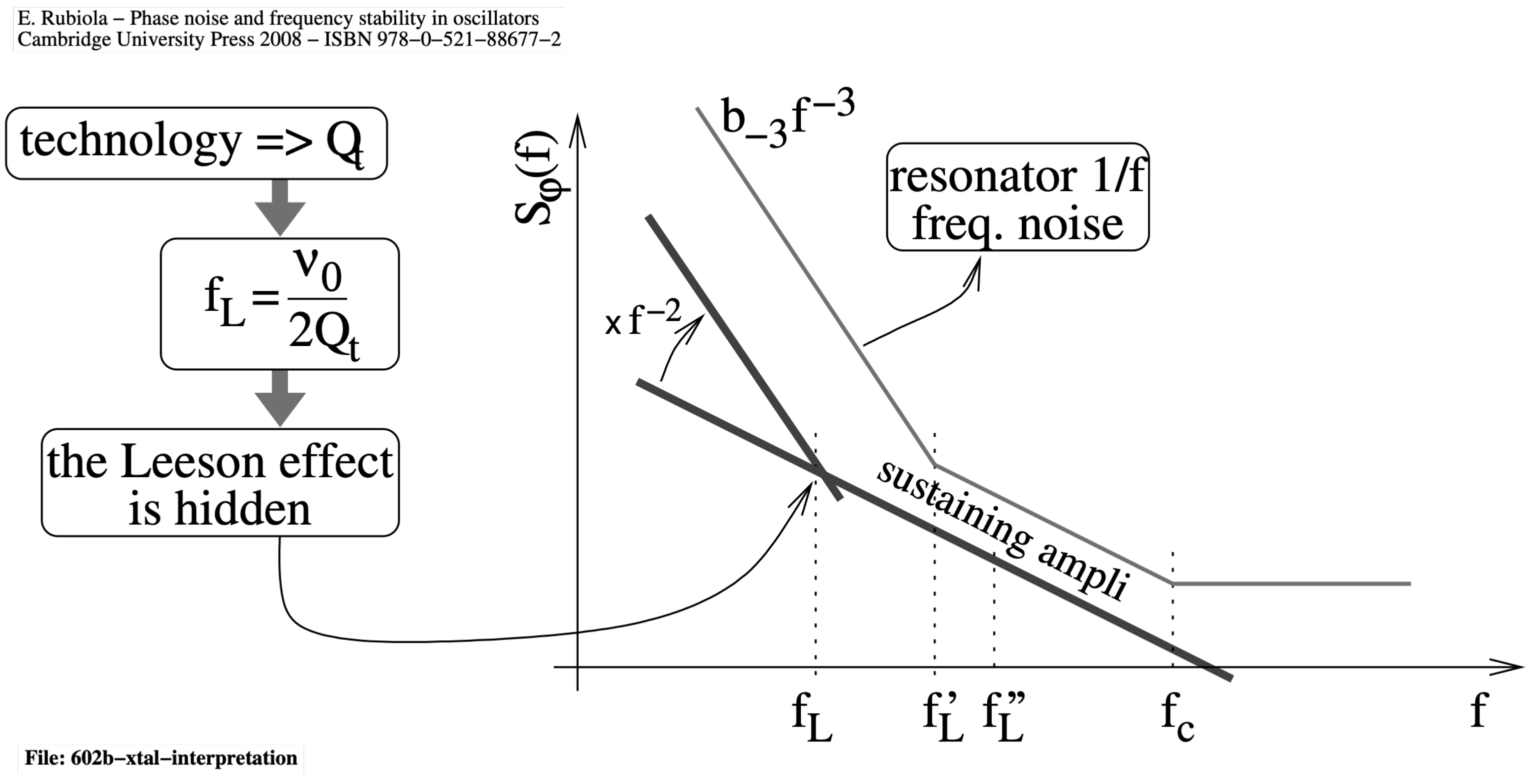

Technology suggests a quality factor Q_t

In all xtal oscillators we find $Q_t \gg Q_s$

Figures are from E. Rubiola, Phase noise and frequency stability in oscillators, © Cambridge University Press

Example – Wenzel 501-04623

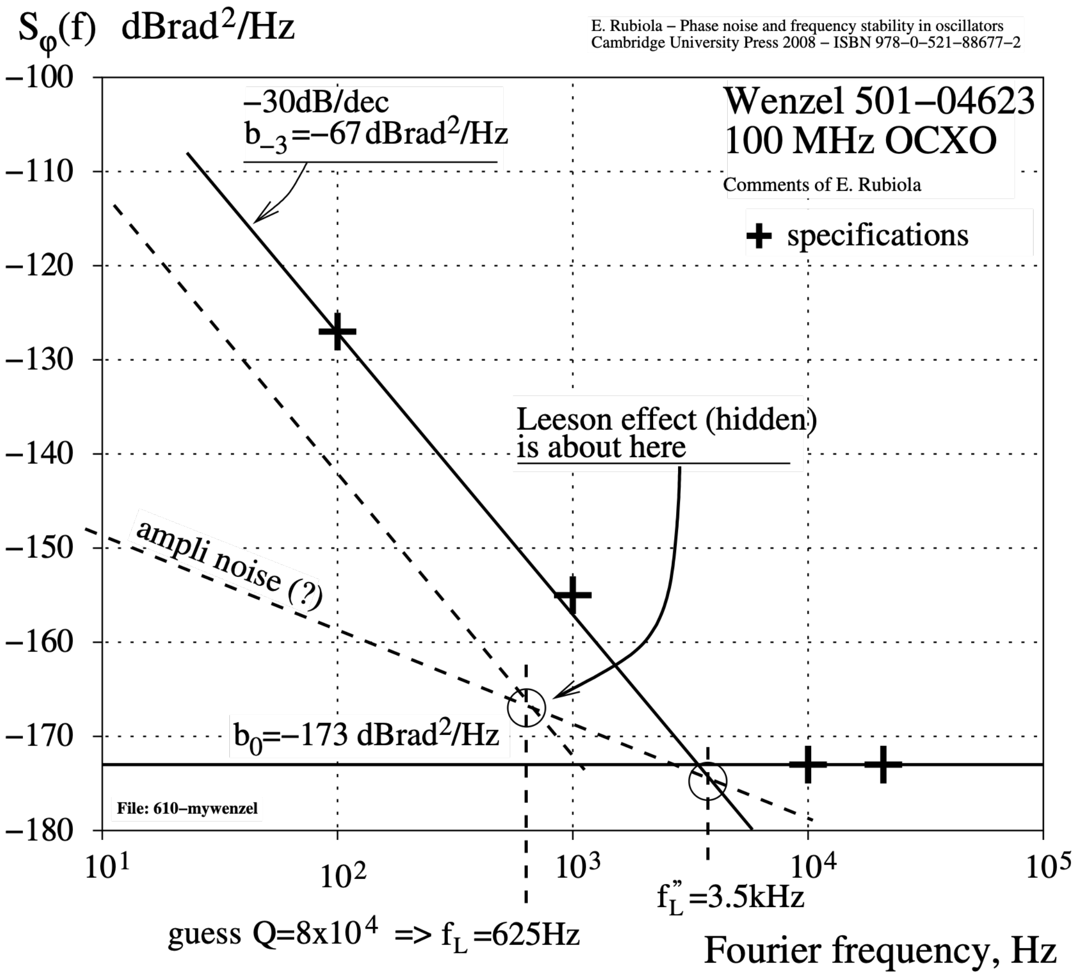

Figures are from E. Rubiola, Phase noise and frequency stability in oscillators, © Cambridge University Press

F=1dB b_0 => P_0=0 dBm

$(b_{-3})_{osc}$ => $\sigma_y = 5.3\times10^{-12}$ $Q = 1.4\times10^4$

$Q \overset{?}{=} 8\times10^4$ => $\sigma_y = 9.3\times10^{-13}$ (Leeson)

Estimating $(b_{-1})_{ampli}$ is difficult because there is no visible 1/f region

Data are from the manufacturer web site.
Interpretation and mistakes are of the author.

Quartz-oscillator summary

The Table is from E. Rubiola, Phase noise and frequency stability in oscillators, © Cambridge University Press

Oscillator	ν_0	$(b_{-3})_{\rm tot}$	$(b_{-1})_{\rm tot}$	$(b_{-1})_{\rm amp}$	f'_L	f''_L	Q_s	Q_t	f_L	$(b_{-3})_{\rm L}$	R	Note
Oscilloquartz 8600	5	−124.0	−131.0	−137.0	2.24	4.5	5.6×10^5	1.8×10^6	1.4	−134.1	10.1	(1)
Oscilloquartz 8607	5	−128.5	−132.5	−138.5	1.6	3.2	7.9×10^5	2×10^6	1.25	−136.5	8.1	(1)
Rakon Pharao	5	−132.0	−135.5	−141.1	1.5	3	8.4×10^5	2×10^6	1.25	−139.6	7.6	(2)
FEMTO-ST LD prot.	10	−116.6	−130.0	−136.0	4.7	9.3	5.4×10^5	1.15×10^6	4.3	−123.2	6.6	(3)
Agilent 10811	10	−103.0	−131.0	−137.0	25	50	1×10^5	7×10^5	7.1	−119.9	16.9	(4)
Agilent prototype	10	−102.0	−126.0	−132.0	16	32	1.6×10^5	7×10^5	7.1	−114.9	12.9	(5)
Wenzel 501-04623	100	−67.0	−132 ?	−138 ?	1800	3500	1.4×10^4	8×10^4	625	−79.1	15.1	(6)
unit	MHz	dB rad²/Hz	dB rad²/Hz	dB rad²/Hz	Hz	Hz	(none)	(none)	Hz	dB rad²/Hz	dB	

Notes

(1) Data are from specifications, full options about low noise and high stability.
(2) Measured by Rakon on a sample. Rakon confirmed that $2\times10^6 < Q < 2.2\times10^6$ in actual conditions.
(3) LD cut, built and measured in our laboratory, yet by a different team. Q_t is known.
(4) Measured by Hewlett Packard (now Agilent) on a sample.
(5) Implements a bridge scheme for the degeneration of the amplifier noise. Same resonator of the Agilent 10811.
(6) Data are from specifications.

$$R = \left.\frac{(\sigma_y)_{\rm oscill}}{(\sigma_y)_{\rm Leeson}}\right|_{\rm floor} = \sqrt{\frac{(b_{-3})_{\rm tot}}{(b_{-3})_L}} = \frac{Q_t}{Q_s} = \frac{f''_L}{f_L}$$

The Rohde Oscillator

The Rohde-Colpitts oscillator

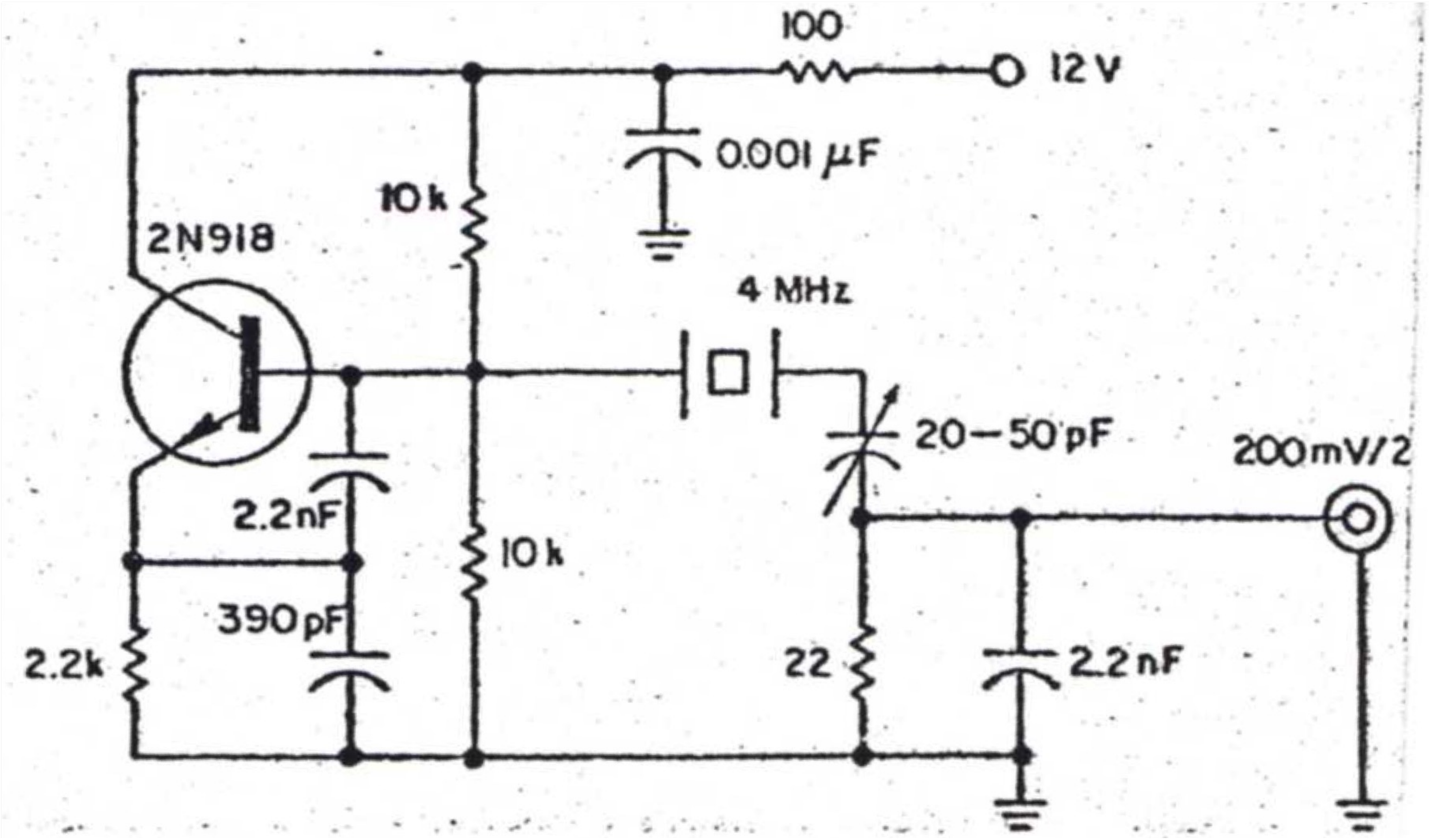

Fig. 1 from U. L. Rohde,
Crystal oscillator provides low noise,
Electronic Design Oct 11, 1975 p.11, 14

- Off resonance, either $X_L \gg R_S$ or $X_C \gg R_S$
- The motional resistance R_S is not coupled to the output
- No thermal noise from R_S to the output
- The quartz also filters out harmonics and spurs

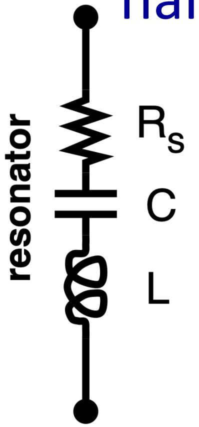

The Rohde oscillator

The weird 100 MHz OCXOs

- Neg-R oscillator, where the resonator also filters the out
- The AC current I_R is transferred from SA to OUT
- At $f > \nu_0/2Q$, the thermal noise of R_S is not coupled
- Magic bias minimizes the buffer noise
- C_{CB} and stray L_{base} originates feedback. Noise is more than just thermal noise

How to get low floor — and the troubles that go with

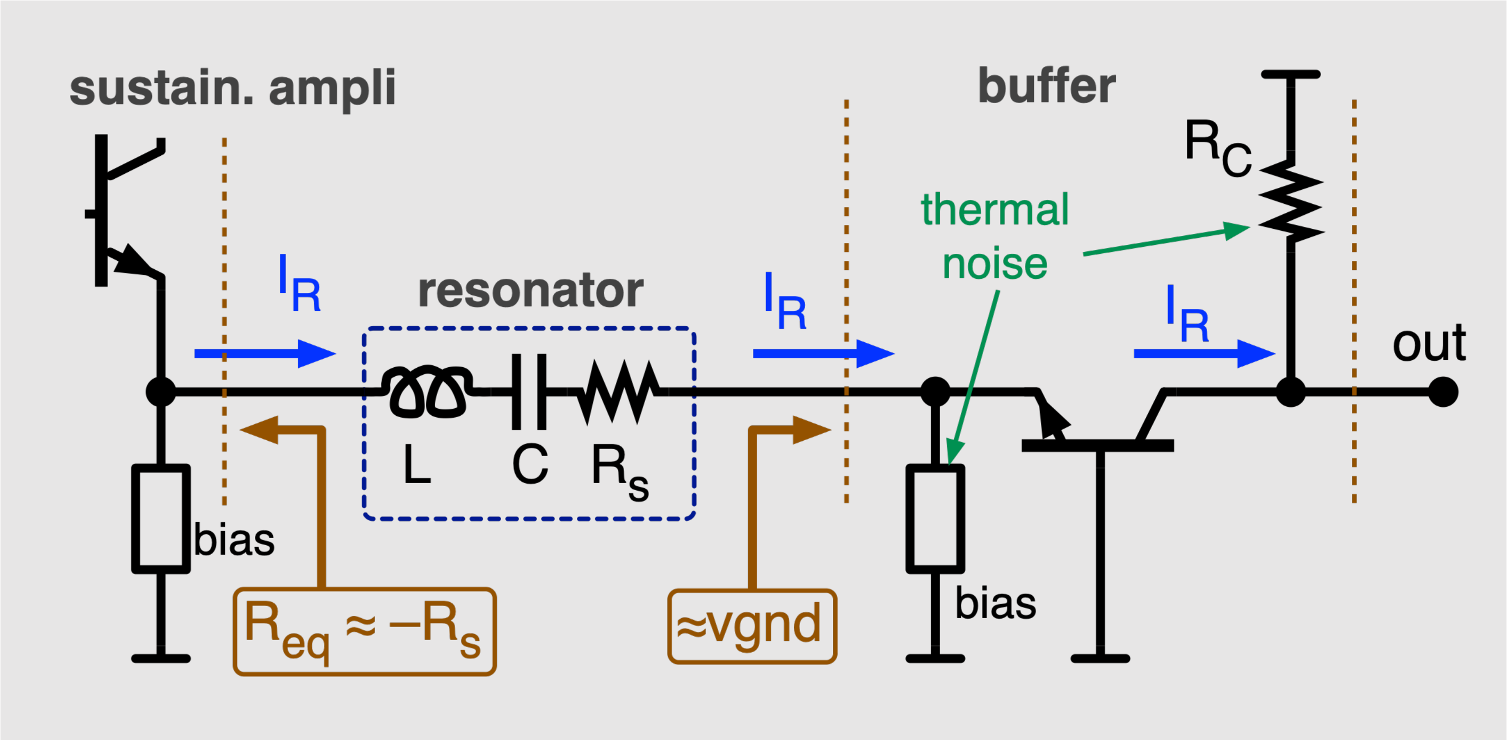

The sub-thermal oscillator

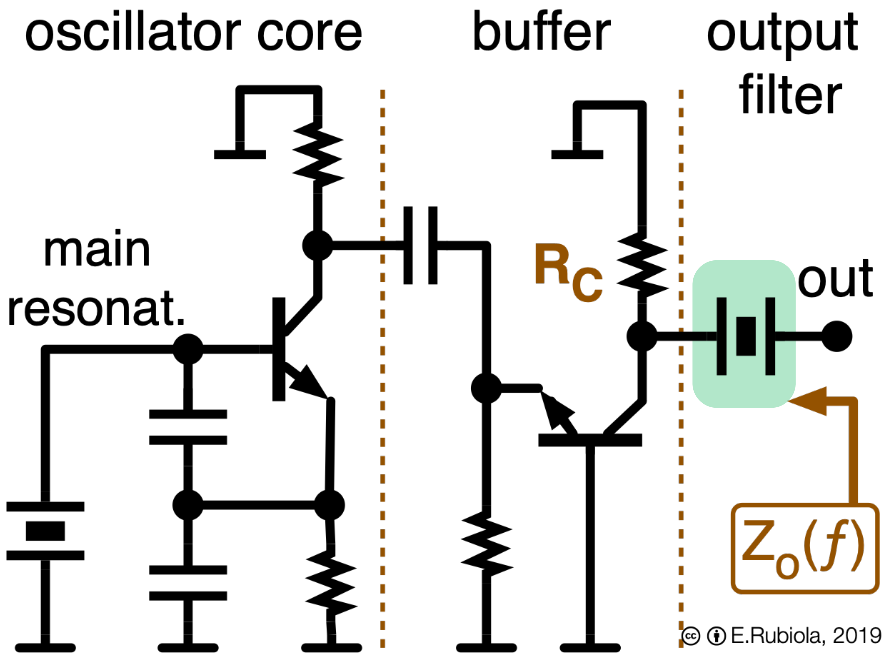

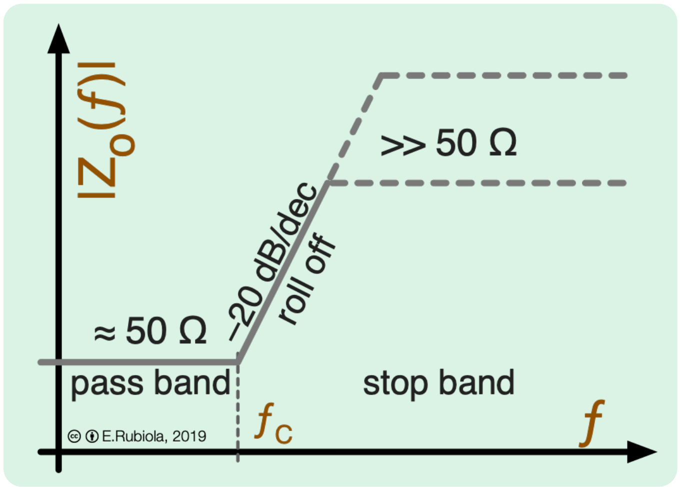

Fig.9 (excerpt), from Y. Gruson et al, Metrologia, 27 April 2020, DOI 10.1088/1681-7575/ab8d7b

- Low white noise achieved with a quartz filter
- $f < f_c$: carrier (and red noise) coupled to out
- $f > f_c$: the filter is open circuit
  - buffer noise and thermal noise of the motional R are not coupled to output
  - Equivalent temperature $T_{eq} < T_{room}$
  - No violation of physics principles!
- Reverse engineering from noise is still unclear
- Actual noise may depend on what is connected at the output
- Odd behavior of commercial phase-noise analyzers

Leeson Effect in the Delay-Line Oscillator

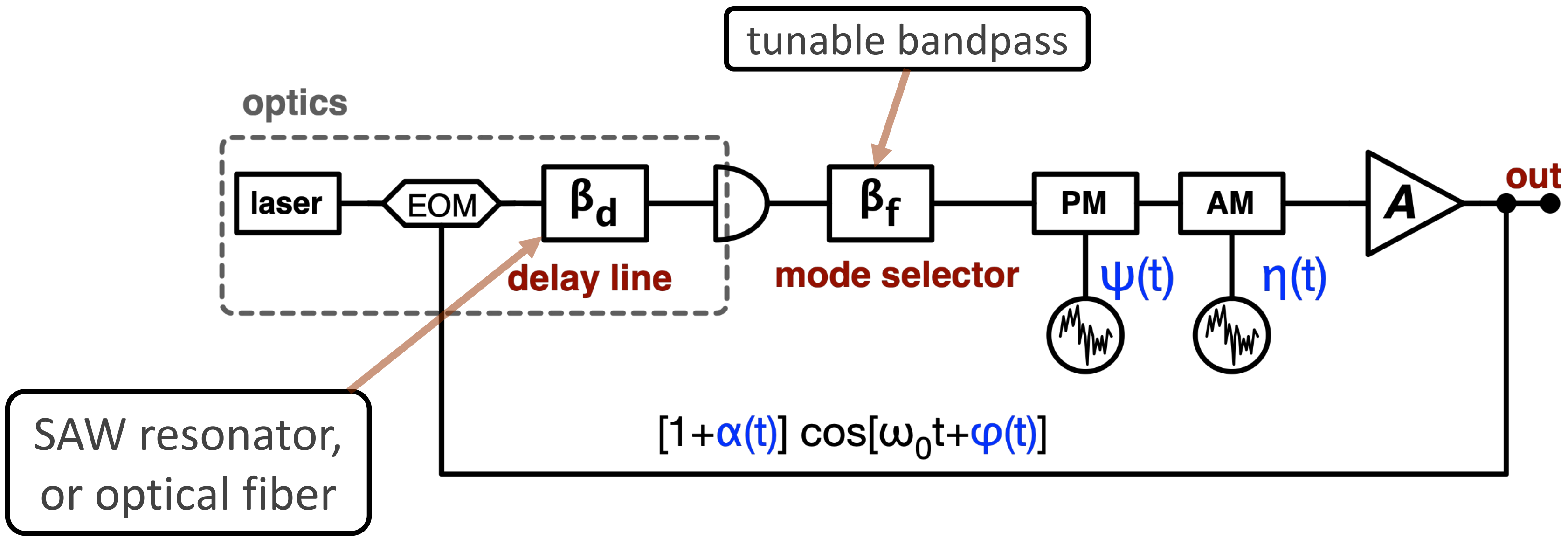

Motivations

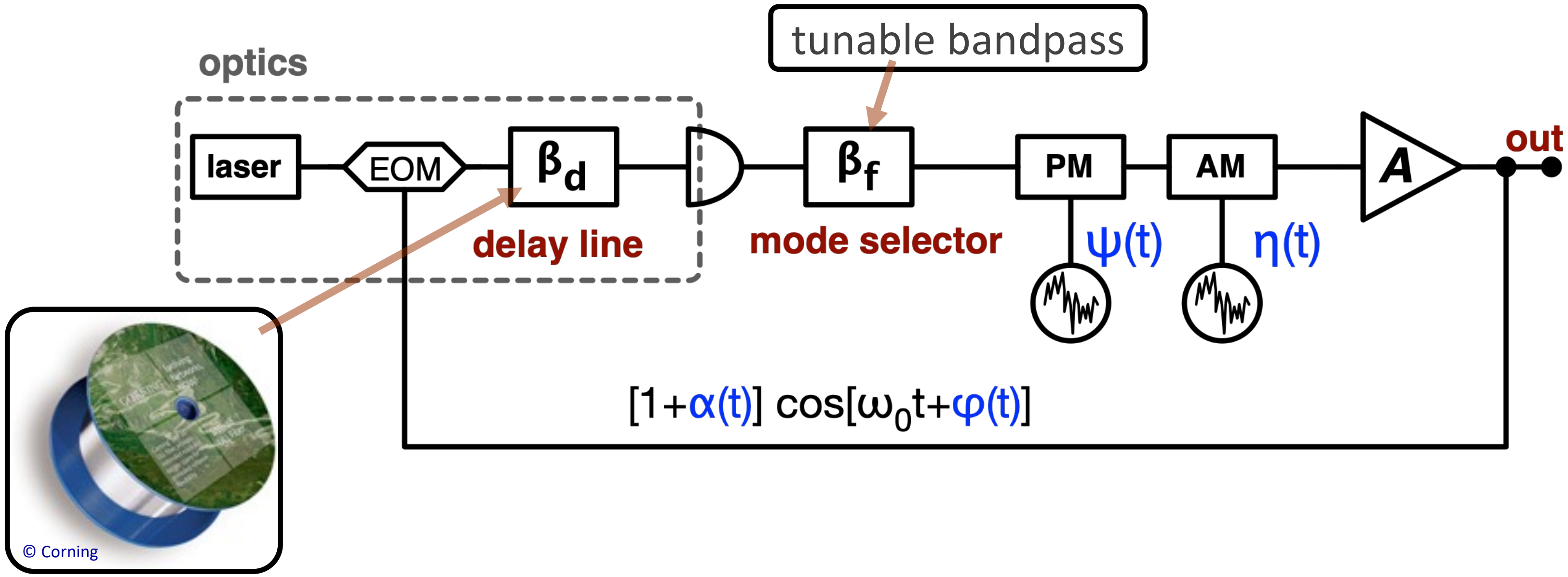

- Potential for very-low phase noise in the 100 Hz – 1 MHz range
- Invented at JPL, X. S. Yao & L. Maleki, JOSAB 13(8) 1725–1735, Aug 1996
- Early attempt of noise modeling, S. Römisch & al., IEEE T UFFC 47(5) 1159–1165, Sep 2000
- PM-noise analysis, E. Rubiola, Phase noise and frequency stability in oscillators, Cambridge 2008 [Chapter 5]
- Since, no progress in the analysis of noise at system level
- Nobody reported on the consequences of AM noise

Low-pass representation of AM-PM noise

E. Rubiola, Phase Noise and Frequency Stability in Oscillators, Cambridge 2008–2012

E. Rubiola & R. Brendel, arXiv:1004.5539v1, [physics.ins-det]

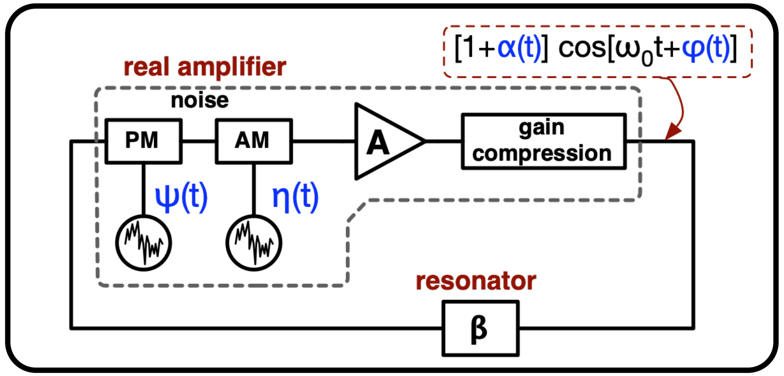

RF, µwaves or optics

The amplifier
- "copies" the input phase to the out
- adds phase noise

low-pass equivalent

The amplifier
- compresses the amplitude
- adds amplitude noise

PM

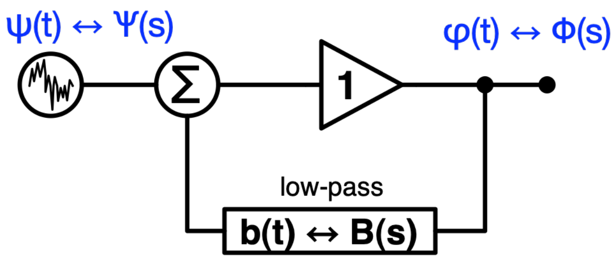

Leeson Effect

AM

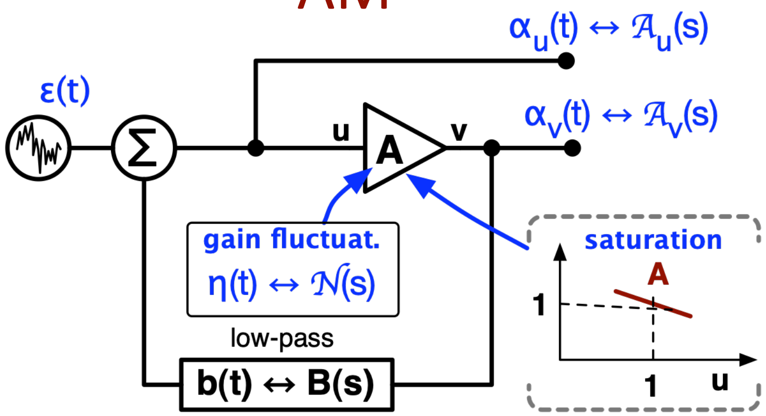

extension of the LE to AM noise

Delay-line oscillator – Operation

Figures from E. Rubiola, Phase Noise and Frequency Stability in Oscillators, Cambridge 2008, ISBN 978-0521-88677-2

Barkhausen condition for oscillation: $A\beta = 1$

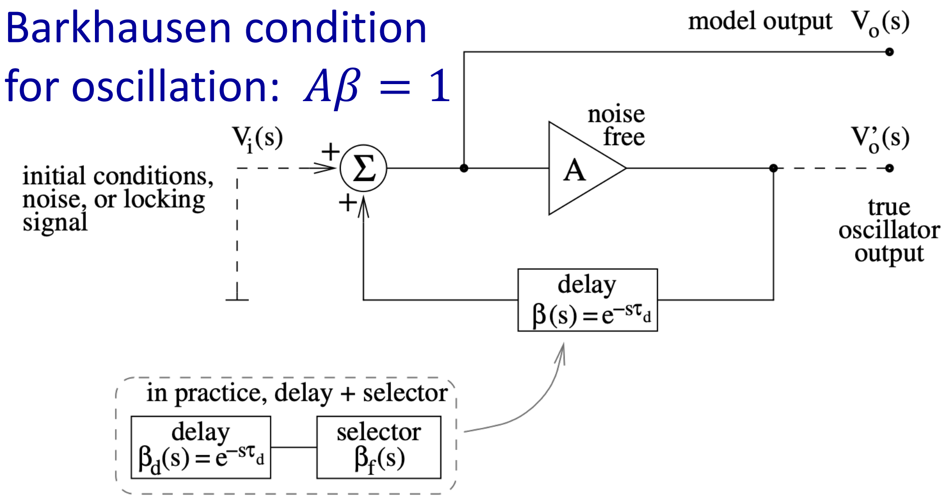

General feedback theory

$$H(s) = \frac{V_o(s)}{V_i(s)} = \frac{1}{1 - A\beta(s)}$$

Delay-line oscillator

$$H(s) = \frac{1}{1 - Ae^{-s\tau_d}}$$

Location of the roots

$$s_l = \frac{1}{\tau_d}\ln(A) + j\frac{2\pi}{\tau_d}l \qquad \text{integer } l \in (-\infty, \infty)$$

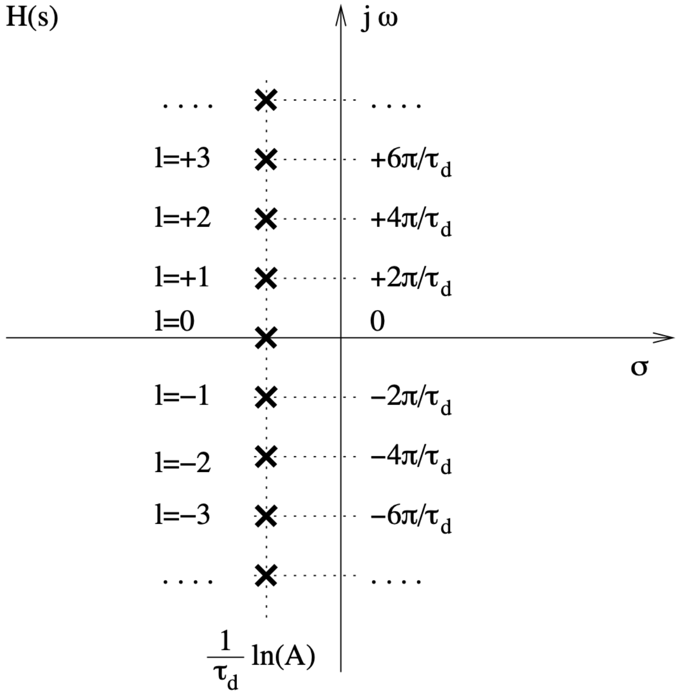

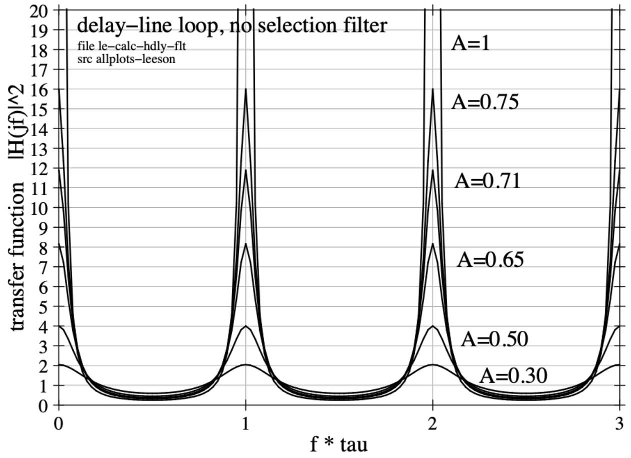

The Leeson effect in the delay-line oscillator

Also describes the laser

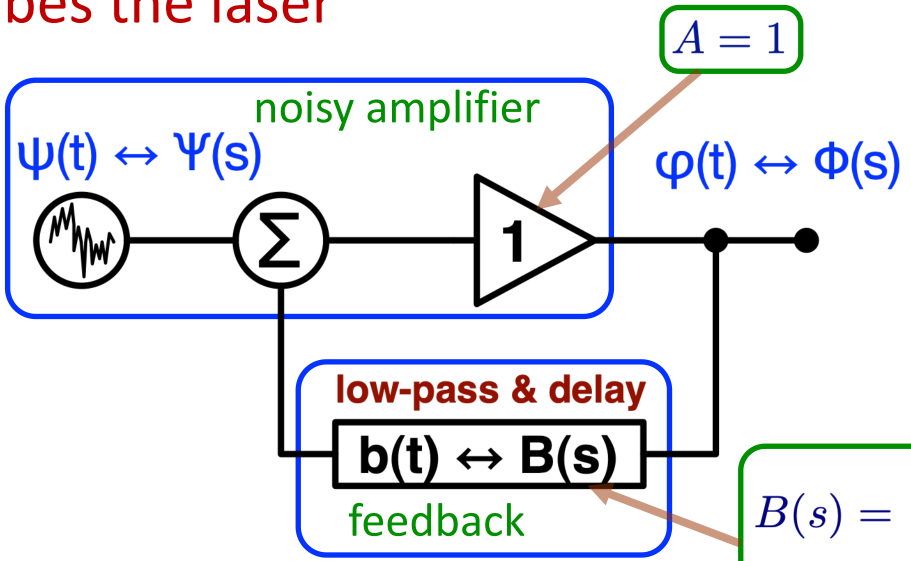

$$B(s) = \frac{e^{-s\tau}}{1+s\tau_f}$$

phase-noise transfer function

$$\mathrm{H}(s) = \frac{\Phi(s)}{\Psi(s)}$$ definition

$$\mathrm{H}(s) = \frac{1}{1+AB(s)}$$ general feedback theory

$$\mathrm{H}(s) = \frac{1+s\tau_f}{1+s\tau_f - e^{-s\tau}}$$ Leeson effect

This figure is from E. Rubiola, Phase noise and frequency stability in oscillators, © Cambridge University Press

H, complex plane

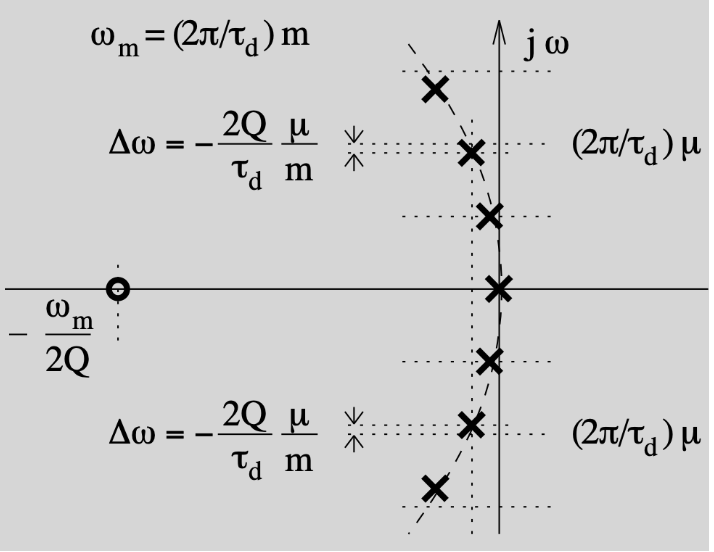

transfer function $|H|^2$

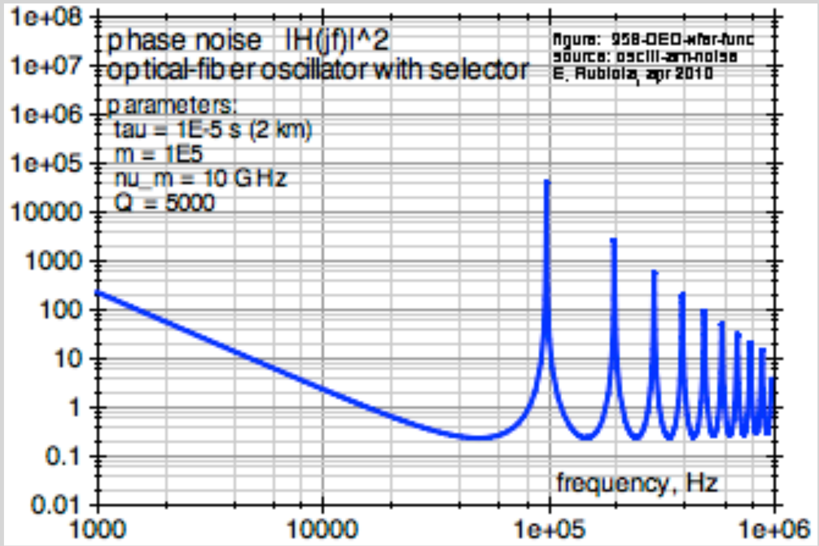

Gain fluctuations – Output is $u(t)$

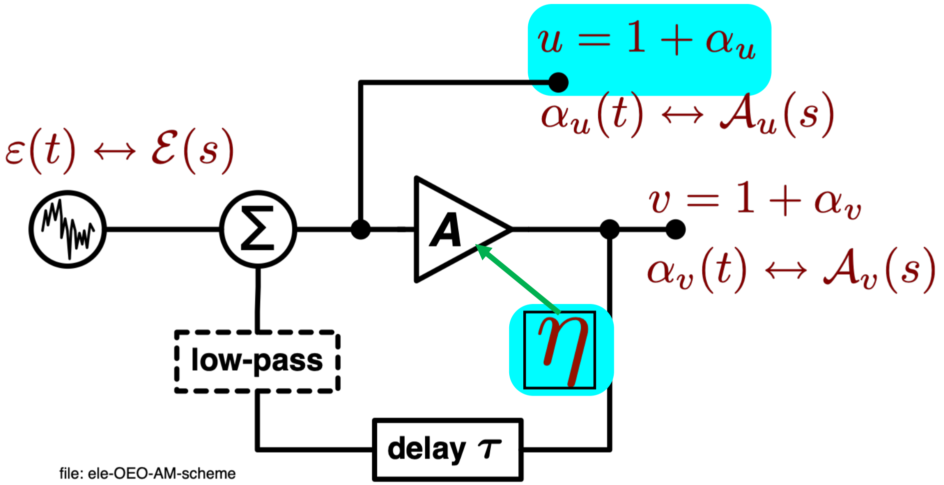

The low-pass has only 2nd order effect on AM

Linearize for low noise and use the Laplace transform

$$\alpha_u(t) \leftrightarrow \mathcal{A}_u(s) \quad \text{and} \quad \eta(t) \leftrightarrow \mathcal{N}(s)$$

$$\mathrm{H}(s) = \frac{\mathcal{A}_u(s)}{\mathcal{N}(s)}$$ definition

$$\mathrm{H}(s) = \frac{1}{1-(1-\gamma)e^{-s\tau}}$$ result

non-linear equation

$$u = A(t-\tau)\,u(t-\tau)$$

$$A = 1 - \gamma(u-1) + \eta$$

use u=α+1, expand and linearize for low noise

$$\alpha(t) = (1-\gamma)\alpha(t-\tau) - \gamma\alpha^2(t-\tau) \rightarrow 0$$

$$+\,\eta(t-\tau) + \eta(t-\tau)\alpha(t-\tau) \rightarrow 0$$

linearized equation

$$\alpha(t) = (1-\gamma)\alpha(t-\tau) + \eta(t-\tau)$$

Laplace transform

$$\mathcal{A}_u(s) = \left[1-(1-\gamma)e^{-s\tau}\right] = \mathcal{N}(s)$$

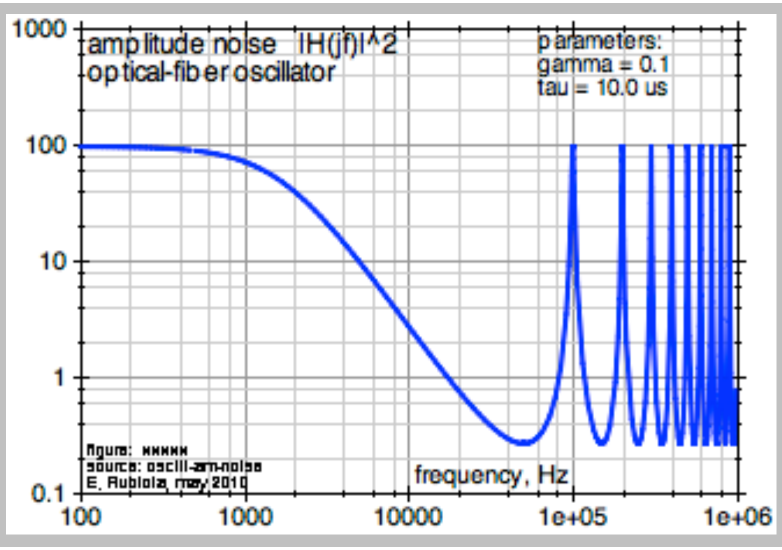

Gain fluctuations – Output is $v(t)$

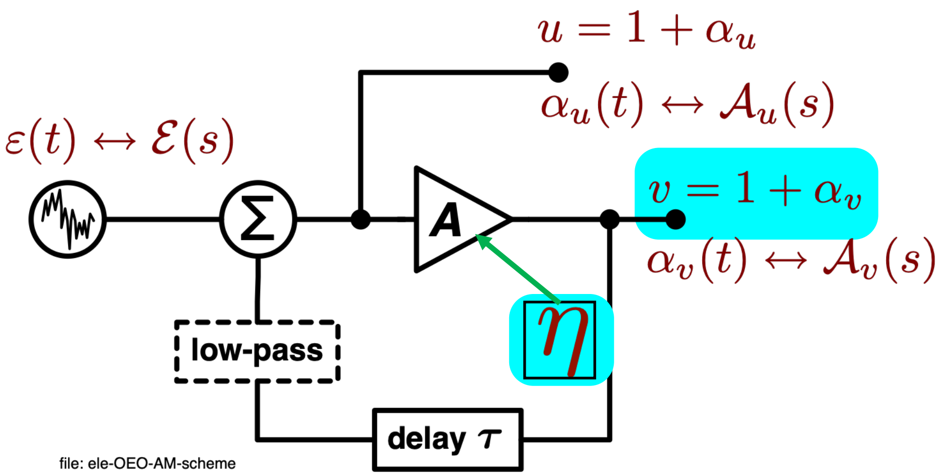

The low-pass has only 2nd order effect on AM

boring algebra relates α_v to α_u

$$v = Au$$

$$A = -\gamma(u-1) + 1 + \eta$$

$$v = [-\gamma(u-1) + 1 + \eta]\, u \qquad \text{use } u=\alpha+1$$

$$v = [-\gamma\alpha_u + 1 + \eta]\, [1 + \alpha_u]$$

$$\cancel{1} + \alpha_v = \cancel{1} + \eta - \gamma\alpha_u + \alpha_u - \cancel{\alpha_u\eta} - \cancel{\gamma\alpha_u^2}$$

$$\alpha_v = (1-\gamma)\alpha_u + \eta$$

$$\alpha_u = \frac{\alpha_v - \eta}{1-\gamma}$$

linearization for low noise

$$\mathcal{A}_u(s)\left[1 - (1-\gamma)e^{-\imath\omega\tau}\right] = \mathcal{N}(s)$$

$$\mathcal{A}_u(s) = \frac{\mathcal{A}_v(s) - \mathcal{N}(s)}{1-\gamma}$$

starting equation

$$\left[1 + (1-\gamma)\left(1 - e^{-s\tau}\right)\right]\mathcal{A}_v(s) = \left[1 - (1-\gamma)e^{-s\tau}\right]\mathcal{N}(s)$$

$$\mathrm{H}(s) = \frac{\mathcal{A}_v(s)}{\mathcal{N}(s)}$$

definition

$$\mathrm{H}(s) = \frac{1 + (1-\gamma)\left(1 - e^{-s\tau}\right)}{1 - (1-\gamma)e^{-s\tau}}$$

result

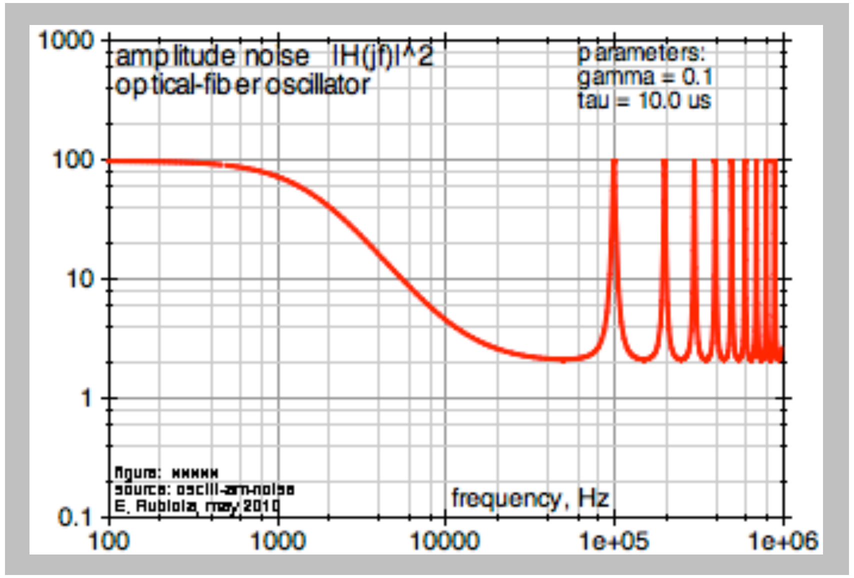

Theoretical prediction of AM & PM spectra

Y.K. Chembo, K. Volyanskiy, L. Larger, E. Rubiola, P. Colet, & al., IEEE J. Quant. Electron. 45(2) p.178-186, Feb 2009

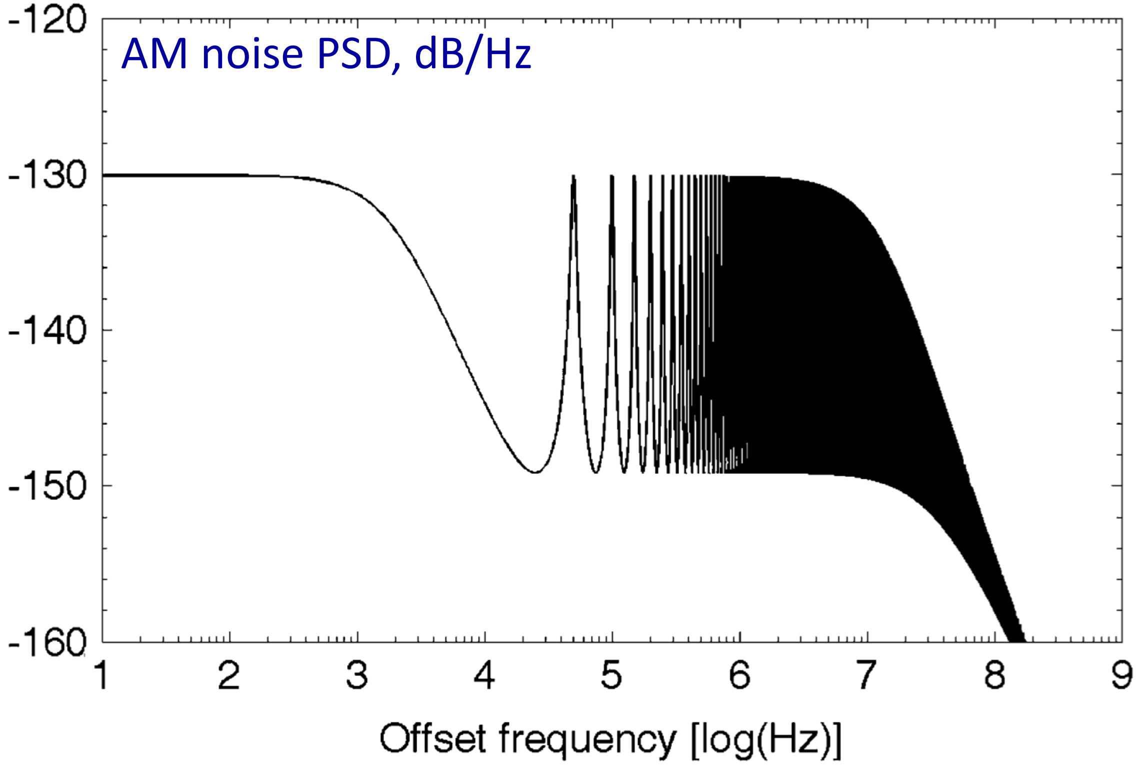

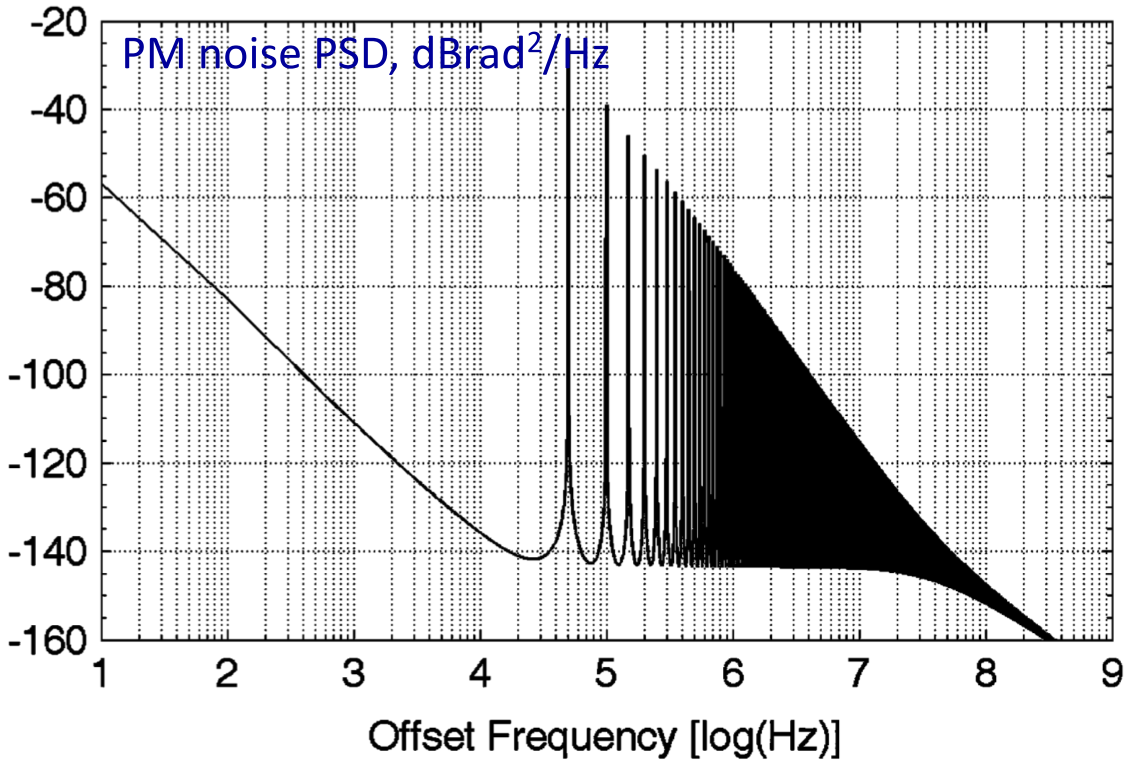

- Prediction is based on the stochastic diffusion (Langevin) theory
- However complex, the Langevin theory provides an independent check

Delay-line oscillator

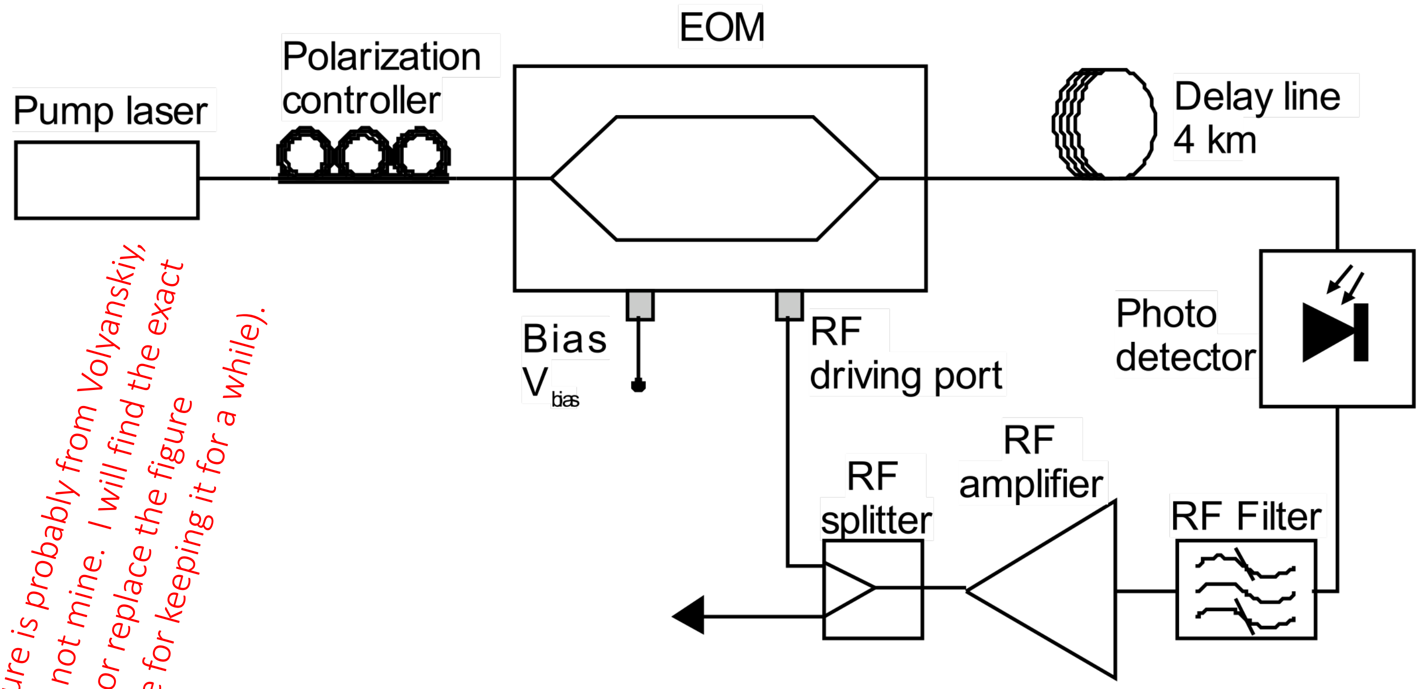

The figure is probably from Volyanskiy, for sure not mine. I will find the exact citation, or replace the figure (apologize for keeping it for a while).

E. Rubiola, *Phase Noise and Frequency Stability in Oscillators*, Cambridge 2008, ISBN13 9780521886772

$$Q_{\mathrm{eq}} = \pi \nu_0 \tau$$

L = 4 km
Q_{eq} = 6.3×10^5

$$f_L = \frac{\nu_0}{2Q}$$

$$f_L = \frac{1}{4\pi^2\tau^2}$$

f_L = 8 kHz

10^{-11}

$$S_\varphi(f) \simeq \frac{f_L^2}{f^2} S_\psi(f) \quad \text{for } f \ll f_L$$

Leeson formula

b_{-3} = 6.3×10^{-4} (–32 dB)

$$h_{-1} = b_{-3}/\nu_0^2$$

6.3×10^{-24}

$$\sigma_y^2 = 2\ln(2)\, h_{-1}$$

808×10^{-24}

$$\sigma_y \simeq 2.9\times10^{-12}$$

Allan deviation

Delay-line oscillator – Measured noise

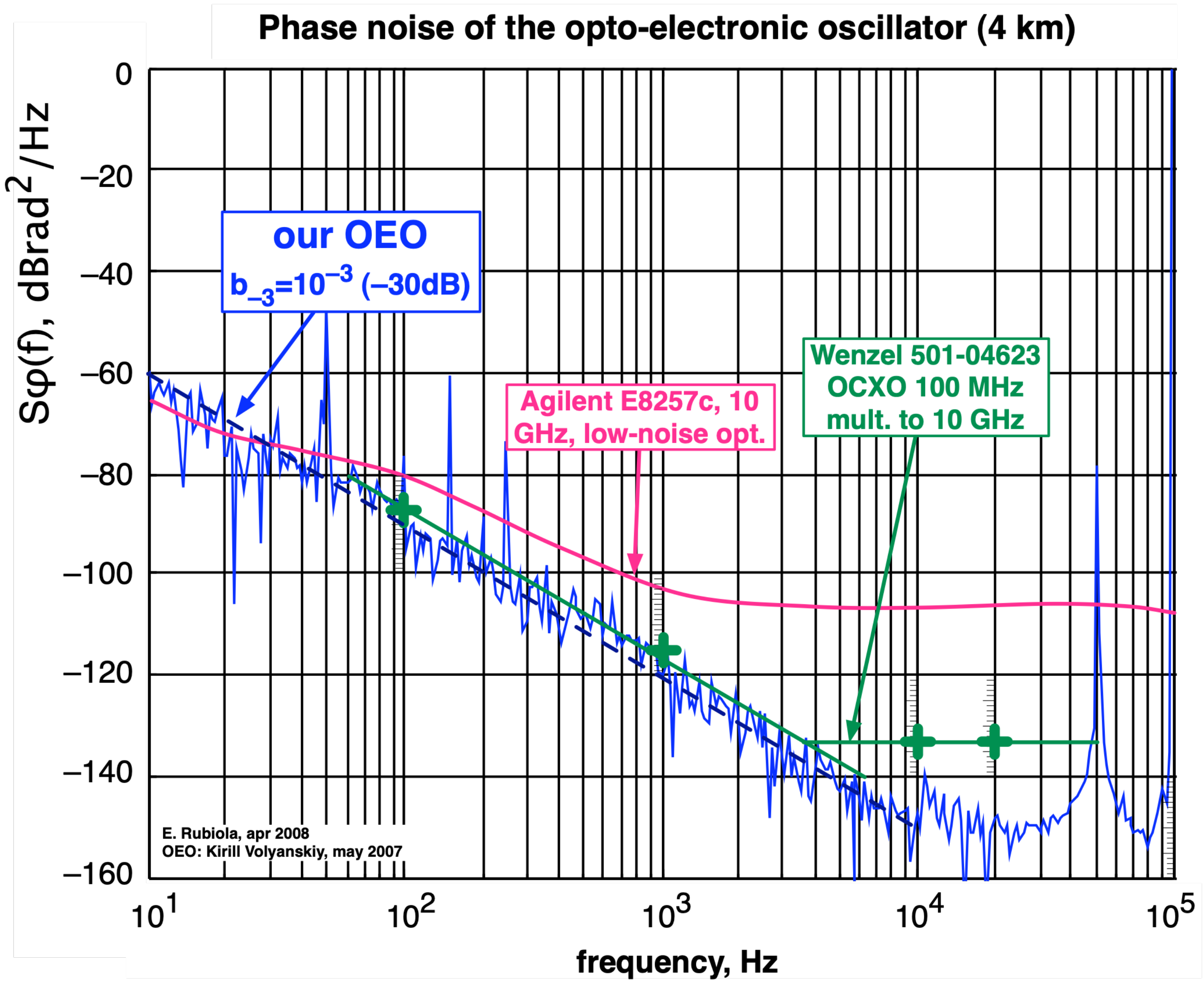

- 1.310 nm DFB CATV laser
- Photodetector DSC 402 responsivity $R = 371$ V/W
- RF filter $\nu_0 = 10$ GHz, $Q = 125$
- RF amplifier AML812PNB1901 (gain +22dB)

expected phase noise
$b_{-3} \approx 6.3\times10^{-4}$ (–32 dB)

NIST Opto-Electronic Oscillator – Simulation

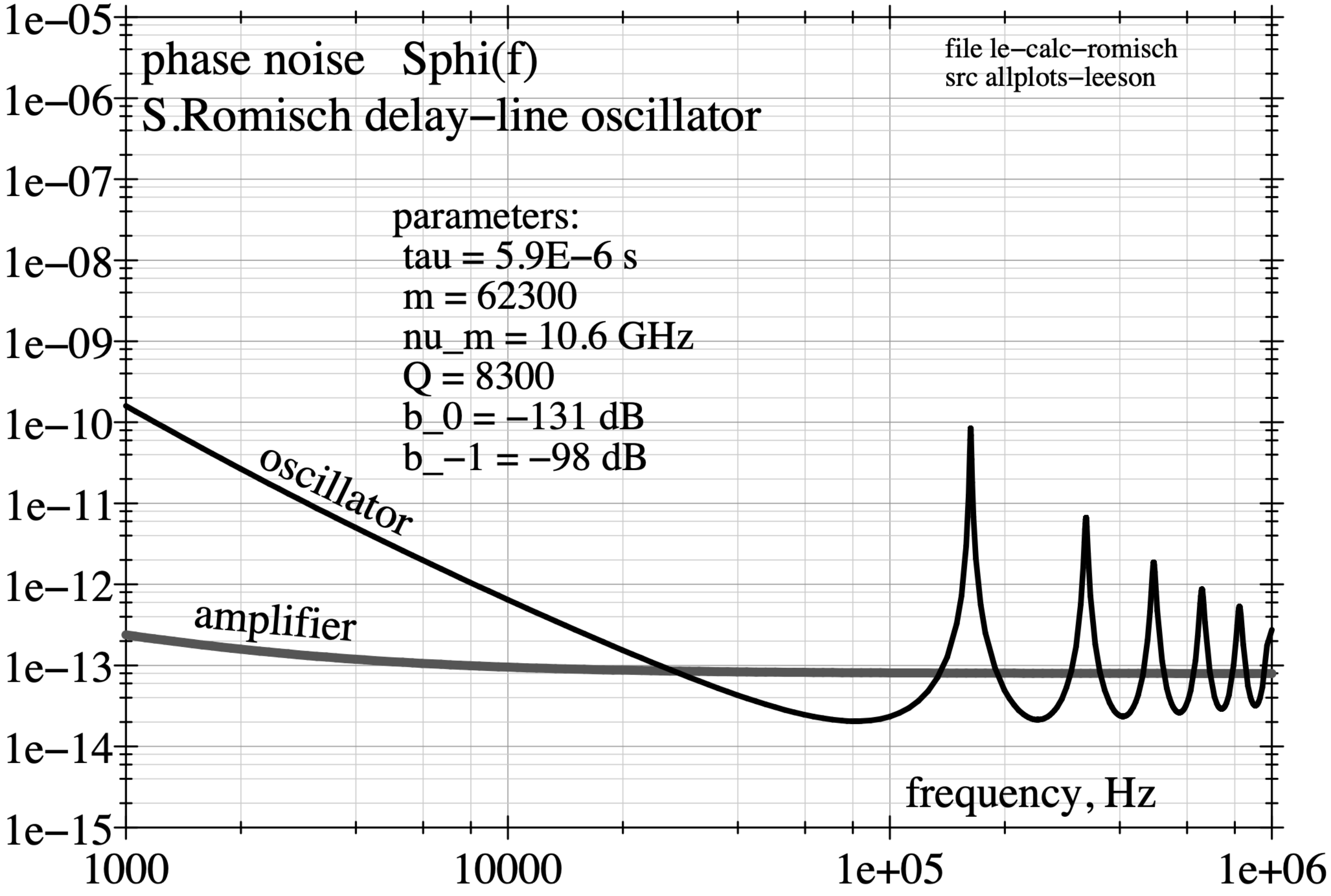

NIST opto-electronic oscillator

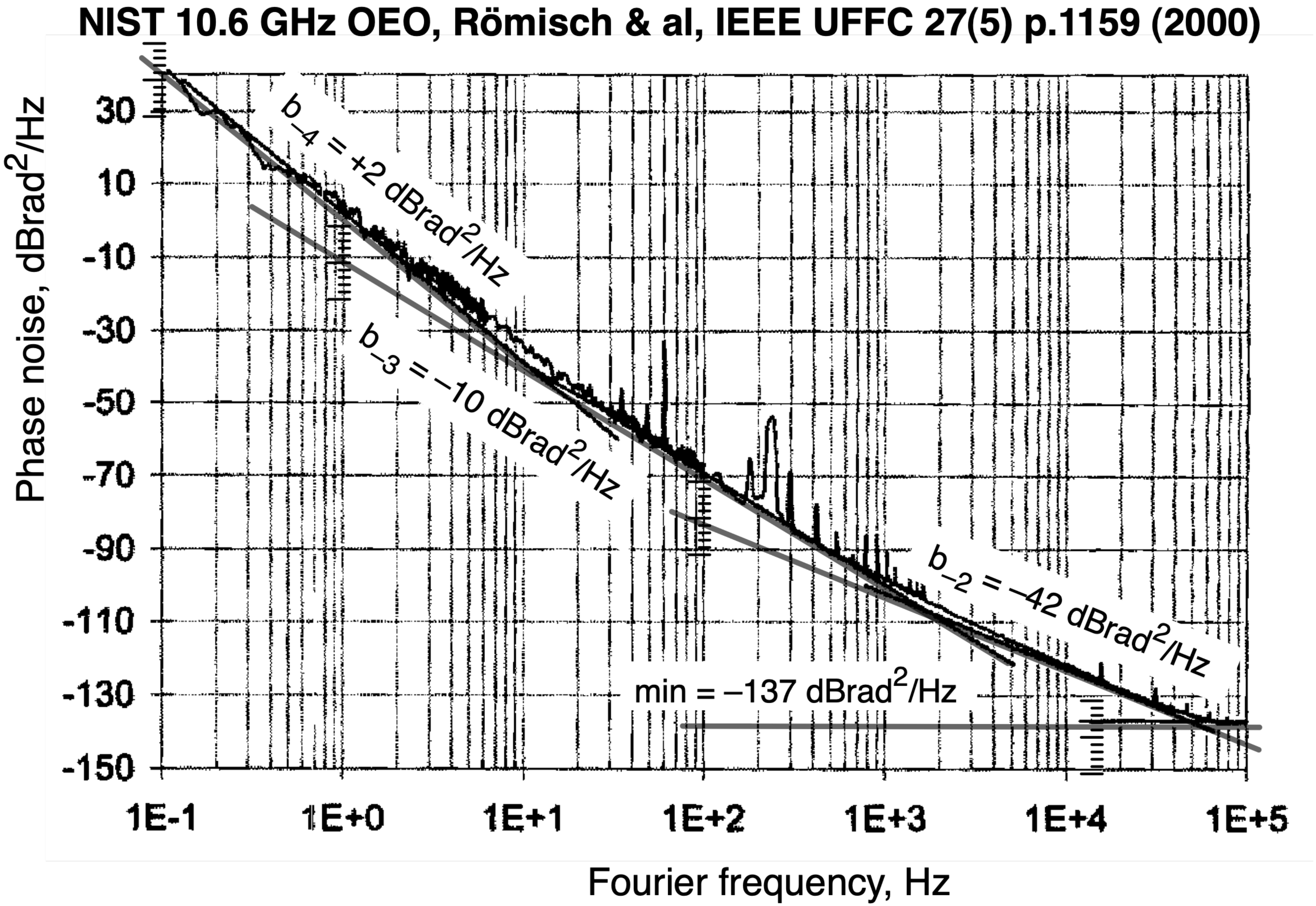

NIST opto-electronic oscillator

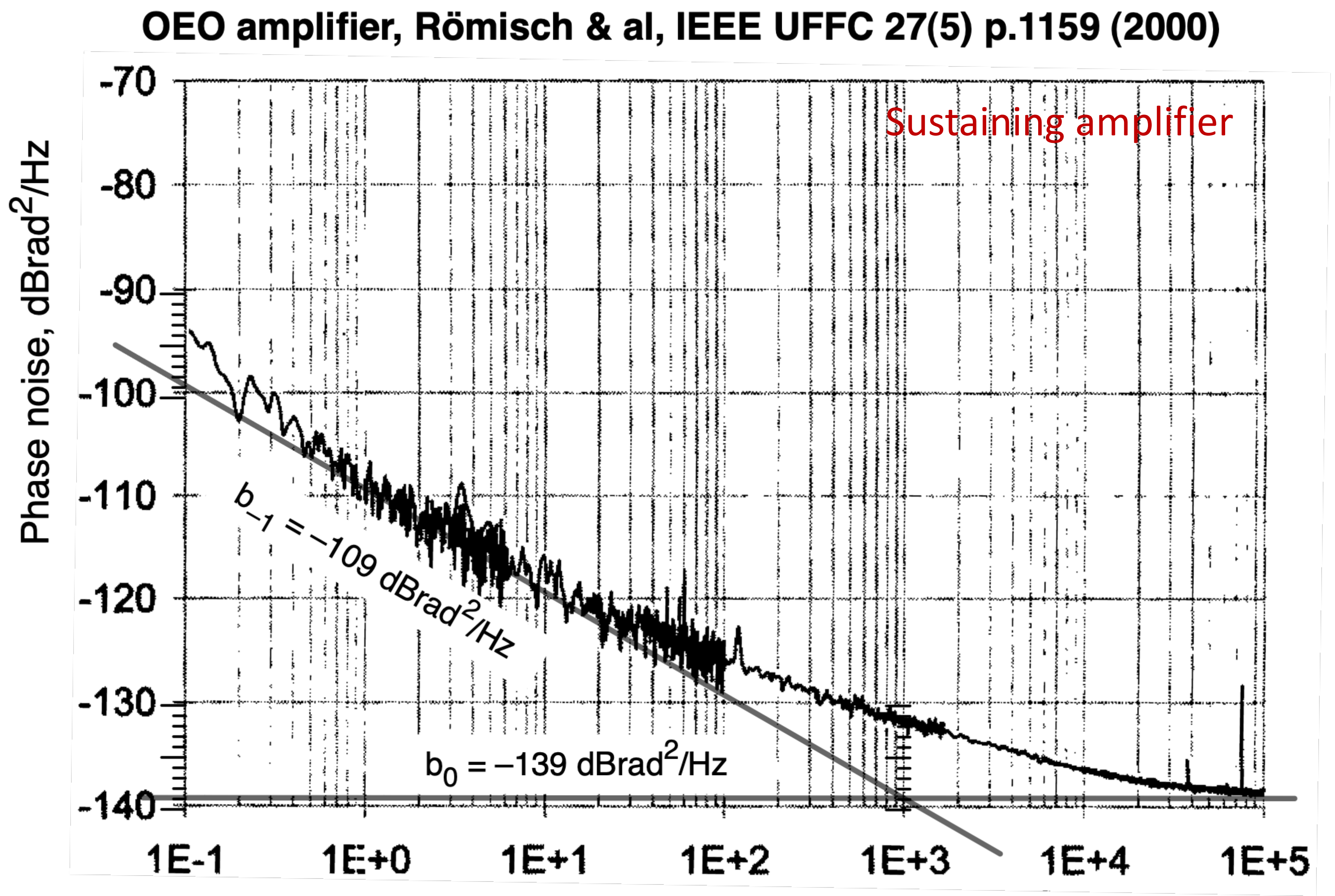

Opto-electronic oscillator

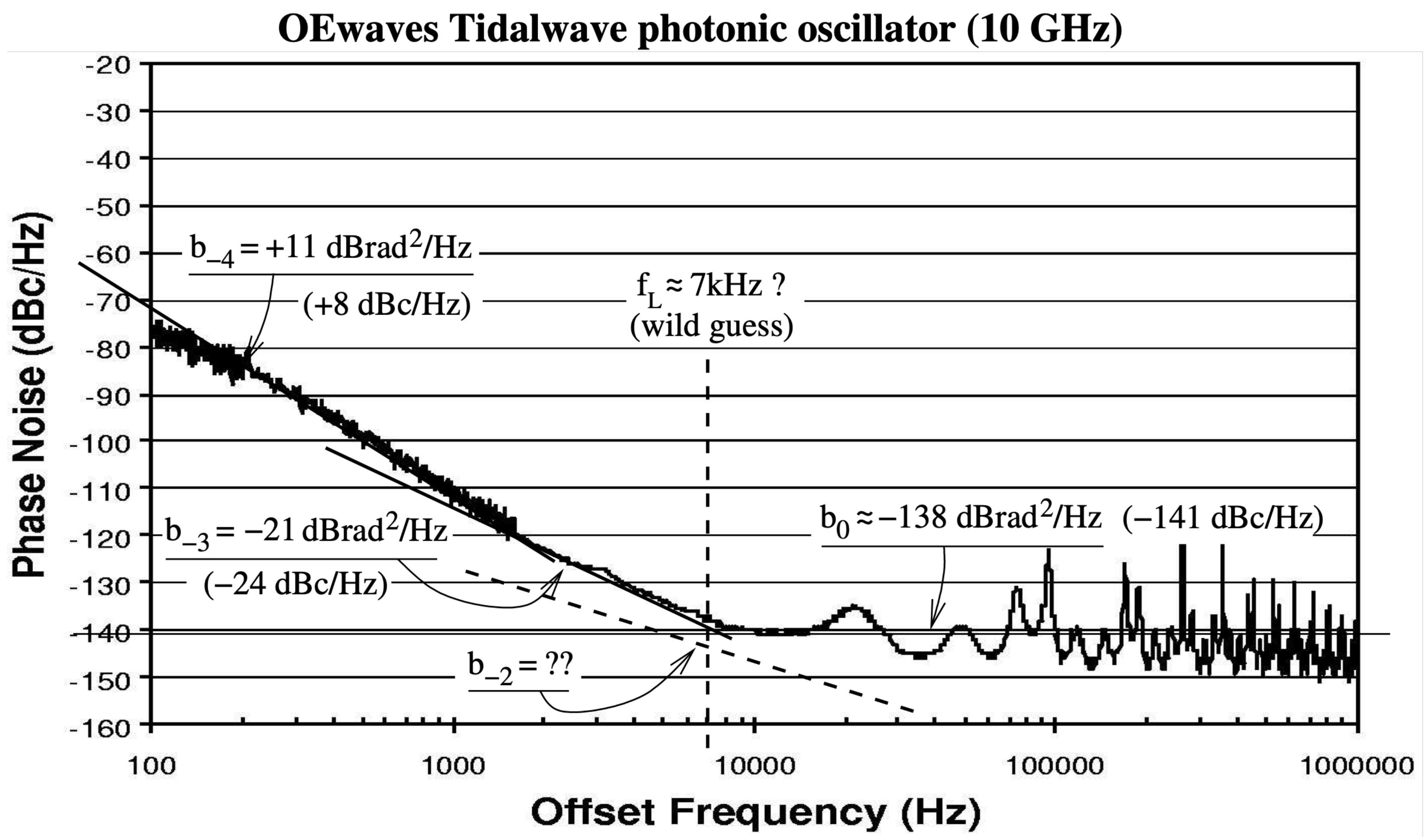

$$Q = \pi \nu_0 \tau$$

$$\tau = \frac{Q}{\pi \nu_0} \approx 16\mu s$$

Courtesy of OEwaves (handwritten notes are mine).
Obsolete product? The specifications are no longer available from the OEwaevs web site

Opto-electronic oscillator

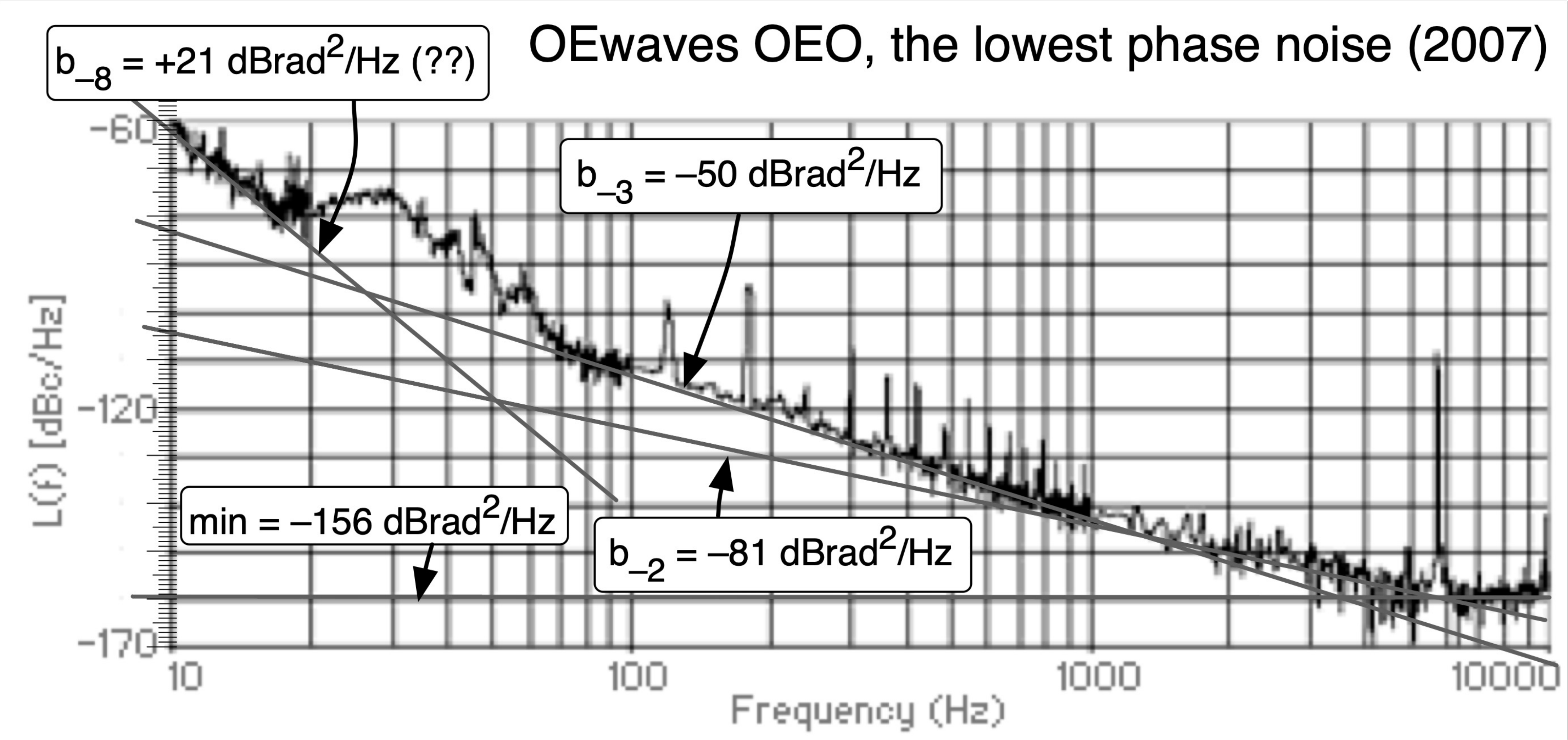

Courtesy of OEwaves, notes are mine

OEwaves, lowest phase noise (2)

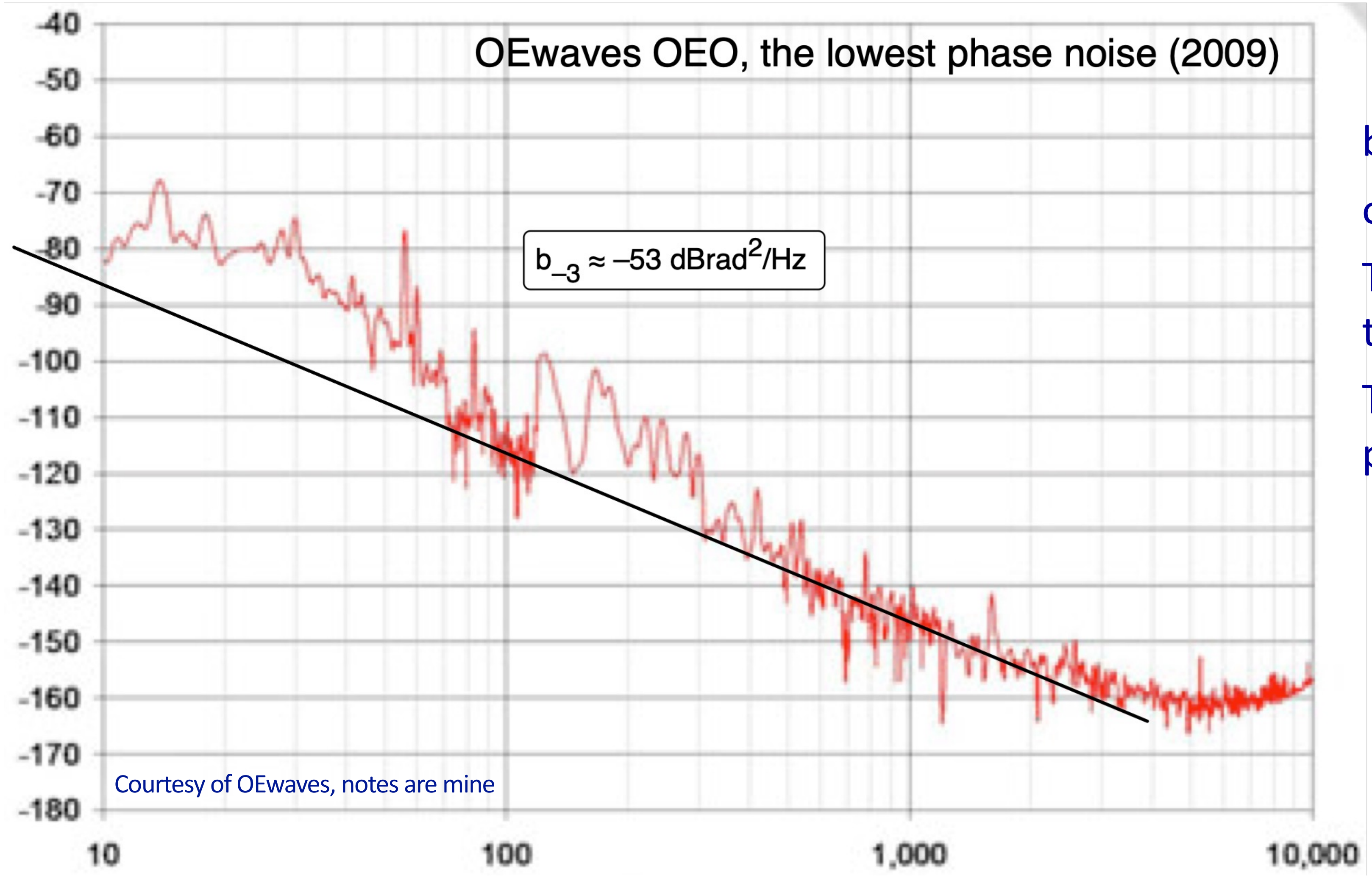

$b_{-3} \approx -53$ dBrad^2/Hz @ 10 GHz   =>

$\sigma_y = 2.6 \times 10^{-13}$

The peak at 5.7 kHz is disappeared. Did they use a shorter fiber?

The high slope is now disappeared, probably filtered by the system

OEwaves compact OEO

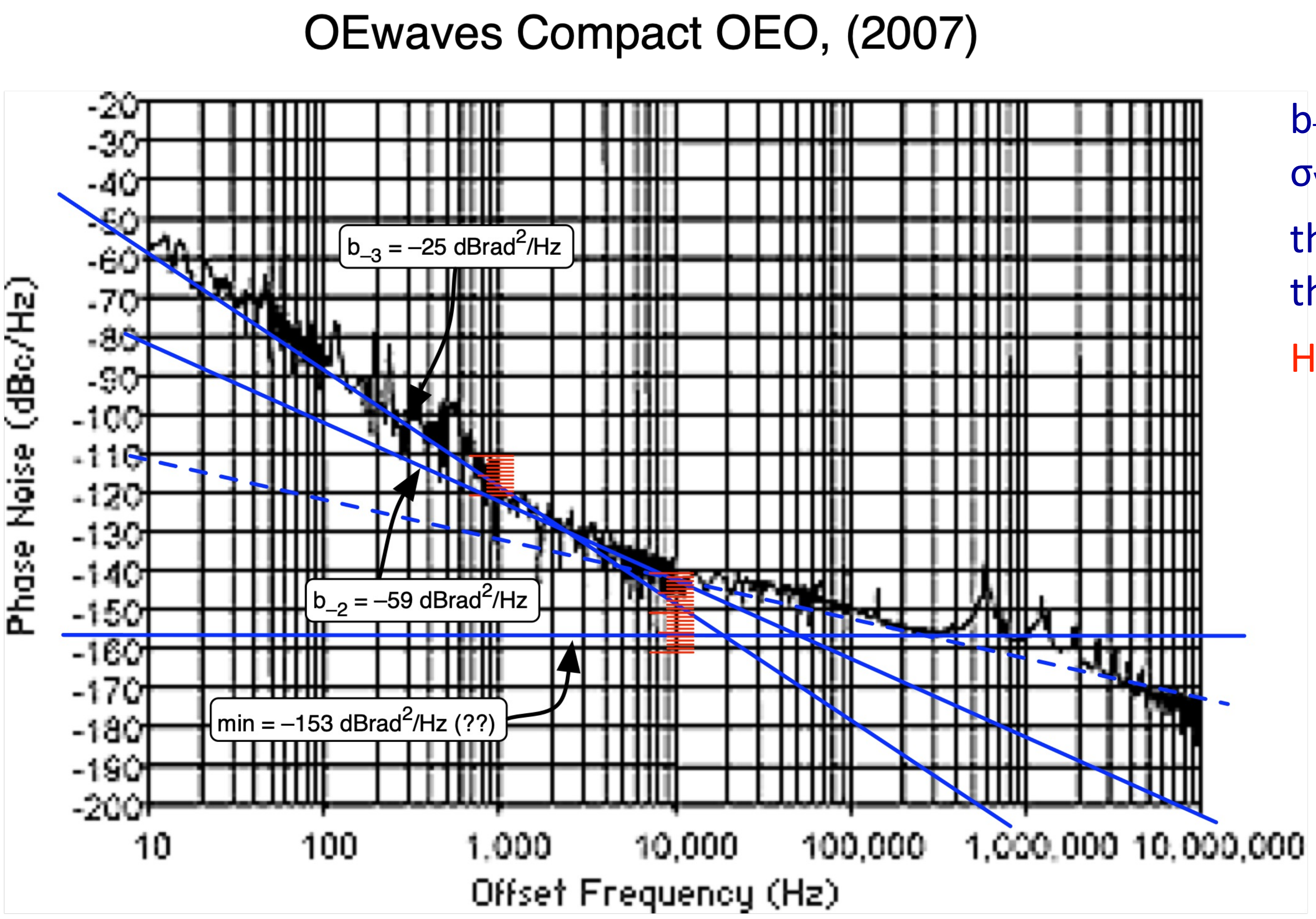

Courtesy of OEwaves, notes are mine

b_{-3} = −25 dBrad^2/Hz @ 10 GHz => $\sigma_y = 6.6\times10^{-12}$

the bump at 580 kHz makes me think about a 340 m fiber

How did they remove the spurious?

Optical-Fiber 10 GHz oscillator

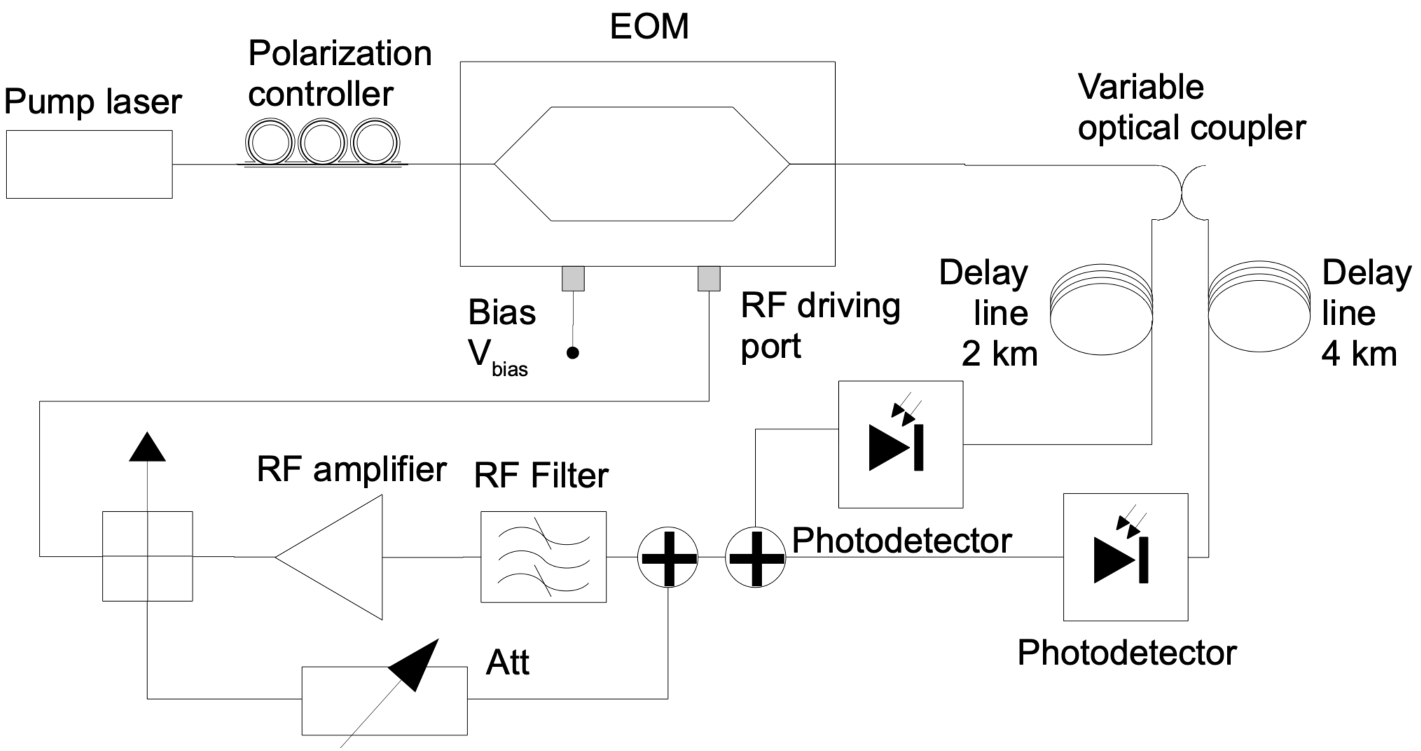

Kiryll Volyanskiy, jan 2008

- use positive feedback with a short cable (3-5 ns) in the feedback path to implement the mode selector filter
- the positive feedback also increase the amplifier gain (AML SiGe parallel amplifiers exhibits lowest flicker, but low have gain 22 dB)
- use the 2-km (10 µs) path to eliminate the 50-kHz noise peak due to the 4-km (20 µs)
- the microwave power is changed by adjusting the laser power
- high noise figure, due to the two power splitters/combiners

Regenerative optical-fiber 10 GHz oscillator

freq. random walk
$b_{-4} = 0.2\ rad^2/Hz$
$h_{-2} = 2\times10^{-21}$
$\sigma_y(\tau) = 1.15\times10^{-10}\ \sqrt{\tau}$

frequency flicker
$b_{-3} = 2.5\times10^{-3}\ rad^2/Hz$
$h_{-1} = 2.5\times10^{-23}$
$\sigma_y(\tau) = 5.9\times10^{-11}$

11 dBm white freq.
$b_{-2} = 2\times10^{-6}\ rad^2/Hz$
$h_0 = 2\times10^{-21}$
$\sigma_y(\tau) = 1\times10^{-13}/\sqrt{\tau}$

9 dBm white freq.
$b_{-2} = 5\times10^{-6}\ rad^2/Hz$
$h_0 = 5\times10^{-26}$
$\sigma_y(\tau) = 1.6\times10^{-13}/\sqrt{\tau}$

8 dBm white freq.
$b_{-2} = 8.9\times10^{-6}\ rad^2/Hz$
$h_0 = 8.9\times10^{-26}$
$\sigma_y(\tau) = 2.1\times10^{-13}/\sqrt{\tau}$

The white f noise follows exactly the quadratic law of the detector

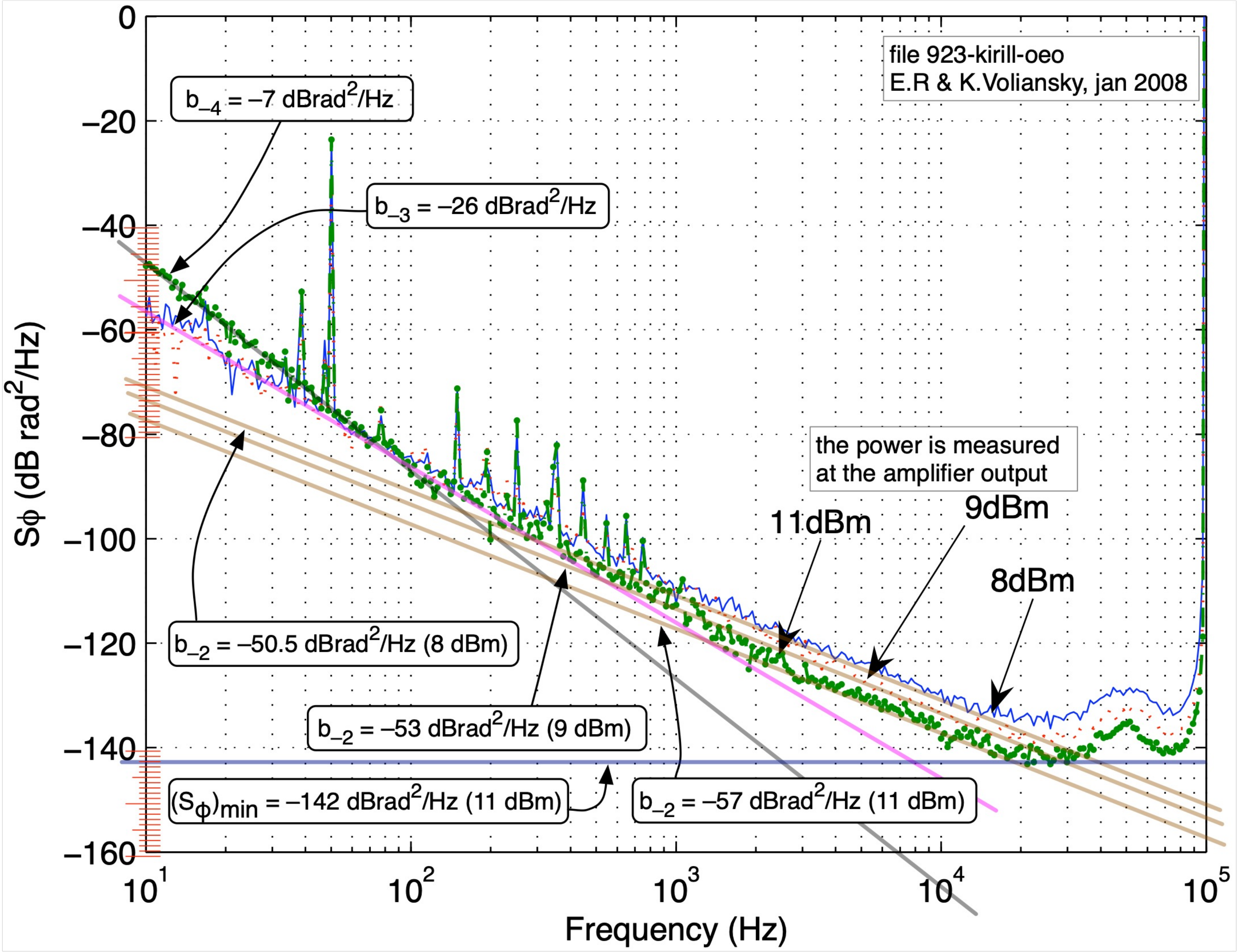

Regenerative optical-fiber 10 GHz oscillator

P_{rf} is given, thus $V_0 = \sqrt{2RP}$
V_π is estimated (4.5 V at 10 GHz)
Use

$$m = 2J_1\left(\frac{\pi V_0}{V_\pi}\right)$$

Get

P, dBm	V_p, V	$\pi V_0/V_\pi$	m
11	1.122	0.86	0.783
9	0.891	0.683	0.644
8	0.794	0.6.09	0.581

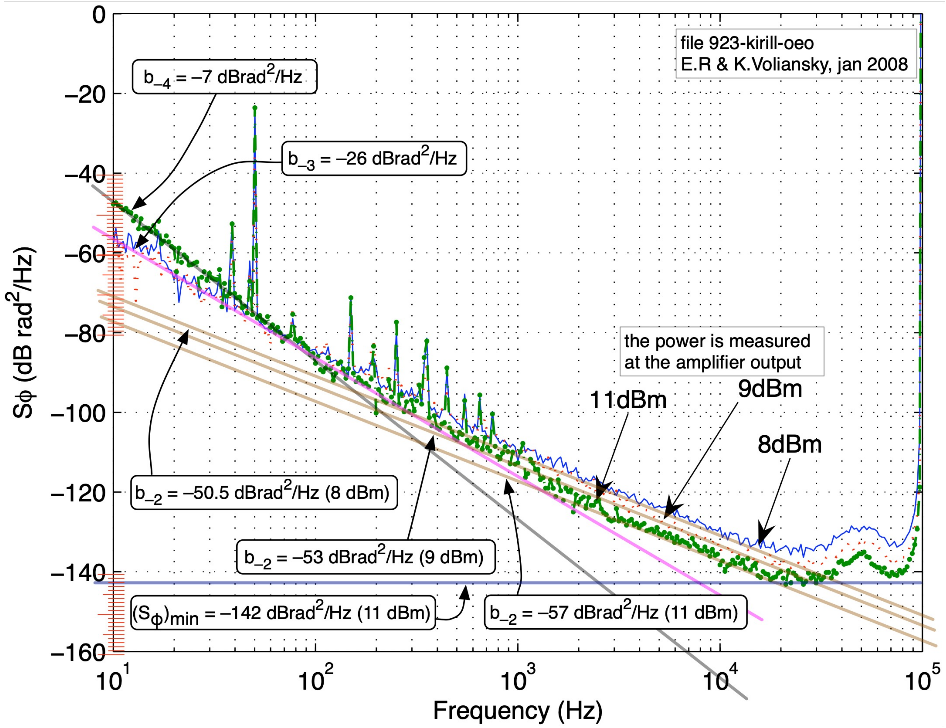

The oscillator phase noise minima are 6 dB lower than $b_0=N/P_0$ (white noise)

$m = 0.725$ (P_{rf}=11 dBm)

$(S_\varphi)_{\min} = -142$ dB

$F = 10$ dB (incl. couplers)

$\eta = 0.6$

$\nu_l = 194$ THz

$$(S_\varphi)_{\min} = \frac{8}{m^2}\left\{\frac{Fk_BT_0}{R_0}\left[\frac{h\nu_l}{q\eta}\right]^2\frac{1}{\overline{P}_l^2} + 2\frac{h\nu_l}{\eta}\frac{1}{\overline{P}_l}\right\}$$

Feeding the available data in the model we get

$P_0 = 6.4$ µW (RF, –22 dBm)

$P_l \approx 0.71$ mW (optical)

There is room for engineering

Noise transfer function – Simulation

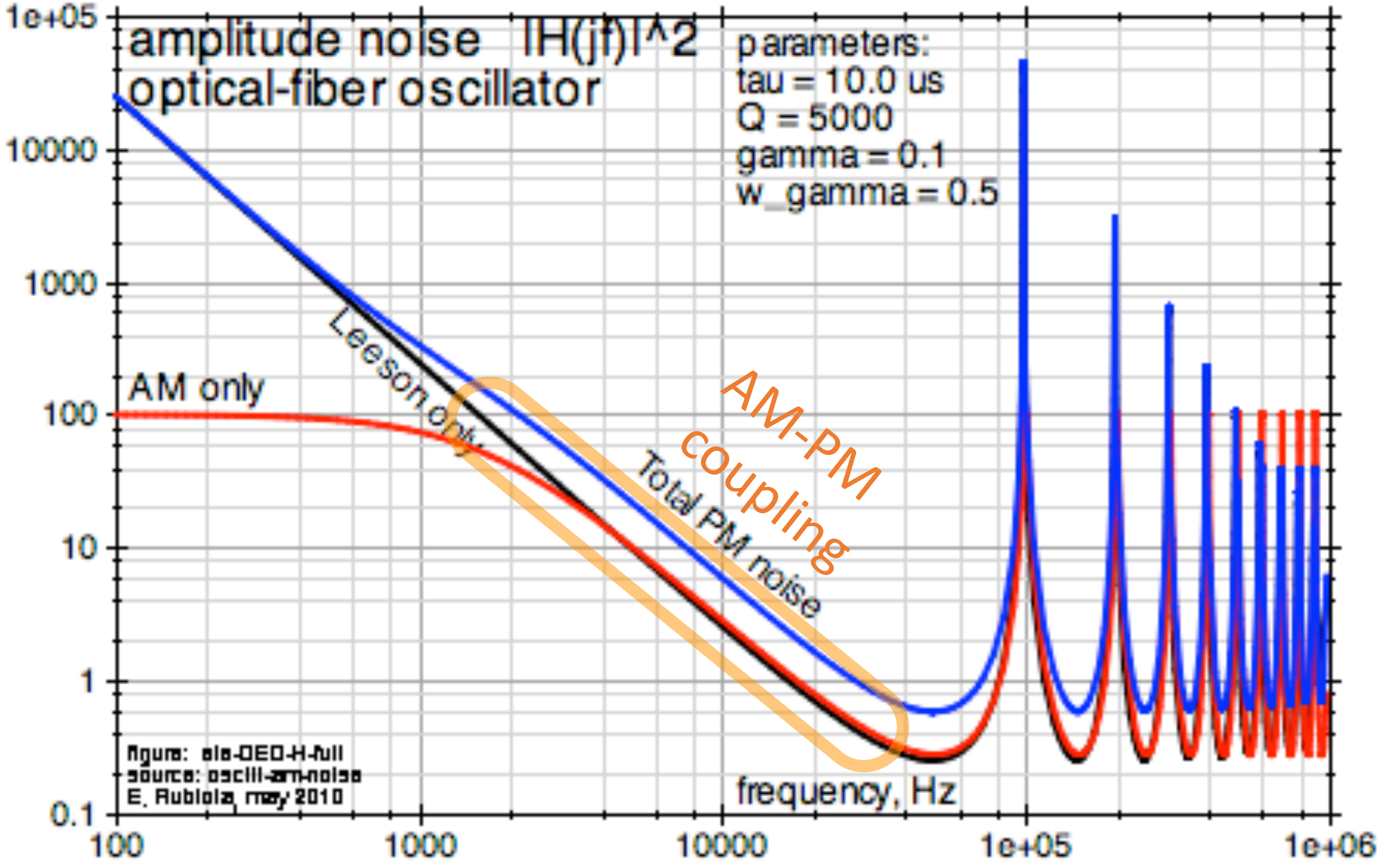

Notice that the AM-PM coupling can increase or decrease the PM noise

In a real oscillator, flicker noise shows up below some 10 kHz
In the flicker region, all plots are multiplied by $1/f$

OEwaves OEO phase noise

A. Savchenkov & al, Opt. Lett 35(10) 1572-74, 15 may 2010, Fig.2

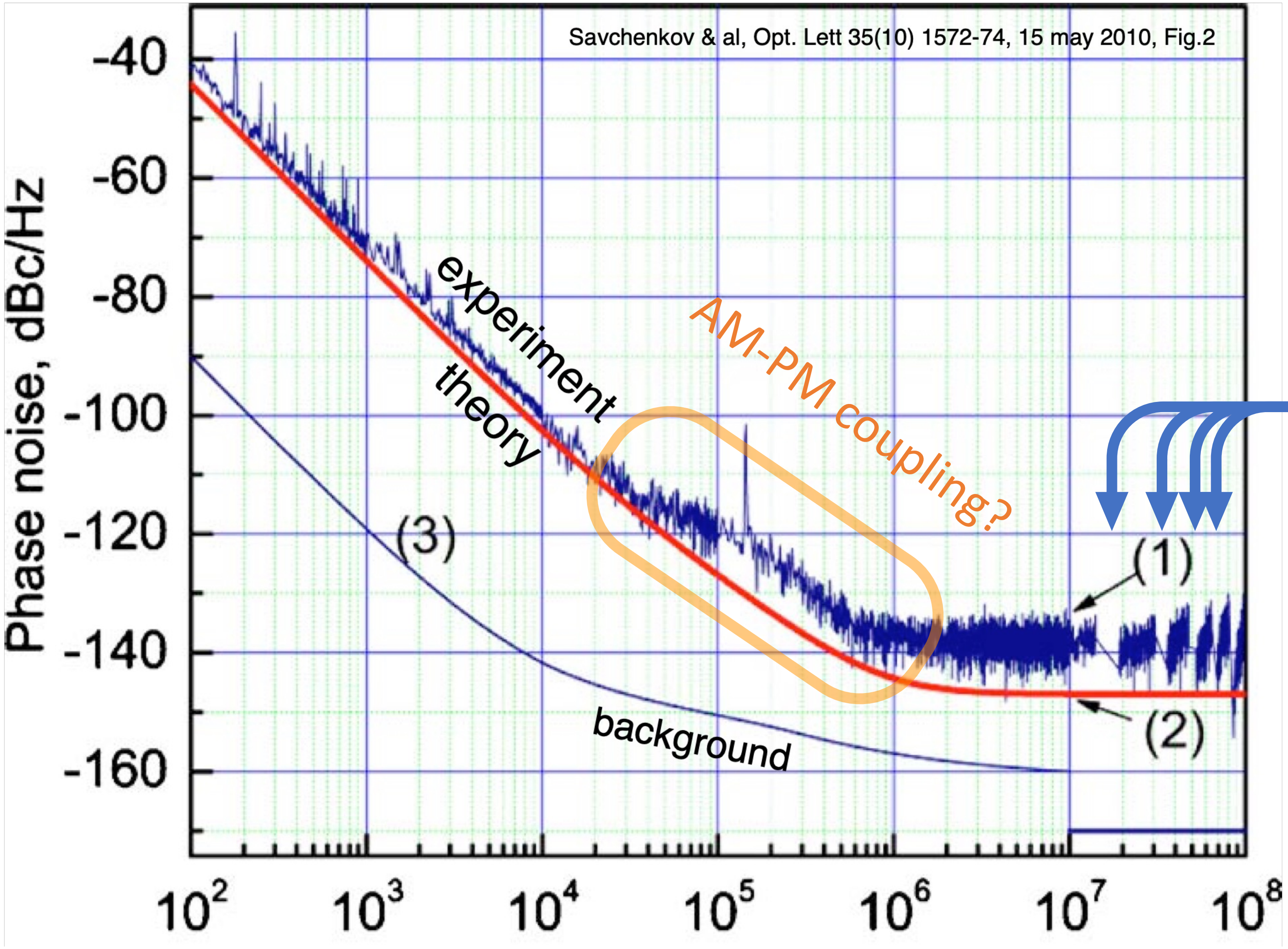

Likely, suppressed data at the noise resonances

Things May Not Be That Simple

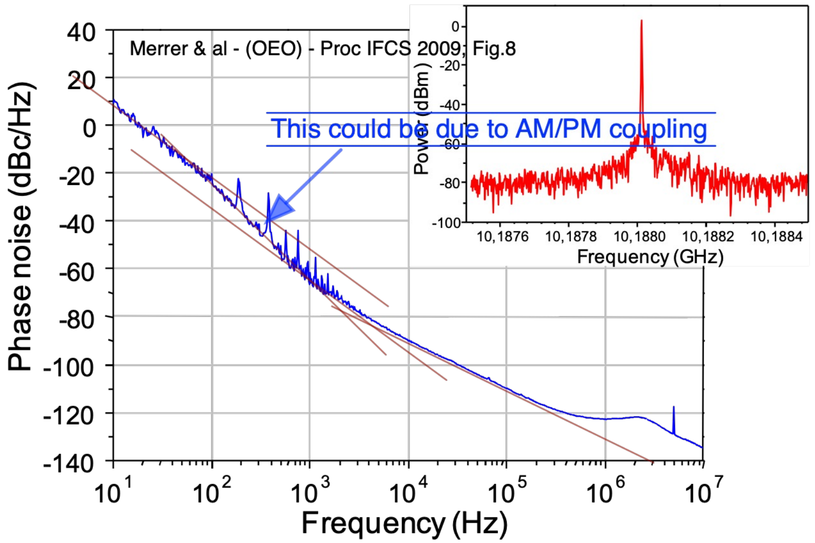

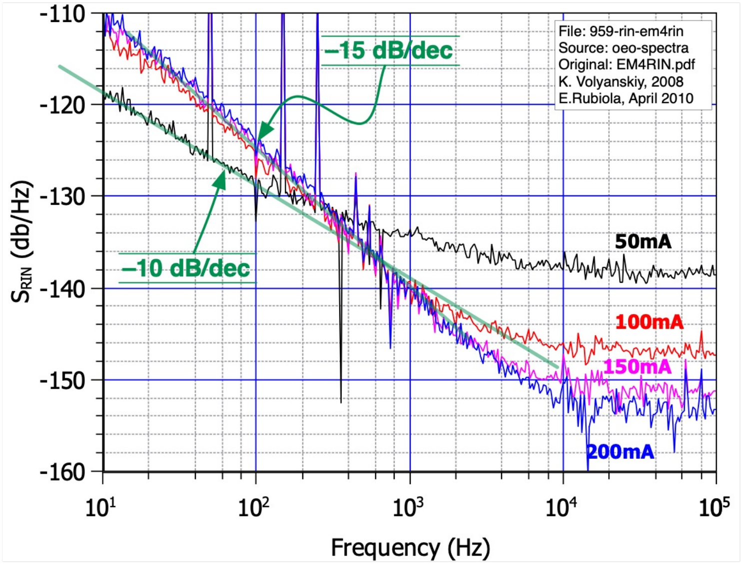

K. Volyanskiy et al, arXiv:0809.4132 [physics.optics], 2008, Fig.3
Also K. Volyanskiy PhD thesis p.51, Fig.3.12(a), 2009

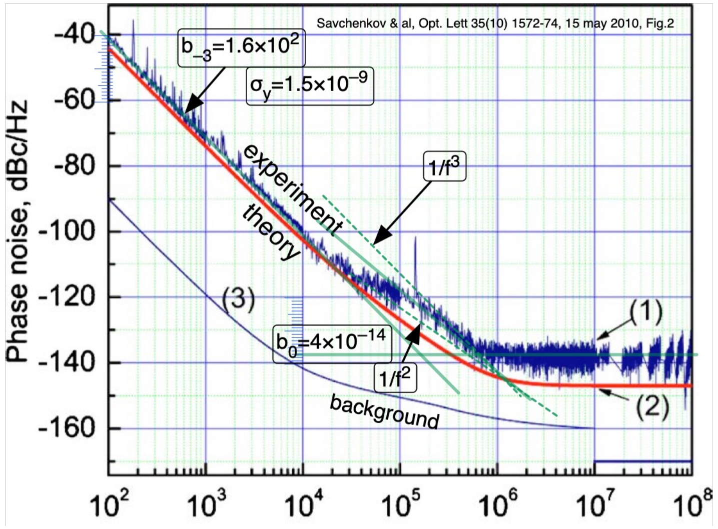

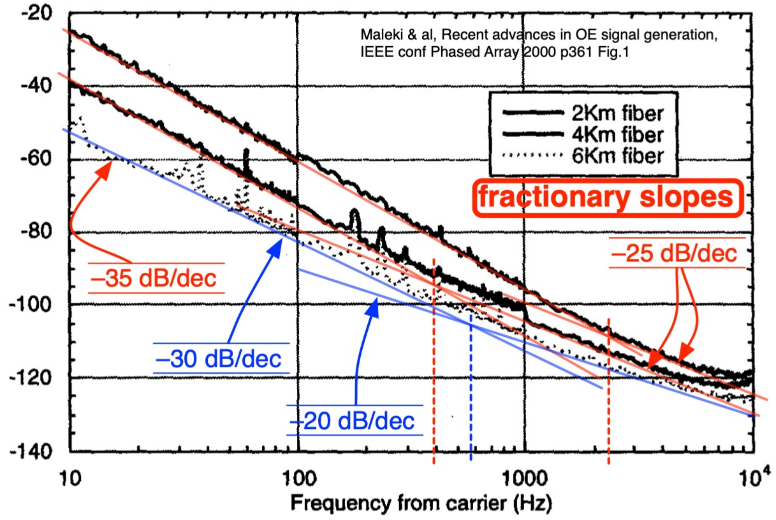

Noise spectra

Spectrum from K. Volyanskiy & al., IEEE JLT, 2010 (double check)

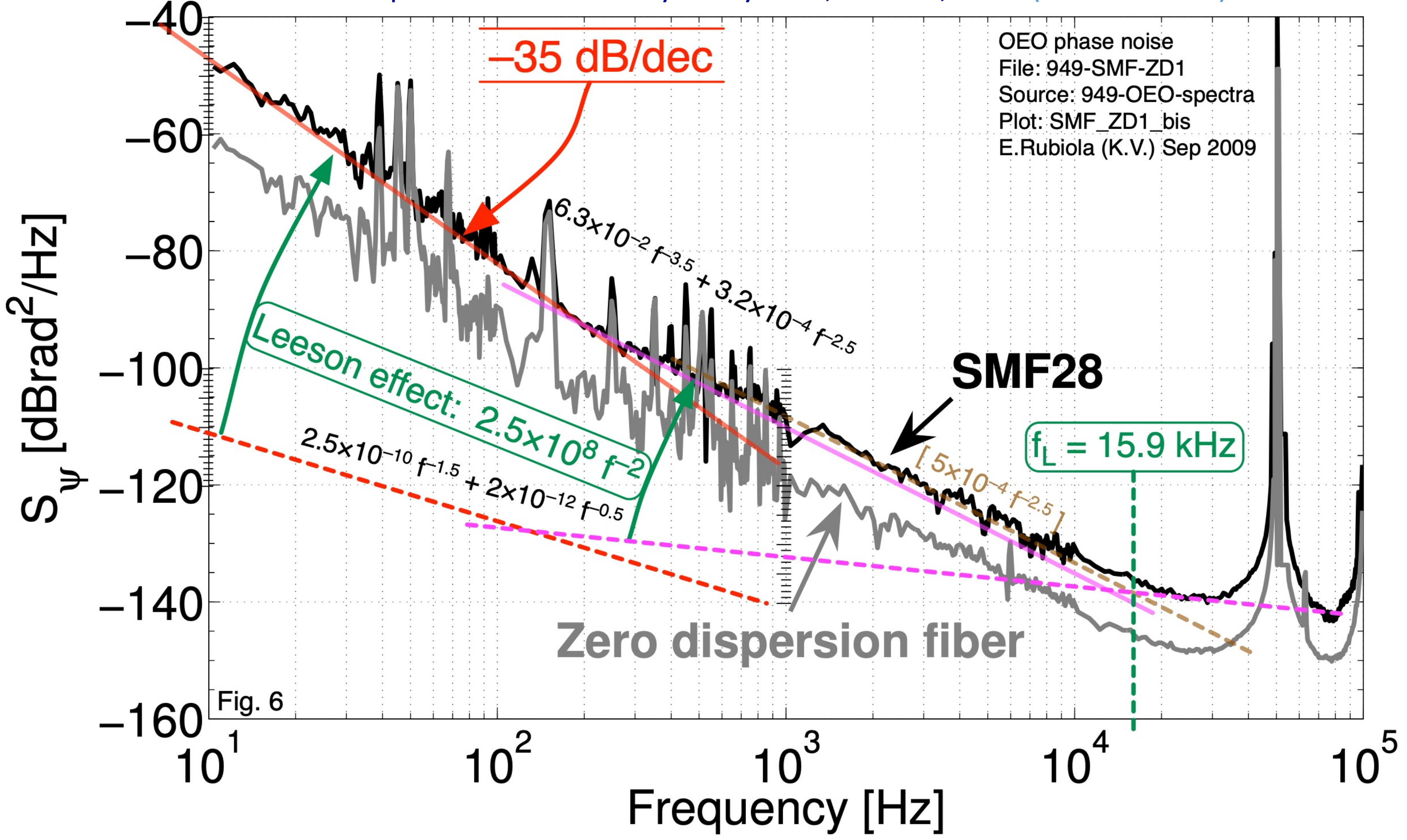

Unfortunately, the awareness of this model come after the end of the experiments

Noise spectra

X.S.Yao & al., NASA TMO Report 42-135 (1998), Fig. 6
The figure is © NASA, comments are mine

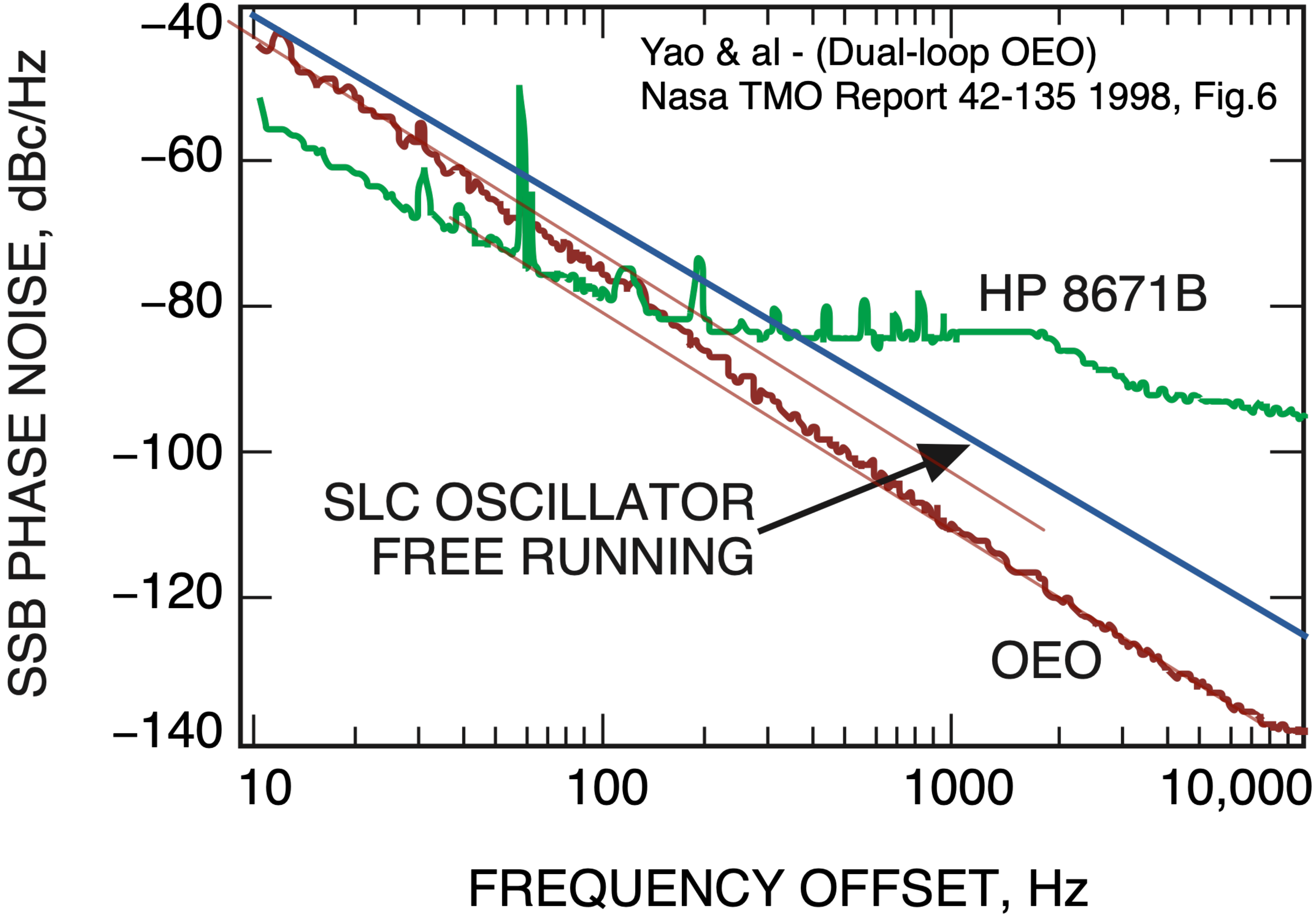

Conclusions

Acknowledgements

I am grateful to Lute Maleki and to John Dick for numerous discussions during my visits at the NASA JPL, which are the first seed of my approach to the oscillator noise

I am indebted to a number of colleagues and friends for invitations and stimulating discussions
- dr. Tim Berenc, ANL, Argonne
- dr. Holger Schlarb, DESY, Hambourg
- prof. Theodor W. Hänsch and dr. Thomas Udem, MPQ, München

This material would never have existed without continuous discussions, help and support of Vincent Giordano, FEMTO-ST, over >20 years

This presentation is based on

E.Rubiola, *Phase noise and frequency stability in oscillators*, Cambridge 2008,

and on the complementary material

E. Rubiola, R. Brendel, A generalization of the Leeson effect, arXiv:1004.5539 [physics.ins-det]

home page http://rubiola.org

Dave and Enrico at the end of a tutorial

IEEE Frequency Control Symposium, S. Francisco, Ca, 1–5 May 2011

Photo by Barbara Leeson, Dave’s wife

Summary of relevant points

- The Leeson effect consists in a phase-to-frequency conversion
- fully explained as a phase (noise) integration
- takes place below $f_L = \nu_0/2Q$
- The step response provides analytical solutions and physical inside.
  (Same formalism introduced by Oliver. Heaviside in network theory)
- Buffer noise and resonator instability add to the Leeson effect
- Amplifier phase noise
- white noise: S_ϕ scales down as the carrier power P_0
- flicker noise: S_ϕ is independent of P0
- Numerous oscillator spectra can be interpreted successfully
- The amplitude-noise response is similar to phase noise, but gain compression provides stabilization at low frequencies
- The theory indicates that amplitude-phase coupling results in a deviation from the polynomial law
- Unified AM/PM noise that applies to resonator-oscillators and to delay-line oscillators, including optical oscillators

End of lecture 9

Lecture 10

Scientific Instruments & Oscillators

Spring 2024

Lectures for PhD Students and Young Scientists

Enrico Rubiola

CNRS FEMTO-ST Institute, Besancon, France

INRiM, Torino, Italy

Contents

- The Pound Drever Hall frequency control

ORCID 0000-0002-5364-1835

home page http://rubiola.org

The Pound-Drever-Hall Frequency Control

Enrico Rubiola

CNRS FEMTO-ST Institute, Besancon, France

INRiM, Torino, Italy

Outline

Basic mechanism
Key ideas
Control loop
Resonators stability
Optimization
Applications
Alternate schemes

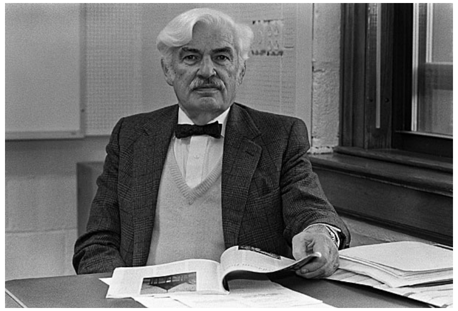

Robert Vivian Pound, 1919-2010
Photo Harvard University
https://news.harvard.edu/gazette/story/2012/10/robert-vivian-pound/

Ronald William P. Drever, 1931-2017
Photo CC-BY-SA 4.0 IDDrever
https://commons.wikimedia.org/wiki/File:Ronald_Drever_Glasgow_2007.jpg

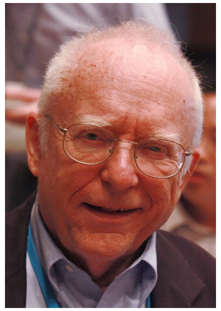

John Lewis “Jan” Hall, 1934-
Photo CC-BY-SA 3.0 Markus Pössel
https://en.wikipedia.org/wiki/John_L._Hall#/media/File:John_L._Hall_in_Lindau.jpg

home page http://rubiola.org

Basic Mechanism

Featured article

Eric D. Black, An introduction to Pound–Drever–Hall laser frequency stabilization, Am J Phys 69(1) January 2001, DOI 10.1119/1.1286663 (paywall)

Also available as Technical Note LIGO-T980045-00-D 4/16/98 (free access)

Overview

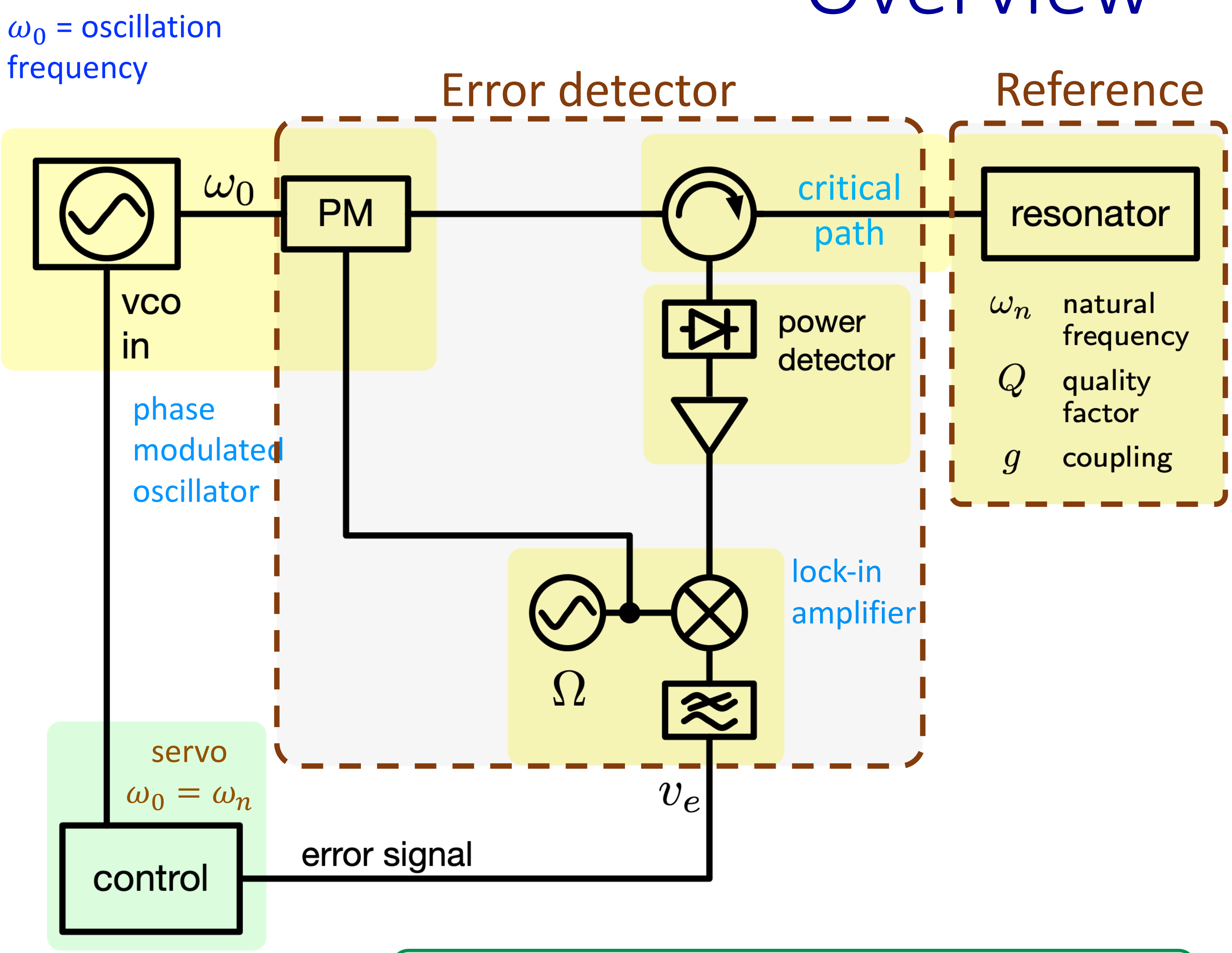

Error signal proportional to frequency error

$$v_e = D(\omega_0 - \omega_n)$$

Points of interest

- Power (intensity) detector is available from RF to optics
- Compensation of the critical path
  - Resonator is large / complex / difficult to access
- Null measurement of the frequency error
- Frequency modulation –> get out of the flicker region
- One-port resonator –> lowest dissipation –> narrowest linewidth
- Multimode resonators –> simple mode selection

Phase modulation, physics

$$v(t) = V_p \cos[\omega t - m \sin(\Omega t)]$$

Phasor diagram

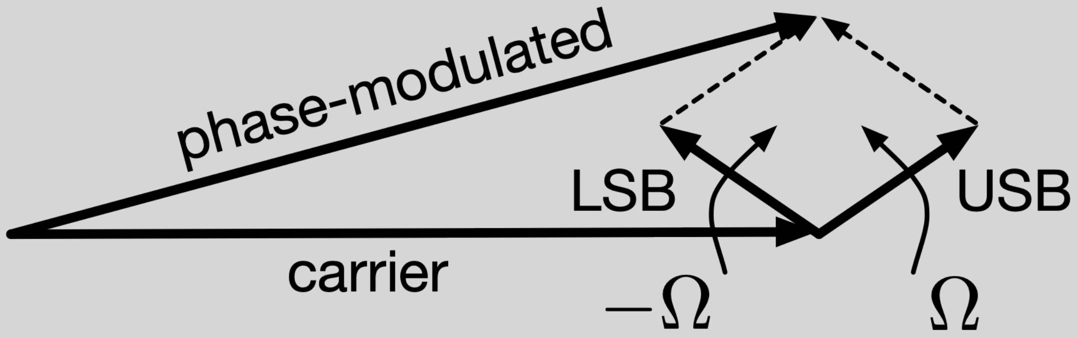

Frequency domain
(small m)

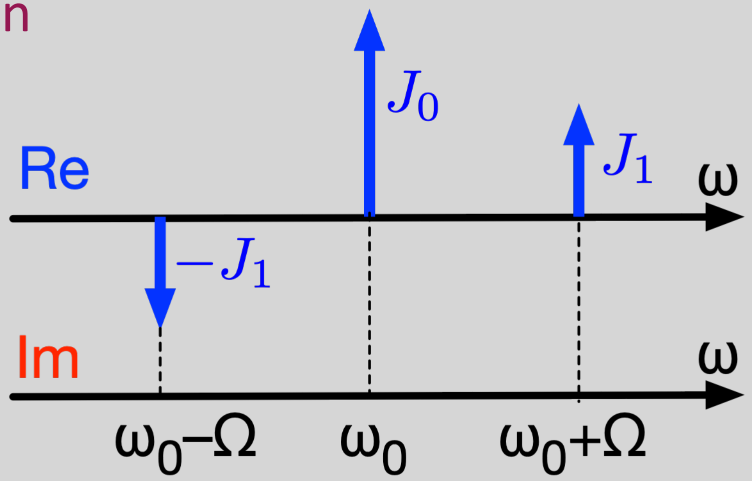

Bessel functions $J_n(m)$

Phase modulation, math

$$V = V_0 e^{i\omega t} e^{im \sin \Omega t}$$

$$= V_0 e^{i\omega t} \sum_{n=-\infty}^{\infty} J_n(m) e^{in\Omega t}$$

small m $$\simeq V_0 e^{i\omega t}\left[J_0(m) + J_{-1}(m) e^{-i\Omega t} - J_1(m) e^{-i\Omega t}\right]$$

$$= V_0\left[J_0(m) e^{i\omega t} - J_1(m) e^{i(\omega-\Omega)t}\right.$$

small m $$\simeq V_0\left[1 + \frac{m}{2}\left(-e^{-i\Omega t} + e^{i\Omega t}\right)\right]$$

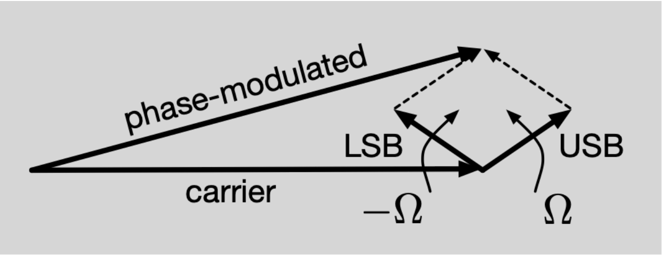

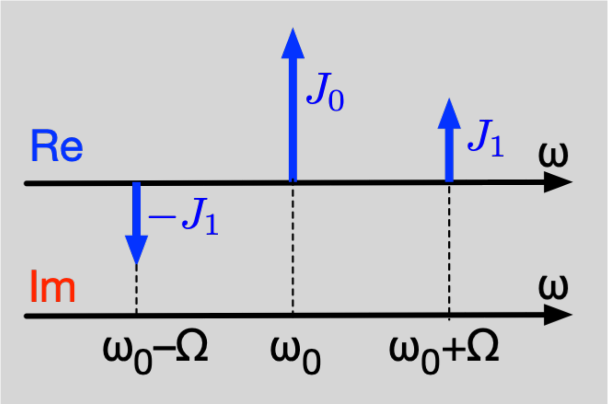

Carrier power

$$P_c = J_0^2(m) P_0 \simeq P_0$$

Sideband power

$$P_s = J_1^2(m) P_0 \simeq \frac{m^2}{4} P_0$$

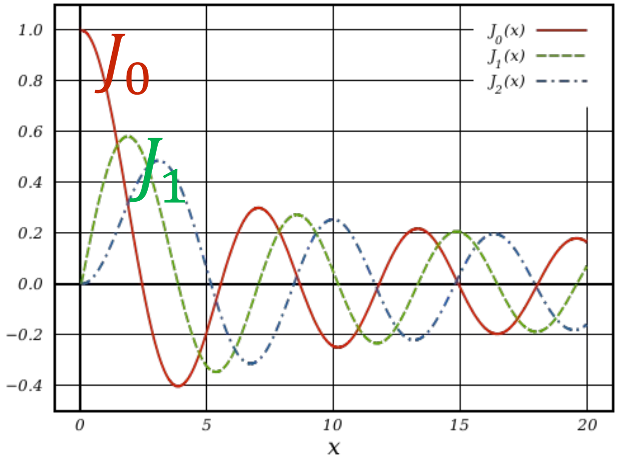

Jacobi-Angers expansion

$$e^{im\cos\phi} = \sum_{n=-\infty}^{\infty} i^n J_n(m) e^{in\phi}$$

$$e^{im\sin\phi} = \sum_{n=-\infty}^{\infty} J_n(m) e^{in\phi}$$

Symmetry, $z \in \mathbb{R}$

$$J_n(z) = \begin{cases} -J_n(z) & \text{odd } n \\ J_n(z) & \text{even } n \end{cases}$$

Small m

$$J_0(m) \simeq 1 - m^2/2$$
$$J_1(m) \simeq m/2$$

The reflection-mode resonator

ω_0 = oscillation frequency

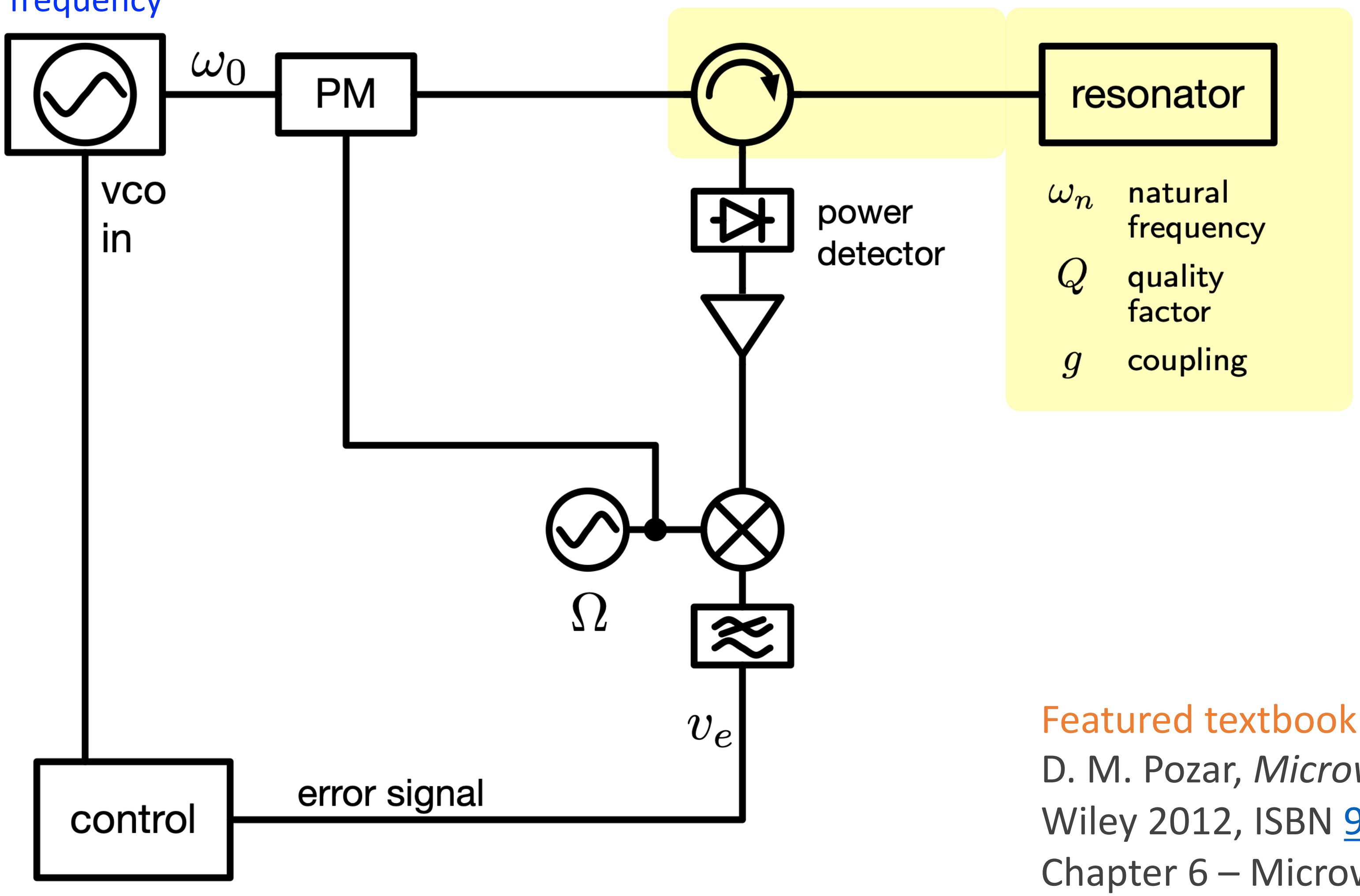

Featured textbook

D. M. Pozar, *Microwave Engineering* 4th ed, Wiley 2012, ISBN 978-0-470-63155-3

Chapter 6 – Microwave Resonators

Notice that the formalism is suitable to optics

Reflection coefficient Γ

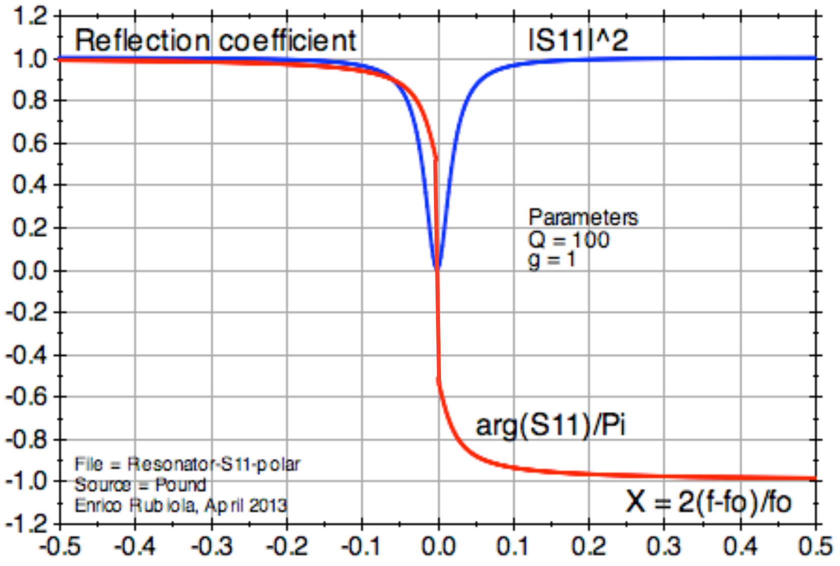

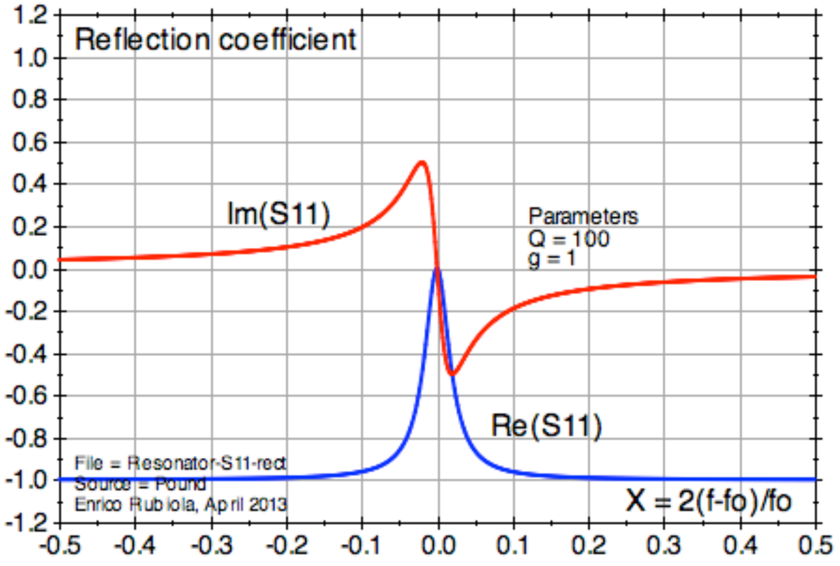

$$\Gamma = V^- / V^+$$

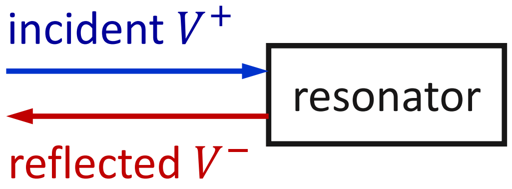

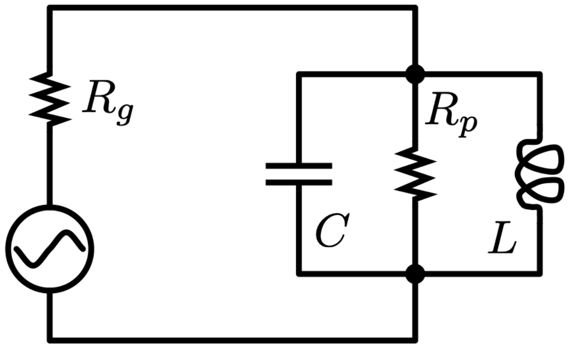

$$\Gamma = \frac{g - 1 - iQ_0\chi}{g + 1 + iQ_0\chi}$$

Proof omitted

Q_0 = unloaded "Q"

$g = R_p / R_g$ coupling

$\chi = \frac{\omega}{\omega_n} - \frac{\omega_n}{\omega}$ detuning

Approximation of Γ for small $Q\Delta\nu/\nu_n$

Start from $\Gamma = \frac{g-1-iQ_0\chi}{g+1+iQ_0\chi}$

use $\chi \simeq \frac{2\Delta\nu}{\nu_n}$

$$\Gamma = \frac{g-1-i2Q_0\,\Delta\nu/\nu_n}{g+1+i2Q_0\,\Delta\nu/\nu_n}$$

collect $g+1$

$$\Gamma = \frac{g-1-i2Q_0\frac{\Delta\nu}{\nu_n}}{(g+1)\left(1+i\frac{2Q_0}{g+1}\frac{\Delta\nu}{\nu_n}\right)}$$

use $\frac{1}{1+\epsilon} \simeq 1-\epsilon$

$$\Gamma = \frac{\left[g-1-i2Q_0\frac{\Delta\nu}{\nu_n}\right]\left[1-\frac{i2Q_0}{g+1}\frac{\Delta\nu}{\nu_n}\right]}{g+1}$$

split $\Re$ and $\Im$

$$\Gamma = \frac{\left\{g-1-\frac{4Q_0^2}{g+1}\left(\frac{\Delta\nu}{\nu_n}\right)^2\right\}-i2Q_0\left\{1+\frac{g-1}{g+1}\right\}\frac{\Delta\nu}{\nu_n}}{g+1}$$

remove the main fraction

$$\Gamma = \left\{\frac{g-1}{g+1}+\frac{4Q_0^2}{(g+1)^2}\left(\frac{\Delta\nu}{\nu_n}\right)^2\right\}-i\frac{2Q_0 g}{(g+1)^2}\frac{\Delta\nu}{\nu_n}$$

drop $(\Delta\nu/\nu_n)^2$

$$\Gamma = \frac{g-1}{g+1}-i\frac{4Q_0 g}{(g+1)^2}\frac{\Delta\nu}{\nu_n}$$

$$\Gamma \simeq \frac{g-1}{g+1}-i\frac{4Q_0 g}{(g+1)^2}\frac{\Delta\nu}{\nu_n}$$

- $\frac{g-1}{g+1}$ → resistance mismatch
- $\frac{4Q_0 g}{(g+1)^2}\frac{\Delta\nu}{\nu_n}$ → frequency error, odd function

Approximations for Γ

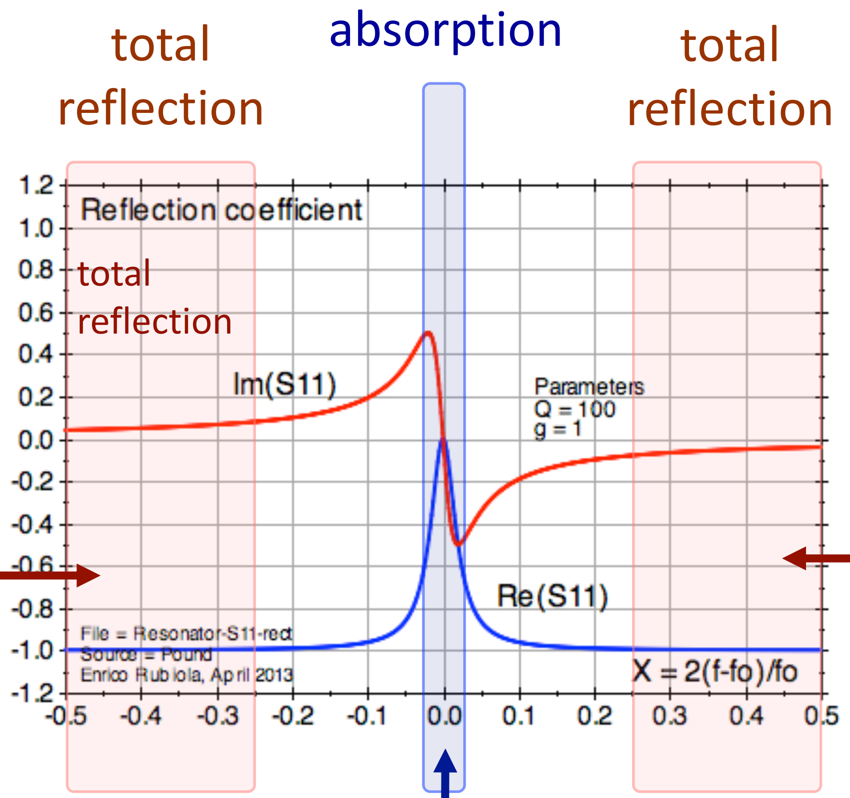

Off-resonance

$\Gamma \simeq -1$

Off-resonance

$\Gamma \simeq -1$

Resonance, close to ω_n

$$\Gamma \simeq \frac{g-1}{g+1} - i\,\frac{4Q_0 g}{(g+1)^2}\,\frac{\Delta\nu}{\nu_n}$$

The reflected signal – Physics

the input signal is phase-modulated

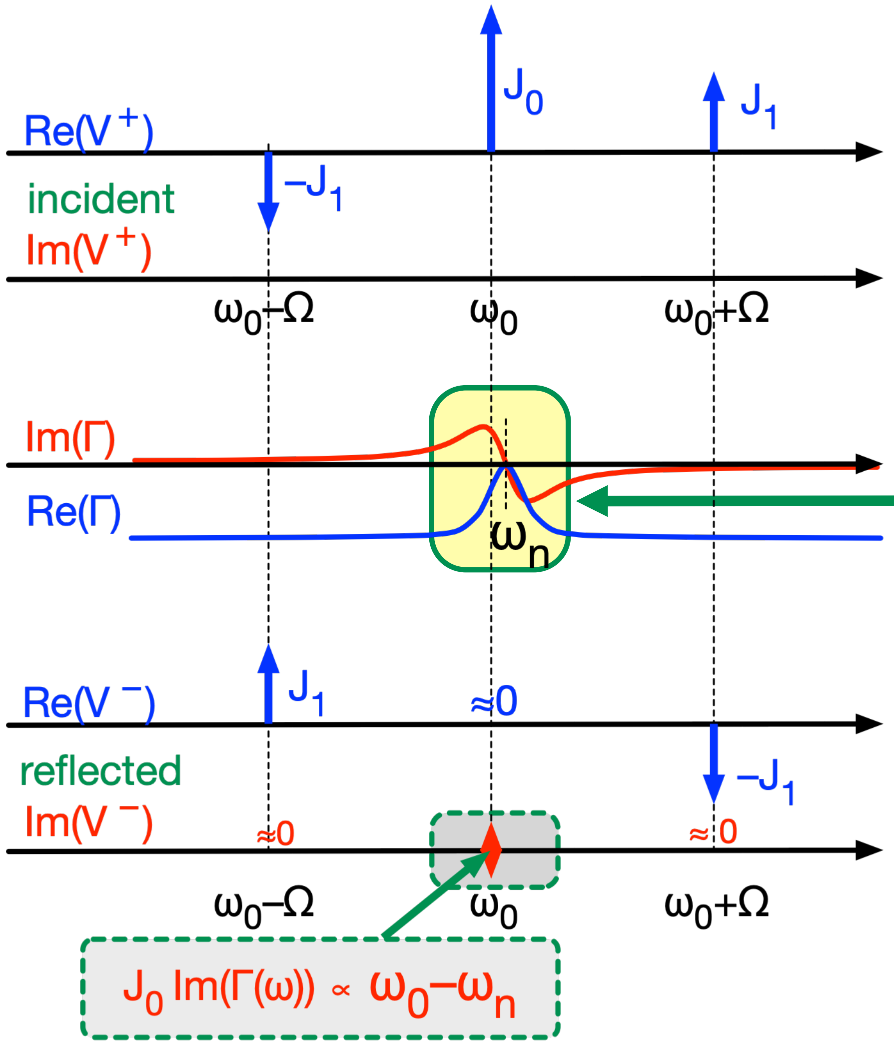

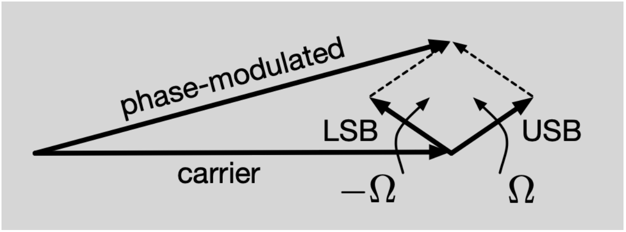

$$\Gamma \simeq \frac{g-1}{g+1} - i\,\frac{4Q_0 g}{(g+1)^2}\,\frac{\Delta\nu}{\nu_n}$$

The reflected signal – Math

the input signal is phase-modulated

Incident wave

$$V^+ = V_0 \left[-J_1(m) e^{i(\omega-\Omega)t} + J_0(m) e^{i\omega t} + J_1(m) e^{i(\omega+\Omega)t} \right]$$

LSB carrier USB

use $\Gamma(\omega \pm \Omega) \simeq -1$ and $\Gamma(\omega) \simeq \frac{g-1}{g+1} - i \frac{4Q_0}{g+1} \frac{\Delta\omega}{\omega_n}$

Reflected wave

$$V^- = V_0 \left\{ J_1(m) e^{i(\omega-\Omega)t} + J_0(m) \left[\frac{g-1}{g+1} - i \frac{4Q_0}{g+1} \frac{\Delta\omega}{\omega_n} \right] e^{i\omega t} - J_1(m) e^{i(\omega+\Omega)t} \right\}$$

LSB carrier USB

impedance mismatch

frequency error, $\propto (\omega - \omega_n)$

Power detector

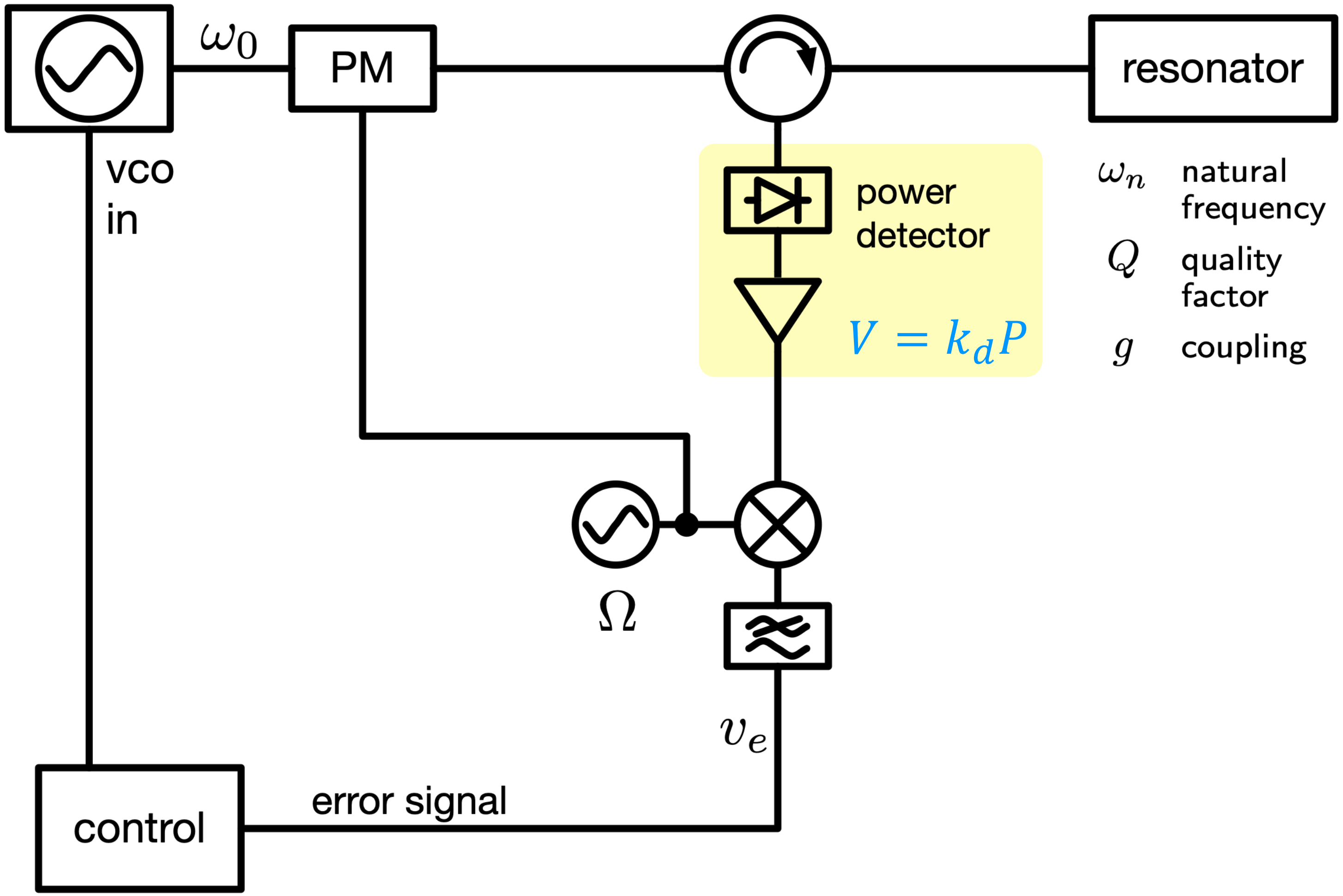

$$\text{Power } P = \frac{1}{2}\Re\{VI^*\} = P\frac{1}{2R_0}\Re\{VV^*\}$$

V and *I* are peak values

Power detector

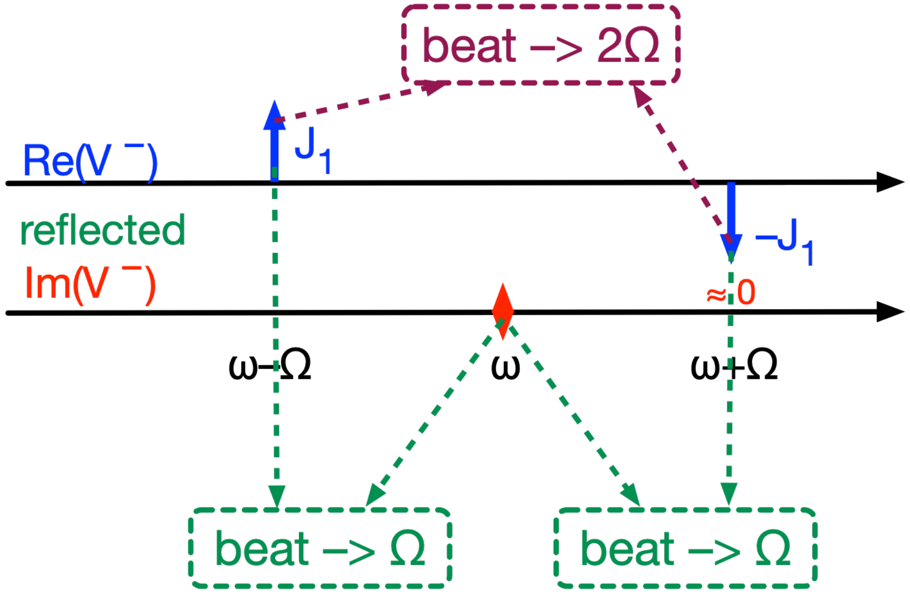

$$P = \frac{1}{2R_0}\Re\{VV^*\}$$

$$(a+b+c)^2 =$$

$$\underbrace{a^2+b^2+c^2}_{\text{DC}} + \underbrace{2ab}_{2\Omega} + \underbrace{2ac+2bc}_{\Omega}$$

dc terms

$$P = \frac{|V_0|^2}{2R_0}\left\{J_1^2(m) + \frac{1}{2}J_0^2(m)\left[\frac{g-1}{g+1}\right]^2 + \frac{1}{2}J_0^2(m)\left[\frac{4Q_0}{g+1}\frac{\Delta\omega}{\omega_n}\right]^2\right\} +$$

$$-\frac{|V_0|^2}{2R_0}J_1^2(m)\cos(2\Omega t) + \frac{|V_0|^2}{2R_0}2J_0(m)J_1(m)\frac{4Q_0}{g+1}\frac{\Delta\omega}{\omega_n}\sin(2\Omega t)$$

diagnostic

error signal

The lock-in amplifier

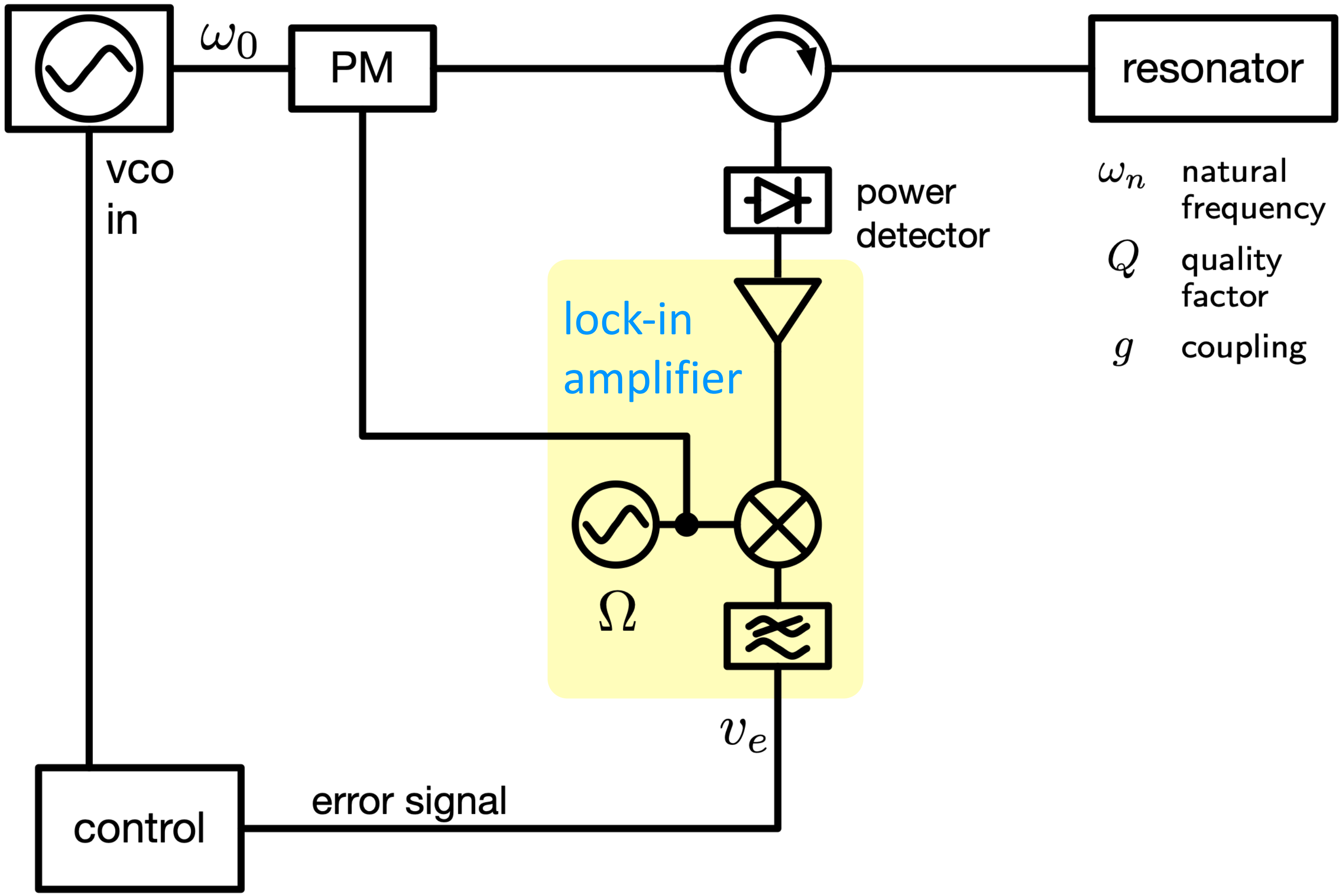

$$v_e \propto \nu_0 - \nu_n$$

The lock-in amplifier

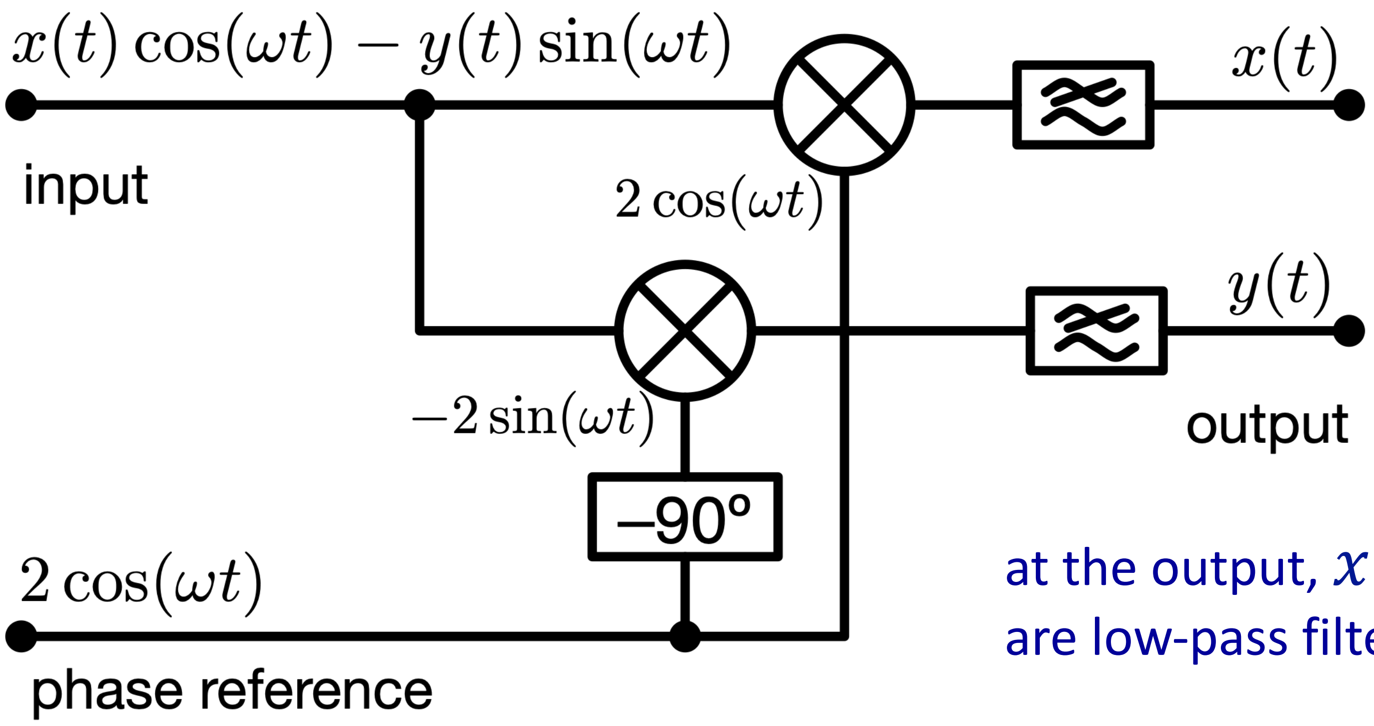

at the output, $x(t)$ and $y(t)$ are low-pass filtered

error ⟶ $$v_e = \frac{|V_0|^2}{2R_0} 2J_0(m)J_1(m)\frac{4Q_0}{g+1}\frac{\Delta\omega}{\omega_n}$$

diagnostic ⟶ $$v_d = -\frac{|V_0|^2}{2R_0} J_1^2(m)$$

Summary

The frequency discriminant D is proportional to

- Oscillator power P_0
- Modulation index m
- Resonator's Q_0/ω_n
- Power-detector gain k_d [V/W]
- RF gain at the detector output (not shown)
- Gain of the lock-in amplifier (not accounted for in equations)

…And affected by the coupling coefficient g

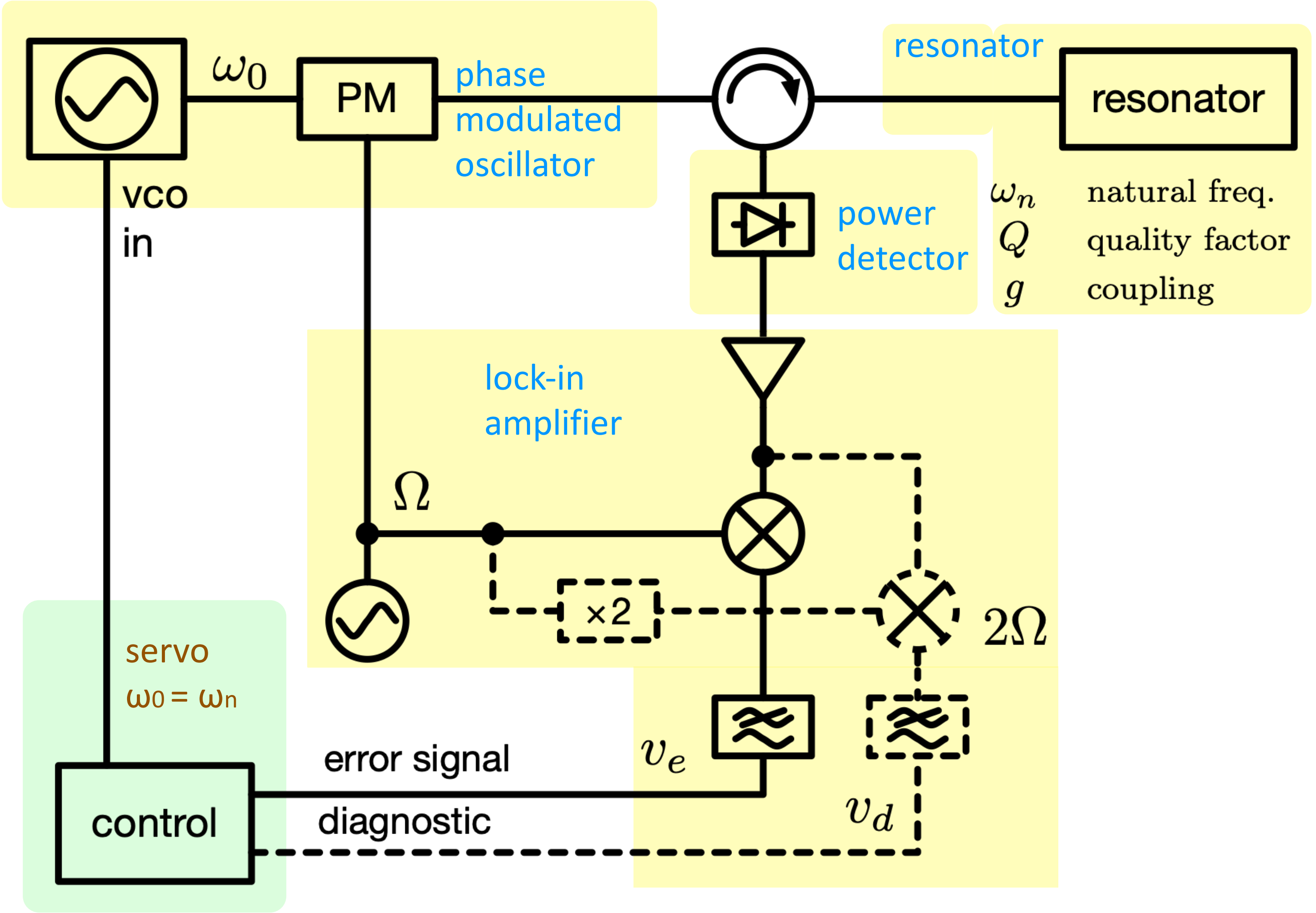

error signal $$v_e = D(\omega_0 - \omega_n)$$

Key Ideas

Use a power detector

- Power detectors are available in the widest frequency range
    - Sub-audio to UV, and more
    - Including the THz band
- The power detector has quadratic response to voltage – or to electric field

Even vs Odd Function

- The detector provides a signal proportional to the power (intensity)
  - Even function at ω_0
  - Unmodulated signal not suitable to feedback control

- The modulation mechanism provides a signal proportional to the imaginary part
  - Odd function at ω_0
  - Great for feedback control

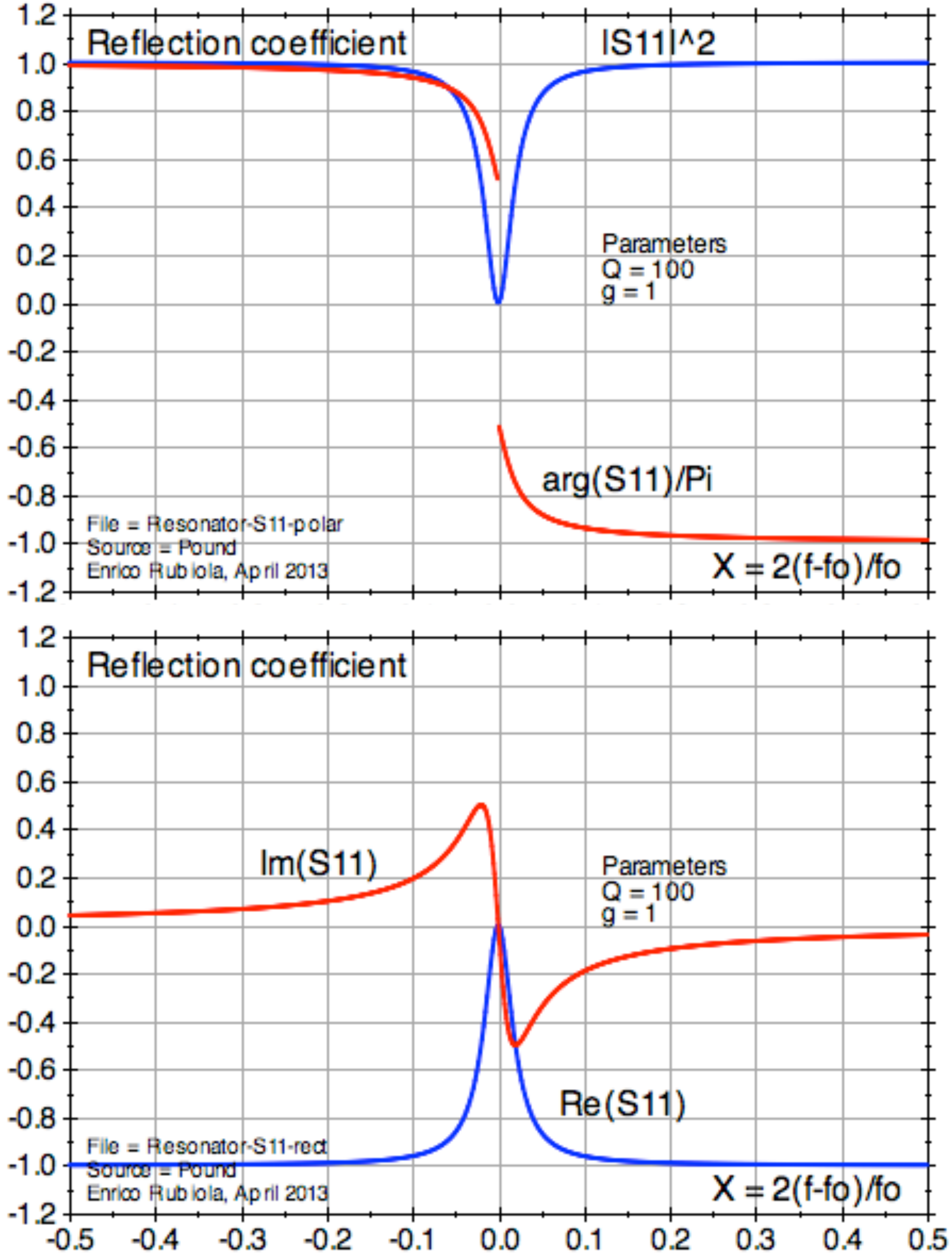

The 10^{-6} golden rule

The oscillator tracks the resonator, and follows its fluctuations
The oscillator contributes too

- It is generally agreed that a microwave frequency control loop can lock within 10^{-6} of the bandwidth
  - Cs standard: 10^{-6} × (100 Hz / 9.2 GHz) ≈ 10^{-14} stability
  - Cryogenic sapphire: 10^{-6} × (10 Hz / 10 GHz) ≈ 10^{-15} stability
- In optics, the 10^{-6} rule yields still unachieved stability
  - Optical FP: 10^{-6} × (10kHz/200THz) ≈ 5×10^{-19} stability
- The resonator fluctuation is not a part of the control, and accounted for separately

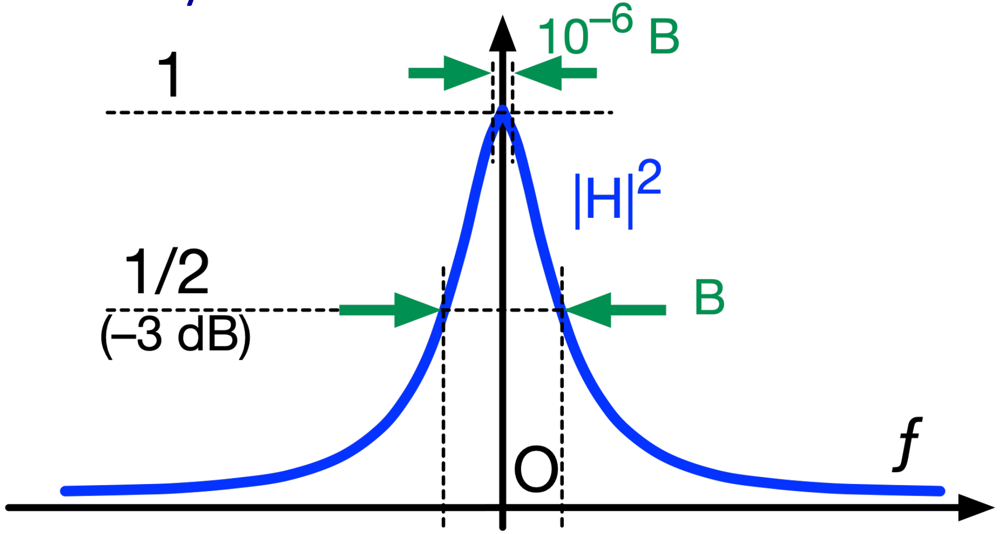

Modulation and flicker

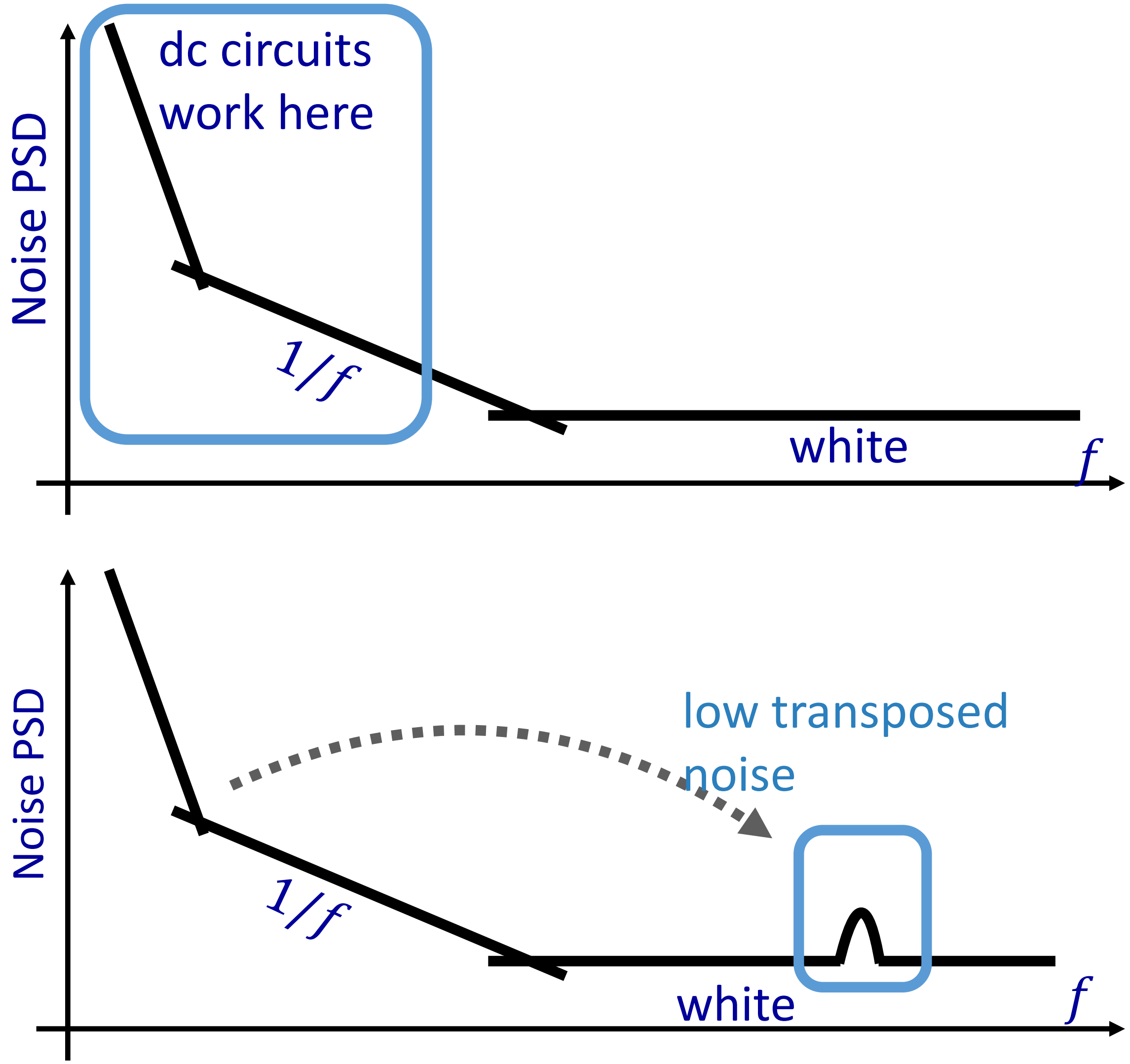

Get out of the flicker and drift region !!!

The virtues of the AC null measurement

- Absolute measurements rely on the "brute force" of instrument accuracy
- Differential measurements rely on the difference of two nearly equal quantities, something like $q_2 - q_1$. However similar, this is not our case!
- Null measurements rely on the measurement of a quantity as close as possible to zero – ideally zero.
- The Pound scheme detects
  - Null of $\Im(\Gamma(\omega))$
  - AC regime, after down-converting to Ω

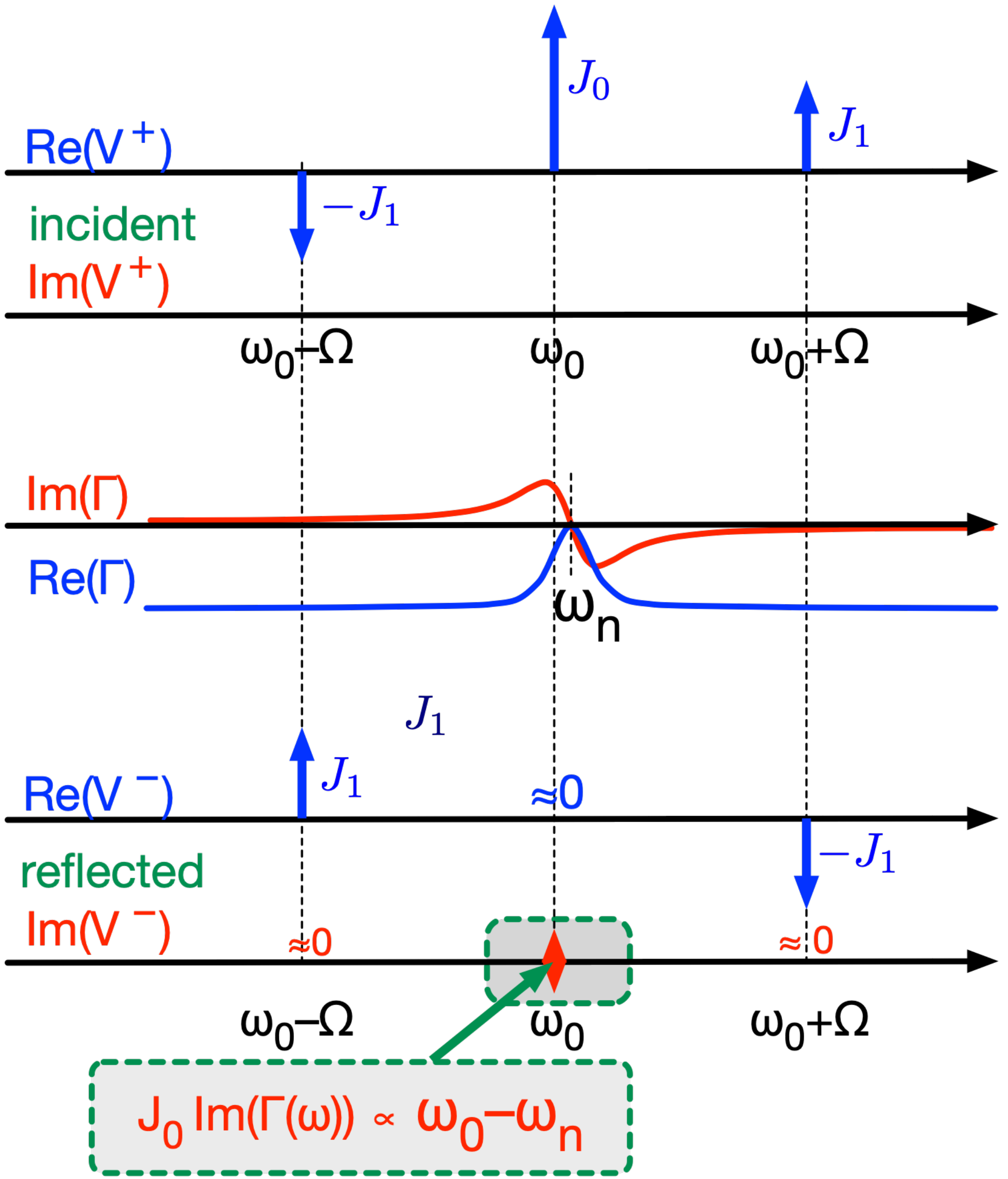

Insensitive to the critical path

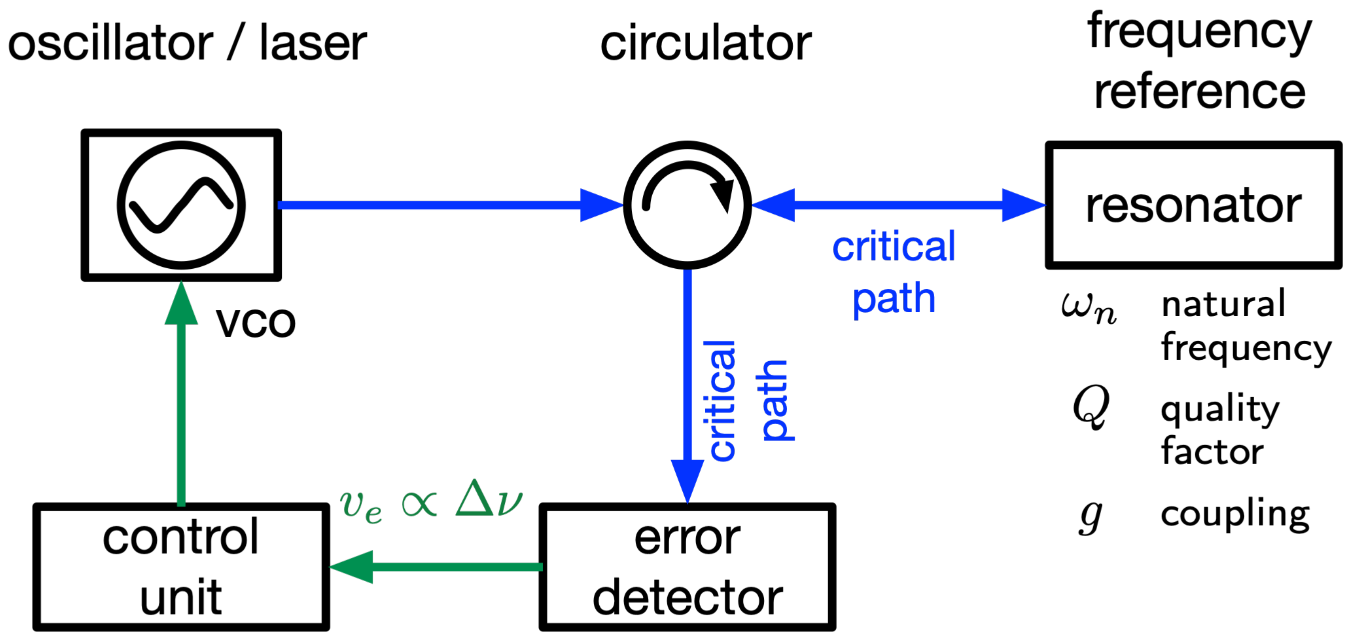

A length fluctuation does not affect

- The phase and amplitude relations between carrier and sidebands
- In turn, the measurement of Δω

(No longer true in the presence of dispersion)

The mechanism is the same of radio emission

The virtues of the one-port resonator

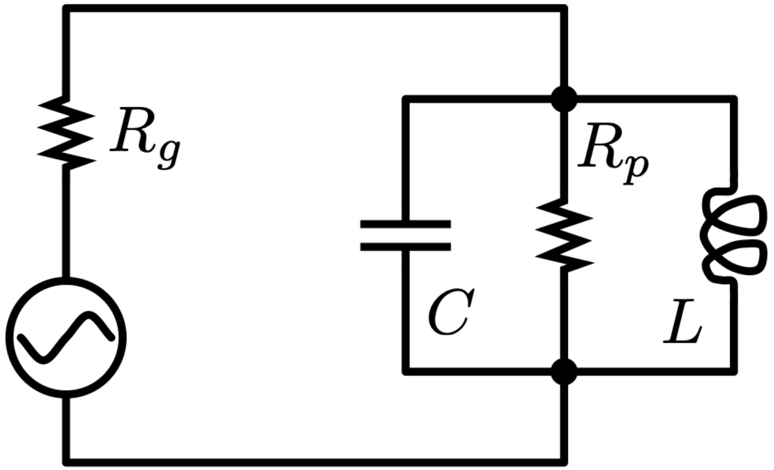

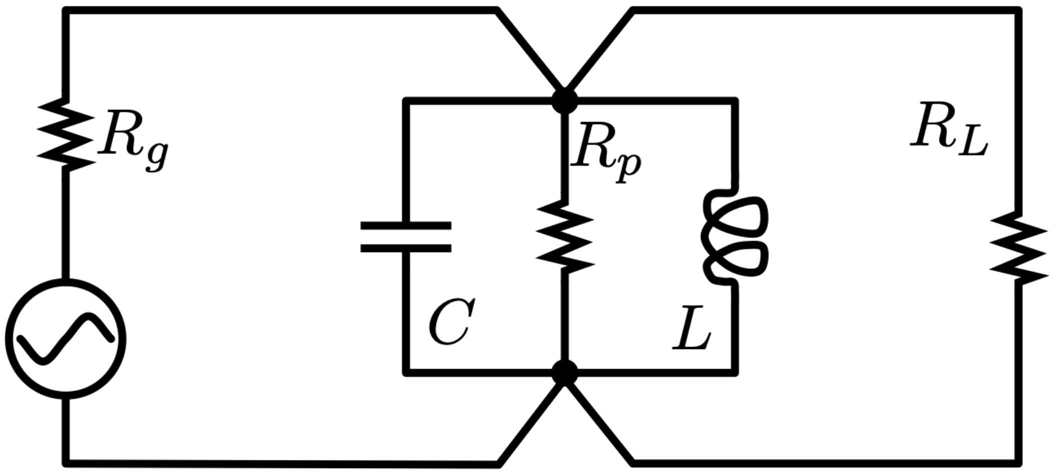

- Electrical
  - Smaller dissipation than the two-port resonator
  - Hence higher Q
- Simpler, related to
  - Vacuum
  - Cryogenic environment
  - Resonator far from the oscillator

Control Loop

Featured book

K.J. Åström, R.M. Murray, Feedback Systems, Princeton 2008

Caveat: however outstanding, this book does not focus on TF applications

Sweep the oscillator frequency

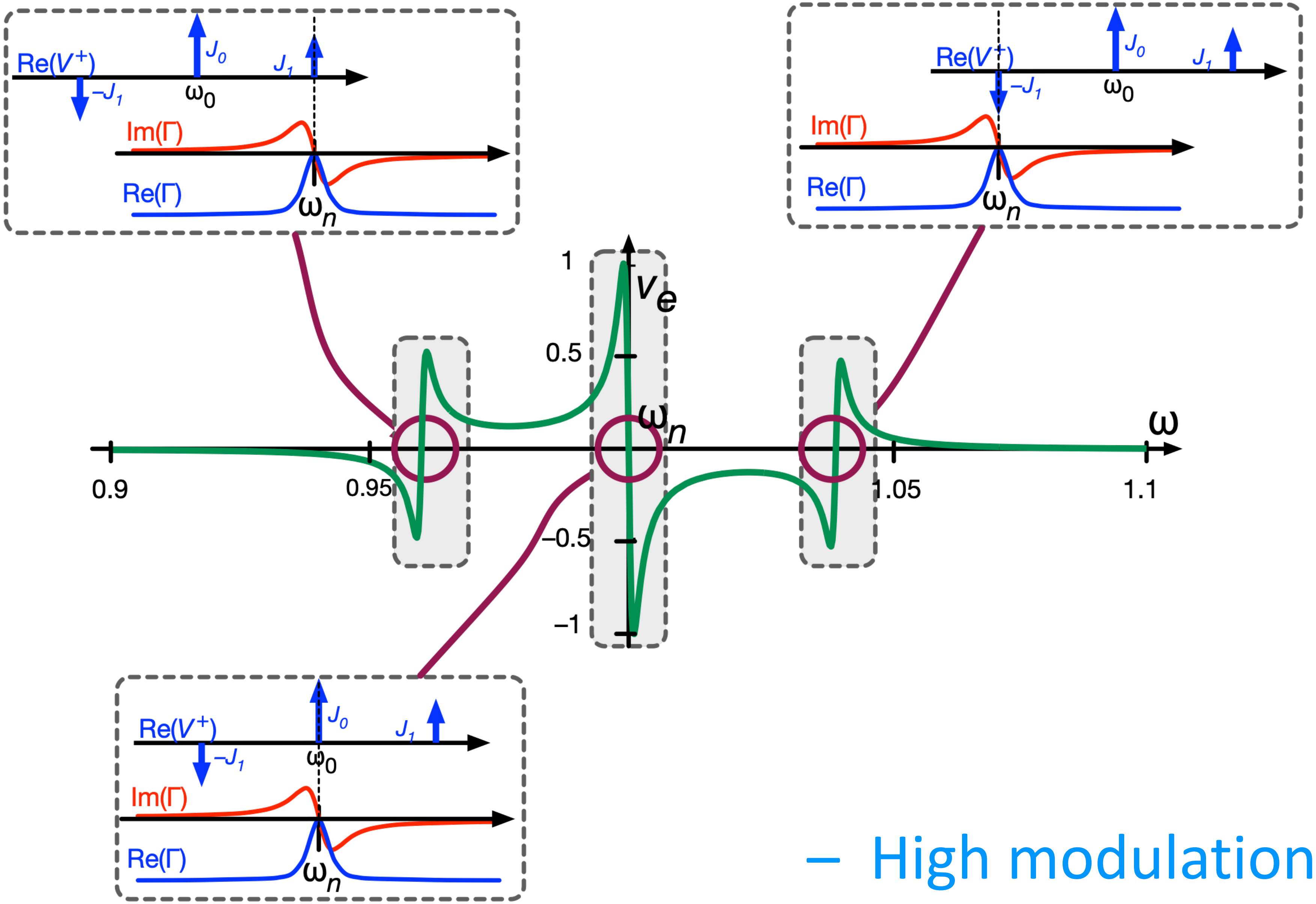

– High modulation frequency –

Sweep the oscillator frequency

Courtesy of Alexandre Didier, FEMTO-ST Institute

Control loop

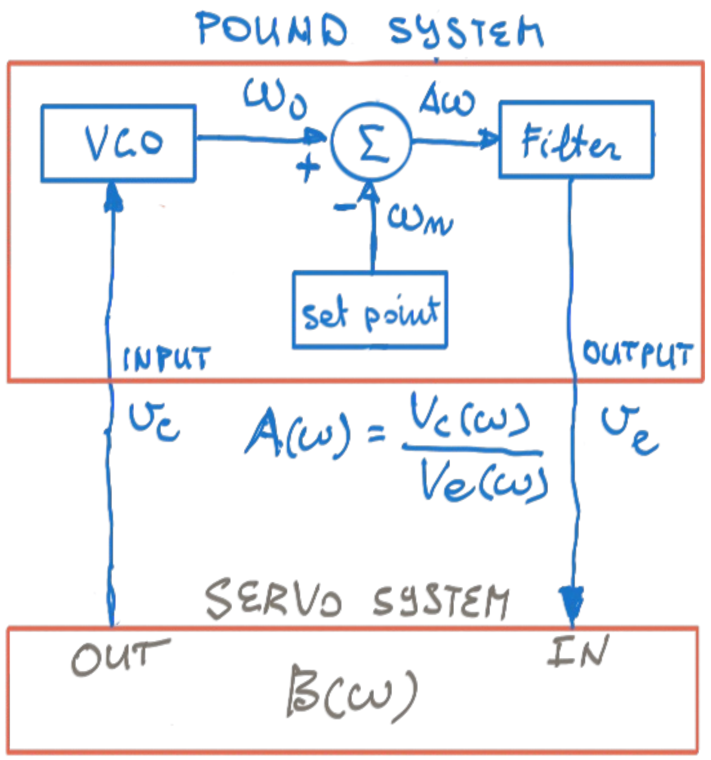

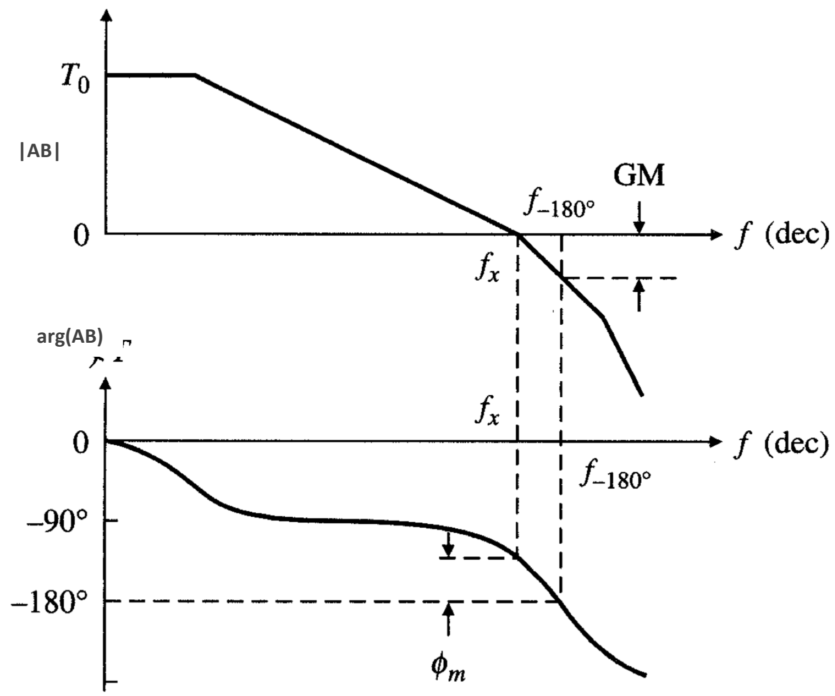

Franco S, Design with operational amplifier and analog integrated circuits 2ed, McGraw Hill 1998 – Fig.8.1.

- The control loop must be stable
  - |AB| < 1 at the critical frequency where arg(AB) = π
  - In practice, ≥ π/4 (45º) phase margin is needed
- Higher dc gain provides higher accuracy

Transfer function

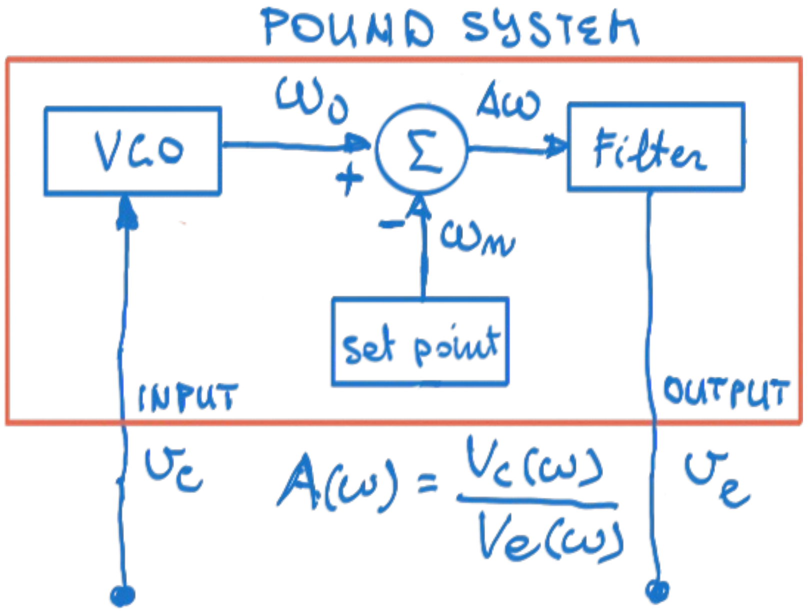

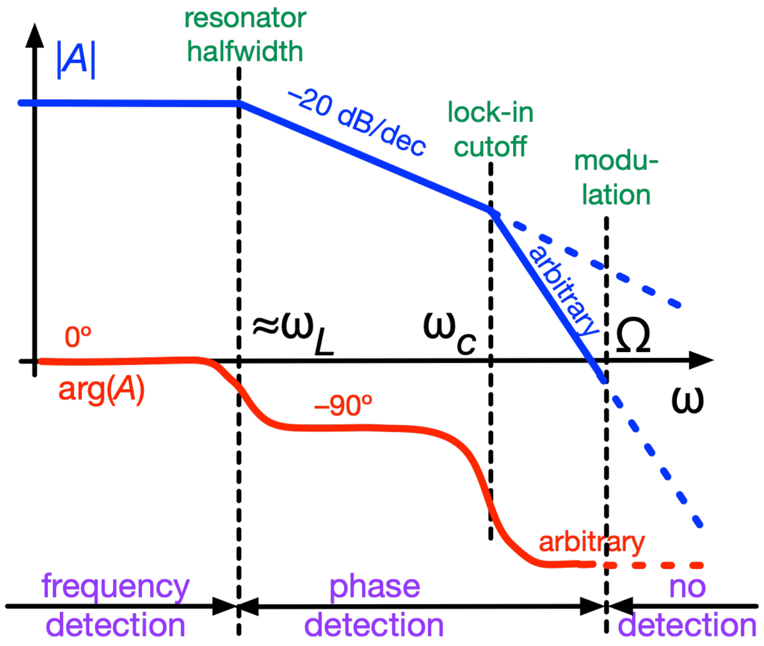

- Quasi-static operation at $\omega < \omega_L$ (resonator half-width)
  - Oscillator frequency-noise detection (as discussed)
- At $\omega > \omega_L$, the resonator reflects the noise sidebands
  - Oscillator phase-noise detection at $\omega_L < \omega < \Omega$ (integrator)
  - The internal lock-in filter rolls off at $\omega > \omega_c$
  - The lock-in amplifier stops working at $\omega \approx \Omega$ and beyond

Design of the servo loop

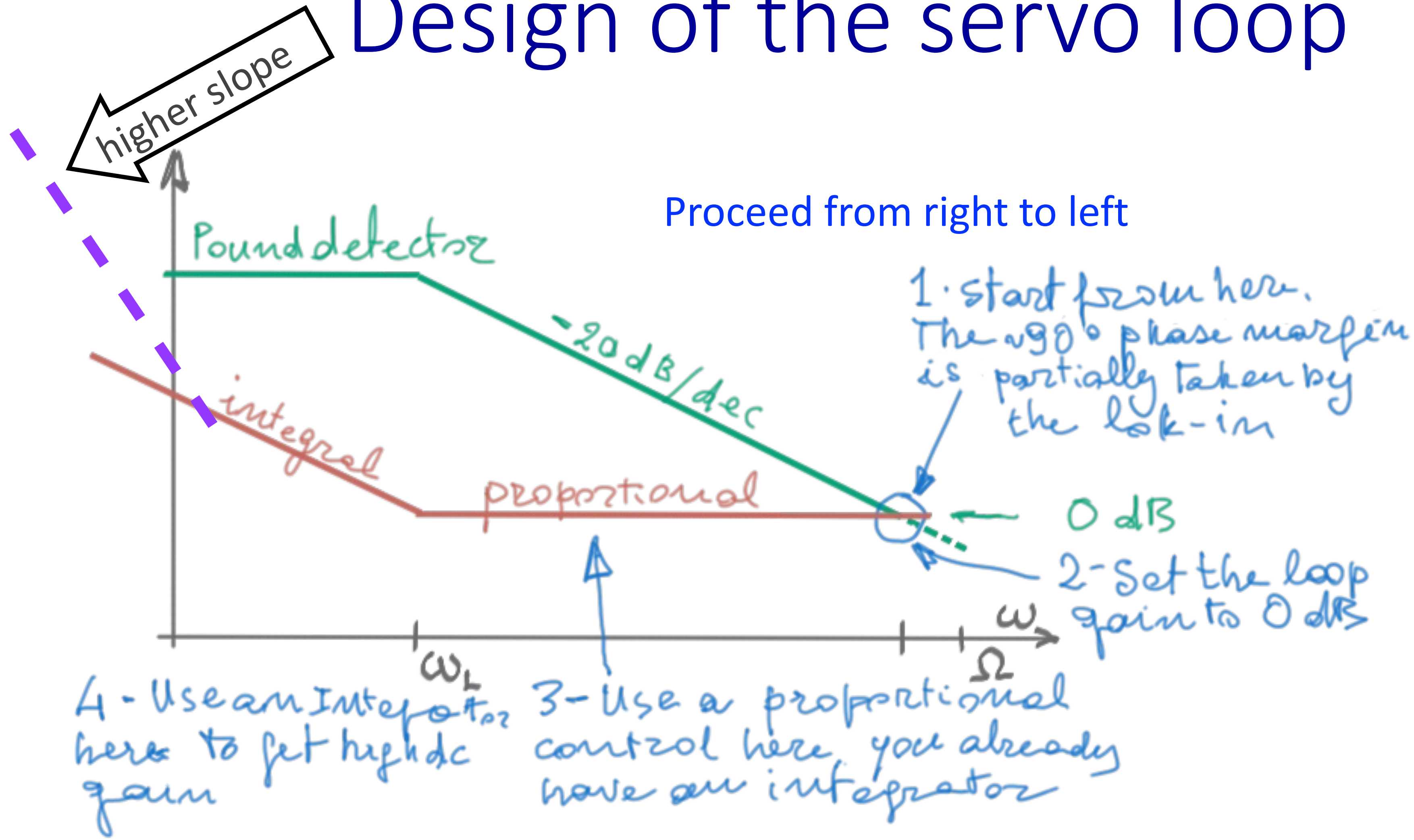

- Start from Ω (or ω_c) and go leftwards
- Set phase margin ≈ π/4 (45º)
- Design the transfer function

Fractional-order servo loop

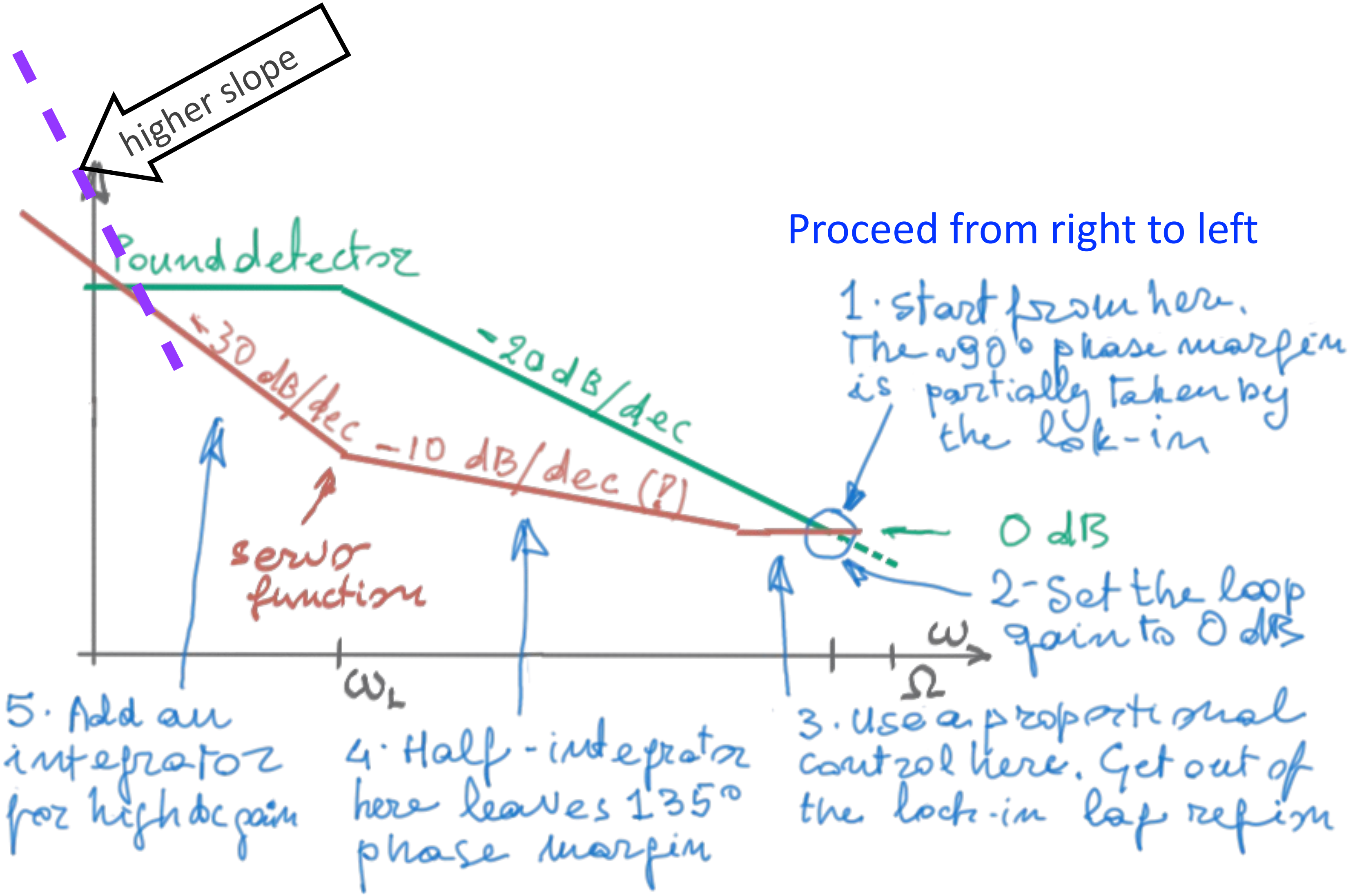

- Resonator –20 dB/decade –> 90º phase lag
- Half integrator 10 dB/decade –> 45º phase lag
- 45º phase margin (to 180º), independent of gain

Delay of the Acousto-Optic Modulator

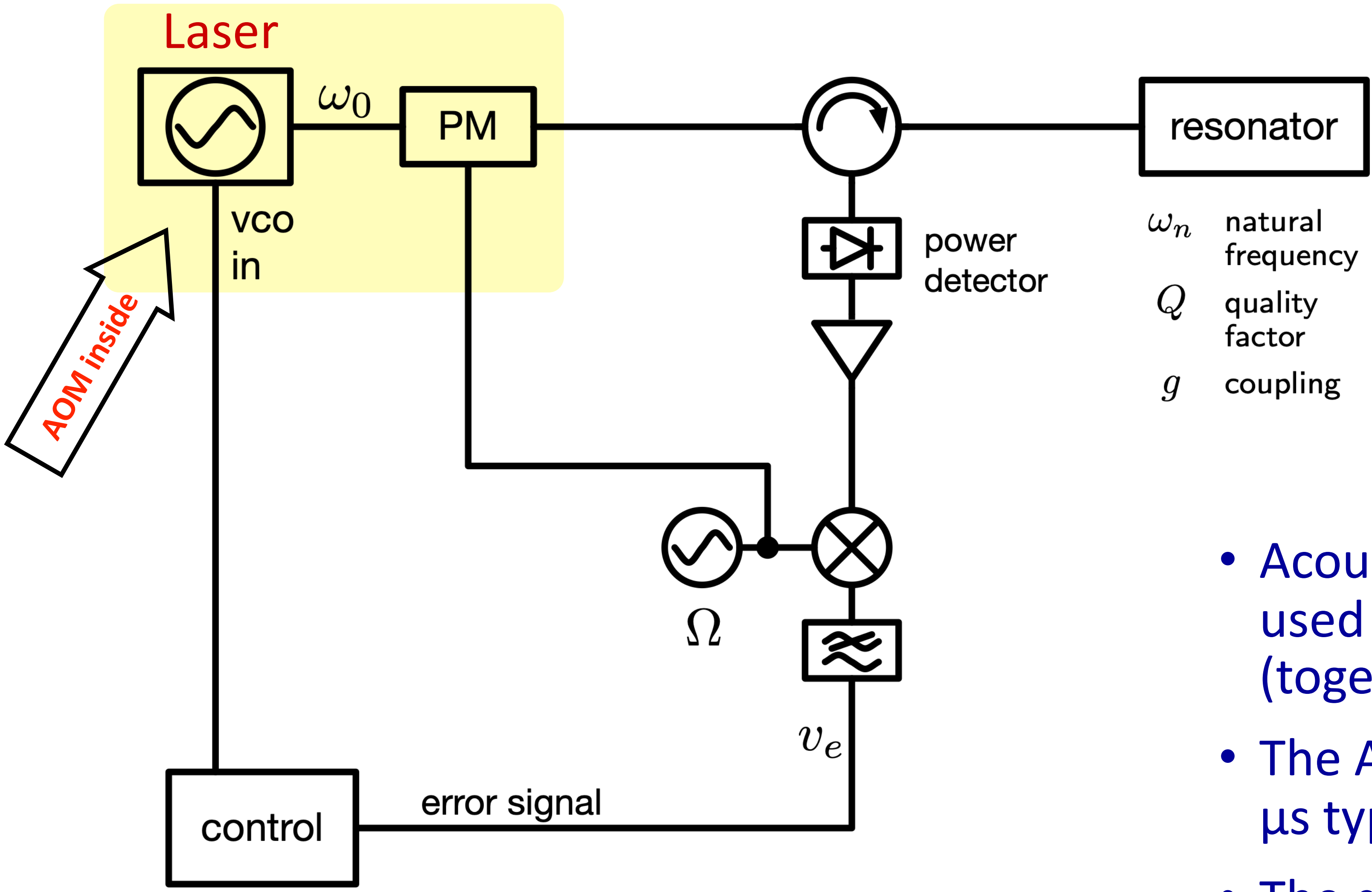

– Warning –

- Acousto-optic modulators are often used to control the laser frequency (together with piezo modulators
- The AOM introduces a delay – a few µs typical
- The delay limits the maximum speed of the control

Resonator Stability

The oscillator stability cannot be better than that of the resonator

Beware of temperature, flicker and drift

Temperature compensation

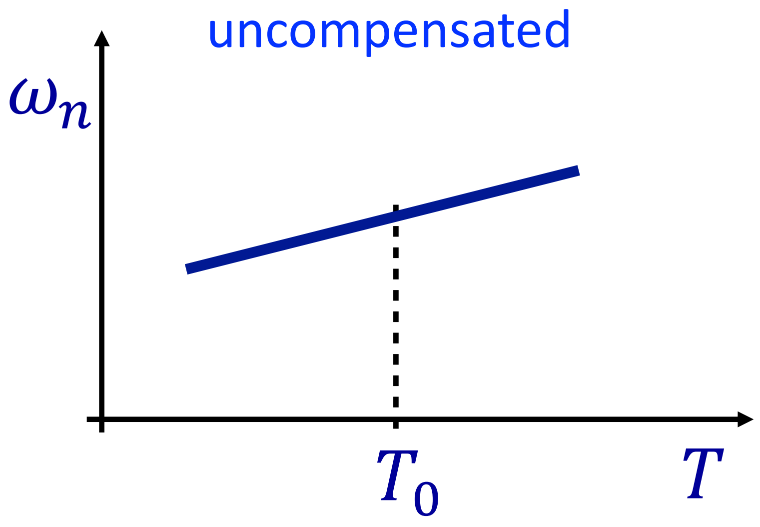

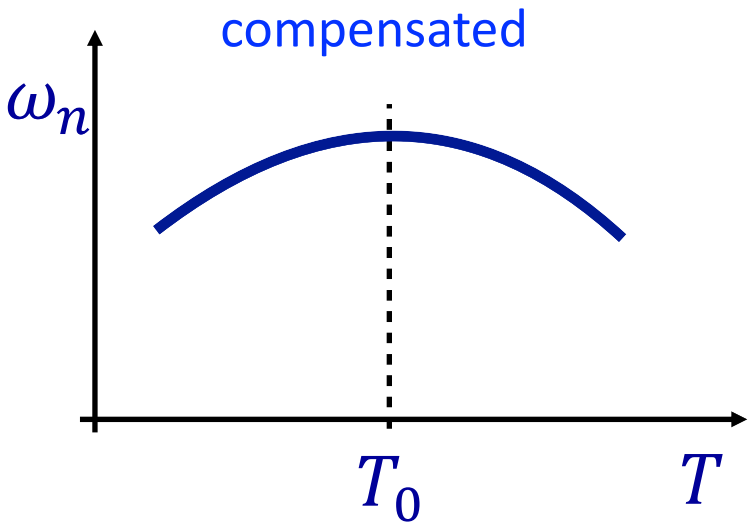

- Most solids (room temperature)
  - dielectric permittivity ε has coefficient of 5–100 ppm/K
  - length has coefficient of 5–25 ppm/K
- Temperature stability < 10–100 μK challenging / impossible
- A turning point is mandatory for high stability

Thermal compensation – Examples

Thermo-mechanical

Dick & al, Proc IFCS 2005

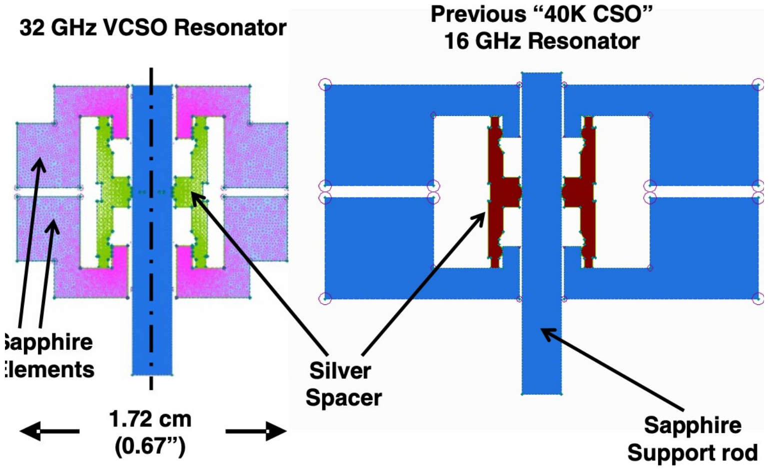

Derived from the old Lampkin oscillator

Paramagnetic

Courtesy of V. Giordano, FEMTO-ST

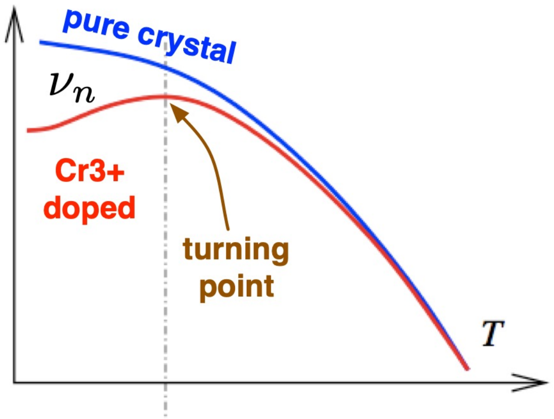

Sapphire Cr3+ impurities @ 6K (V.Giordano / M.Tobar)
Also rutile/sapphire compound @ 80 K (V.Giordano)

Natural – Refraction index

A. Savchenkov et al, JOSAB 24(12), December 2007

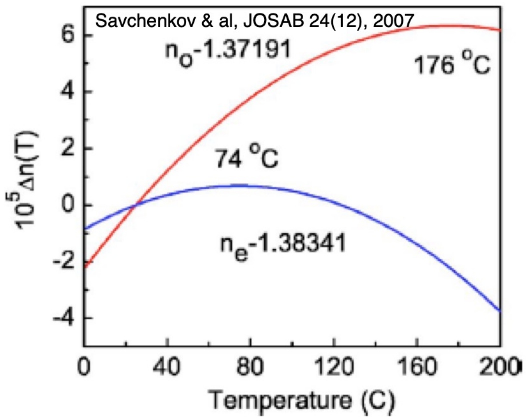

MgF2 whispering gallery (A. Savchenkov)

Natural – Thermal expansion

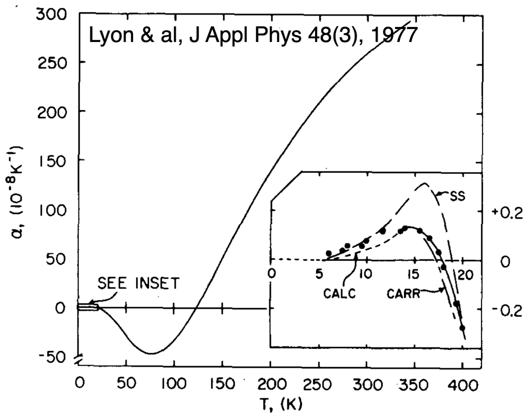

Semiconductor-grade Si @ 124 K (PTB) & @ 17 K

In some fortunate cases, the origin of $1/f$ frequency noise is known

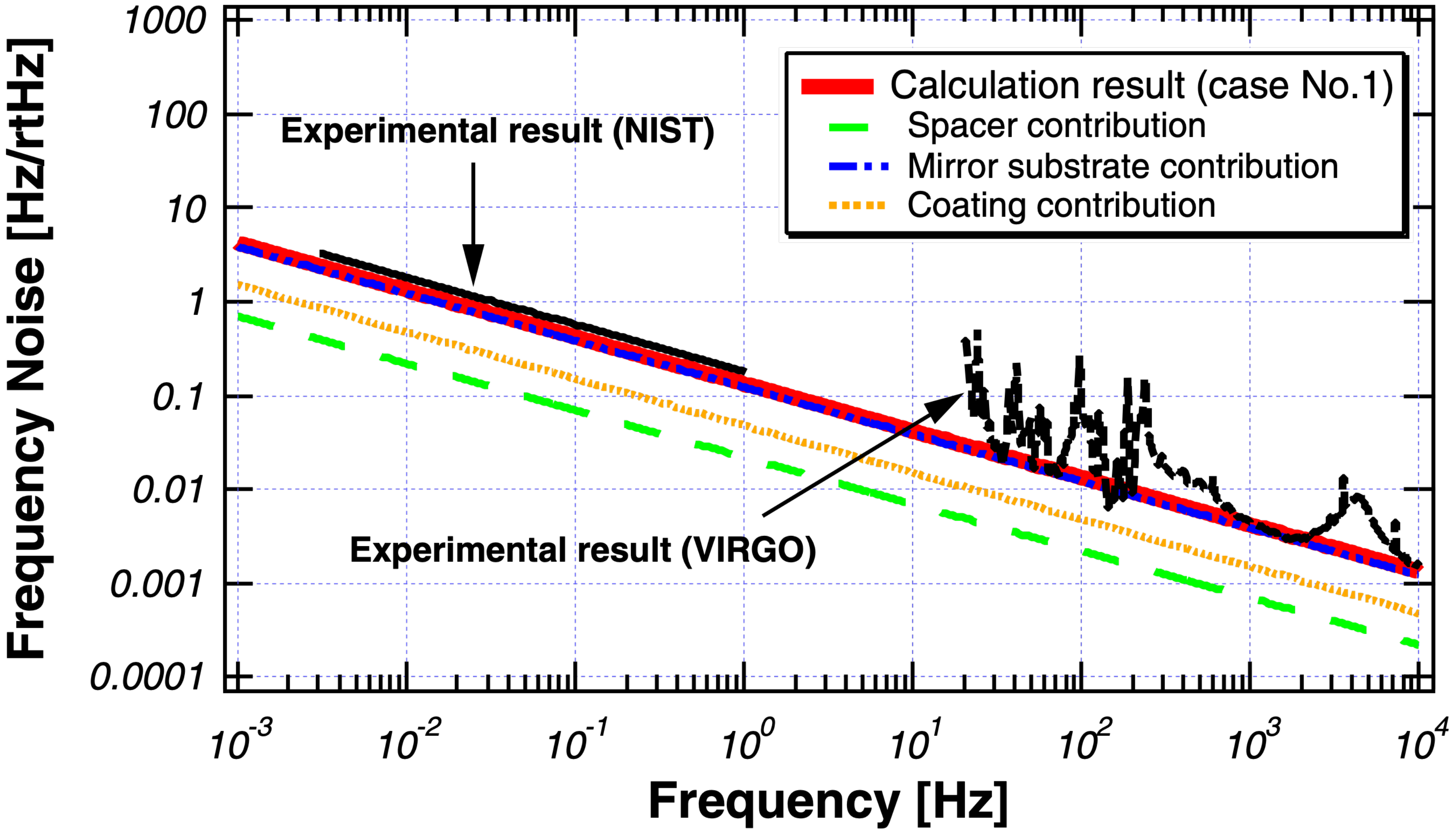

Figure from: Numata K, Kemery A, Camp J, Thermal-noise limit in the frequency stabilization of lasers with rigid cavities, PRL 93(25) 250602, Dec 2004

Featured article: T. Kessler, T. Legero, U. Sterr, Thermal noise in optical cavities revisited, JOSA-B 29(1), 2012

$1/f$ noise and the FD theorem

Debye-Einstein theory for heath capacity

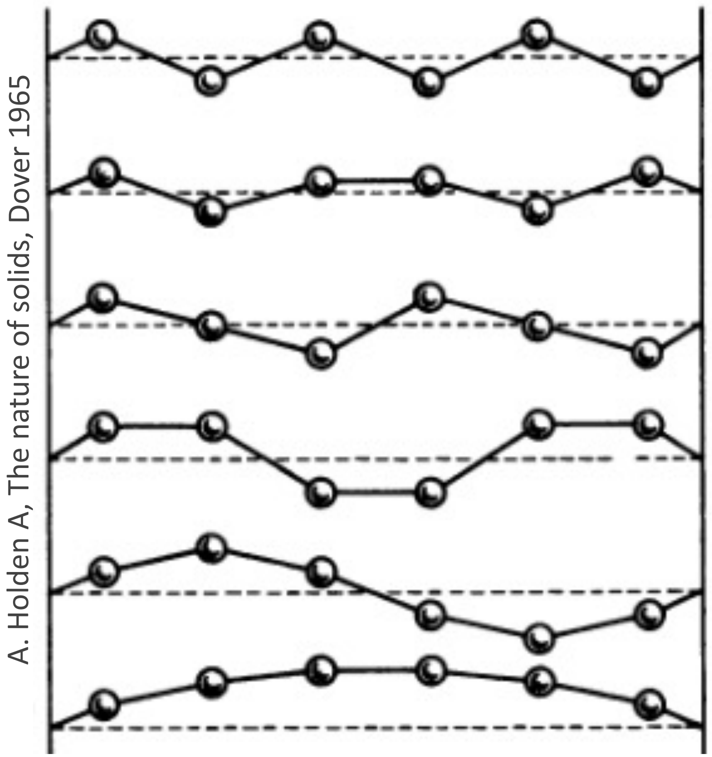

A single theory explains

- Heath capacity
- Elasticity
- Thermal expansion
- … and fluctuations

Fluctuation Dissipation

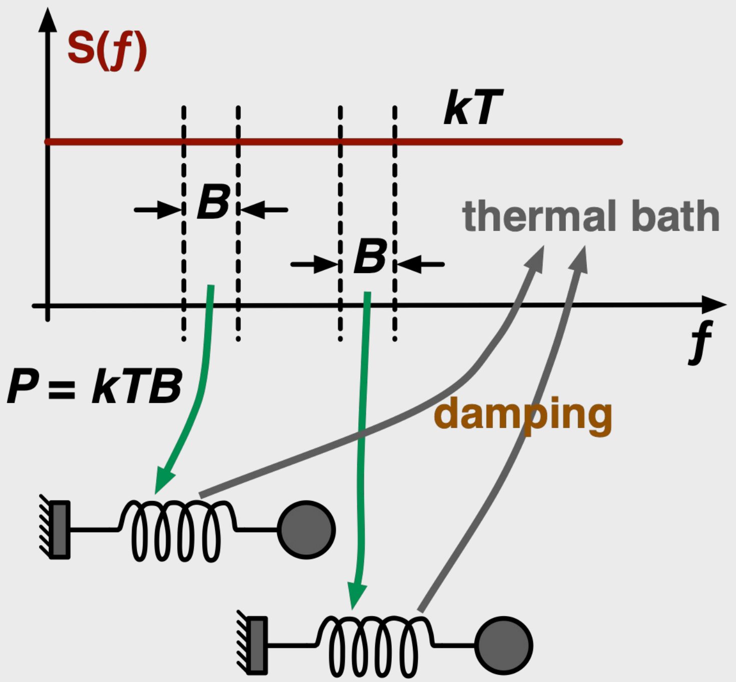

Thermal equilibrium applies to all parts of spectrum

$1/f$ noise and structural damping

$$\ddot{x} + 2\xi\omega_m \dot{x} + \omega_m^2 x = 0$$ homogeneous

dry friction
$F = -c\,\mathrm{sgn}(\dot{x})$

viscous
$F = -H\dot{x}$

Structural dissipation
$\approx$ in-phase with x

Thermal $1/f$ noise

$\ddot{x} + 2\zeta\omega_M\dot{x} + \omega_M^2 x = 0$	general
$\ddot{x} + \frac{H}{m}\dot{x} + \frac{K}{m}x = 0$	(mechanics)
$Q = \frac{1}{2\zeta}$ quality factor	$\tau = \frac{2Q}{\omega_M} = \frac{1}{\zeta\omega_M}$ relaxation time

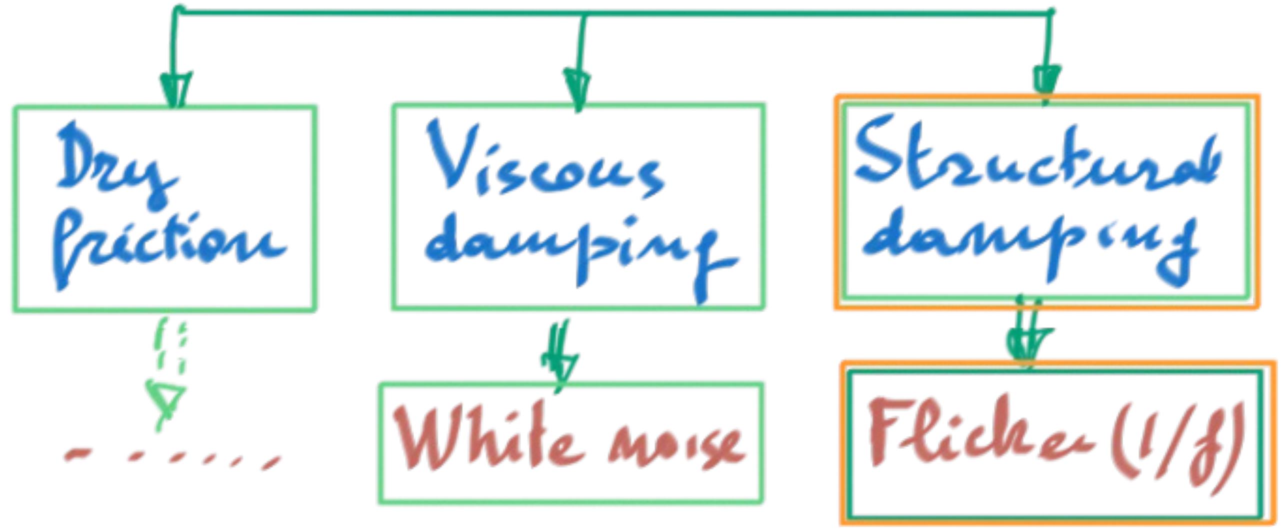

Thermal $1/f$ from structural dissipation

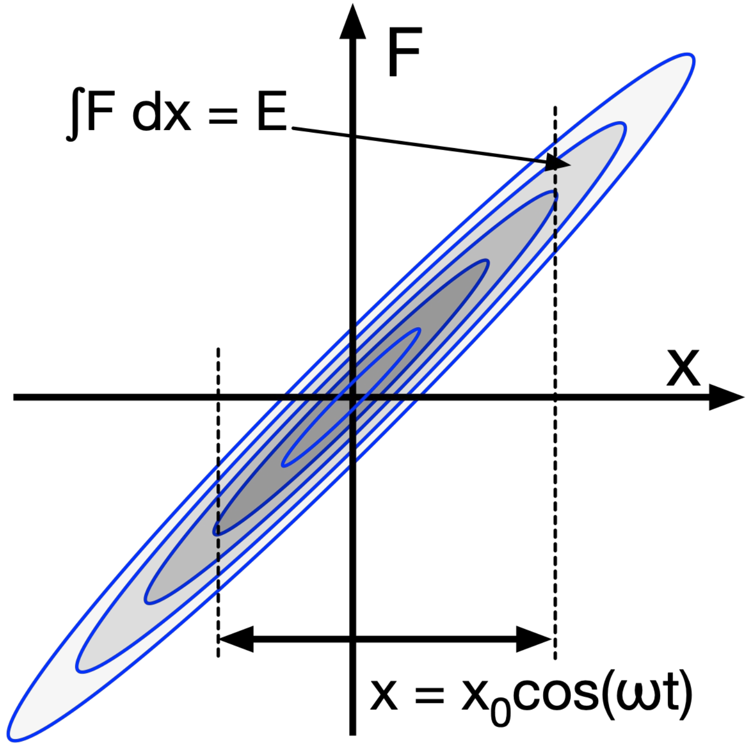

Dissipation in solids is structural (hysteresis)

There is no viscous dissipation

Structural dissipation

nanoscale, instantaneous

Dissipated energy $E = \int F dx$

Small vibrations

The hysteresis cycle keeps the aspect ratio

$E \propto x_0^2$ lost energy in a cycle

Thermal equilibrium

$P = kT$ in 1 Hz BW

$P \propto kT x_0^2$

$x_0^2 \propto 1/f$ —> flicker

A weird exercise

Dissipation in quartz resonators comes from phonon-phonon interaction
– Let's look at what it would happen if it was about breaking bonds –

High-stability 5 MHz quartz resonator

- Active volume 10^{-8} m^3 (1 cm^2 × 100 µm)
- Mass of 25 mg (≈2.5 kg/dm^3)
- N ≈ 7.5×10^{17} atoms (quartz $^{28}Si\,^{16}O_2$ –> ⟨A⟩=20)
- Drift D = 10^{-15} / s (i.e., 10^{-10}/day, or 10^{-6} in 30 years)
- P = 10 µW RF power
- Melting point 1670 ºC (1943 K)
  kT = 2.68×10^{-20} J = 167 meV

The number of bonds of energy E broken in 1 s by structural damping is

$$n = P/E$$

Taking E = 2.7×10^{-20} J (167 meV)

n ≈ 3.7×10^{14} bonds / s

n/f ≈ 3.7×10^{14} / 5×10^{6} = 7.5×10^{6} bonds/cycle

If the bonds are not repaired, the crystal is "atomized" after

$$T = N/n \approx 2 \times 10^{3}\ \text{s} \quad (34\ \text{M})$$

Optimization Issues

Setting up a Pound control is decently simple

Optimization is disappointingly complex

In situ testing: the ringdown method

Purpose: measure Q (or finesse)

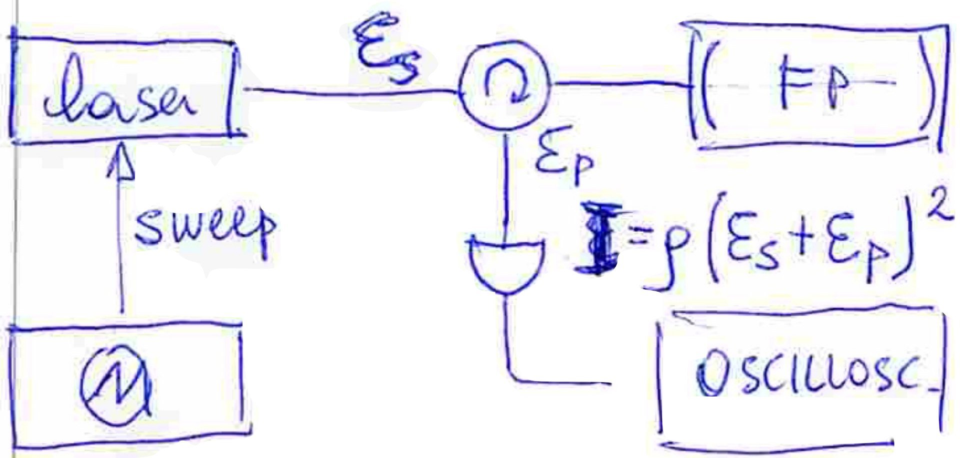

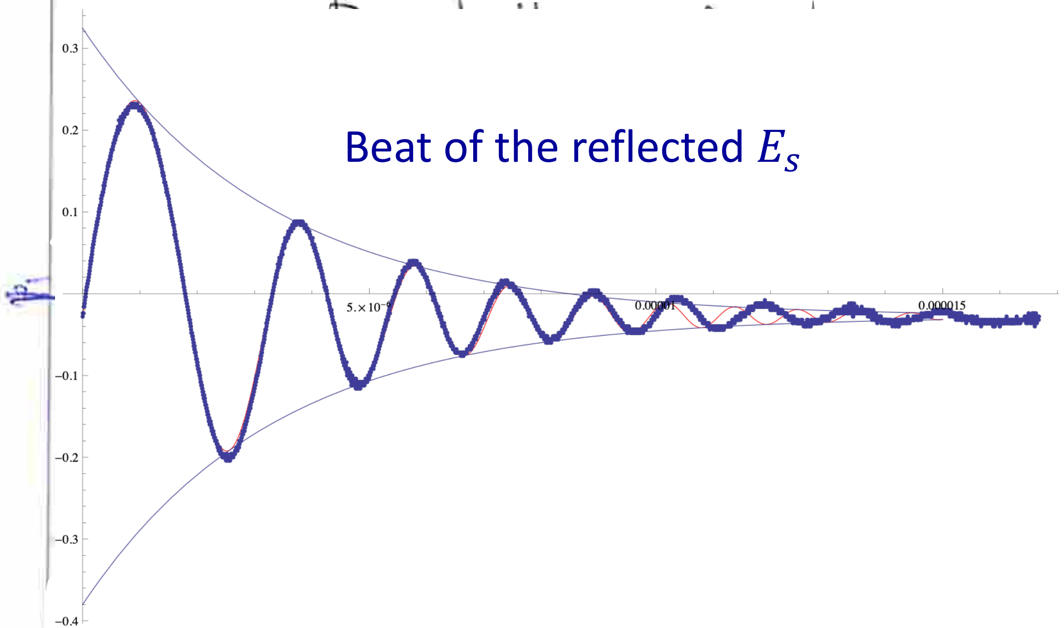

Beat of the reflected E_s

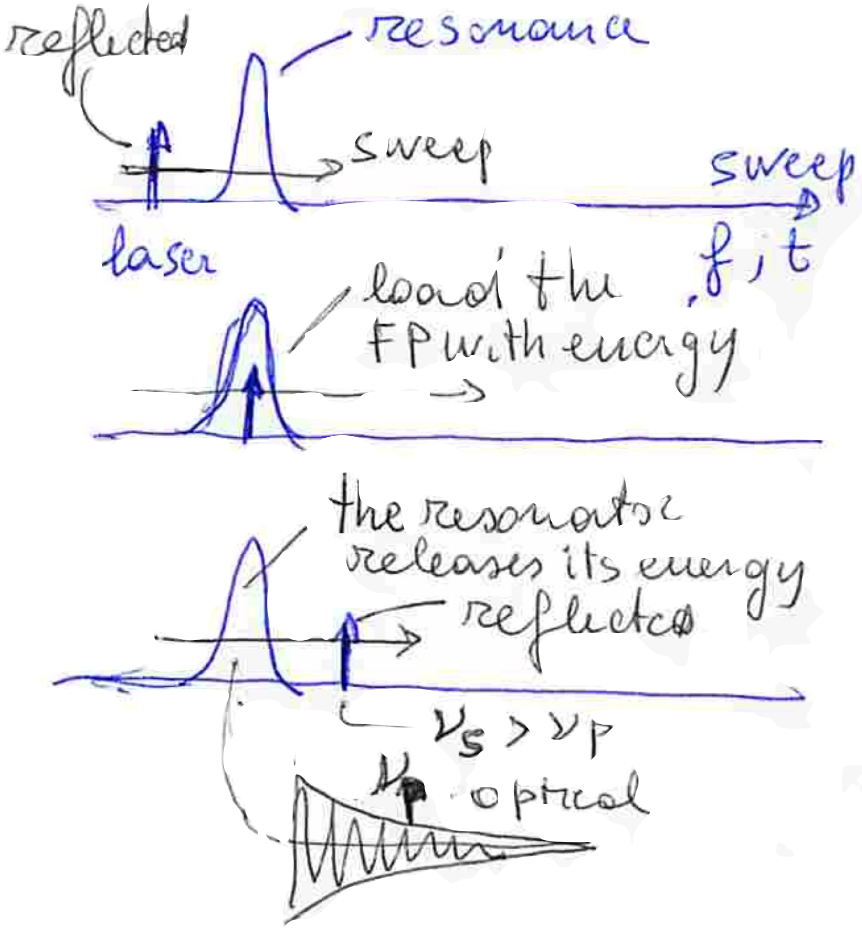

Ringdown method

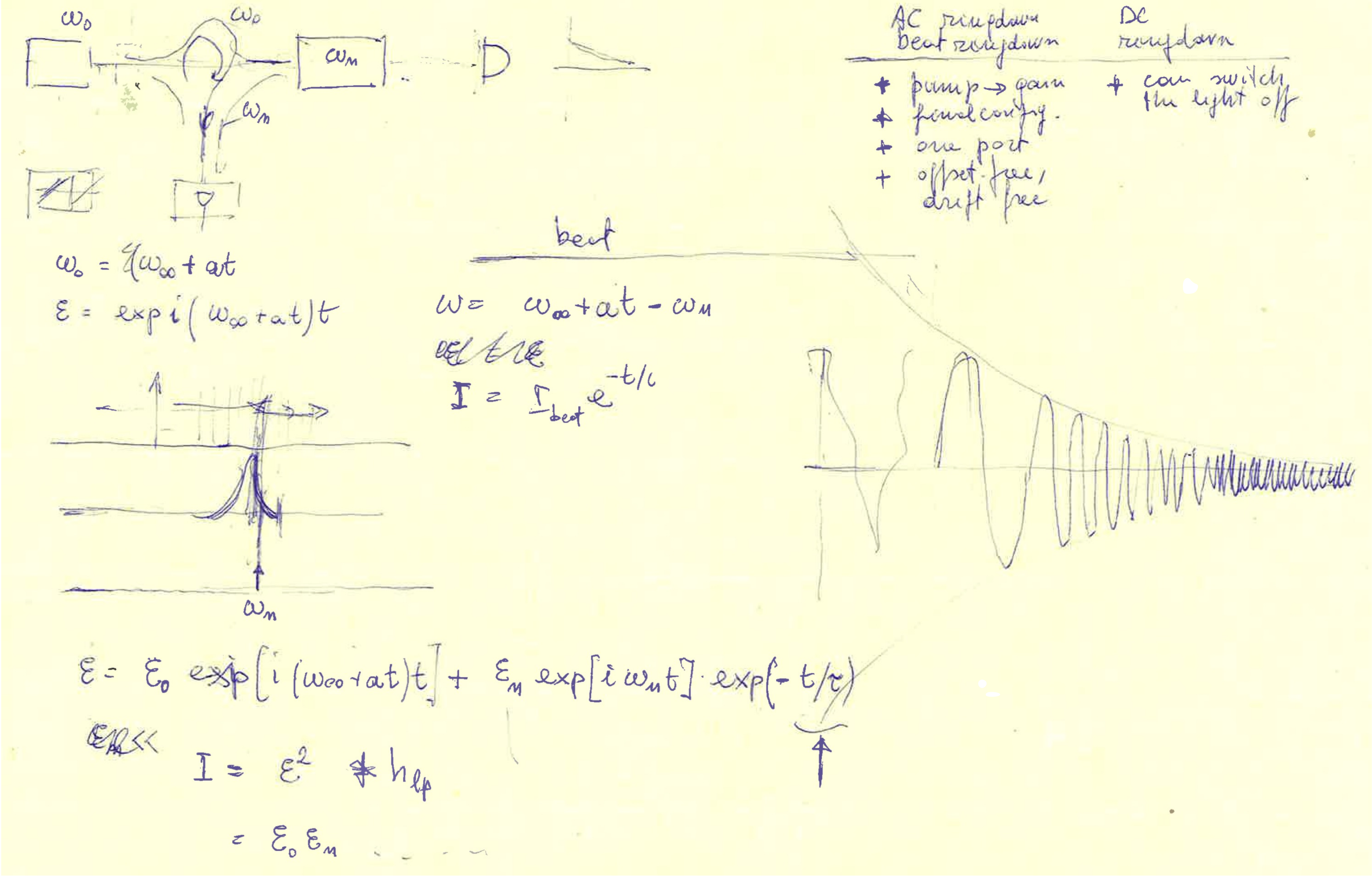

Ringdown method

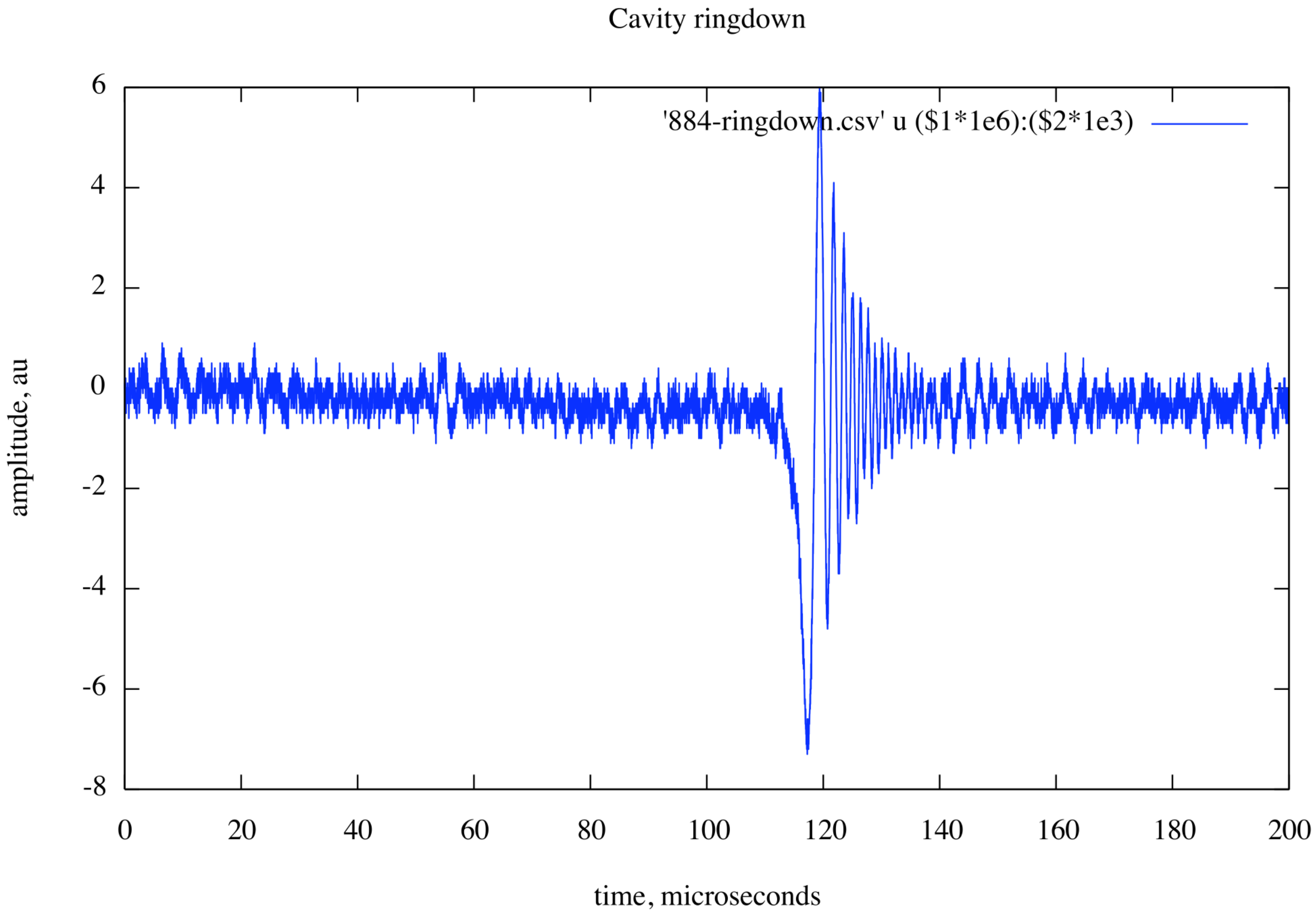

- works only with high Q cavities
- makes the measurement possible even if frequency is not stable enough for other methods
- wavelength sweep –> beat sweep vs decay
- the exponential decay time is τ (amplitude, not intensity!)

J. Poirson, F. Bretenaker, M. Vallet, and A. Le Floch, J. Opt. Soc. Am. B 11, 2811 (1997).

Critical coupling $(g = 1)$

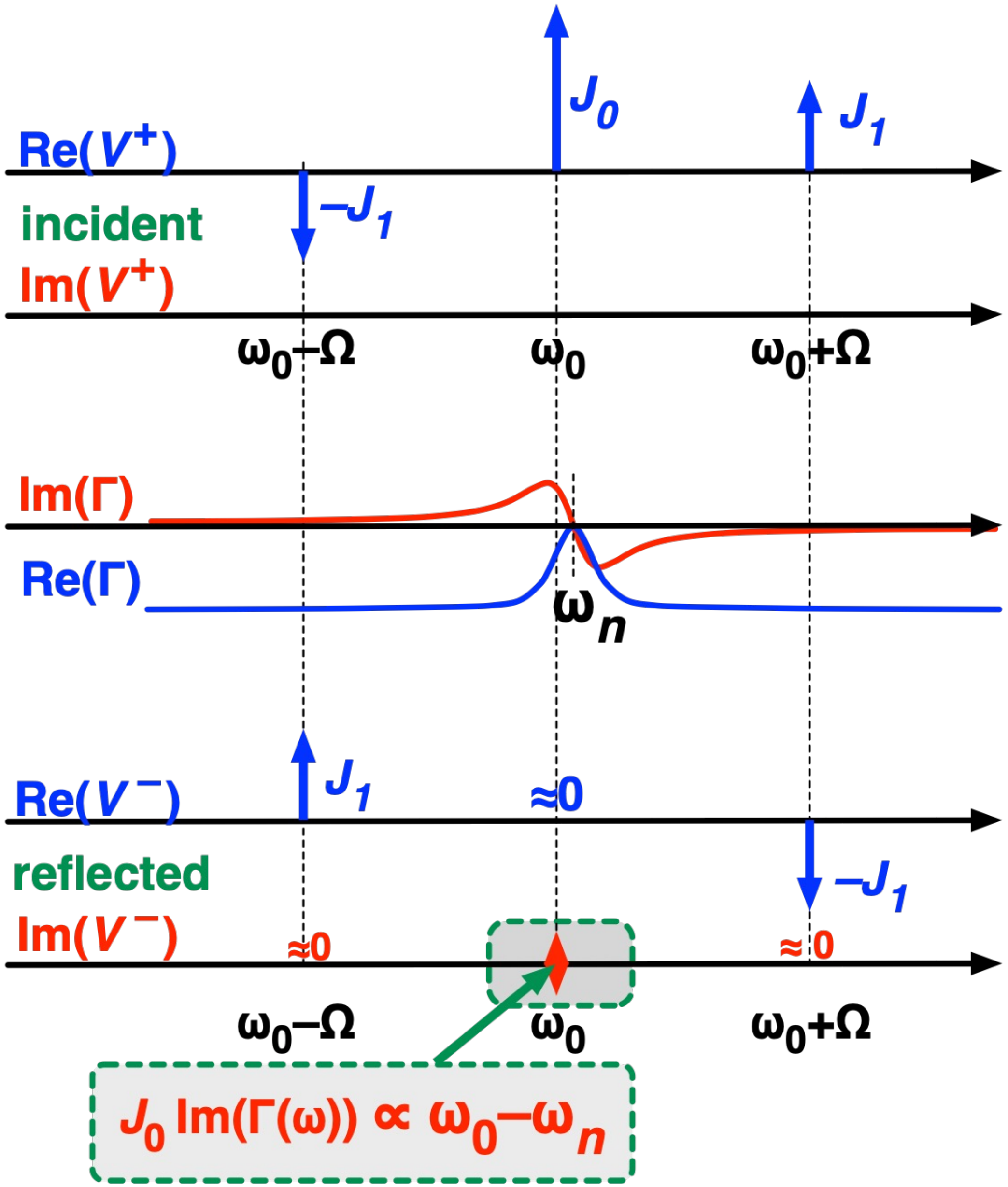

$$\Gamma \simeq \frac{g-1}{g+1} - i\,\frac{4Q_0 g}{(g+1)^2}\,\frac{\Delta\omega}{\omega_n}$$

close to ω_n

- Maximum gain.
  Immediately seen on Im{Γ}
- Lowest "useless" power in the quadratic detector.
  Immediately seen on Re{Γ}
- The frequency error due to residual AM vanishes
  Some math – not shown

Detector responsivity

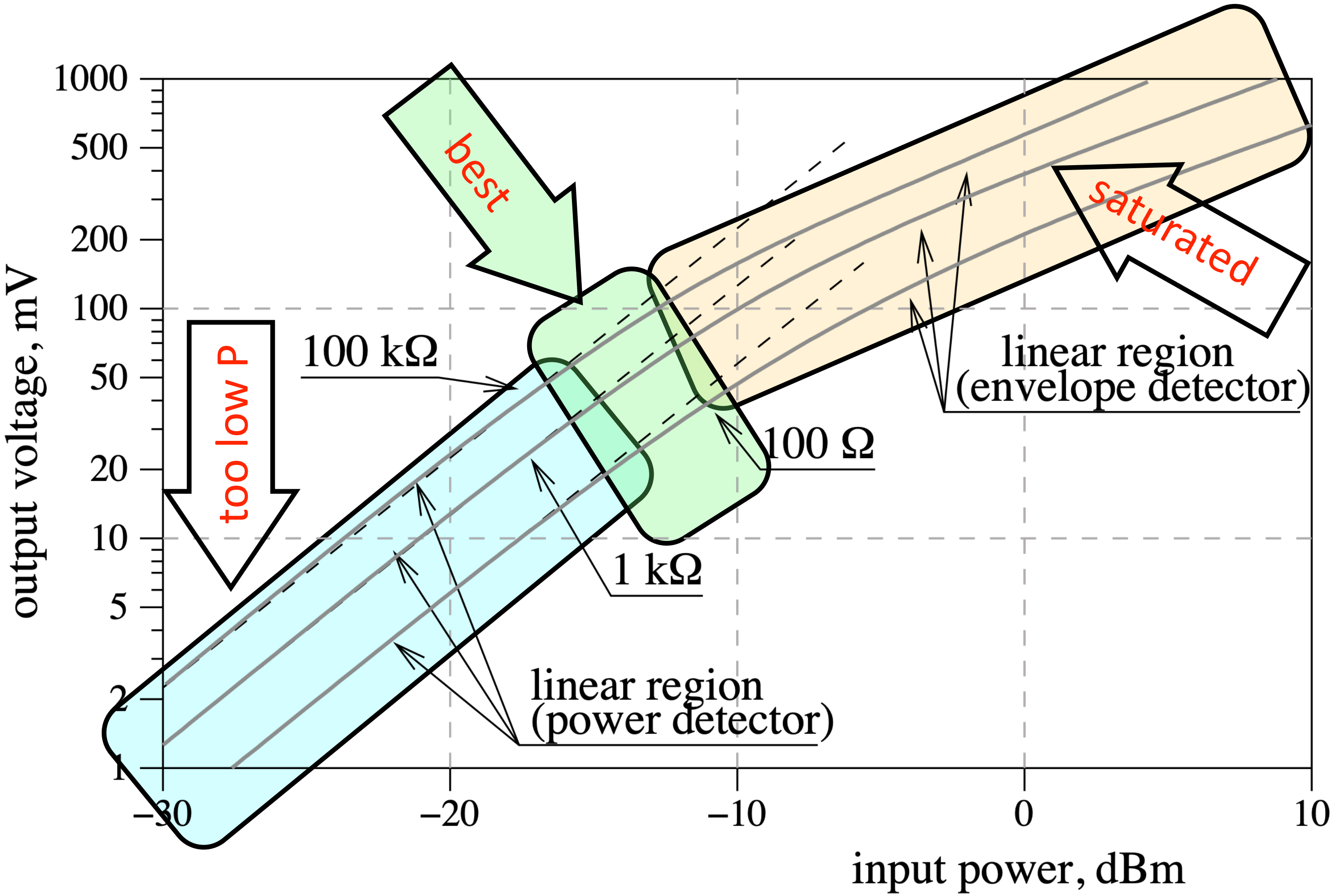

- The error signal comes from the 2ac + 2bc terms
- Highest sensitivity just below the corner

E. Rubiola, *The Measurement of AM noise of Oscillators*, arXiv:physics/0512082 [physics.ins-det]. Fig. 5.
Also S.Grop, E.Rubiola, Proc.2009 IFCS Fig.1 (≠artwork)

$$(a+b+c)^2 = a^2 + b^2 + c^2 + 2ab + 2ac + 2bc$$

Identify the detector's optimum power

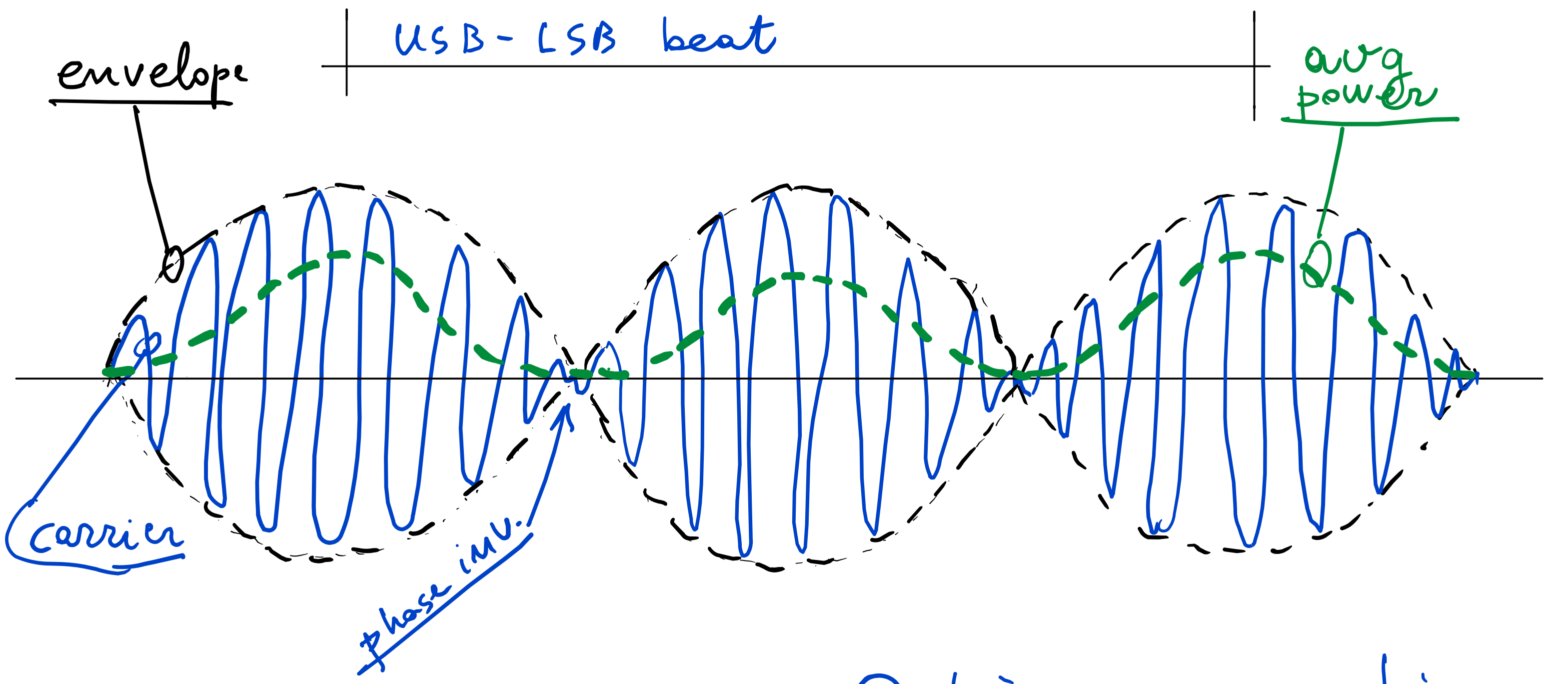

optics
$\bar{P} \rightarrow$ photon flux
& saturation

μwaves/RF
$v \rightarrow$ saturation

Optimum working point:
maximize the 2Ω beat note

$$(a+b+c)^2 = \underbrace{a^2+b^2+c^2}_{\text{dc and } 2\omega_0} + \underbrace{2ab}_{\Omega} + \underbrace{2ac+2bc}_{2\Omega}$$

Maximum power in the resonator

- Dissipated P –> Thermal instability (obvious)
- Traveling P –> Instability
    - Electrooptic effect: field affects the dielectric constant
    - Radiation-pressure
      Chang & al., …radiation pressure effect…, PRL 79(11) 1997
- Difficult to lock (ω_n runaway)
    - Control instability and failure
- "Maximum P" applies to the carrier, not to sidebands
    - The carrier gets in the resonator, the sidebands are reflected
- Look carefully at the resonator physics
    - Loss and dissipation are not the same thing

Modulation index

- The sidebands are reflected
- High modulation index –> high sideband power
  - Higher gain without increasing P inside the resonator
- Effect of higher-order sidebands ($\pm 2\Omega$, $\pm 3\Omega$, etc.)
  - Not documented – though conceptually simple
- DSB modulation, instead of true PM
  - A pair of sidebands is simpler than true PM
  - Modulator $1/f$ noise?

Modulation frequency

Lower bound for Ω

- Total reflection at $\omega_n \pm \Omega$ is necessary
  - Thus, $\Omega \gg B/2\pi$, B = resonator bandwidth

Why to choose the largest possible Ω

- Larger control bandwidth
  - Higher dc gain –> higher stability

Why not to choose the largest possible Ω

- Avoid dispersion (PM –> AM conversion)
- Technical issues / Design issues

My experience – at Femto-ST

- 95–99 kHz for the sapphire oscillators (10 GHz, B=10 Hz)
- 22 MHz for the optical FP (193 THz, $B \approx$ 30 kHz)

Residual amplitude modulation (RAM)

- Residual AM yields a detected signal at the modulation frequency Ω
  - Generally poorer operation
  - Frequency error –> $\omega 0 \neq \omega n$ at the null point
  - Frequency fluctuation if the AM fluctuates
- Dispersion results in PM –> AM conversion
  - Breaks the non-distortion condition

Basu R, Wang R, Dick GJ, Novel design of an all-cryogenic RF Pound circuit, Proc IEEE IFCS 2005
Marra G & al, Reduction of residual amplitude modulation …, Proc. EFTF 2004

Removing the residual AM

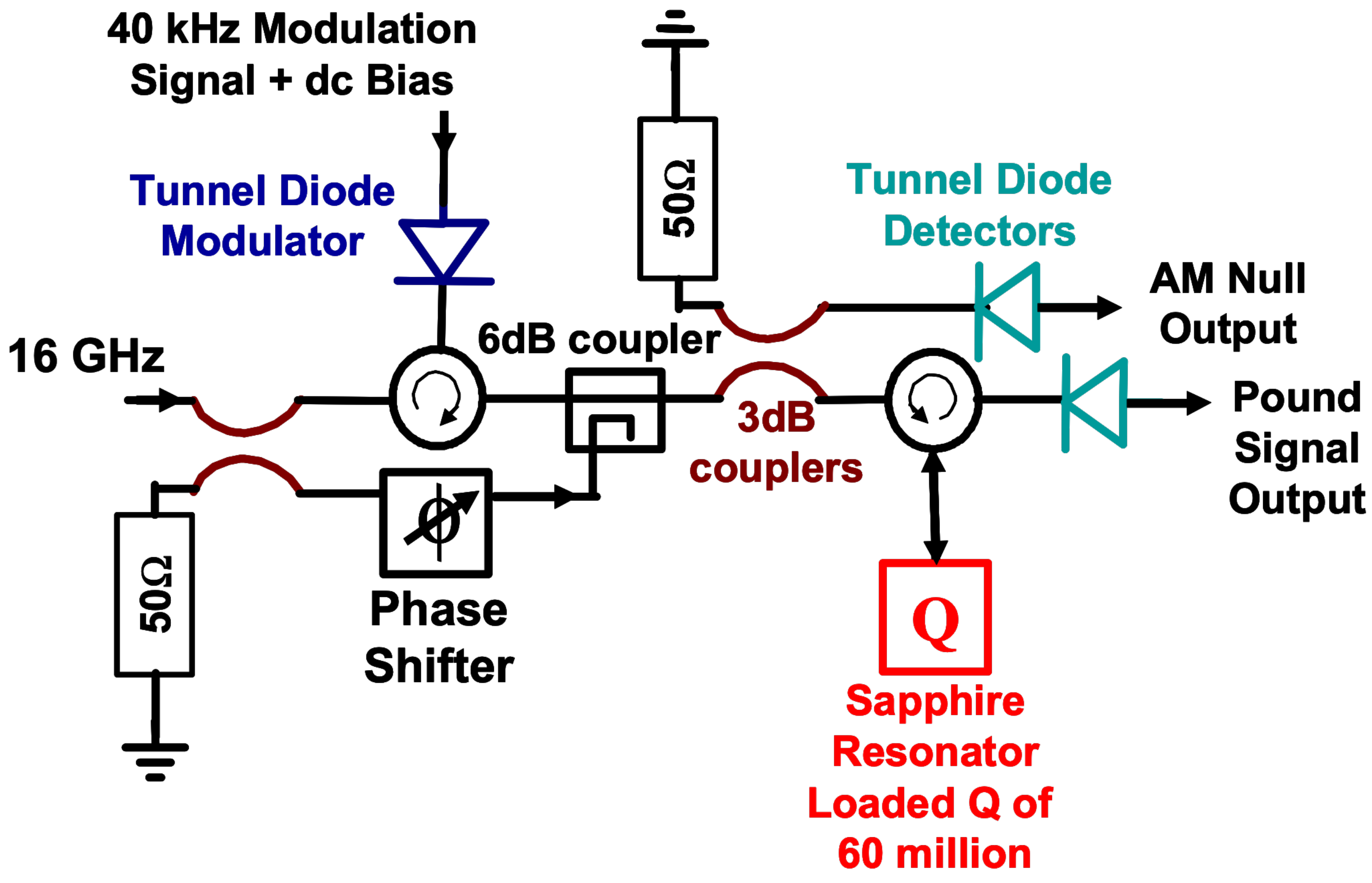

Figure from R. Basu, R. Wang, G. J. Dick, Novel design of an all-cryogenic RF Pound circuit, Proc IEEE IFCS 2005

- Additional detector enables nulling the AM in closed loop
- The power detector is reversible
- Reversed, is used as a variable stub

Filter the detector output

dc terms

$$P = \frac{|V_0|^2}{2R_0}\left\{J_1^2(m) + \frac{1}{2}J_0^2(m)\left[\frac{g-1}{g+1}\right]^2 + \frac{1}{2}J_0^2(m)\left[\frac{4Q_0}{g+1}\frac{\Delta\omega}{\omega_n}\right]^2\right\} +$$

$$- \frac{|V_0|^2}{2R_0}J_1^2(m)\cos(2\Omega t) + \frac{|V_0|^2}{2R_0}2J_0(m)J_1(m)\frac{4Q_0}{g+1}\frac{\Delta\omega}{\omega_n}\sin(2\Omega t)$$

diagnostic — error signal

Large, 2Ω — Small, Ω

Separating the Ω and 2Ω signals with passive filter helps in getting clean, simple and effective electronics

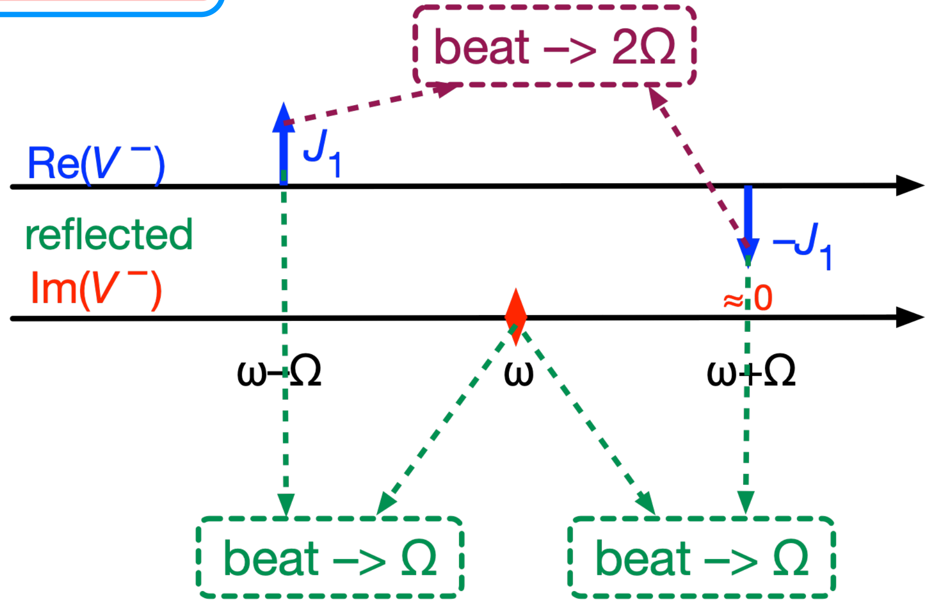

More optimization issues

- Given the laser power –> best modulation index (Eric Black)
- Detector saturation power –> best modulation scheme
- Resonator max power –> best modulation
- Quadrature modulation (μwaves) – does it really make sense?

Alternate Schemes

The original Pound scheme

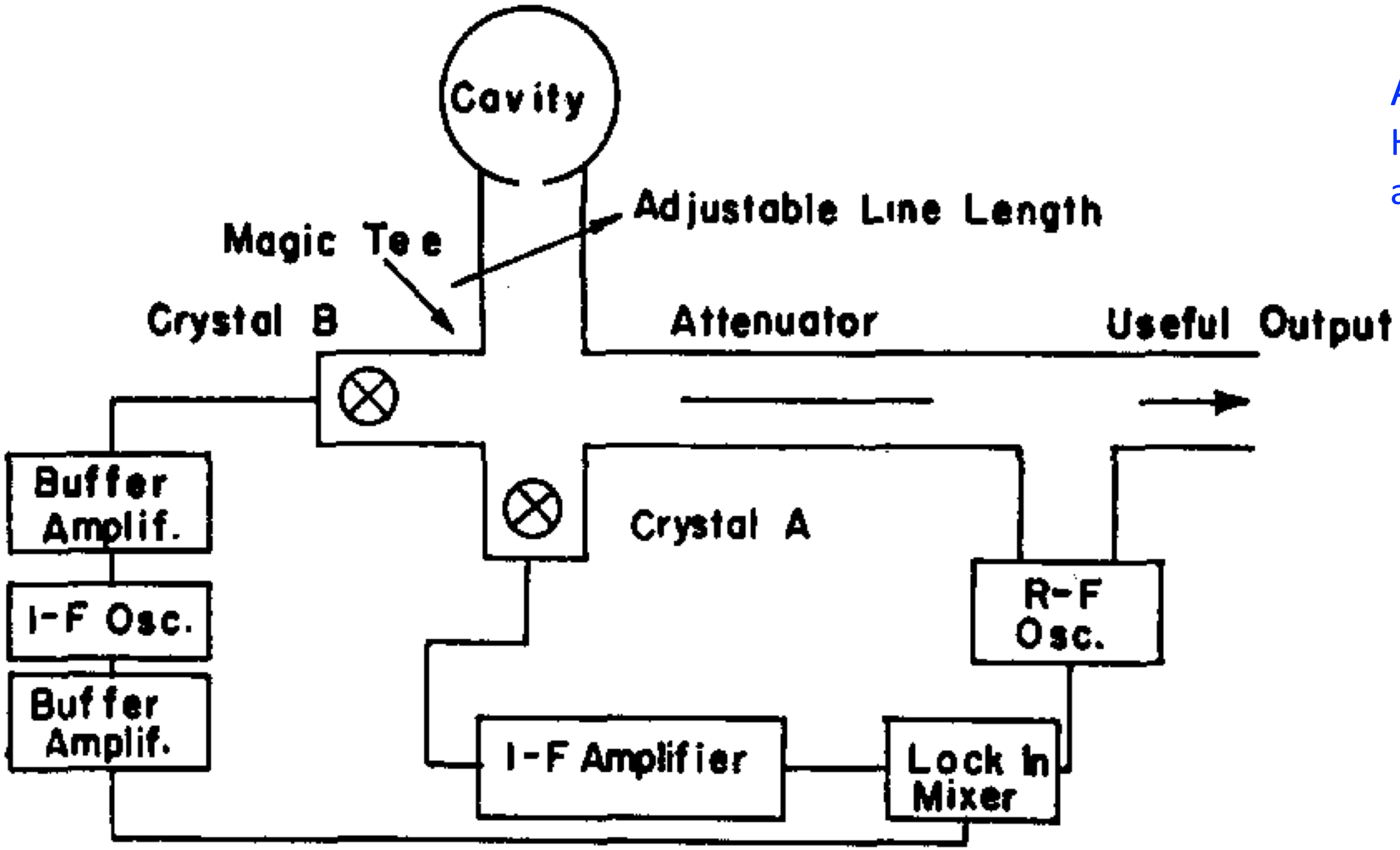

All the key ideas are here

However technology, electrical symbols, and writing style are quite different

R. V. Pound, Rev Sci Instruments 17(11) p. 490–505, Nov. 1946

The Pound-Drever-Hall scheme

The Pound scheme ported to optics

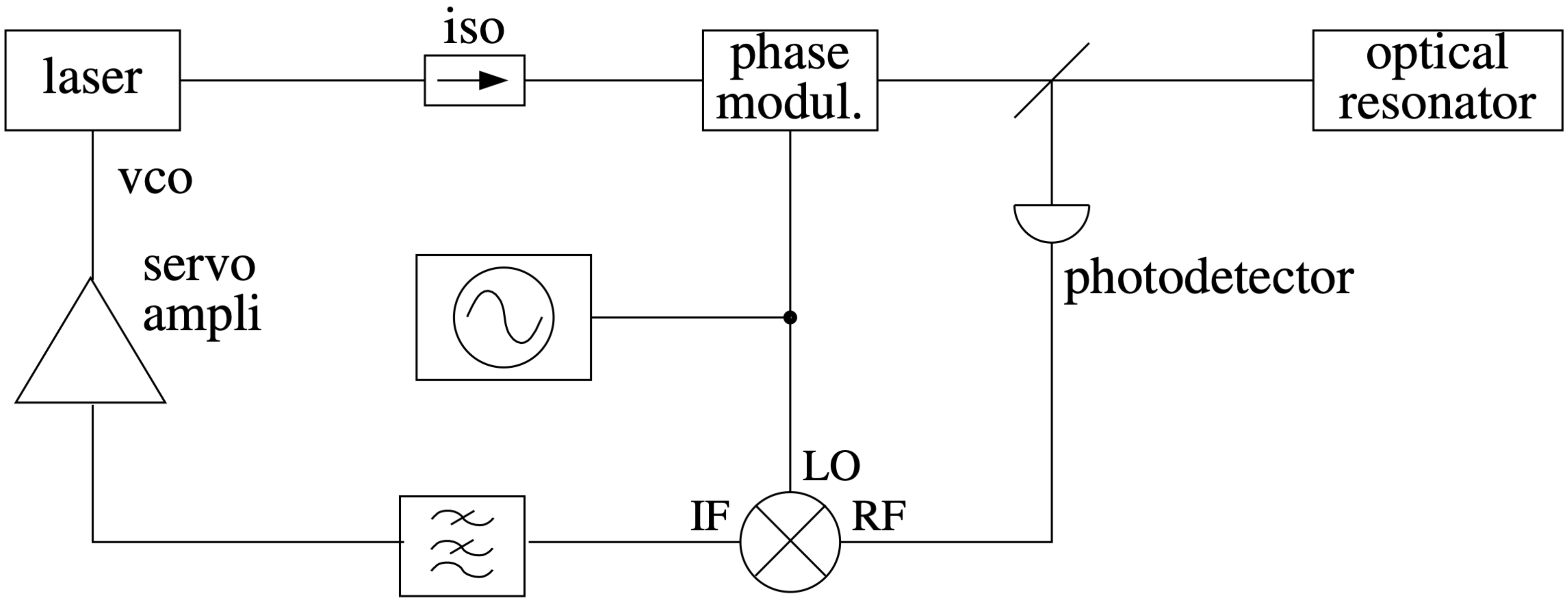

Figure from E. Rubiola, Phase noise and frequency stability in oscillators, © Cambridge University Press

R.P.V. Drever, J.L. Hall & al., Appl. Phys. Lett. 31(2) p.97–105, June 1983

The Pound-Galani oscillator

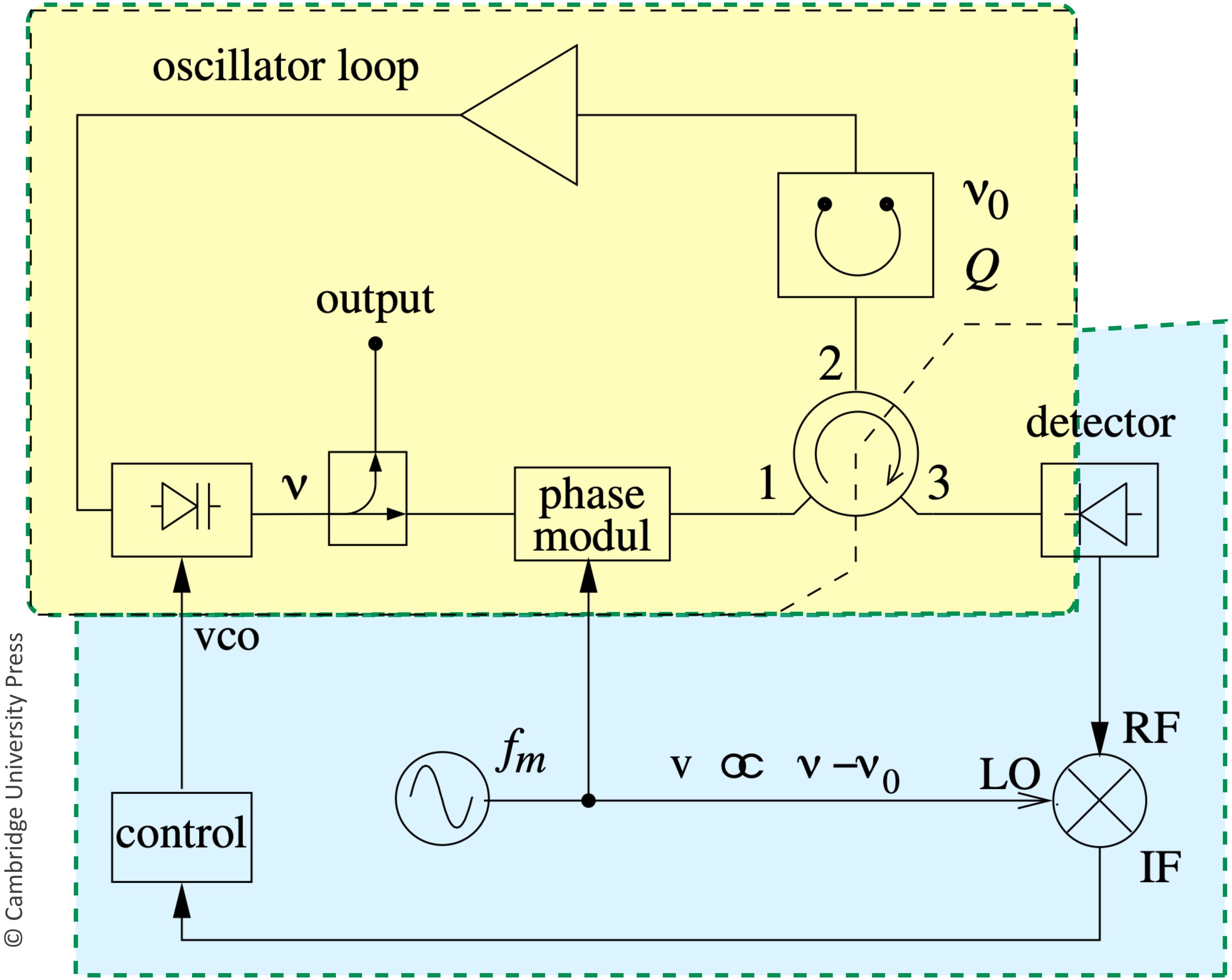

- Great VCO for cheap
- Easier to control
- Two-port resonator
  - More complex
  - Lower Q

Z. Galani & al, Analysis and design of a single-resonator GaAs FET oscillator with noise degeneration, IEEE-T-MTT 39(5), May 1991

Pound-Galani transfer function

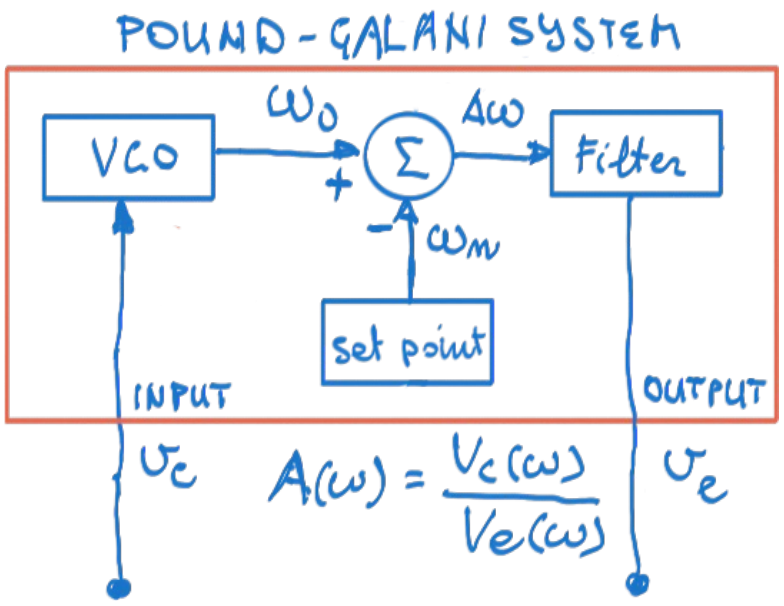

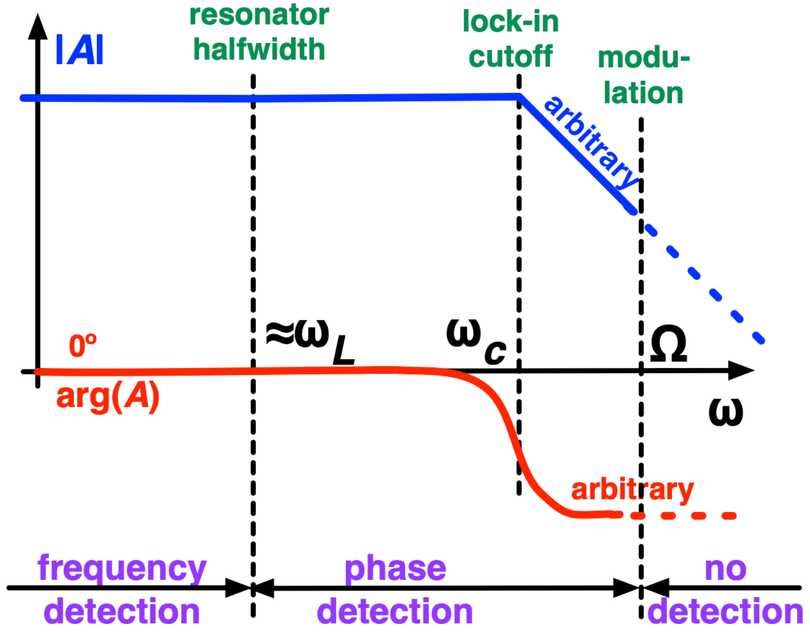

- FD region –> full performance
- PD region
  - Flat frequency response, not for free
  - Poor response of the frequency-error detection
  - Higher noise

The Pound-Sulzer oscillator

Figure from E. Rubiola, Phase noise and frequency stability in oscillators, © Cambridge University Press

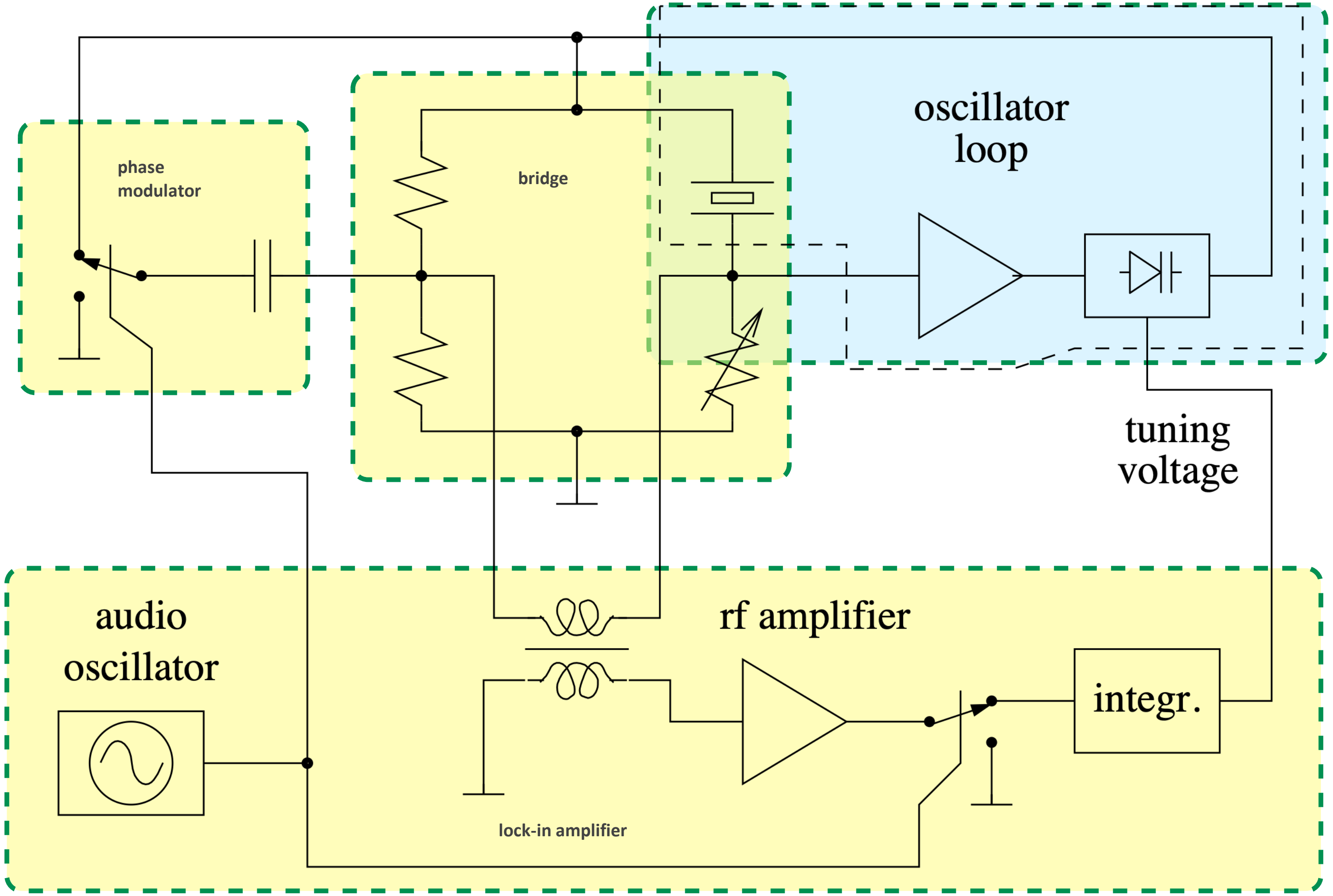

P. Sulzer, Proc. IRE 43(6) p.701-707, June 1955

Resonators and Oscillators

Microwaves

Whispering gallery resonator

Geometrical optics interpretation

Full reflection

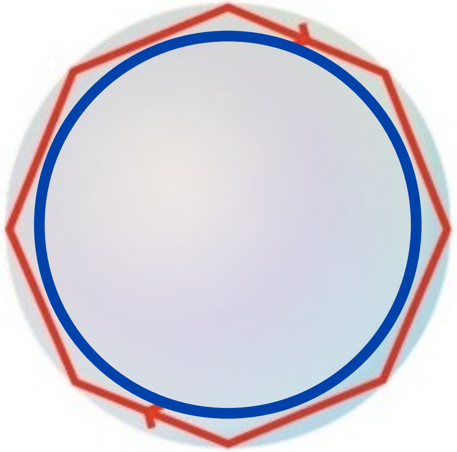

Energy trapped inside the dielectric

All figures of this page are courtesy of V. Giordano, FEMTO-ST

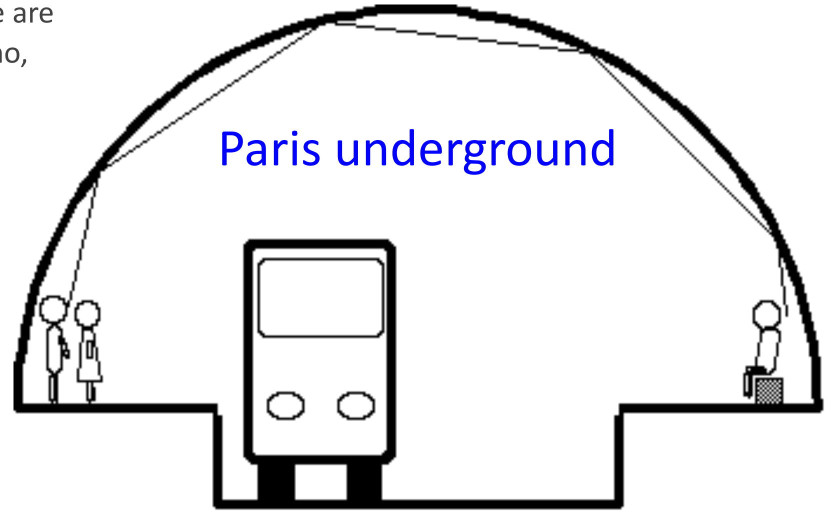

Energy

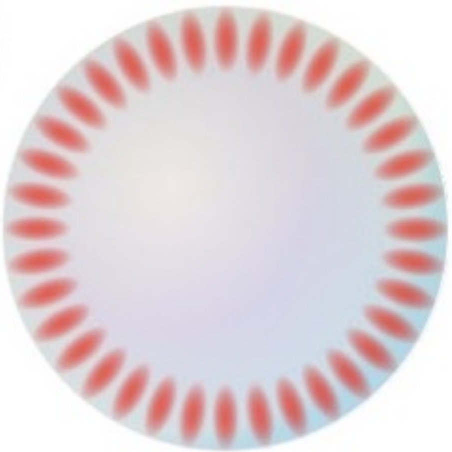

Electromagnetic field

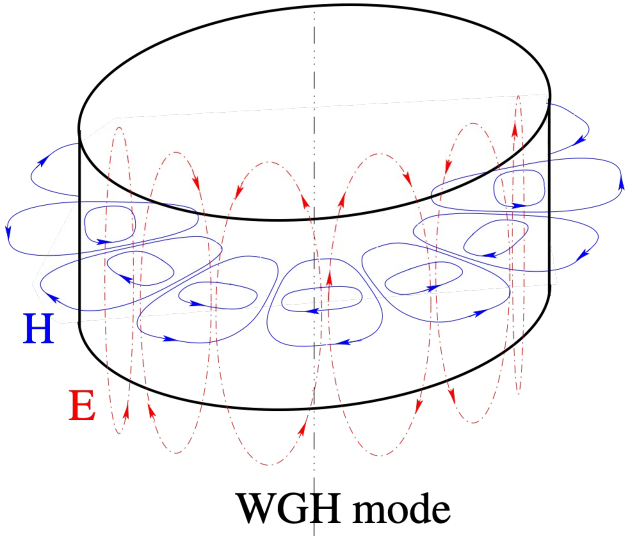

$$Q_0 \sim \frac{1}{\mathrm{tg}\delta} \quad \rightarrow \quad \sim 10^9 \text{ @ } 4\text{K}$$

Temperature compensation

All figures of this pages are courtesy of V. Giordano, FEMTO-ST

Compensation exploits impurities, ≈6 K

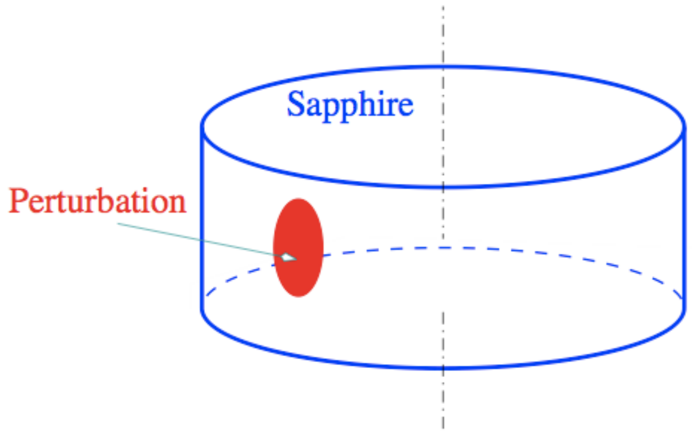

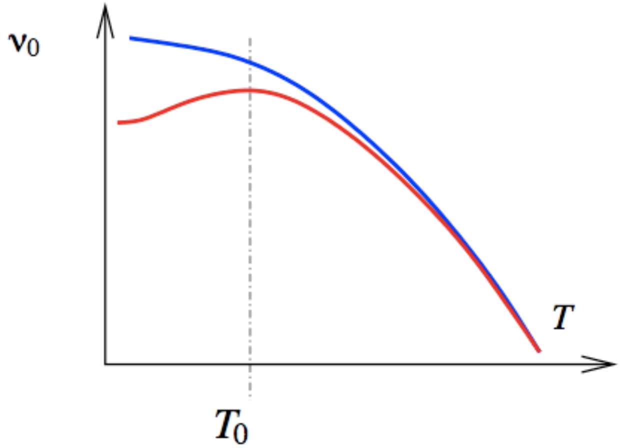

Two ideas tested above 30K

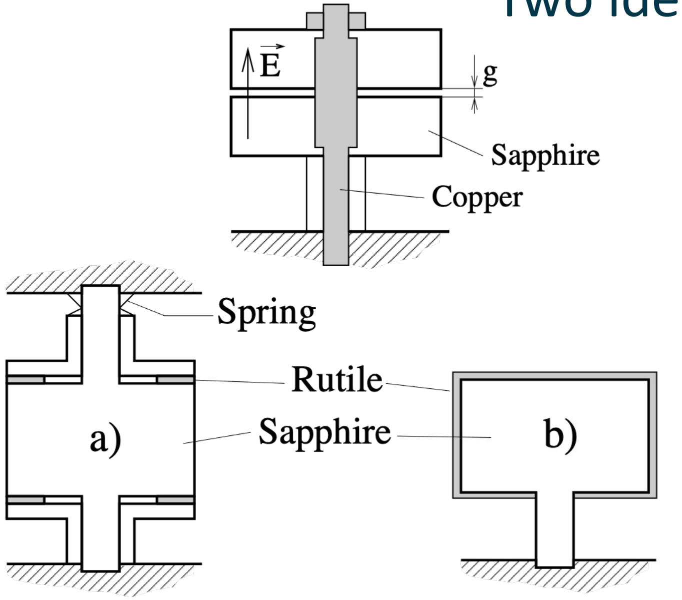

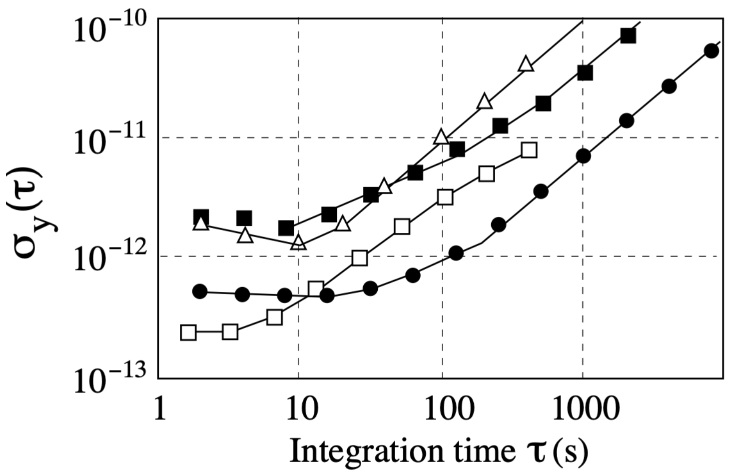

Temperature compensation

paramagnetic impurities: Fe^{3+} Cr^{3+}, Mo^{3+}, Ti^{3+}

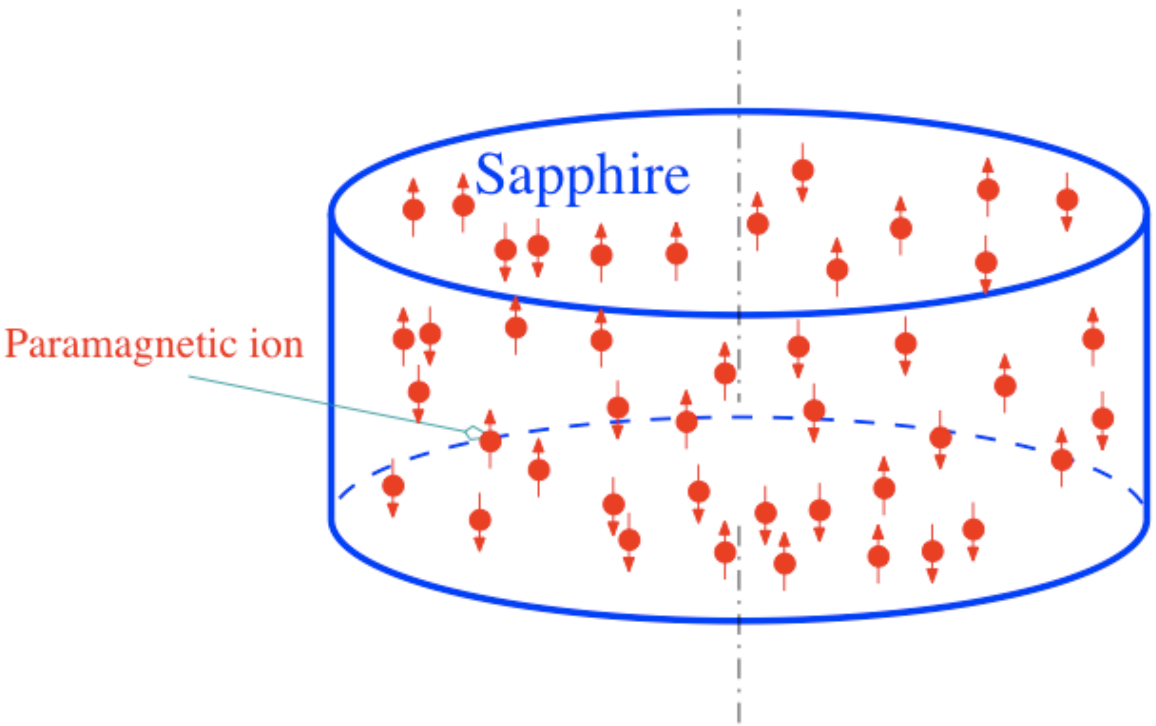

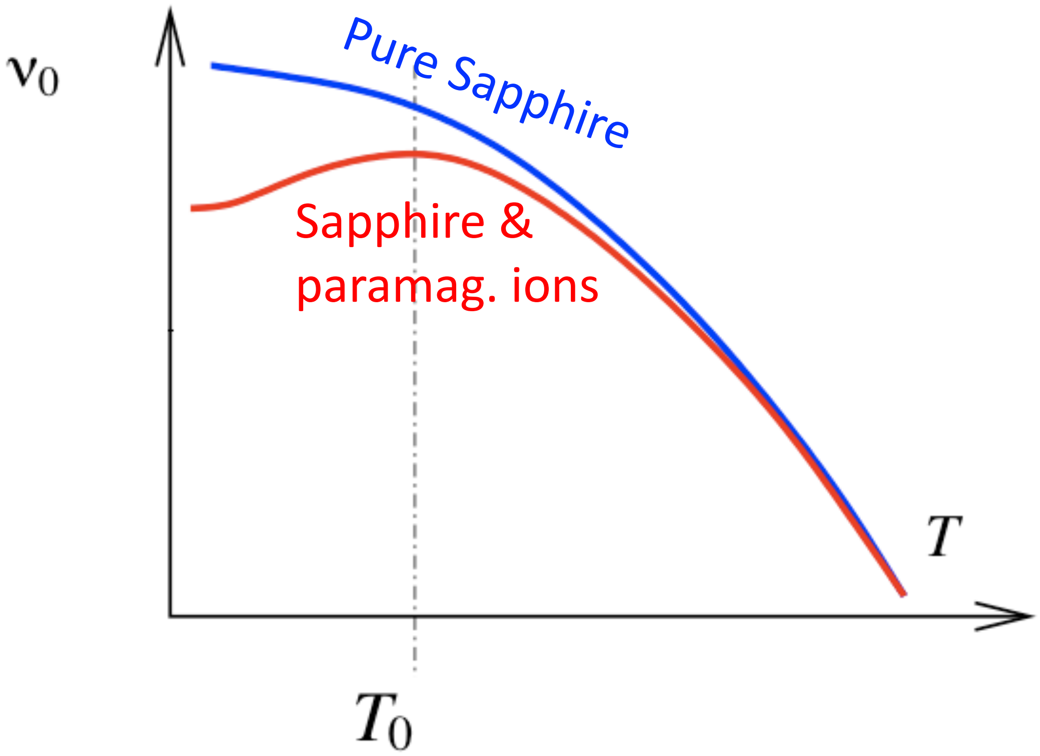

$$T_0 \sim 6\text{ K}$$

All figures of this page are courtesy
of V. Giordano, FEMTO-ST

CSOs exhibit ultimate stability

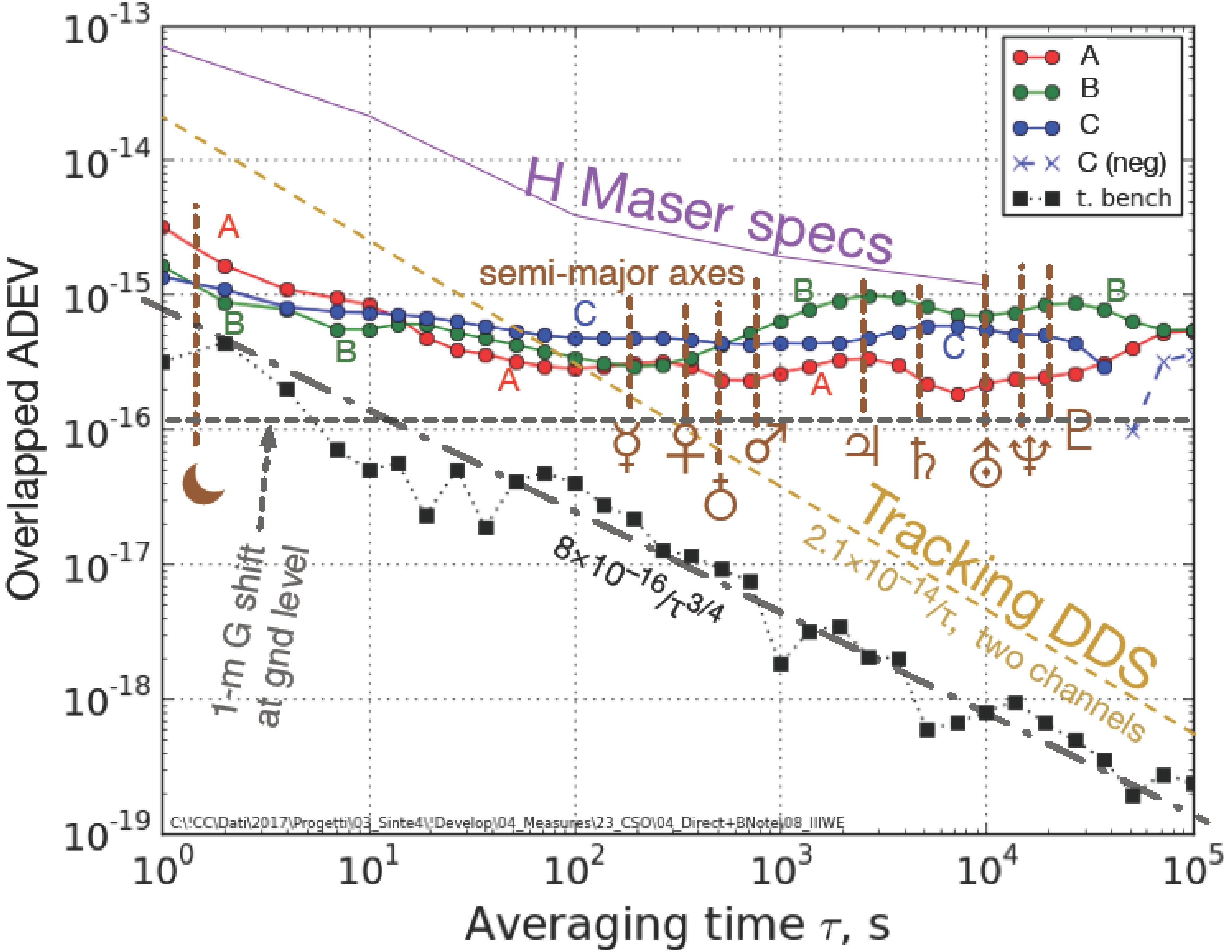

ELISA, before going to Argentina

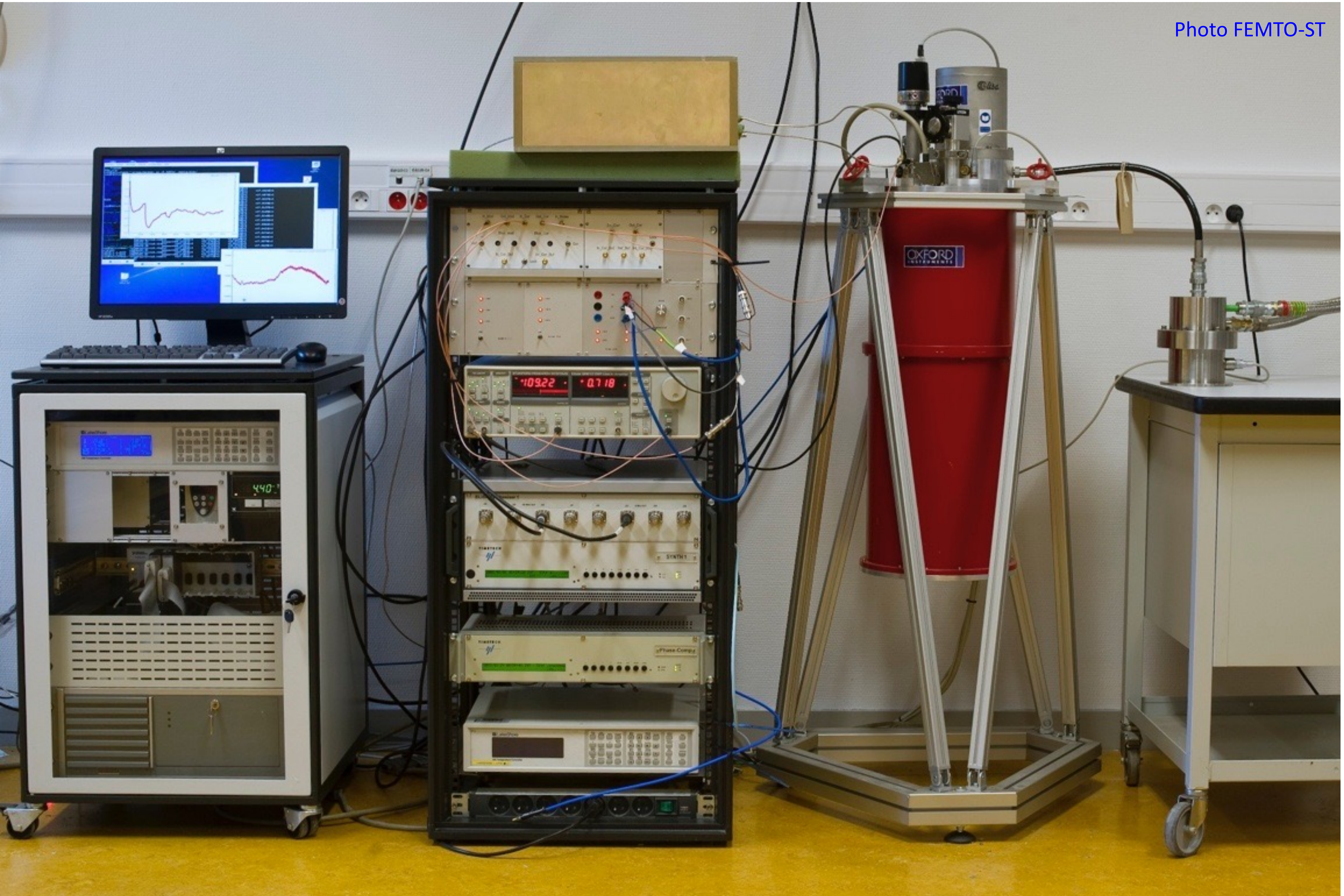

Photo FEMTO-ST

2-inch sapphire monocrystal

Photo V. Giordano

ULISS

Double check on the Figures

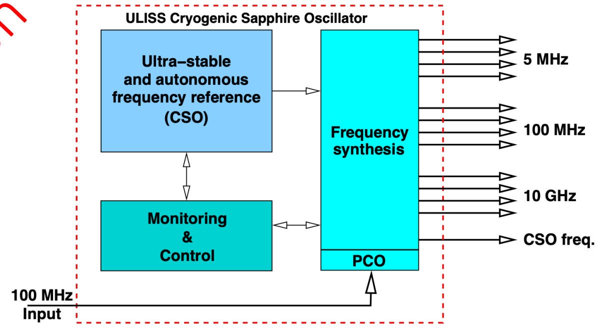

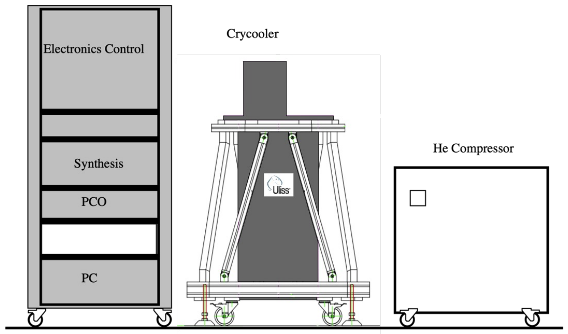

ADEV measurement ELISA/ULISS

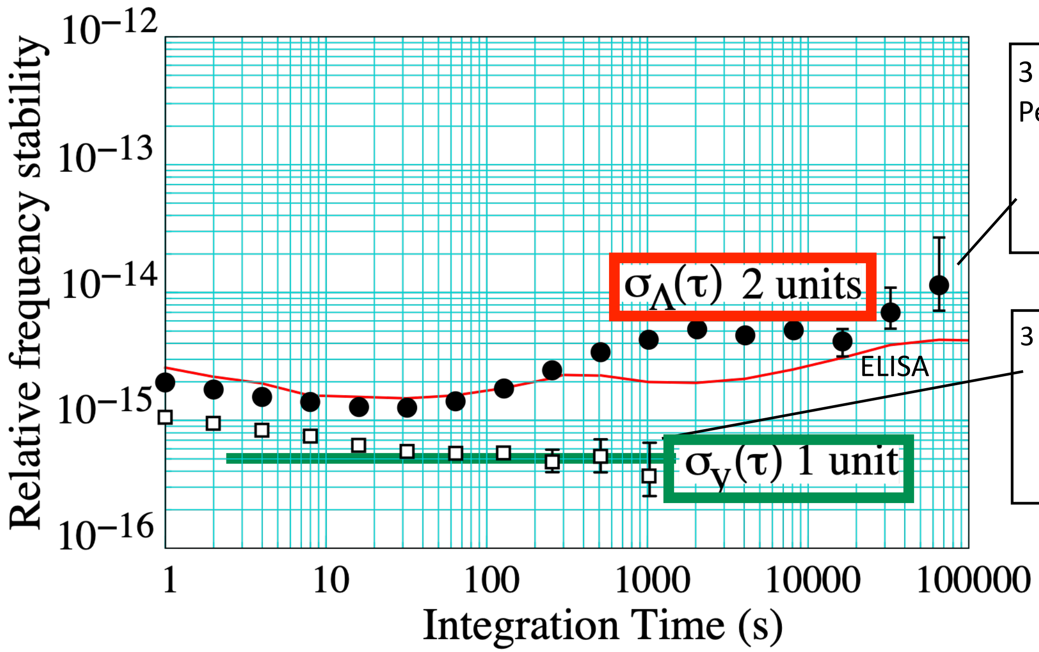

3 days measurement without post-processing
Perturbed environment:
- Technical university (ENSMM), ≥ 800 students
- Air conditioning still not operational during measurements

3 hours extracted from the entire data set
- Quiet environment, nighttime
- Take away 3dB for two equal units
- Λ-counter compensated: for flicker: $\sigma_\Lambda(\tau) \simeq 1.3 \times \sigma_y(\tau)$

flicker floor: 4×10^{-16} 10 s < τ < 1,000 s

The Flory-Taber Bragg resonator

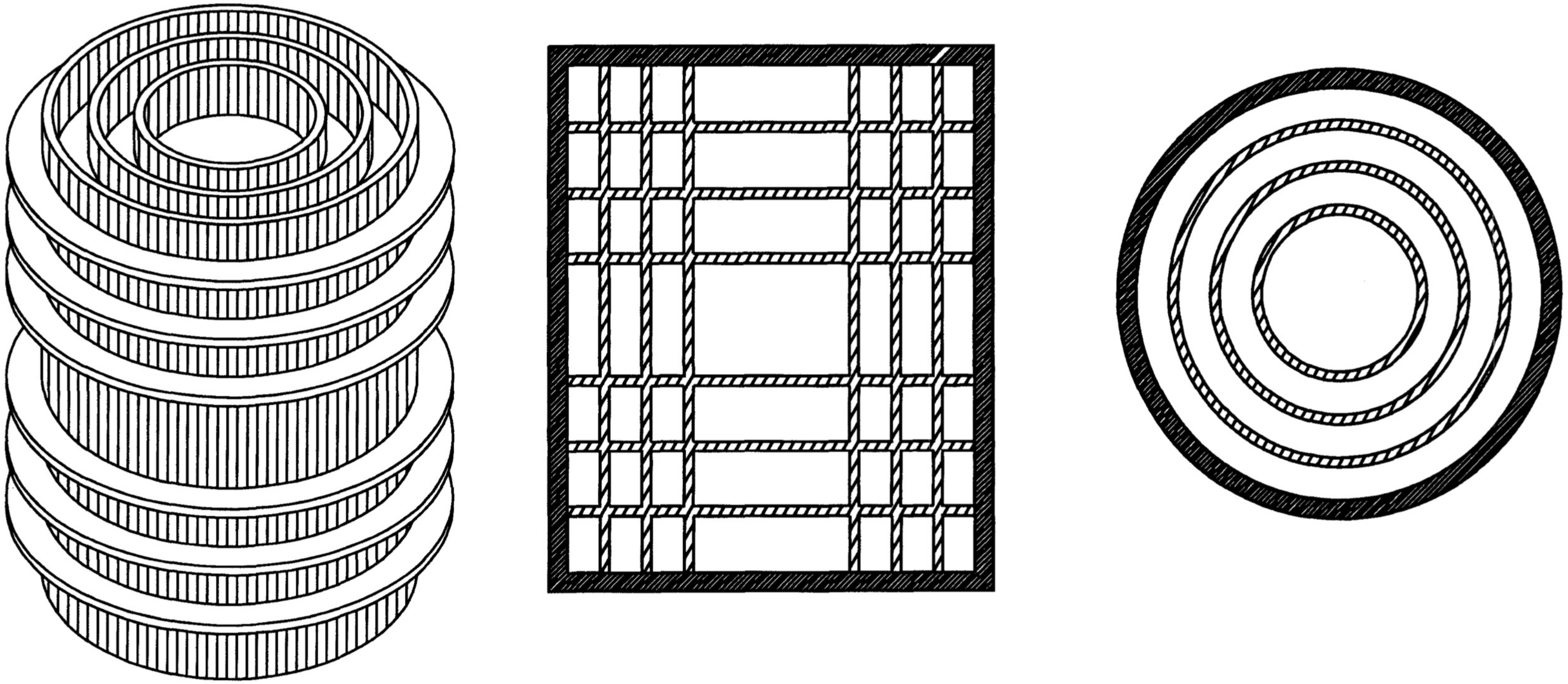

- Measured Q = 6.5×105 at 9 GHz, and 4.5×105 at 13.2 GHz
- Oscillator stability and noise not reported (yet)
- Project dropped

Figures / Featured article: Flory CA, Taber RC, IEEE T UFFC 44(2), March 1997

The Bale-Everard aperiodic Bragg resonator

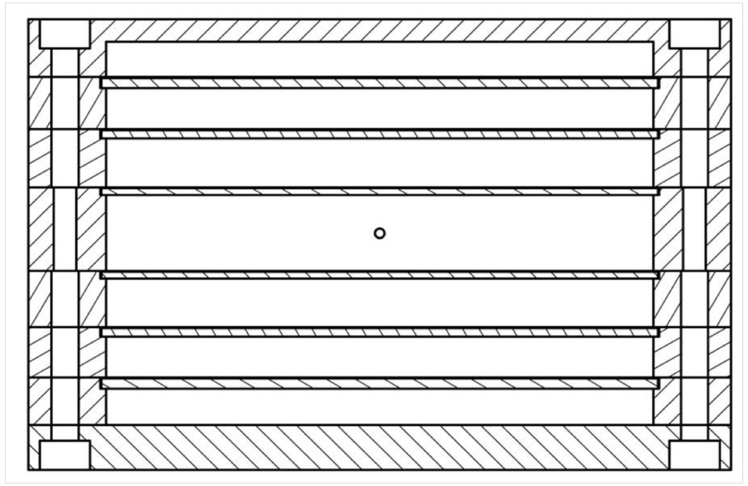

Suitable to Pound lock

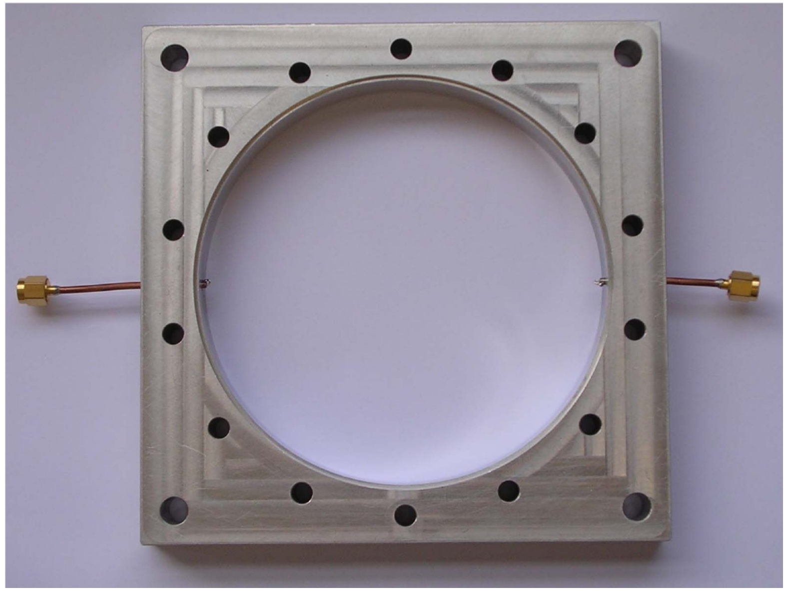

- 6-plates 10 GHz resonator
  - Q > 3×105 (simulated)
  - Q ≈ 2×105 (measured)
- Oscillator stability and noise not reported yet

Featured articles / Figures from:
S. Bale, J. K. A. Everard, High Q X-band distributed Bragg resonator utilising an aperiodic alumina plate arrangement, Proc IFCS-EFTF 2009
J. K. A. Everard, Proc. IFCS-EFTF 2015

Small superconducting Resonator

Superconducting resonator (NPL, UK)

Nb on Al_2O_3, 300x300 μm^2. 7.5 GHz, Q = 5E4,

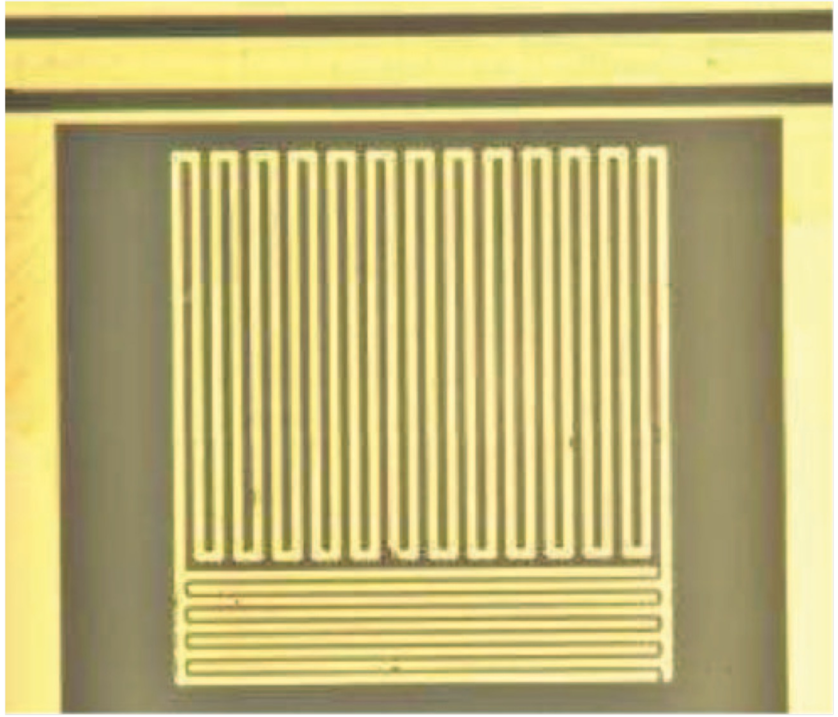

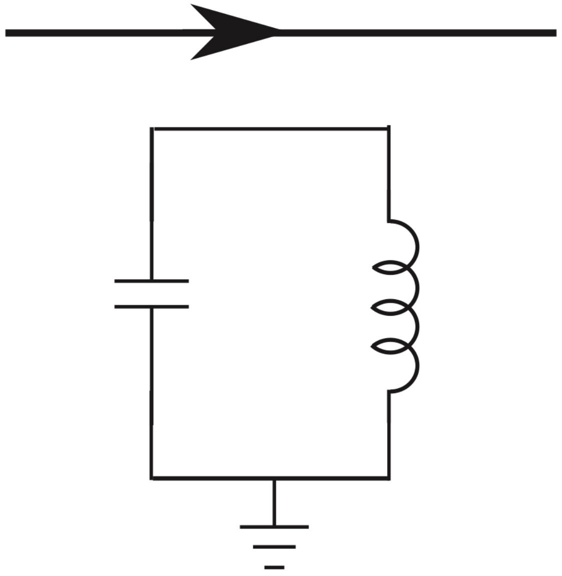

Lindstrom, Oxborrow & al, Rev Sci Instrum 82, 104706 (2011)

Resonators and Oscillators

Optics

Stabilization of the FS comb

- The FS comb enables frequency synthesis from RF to optics
  - Major breakthrough
  - 2005 Nobel prize, Roy J. Glauber, John L. Hall, Theodor W. Hänsch
- Stability and noise
  - Low noise in the sub-millisecond region
  - Drift and walk
  - Need stabilization
- Common practice
  - CW laser stabilized to a FP etalon
  - PDH control – of course
  - Compare/stabilize the FS comb to the CW laser

Featured book

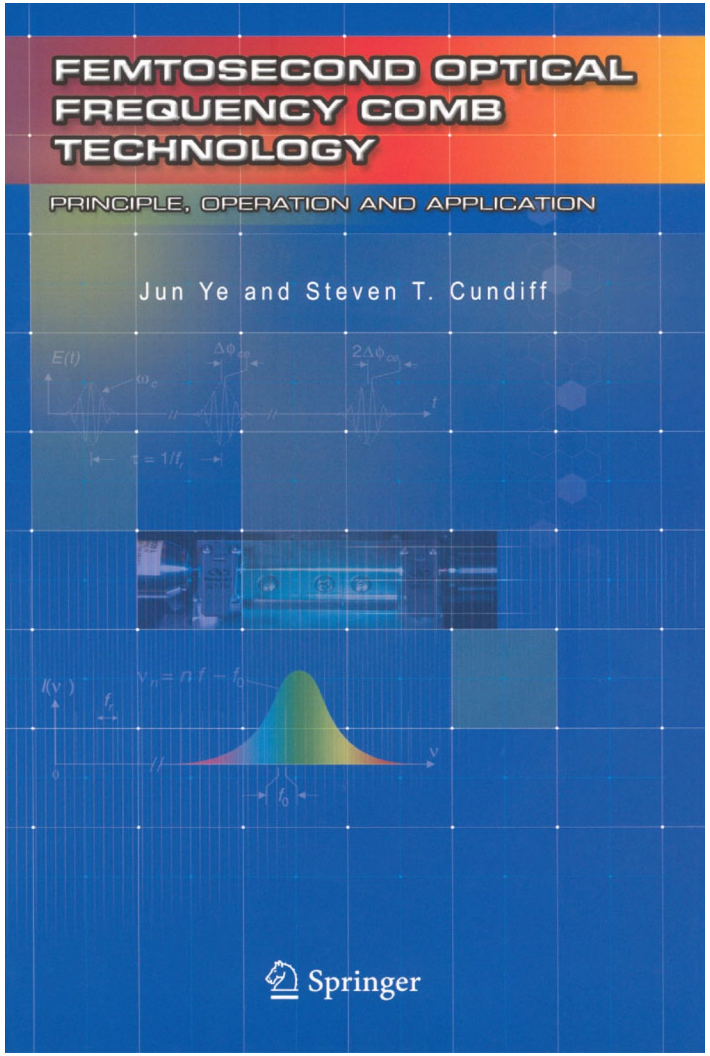

Fabry Pérot cavity

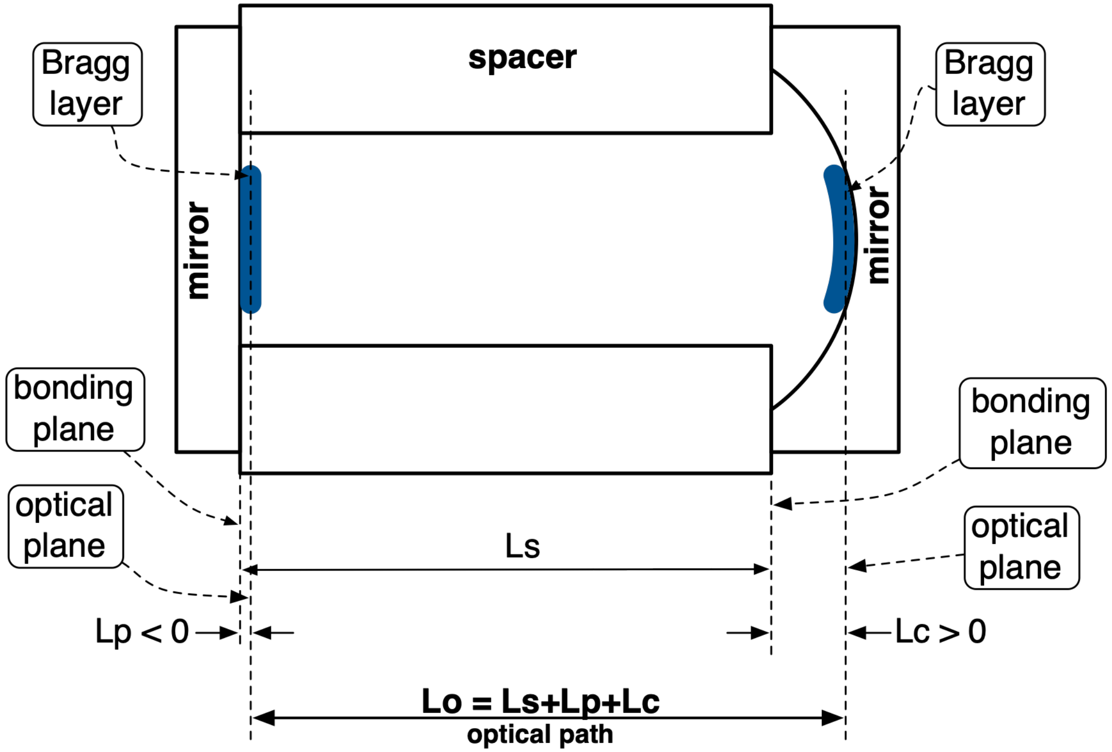

- Smart design of the spacer provides
  - Low sensitivity to acceleration
  - Temperature compensation
    - ULE and Zerodur
    - Many materials (Si, Ge, …) have natural turning point
- High Q is possible, ≥ 1010 (≈10 kHz optical bandwidth)

Optical transmission

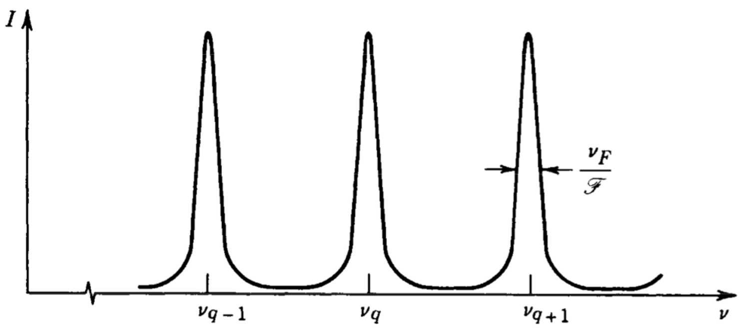

The JILA bicone spacer

March 15, 2007 / Vol. 32, No. 6 / OPTICS LETTERS 641

Compact, thermal-noise-limited optical cavity for diode laser stabilization at 1×10^{-15}

A. D. Ludlow, X. Huang,* M. Notcutt, T. Zanon-Willette, S. M. Foreman, M. M. Boyd, S. Blatt, and J. Ye

JILA, National Institute of Standards and Technology, and University of Colorado Department of Physics, University of Colorado, Boulder, Colorado 80309-0440, USA

Received October 30, 2006; accepted November 25, 2006; posted December 20, 2006 (Doc. ID 76598); published February 15, 2007

We demonstrate phase and frequency stabilization of a diode laser at the thermal noise limit of a passive optical cavity. The system is compact and exploits a cavity design that reduces vibration sensitivity. The subhertz laser is characterized by comparison with a second independent system with similar fractional frequency stability (1×10^{-15} at 1 s). The laser is further characterized by resolving a 2 Hz wide, ultranarrow optical clock transition in ultracold strontium.

OCIS codes: 140.2020, 030.1640, 300.6320.

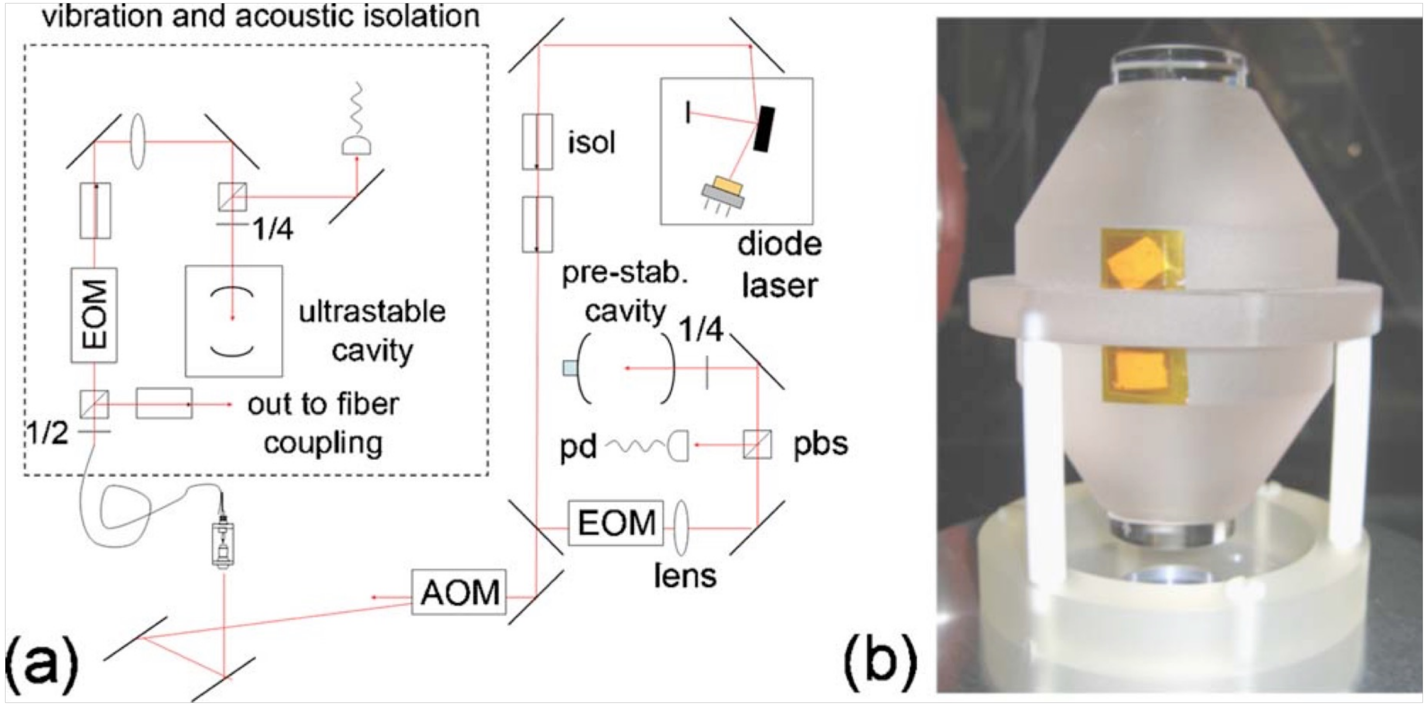

Field-test of a robust, portable, frequency-stable laser

David R. Leibrandt,* Michael J. Thorpe, James C. Bergquist, and Till Rosenband
National Institute of Standards and Technology, 325 Broadway Street, Boulder, Colorado 80305, USA
**david.leibrandt@nist.gov*

Abstract: We operate a frequency-stable laser in a non-laboratory environment where the test platform is a passenger vehicle. We measure the acceleration experienced by the laser and actively correct for it to achieve a system acceleration sensitivity of $\Delta f/f = 11(2) \times 10^{-12}$/g, $6(2) \times 10^{-12}$/g, and $4(1) \times 10^{-12}$/g for accelerations in three orthogonal directions at 1 Hz. The acceleration spectrum and laser performance are evaluated with the vehicle both stationary and moving. The laser linewidth in the stationary vehicle with engine idling is 1.7(1) Hz.

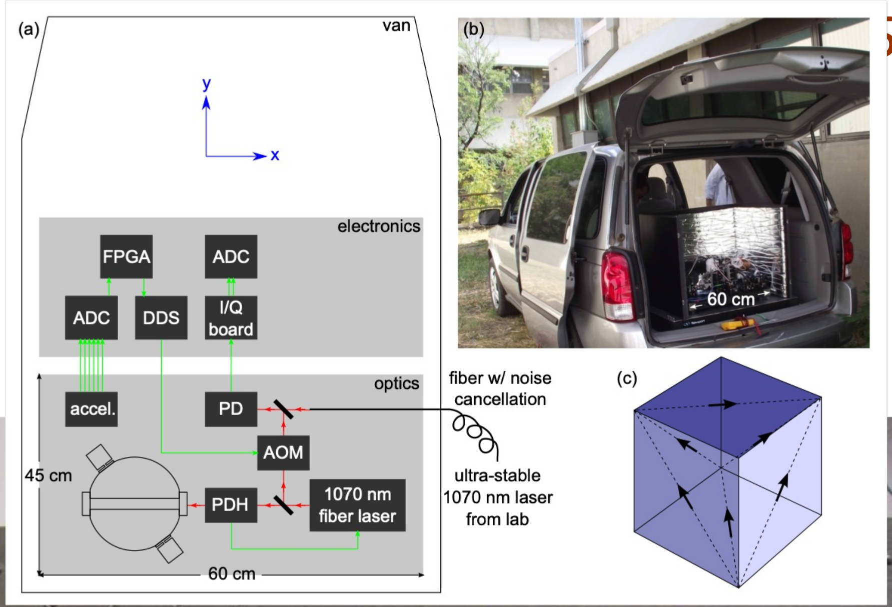

The NIST spherical spacer

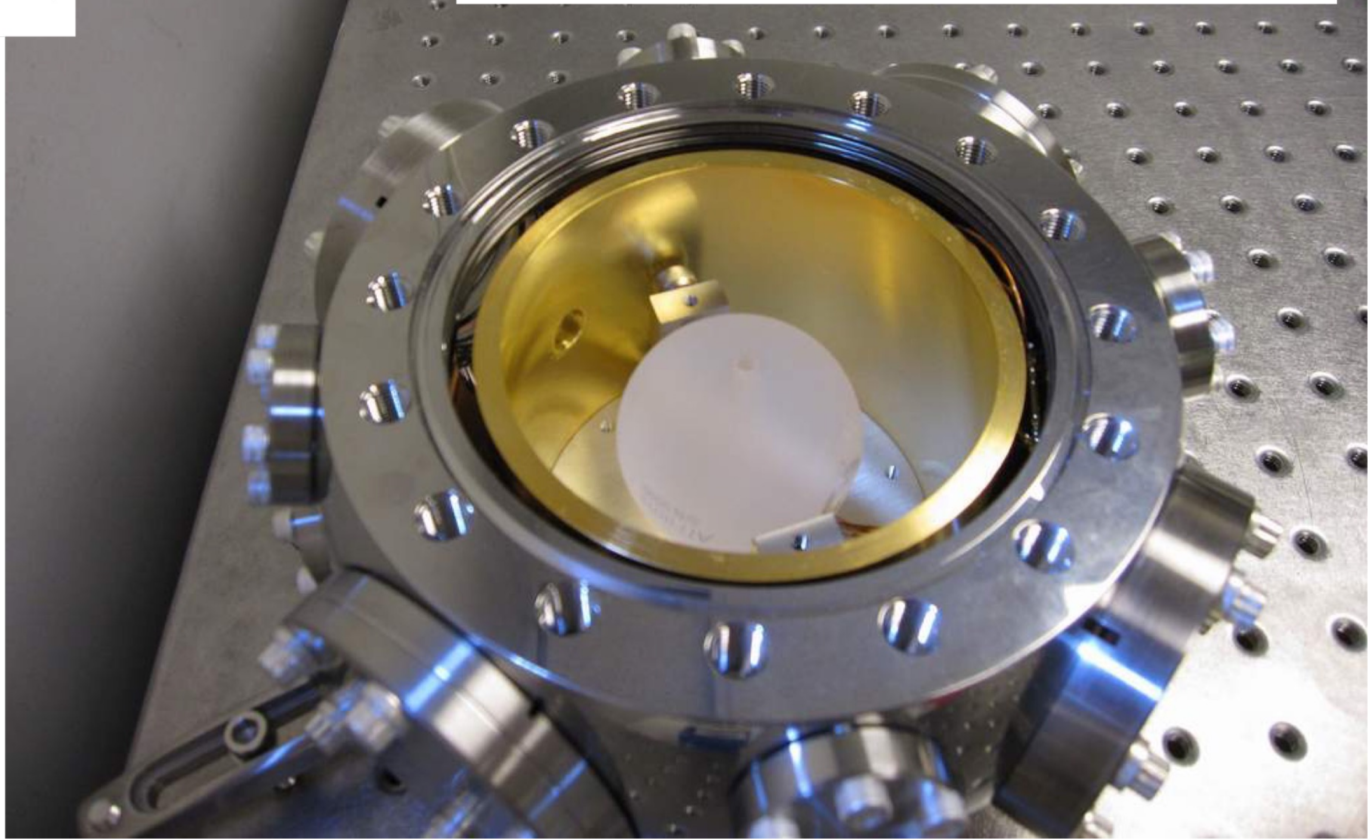

The improved NIST spherical spacer

PHYSICAL REVIEW A **87**, 023829 (2013)

Cavity-stabilized laser with acceleration sensitivity below 10^{-12} g^{-1}

David R. Leibrandt,* James C. Bergquist, and Till Rosenband
National Institute of Standards and Technology, 325 Broadway Street, Boulder, Colorado 80305, USA
(Received 31 December 2012; published 21 February 2013)

We characterize the frequency sensitivity of a cavity-stabilized laser to inertial forces and temperature fluctuations, and perform real-time feedforward to correct for these sources of noise. We measure the sensitivity of the cavity to linear accelerations, rotational accelerations, and rotational velocities by rotating it about three axes with accelerometers and gyroscopes positioned around the cavity. The worst-direction linear acceleration sensitivity of the cavity is $2(1) \times 10^{-11}$ g^{-1} measured over 0–50 Hz, which is reduced by a factor of 50 to below 10^{-12} g^{-1} for low-frequency accelerations by real-time feedforward corrections of all of the aforementioned inertial forces. A similar idea is demonstrated in which laser frequency drift due to temperature fluctuations is reduced by a factor of 70 via real-time feedforward from a temperature sensor located on the outer wall of the cavity vacuum chamber.

DOI: 10.1103/PhysRevA.87.023829 PACS number(s): 42.62.Eh, 42.60.Da, 46.40.−f, 07.07.Tw

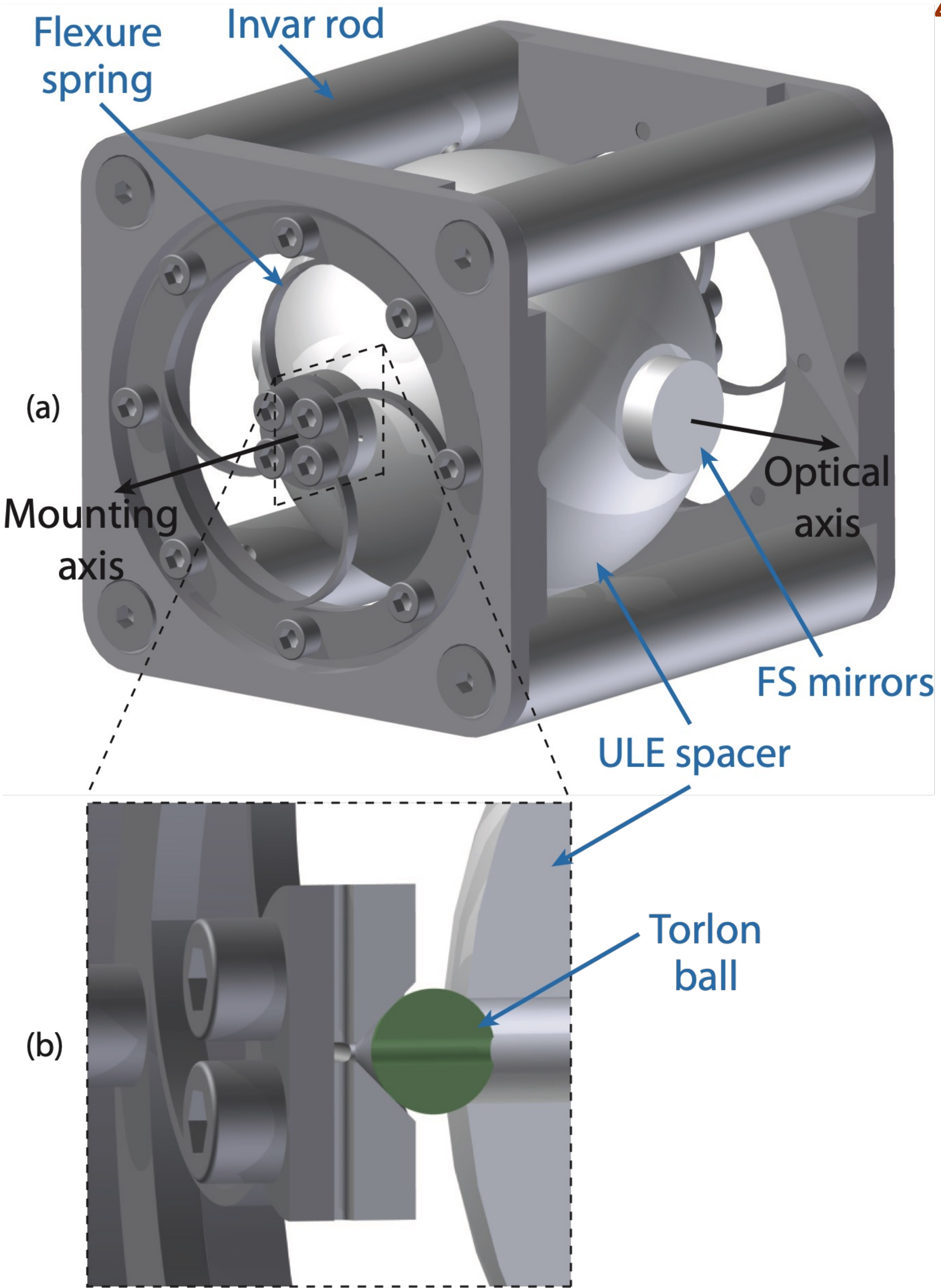

The NPL horizontal cavity

PHYSICAL REVIEW A **75**, 011801(R) (2007)

Vibration insensitive optical cavity

S. A. Webster, M. Oxborrow, and P. Gill
National Physical Laboratory, Hampton Road, Teddington, Middlesex, TW11 0LW, United Kingdom
(Received 31 October 2006; published 9 January 2007)

An optical cavity is designed and implemented that is insensitive to vibration in all directions. The cavity is mounted with its optical axis in the horizontal plane. A minimum response of 0.1 (3.7) kHz/ms^{-2} is achieved for low-frequency vertical (horizontal) vibrations.

DOI: 10.1103/PhysRevA.75.011801 PACS number(s): 42.60.Da, 07.60.Ly, 06.30.Ft

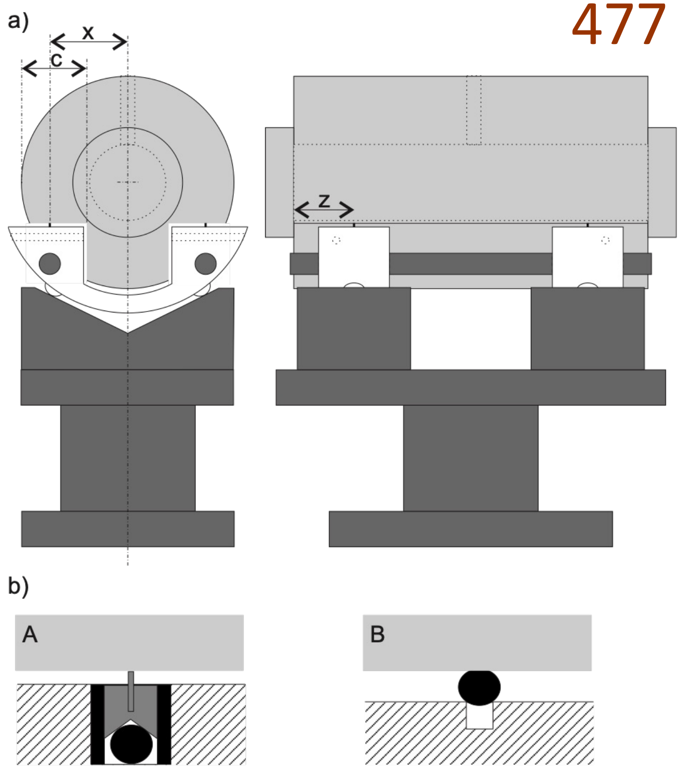

PHYSICAL REVIEW A **77**, 033847 (2008)

Thermal-noise-limited optical cavity

S. A. Webster,[1] M. Oxborrow,[1] S. Pugla,[2] J. Millo,[3] and P. Gill[1]
[1]*National Physical Laboratory, Hampton Road, Teddington, Middlesex, TW11 0LW, United Kingdom*
[2]*Blackett Laboratory, Imperial College London, South Kensington Campus, London, SW7 2BZ, United Kingdom*
[3]*SYRTE, Observatoire de Paris, 61, Avenue de l'Observatoire, 75014, Paris, France*
(Received 31 October 2007; published 27 March 2008)

A pair of optical cavities are designed and set up so as to be insensitive to both temperature fluctuations and mechanical vibrations. With the influence of these perturbations removed, a fundamental limit to the frequency stability of the optical cavity is revealed. The stability of a laser locked to the cavity reaches a floor $<2 \times 10^{-15}$ for averaging times in the range 0.5–100 s. This limit is attributed to Brownian motion of the mirror substrates and coatings.

DOI: 10.1103/PhysRevA.77.033847 PACS number(s): 42.60.Da, 07.60.Ly, 07.10.Fq, 06.30.Ft

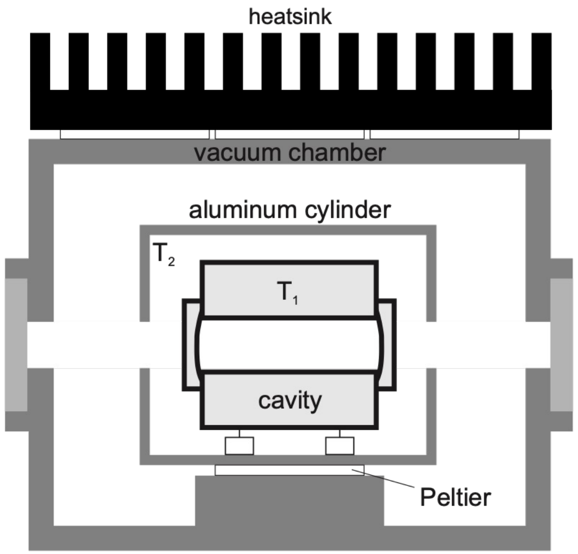

The NPL small cubic cavity

Force-insensitive optical cavity

Stephen Webster* and Patrick Gill

National Physical Laboratory, Hampton Road, Teddington, Middlesex, TW11 0LW, UK

**Corresponding author: stephen.webster@npl.co.uk*

Received June 20, 2011; revised August 11, 2011; accepted August 11, 2011;
posted August 12, 2011 (Doc. ID 149376); published September 9, 2011

We describe a rigidly mounted optical cavity that is insensitive to inertial forces acting in any direction and to the compressive force used to constrain it. The design is based on a cubic geometry with four supports placed symmetrically about the optical axis in a tetrahedral configuration. To measure the inertial force sensitivity, a laser is locked to the cavity while it is inverted about three orthogonal axes. The maximum acceleration sensitivity is $2.5 \times 10^{-11}/g$ (where $g = 9.81\,\mathrm{ms}^{-2}$), the lowest passive sensitivity to be reported for an optical cavity.

OCIS codes: 140.4780, 140.3425, 120.3940, 120.6085.

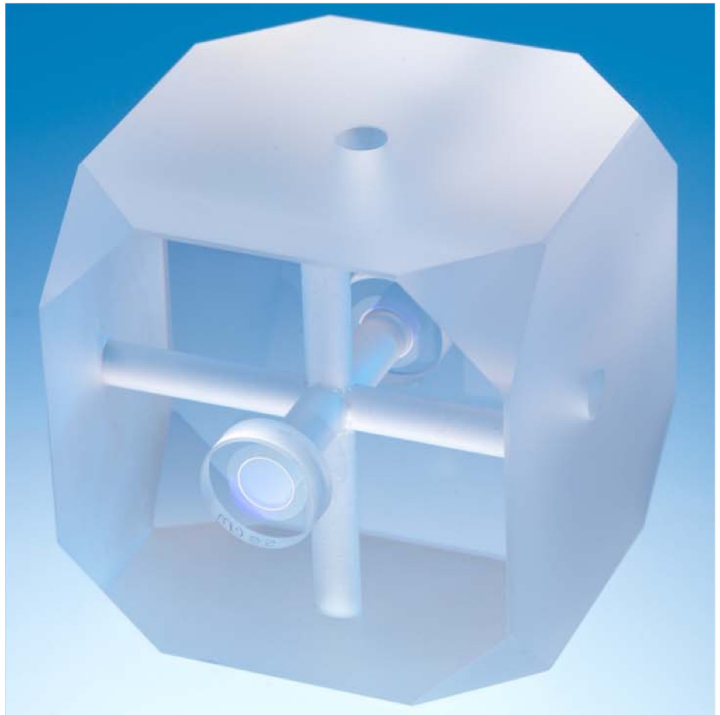

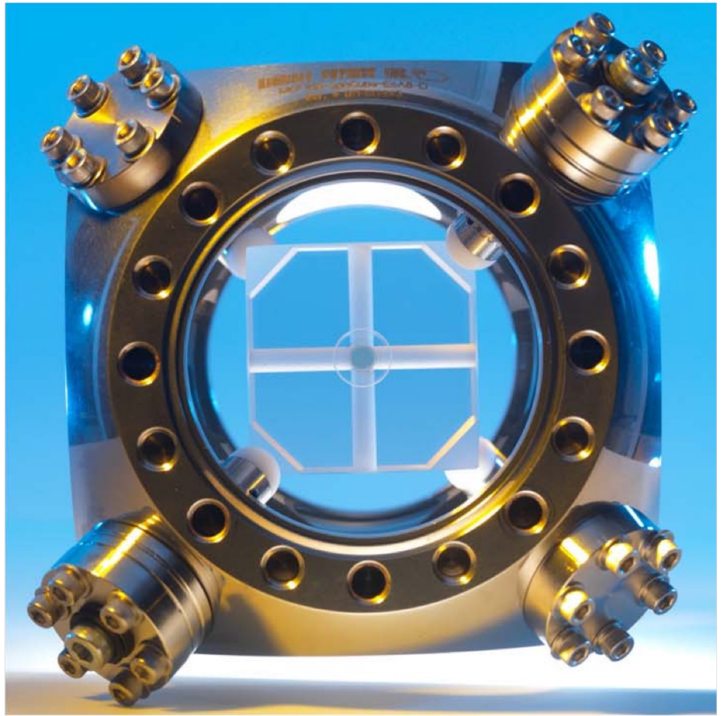

The SYRTE horizontal cavity

PHYSICAL REVIEW A **79**, 053829 (2009)

Ultrastable lasers based on vibration insensitive cavities

J. Millo, D. V. Magalhães, C. Mandache, Y. Le Coq, E. M. L. English,* P. G. Westergaard, J. Lodewyck, S. Bize, P. Lemonde, and G. Santarelli

LNE-SYRTE, Observatoire de Paris, CNRS, UPMC, 61 Avenue de l'Observatoire, 75014 Paris, France

(Received 5 February 2009; published 18 May 2009)

We present two ultrastable lasers based on two vibration insensitive cavity designs, one with vertical optical axis geometry, the other horizontal. Ultrastable cavities are constructed with fused silica mirror substrates, shown to decrease the thermal noise limit, in order to improve the frequency stability over previous designs. Vibration sensitivity components measured are equal to or better than $1.5\times10^{-11}/\text{m s}^{-2}$ for each spatial direction, which shows significant improvement over previous studies. We have tested the very low dependence on the position of the cavity support points, in order to establish that our designs eliminate the need for fine tuning to achieve extremely low vibration sensitivity. Relative frequency measurements show that at least one of the stabilized lasers has a stability better than 5.6×10^{-16} at 1 s, which is the best result obtained for this length of cavity.

DOI: 10.1103/PhysRevA.79.053829 PACS number(s): 42.60.Da, 07.60.Ly, 42.62.Fi

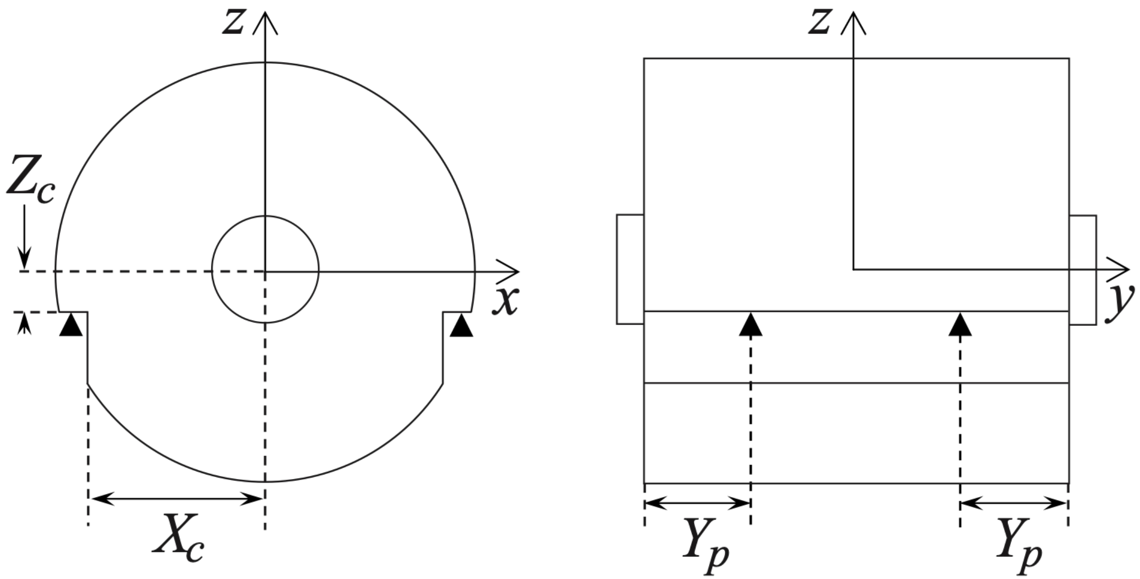

The PTB transportable laser

Demonstration of a Transportable 1 Hz-Linewidth Laser

Stefan Vogt, Christian Lisdat, Thomas Legero, Uwe Sterr, Ingo Ernsting, Alexander Nevsky, Stephan Schiller

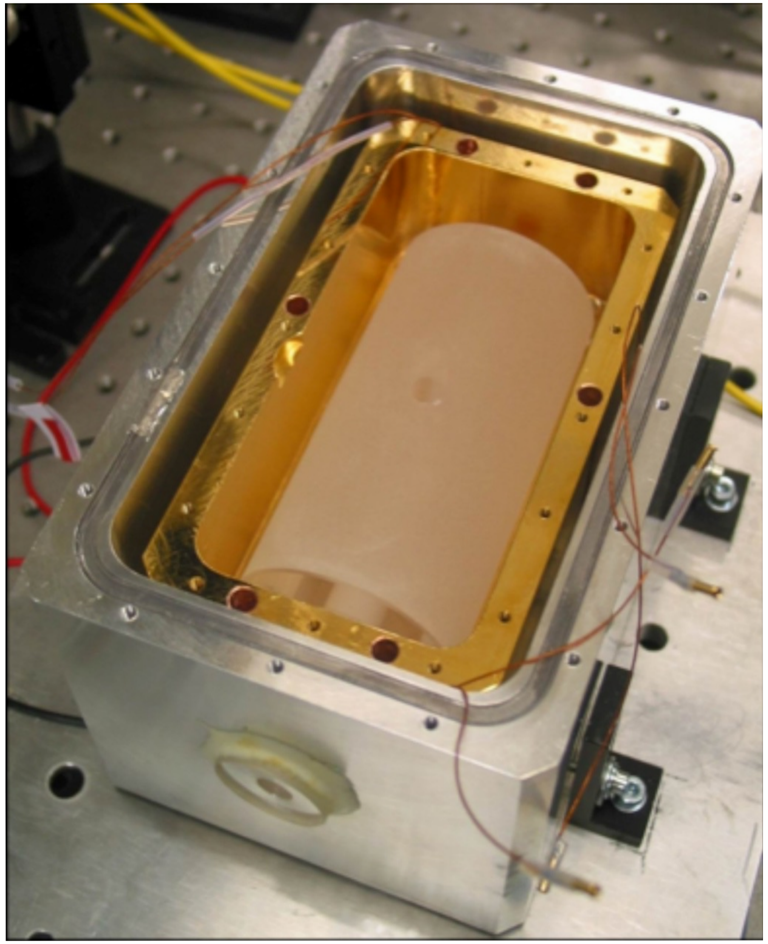

APPLIED PHYSICS B: LASERS AND OPTICS
Volume 104, Number 4, 741-745, DOI: 10.1007/s00340-011-4652-7

Natural Si has zero expansion at 17 K and 124 K

Figure from: K. G Lyon & al, JAP 48(3) p.865, 1977

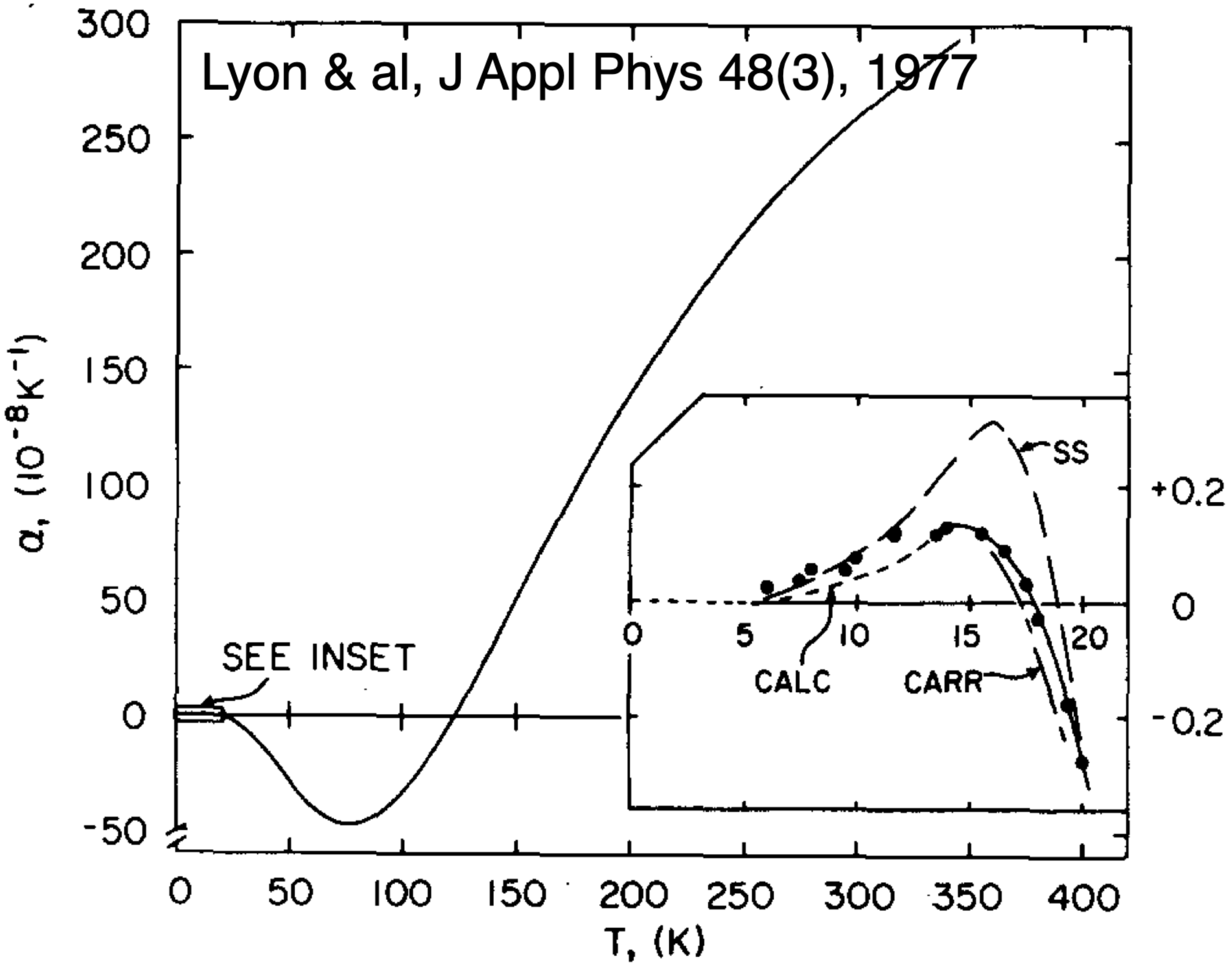

T = 124 K –> T. Kessler & al., PTB / QUEST - Proc. 2011 IFCS

K. G Lyon & al, Linear thermal expansion measurements on silicon from 6 to 340 K - J Appl. Phys 48(3) p.865, 1977

Swenson CA - Recommended values for the thermal expansivity of Silicon from 0 to 1000 K - JPCRD 12(2), 1983

The PTB 124-K Si cavity

TABLE II. Parameters for optical resonators.

Parameter	Value
21-cm cavity	
Cavity length	0.212 m
Spacer radius	0.04 m
Radius of central bore	5 mm
ROC of mirror	2 m
Beam radius on mirror	482 μm
Cavity temperature	124 K
Cavity finesse	3.6×10^5
Laser wavelength	1542 nm
6-cm cavity	
Cavity length	0.06 m
ROC of mirror	1 m
Beam radius on mirror	294 μm
Cavity temperature	4 or 16 K
Cavity finesse	2.9×10^5
Laser wavelength	1542 nm
Single-crystal silicon	
Young's modulus	188 GPa [65]
Poisson ratio	0.26 [65]
Density	2331 kg/m^3 [66]
Thermal conductivity	600 W/m K [67]
Specific heat	330 J/kg K [68]
Mechanical loss	0.83×10^{-8} [69]

Table II from J. Yu et al, Excess Noise and Photoinduced Effects in Highly Reflective Crystalline Mirrror Coatings, Phys Rev X 13(4) 2023

Experimental setup

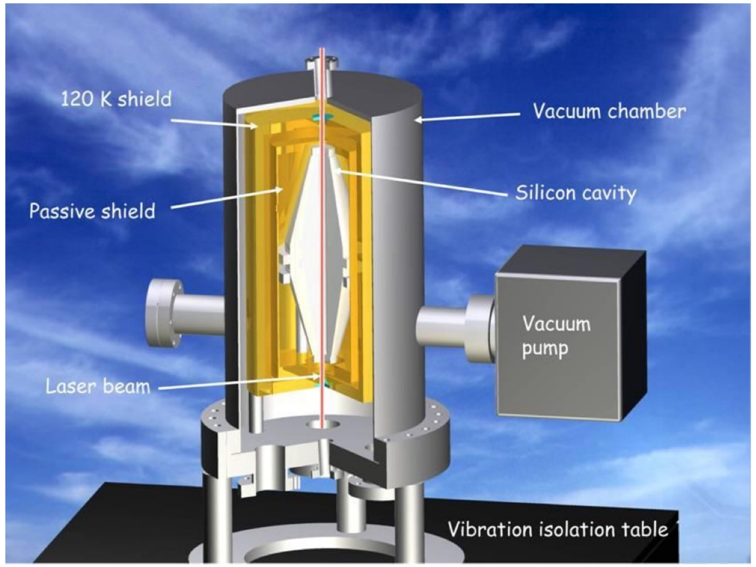

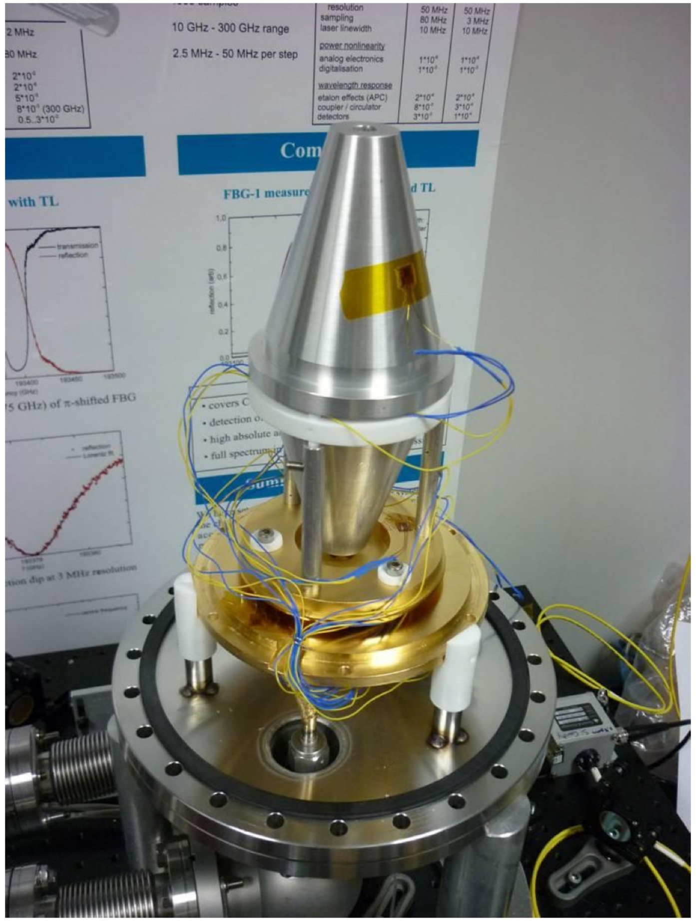

Silicon cavity is thermally isolated by two gold-plated copper shields.

femto-st SCIENCES & TECHNOLOGIES

Spherical FP etalon

Implemented at FEMTO-ST Institute, using a kit from
Stable Lasers Sistem, Boulder, CO, USA

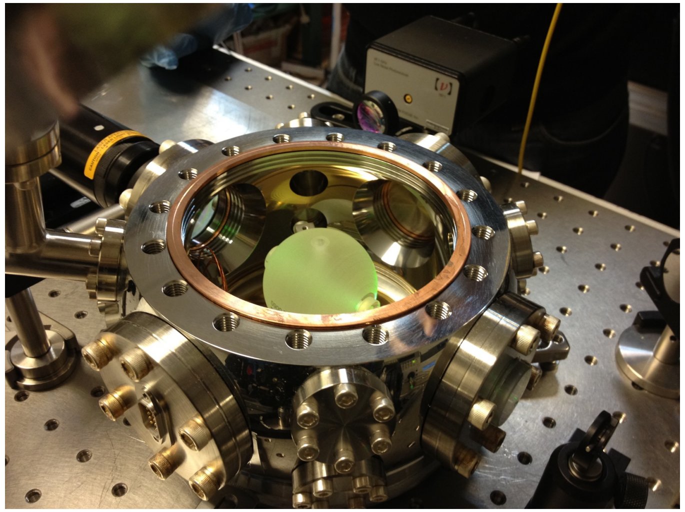

A. Didier et al., Photo from the authors

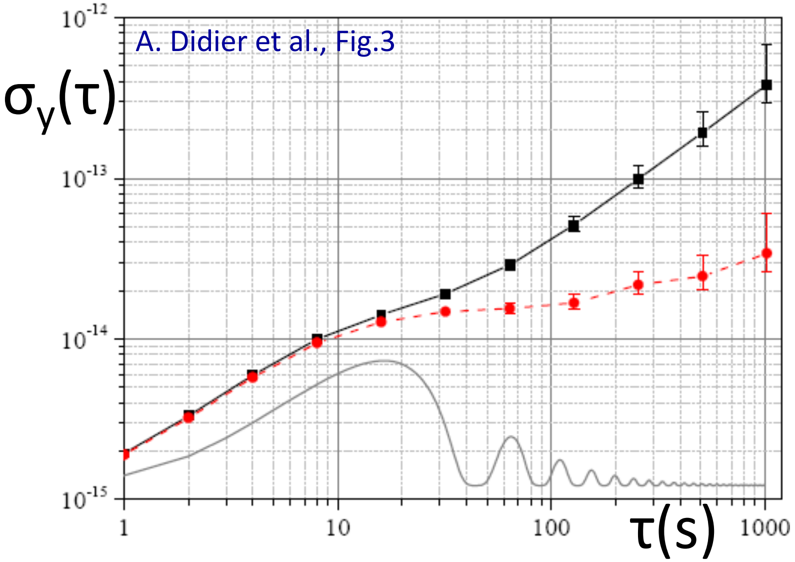

A. Didier et al., Fig.3

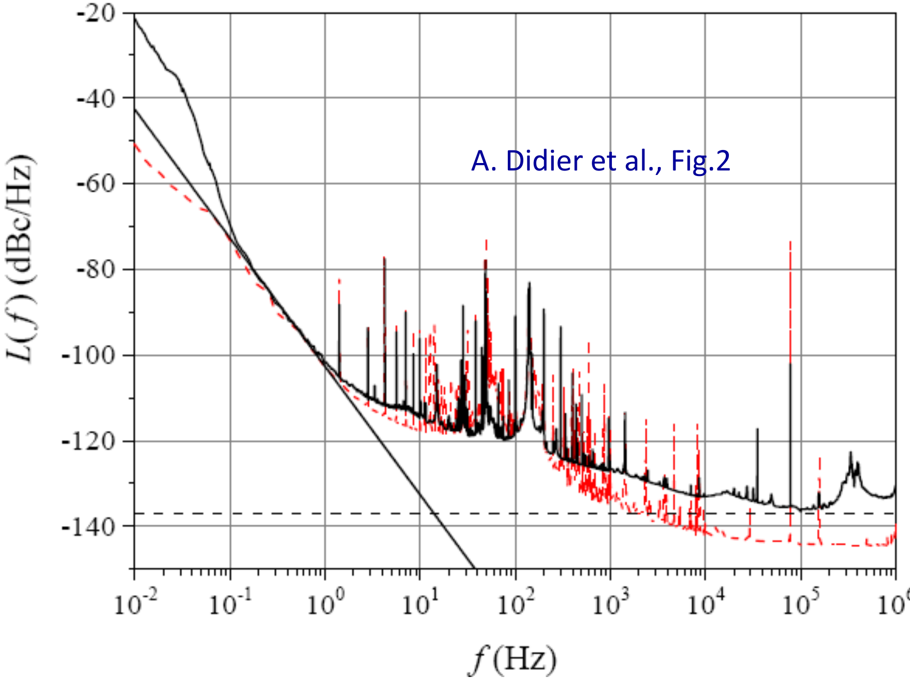

A. Didier et al., Fig.2

Phase noise –104 dBc/Hz, state of the art

Frequency instability limited by the lab temperature fluctuations

Operational, $\sigma_y(\tau) \approx 2\text{x}10^{-15}$

A. Didier, J. Millo, S. Grop, B. Dubois, E. Bigler, E. Rubiola, C. Lacroûte, Y. Kersalé, Ultra-low phase noise all-optical microwave generation setup based on commercial devices, Applied Optics 54(12) pp.3682-3686, April 2015.

Compact FP etalon

Original project at FEMTO-ST Institute

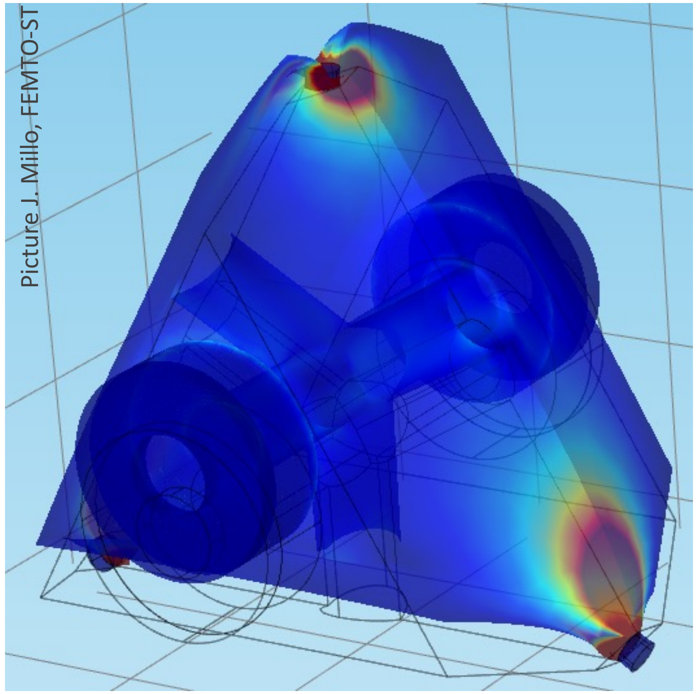

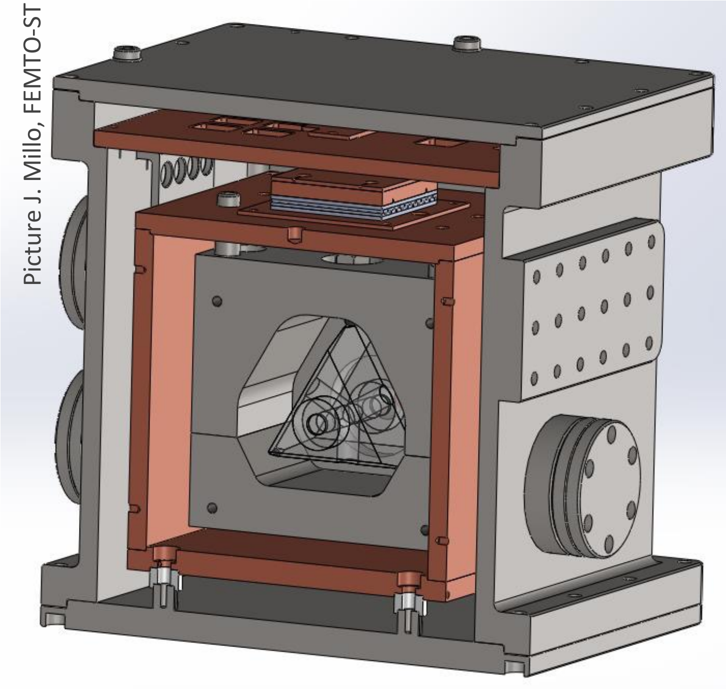

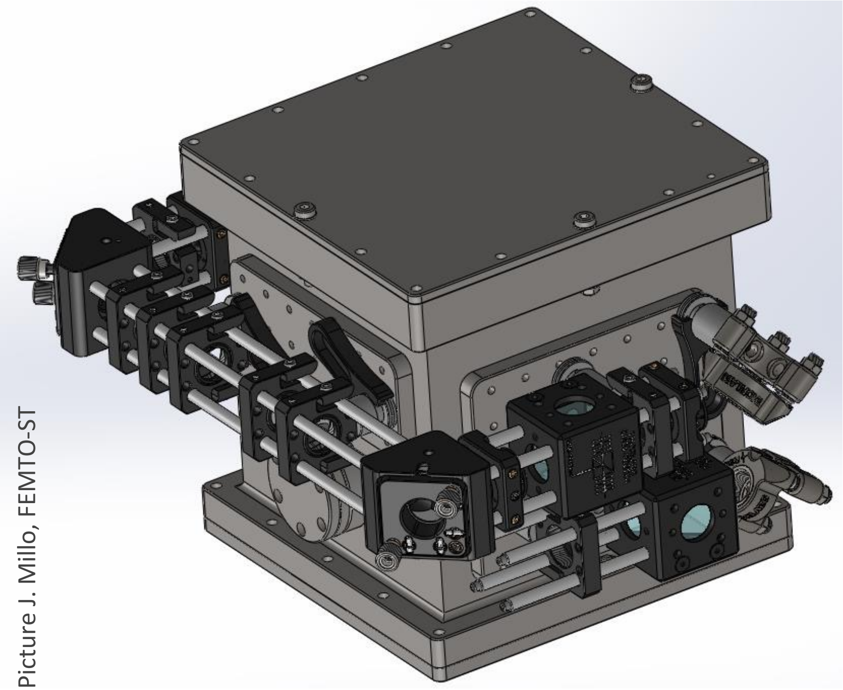

Target $\sigma_y(\tau) \approx 2\text{x}10^{-15}$

Silicon FP Etalon

Original project at FEMTO-ST Institute

Photos/pictures from the OHMS team, FEMTO-ST Institute

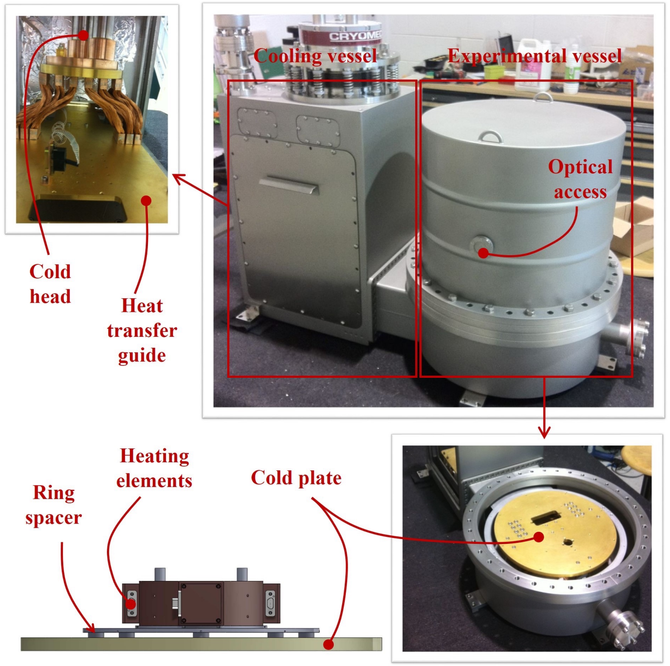

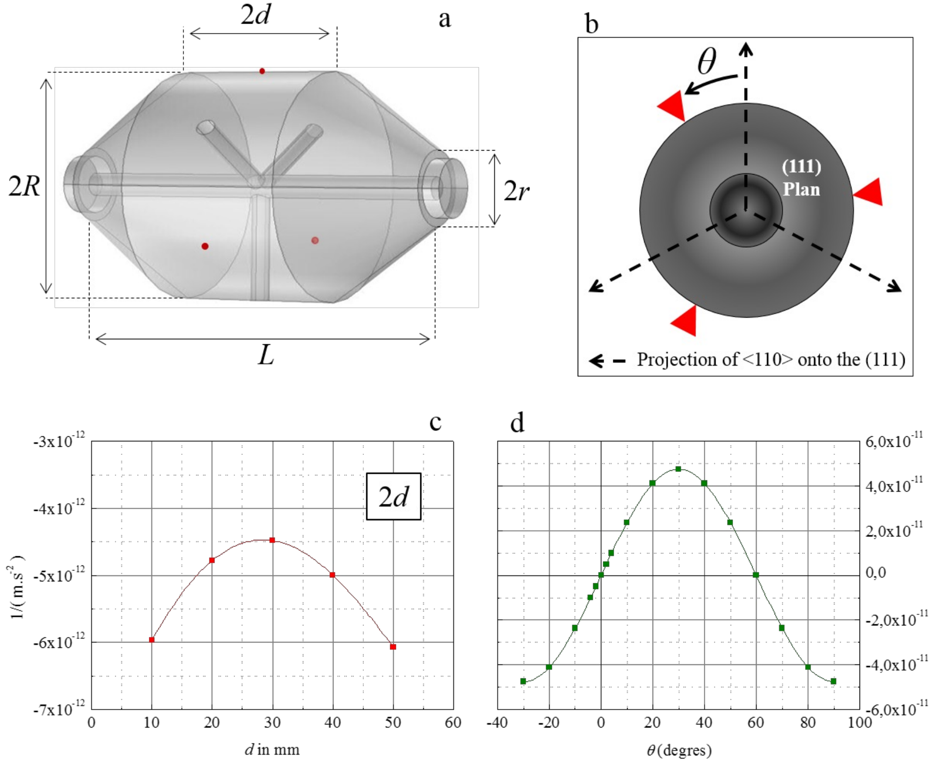

Cavity

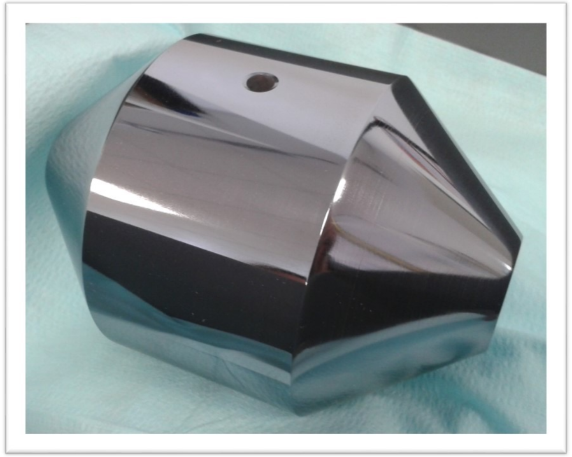

Low vibrations cryocooler: displacement less than 40 nm

Temperature instability less than 100 μK

Sensitivity to vibrations less than $4x10^{-12}$ /m.s^{-2}

Target $\sigma_y(\tau) \approx 3x10^{-17}$

Fundamental Physics

VIRGO – Gravitational waves

Duplicated

September 14, 2015
twin LIGO interferometers,
Livingston, LA, Hanford, WA

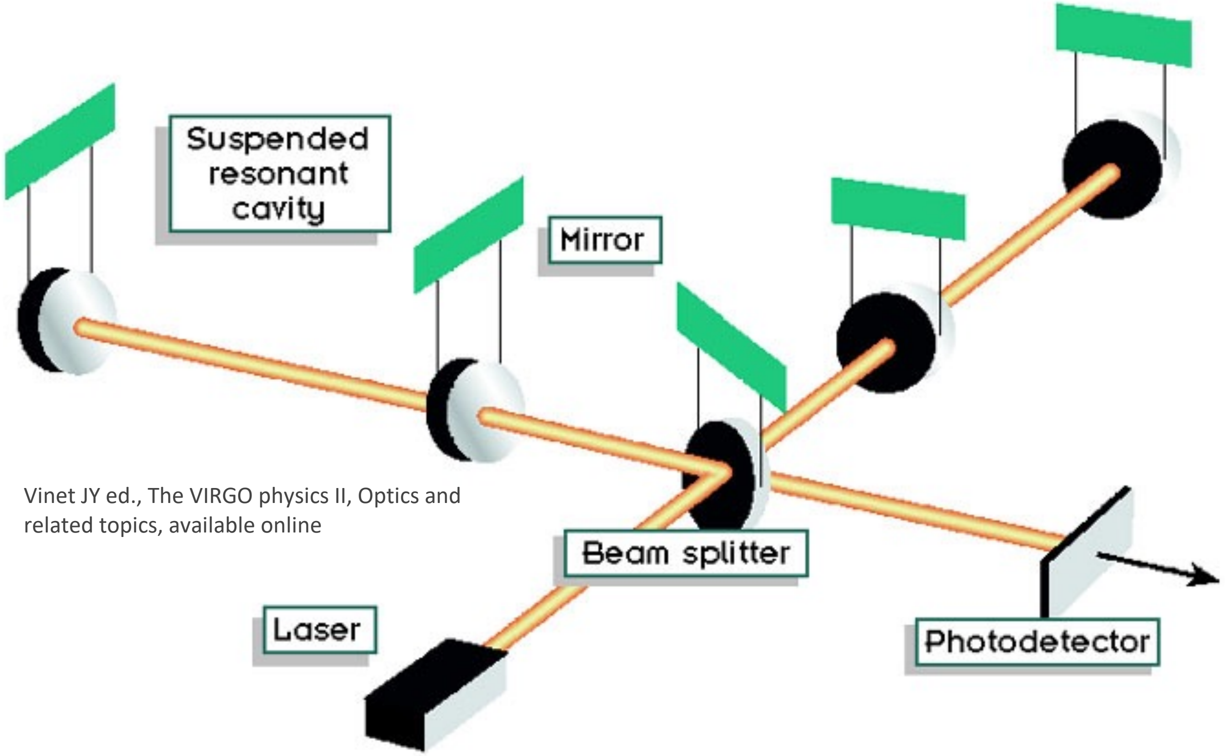

Vinet JY ed., The VIRGO physics II, Optics and related topics, available online

- Large Michelson interferometers detect the space-time fluctuations
- PDH control is used to lock ultra-stable lasers to the interferometer

https://www.virgo-gw.eu/

https://www.ego-gw.it

Lorentz invariance

PHYSICAL REVIEW D **80,** 105011 (2009)

Rotating optical cavity experiment testing Lorentz invariance at the 10^{-17} level

S. Herrmann,[1,2] A. Senger,[1] K. Möhle,[1] M. Nagel,[1] E. V. Kovalchuk,[1] and A. Peters[1]
[1]*Institut für Physik, Humboldt-Universität zu Berlin, Hausvogteiplatz 5-7, 10117 Berlin*
[2]*ZARM, Universität Bremen, Am Fallturm 1, 28359 Bremen*
(Received 10 August 2009; published 12 November 2009)

We present an improved laboratory test of Lorentz invariance in electrodynamics by testing the isotropy of the speed of light. Our measurement compares the resonance frequencies of two orthogonal optical resonators that are implemented in a single block of fused silica and are rotated continuously on a precision air bearing turntable. An analysis of data recorded over the course of one year sets a limit on an anisotropy of the speed of light of $\Delta c/c \sim 1 \times 10^{-17}$. This constitutes the most accurate laboratory test of the isotropy of c to date and allows to constrain parameters of a Lorentz violating extension of the standard model of particle physics down to a level of 10^{-17}.

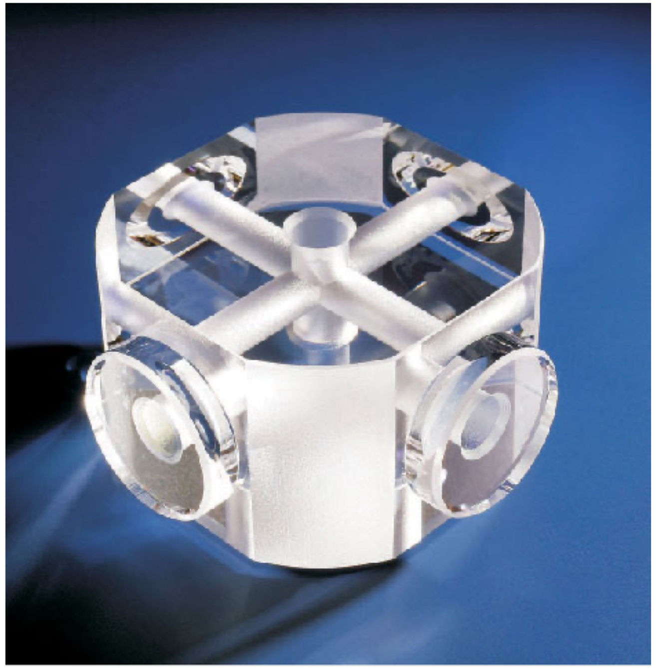

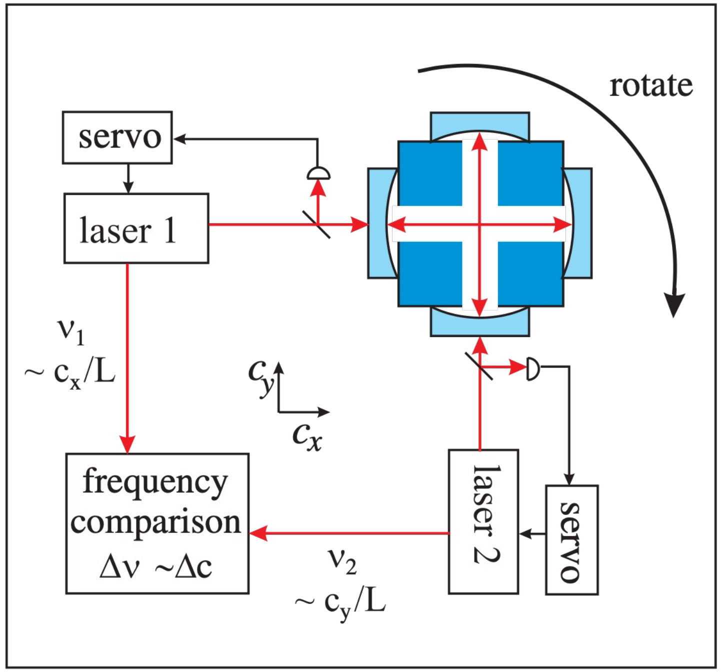

Small Crystalline Optical Resonators

Optical materials

	MgF_2	CaF_2	Fused silica	Quartz
Transparency range	0.12 to 8.5 µm	0.2 to 9 µm	0.18 to 2.5 µm	0.19 to 2.9 µm
Refractive index @ 1550 nm	n_o = 1.37 n_e = 1.38	n = 1.42	n = 1.44	n_o = 1.54 n_e = 1.53
Hardness (Mohs)	6	4	6-7	7
Crystal Class	Tetragonal	Cubic	Non crystalline	Hexagonal
H_2O pollution	Good	Good	Bad	Bad
Mechanical shock	Good	Bad	Good	good

Q = 6 x 1010 demonstrated with CaF2 disk
I. S. Grudinin, V. S. Ilchenko, and L. Maleki, Phys. Rev. A 74, 063806(9) (2006).

MgF_2 turning point

Whispering-gallery-mode resonators as frequency references. II. Stabilization

J. Opt. Soc. Am. B/Vol. 24, No. 12/December 2007

Anatoliy A. Savchenkov, Andrey B. Matsko,* Vladimir S. Ilchenko, Nan Yu, and Lute Maleki

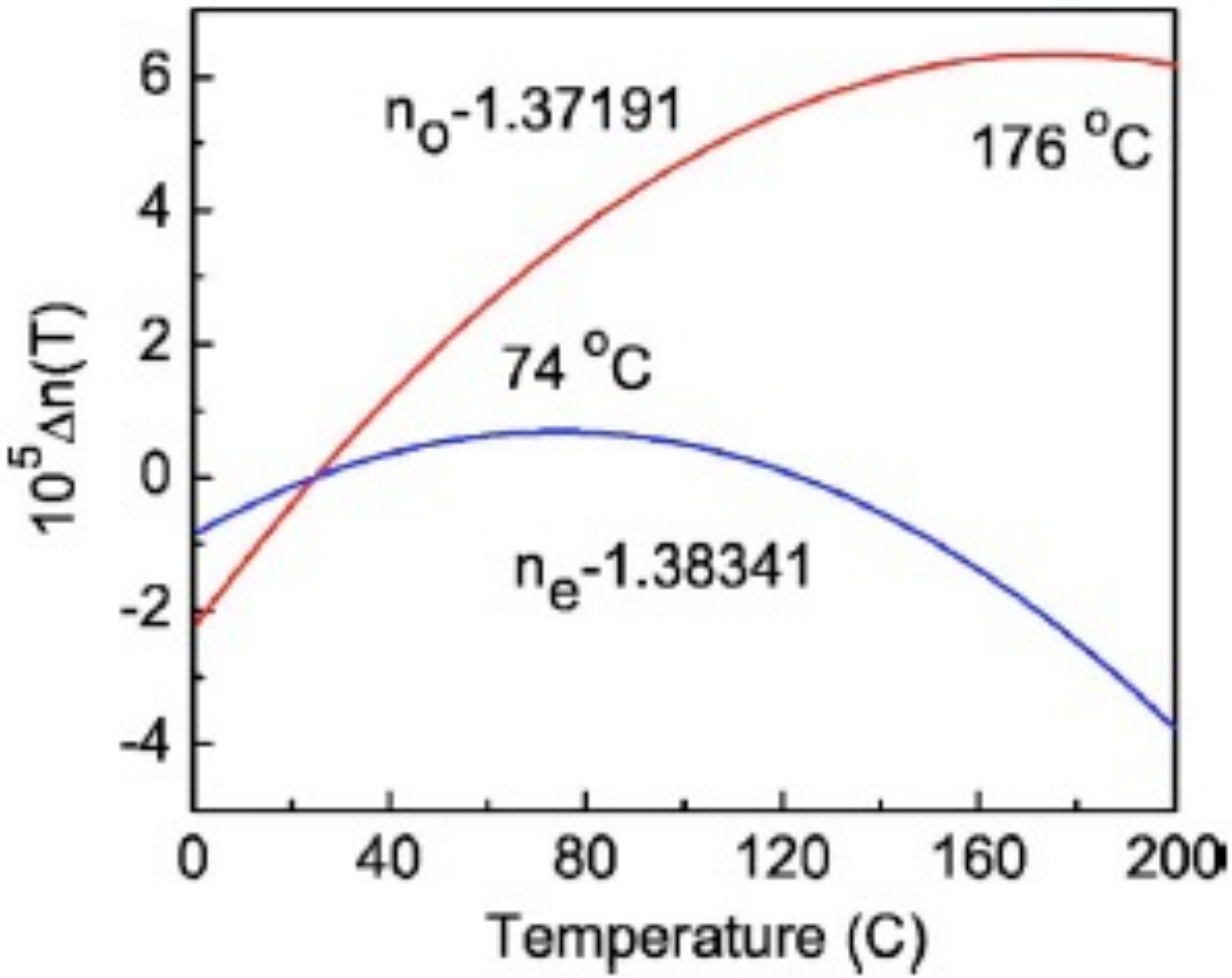

relevant to Pound-Drever-Hall stabilization

Optical whispering gallery

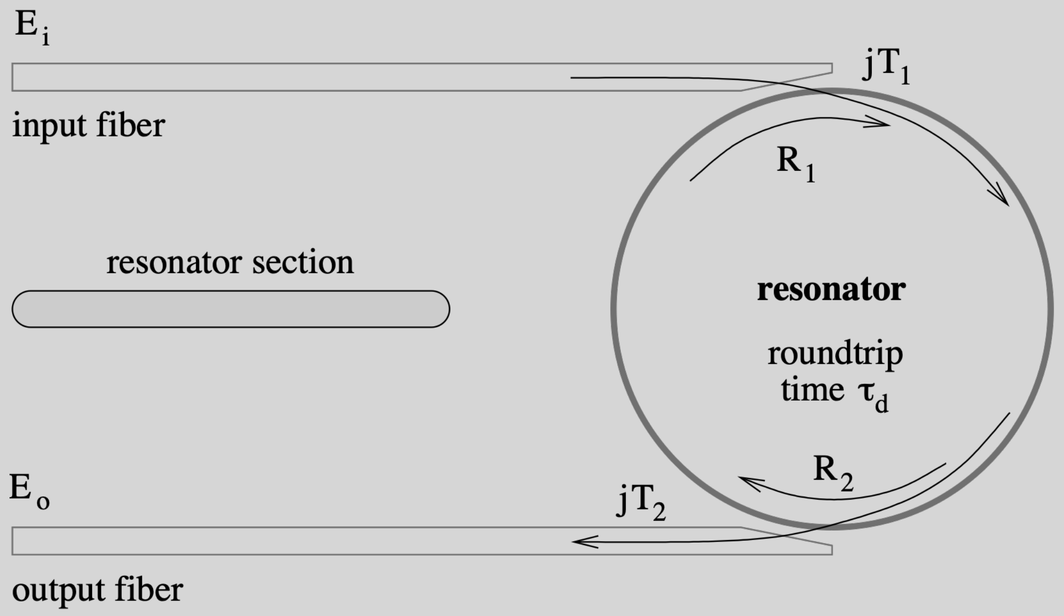

Fig.5.5, E. Rubiola, Phase noise and frequency stability in oscillators, © Cambridge University Press

Alnis & al., PRA 4, 011804(R) (2011)

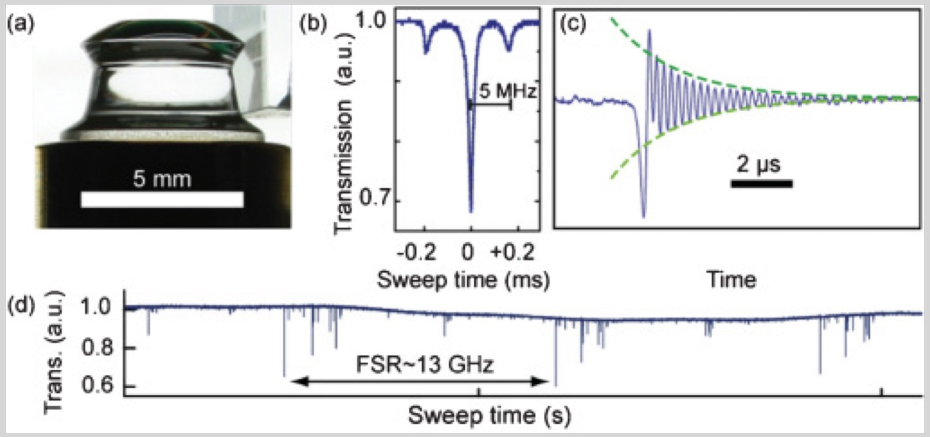

- Pioneering work by Braginsky (Moscow)
- Made popular by Maleki and Ilchenko (JPL/OEwaves)
- Similar to a Fabry Perot
- Q = $10^9 \ldots 10^{11}$ has been reported
- Poor power handling
- Temperature compensation is challenging

Prism-shaped fiber coupler

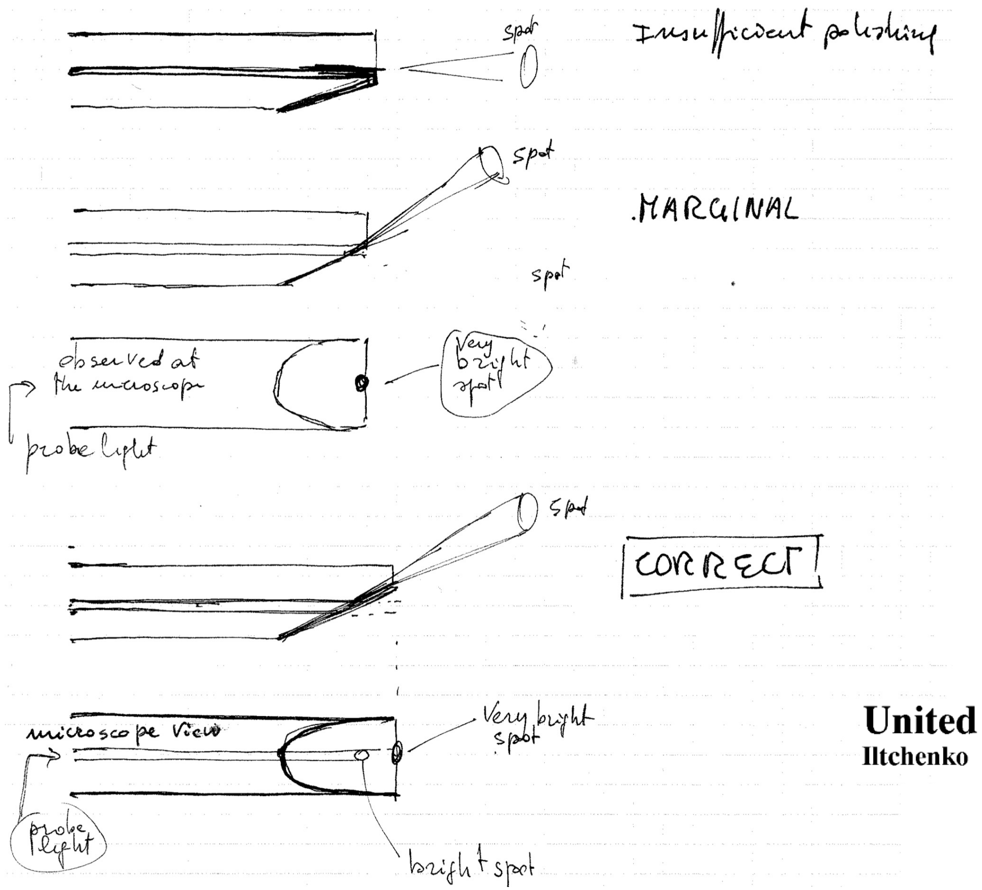

Invented by Vlad Ilchenko & coworkers
Hand making this coupler is amazingly simple

Sticking the fiber with thermoplastic glue on a microscope glass slide is an efficient way to sand and polish the fiber with the appropriate angle, without breaking

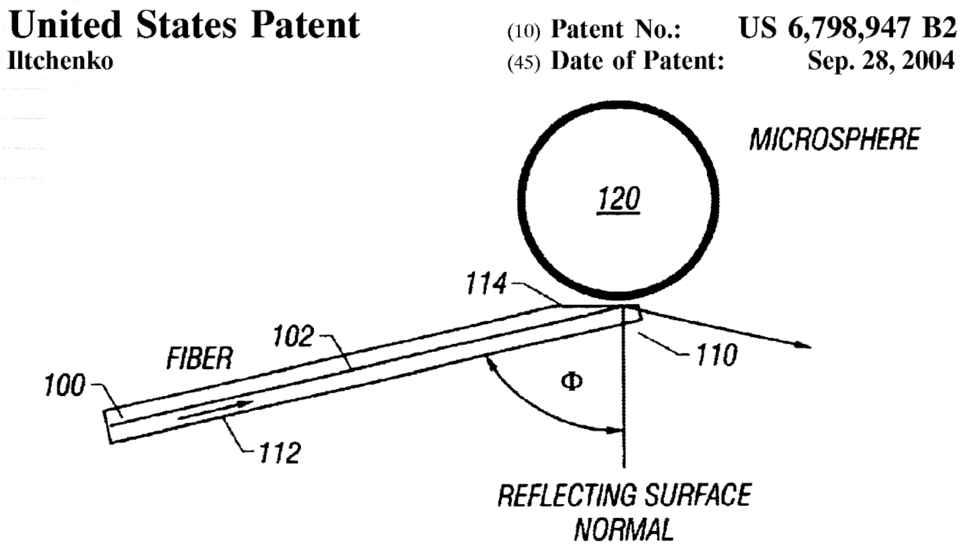

Photo from the Vlad Ilchenko's Linkedin public profile

Dedicated lathe

Brushless motor
Air-bearing to guarantee low vibrations
Small eccentricity error (200 nm)
Precision collet to position the resonator holder

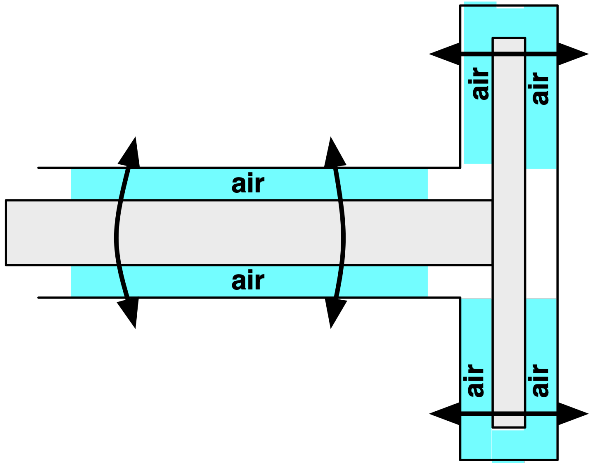

Derives from hard-disk test equipment
Can you figure out what a hard disk is?
3.5” & 7200 rpm => ~ 200 km/h
1 (µm)2 bit area, 50 nm head–disk distance

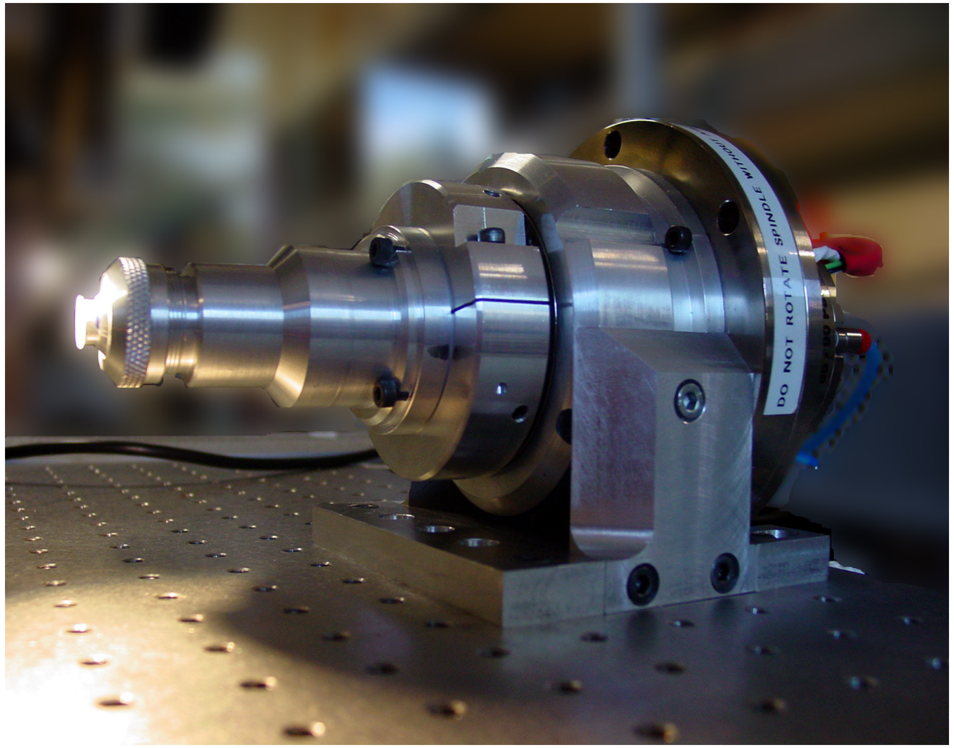

Good air bearings available from the technology of progressive lenses for glasses

Small resonators

- Technology: dedicated lathe
- an air-spindle motor for lowest vibration
  (from a hard-disk test equipment)
- btw, can you figure out what a hard disk is?
- 3.5” & 7200 rpm => ~ 200 km/h
- 1 (μm)2 bit area, 50 nm head–disk distance
- Surface metrology: ready
- A few resonator already made
- quartz, 7 ° Mohs (technology training, not for serious oscillators)
- CaF2 4 ° Mohs, too soft for serious precision machining
- MgF2 (~6 ° Mohs) harder than CaF2, more suitable to machining
- Achieved Q=3x108 with MgF2 resonator
  (still low, but it goes with tapered-fiber coupling)
- Achieved stable coupling with tapered fiber (H. Tavernier)
- Let us dream
- diamond: probably chemical purity may be a problem
  (insufficient transparence)
- sapphire: think more about it
  (we can learn a lot from the microwave technology)
- MgF2 seems to have a turning point of the thermorefractive index
- 74 °C, extraordinary wave
- 176 °C, ordinary wave

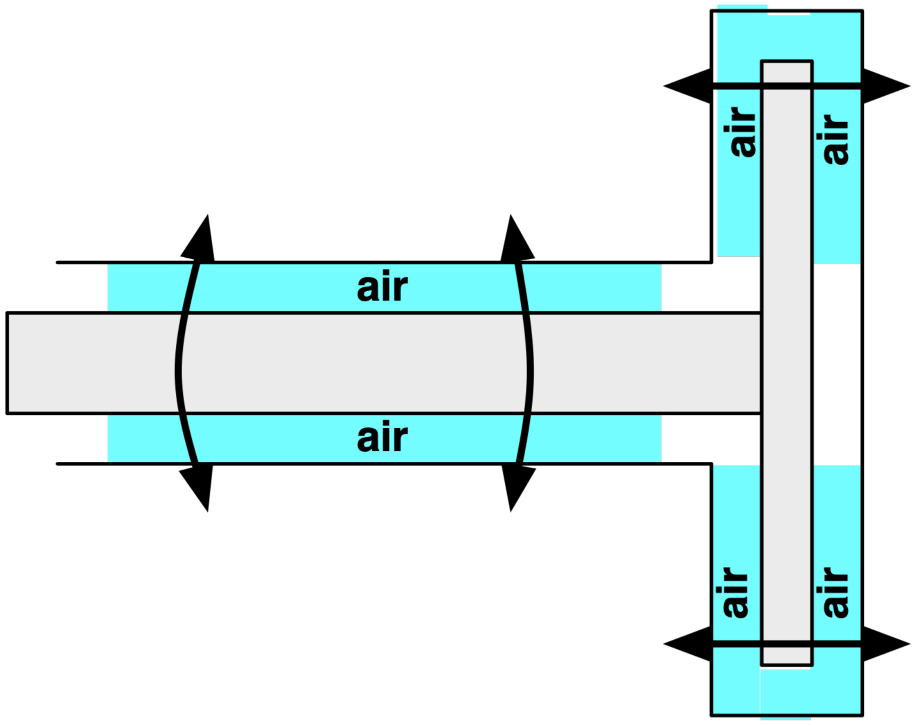

Resonator preforming and polishing

Stick a 6 mm MgF_2 optical window on a metal holder (0.5 - 1 mm thick)

Correct for the centering error by grinding with several diamond grains size (40 - 20 µm)

Create two 20° bevels to get a thin edge (about 30 µm, depending on crystal splinters)

Figures/photos: FEMTO-ST Institute (project canceled)

Several polishing powders in decreasing grains size (diamond, colloidal silica, cerium oxide, alumina) diluted in distilled water (6 µm to 30 nm)

Polishing baize used as powder holder

Rotation speed depends on grain size

Surface roughness & Newton rings

White light phase-shifting microscope
with 1 nm of resolution.
(FEMTO-ST instrument, based on the idea of phase-contrast microscope)

Interference fringes as contour curves.
Smooth contour curves indicates
roughness less than 20 nm.

200 nm surface roughness

< 20 nm surface roughness

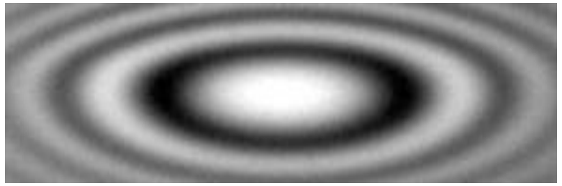

Figures/photos: FEMTO-ST Institute
(project canceled)

Surface roughness

White light phase-shifting microscope with piezo control, after scan and image processing

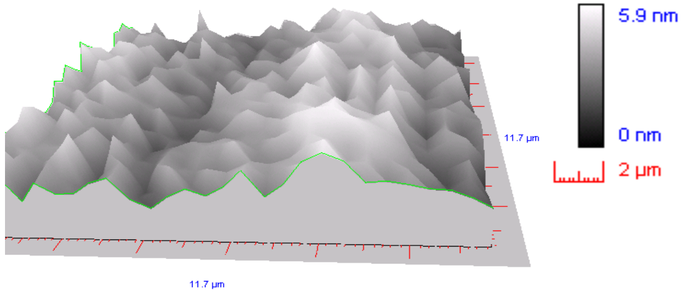

3D surface of the disk

Figures/photos: FEMTO-ST Institute
(project canceled)

Roughness: 6 nm peak-to-peak, 0.92 nm rms.

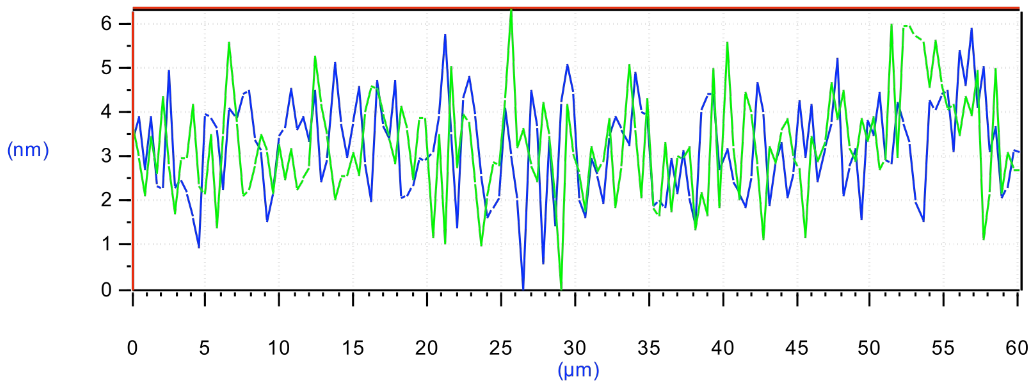

Rt	5,857	6,344
Ra	0,917	0,923
Rq	1,106	1,172
Rsk	-0,089	0,266
Rku	2,563	3,041
Rp	2,652	3,119
Rv	3,205	3,225
Rz	4,309	4,816
Rtm	4,309	4,816

Small quartz resonator

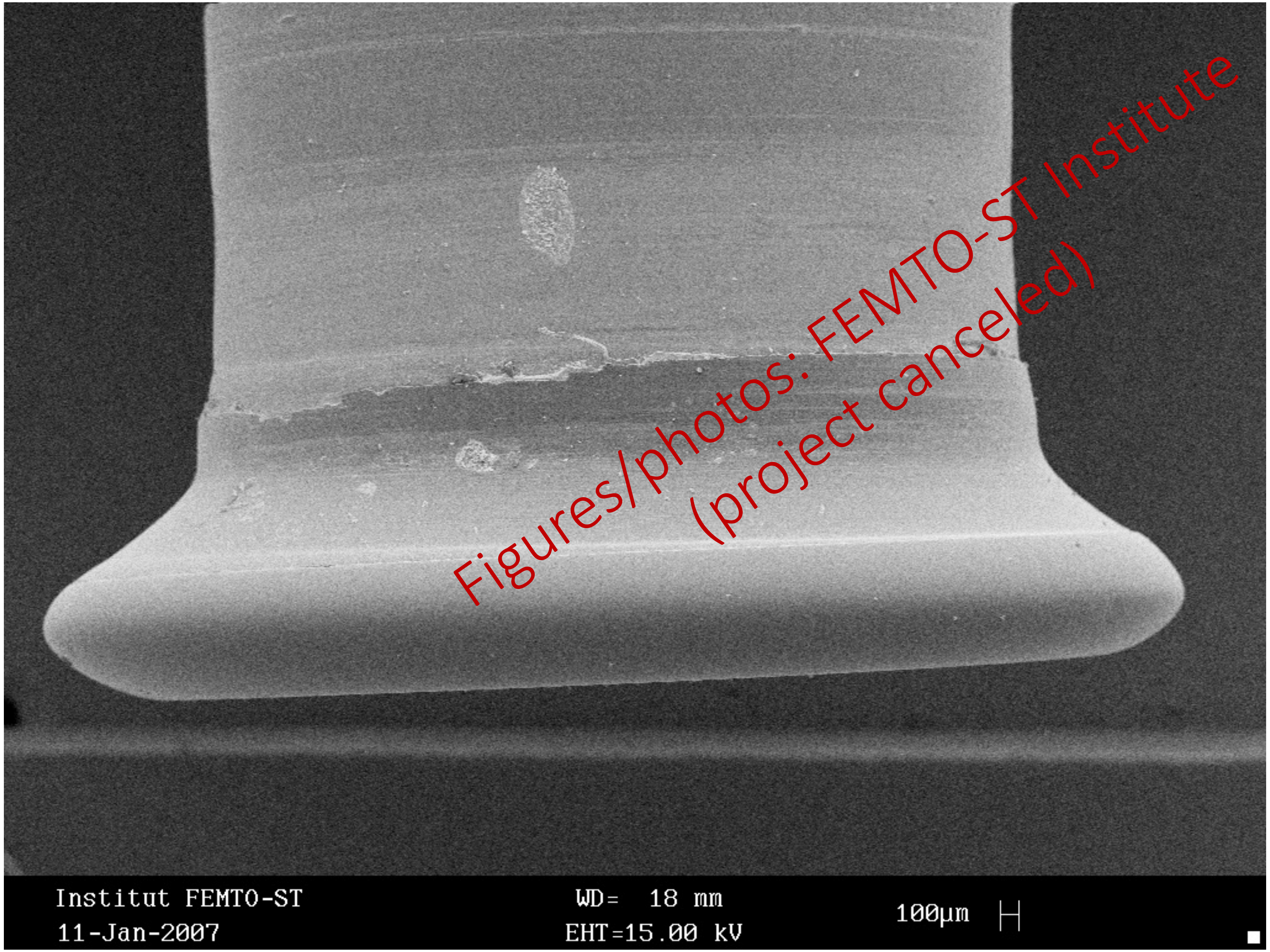

Taper coupling

Tapered SMF28 fiber glued on the holder.
Manufactured by LASEO (Lannion, FR)
For lowest stress, holder geometry and alloy match the thermal expansion of glass.
Waist < 3 µm.
3-axis nano-positioning with 20 nm resolution.

Taper glued on the holder

Nano-positioning system

Figures/photos: FEMTO-ST Institute
(project canceled)

Advantages vs. prism-shaped fiber:
+ higher modal selectivity
+ clean mechanical design
+ one coupler serves as in/out

Disk resonator – Surface characterization

disk
surface

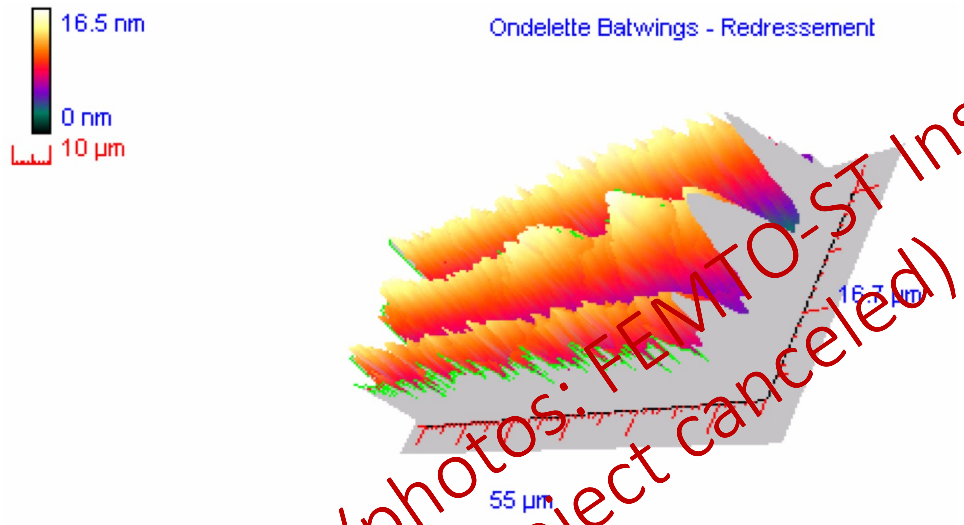

surface
rugosity

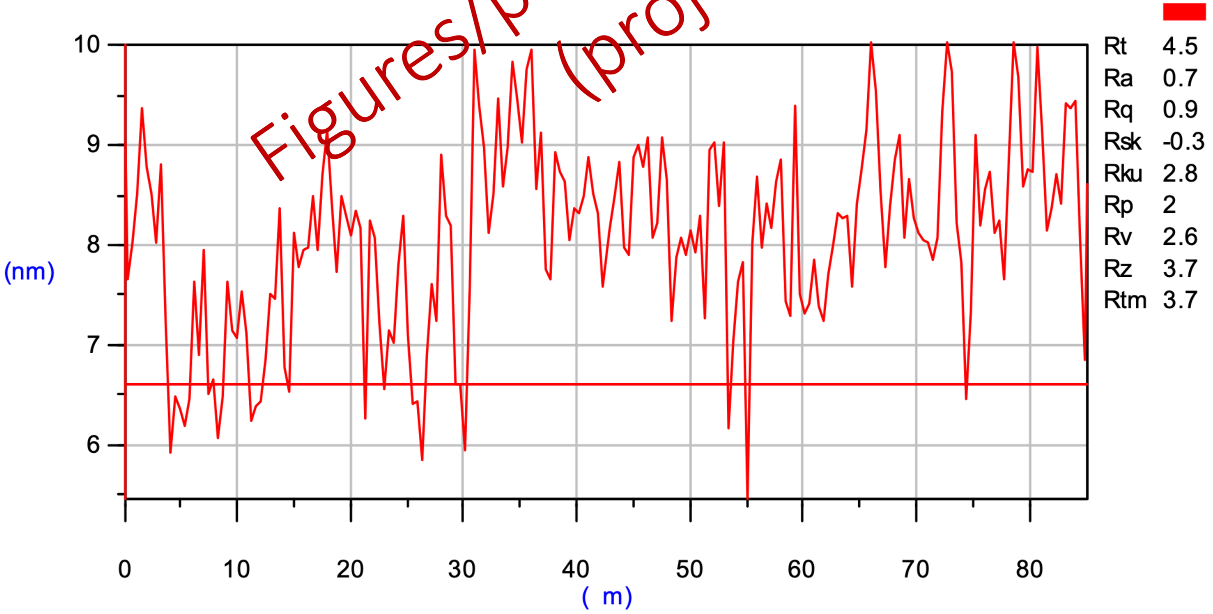

Figures/photos: FEMTO-ST Institute
(project canceled)

Coupling: prism-shaped optical fiber

electron-beam microscope photo

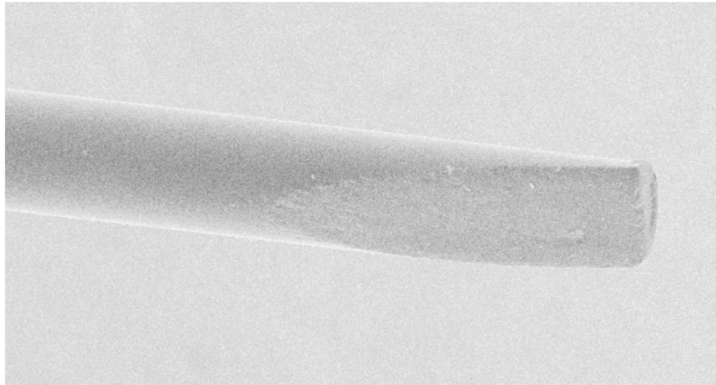

precision
saw

Figures/photos: FEMTO-ST Institute
(project canceled)

surface
rugosity

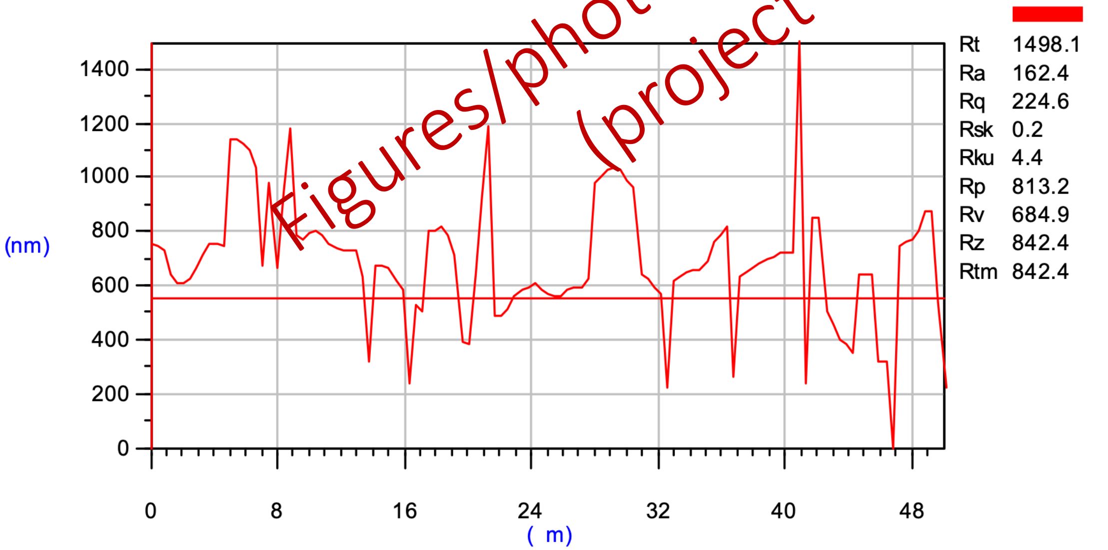

Let technologists have fun with their weird equipment
I don’t think that the fiber machining is that critical (also experience)

Raman oscillations

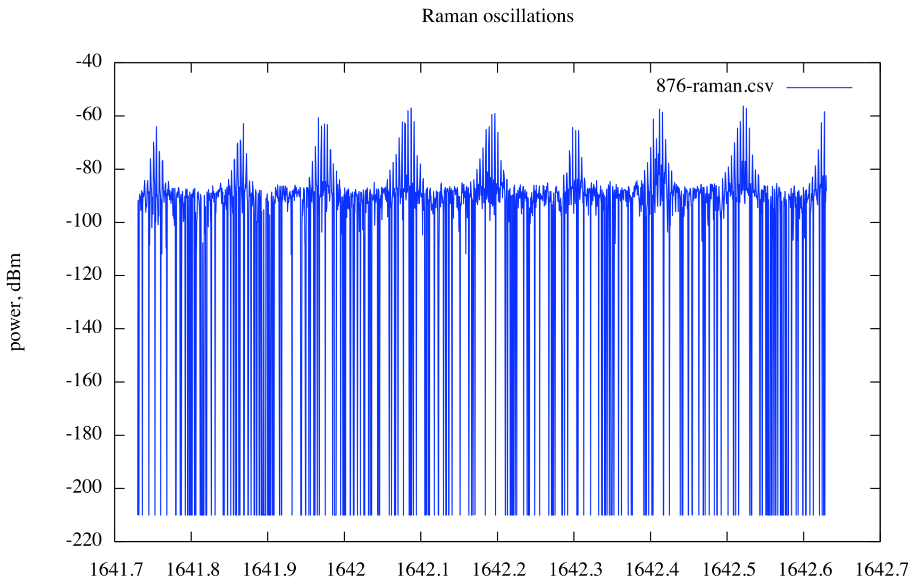

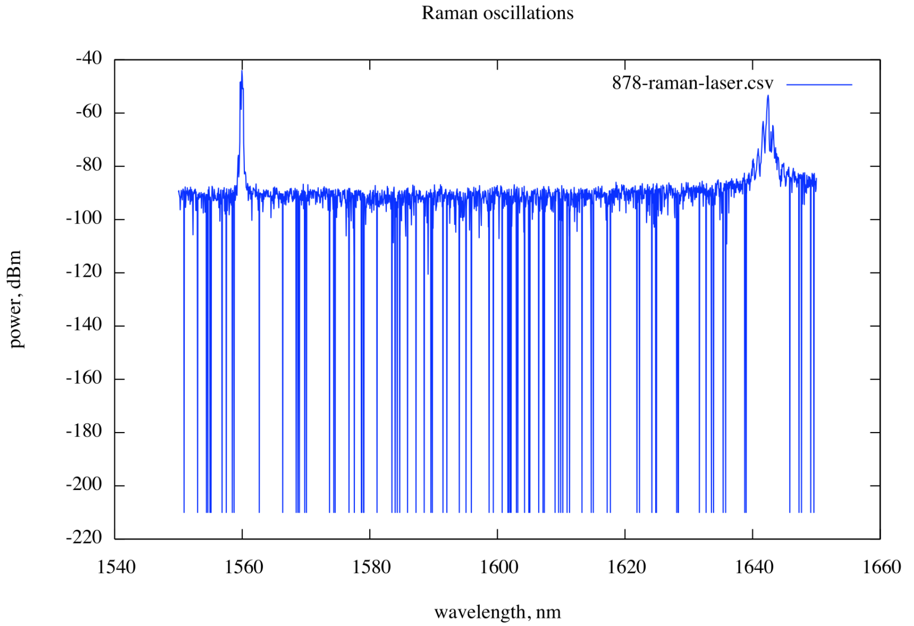

- The Raman amplification is a quantum phenomenon of nonlinear origin that involves optical phonons.
- Raman amplification in a high-Q cavity yields oscillation.
- Oscillation threshold ~ $1/Q^2$ (Anrey Matsko said)
- For reference with $Q \approx 5\times10^9$, the maximum optical power is of 20 μW
- In CaF2 pumped at 1.56 μm, Raman oscillation occurs at 1.64 μm
- Due to the large linewidth, the Raman oscillation appears as a bunch of (noisy) spectral lines spaced by the FSR (12 GHz, or 100 pm for 5.5 mm diam)
- Raman phonons modulate the optical properties of the crystal, which induces noise at the pump frequency (1.56 μm)

Thermal effects on frequency

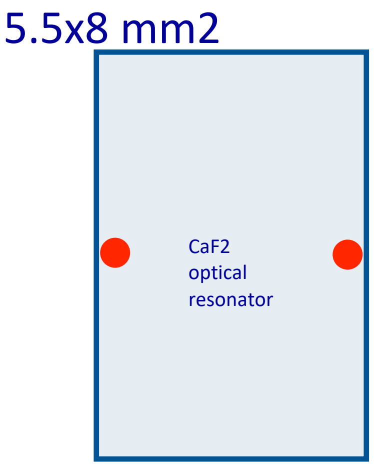

1.56 μm wavelength (192 THz)
Q=5x109 –> BW=40 kHz
300 μW power shifts the resonant frequency by 1.2 MHz
(6x10–9), i.e., 37.5 x BW
Time scale about 60 μs
[Q = 6x1010 demonstrated with CaF2 (I. Grudinin)]

laser scan

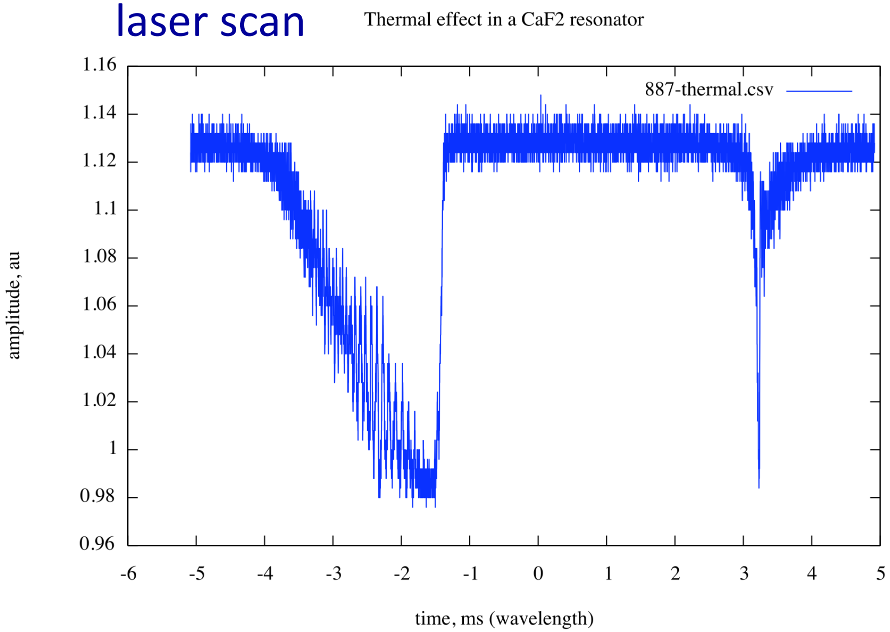

calibration (2 MHz phase modulation)

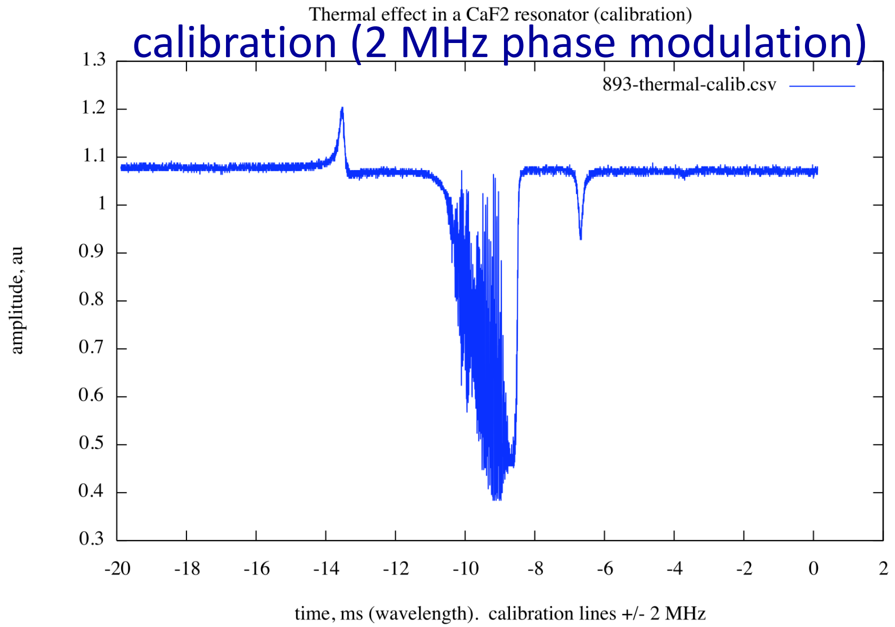

Thermal effect on frequency (MgF_2)

- Asymmetric shape.
- Positive TC (λ) of the
- resonance.
- Triangle sweep.
- First half of resonance shape: t
  energy region.
- The resonance tracks the carrie
- Second half: heating decrease
- The resonance steps back

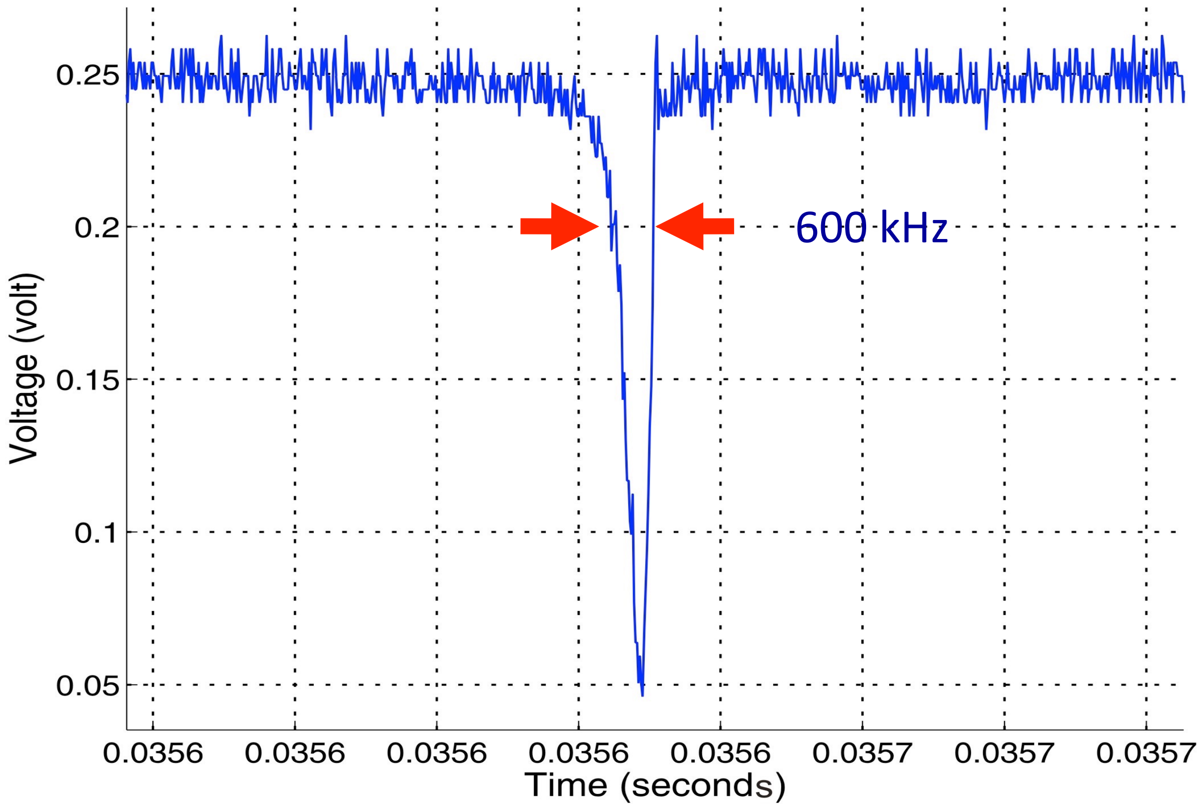

Low-power oscillator operation

Assume: λ = 1560 nm, ρ = 0.8 A/W, R = 50 Ohm, $(P_\lambda)_{peak} = 2\times10^{-5}$ W (20 µW)

Shot noise (m=1)

$$I_{RMS} = \frac{1}{\sqrt{2}}\rho\overline{P}_\lambda$$

$$S_I = 2q\overline{I} = 2q\,\rho\overline{P}_\lambda$$

$$SNR = \frac{1}{4}\frac{\rho\overline{P}_\lambda}{q}$$

Thermal noise (m=1)

$$I_{RMS} = \frac{1}{\sqrt{2}}\rho\overline{P}_\lambda$$

$$S_I = \frac{4kT}{R} \quad \text{or} \quad \frac{4FkT}{R}$$

$$SNR = \frac{1}{8}\frac{\rho^2\overline{P}_\lambda^2 R}{kT}$$

In practice, –131 dBrad^2/Hz

In practice, –110 dBrad^2/Hz with F=0 dB (!!!)

- Thermal noise is dominant: below threshold, SNR ~ $1/P^2$
- Thermal noise can be reduced (10 dB or more?) using VGND amplifiers
- What about flicker of photodetectors with integrated VGND amplifier?
- Dramatic impact on the (phase) noise floor

Extreme nonlinearity

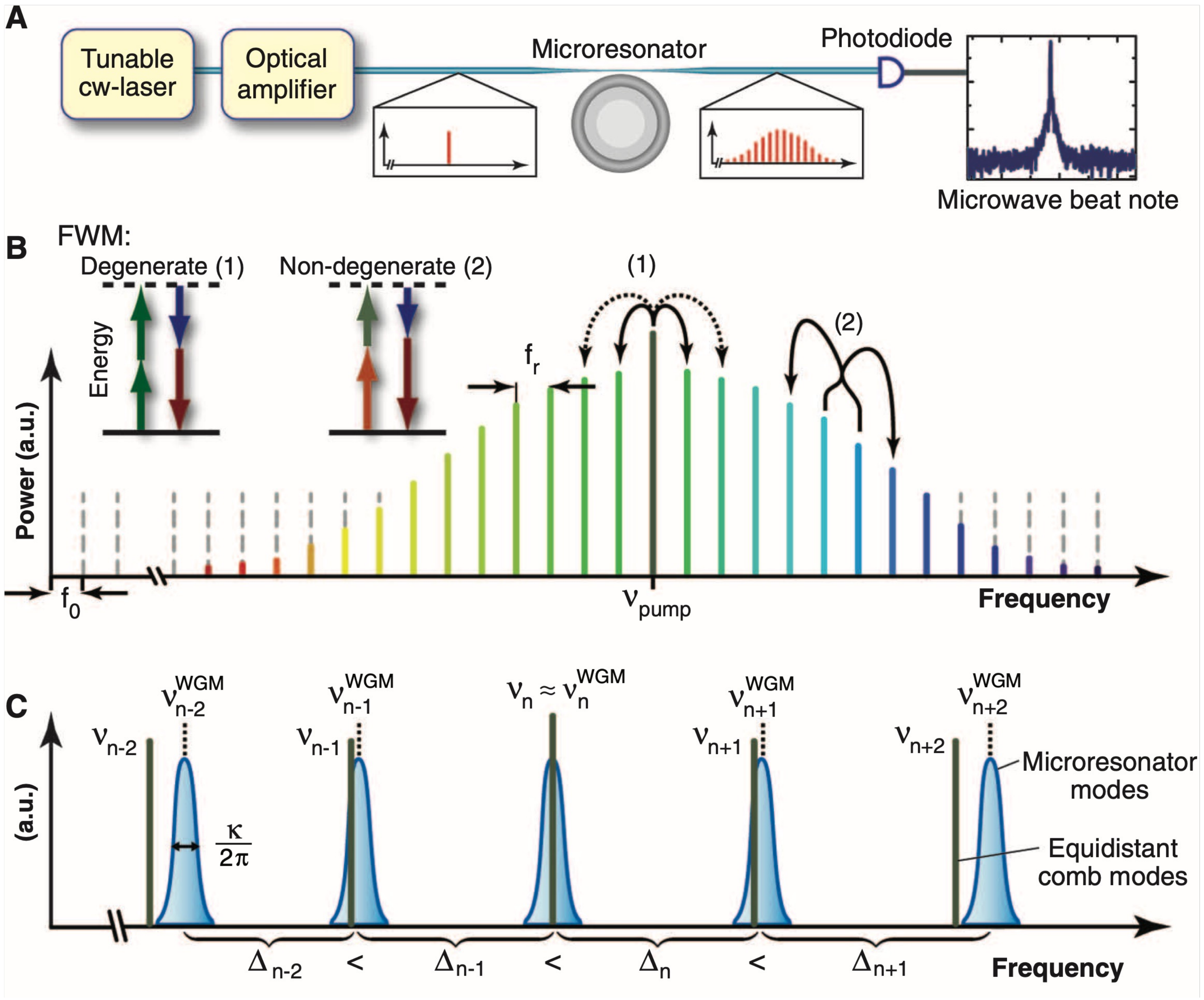

T.J.Kippenberg, R.Holzwarth, S.A.Diddams, Microresonator-based optical frequency combs, Science 332:555, Apr.2011

References

- Black ED, An introduction to Pound–Drever–Hall laser frequency stabilization, Am J Phys 69(1) January 2001
- R.P.V. Drever, J.L. Hall & al., Appl. Phys. Lett. 31(2) p.97–105, June 1983
- Hall JL & al, Laser stabilization, Chapter 27 of Bass et al, Handbook of optics, McGraw Hill 2001
- Mor O, Arie A, JQE 33(4), April 1997
- R.V. Pound, Rev. Sci. Instrum. 17(11) p. 490–505, Nov. 1946
- Z. Galani & al, IEEE-T-MTT 39(5), May 1991
- P. Sulzer, Proc. IRE 43(6) p.701-707, June 1955

Accuracy and Noise

- Bahoura M, Clairon A - Ultimate linewidth reduction of a semiconductor laser frequency-stabilized to a Fabry-Perot Interferometer - IEEE TUFFC 50(11), November 2003
- Vinet JY ed., The VIRGO physics II, Optics and related topics, available online
- Black ED, An introduction to Pound–Drever–Hall laser frequency stabilization, Am J Phys 69(1) January 2001

Immunity to Cable Length

- Modulation is not affected by a delay
  - In telecommunication, (amplitude stretch and) delay is called “non-distortion condition”
  - Radio communications provide evidence
- Enables high stability with the resonator in vacuum, in cryogenic environment, or far from the oscillator

optical FP in vacuum

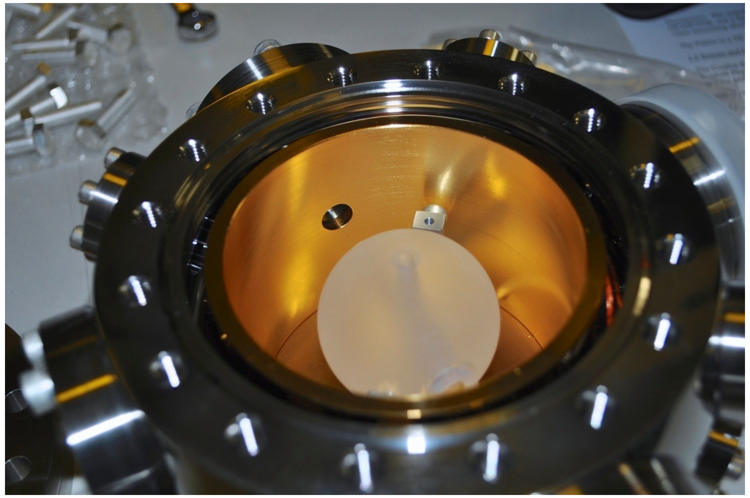

cryogenic microwave sapphire

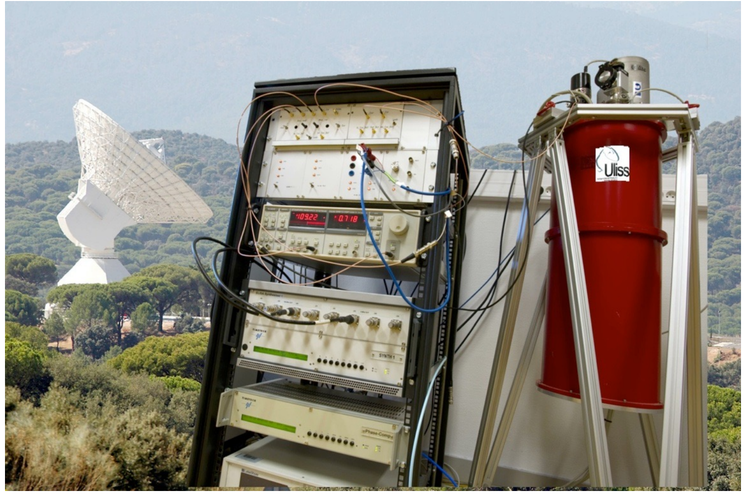

Atomic Frequency Standards!

Totally different physics – Similarity with the detection process

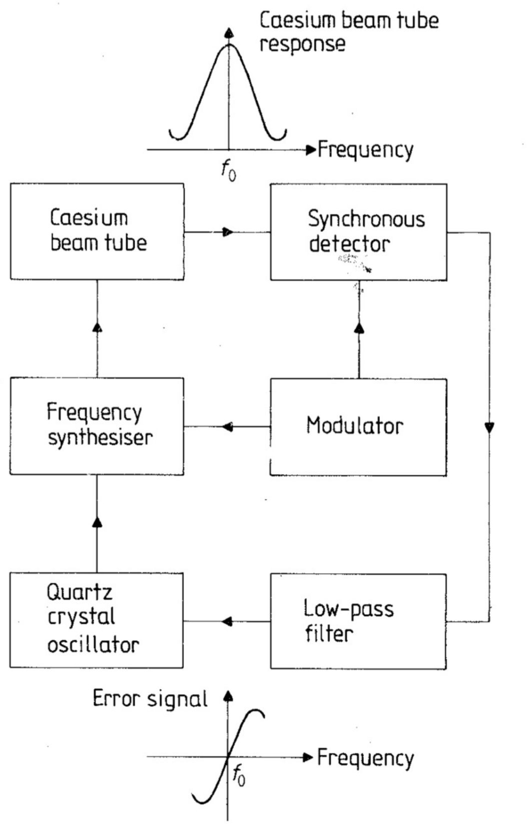

Vanier J, Audoin C, The quantum physics of atomic frequency standards v2, Adam Hilger 1989 – p.617

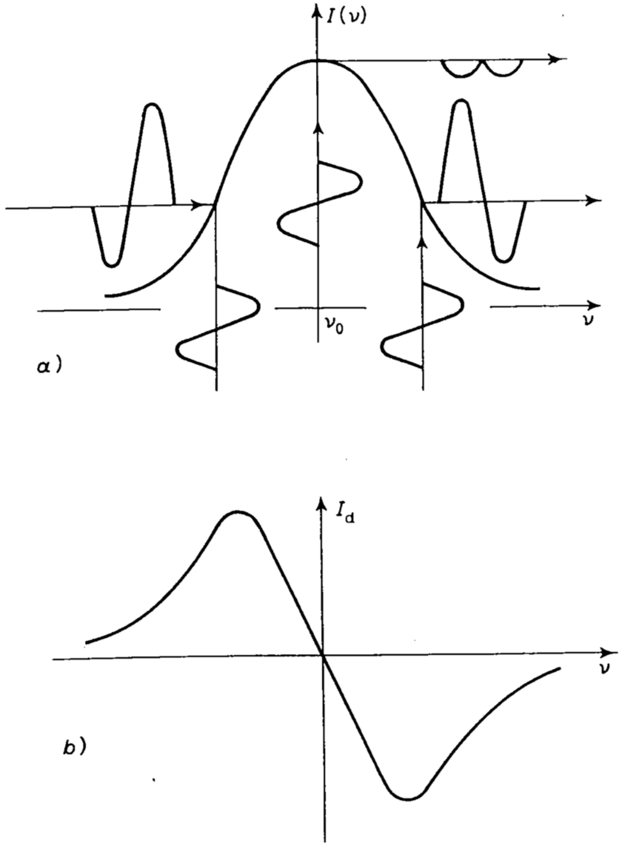

Vanier J, Audoin C, The quantum physics of atomic frequency standards v2, Adam Hilger 1989 – p.614

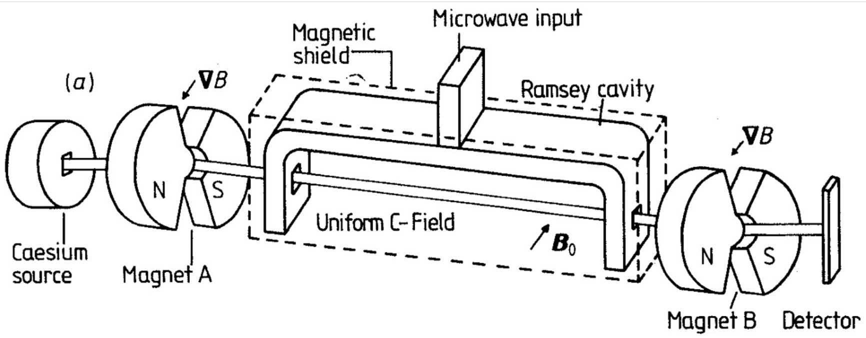

Ferro-Milone A, Giacomo P, Metrology and fundamental constants, North Holland 1980 – p.192 0-444-85467-3

Pound vs Interferometer

Carrier suppression techniques now make possible a dramatic reduction in flicker noise. This has complemented the high Q of sapphire to allow unprecedented oscillator performance.

- Passive sources already make possible very low phase noise.
- Flicker noise in passive mixers is 20 to 30 dB lower than for microwave amplifiers required by an active oscillator.

John Dick, NASA/JPL

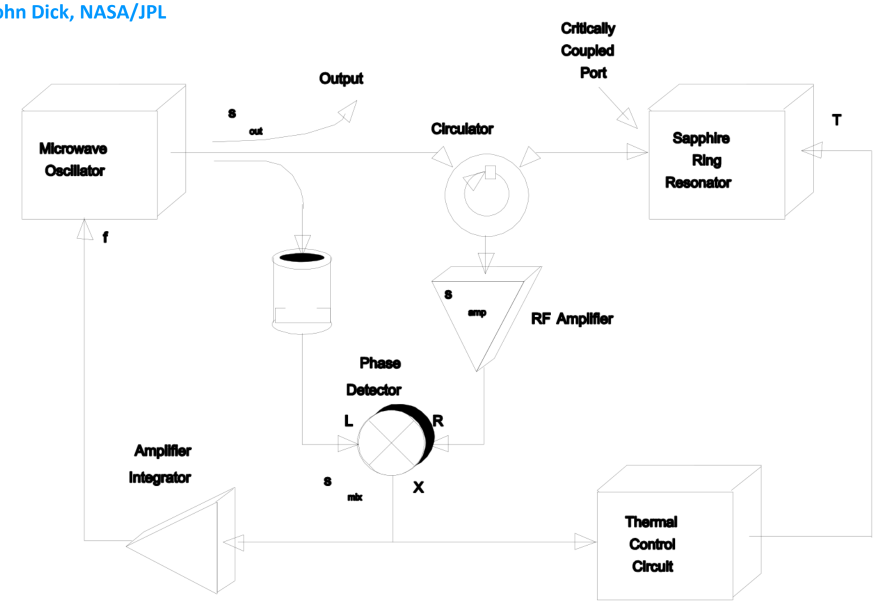

Block Diagram - Sapphire Phase Stabilizer (SPS)

However, the interferometer works in dc, it cannot get out of the flicker region

Unused Material

Duplicated

The Pound-Sulzer oscillator

I already have a slide like this, with the picture taken from the Cambridge book

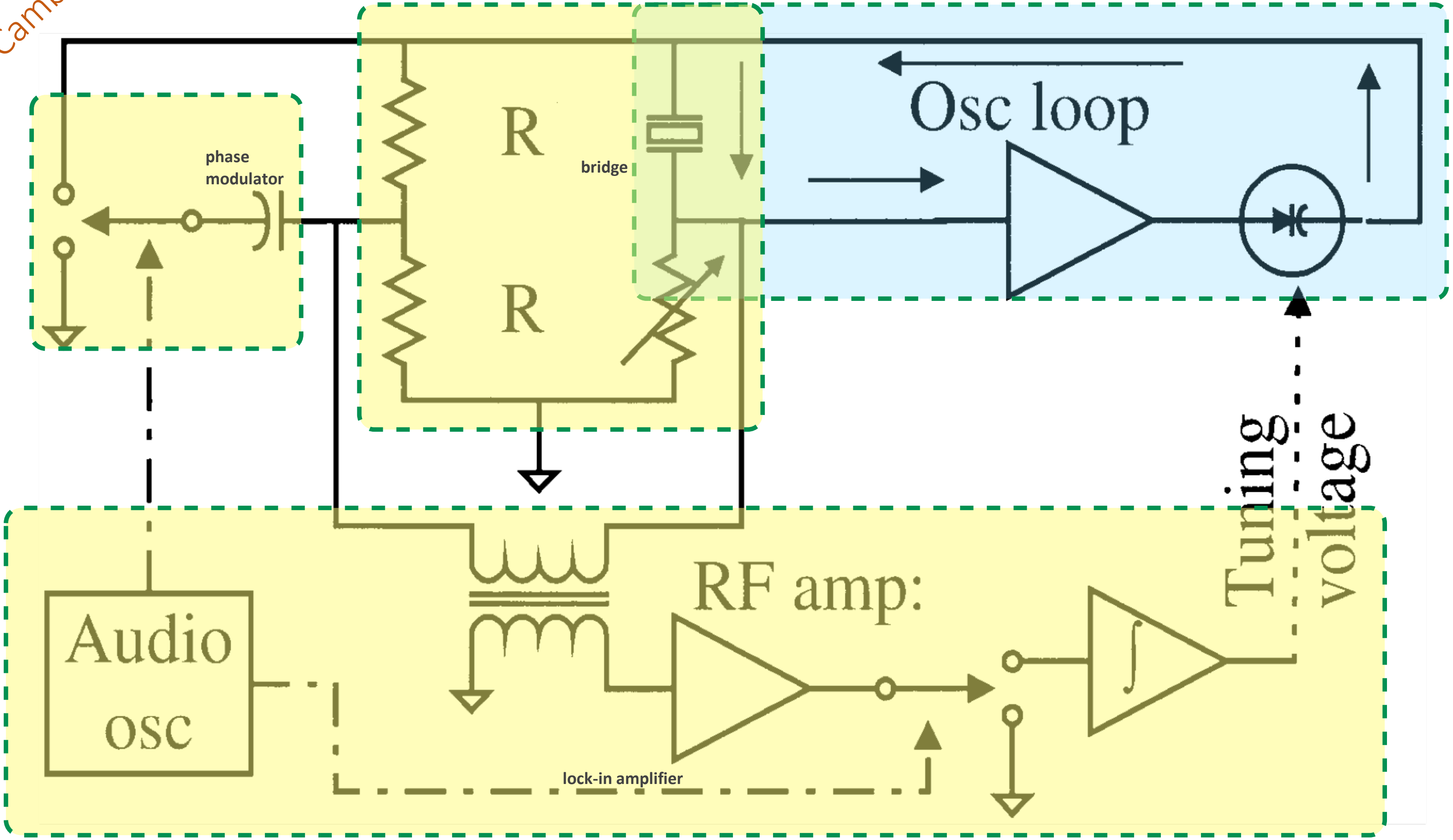

Figure from P. Sulzer, Proc. IRE 43(6), June 1955

P. Sulzer, "High stability bridge balancing oscillator," Proc. IRE 43(6), pp. 701–707, June 1955.

End of lecture 10